NONLINEAR SITE AMPLIFICATION FUNCTIONS FOR CENTRAL AND EASTERN NORTH AMERICA

BY

JOSEPH A. HARMON

DISSERTATION

Submitted in partial fulfillment of the requirements
for the degree of Doctor of Philosophy in Civil Engineering
in the Graduate College of the
University of Illinois at Urbana-Champaign, 2017

Urbana, Illinois

Doctoral Committee:

Professor Youssef M. A. Hashash, Chair
Associate Professor Scott M. Olson
Assistant Professor Ahmed E. Elbanna
Professor Jonathan P. Stewart, University of California, Los Angeles
Professor Ellen M. Rathje, University of Texas at Austin

Abstract

Site amplification functions are used to modify ground motions from a reference bedrock condition to a surface condition based on the geologic features of the site of interest. Site amplification has been extensively studied and evaluated empirically for seismic regions such as the Western United States where there are abundant ground motion recordings for many sites and earthquake events. In regions of relatively lower or infrequent seismicity, such as Central and Eastern North America (CENA), the lack of ground motion recordings and seismic site properties severely limits the empirical characterization of site amplification. This research uses site response simulations to develop site amplification functions for CENA.

The first part of this study is the development of 1,747,278 1-D linear elastic, equivalent linear, and nonlinear site response analyses. Simulations are designed to capture the variability in site conditions in CENA and the uncertainty in soil properties at individual sites. Site profiles are developed for 1,747,278 site response analyses, 582,426 each of linear elastic, equivalent linear and nonlinear 1-D analyses for 70,650 unique site profiles. The database of simulations is the largest of its kind. This study describes the process for generating V_S profiles, soil and weathered rock material properties, and ground motions to represent the variability and uncertainty of site conditions in CENA.

The second part of this study is the modeling of the site response simulation data with linear and nonlinear site amplification functions for the response spectrum (RS) and Fourier amplitude spectrum (FAS) and a correction factor to convert site amplification from a 3000 m/s CENA hard rock condition to a 760 m/s condition. The modular RS amplification model includes terms for time averaged shear wave velocity in the top 30 m of a site (V_{S30}), site natural period, soil depth, and site nonlinearity which can be coupled with empirically-developed linear empirical amplification models. Including site natural period into the amplification function is shown to greatly improve estimates of site response over models dependent only on V_{S30}. The FAS site amplification model is the first model developed from simulations, and the first to include nonlinear amplification.

Acknowledgements

I would like to my appreciation and respect for my advisor, Professor Youssef M. A. Hashash for his guidance and support throughout the period of study. His critiques and investment of time and energy in the support of this research have been a source of professional and personal inspiration. I would like to extend my appreciation to Professors Jonathan P. Stewart of the University of California, Los Angeles and Ellen M. Rathje of the University of Texas at Austin who have provided immense value to this work through their alternative viewpoints and constructive criticism.

I would also like to extend my appreciation to the members of my committee: Professor Scott M. Olson, and Professor Ahmed E. Elbanna for their interest in my research.

My appreciation is extended to the many talented researchers who I have had the pleasure of collaborating with including Albert Kottke of Bechtel, Ken Campbell of CoreLogic, Walt Silva of Pacific Engineering and Christine Goulet of SCEC.

Special thanks is extended to the many talented graduate and undergraduate researchers who have contributed greatly to my education, especially Michael M. Musgrove, Okan Ilhan, and Hua Shao, who have contributed enormously to both the work I have done and my personal development as a researcher. I thank my research group members Byungmin Kim, Ozgun A. Numanoglu, Eun Hyun Park, and Omar Al Baltaji for their insight and perspective.

I would like to thank my parents and my sister, Ivy, for their unwavering support and encouragement.

The support from the University of Illinois and the USGS and NEHRP under grants G14AP00102, G14AP00103, G14AP00104 is also gratefully acknowledged.

Table of Contents

List of Figures

List of Tables

List of Symbols

Symbol	
$C_{760-3000}$	Correction factor between 760 m/s V_{S30} and 3000 m/s V_{S30}
$F_{S,B}$	Response Spectrum base-case site amplification without basin effects
F_{lin}	Response Spectrum Linear Amplification
F_{nl}	Response Spectrum Nonlinear Amplification
H_{sed}	Thickness of sediments
V_c	V_S above which no increase in amplification with V_{S30} is observed
c_{V_S}	Cohesive shear strength from V_S
n_v	Exponent of V_S increase as function of depth or confining pressure
σ_v'	Vertical effective stress
D	Small-strain damping
E_{lin}	Fourier Amplitude Spectrum Linear Amplification
E_{nl}	Fourier Amplitude Spectrum Nonlinear Amplification
$E_{S,B}$	Fourier Amplitude Spectrum base-case site amplification without basin effects
f	Cycle frequency
f_{max}	Maximum frequency that a material layer can propagate in site response
G/G_{max}	Ratio of secant shear stiffness to maximum shear stiffness
I_r	Ground motion intensity parameter that drives site nonlinearity
I_y	Strain index
K_0	At-rest earth pressure
M_w	Earthquake moment magnitude
N	Number of Cycles
Q:	Anelastic attenuation factor
T_{nat}	Site natural period
T_{OSC}	Response Spectrum Oscillator period
V_{LIN}	V_S threshold for nonlinear site amplification to be observed
V_{ref}	Reference V_S
V_S	Shear wave velocity
V_{S30}	Time-averaged shear wave velocity in the top 30 m of a site
Z_{soil}	Depth of soil
α	Width of Riker wavelet
β	Offset of central peak of Riker wavelet
γ	Unit weight of soil
Δκ	Change in κ between rock outcrop and ground surface due to site effects
ε_D	Random number generated for damping curve randomization
ε_G	Random number generated for G/G_{max} curve randomization
κ	Exponential decay of FAS at high frequency
ρ	Material density
σ	Standard Deviation
τ	Shear Strength
φ	Friction Angle
r	Radial Earthquake Distance

List of Abbreviations

Abbreviation	
amp	Amplification
BSSA14	Boore et al. (2014)
CENA	Central and Eastern North America
CS05	Choi and Stewart (2005)
EL	Equivalent Linear
FAS	Fourier Amplitude Spectrum
GEM	Global Earthquake Model
GMIM	Ground Motion Intensity Measure
GMM	Ground Motion Model
GQ/H	General Quadratic / Hyperbolic
GWG	Geotechnical Working Group
LE	Linear Elastic
MASW	Multiple Analysis of Surface Waves
NEHRP	National Earthquake Hazard Reduction Program
NGA	Next Generation Attenuation Relations
NL	Nonlinear
NUREG	Nuclear Regulatory Guides
OCR	Overconsolidation Ratio
PGA	Peak Ground Acceleration
PGD	Peak Ground Displacement
PGV	Peak Ground Velocity
PI	Plasticity Index
PSA	Pseudo-spectral Acceleration
RS	Response Spectrum
SA	Spectral Acceleration
SCR	Stable Continental Region
SMSIM	Stochastic Method Simulation
SS14	Seyhan and Stewart (2014)
USGS	United States Geological Survey

Chapter 1. Introduction

1.1 Problem Statement

Site amplification functions are used to modify ground motions from a reference bedrock condition to a surface condition based on the geologic features of the site of interest. Site amplification has been extensively studied and evaluated empirically for seismic regions such as the Western United States (WUS) where there are abundant ground motion recordings for many sites and events. In regions of relatively lower or infrequent seismicity, such as Central and Eastern North America (CENA), the lack of ground motion recordings and seismic site properties severely limits the empirical characterization of site amplification. Additionally, differences in geologic regimes limit the applicability of site amplification models developed for active seismic regions to stable regions. Earthquakes in stable continental regions are usually infrequent, but still contribute to seismic hazard for infrastructure and lifelines, and a quantification of site behavior is required for engineering design and seismic hazard mapping.

The Next Generation Attenuation Relationships for Central and Eastern North America (NGA-East) project coordinated by the Pacific Earthquake and Engineering Research center (PEER) have developed models that characterize ground motions in CENA (PEER 2015). The site effects of the ground motion models (GMM's) developed as a part of the NGA-East project for the entire CENA region are constrained by measurements at 84 of 1379 stations (Goulet et al. 2014) and with mostly weak motions. Site response behavior of a much larger range of site conditions and ground shaking levels are needed to supplement this limited dataset.

1.2 The NGA-East Geotechnical Working Group

The work presented in this study was completed as a part of the Next Generation Attenuation Relationships for Central and Eastern North America (NGA-East) as a collaborative project with the NGA-East Geotechnical Working Group. The NGA-East is a multi-disciplinary research project coordinated by the Pacific Earthquake Engineering Research center (PEER), and is jointly sponsored by the US Nuclear Regulatory Commission (NRC), the US Department of Energy, the Electric Power Research Institute, and the US Geological Survey (USGS) and is

tasked with the development of a ground motion characterization model for CENA. The NGA-East Geotechnical Working Group (GWG) serves as resource experts that focus on a specific technical area of the NGA-East Project. The NGA-East GWG was tasked with defining the reference rock shear wave velocity and kappa values and developing a model for site effects. The members of the Geotechnical Working Group are: Professor Youssef M. A. Hashash of the University of Illinois at Urbana-Champaign, Professor Jonathan P. Stewart of the University of California, Los Angeles, Professor Ellen M. Rathje of the University of Texas at Austin, Ken W. Campbell of CoreLogic, and Walt J. Silva of Pacific Engineering. Many other collaborators from industry and graduate students have been involved with the NGA-East GWG since it was formed.

Work produced from the NGA-East GWG that is used directly in this study are the definition of the 3000 m/s reference rock condition in Hashash et al. (2014a), the classification of site V_{S30} by geology in Kottke et al. (2012), and the establishment of an *a priori* threshold that describes the differences between EL and NL site response analyses in Kim et al. (2015).

Several sections presented in this thesis were developed by others as a part of the collaborative effort of the NGA-East GWG, notably Chapter 4, Chapter 6, and Section 10.2.1 which were developed originally by E. Rathje and B. Xu of the University of Texas at Austin. The work presented in these sections is as yet unavailable elsewhere but integral to the study as a whole. For this reason, these sections are included in this thesis for completeness.

1.3 Objectives and Scope of Study

The main purpose of this study is to develop robust, statistically significant site amplification functions from simulations of site conditions in CENA for the response spectrum (RS) and Fourier Amplitude Spectrum (FAS). To achieve this goal a parametric study of 1-D site response analysis simulations is conducted and the simulation results regressed and modeled to develop a suite of site amplification functions relative to the V_S = 3000 m/s hard rock condition of CENA.

Data of site conditions in CENA is collected and used to develop inputs to the parametric study. Input data required for this study are shear wave velocity (V_S) profiles, material properties, and bedrock motions.

The response spectral site amplification models developed have one nonlinear amplification component and three linear amplification components: (1) V_{S30} (time-average shear wave velocity of the top 30 m of a site) scaling, (2) soil depth effects, and (3) soil column natural period (T_{nat}) effects. The Fourier amplitude spectral site amplification model has linear and nonlinear components. Period-dependent coefficients are provided for the FAS and RS amplification models.

1.4 Organization of Thesis

Chapter 2 introduces the current state of practice for conducting site response analyses and site amplification. Chapter 3 describes the structure of the parametric study and an overview of the site response analyses conducted. Chapters 4 through 7 describe the development and selection of input properties to the parametric study. Chapter 4 describes the selection of rock outcrop motions, Chapter 5 describes the development of V_S profiles from data, Chapter 6 describes the selection of small strain damping, and Chapter 7 describes the selection of material properties including nonlinear behavior.

The simulation dataset is presented in Chapter 8. Chapter 9 describes the development of the linear and nonlinear RS site amplification functions, and Chapter 10 describes the development of the linear and nonlinear FAS site amplification function.

Finally, conclusions are reached in Chapter 11 and future developments are suggested for work that builds on the simulation dataset and site amplification models presented in this study.

Chapter 2. Site Response Analyses and Site Amplification

2.1 Use of Simulations in GMM Development in CENA

Simulations have previously been used to develop site amplification functions and constrain empirical site amplification functions in the WUS and CENA. Stochastic simulations have been widely used in evaluating linear amplification in both the WUS and CENA (e.g. Boore 1983, 2003, and 2015b, Campbell (2003), Pezeshk et al. (2011), and others). One-dimensional site response simulations have been used in the WUS in the assessment of site amplification in the San Francisco Bay area and Los Angeles Basin (Silva et al. 1999) and the Next Generation Attenuation Relationships for Western US (NGA-West) project where equivalent linear (EL) simulations from Walling et al. (2008) were used to constrain the nonlinearity of GMM's. The constraints on nonlinearity were updated for the NGA-West2 project by Kamai et al. (2014) by using 1-D simulations of a wider range of site conditions and a more versatile functional form for nonlinear site amplification. The Kamai et al. (2014) model is designed for use within the context of GMM development, and as such, only the model coefficients related to nonlinear site amplification are provided. The linear site amplification model coefficients to be regressed from ground motion data at the same time as other GMM model parameters. For the NGA-East project the GMM developed by Graizer (2015) used a site correction developed from EL analyses of representative soil profiles.

In CENA, simulation-based site amplification functions for NEHRP-style site amplification factors have been developed for specific regions. Moon et al. (2016) used nonlinear site response (NL) analyses to develop depth-dependent site factors for the Mississippi Embayment, and Aboye et al. (2015) used 13,000 nonlinear and equivalent linear site response analyses to develop site amplification functions for the Charleston, South Carolina area. Neither of these sets of simulations are intended to characterize the entire CENA region, and as 1-D site response capabilities have advanced, these previous studies lack features of current best-practice nonlinear site response analyses such as constraints on shear strength and a low maximum usable frequency, f_{max}.

A large scale parametric study of 1D site response simulations to develop ergodic amplification functions for CENA is presented. The site response simulations presented in this study are used to develop base case (i.e. the free field amplification without basin effects) linear and nonlinear site amplification models for CENA that can be used independently of GMM development and use the current best-practice nonlinear site response analyses procedures. To capture the range of site condition and seismic hazard variability and uncertainty in CENA, many more simulations are used than previous studies. This study presents 1.7 million site response simulations, more than the next largest study of 324,000 simulations of Moon et al. (2016). Parameters required to define a site response simulation can broadly be split into two categories: rock outcrop ground motions and soil site conditions. A database of ground motions characteristic of the bedrock condition in CENA is developed with a range of intensities, spectral shapes, magnitudes, and distance. Site profiles with representative CENA site properties are systematically developed and their properties varied including V_S profile and soil properties.

The site response analysis software DEEPSOIL V6.1 (Hashash et al. 2016) is used to perform linear elastic (LE), EL and NL 1-D simulations of CENA site response in this study. DEEPSOIL has been extensively verified and validated (i.e. demonstrated to reproduce observed site response at known soil sites). Verification studies such as Stewart et al. (2008) and Regnier et al. (2016) have shown that the calculation algorithms used in DEEPSOIL correctly reproduce theoretical site response. DEEPSOIL has been used in site-specific calculations of site response and compared to observed field site response (Kim and Hashash (2013), Yee et al. (2013)) and centrifuge site response (Hashash et al. 2015a).

2.2 Geologic and Seismic Setting of CENA

The seismic hazard in CENA comes from different sources and affects different geologic site conditions than what is typically observed in active seismic regions such as the WUS. The hard rock condition of the stable continental crust causes slower attenuation of waves from major seismic events and therefore affect a much larger region in CENA than would be expected for the WUS as was observed with the 2011 Mineral, VA earthquake (Nikolaou et al. 2012). Sites affected by an event may have variable geologic structures resulting from different histories,

affecting properties that influence site response such as V_S which is affected by glaciation in CENA (Kottke et al. 2012).

CENA is a SCR and located far from the plate boundaries that are typically the source of earthquakes in active continental regions. The intraplate seismicity in CENA comes from roughly three types of sources, background seismicity that is randomly distributed through the region, potentially induced earthquake events from hydrocarbon production and wastewater disposal, and seismic zones capable of producing large earthquakes that are not associated with major identified faults (Petersen et al. 2014). Seismic hazard throughout most of CENA is dominated by events originating from seismic zones such as New Madrid and Charleston (Petersen et al. 2014). The sources of seismicity can produce a variety of earthquakes that propagate through the hard bedrock to produce a large range of rock outcrop motions beneath any particular site.

The surficial geology in CENA is diverse and can greatly influence the response of a site to a seismic event. In CENA, studies by Kottke et al. (2012) and Parker et al. (2017) found correlations between V_{S30} and the geologic age and prior glaciation of a site. Glaciation can cause consolidation of surface sediment from the weight of thick sheets of ice and the advancing and retreating of glaciers can scrape and exhume sediment from the bedrock, and the variability of V_{S30} within glaciated regions is higher than in non-glaciated regions. A seismic event may affect sites in both glaciated and non-glaciated regions with very different geologic histories and V_S structures.

Variability in V_S structure in CENA comes in part from the location of bedrock below the ground surface. Some sites, notably in New England and southern Canada have hard bedrock near the ground surface, while in other places in CENA, bedrock is only encountered below 1 km from the ground surface. Three V_S profiles with similar V_{S30} from the Mississippi Embayment, the North Anna Nuclear Power Plant (NPP) near Mineral Virginia, and Royal Center, Indiana highlighting this difference condition are shown in Figure 2.1. The NEHRP site class D (BSSC 2009) Mississippi embayment uplands V_S profile from Romero and Rix (2001) is constructed from measurements of V_S within the Mississippi Embayment and has 1 km of soil material before an abrupt change to a much stiffer rock condition at the bottom of the profile. The North

Anna V_S profile from suspension logging of the Boring M-10DH from Dominion Virginia Power (2009) has an abrupt change in V_S at around 35 m depth and increasing to 3000 m/s near 50 m depth. The V_S profile from Royal Center, IN from Kayen et al. (2013) features a V_S profile from the multichannel analysis of surface waves (MASW) technique that at a depth of 40 m does not show any high V_S values indicative of bedrock, and the depth to bedrock is unknown. All three sites have similar V_{S30}, with V_{S30} values of 220 m/s, 250 m/s and 325 m/s for the Mississippi Embayment, Royal Center, and North Anna NPP V_S profiles, respectively, and very different bedrock conditions. The depth of bedrock for the sites is expected to have a significant effect on the surface response, yet all three sites would be classified similarly by V_{S30}.

The variability in seismic hazard and geologic conditions in CENA present a challenge in the development of ergodic amplification factors for the region because of the number of events and sites that must be represented. One approach to addressing this problem is to perform many simulations of CENA site conditions in a large-scale parametric study.

2.3 Site Amplification

Central and Eastern North America (CENA) is considered a stable continental region (SCR) from the perspective of ground motion prediction. Without tectonic plate boundaries and regular seismic events, ground motion models (GMM's) for SCR's have historically been dependent on sparse datasets or modifications to GMM's developed for active seismic regions. In GMM's the site term or site amplification is the effect of the surface soil material on the modeled ground motion and is typically dependent on the shear wave velocity (V_S), strain-dependent material behavior of soil at the site, and the effects of multidimensional wave propagation. The site amplification of a particular ground motion intensity measure (GMIM) is the ratio of surface response to outcrop ground response and is usually expressed as a natural log of the ratio.

For relatively weak ground motions, the soil at the site experiences low levels of strain and responds mostly linearly, and the response of the site is the linear site amplification. For stronger ground motions, the soil at the site begins to experience modulus reduction behavior as it shears which affects the surface ground motion. The difference between the linear site amplification and the site amplification that occurs when nonlinear soil effects are considered is the nonlinear site amplification. The response spectrum amplification absent of multidimensional and basin effects,

($F_{S,B}$) is commonly represented as the sum of a linear amplification component (F_{lin}) and a nonlinear site amplification (F_{nl}) component as given in eq. 2.1 after Seyhan and Stewart (2014) as

$$F_{S,B} = F_{lin} + F_{nl} \qquad \text{eq. 2.1}$$

The linear amplification component is the intensity-independent site amplification for a linear site condition. The accurate modeling of site effects is an important element of geotechnical engineering to quantify design loads for structures and in the development of GMM's where the effects of the site must be removed from ground motion recordings.

This study develops robust, statistically significant site amplification functions from simulations of site conditions in CENA for the response spectrum (RS) and Fourier Amplitude Spectrum (FAS). The site amplification models presented in this study are developed from the parametric study of 1-D site response analyses relative to the V_S = 3000 m/s hard rock condition of CENA.

The response spectral site amplification models developed have one nonlinear amplification component and three linear amplification components: (1) V_{S30} (time-average shear wave velocity of the top 30 m of a site) scaling, (2) soil depth (Z_{soil}) effects, and (3) soil column natural period (T_{nat}) effects. The Fourier amplitude spectral (FAS) site amplification model has one nonlinear component and a component as a function of V_{S30} in tabular form. Site amplification models presented in this can be used both independently and in conjunction with other, empirically-based site amplification models for CENA.

2.4 Review of CENA Response Spectrum Site Amplification Models

The NGA-East Project coordinated by the PEER has resulted in a suite of GMM's for CENA relative to a 3000 m/s reference rock condition (Hashash et al. 2014a) from various authors using a common dataset. GMM's relevant to CENA can therefore be broadly separated into two categories: models available before the NGA-East project and models produced since and including the NGA-East project.

Prior to the NGA-East project an international team of experts developed a list of the highest quality technically viable GMM's for SCR's as a part of the Global Earthquake Model (GEM)

project (Stewart et al. 2013). These models are listed in Table 2.1. Many of these models are currently used for the USGS national hazard maps (Petersen et al. 2014) in the CENA region, namely Frankel et al. (1996), Somerville et al. (2001), Campbell (2003), Toro et al. (1997), Atkinson and Boore (2006), Tavakoli and Pezeshk (2005), Silva et al. (2002a), and Pezeshk et al. (2011).

The models shown in Table 2.1 are developed for a hard rock condition similar to the Hashash et al. (2014a) reference rock condition of 3000 m/s but generally lack model terms for site effects. The models which include site effects are not necessarily applicable for use in CENA either because they are developed for other regions (as in Raghu Kanth and Iyengar (2007)) or are developed from models in active regions (as in Atkinson and Boore (2011)).

GMM's for CENA produced as during the NGA-East project are shown in Table 2.2. Of the GMM's developed, only 5 of the 10 have linear site terms to correct site to a 760 m/s condition. The Yenier and Atkinson (2015), Al Noman and Cramer (2015), Hassani and Atkinson (2015), and Hollenback et al. (2015) models all use linear site amplification as a function of the time-averaged V_S in the top 30 meters of a site, V_{S30}. All models use a linear increase in the natural log of site amplification as a function of the ratio of site V_{S30} to a reference V_S condition (V_{ref}) as shown in eq. 2.2, and commonly referred to as V_{S30} scaling. The linear scaling coefficients and reference velocity (c, and V_c, repsectively in eq. 2.2, but having model-specific symbols) are either taken from Seyhan and Stewart (2014), or derived from the regression of the GMM as noted in Table 2.2.

$$\ln(amp) = \begin{cases} c \ln\left(\frac{V_{S30}}{V_{ref}}\right) & V_{S30} \leq V_c \\ c \ln\left(\frac{V_c}{V_{ref}}\right) & V_{S30} > V_c \end{cases} \qquad \text{eq. 2.2}$$

where V_c is V_{S30} above which no amplification of a site is observed. The Graizer (2015) linear site correction is also a function of V_{S30} but instead of period-dependent coefficients, includes frequency in the equation for site correction.

The CENA site database (Goulet et al. 2014) used in the NGA-East GMM development process lacks the strong shaking data to constrain nonlinearity for CENA site conditions. In the GMM's shown in Table 2.2, the nonlinear site amplification comes from the Seyhan and Stewart (2014) model developed from site amplification in active crustal regions.

Site amplification model forms commonly use V_{S30} and PGA to capture linear and nonlinear effects, respectively for the natural log of site amplification. Several previously-used and current site amplification model forms are shown in Table 2.3. The Boore et al. (1997) and Abrahamson and Silva (1997), model forms express site amplification as a function of V_{S30} and PGA_{rock}, respectively, but do not distinguish linear and nonlinear site amplification. The Choi and Stewart (2005) site amplification models include separate model terms for the linear amplification as a function of the V_{S30} scaling and nonlinear amplification as a function of the PGA of the rock outcrop ground motion, PGA_{rock}. PGA_{rock} is used as the driver of nonlinearity for these models (i.e. an indicator for the amount of nonlinear site amplification).

The Walling et al. (2008) functional form in Table 2.3 uses linear V_{S30} scaling and model terms that capture nonlinear site amplification effects as a function of both V_{S30} and PGA_{rock}. The inclusion of V_{S30} into the nonlinear site amplification model term reflects the idea that a site with more stiff material (i.e. higher V_{S30}) will experience less strain during ground motion shaking, and less nonlinear site amplification will be observed. The Walling et al. (2008) functional form used in NGA-West is nearly identical to the Kamai et al. (2014) functional form used in NGA-West2. The Kamai et al. (2014) formulation uses two alternative formulations, one which uses PGA_{rock} as the driver of nonlinearity and the other which uses Sa(T) where Sa(T) is the PSA from the 5% damped response spectrum at the period (T) of interest. The Seyhan and Stewart (2014) model from distinguishes linear and nonlinear site amplification using eq. 2.1 and the terms for $\ln(F_{lin})$ and $\ln(F_{nl})$ shown in Table 2.3.

The GMM's for CENA shown in Table 2.1 and Table 2.2 have been developed for a hard rock reference condition similar to the recommendation of 3000 m/s in Hashash et al. (2014a). However, national ground motion hazard maps have been developed relative to a V_{S30} = 760 m/s reference condition (Frankel (1996),Petersen et al. (2014), Petersen et al. (2008)) and there is a longstanding need to be able to correct hard rock GMM's to a 760 m/s condition. The reverse is

also true, as for the development of CENA GMM's in NGA-East, there was a need to correct soft soil sites to a 3000 m/s reference condition. Most existing models for the 760/3000 correction for GMM's are developed from simulations using the quarter-wavelength method (e.g. Frankel (1996), Campbell (2003), Atkinson and Boore (2006), Boore (2015a)). Controlling factors in these simulations are the V_S profiles, soil damping, and spectral shape of the rock motions including any distance and magnitude effects.

Quantifications of the site amplification in CENA outside of the context of GMM development include the use of discrete factors in National Earthquake Hazards Reduction Program (NEHRP)-style (BSSC 2015) amplification factors and region-specific amplification studies. The site coefficients used in NEHRP amplification are for a limited and discrete range of periods, site V_{S30}, and ground motion intensity conditions. Discrete amplification functions may not provide high enough resolution to fully capture important site effects that may affect building design. Moon et al. (2016) used nonlinear site response (NL) analyses to develop NEHRP-style depth-dependent site factors for the Mississippi Embayment, and Aboye et al. (2015) used 13,000 nonlinear and equivalent linear site response analyses to develop site amplification functions for the Charleston, South Carolina area. Region-specific site amplification studies may not be appropriate for use at sites outside their respective regions in CENA.

In CENA, the effects of site natural period and soil column depth have been evaluated and shown to have considerable effect on linear site amplification. Following the work in NGA-East Hassani and Atkinson (2016) recognized that site fundamental frequency, f_{peak}, as estimated from horizontal-to-vertical component response spectral ratios played an important part in site amplification and introduced a model for linear amplification relative to a hard-rock and NEHRP B/C boundary conditions as a function of f_{peak}. Moon et al. (2016) introduced depth-dependency into NEHRP-style amplification functions to account for decreases in amplification at low period and increases in amplification at long period for deep sites in the Mississippi Embayment. These site effects may be implicitly included in simulation-based amplification models currently used in CENA, such as the NGA-East Darragh et al. (2015) model, but are not currently included in V_{S30}-based amplification models for CENA.

2.5 Threshold for Difference between Equivalent Linear and Nonlinear Site Response Analyses

To simulate the amplification of ground motions at soil sites, parametric studies of one-dimensional site response analyses have been used in the development of site amplification functions in both stable and active continental regions to constrain soil nonlinearity (Walling et al. (2008), Navidi (2012), Bozorgnia and Campbell (2015)). Soil displays nonlinearity in ground motion response even at relatively small strains, so it is necessary to incorporate nonlinearity into 1-D site response analyses. The two commonly used types of analyses for one-dimensional site response calculations that capture nonlinearity are frequency-domain equivalent linear (EL) analyses and time-domain nonlinear (NL) analyses. EL analyses tend to over-damp high frequency content but are computationally efficient. NL analyses preserve high frequency content, but are more computationally expensive and tend to require better control of input parameters than EL analyses (Hashash et al. 2010). As EL analyses are significantly less computationally expensive than NL analyses, they have been used extensively in the development of current-generation site amplification factors.

Systematic differences between EL and NL site response analyses have been investigated in a number of studies (Stewart et al. (2008), Assimaki and Li (2012)) and for most conditions EL response analyses are appropriate for use in conditions with relative weak ground motions and relatively stiff soil conditions. Kim et al. (2015) developed an *a priori* methodology for evaluating the expected differences between the FAS of EL and NL site response analyses to determine when EL analyses are sufficient and when more computationally expensive NL analyses are required. The proposed threshold as a function of shear strain index $I_\gamma = \mathrm{PGV_{in}}/V_{S30}$ and maximum desired reliable frequency of analysis, f, and is given in eq. 2.3 below.

$$I_\gamma = 0.09 f^{-0.8}. \qquad \text{eq. 2.3}$$

2.6 Site Amplification in FAS-Based GMM Development

Most GMM's are developed for the response spectrum (RS) using GMIM's from the response spectrum. However, because GMM creation using the Fourier Amplitude Spectrum (FAS) is less

affected by nonlinear complexities, there is an increasing interest in GMM development for the FAS (Hollenback et al. 2015). For the NGA-East project, Hollenback et al. (2015) developed a GMM in FAS space following the work of Bora et al. (2014) then used random vibration theory to translate the FAS to RS GMIM's. In both Hollenback et al. (2015), and Bora et al. (2014) , the site amplification for the FAS uses the functional form in eq. 2.4.

$$\ln(amp) = c \ln(V_{S30}) \qquad \text{eq. 2.4}$$

This functional form was shown in Hollenback et al. (2015) to not produce any strong biases in the model residuals as a function of V_{S30}, but has not been as extensively quantified as the site amplification terms used for the response spectrum in the WUS.

Table 2.1: Global Earthquake Model Selected GMM's for Stable Continental Regions developed prior to NGA-East (Stewart et al. 2013) where model types are defined as follows: RE is Referenced Empirical, S is Stochastic, H is Hybrid, and M is Simulation-based.

Model Reference	Region	Model Type	Site Parameters		Site Amplification Function	
			Discrete Categories	Continuous Variables	Non-Linearity	Reference Site Condition
Atkinson (2008), Atkinson & Boore (2011)	CENA	RE	NEHRP B/C only	-	N/A	NEHRP B/C
Atkinson & Boore (2006, 2011(2011))	CENA	S	Hard Rock; NEHRP B/C	V_{S30}	Yes	Hard Rock (V_S > 2000 m/s), B/C (V_S = 760 m/s)
Campbell (2003)	CENA	H	Hard Rock Only	-	N/A	Hard Rock (V_S > 2800 m/s)
Douglas et al. (2006)	South Norway	H	Hard Rock Only	-	N/A	Hard Rock (V_S > 2800 m/s)
Frankel et al. (1996)	CENA	S	Hard Rock; NEHRP B/C	-	N/A	Hard Rock (V_S > 2800 m/s)
Raghu Kanth and Iyengar (2007)	Peninsular India	S	Hard Rock; NEHRP A-D	-	Yes	Hard Rock (V_S > 3600 m/s)
Silva et al. (2002b)	CENA	S	Hard Rock Only	-	N/A	Mid-Continent: V_S = 2830 m/s, Gulf Coast: V_S = 2310 m/s
Somerville et al. (2009)	Australia	M	Rock Only	-	N/A	Rock (V_S = 865 m/s)
Pezeshk et al. (2011)	CENA	H	Hard Rock Only	-	N/A	Hard Rock (V_S > 2000 m/s)
Toro et al. (1997)	CENA	S	Hard Rock Only	-	N/A	Hard Rock (V_S > 2800 m/s)

Table 2.2: GMM's produced as a part of the NGA-East Project. All models can be found in PEER (2015/04).

NGA-East Model (2015)	Site Term	Site Term Parameter	Site correction to 760 m/s	Site correction to 3000 m/s
Boore (2015b)	No	N/A	N/A	Boore (2015)
Darragh et al. (2015).	No	N/A	1-D Site Response Analysis for NEHRP Categories up to 4.8k m/s	
Yenier and Atkinson (2015)	Yes	V_{S30}	SS14	Atkinson and Boore (2006) BC Crustal Amp (Atkinson 2012)
Pezeshk et al. (2015)	No	N/A	SS14 (validation only)	Boore and Thompson (2015)
Frankel (2015)	No	N/A	N/A	Frankel et al. (1996)
Shahjouei and Pezeshk (2015)	No	N/A	SS14 (validation only)	Atkinson and Boore (2006), and Boore and Thompson (2015)
Al Noman and Cramer (2015)	Yes	V_{S30}	Regression Parameter d_1	NA
Graizer (2015)	Yes	V_{S30}	1-D Site Response Analysis	Site Response Analysis-Based (Similar to Atkinson and Boore (2006), Atkinson and Boore (2011)
Hassani and Atkinson (2015)	Yes	V_{S30}	SS14	Atkinson and Boore (2006), BC Crustal Amp (Atkinson 2012)
Hollenback et al. (2015)	Yes	V_{S30}	Regression Parameter c_8	Boore (2015)

Table 2.3: Common site amplification functions where a, b, c, c_1, and d, are frequency-dependent constants, PGA_{rock} is the PGA of the ground motion at a reference rock condition, V_{LIN} is the shear wave velocity in a soil column nearest to the ground surface where linear soil response is expected, and V_{ref} is the shear wave velocity of the reference rock condition.

Model	Functional Form
Boore et al. (1997)	$\ln(Amp) = a \ln\left(\frac{V_{S30}}{V_{REF}}\right)$
Abrahamson and Silva (1997)	$\ln(Amp) = a + b \ln(PGA_{rock} + c)$
Choi and Stewart (2005)	$\ln(Amp) = a \ln\left(\frac{V_{S30}}{V_{ref}}\right) + b \ln\left(\frac{PGA_{rock}}{0.1}\right)$
Walling et al. (2008)	$\ln(Amp) = \begin{cases} a \ln\left(\frac{V_{S30}}{V_{LIN}}\right) - b \ln(PGA_{rock} + c_1) \\ +b \ln\left(PGA_{rock} + c\left(\frac{V_{S30}}{V_{LIN}}\right)^n\right) + d \; for \; V_{S30} < V_{LIN} \\ (a + bn) \ln\left(\frac{V_{S30}}{V_{LIN}}\right) + d \;\; for \; V_{S30} \geq V_{LIN} \end{cases}$
Seyhan and Stewart (2014)	$\ln(F_{lin}) = \begin{cases} c \ln\left(\frac{V_{S30}}{V_{ref}}\right) & V_{S30} \leq V_c \\ c \ln\left(\frac{V_c}{V_{ref}}\right) & V_{S30} > V_c \end{cases}$
	$\ln(F_{nl}) = f_1 + f_2 \ln\left(\frac{PGA_r + f_3}{f_3}\right) \; where$ $f_2 = f_4[\exp\{f_5(\min(V_{S30}, 760) - 360)\} - \exp\{f_5(760 - 360)\}]$

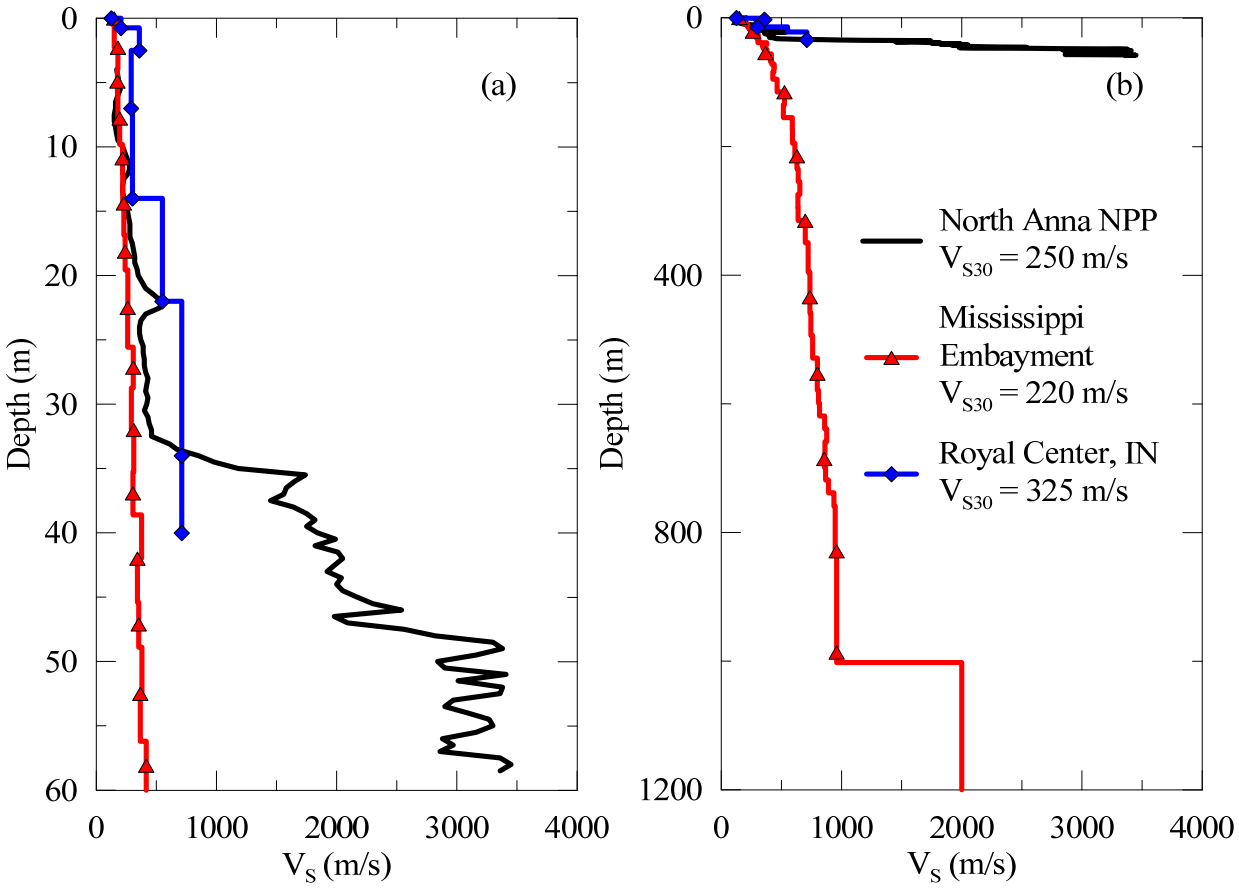

Figure 2.1: CENA V_S profiles for North Anna NPP (Dominion Virginia Power 2009), the Mississippi Embayment (Romero and Rix 2001), and Royal Center, IN (Kayen et al. 2013) to a depth of 60 m (a) and 1200 m (b).

Chapter 3. Parametric Study Design

A parametric study is designed to capture the range of geologic site profiles expected in CENA (i.e. the variability in site conditions) as well as the degree to which those site conditions are known (i.e. the uncertainty in the site conditions). Figure 3.1 shows a pseudo-factorial tree structure for the parametric study. The parametric study tree details the design factor levels used to generate site profiles for use in 1-D site response analysis (i.e. the representation of a single site V_S and soil properties) that reflect the variability of site conditions in CENA. In total, Figure 1 represents 1,747,278 site response analyses, 582,426 of each LE, EL and NL analyses corresponding to 70,650 unique site profiles.

Site profiles in this study consist of three main V_S horizons: a horizon at the ground surface representative of soil material, a stiffer weathered rock horizon under the soil region to transition to the reference rock horizon with V_S = 3000 m/s. The site profile is the representation of all three horizons and their material properties. Material properties in the site profile include soil index properties, nonlinear curves generated from soil index properties, shear strength, and damping ratio, D_{min}. A set of 10 V_S profiles for the soil horizon are developed to be used as inputs for randomization and are described as representative seed profiles. In this study, an analysis consists of a 1-D LE, El, or NL calculation of site response of a site profile to a rock outcrop ground motion occurring at the reference rock condition at the bottom of the profile.

The parametric study tree consists of two main branches, an upper branch is used to generate sites with soil at the ground surface that then transition to weathered rock and bedrock at depth, and a lower branch for generating sites with weathered rock material at the ground surface that transitions to bedrock at depth (i.e. there is no soil horizon in the site profile). The upper branch of Figure 3.1 represents the generation of 70,200 profiles as listed below and described in greater detail in later sections:

- Ground Motions: A suite of 247 ground motions representative of a range of durations and intensities with frequency content characteristic of the geologic conditions in CENA is developed (Chapter 4)

- Representative Seed V_S Profiles: Ten V_S profiles representative of soil material derived from measured V_S profiles in CENA to be used as seeds to V_S randomization (Chapter 5),
- Material Properties: Nine geology-based combinations of soil index and strength properties. Material properties are matched with representative seed V_S profiles for a total of 13 unique combinations of representative seed profiles and material properties (Chapter 7),
- Randomized V_S profiles: Thirty random realizations of the representative seed V_S profiles for each pairing of representative seed V_S profile and material properties. Ground motions are evenly and randomly distributed to the random V_S realizations. Each random site profile is therefore paired with 8-9 rock outcrop ground motions and the analysis tree presented in Figure 3.1 is only pseudo-factorial (i.e. each branch of the study tree is not evaluated with all levels of each other branch). Rock outcrop ground motions are evenly and randomly selected from the set of motions developed in Chapter 4. Random V_S profiles are described in Section 5.4
- Randomized Dynamic Curves: Three random realizations of the nonlinear curves of each random V_S profile (Section 7.5),
- Profile Depth: Ten soil depth bins. The representative seed soil velocity profiles will extend from the ground surface to the bottom of the depth bin (Chapter 5),
- Weathered Rock Zone Model: Six models for V_S structure of the bottom of the soil velocity profiles above the reference rock condition. All weathered rock zone models share the same soil index properties which are separate from the soil index properties of the soil material above (Section 5.3),
- Analysis Type: Three analyses methods are used including frequency domain linear elastic (LE), frequency domain equivalent linear (EL) and time domain nonlinear (NL). Parameters used in the solution of the EL, NL and LE analysis methods are provided in Table 3.1.

The lower branch of Figure 3.1 closely follows the structure of upper branch and represents the generation of 450 profiles with only weathered rock over reference rock. The levels of the lower branch are analogous to the upper branch.

The 1-D site condition is represented by a single vertical site profile defined between the ground surface and a reference bedrock condition for simulation of a vertically propagating shear wave in one direction. The modeling of a single site for 1-D site response analysis requires capturing the geologic structure of the site profile including the V_S and, in the case of EL and NL analyses, nonlinear material behavior. The relatively low computational cost and simplifying assumptions of 1-D site response analyses allows for the simulation of site amplification at many different sites using a large number of analyses.

Table 3.1: EL, NL, and LE analysis parameters for site response calculation. Detailed explanations of the chosen analysis parameters are available in the DEEPSOIL manual (Hashash et al. 2015c).

Analysis Parameter	Analysis Type	Value
Number of iterations	EL	16
	LE	1
Shear Stress Strain Ratio	EL	0.65
Complex Shear Modulus Type	LE	Frequency Independent
	EL	Frequency Independent
Step Control	NL	Flexible
Maximum Strain Increment	NL	0.005
Time History Interpolation	NL	Linear

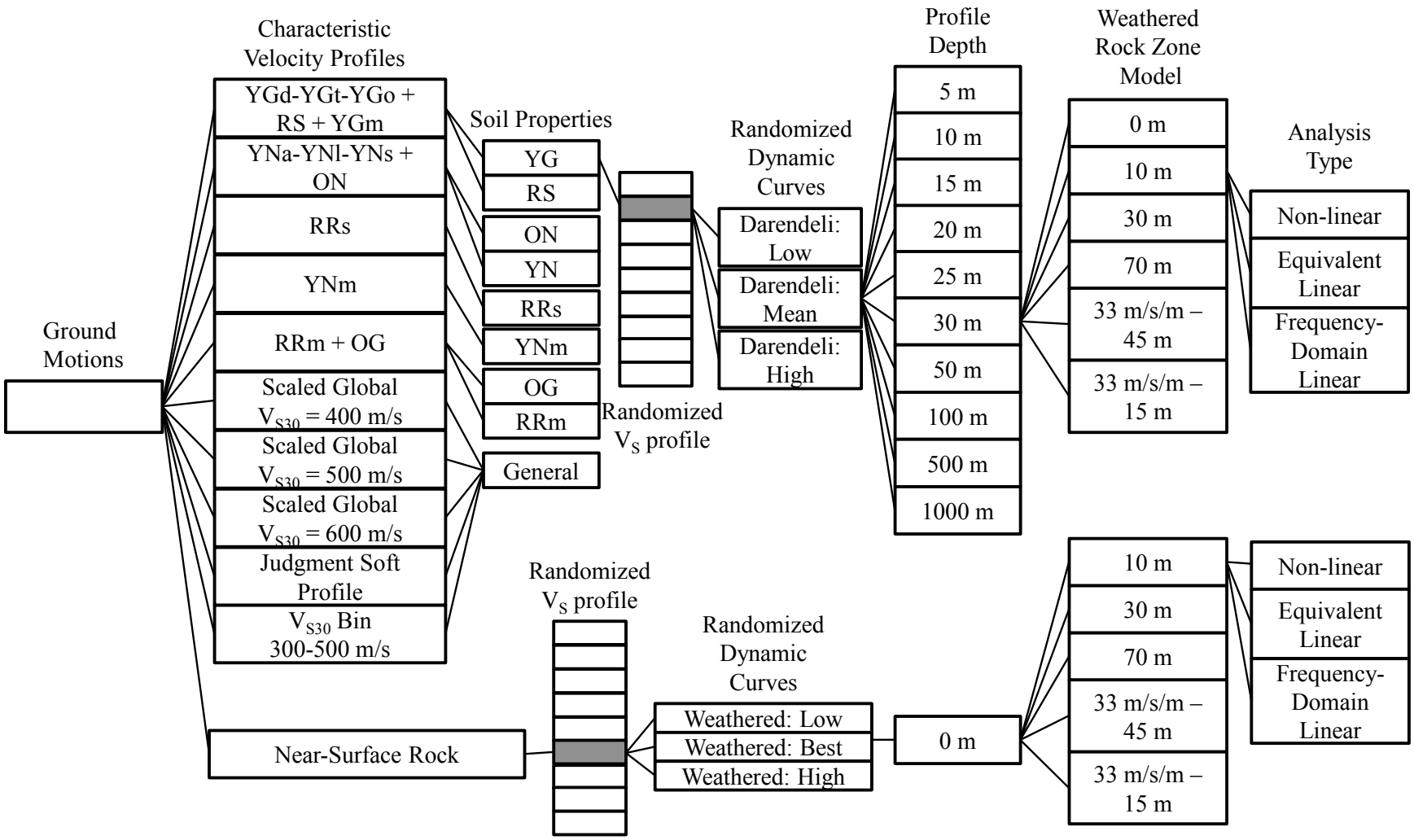

Figure 3.1: Parametric study analysis tree.

Chapter 4. Rock Outcrop Ground Motions

The work presented in this chapter was developed by E. Rathje and B. Xu of the University of Texas at Austin as a part of the collaboration with the NGA-East Geotechnical Working Group.

Rock outcrop ground motions are a selection of 186 synthetic and recorded rock motions developed in NUREG-6729 McGuire et al. (2001) and 61 motions generated stochastically with SMSIM (Boore 2005) for CENA rock conditions. These motions have been selected to cover a range of intensities and be representative of CENA bedrock conditions.

Rock outcrop ground motions from NUREG-6729 are synthetic and modified motions from the WUS to include more high frequency content and be representative of CENA bedrock conditions. All motion pairs (i.e. two horizontal components of a ground motion) with Nyquist frequencies of 100 Hz (time step = 0.005 s) are selected from McGuire et al. (2001) for 10 magnitude-distance combinations shown in shown in Table 4.1, with magnitudes ranges M_w = 4.5-6, 6-7, and 7+ and distances from 0 km to 100 km. In total, 93 motion pairs (186 unique horizontal rock outcrop ground motions) have been selected from McGuire et al. (2001). Smoothed FAS for the NUREG-6729 motions are shown in Figure 4.1a, and response spectra are shown in Figure 4.2a.

Rock outcrop ground motions from SMSIM have been generated stochastically based on rupture and wave propagation characteristics of the CENA bedrock condition. The stochastic parameters for the generation of these motions are based on the published values of Boore and Thompson (2015) and included in shown in Table 4.2 for the magnitude and distances shown in Table 4.3. Motions were generated for four earthquake magnitudes (M_w = 4.5, 5.5, 6.5, and 7.5) and distances ranging from 5 km to 250 km. Distance ranges were chosen such that the SMSIM rock outcrop ground motions generated PGA and PGV values that complement the range of PGA and PGV values of the NUREG-6729 motions. Figure 4.3a and Figure 4.3b show the range of values of PGD and PGV, respectively, as functions of PGA for the NUREG-6729 and SMSIM rock outcrop ground motions. Rock outcrop ground motions from SMSIM all have a Nyquist frequency of 125 Hz (time step = 0.004 s). Smoothed FAS for the SMSIM motions are shown in Figure 4.1b, and response spectra are shown in Figure 4.2b.

The combined bedrock outcrop motion dataset includes 247 horizontal motions for use in site response simulation. The PGA, PGV, and PGD of the rock outcrop ground motions are shown in Figure 4.3. The motions are evenly distributed across PGA from 0.01 g to 4 g, and PGA is correlated to PGV and PGD. The duration (total length of the rock outcrop ground motion used in analysis) of the rock outcrop motions as a function of PGA is shown in Figure 4.3, and there is no correlation.

Table 4.1: Summary of selected NUREG motions.

Magnitude	Number of motion sets*	Distance (km)**
4.5-6	0 (14)	0-50 (ab)
	4 (7)	50-100 (c)
6-7	2 (5)	0-10 (a)
	1 (8)	10-50 (b)
	0 (5)	50-100 (c)
	0 (6)	100-200 (d)
7+	0 (12)	0-10 (a)
	0 (10)	10-50 (b)
	0 (10)	50-100 (c)
	0 (9)	100-200 (d)
Total	93 sets	

***** The number in the brackets is the number of simulated motions, while the number outside the brackets is the number of recorded motions.
****** The distance bins are labeled as a: 0-10 km, b: 10-50 km, ab: 0:50 km c: 50-100 km, d: 100-200 km.

Table 4.2: SMSIM input parameters for synthetic ground motions for CENA based on recommendations of Boore and Thompson (2015).

Source Parameters	
Single Corner Model	
ρ (g/cm^3)	2.8
β (km/s)	3.7
Stress drop (bars)	400
Quality factor, Q	525 f$^{0.45}$
kappa	0.006

Path Duration	
nknots	8
Rdur (i)	Dur (i)
0	0
15	2.6
35	17.5
50	25.1
125	25.1
28.5	28.5
392	46
600	69.1
> 600 slope	0.111

Crustal Amplification	
namps	14
Freq (i)	Amp (i)
0.001	1
0.00783	1.003
0.0233	1.010
0.04	1.017
0.0614	1.026
0.108	1.047
0.234	1.069
0.354	1.084
0.508	1.101
1.09	1.135
1.37	1.143
1.69	1.148
1.97	1.150
2.42	1.151

Table 4.3: Magnitude and Distance of simulated SMSIM motions.

Magnitude:	M=7.5	M=6.5	M=5.5	M=4.5
Distance (km)	6	5	10	10
	7.1	6	12.0	12.0
	8.4	7.2	14.3	14.3
	10	8.6	17.1	17.1
	11.8	10.2	20.4	20.4
	14	12.2	24.5	22
	16.6	14.6	29.2	24.5
	19.6	17.5	35.0	28
	23.3	20.9	41.8	/
	27.6	25.0	50	/
	32.6	30	/	/
	38.7	35.8	/	/
	45.8	42.8	/	/
	54.3	51.2	/	/
	64.3	61.3	/	/
	76.2	73.3	/	/
	90.2	87.7	/	/
	106.9	104.9	/	/
	126.6	125.4	/	/
	150	150	/	/
	177.7	/	/	/
	210.5	/	/	/
	249.4	/	/	/

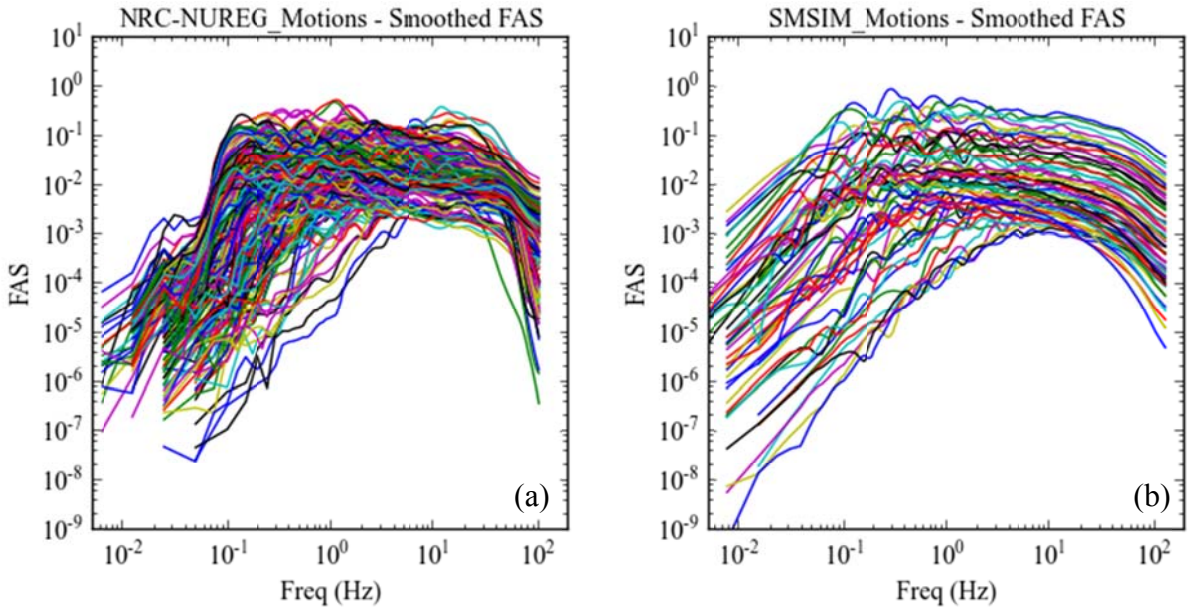

Figure 4.1: Smoothed Fourier amplitude spectra of selected input motions for site response analyses (a) selected from McGuire et al. (2001), and (b) generated stochastically with SMSIM.

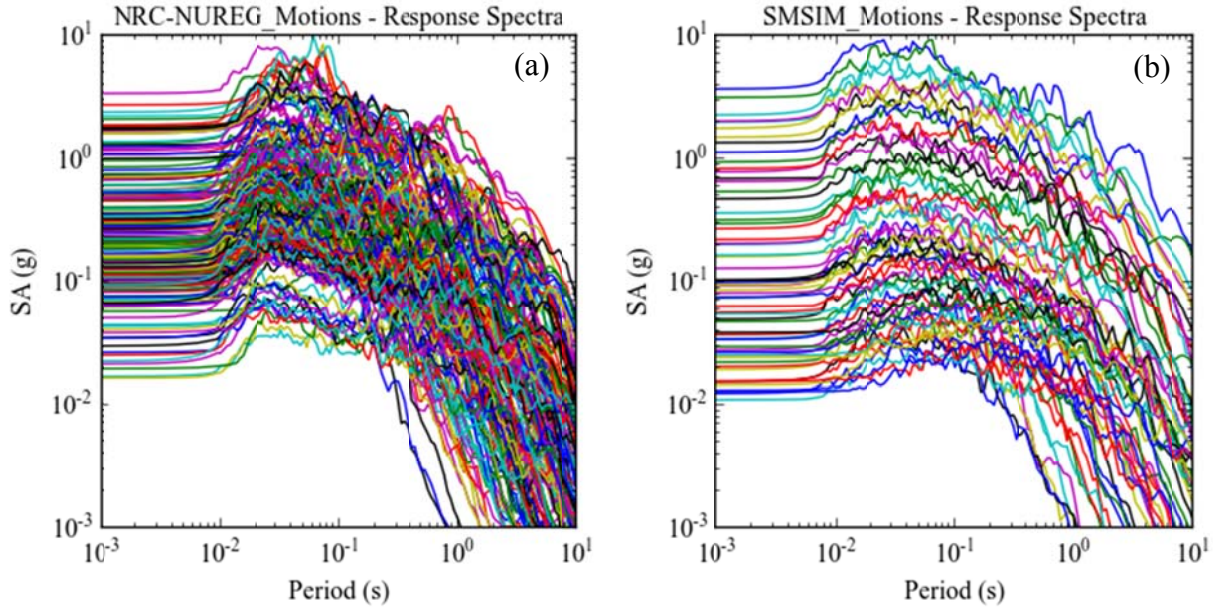

Figure 4.2: Response spectra of selected input motions for site response analyses (a) selected from McGuire et al. (2001), and (b) generated stochastically with SMSIM.

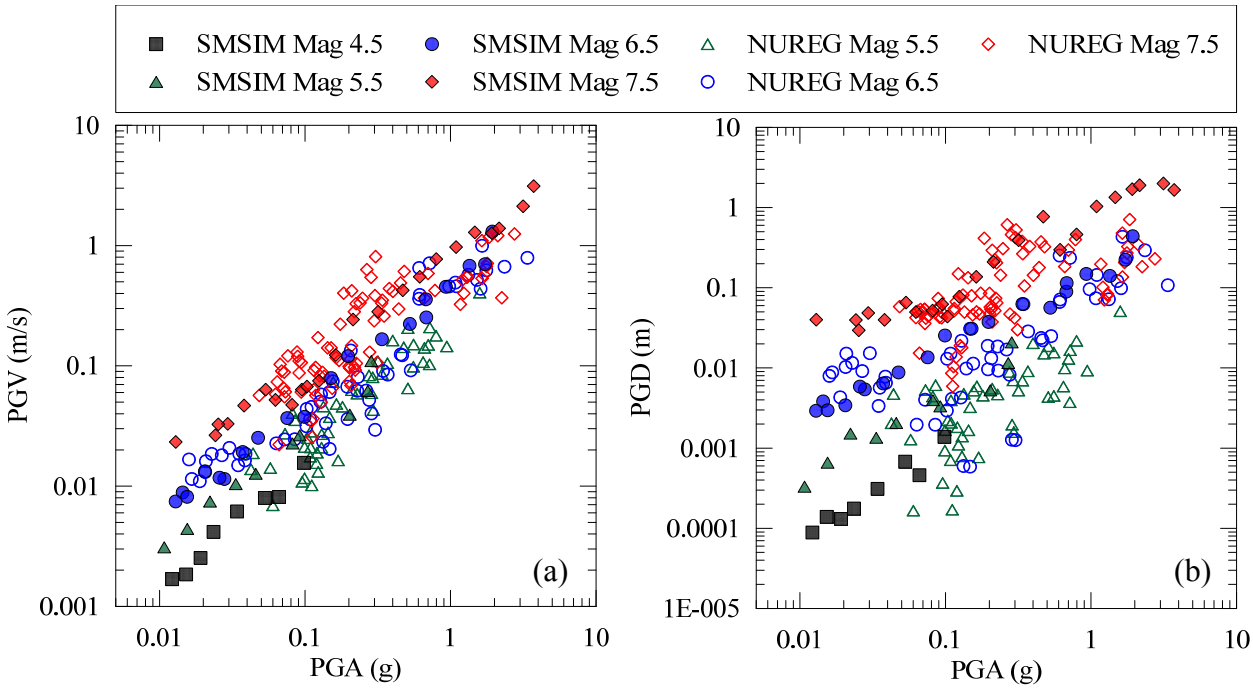

Figure 4.3: PGV (a) and PGD (b) as a function of PGA of rock outcrop ground motions for use in site response analysis. Filled symbols are rock outcrop ground motions generated stochastically with SMSIM, and open symbols are motions selected from NUREG-6729 (McGuire et al. 2001).

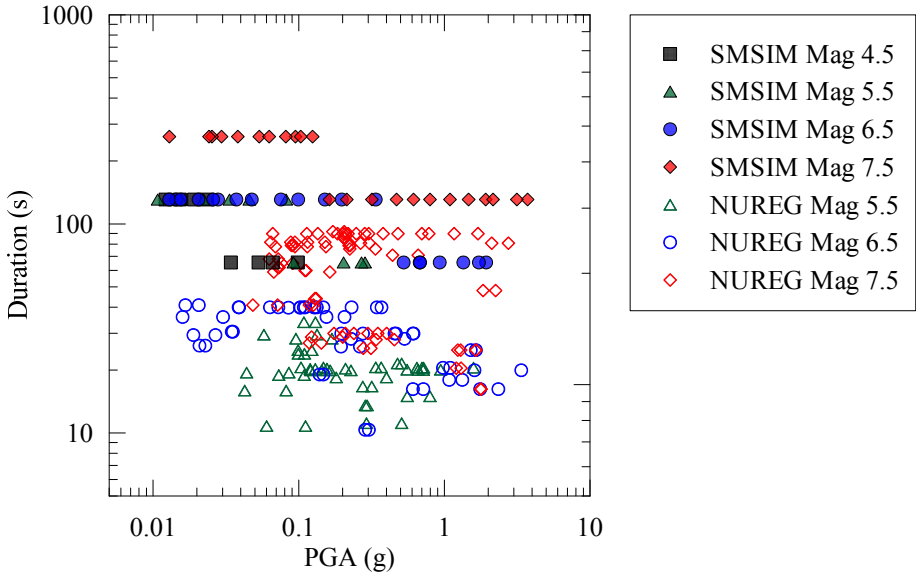

Figure 4.4: Duration of selected rock outcrop motions as a function of PGA.

Chapter 5. Shear Wave Velocity Profiles

5.1 Introduction

Shear wave velocity is an important parameter in the quantification of site effects as it describes the small-strain shear stiffness of soil and rock. This section details how V_S is included in the parametric study of 1D site response analyses. The representative seed V_S profiles used as input to randomization are representative of the soil horizon, and their development is detailed in Section 5.2. At the bottom of the soil horizon, a model for the weathered rock horizon is described in Section 5.3. The randomization procedure used for the entire site profile consisting of the soil and weathered rock horizons is detailed in Section 5.4. All V_S profiles developed in this study terminate at the reference rock condition of 3000 m/s established by Hashash et al. (2014a).

5.2 Development of Representative Seed Shear Wave Velocity Profiles

A total of ten V_S profiles are derived from 821 V_S profiles in CENA from literature and open file reports to represent the soil V_S in CENA and are shown in Figure 5.1 to be used as seeds for V_S randomization. The list of references for the V_S profiles collected is shown in Table 5.1. The profiles are from a variety of locations in the central and eastern United States and Canada as shown in Figure 5.2. Much of the work in this study builds on the report of reference rock condition of CENA in Hashash et al. (2014a) including use of much the shear wave velocity (V_S) profile data collected for that study.

The steps used to create the ten representative seed V_S profiles based on geologic classifications and the sections that describe these steps in detail are:

- Remove rock-like material from the V_S profile data (Section 5.2.1)
- Sort profiles by geology and calculate the log-mean of V_S as a function of depth (Section 5.2.2)
- Smooth the log-mean profiles to remove features in the mean V_S profiles resulting from changing amounts of data as a function of depth such as sharp changes in V_S near the

ground surface and regions within the profile where V_S decreases as a function of depth (Section 5.2.2)

- Extend the smoothed log-mean V_S profiles to a depth of 1000 m. (Section 5.2.3)
- Combine similar smoothed, extended log-mean V_S profiles (Section 5.2.4)
- Sample the smoothed, extended log-mean V_S profiles as a function of depth to create units of continuous V_S within the profile. The sampled V_S profiles are the representative seed V_S profiles. (Section 5.2.4)

The representative seed V_S profiles developed fall into two categories: Five V_S profiles are based on CENA geologic classes (Young nonglaciated marine material, Residual material from sedimentary rock, Young nonglaciated Alluvium, loess, and sands and Old Nonglaciated material, Residual material from metamorphic rock and old glaciated material, and young glaciated discontinuous till, till, and outwash and residual material from soils and young glaciated marine material, abbreviated as YNm, RRs, YNa-YNl-YNs+ON, RRm+OG, and YGd-YGt-YGo+RS+YGm, respectively) derived and named after the geologic classes presented in Kottke et al. (2012) and shown in Table 5.1, and five V_S profiles are judgement based (Judgement Soft, V_{S30} binned, and the Scaled Global Log-Mean profiles) derivations of the V_S profile data to capture a range of V_S behaviors as a function of depth and V_{S30} values as described in Section 5.2.4.

5.2.1 Removal of Rock-Like Material

Rock-like material (i.e. material with high V_S) is sampled in many of the collected V_S profiles. The representative seed V_S profiles represent the soil horizon of the site profile, a procedure is used to remove the rock-like material from the collected V_S profiles prior to combining them into representative seed profiles. A V_S value of 760 m/s is on the boundary between NEHRP site classes B and C (FEMA (1997)) and is typically considered the reference rock condition for the Western United States. Rock-like material was removed from the V_S profile data by truncating the profile at the deepest V_S values greater than 800 m/s or at the deepest increase of more than 500 m/s between adjacent V_S values to capture the high impedance contrasts expected between rock and soil material. The values of 800 and 500 m/s for the removal of rock-like data are judgment based. Material with V_S greater than 760 m/s would be classified into NEHRP site

class B and is considered rock for the purposes of WUS site amplification. A jump in 500 m/s or greater in V_S suggests a significant change in stiffness between geologic layers. Figure 5.3 shows the results of this rock-removal process for the geologic classes YGd, YGo, and YGt.

5.2.2 Geology-Based Representative Shear Wave Velocity Profiles

V_{S30} values in CENA can be related to surficial geology age and origin (Kottke et al. 2012). An investigation by Kottke et al. (2012) found that surficial geology classifications could be used as a proxy for time-averaged shear wave velocity in the top 30 m of soil (V_{S30}). Surficial geology information from Fullerton et al. (2003) for the United States and Fulton (1995) for Canada was used to develop geologic classes of surficial materials in CENA that shared similar V_S characteristics for use in site amplification. The CENA geology classifications from Kottke et al. (2012) are shown in Table 5.2 and are adopted for this study.

V_S profile data collected does not provide even coverage of all geologic classes shown in Table 5.3. Some geologic sub-units with similar velocity and geologic characteristics were combined to create more stable log-mean profiles. In Figure 5.4 the rock-removed velocity profiles from geology classes YGd, YGo, and YGt are combined to increase the stability of the log-mean (e.g. the log-mean does not significantly change with the addition or removal of data). Additional geologic sub-units that are combined in this way are: ONa, ONc, ONl, and ONm; OGm, OGo, and OGt; and YNa, YNl, and YNs.

Once sorted, the log-mean of the V_S profiles was calculated as a function of depth. Log-Mean V_S values were calculated at a 1 m interval from 0 m to 10 m depth, then at a 5 m interval below 10 m. The log-mean V_S profiles to 100 m are shown in Figure 5.4 through Figure 5.14 for each of the geologic classes.

Certain characteristics of the representative seed V_S profiles to be used as inputs to randomization schemes for the parametric study are desirable, and the strict log-mean V_S profiles of the collected data needed to be adjusted to have these characteristics. The log-mean V_S profiles were “smoothed” to be monotonically increasing with depth. If a region of the log-mean profiles would exhibit a decrease in V_S with depth, the V_S is held constant with depth over the affected layers. The log-mean V_S profiles also had abrupt changes in V_S with depth reduced.

Because of the dependency of the shape of the log-mean V_S profiles on the number of V_S profiles collected at each depth, the final adjustments to the log mean V_S profiles are made near the ground surface and at depth where the number of collected V_S profiles controls the shape of the log-mean profile. At the ground surface, abrupt changes in V_S were ignored and the V_S profiles were extrapolated to the ground surface depth from a deeper area with more data and the log mean V_S is better constrained. At depth, where there is little V_S data, or where the V_S data available only comes from one or two sites, the profile extrapolation technique described in Section 5.2.3 is used. Typically if there are fewer than five collected V_S profiles for a given depth, profile extrapolation is used. Figure 5.4 shows an example of the log-mean V_S profile of the collected data, and its adjustment.

5.2.3 Depth Extension of Characteristic Profiles

Of the V_S profile data collected, none reaches a depth of 1000 m, the greatest soil profile depth to be considered in this study. V_S profiles are commonly fit to an equation of the form

$$\log(V_S) = n_v \times log(z) + C \qquad \text{eq. 5.1}$$

where V_S is shear wave velocity, z is depth or confining pressure, and C is a constant (Sykora 1983 , Darendeli 2001, Menq 2003). A review of literature using this functional form to fit was performed; sources are shown in Table 5.4. The functional form of shear wave velocity shown in eq. 5.1 was fit using a least-squares method to the log-mean velocity profiles of each combined geologic classification described in Section 5.2.4 and the n_v values are shown with the literature values of n_v in Figure 5.15.

When the log-mean of all rock-removed velocity profiles is fit to eq. 5.1, $n_v = 0.293$ which falls in the range of values observed in literature. The value of C in eq. 5.1 can be adjusted to cause the fit profile to intersect the log-mean profile where the profile terminates, as shown in Figure 5.16. Smoothed log mean V_S profiles are extrapolated to depths beyond where there is reliable data from the slope of the curve with $n_v = 0.293$ fit to the log-mean of all velocity profile data shown in Figure 5.16. This extension procedure can be applied consistently to the smoothed V_S profiles and results in reasonably-shaped velocity profiles as a function of depth. An example of a smoothed log mean V_S profile extension from 20 m to 100 m is shown in Figure 5.4.

5.2.4 Additional Representative Seed V_S profiles

Additional smoothed log mean V_S profiles for use in site response analyses are derived from the log mean of collected velocity profile data at discrete depths across geologic classes and values of V_{S30}, from scaling the log mean profile of all collected V_S profiles, and using engineering judgment to come up with a soft V_S profile. The smoothed log mean V_S profiles V_S profiles from the binning, judgment, and scaling procedures are used to provide coverage of V_S not captured by collected data, but desired for use in developing site amplification functions.

The smoothed log mean V_S profiles derived from the geologic classes presented in Kottke (2012) do not provide the coverage of higher V_S values observed in the data, and do not provide sufficient coverage of V_{S30} desired for use in the parametric study. Three additional velocity profiles were created by uniformly scaling the smoothed (through the process detailed in Section 5.2.2) log-mean profile calculated from all collected V_S profiles to produce smoothed log mean V_S profiles with V_{S30} values of 400 m/s, 500 m/s, and 600 m/s. The scaled global mean profiles are shown in Figure 5.18.

A smoothed log mean V_S profile was also created from the log-mean velocity profile of rock-removed velocity profile data with V_{S30} values between 300 m/s and 500 m/s to capture more intermediate V_S behavior. The smoothed log mean V_S profile from binning by V_S is shown in Figure 5.14.

To capture the lower V_S values observed in the data, an additional judgment-based profile was created from the lower bound of the collected rock-removed profile data and a smoothed log-mean binned velocity profile developed from the rock-removed velocity profile data with V_{S30} values between 0 m/s and 300 m/s. The soft judgment-based profile was created by taking the geometric mean of the lower bound and binned profile and imposing a few additional constraints: the maximum increase in velocity between 5 m layers is 30 m/s and velocity is monotonically increasing with depth. The V_{S30} of the soft judgment profile is 142 m/s. Figure 5.17 shows the binned and minimum bound velocity profiles used to create the judgment-based soft velocity profile.

The smoothed log mean V_S profiles calculated for the similar geology classes described in Section 5.2.2 were combined to reduce the number of representative seed velocity profiles used in site response analysis. The combined profiles were created by taking the log-mean of the two or three adjusted log-mean profiles similar in V_S structure. Geology-sorted adjusted log-mean profiles combined in this way are RRm and OG (shown in Figure 5.21), YNa-YNl-YNs and ON (shown in Figure 5.19), and YGd-YGt-YGo, RS, and YGm (shown in Figure 5.20).

A V_S profile is developed similar to the other smoothed log mean V_S profiles and used as a lower-bound of V_S profile randomization. The lower bound profile comes from lowest value of the collected V_S profile data at the center of each sublayer used for profile averaging. This profile then has reversals removed and is extended to 1000 m same as the other smoothed log mean V_S profiles. The minimum bound V_S profile is shown in Figure 5.1 Any randomized V_S profile generated with V_S lower than the minimum bound profile at the midpoint of a layer is discarded and resampled.

5.3 Weathered Rock Zone Velocity Structure

Above the hard reference rock conditions in CENA is a zone of weathered rock of varying thickness and velocity structure. To capture the range of characteristics of the weathered zone in the parametric study, six velocity gradients and zone thicknesses are selected to reach the V_S = 3000 m/s value of reference rock. Four depth-based velocity structures in the weathered rock zone are selected to capture observed weathered-rock zone thicknesses and two gradient-based models are selected to capture varying impedance ratios at the top of the weathered rock zone.

Weathered rock zone models are selected to cover the range of weathered rock zone conditions described in Hashash et al. (2014a) and either have a prescribed depth or prescribed gradient. The depth-based structures all have median V_S at the top of the weathered zone of 2000 m/s. This is a typical value as described in Hashash et al. (2014). The chosen thicknesses of the weathered rock zone are 0 m, 10 m, 30 m, and 70 m. The gradient-based structures all have a constant V_S gradient with depth of 33 (m/s)/m. This value was selected to capture variability in the V_S of the top of the weathered rock zone. For V_S values of 1500 and 2500 m/s at the top of the weathered rock zone, the chosen gradient model results in thicknesses of the weathered rock

zone of 45 m and 15 m, respectively. Figure 5.22 shows a comparison of the selected weathered rock zone models with the collected data from the report on reference rock condition.

The weathered rock models are applied to the bottom of each representative seed V_S profile for each depth bin in the parametric study. The weathered rock models are randomized as a part of the representative seed velocity profile. Figure 5.23 shows the application of the six weathered rock zone models to the bottom RRs representative seed V_S profiles truncated at the 50 m depth bin to provide a transition from the soil horizon to the 3000 m/s reference rock horizon. The weathered rock zone models are randomized simultaneously with the V_S and added to the bottom of each representative seed V_S profile at each profile depth investigated.

The weathered rock zone models are also used in a set of profiles with no soil horizon at the ground surface, shown as the bottom branch of Figure 3.1 detailed in Chapter 3. The weathered rock zone models are randomized the same way as the representative seed V_S profiles as described in Section 5.4.

5.4 Randomization of Shear Wave Velocity Profiles

5.4.1 Introduction

In the development of site amplification functions, spatial variability in soil structure is typically modeled by using randomized V_S profiles with a procedure similar to Toro (1995) in a Monte Carlo simulation. The Toro (1995) randomization scheme allows for V_S profile structures where deeper layers can have lower V_S than more shallow layers, creating a reversal with V_S as a function of depth. Within this model, statistical correlation coefficients limit the frequency with which these V_S reversals occur, but in large-scale studies, site amplification behavior for sites with V_S reversals can be systematically different than those without.

A study by Pehlivan et al. (2015) found that reversals in shear wave can lower the median surface response up to 10% at periods shorter than the site period. The Pehlivan et al. (2015) study used ground motions and soil columns similar to those derived for this study in 1-D EL site response analyses. The profiles randomized with coefficients of Toro (1995) that allow reversals

in V_S as a function of depth showed lower median surface responses than profiles without V_S reversals.

There are two systematic problems with V_S profiles generated with the Toro (1995) scheme: individual profiles can have unrealistic shapes, and when many realizations are created, the median of the simulations does not converge to the input median when V_S layer thickness is randomized as noted in Pehlivan (2015).

In the Toro (1995) V_S for each soil layer is assigned from a lognormal distribution with median V_S from an input median profile and either a prescribed standard deviation as a function of depth or a standard deviation related to surficial geology and site classification recommended from the data collected for the Toro (1995) model derivation. The randomized assigned V_S is correlated to the V_S of the previous layer, with the strength of the correlation depending on depth. When this model is used without layer thickness randomization, the input median and standard deviation are stable and returned when a sufficient number of random velocity profiles are generated, but the profiles may be unrealistic. V_S values at most sites increase as a function of depth and reversals in V_S are usually attributable to well-documented, specific geologic site conditions. It is possible, even with high inter-layer velocity correlation coefficients for the Toro (1995) model to generate layers with overly high or low V_S relative to the surrounding layers at any depth. The Toro (1995) model also has no built-in boundaries on reasonable soil behavior. The log-normal distribution of V_S in the model can generate rock-like V_S values at shallow depths. If the randomization model is constrained with upper or lower bounds, the median profile and standard deviation inputs are not returned by the randomization scheme. Additionally, in nonlinear site response analysis, a sharp change in V_S with depth can create numerical difficulties, as ground motion frequency can get trapped in the soft layer.

In this study, the representative seed V_S profiles are randomized using guidelines from Toro (1995) V_S randomization model with three notable differences: (1) the random V_S profiles have geologically-based upper and lower bounds, (2) V_S distribution is perfectly correlated as a function of depth, and (3) V_S layer thickness is not randomized as described in sections 5.4.2, 5.4.3, and 5.4.4, respectively. The combined effects of perfectly correlating V_S as a function of depth and removing layer thickness randomization results produces randomized V_S profiles that

are lognormally distributed and geometrically scaled (i.e. multiplied by a constant) from the representative seed V_S profiles.

Figure 5.24a shows the 30 random V_S realizations of the YNm representative seed V_S profile with 100 m depth and 30 m thick weathered rock zone are shown as a function of depth with their log-mean and log mean ± one log standard deviation (σ). The random realizations of each of the representative seed V_S profiles are shown in Figure 5.26 through Figure 5.35 to a depth of 100 m (a) and 1000 m (b). The random realizations of the surface weathered rock profiles described by the lower branch of Figure 3.1 are shown in Figure 5.36 through Figure 5.40.

5.4.2 Randomization Bounds

The randomized V_S profiles in this study are bounded at both high and low V_S to better reflect V_S conditions in CENA. The lower bound of the randomized V_S profiles comes from a profile of the lower bound of V_S profile data collected in CENA. If any V_S realization has V_S lower than the minimum bound profile, the realization is resampled. If any V_S realization has V_S higher than 3000 m/s, the profile is truncated at the deepest layer with a V_S less than 3000 m/s.

These bounds have the potential to introduce bias into the random realizations that cause them to deviate from the representative seed profiles for the soil models, or the weathered rock zone V_S models. The soil horizon of the random V_S profiles is most likely to be affected by the lower bound of randomization. The influence of this lower bound in the random V_S data will be manifested by the log-mean of the randomized profiles being higher than the source representative seed V_S profiles. The log mean and 95% confidence interval (CI) on the log mean of the realizations each of the representative seed profiles is shown with the source seed V_S profile in each of Figure 5.26 through Figure 5.35. With the exception of the RRs representative seed profile, all other representative seed V_S profiles fall within the 95% CI of the mean of the realizations. Across all of the representative seed V_S profiles, this is sufficient evidence to suggest that there is relatively little bias introduced into the realizations by the inclusion of the lower bound of V_S.

The upper bound of V_S of 3000 m/s will manifest differently than the lower bound because profiles are truncated and not resampled. This will result in the log-mean of the random

realizations deviating from the weathered rock zone V_S models as a function of depth as profiles that reach 3000 m/s are truncated as shown in Figure 5.24a for a weathered rock zone at the bottom of a soil column and in Figure 5.36 through Figure 5.40 for the surface rock V_S randomizations. The truncation of the weathered rock models at 3000 m/s results from the lack of reference rock randomization. Without truncation, V_S values for the weathered rock could be generated greater than the 3000 m/s reference rock condition.

Deviation from the randomization inputs for the V_S randomizations of the soil or weathered rock horizons will have no effect on the usability of the site profile in the modeling of amplification functions. The site parameters such as V_{S30} used in the amplification function development in this study come only from the site realizations and are not influenced by the source representative seed V_S profiles and weathered rock zone V_S model.

5.4.3 V_S Distribution

When the Toro (1995) V_S randomization model is used with perfect V_S correlation between layers, the random number assigned to each soil layer is identical to the layer above it, and a single random number generated for the first layer is used to generate the random V_S profile. All soil layers after the first are perfectly correlated and identical to the random number generated at the surface of the profile. Following the procedure of randomization from Toro (1995), the random number at the surface will be lognormally distributed with some specified log standard deviation and a log mean equal to the representative seed V_S profile at the surface.

The log standard deviation, commonly $\sigma_{ln(v)}$ used was 0.2. This value is higher than the $\sigma_{ln(v)}$ = 0.1 typically associated with measurements (Ancheta et al. 2013), but lower than the $\sigma_{ln(v)}$ typically associated with V_{S30} proxies which range from 0.2 to 0.6 in the WUS (Ancheta et al. 2013), and from 0.4 to 0.6 in CENA (Goulet et al. 2014). The selection of $\sigma_{ln(v)}$ = 0.2 produces good coverage of V_{S30} as shown in Figure 5.25.

5.4.4 V_S Layer Thickness

The V_S profiles developed in Section 5.2 use a very fine resolution of V_S as a function of depth that does not necessarily represent realistic V_S profiles where units of relatively constant V_S are

expected. The representative seed V_S profiles used in randomization sample the smoothed, depth-extended log-mean V_S profiles to better reflect the idea that V_S is not continuously smooth, and that thicker units of V_S are expected at greater depth. The mean expected values from the Toro (1995) layer randomization scheme is used to define layer thickness of the representative seed V_S profiles as a function of depth.

The layer thickness randomization scheme in the Toro (1995) model uses a nonhomogeneous Poisson process to predict the rate of soil layers with soil column depth. These layers are then assigned a V_S value from the V_S randomization model. The rate function of the Toro (1995) model is given by

$$\lambda(d) = a(d + b)^c \qquad \text{eq. 5.2}$$

where λ is the expected layer rate, d is depth, and a and b are constants. Using the recommended values for a, b, and c shown in Table 5.5, the expected layer thickness at 1000 m is 239 m. It is unusual that the velocity structure of a soil column would have a constant velocity for over 200 m, even at great depth. Because the increase in layer thickness with depth is greatly dependent on the c exponent, if the exponent is increased to -0.7, and a and b are unchanged, the expected layer thickness at 1000 m is reduced to 64 m, a more reasonable unit to have a uniform V_S. The layer thickness of V_S profiles used in this study are not randomized and all have the same layer thicknesses as a function of depth, where the V_S layer thickness at each depth is the expected layer thickness for that depth given by eq. 5.2 using the coefficients shown in Table 5.5.

The V_S layer thicknesses are assigned to the representative seed V_S profiles from the smoothed, depth-extended log mean V_S profiles in Section 5.2.3, resulting in slightly different V_{S30} values for each of the sets of profiles. The V_{S30} values of the representative seed V_S profiles after assigning layer thicknesses from Toro (1995) is provided in Table 5.6 below.

The weathered rock models do not follow this procedure for layer thickness assignment. All layers in the weathered rock zone have a thickness of 5 m to capture the gradient and V_S structure between the bottom of the soil profile and the 3000 m/s reference rock.

After randomization of V_S, model layers are subdivided to control the propagation of high frequency through the soil column. The maximum frequency a model soil layer can propagate in a time domain analysis, f_{max}, is given by eq. 5.3 (Kramer 1996).

$$f_{max} = \frac{V_S}{4H} \qquad \text{eq. 5.3}$$

where H is the thickness of the model layer, and V_S is the shear wave velocity of that layer. The maximum frequency that can be reliably propagated by an entire soil profile in a time domain site response analysis is the minimum f_{max} of the soil profile's layers. Soil profiles in this study were subdivided such that the maximum frequency of the soil profile was 50 Hz.

Table 5.1: List of V_S profiles references.

• Anderson et al. (2003) • Anderson and Thitimakorn (2004) • Anderson et al. (2005) • Andrus et al. (2006) • Bauer et al. (2004) • Beresnev and Atkinson (1997) • Calvert Cliffs 3 Nuclear Project LLC and UniStar Nuclear Operating Services LLC (2011) • Dames and Moore (1974) • Detroit Edison Company (2010) • Dominion Virginia Power (2009) • Duke Energy (2010) • Entergy Operations Florida Inc. (2011) • Entergy Operations Inc. (2008) • Exelon Generation Company (2006) • Exelon Nuclear Texas Holdings LLC (2008) • Florida Power and Light Company (2010) • Ge et al. (2007) • Gomberg et al. (2003) • Herrmann and Crossely (2008) • Hoar and Stokoe (1982) • Hoffman et al. (2008) • Jaume (2006) • Kaka (2005) • Kayen et al. (2013) • Lester (2005) • Liu et al. (1997) • Luminant Generation Company LLC (2009) • Mohanan et al. (2006) • Moos and Zoback (1983)	• Nine Mile Point Nuclear Project LLC and UniStar Nuclear Operating Services LLC (2011) • Odum et al (2003) • Ohio Geologic Survey (2011) • Olson and Hashash (2009) • Progress Energy Carolinas (2011) • Progress Energy Florida Inc. (2011) • PSEG Power (2011) • Read et al. (2008) • Rosenblad (2006) • Salomone et al. (2012) • Santagata and Kang (2007) • Shneider et al. (2001) • South Carolina Electric & Gas (2011) • Southern Nuclear Operating Company (2008) • Stokoe (1983) • Stokoe and Mok (1987) • Stokoe and Turner (1983) • Stokoe et al. (1983) • Stokoe et al. (1985) • Stokoe et al. (1989) • Stokoe et al. (1992) • Stokoe et al. (1994) • STP Nuclear Operating Company (2011) • Street et al. (1995) • Sykora and Davis (1993) • Tennessee Valley Authority (2009) • Union Electric Company (2009) • UniStar Nuclear Services LLC (2010) • Woolery and Wang (2005) • Xia et al. (2002)

Table 5.2: CENA Geology types used to sort V_S profile data collected for derivation of geology-based characteristic V_S profiles. Modified after (Kottke et al. 2012).

Major Unit and Age	Sub-Unit	Abbreviation
Old Glacial Sediments (Older than Wisconsin)	None	OG
Young Glacial Sediments (Wisconsin and younger)	Glaciomarine and Lacustrine	YGm
	Outwash and alluvium	YGo
	Tills	YGt
	Discontinuous Till	YGd
Old Non-Glacial Sediments (Mid-Pleistocene and older)	None	ON
Young Non-Glacial Sediments (Holocene and late Pleistocene)	Alluvium	YNa
	Loess	YNl
	Lacustrine, Marine and Marsh	YNm
	Beach, dune, and sheet sands	YNs
Residual Material	Residual material from metamorphic and igneous rock	RRm
	Residual material from sedimentary rock	RRs
	Residual from soils	RS

Table 5.3: CENA Geology types for site amplification (Kottke et al. 2012).

Major Unit and Age	Sub-Unit	Abbreviation
Old Glacial Sediments (Older than Wisconsin)	Glaciomarine and Lacustrine	OGm
	Outwash and alluvium	OGo
	Tills	OGt
Young Glacial Sediments (Wisconsin and younger)	Glaciomarine and Lacustrine	YGm
	Outwash and alluvium	YGo
	Tills	YGt
	Discontinuous Till	YGd
Old Non-Glacial Sediments (Mid-Pleistocene and older)	Alluvium	ONa
	Colluvium	ONc
	Loess	ONl
	Lacustrine, Marine and Marsh	ONm
Young Non-Glacial Sediments (Holocene and late Pleistocene)	Alluvium	YNa
	Colluvium	YNc
	Loess	YNl
	Lacustrine, Marine and Marsh	YNm
	Beach, dune, and sheet sands	YNs
Residual Material	Residual material from metamorphic and igneous rock	RRm
	Residual material from sedimentary rock	RRs
	Residual from soils	RS
Not Classified	Not Classified	NC

Table 5.4: List of references of n_v values.

• Ashland and McDonald (2003),	• Marcuson and Wahls (1972)
• Brandenberg et al. (2010)	• Menq (2003)
• Choi (2008)	• Ohta and Goto (1978)
• Dickenson (1994)	• Rosenblad (2006)
• Fumal (1978)	• Seed and Idriss (1970),
• Hamilton (1976)	• Sykora and Stokoe (1983)
• Hardin and Drnevich (1972)	• Wills and Clahan (2006)
• Jeon (2008)	• Yamada et al. (2008)
• Kokusho et al. (1982)	• Wilder (2007)
• Lew and Campbell (1985)	• Zen et al. (1987)

Table 5.5: Coefficients for use with Toro (1995) layer thickness randomization scheme.

Coefficient	Toro (1995) recommended values	Values used in this study
a	1.98	1.98
b	10.86	10.86
c	-0.89	-0.7

Table 5.6: V_{S30} of representative seed profiles after layer thickness assignment.

Profile Name	V_{S30} of smoothed, depth-extended log mean V_S profile before layer thickness assignment (m/s)	V_{S30} of representative seed profile after layer thickness assignment (m/s)
YNm	229	240
RRs	356	356
YNa-YNl-YNs +ON	245	252
RRm + OG	380	391
YGd-YGt-YGo + RS + YGm	329	333
V_{S30} Bin = 300-500 m/s	375	383
Scaled Global Log-Mean to V_{S30}= 600 m/s	600	616
Scaled Global Log-Mean to V_{S30}= 500 m/s	500	513
Scaled Global Log-Mean to V_{S30}= 400 m/s	400	411
Judgment Soft	143	148

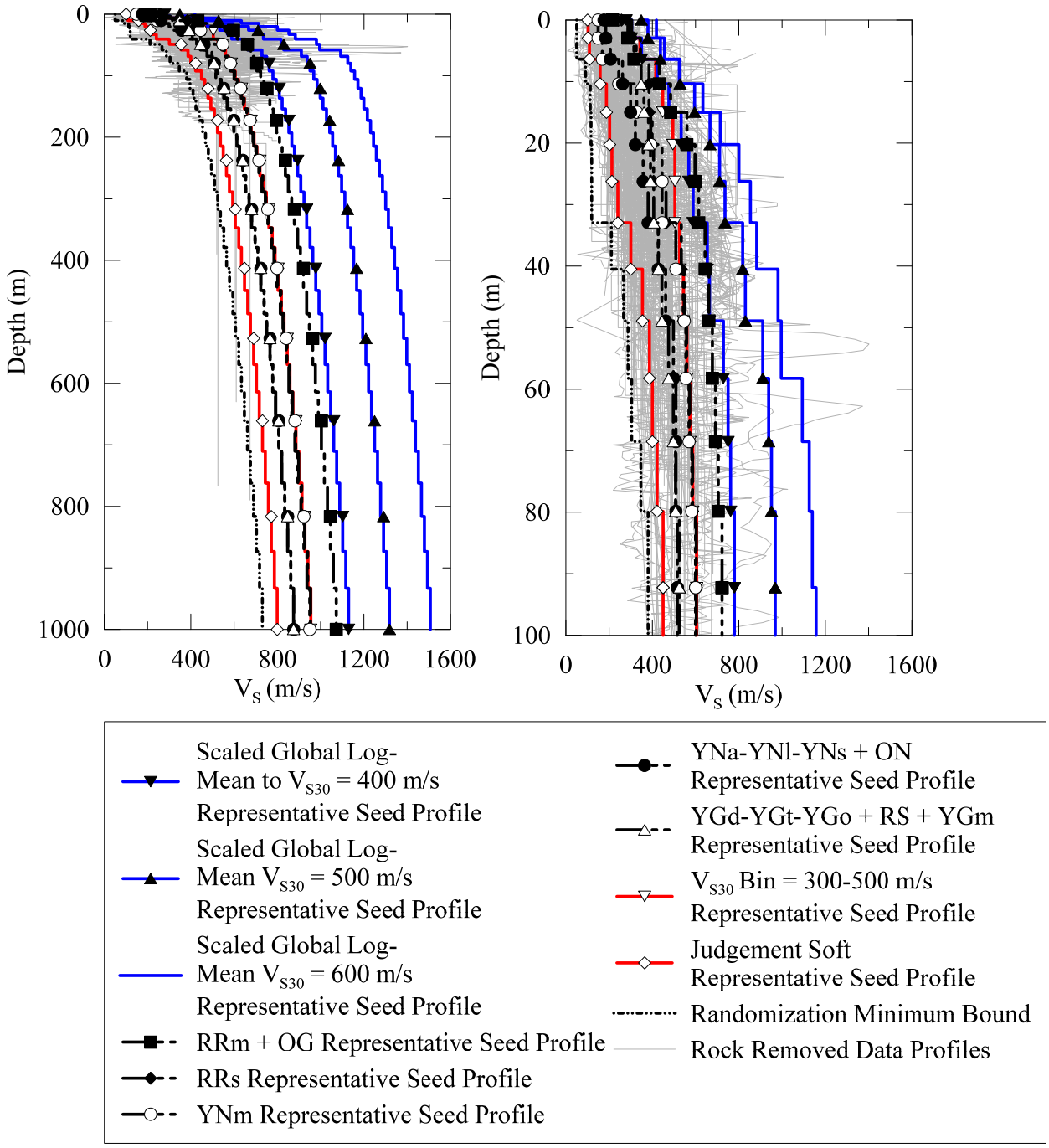

Figure 5.1: Representative Seed V_S profiles to a depth of 1000 m (a) and 100 m (b) with collected CENA V_S profile data.

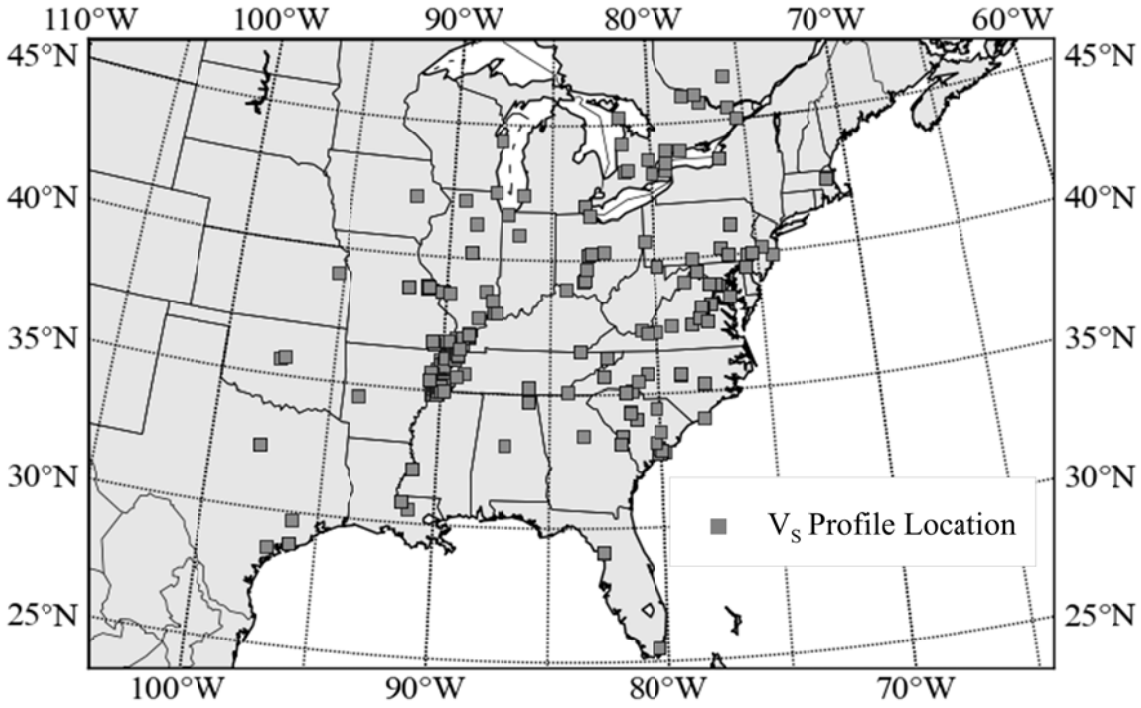

Figure 5.2: Locations of V_S profiles in CENA from literature and open file reports.

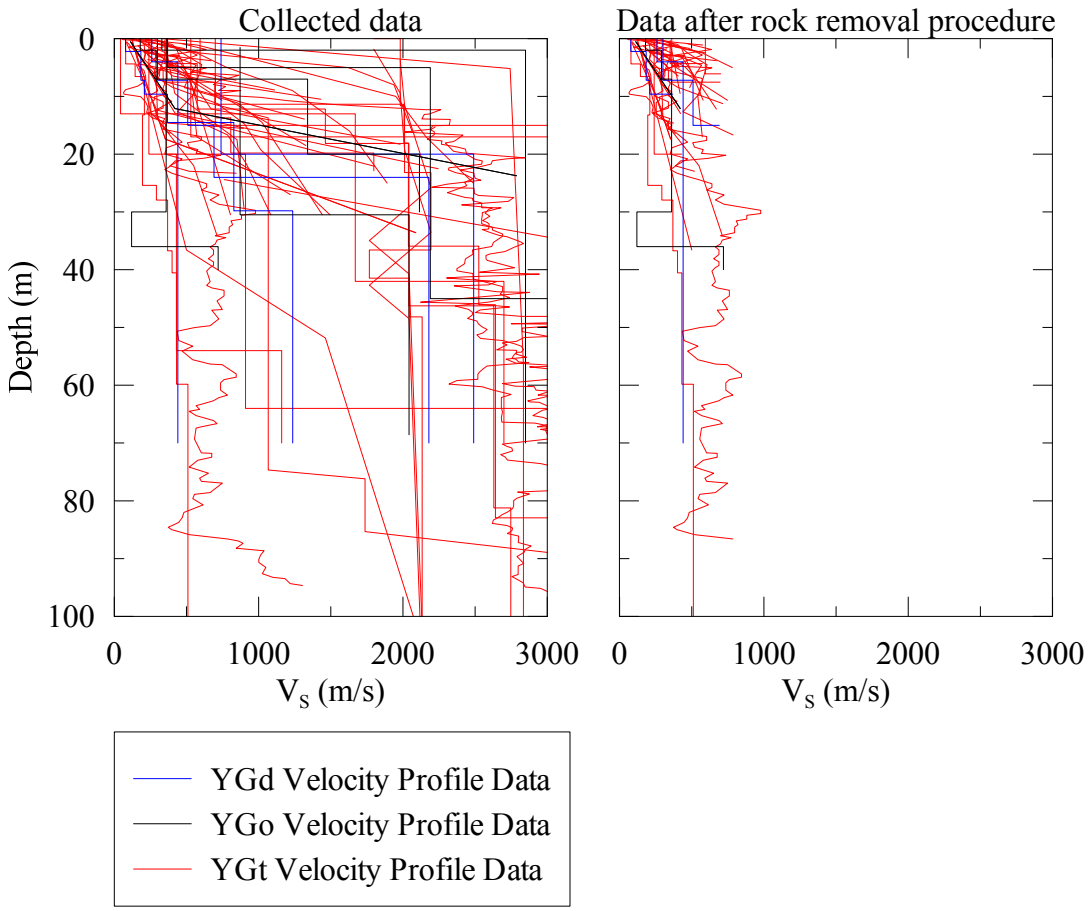

Figure 5.3: Results of rock removal procedure for velocity profiles collected in geologic classes YGd, YGo, and YGt.

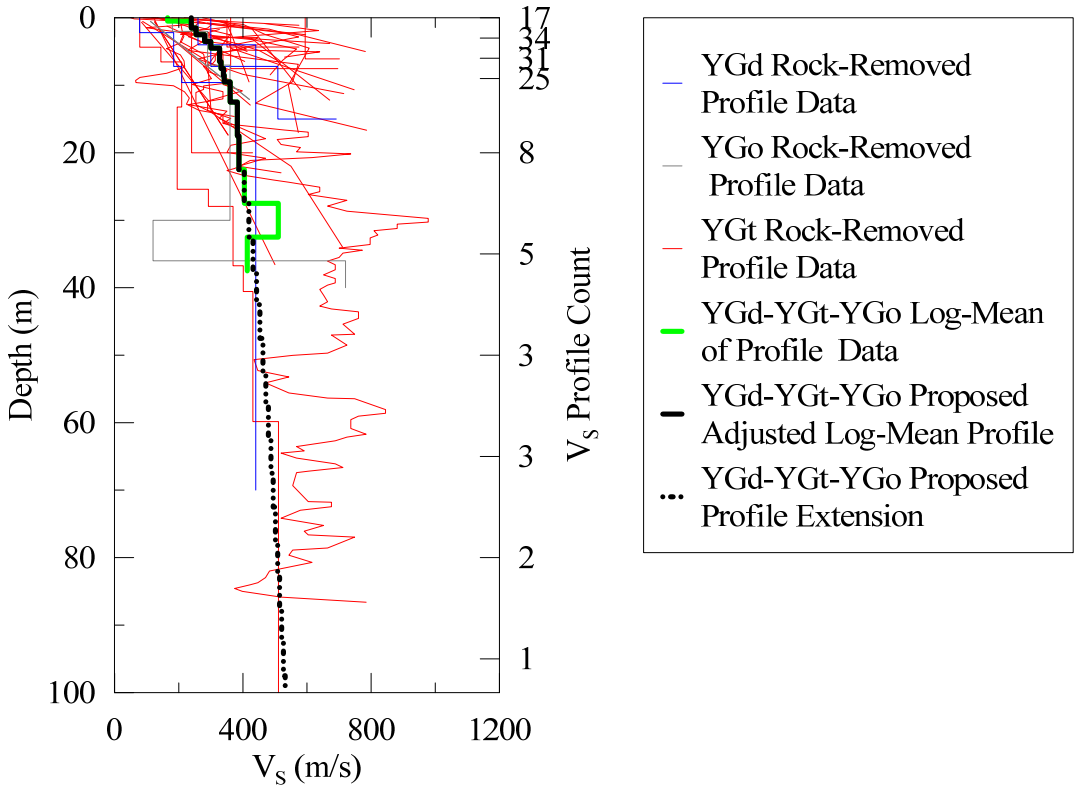

Figure 5.4: YGd-YGt-YGo adjusted log mean velocity profile. Profile data and log mean of geologic classes YGd, YGo, and YGt shown.

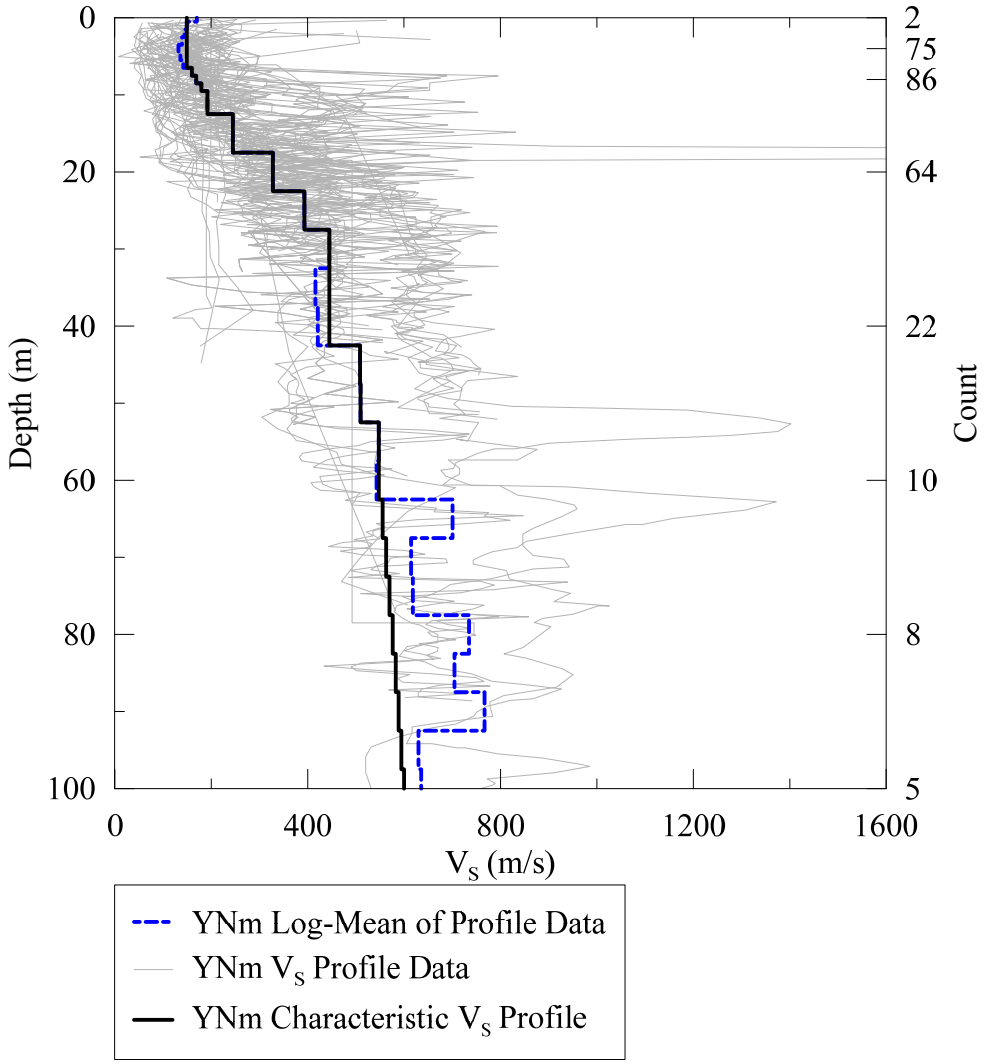

Figure 5.5: YNm smoothed, depth extend log mean V_S profile with count of V_S profile data as a function of depth.

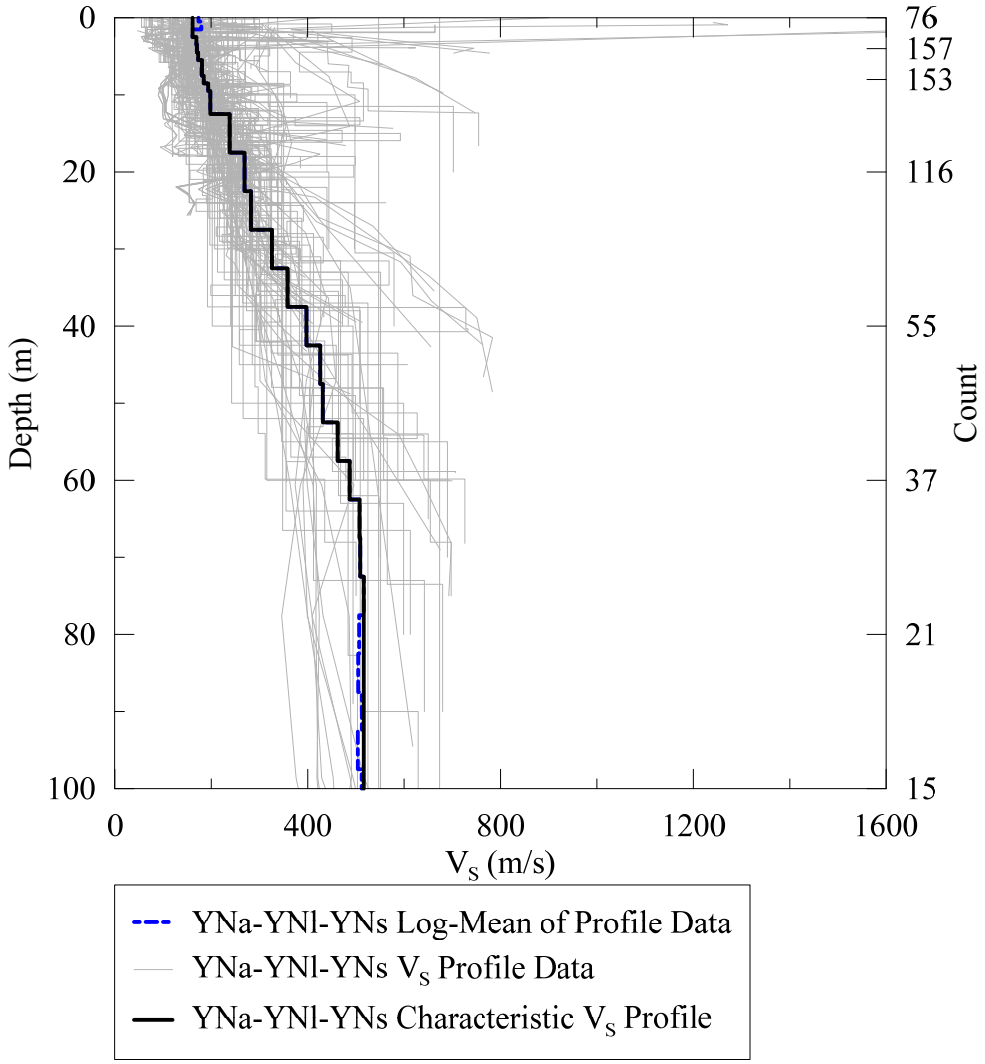

Figure 5.6: YNa-YNl-YNs smoothed, depth extend log mean V_S Profile with count of V_S profile data as a function of depth.

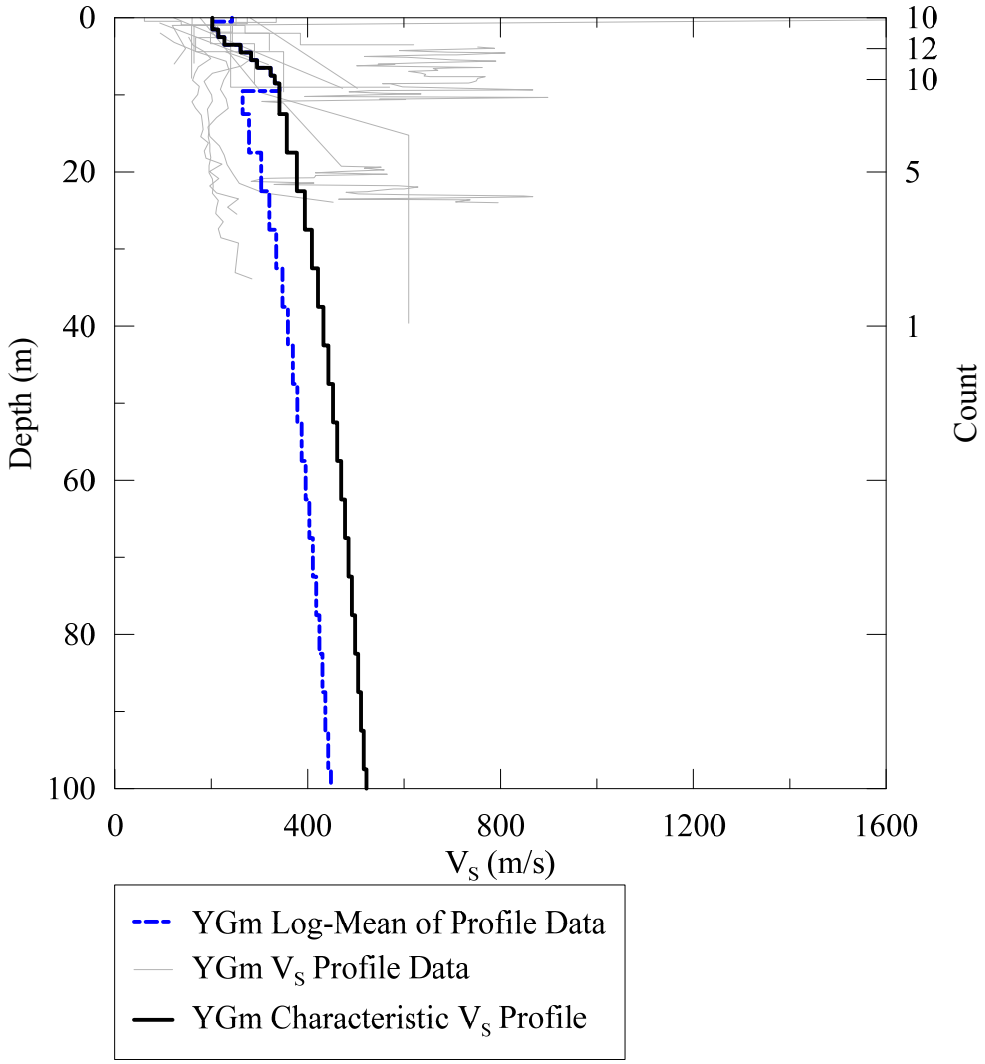

Figure 5.7: YGm smoothed, depth extend log mean V_S Profile with count of V_S profile data as a function of depth.

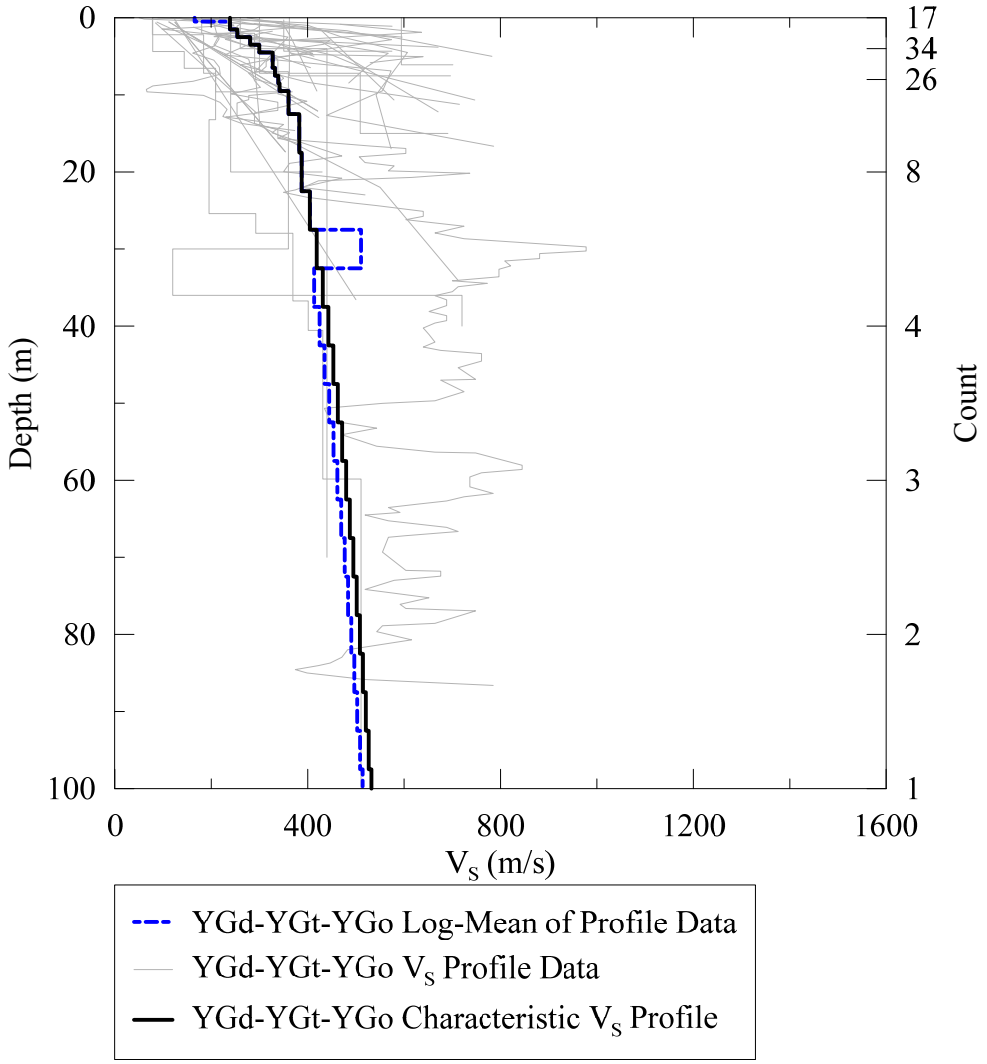

Figure 5.8: YGd-YGt-YGo smoothed, depth extend log mean V_S Profile with count of V_S profile data as a function of depth.

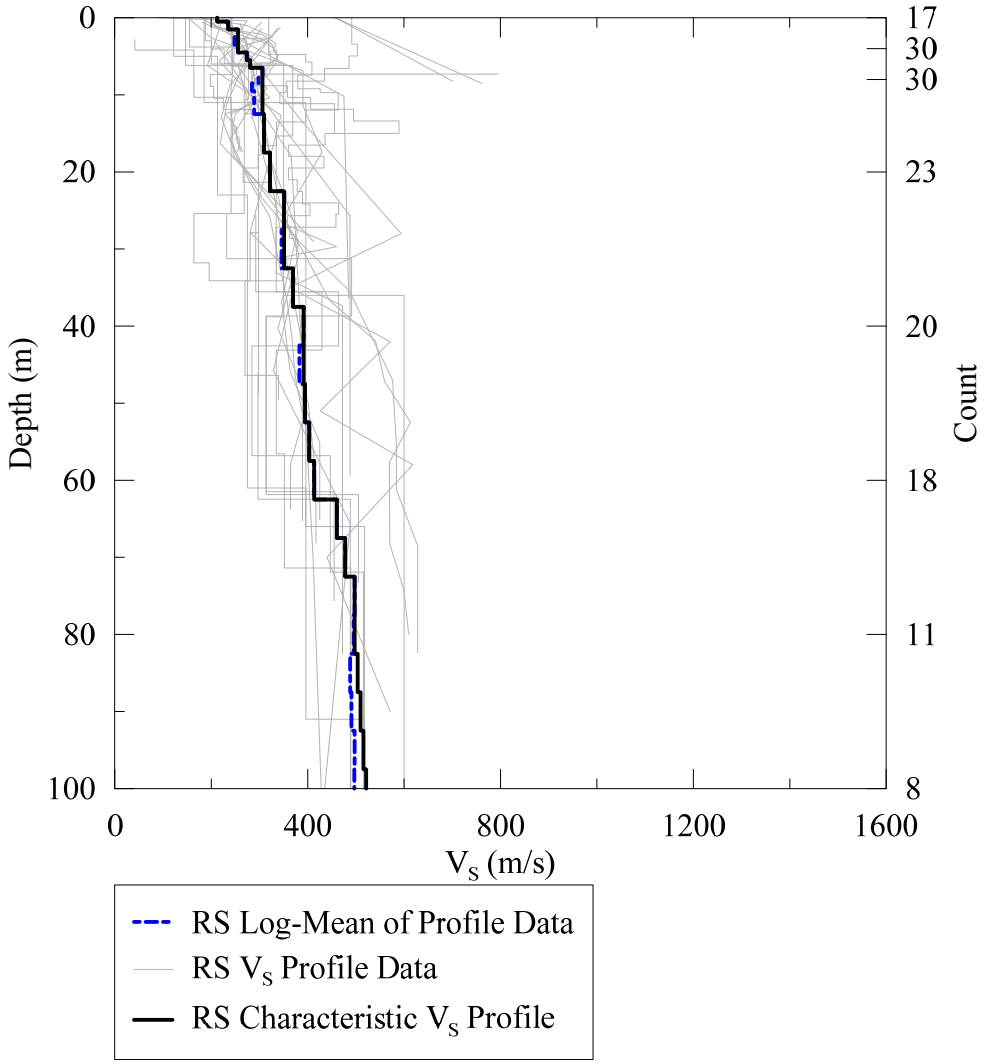

Figure 5.9: RS smoothed, depth extend log mean V_S Profile with count of V_S profile data as a function of depth.

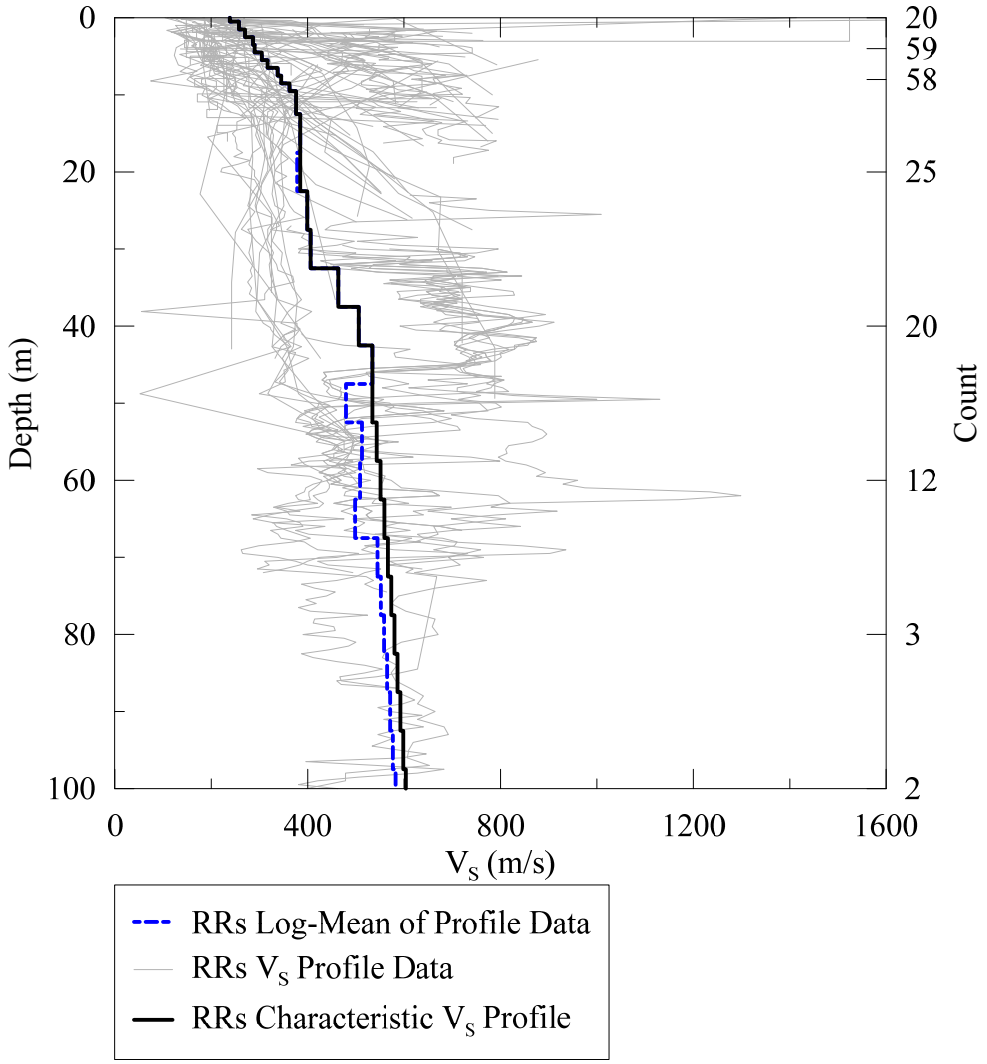

Figure 5.10: RRs smoothed, depth extend log mean V_S Profile with count of V_S profile data as a function of depth.

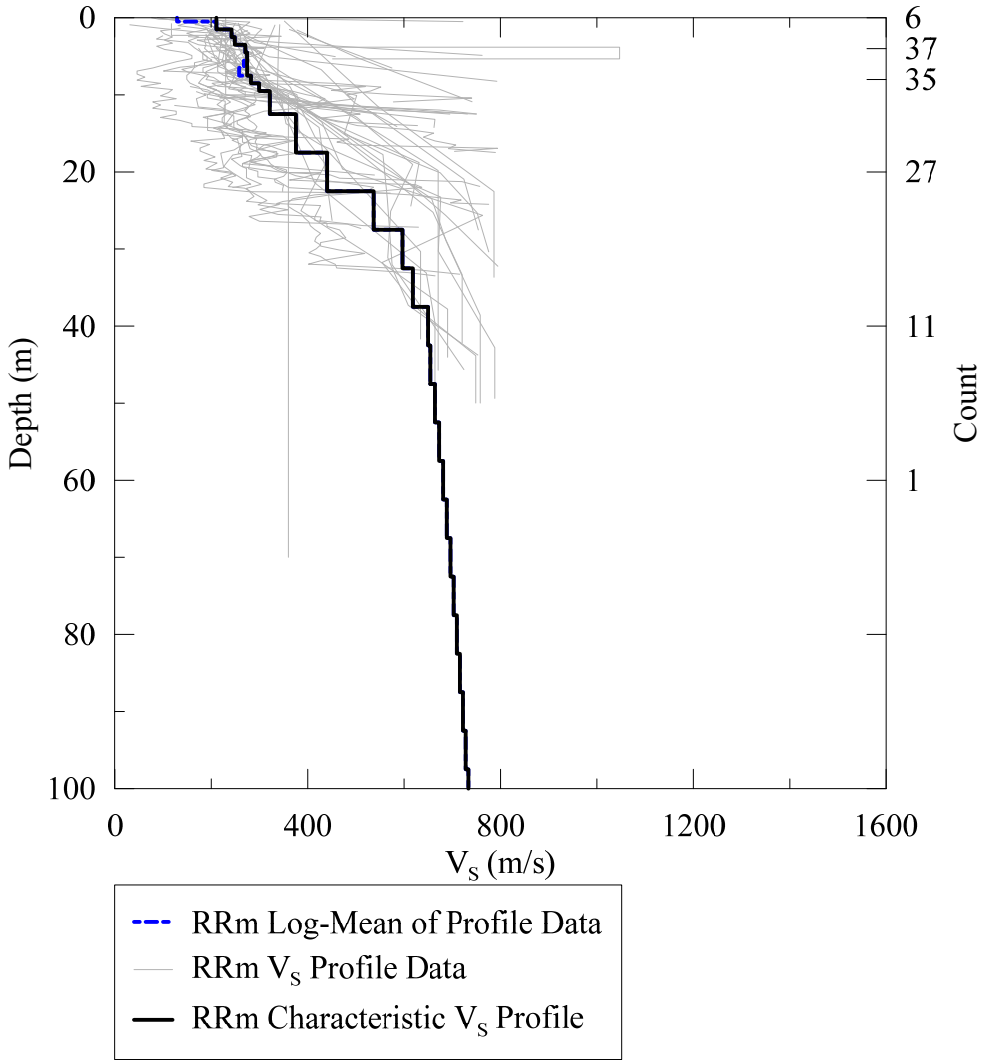

Figure 5.11: RRm smoothed, depth extend log mean V_S Profile with count of V_S profile data as a function of depth.

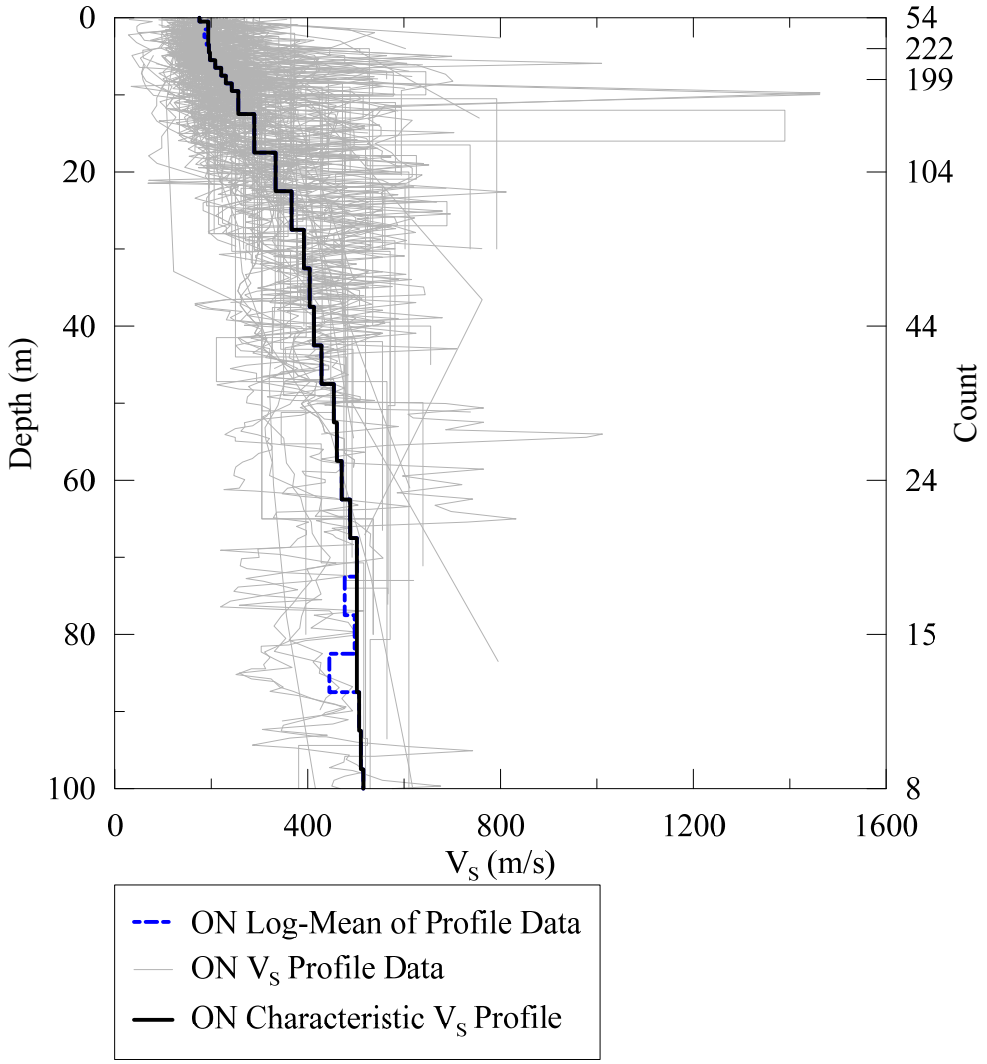

Figure 5.12: ON smoothed, depth extend log mean V_S Profile with count of V_S profile data as a function of depth.

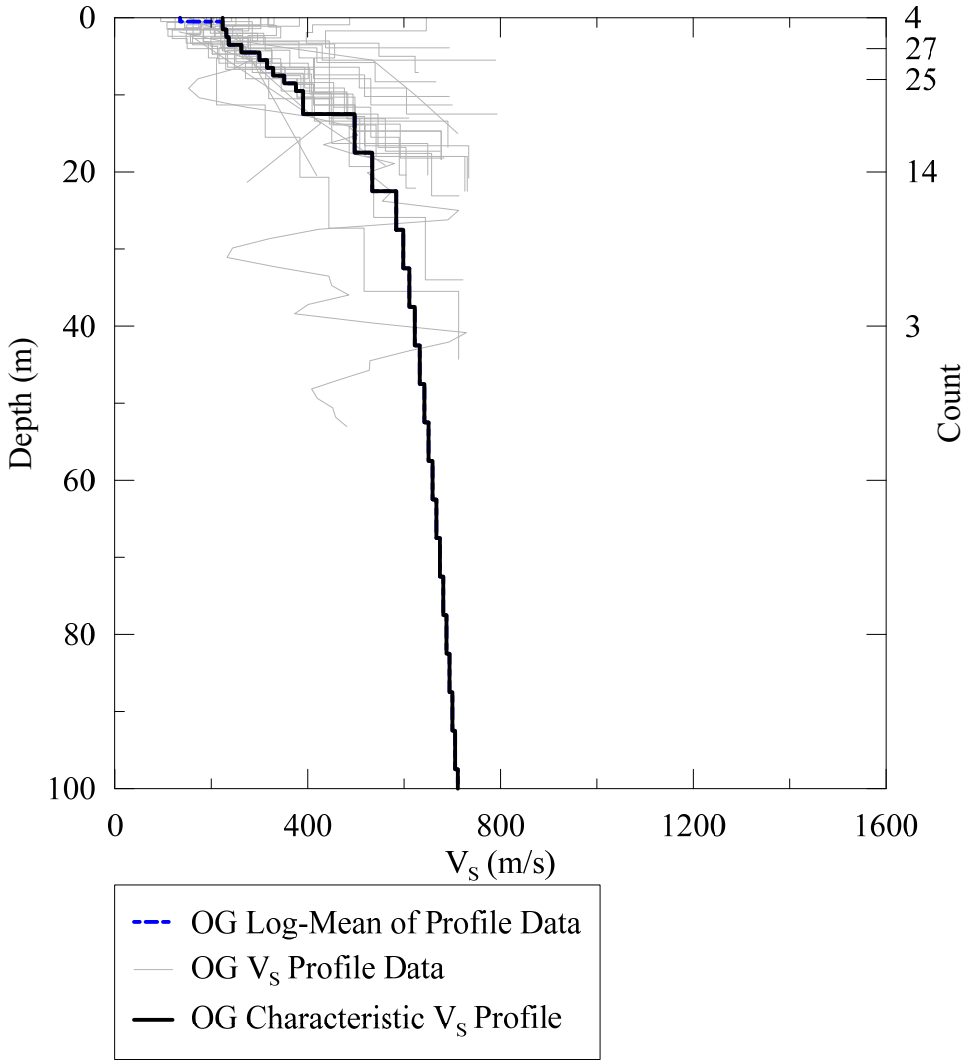

Figure 5.13: OG smoothed, depth extend log mean V_S Profile with count of V_S profile data as a function of depth.

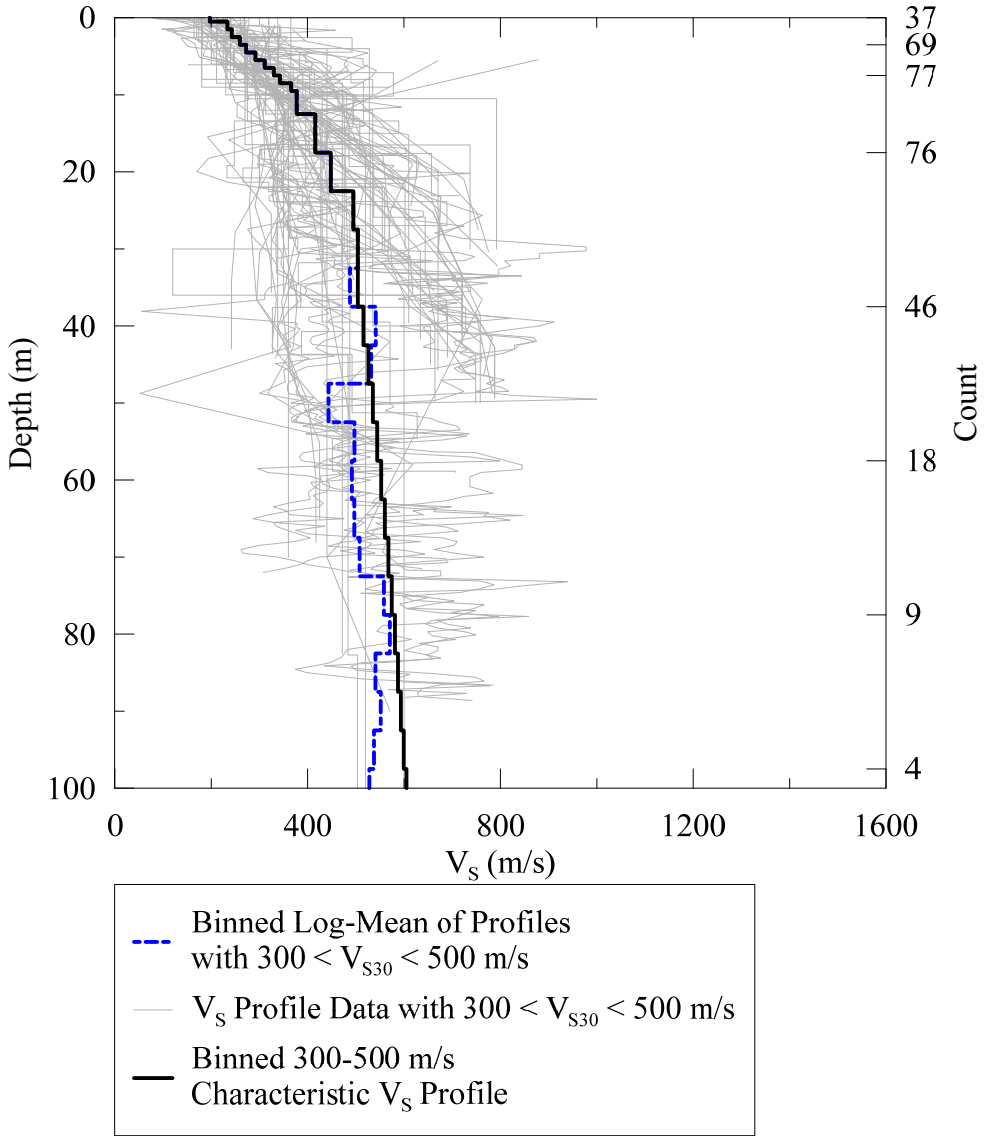

Figure 5.14: Smoothed, depth extend log mean V_S Profile of Binned data with 300 m/s < V_{S30} < 500 m/s with count of V_S profile data as a function of depth.

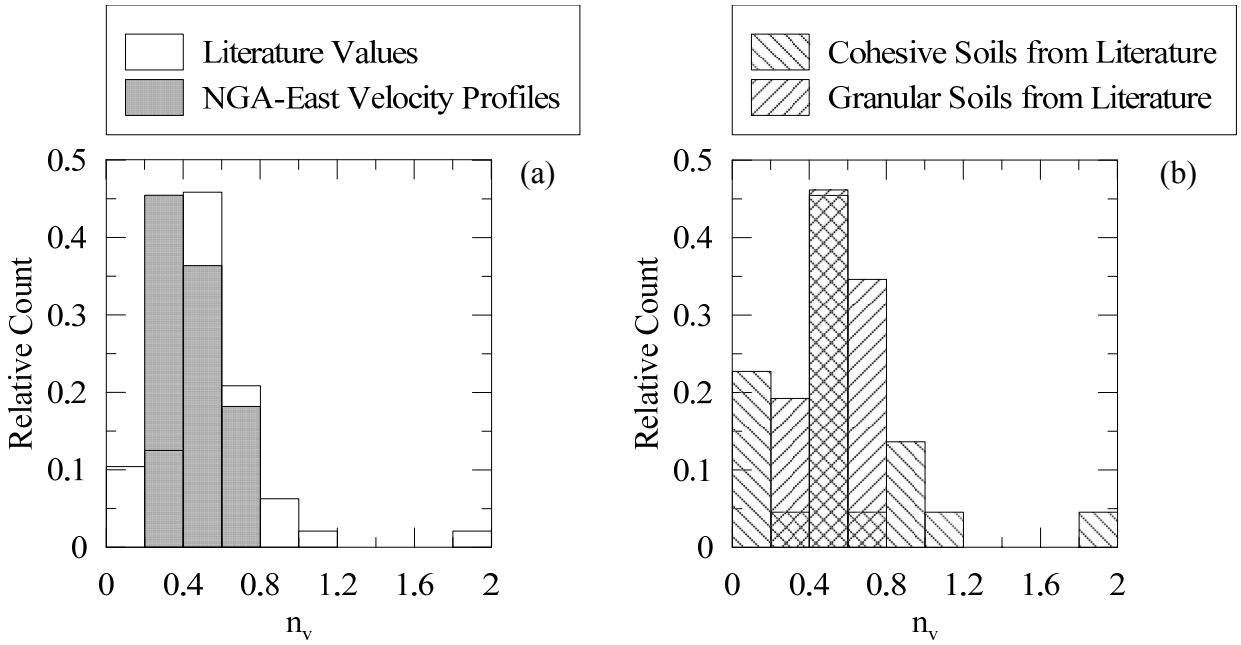

Figure 5.15: Relative histograms of n_v values from literature and collected velocity profiles. Relative histograms shown for cohesive and granular soils in literature where soil classification is known.

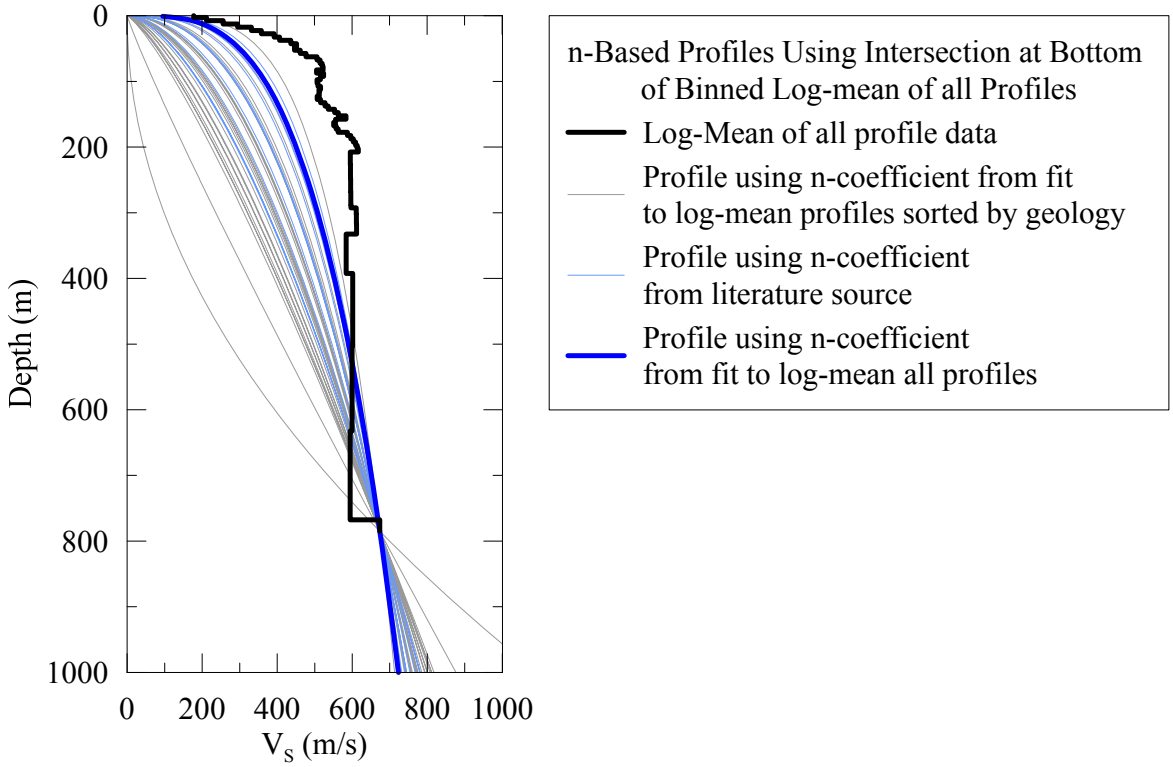

Figure 5.16:Velocity profiles generated for literature and data nv-coefficient values fit to the termination point of the log-mean of all velocity profile data.

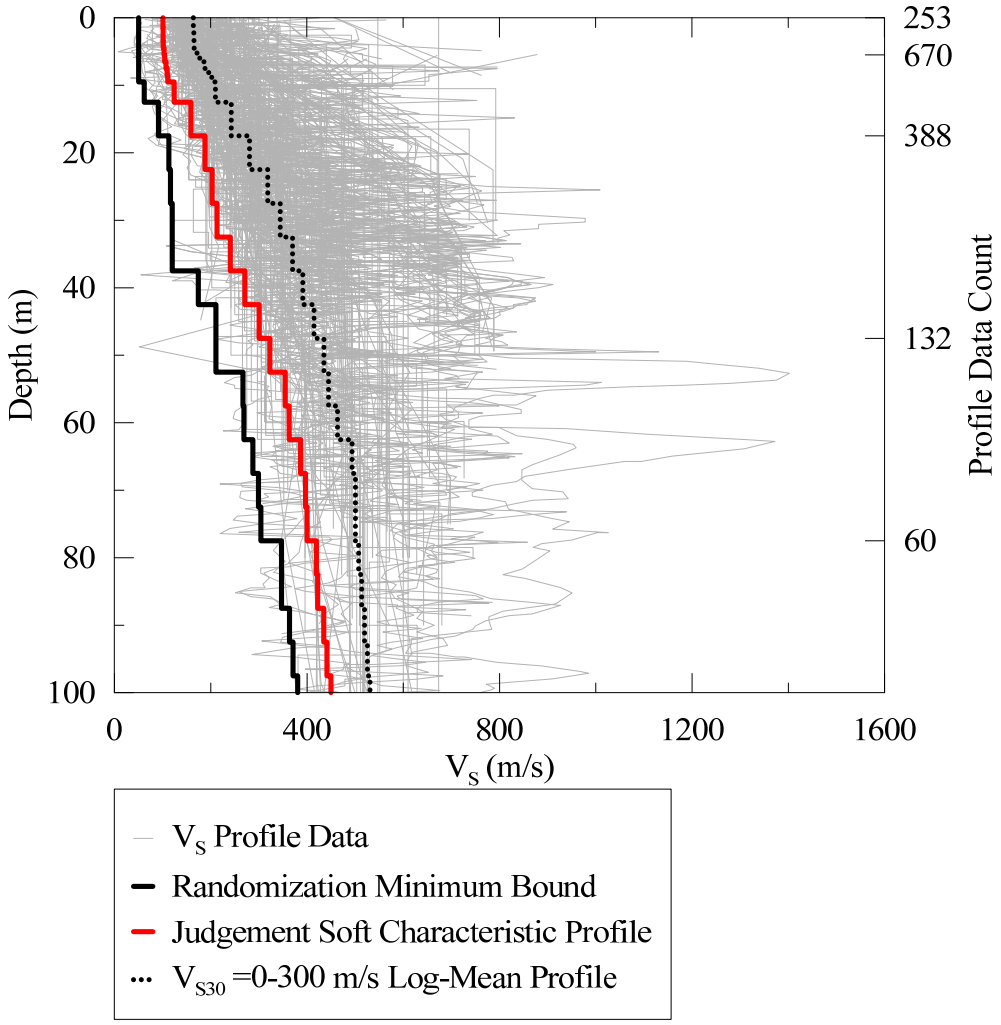

Figure 5.17: Creation of Judgment Soft profile for use as a representative seed profile in parametric study from the minimum bound profile and the adjusted log mean of rock-removed velocity profiles with V_{S30} values between 0 and 300 m/s.

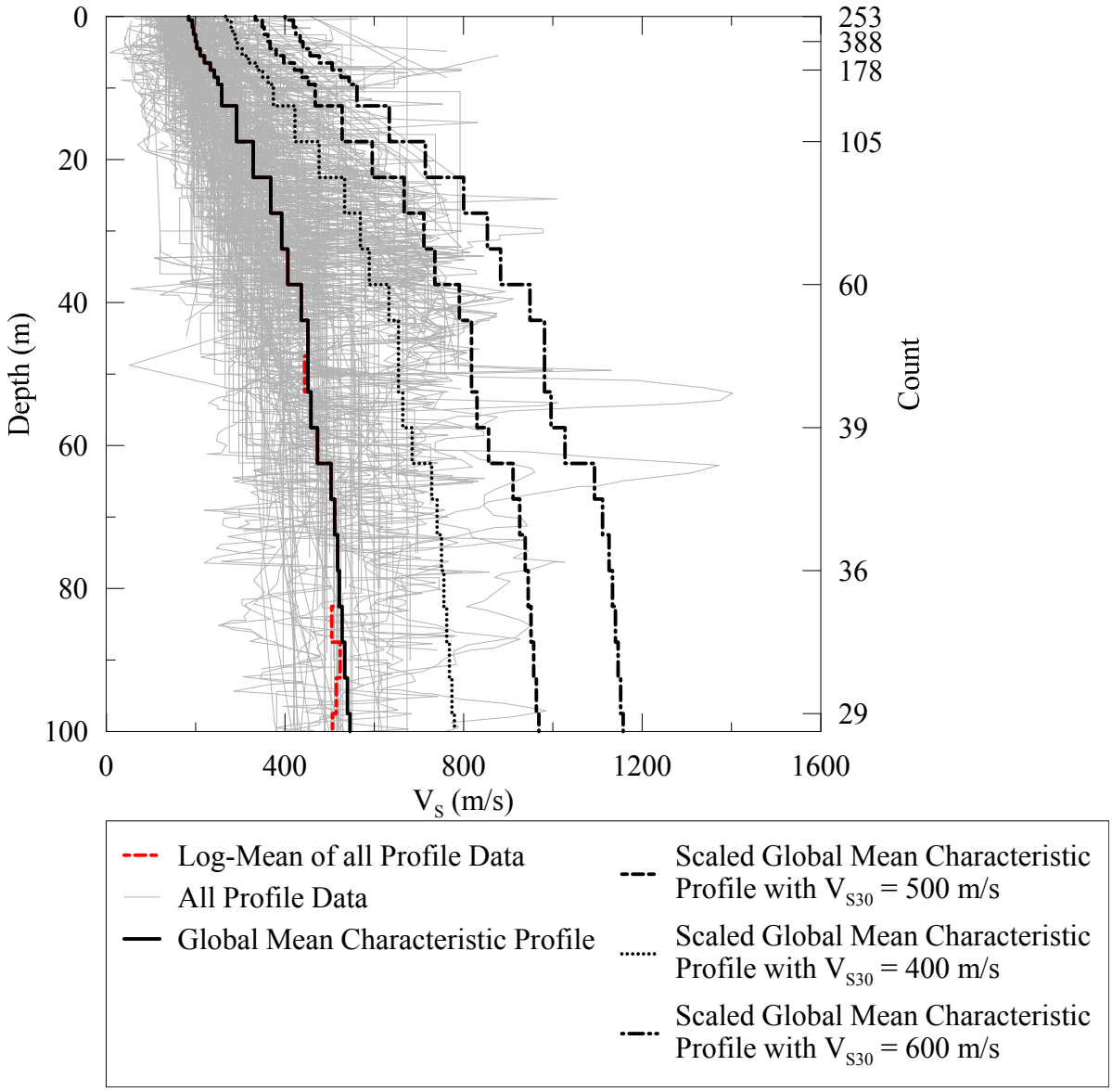

Figure 5.18: Smoothed log mean V_S Profiles from scaled global log-mean profile with count of all V_S profile data as a function of depth.

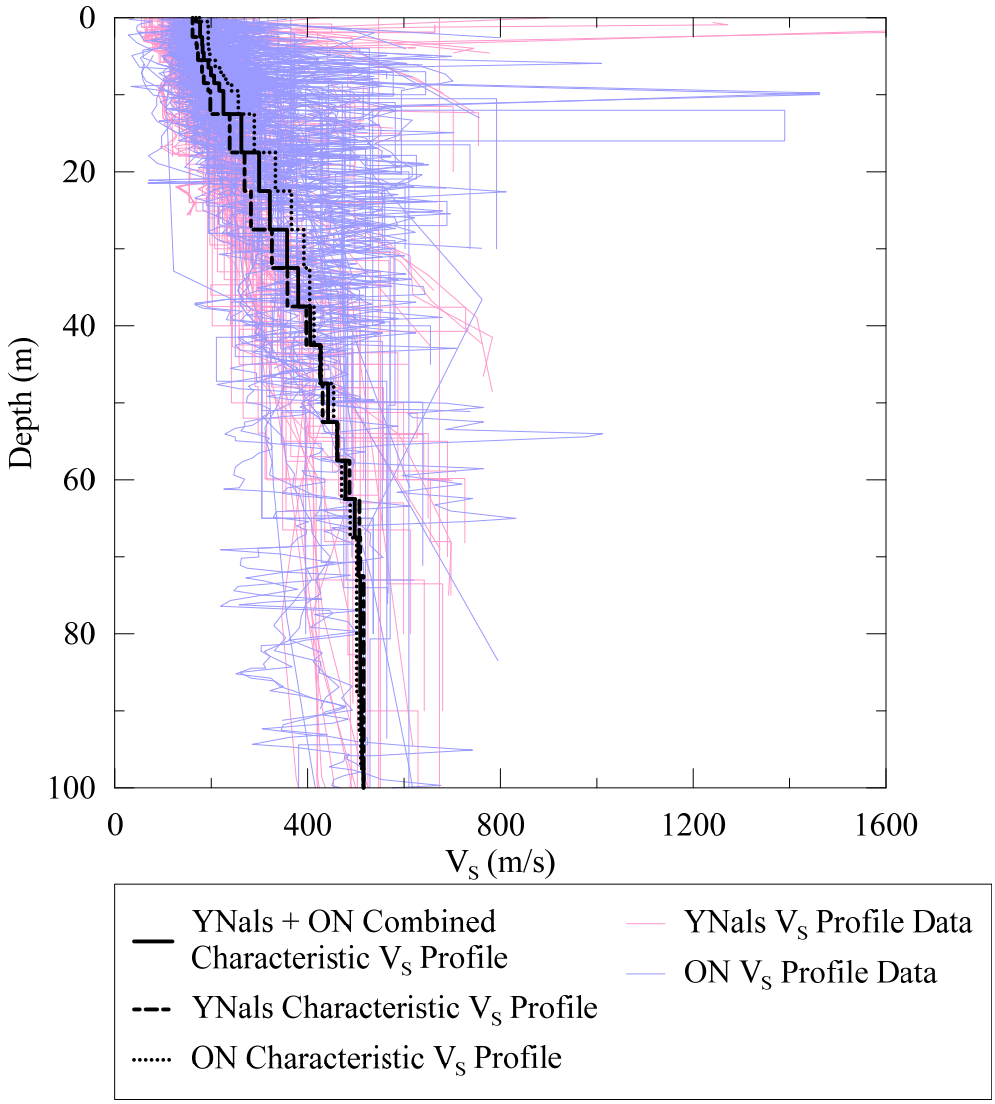

Figure 5.19: Combination of YNa-YNl-YNs smoothed log mean profile and ON profile for YNals+ON smoothed log mean Profile.

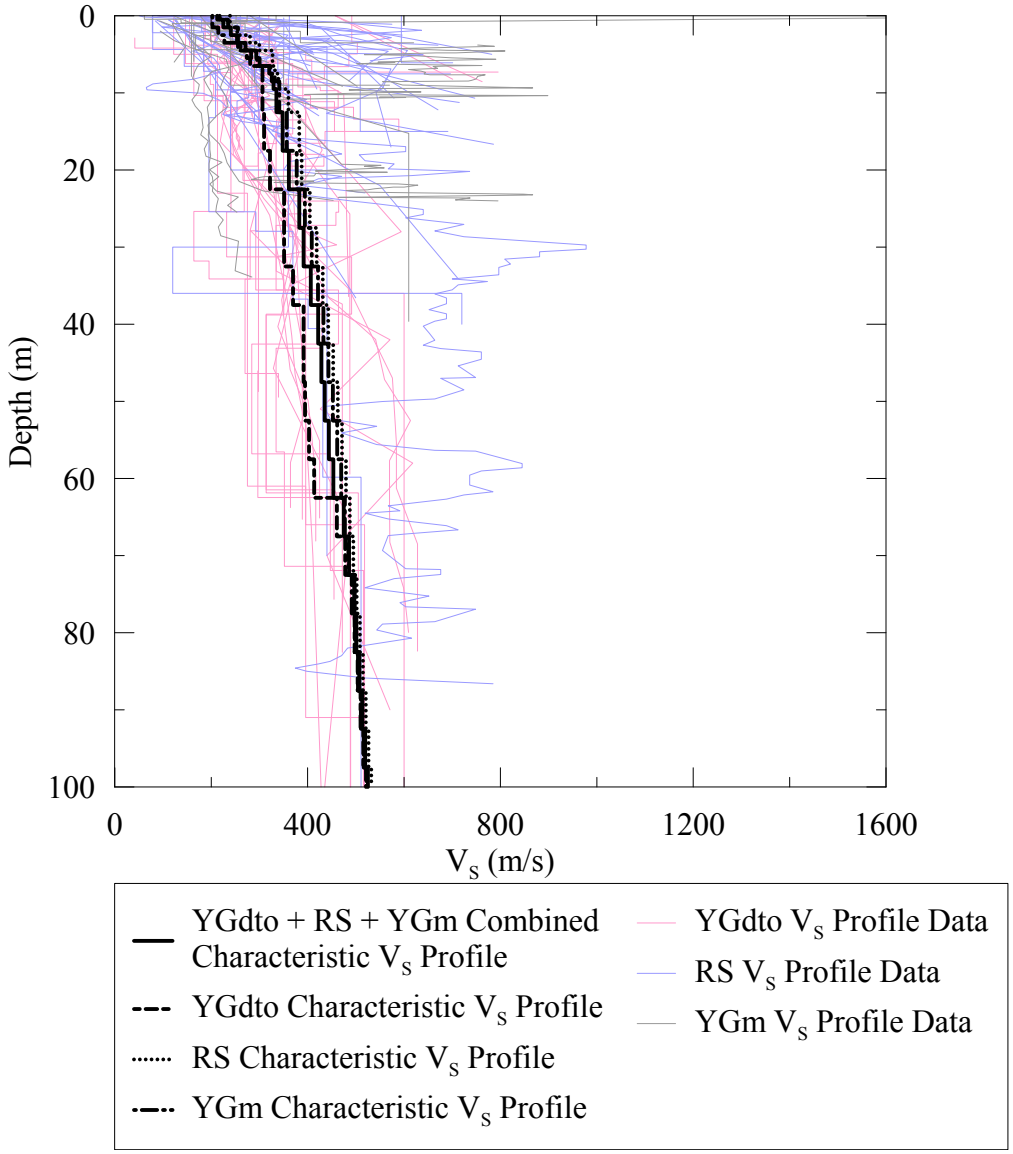

Figure 5.20: Combination of YGd-YGt-YGo, RS, and YGm smoothed log mean profiles to form YGdto+RS+YGm smoothed log mean profile.

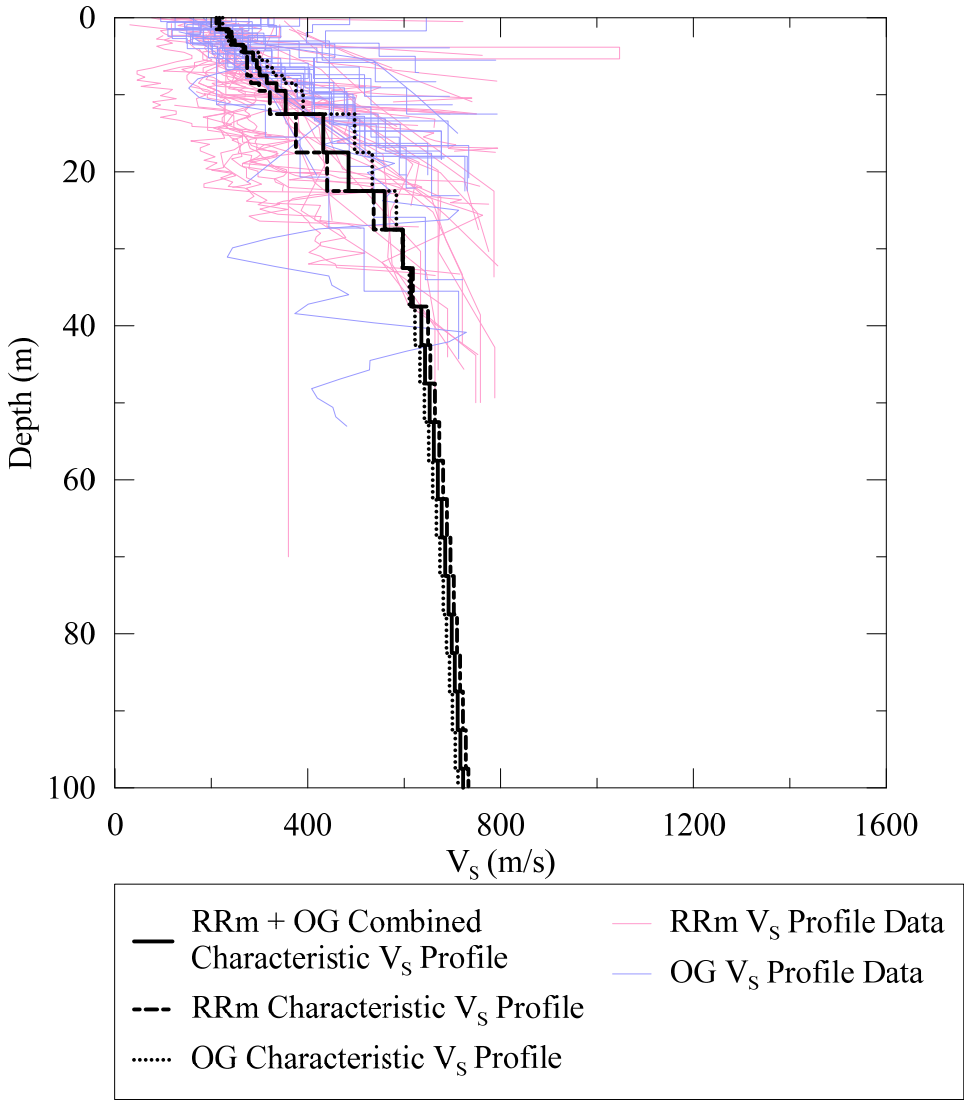

Figure 5.21: Combination of RRm and OG smoothed log mean profiles to form RRm+OG smoothed log mean profile.

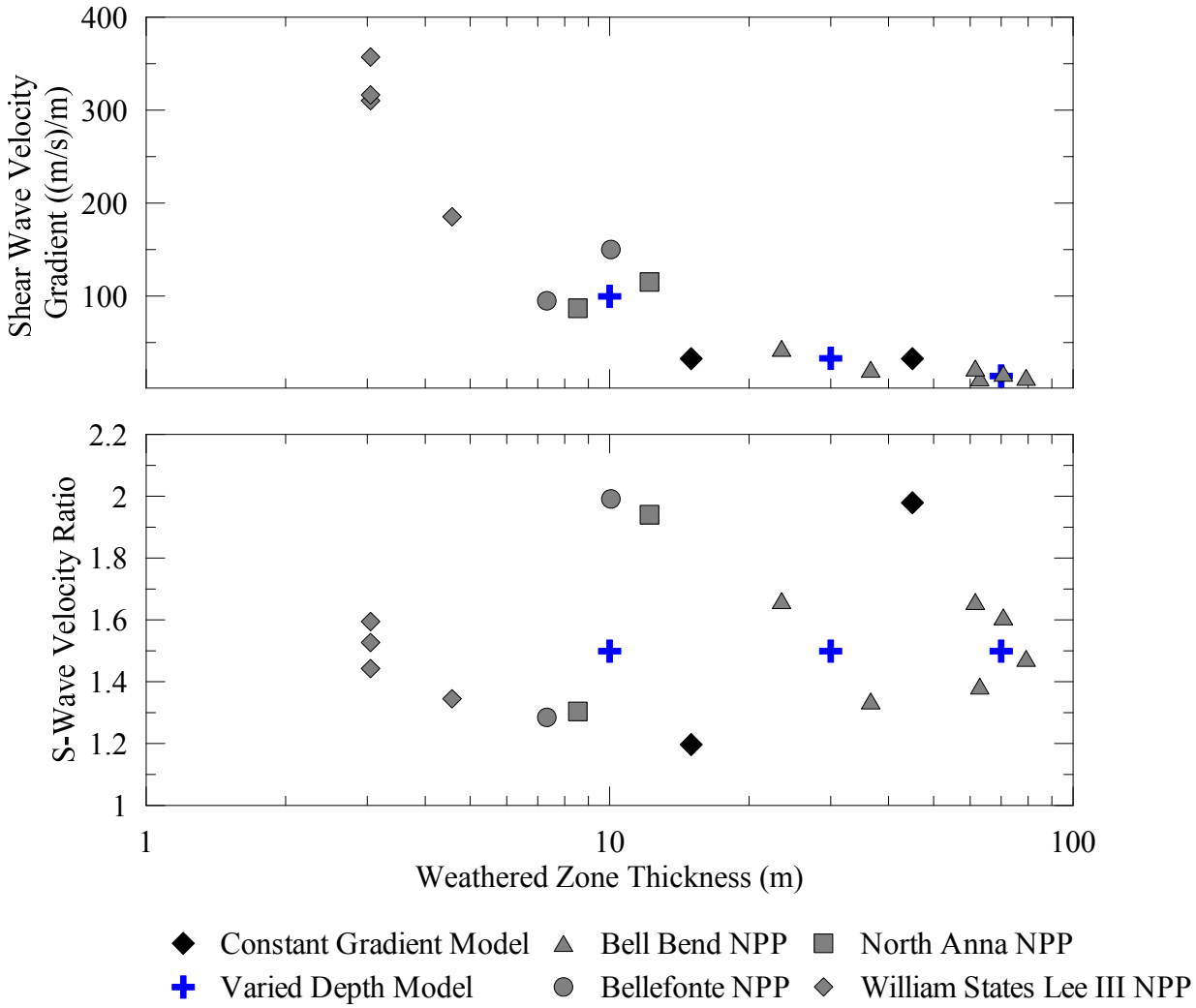

Figure 5.22: Weathered Rock Zone Properties (Data from Hashash et al. (2014b)). S-Wave Velocity Ratio describes the ratio between the V_S at the top of the weathered rock zone and the bottom at the reference condition.

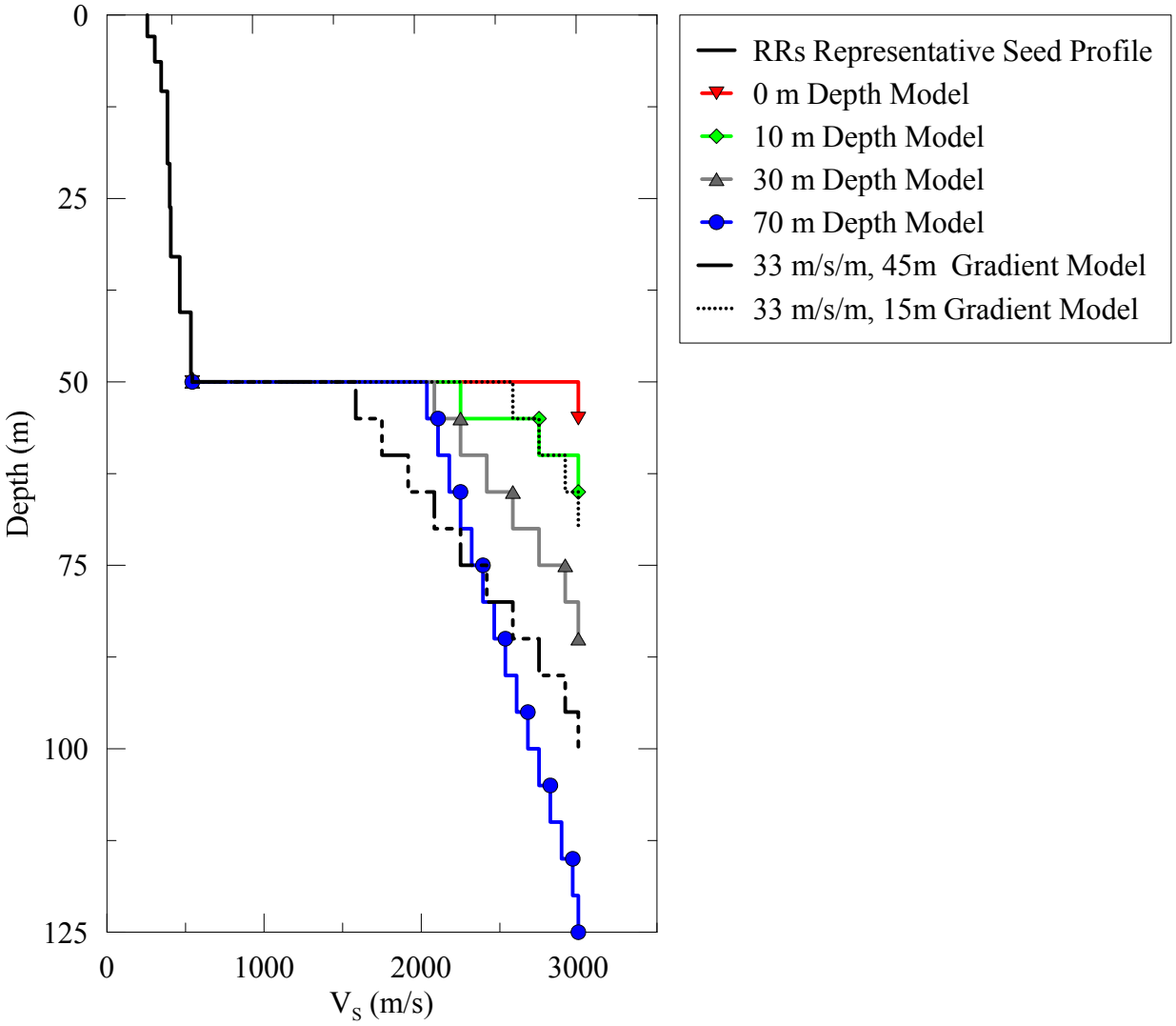

Figure 5.23: Weathered Rock Models applied to RRs representative seed profile at the 30 m depth bin.

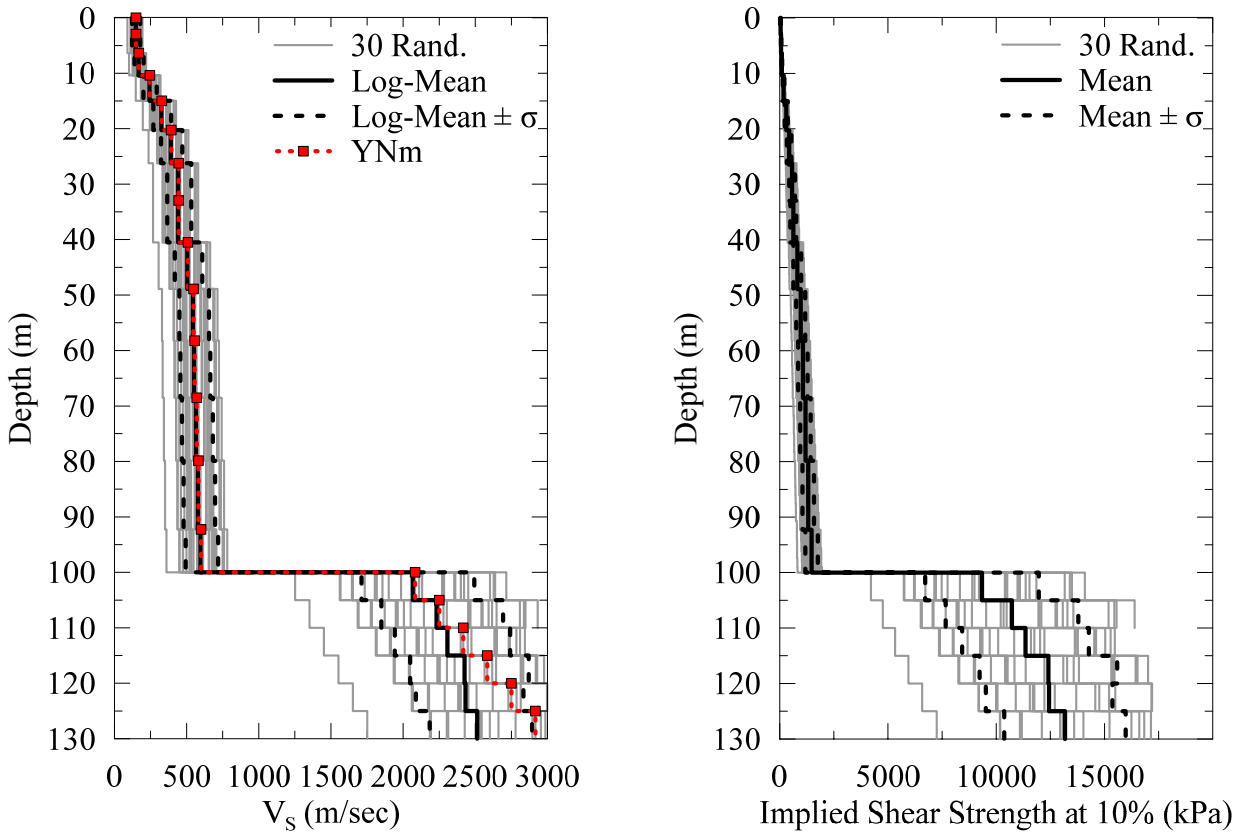

Figure 5.24: Realizations of the 100 m soil depth YNm representative seed V_S profile with 30 m thick weathered rock zone. Random V_S realizations with log-mean of randomly generated profiles and $\pm$ 1 log-standard deviation (a) and corresponding implied shear strength of randomized nonlinear curves with mean and $\pm$ 1 standard deviation (b).

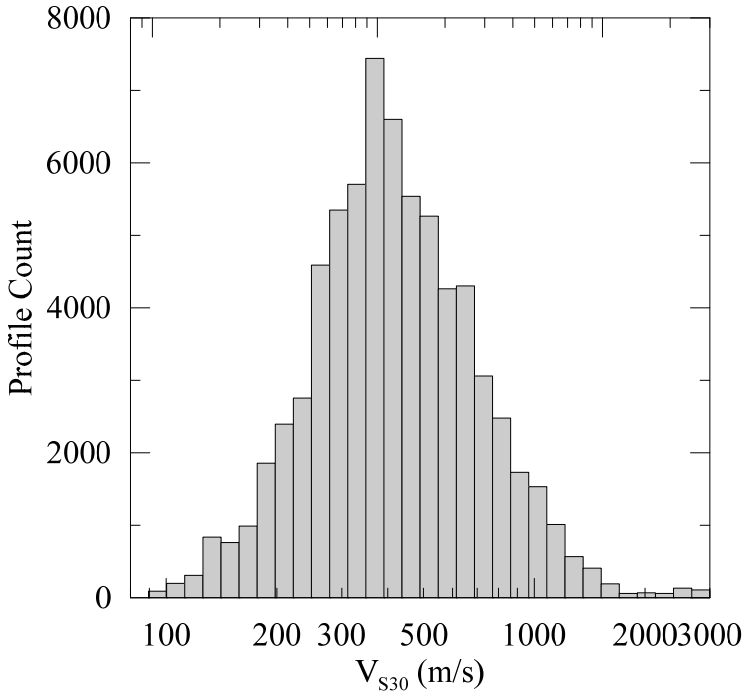

Figure 5.25: Distribution of V_{S30} of all randomized V_S profiles.

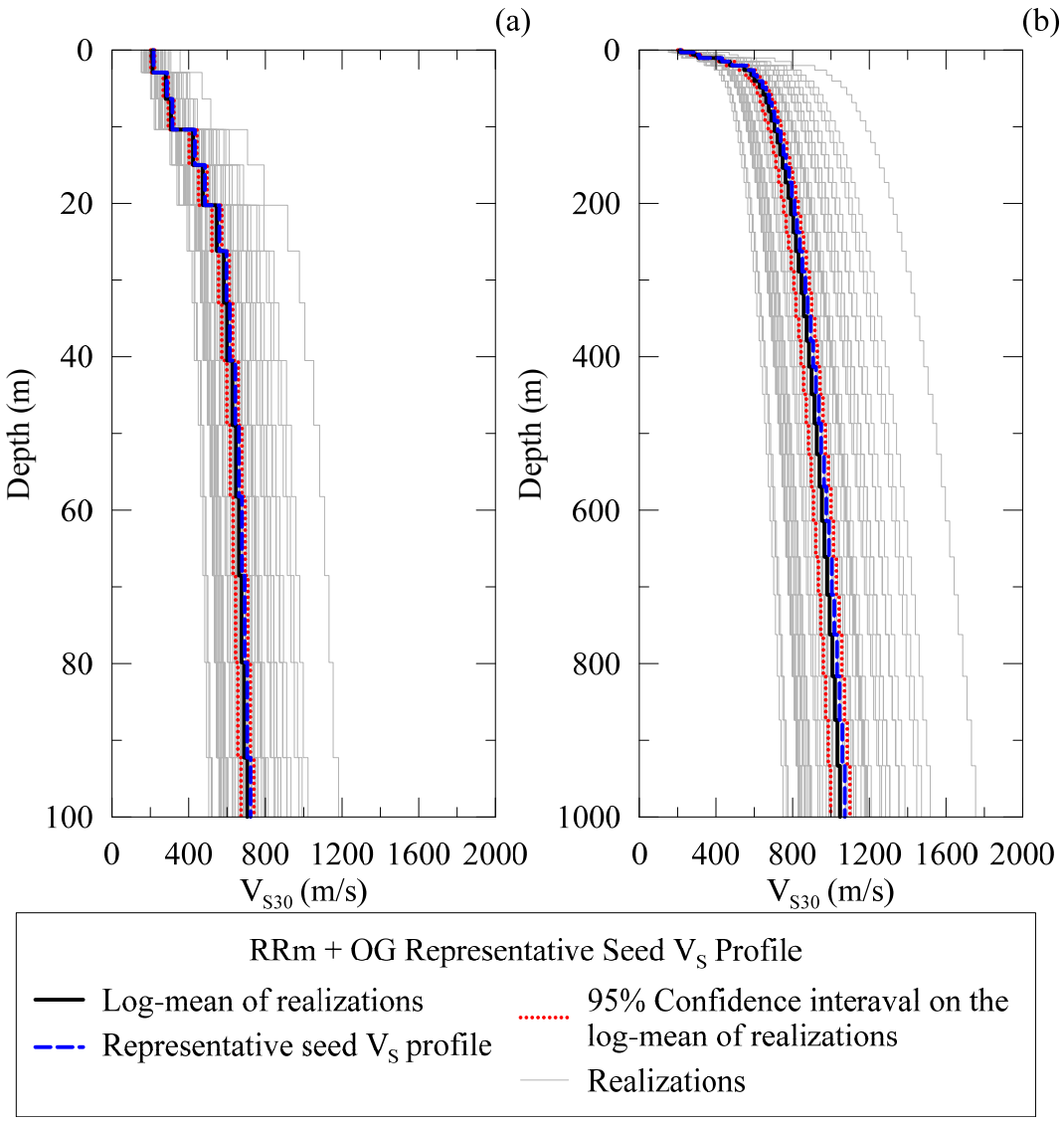

Figure 5.26: Realizations of the RRm+OG representative seed V_S profile with log mean and 95% confidence interval of the log mean of the realizations shown as a function of depth, and the RRm+OG representative seed V_S profile to a depth of 100 m (a), and 1000 m (b).

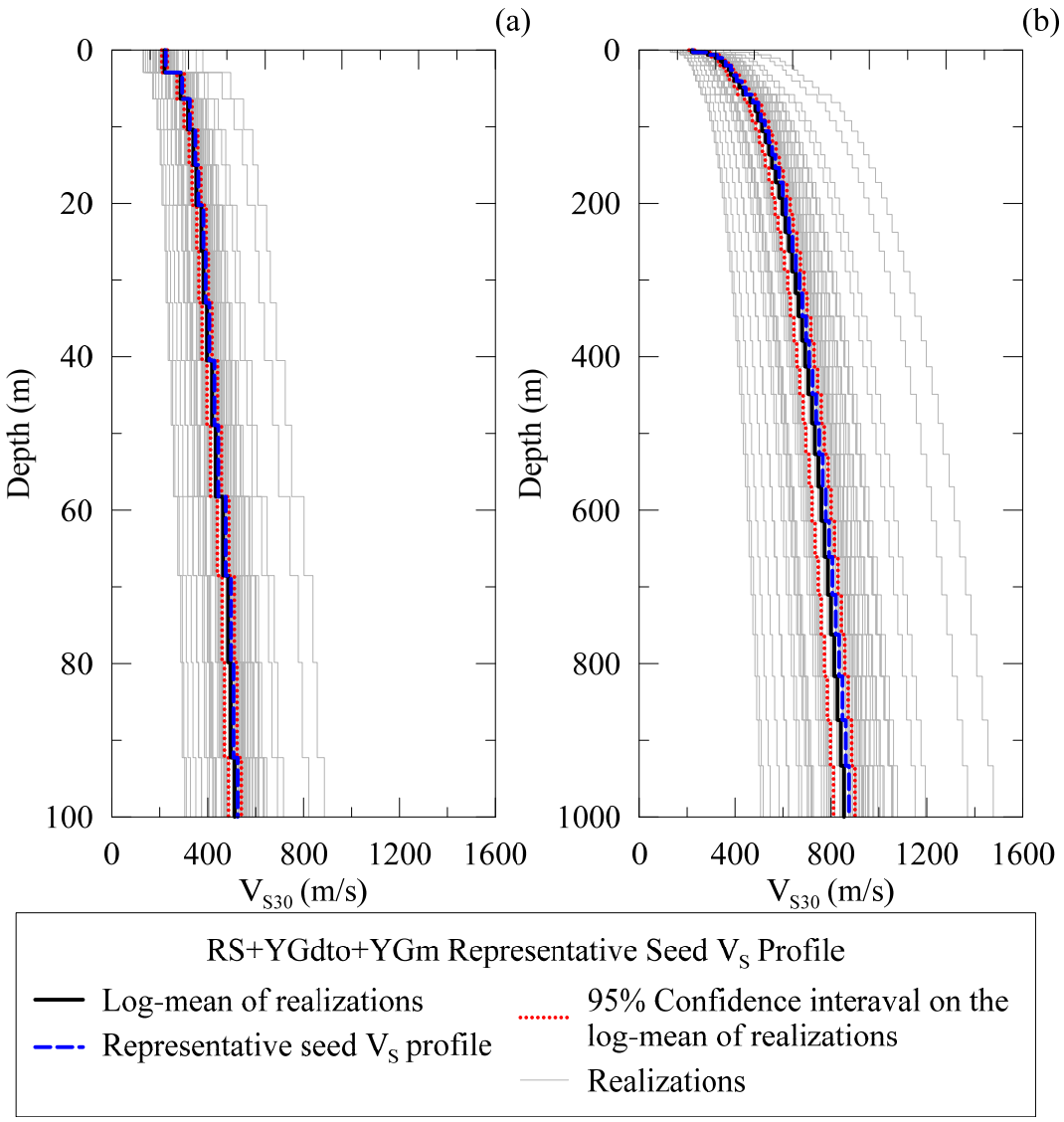

Figure 5.27: Realizations of the RS+YGdto+YGm representative seed V_S profile with log mean and 95% confidence interval of the log mean of the realizations shown as a function of depth, and the RS+YGdto+YGm representative seed V_S profile to a depth of 100 m (a), and 1000 m (b).

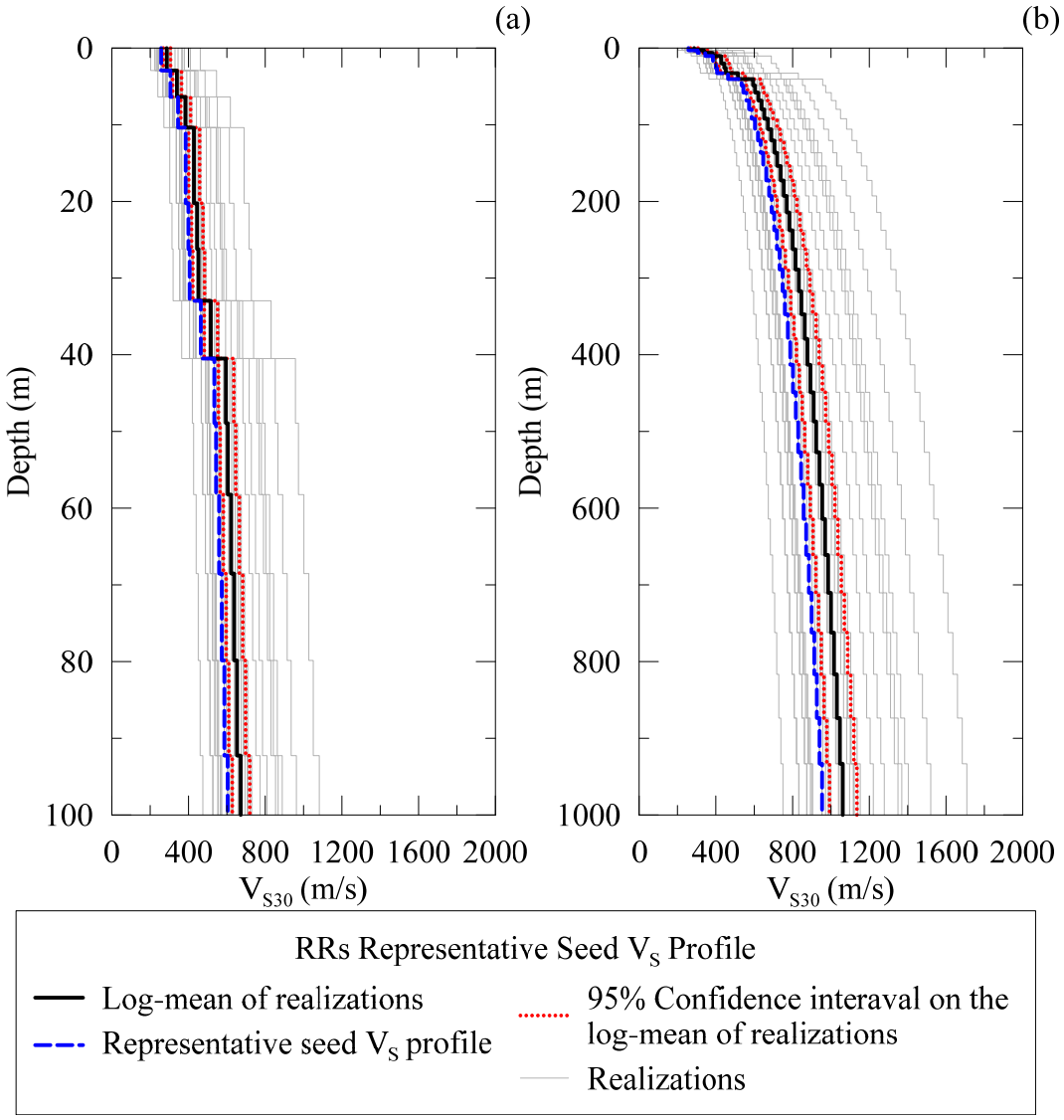

Figure 5.28: Realizations of the RRs representative seed V_S profile with log mean and 95% confidence interval of the log mean of the realizations shown as a function of depth, and the RRs representative seed V_S profile to a depth of 100 m (a), and 1000 m (b).

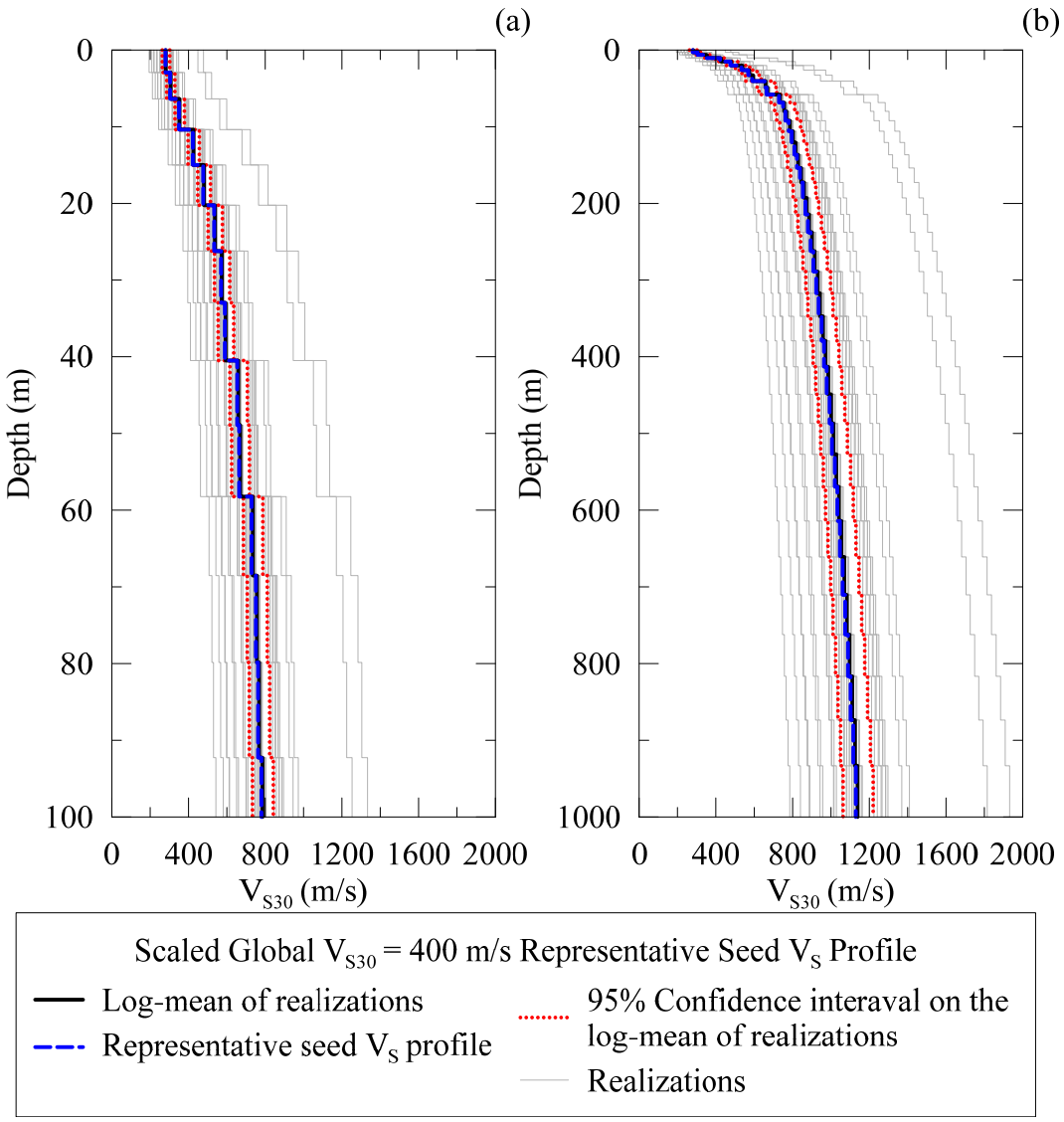

Figure 5.29: Realizations of the scaled global log-mean to V_{S30}=400 m/s representative seed V_S profile with log mean and 95% confidence interval of the log mean of the realizations shown as a function of depth, and the scaled global log-mean to V_{S30}=400 m/s representative seed V_S profile to a depth of 100 m (a), and 1000 m (b).

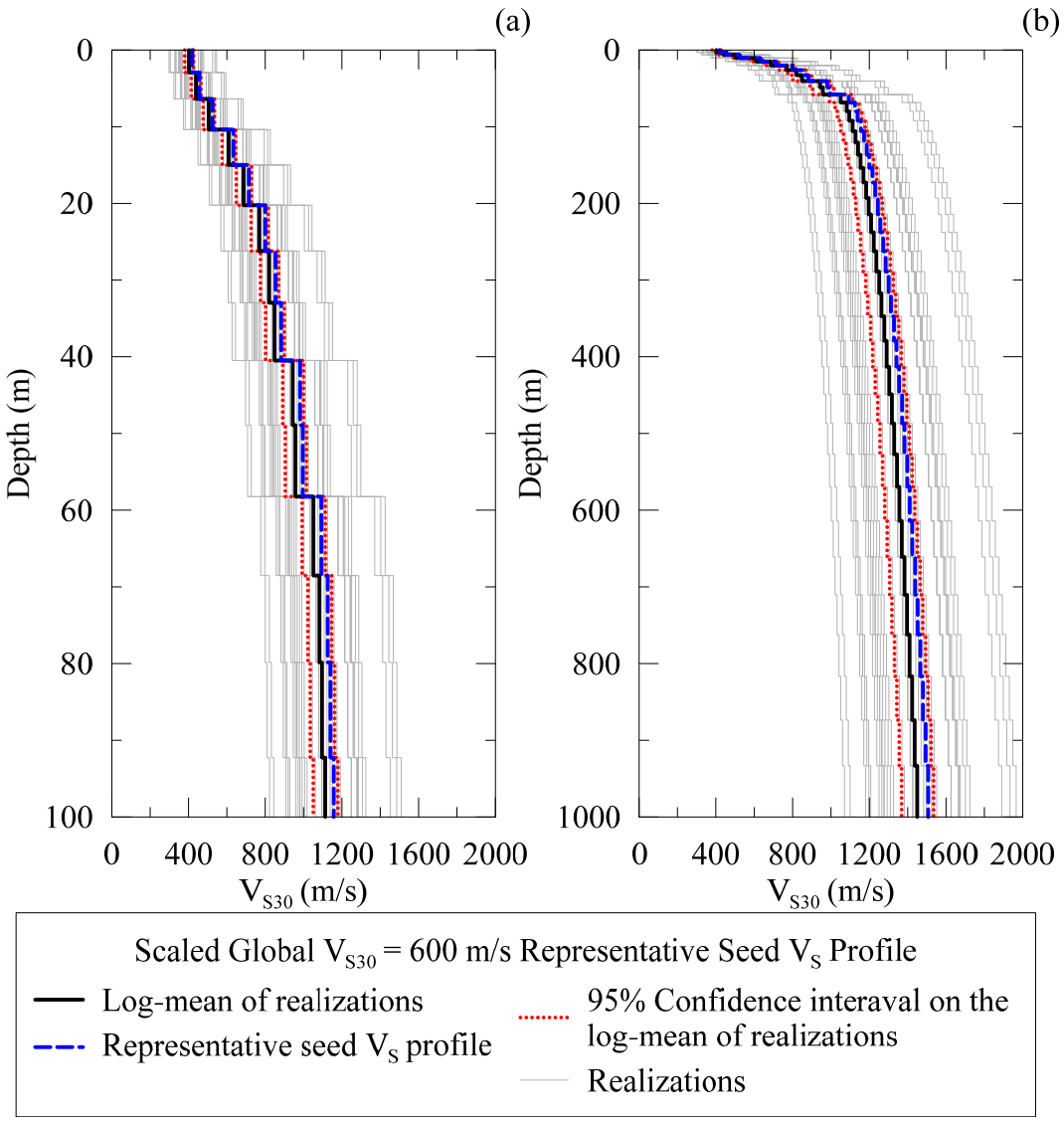

Figure 5.30: Realizations of the scaled global log-mean to V_{S30}=600 m/s representative seed V_S profile with log mean and 95% confidence interval of the log mean of the realizations shown as a function of depth, and the scaled global log-mean to V_{S30}=600 m/s representative seed V_S profile to a depth of 100 m (a), and 1000 m (b).

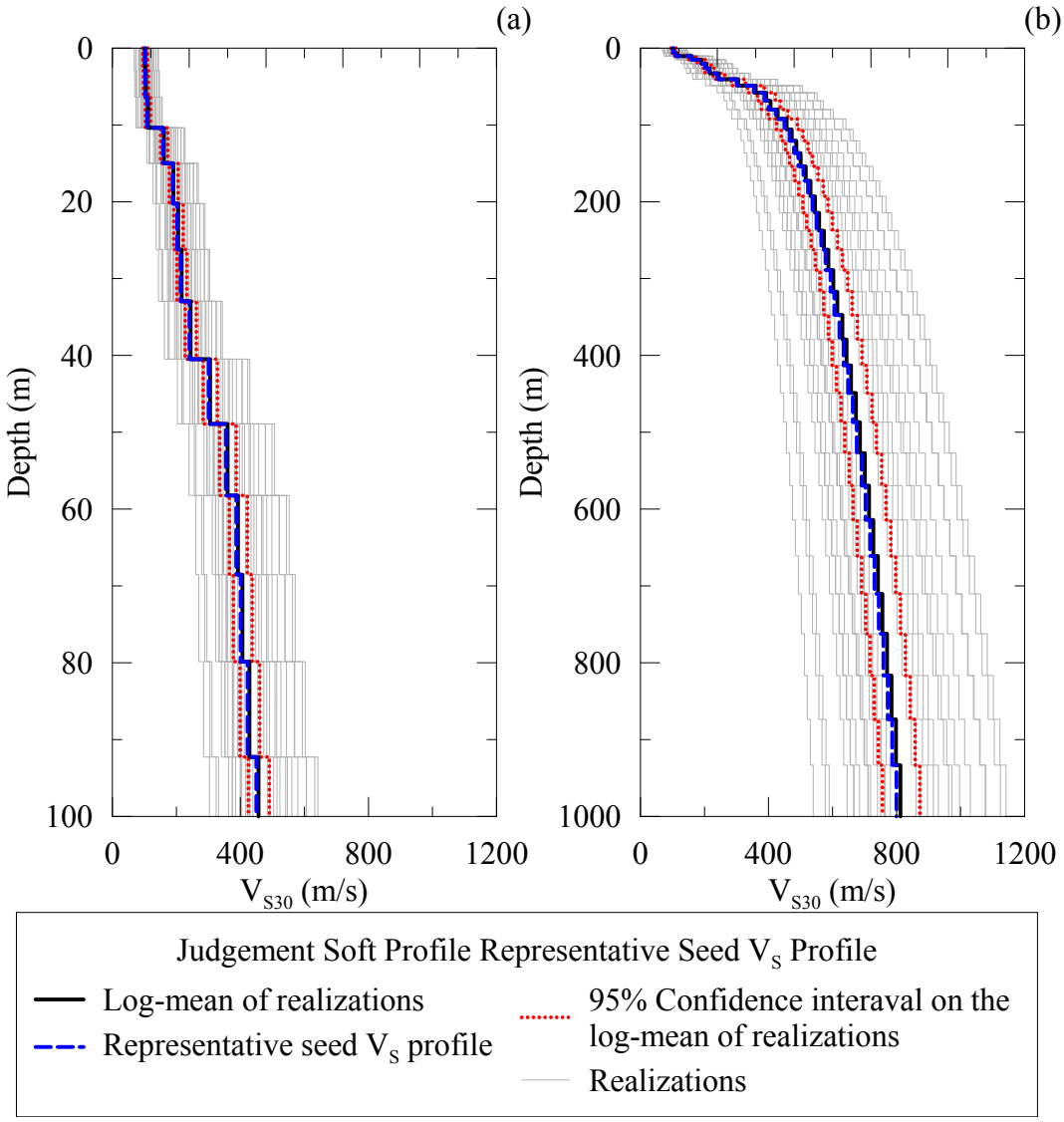

Figure 5.31: Realizations of the judgement soft representative seed V_S profile with log mean and 95% confidence interval of the log mean of the realizations shown as a function of depth, and the judgement soft representative seed V_S profile to a depth of 100 m (a), and 1000 m (b).

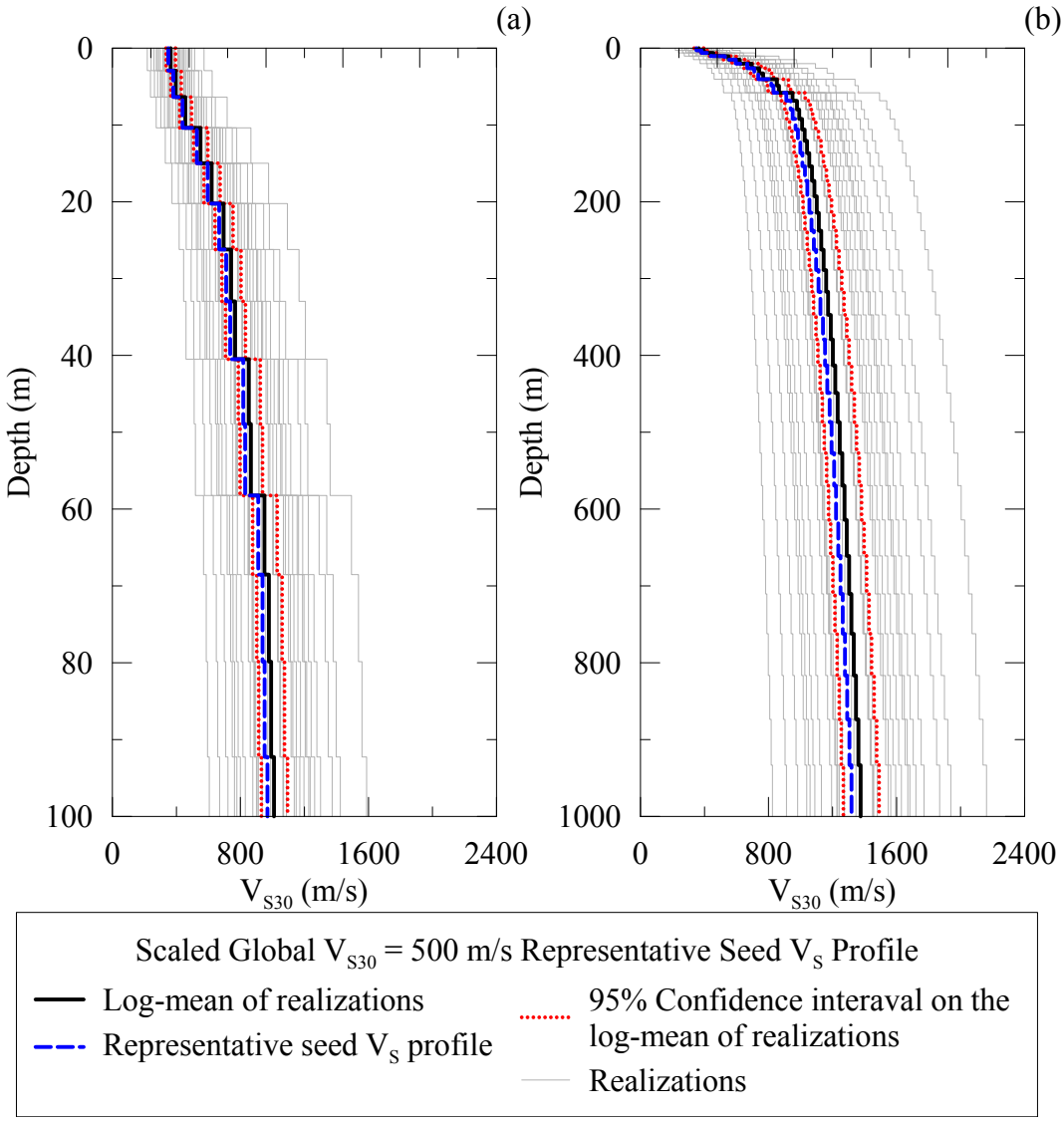

Figure 5.32: Realizations of the scaled global log-mean to V_{S30}=500 m/s representative seed V_S profile with log mean and 95% confidence interval of the log mean of the realizations shown as a function of depth, and the scaled global log-mean to V_{S30}=500 m/s representative seed V_S profile to a depth of 100 m (a), and 1000 m (b).

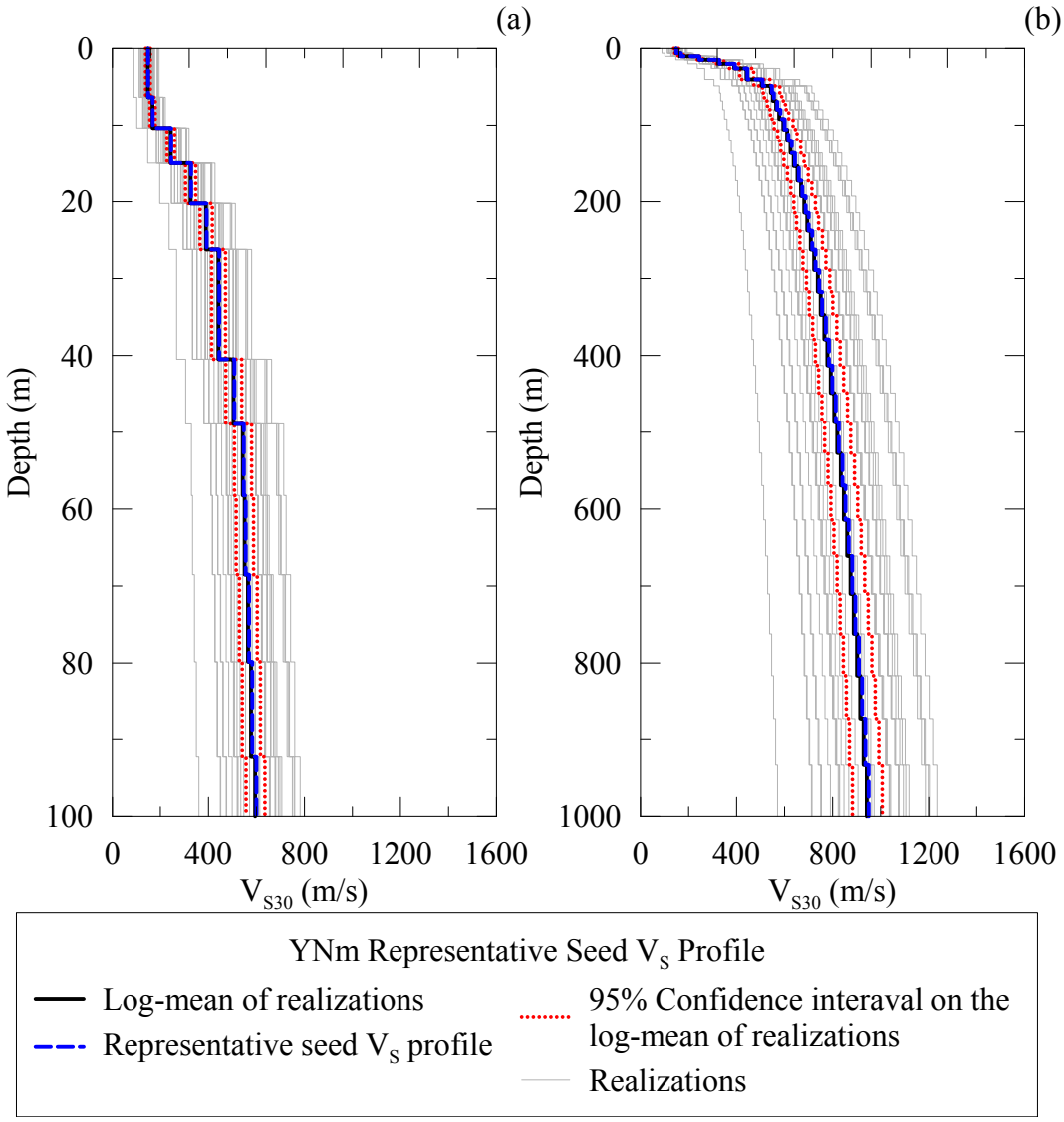

Figure 5.33: Realizations of the YNm representative seed V_S profile with log mean and 95% confidence interval of the log mean of the realizations shown as a function of depth, and the YNm representative seed V_S profile to a depth of 100 m (a), and 1000 m (b).

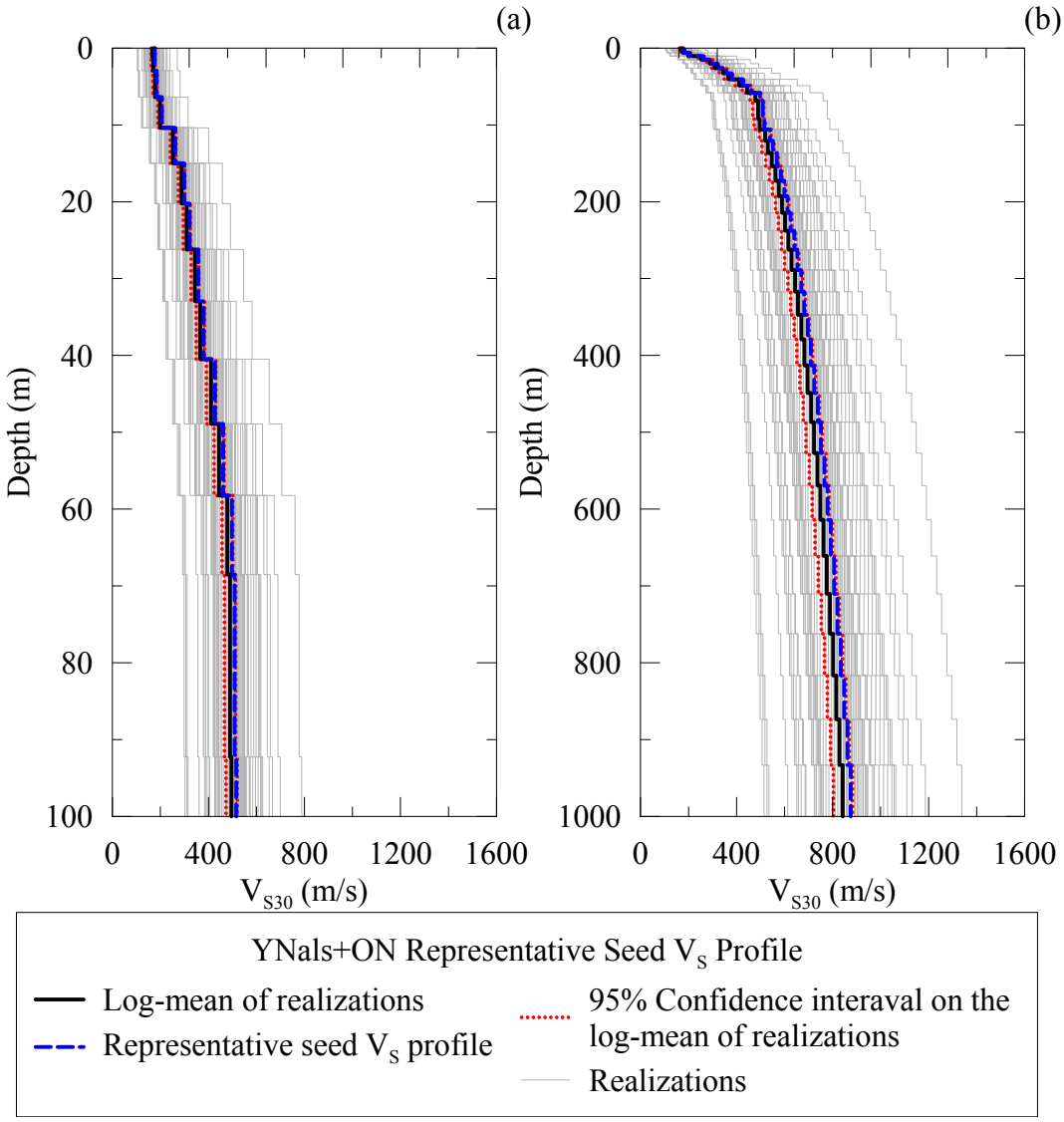

Figure 5.34: Realizations of the YNals+ON representative seed V_S profile with log mean and 95% confidence interval of the log mean of the realizations shown as a function of depth, and the YNals+ON representative seed V_S profile to a depth of 100 m (a), and 1000 m (b).

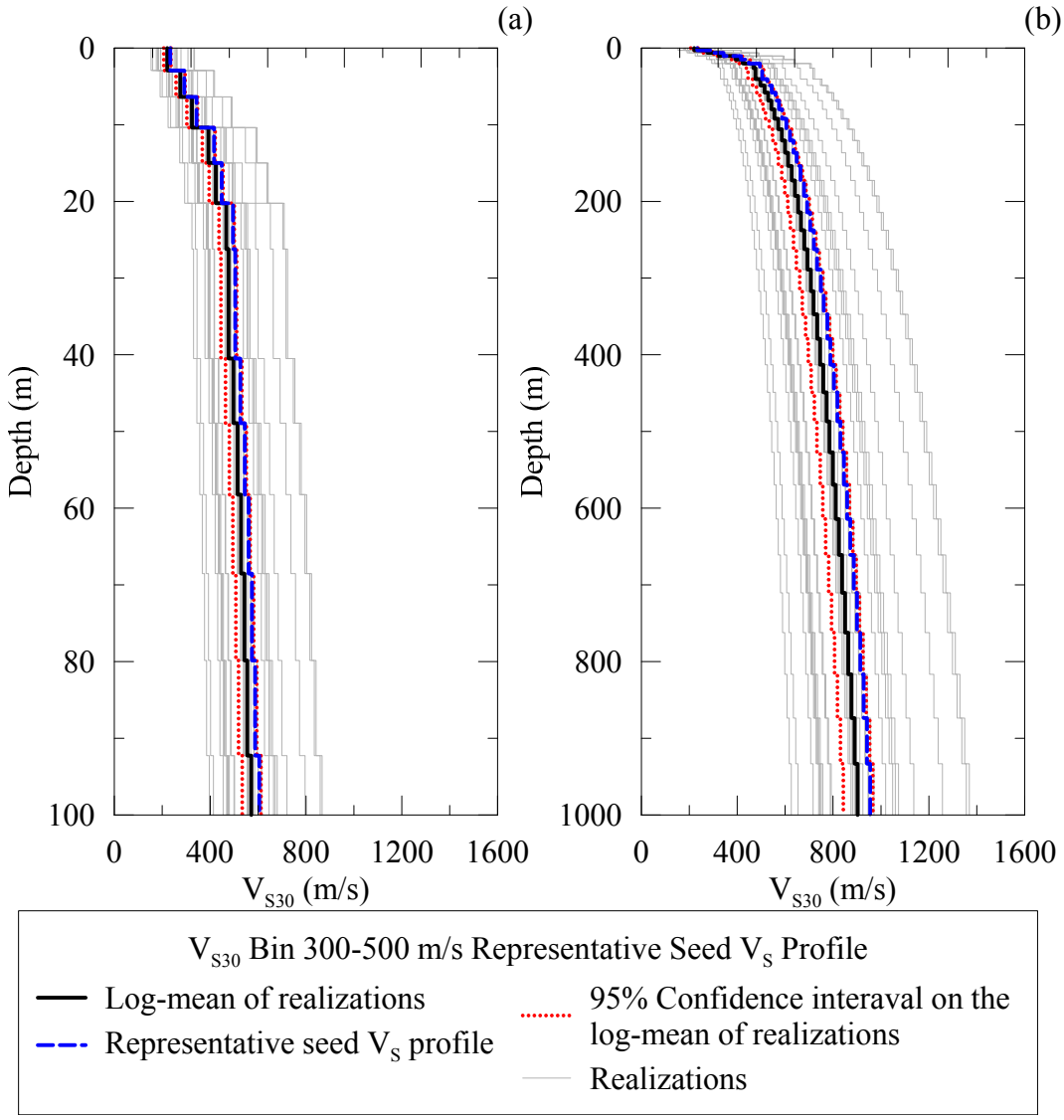

Figure 5.35: Realizations of the V_{S30} Bin = 300-500 m/s representative seed V_S profile with log mean and 95% confidence interval of the log mean of the realizations shown as a function of depth, and the V_{S30} Bin = 300-500 m/s representative seed V_S profile to a depth of 100 m (a), and 1000 m (b).

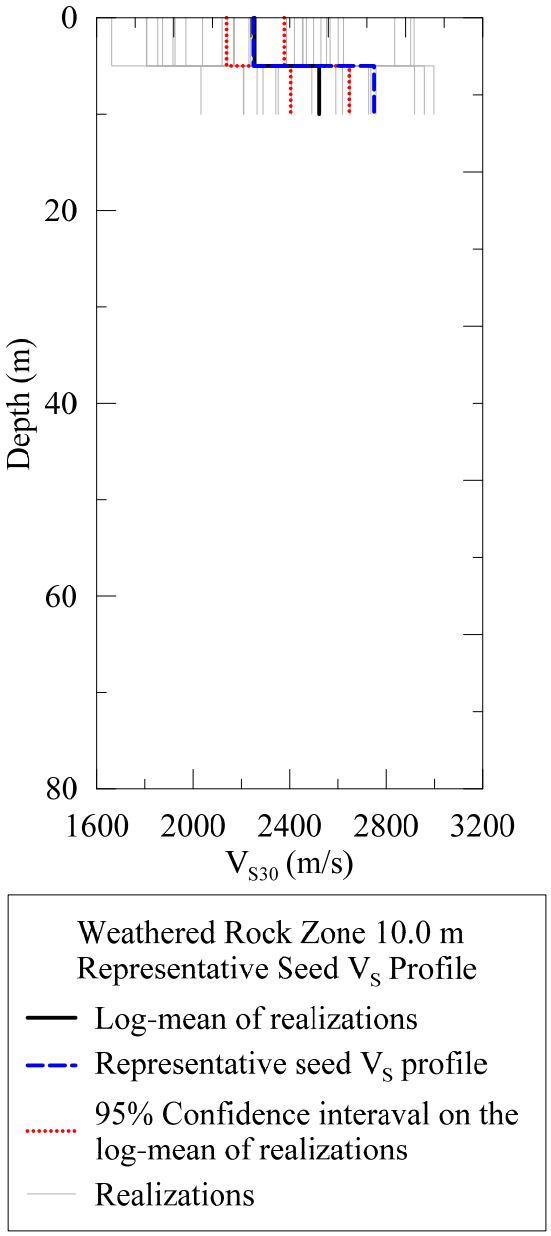

Figure 5.36: Realizations of the surface rock 10 m thick weathered rock zone with 0 m of soil profile with log mean and 95% confidence interval of the log mean of the realizations shown as a function of depth, and the 10 m thick weathered rock zone V_S model.

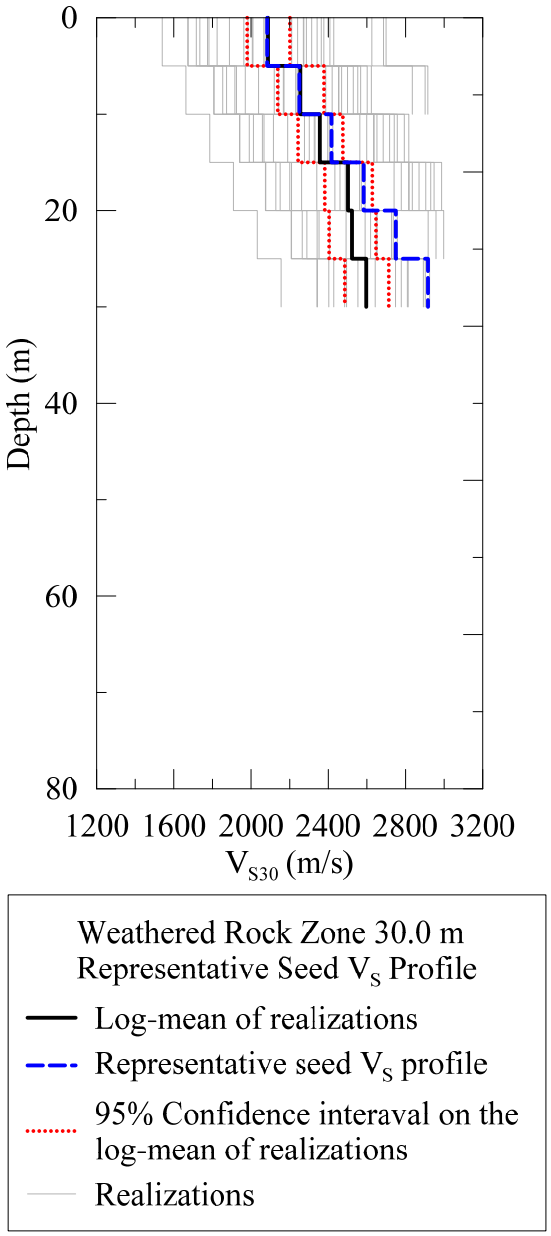

Figure 5.37: Realizations of the surface rock 30 m thick weathered rock zone with 0 m of soil profile with log mean and 95% confidence interval of the log mean of the realizations shown as a function of depth, and the 30 m thick weathered rock zone V_S model.

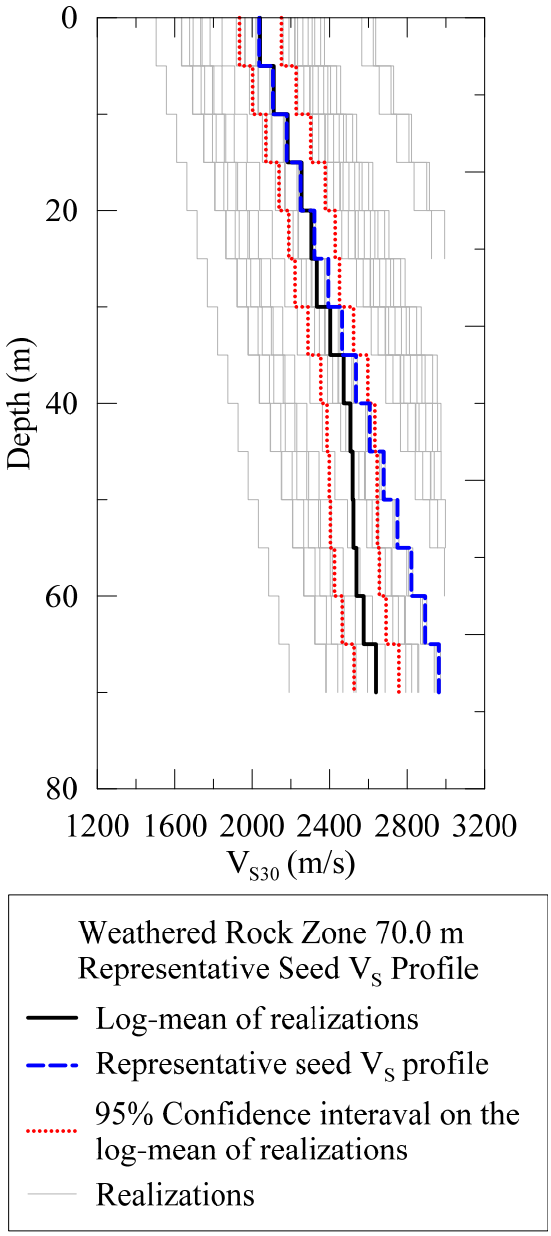

Figure 5.38: Realizations of the surface rock 70 m thick weathered rock zone with 0 m of soil profile with log mean and 95% confidence interval of the log mean of the realizations shown as a function of depth, and the 70 m thick weathered rock zone V_S model.

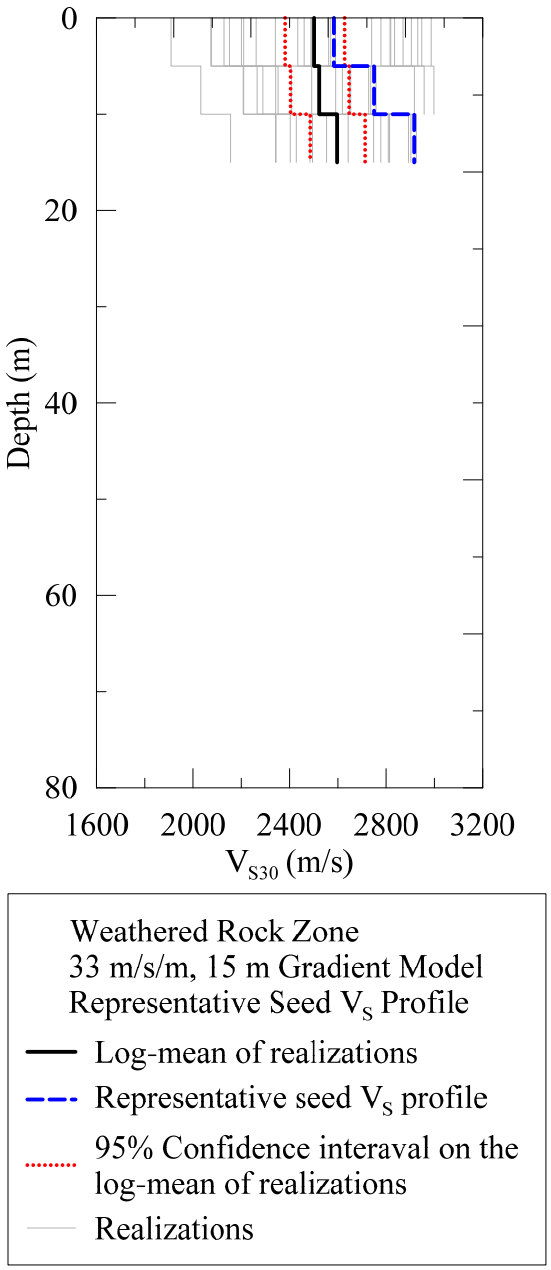

Figure 5.39: Realizations of the surface rock 15 m thick, 33m/s/m gradient weathered rock zone with 0 m of soil profile with log mean and 95% confidence interval of the log mean of the realizations shown as a function of depth, and the 15 m thick, 33m/s/m gradient weathered rock zone V_S model.

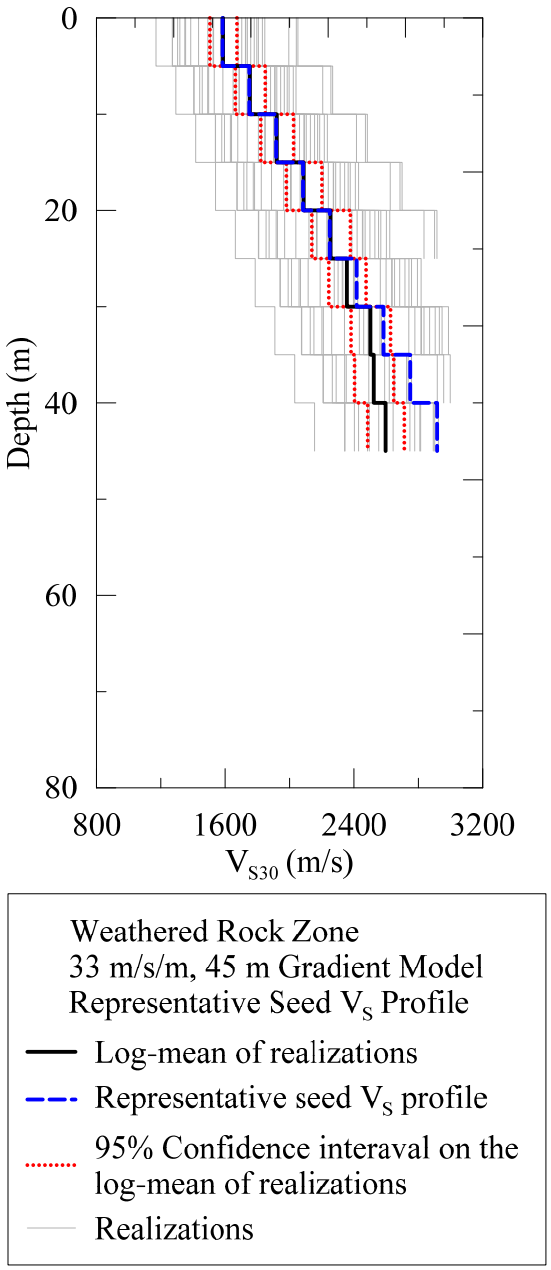

Figure 5.40: Realizations of the surface rock 45 m thick, 33m/s/m gradient weathered rock zone with 0 m of soil profile with log mean and 95% confidence interval of the log mean of the realizations shown as a function of depth, and the 45 m thick, 33m/s/m gradient weathered rock zone V_S model.

Chapter 6. Small Strain Damping Profiles

The work presented in this chapter was developed by E. Rathje and B. Xu of the University of Texas at Austin as a part of the collaboration with the NGA-East Geotechnical Working Group.

At high frequencies the shape of the Fourier amplitude spectrum of the S-wave acceleration can be characterized by exponential decay (Anderson and Hough 1984). Anderson and Hough (1984) introduced κ as a spectral decay factor to model this exponential decay, $e^{-\pi\kappa f}$. They also observed that κ increases with distance from the source (r), and proposed a linear relationship between κ and r, $\kappa(r) = \kappa_0 + \kappa_1 * r$. In this expression, κ_0 is the zero-distance κ, representing the attenuation of seismic waves within the geological structure beneath the site. The slope κ_1 represents the attenuation due to the horizontal propagation of seismic waves within the crust.

The value of κ_0 at the surface of a site can be computed from the shear wave velocity (V_s) profile and the anelastic attenuation factor (Q) profile using (Hough and Anderson 1988):

$$\kappa_0 = \int \frac{1}{Q(z) \cdot Vs(z)} \cdot dz \qquad \text{eq. 6.1}$$

The attenuation factor, Q, can be related to the small-strain damping ratio, D_{min}, which is more commonly used in engineering to represent energy dissipation. This relationship is $Q=1/(2D_{min})$. When considering the contribution to κ_0 from the soil layers overlying a rock half space, eq. 6.1 can be modified to:

$$\kappa_0 = \kappa_{0,rock} + \int \frac{2 \cdot D_{min}(z)}{Vs(z)} \cdot dz \qquad \text{eq. 6.2}$$

Thus, given the velocity profile and damping profile at a soil site and estimate of κ_0 for the underlying rock half space ($\kappa_{0,rock}$) the high frequency decay of Fourier amplitude spectrum, as modeled through the parameter κ_0 , can be computed from eq. 6.2. In CENA, an investigation by Hashash et al.(2014a) on the reference rock condition of CENA found that the expected $\kappa_{0,rock}$ is 0.006 s.

In this study, the damping profiles used in site response are constrained by κ. Values of κ_0 values are computed for the 10 representative seed shear wave velocity profiles for different D_{min} approaches. These κ_0 values are compared with κ_0 values in literature and those measured from earthquake recordings at soil sites.

6.1 Kappa$_0$ Values of Site Response Models

Ten representative seed shear wave velocity models were developed as part of this study using a shear wave velocity database for the CENA (5.2). These shear wave velocity profiles represent different geologic conditions and are shown in Figure 5.1. Each of the representative seed profiles is underlain with a hard-rock half space of Vs = 3,000 m/s. Analyses of resulting surface frequency content were performed with these profiles extending to 1,000 m, and also truncated at depths of 10 m, 30 m, 50 m, 100 m, and 500 m. Properties of each of the representative seed profiles to be used in this investigation are listed in Table 6.1 for V_{S30}, plasticity index (PI), unit weight, and over-consolidation ratio (OCR).

Different options are available to model the profile of D_{min} for use in equation (2) to compute κ_0. From a seismological perspective, Campbell (2009) developed four models that relate Q to Vs, with the different models capturing the significant uncertainty in the data. Figure 6.1a shows plots of the four Q-Vs relationships. Model 1 is a linear relationship between Q and Vs across all Vs ($Q = 7.17 + 0.0276V_s$). Model 2 is the same as Model 1 except that Q is constrained to 50 when V_s > 800 m/s. Model 3 assigns Q=10 when $Vs \leq 366\ m/s$,, and $Q = 0.00382\ {V_s}^{1.333}$ when $Vs > 366\ m/s$. Model 4 is the same as Model 3, except that it constrains Q = 50 when V_s > 800 m/s, similar to Model 2. Figure 6.1b shows the corresponding D_{min} vs. Vs relationships. The damping values generally are between 1% and 2% for Vs greater than 800 m/s, and increase to values above 3% for Vs less than about 500 m/s. For this study we used Model 1 to represent the Q-Vs relationship. Models 2 and 4 were not used because they include an instantaneous increase in Q at Vs = 800 m/s, and Model 3 was not used because of the very large damping values predicted for Vs between 100 and 500 m/s.

From a geotechnical perspective, Darendeli (2001) developed a D_{min} model based on measured values from laboratory testing of soil samples obtained from geotechnical sites. This model

predicts D_{min} as a function of PI, OCR, and mean effective stress (σ'_o) using $D_{min} = (0.8 + 0.0129 * PI * OCR^{-0.1}) * {\sigma'_o}^{-0.29}$. This model generally predicts D_{min} values between 0.3% and 2%, with the values decreasing with increasing depth. These values tend to be smaller than those predicted by the Campbell (2009) models. The Darendeli (2001) model predicts smaller damping because it is based on laboratory measurements of damping, which only capture material damping and not the attenuation caused by wave scattering in the field.

Using the 10 representative seed Vs profiles, corresponding D_{min} profiles were developed using the Campbell (2009) Q-Vs Model 1 (Figure 6.2a). Using the geotechnical parameters in Table 1 and the mean effective stress computed from an assumed ground water table of 0 m and K_0= 0.5, D_{min} profiles were developed using the Darendeli (2001) model (Figure 6.2b). The D_{min} profiles developed from Campbell (2009) vary noticeably between the sites because the damping model is proportional to Vs, which varies considerably from site to site. The D_{min} profiles developed from Darendeli (2001) do not vary considerably between sites because the geotechnical parameters (Table 6.1) do not vary significantly from site to site.

As noted earlier, site response analyses are performed with the 10 representative seed profiles truncated at different depths between 10 m and 1000 m. The Vs profiles and D_{min} profiles truncated at different depths are used with eq. 6.1 to compute k_0. For these analyses $\kappa_{0,rock}$ is taken as 0.006 s, which is consistent with the value for CENA hard rock recommended by the NGA-East Geotechnical Working Group (Hashash et al. 2014). Figure 6.3 shows the computed k_0 values as a function of soil depth for the Campbell (2009) and Darendeli (2001) damping profiles. For both damping models, k_0 increases with soil depth due to the increase in the travel path over which the damping acts. However, the k_0 values derived from the Campbell (2009) damping model are significantly larger and vary more considerably among the sites than the values derived from the Darendeli (2001) model. This effect is a direct result of the differences in the D_{min} profiles shown in Figure 6.2.

6.2 Comparisons of kappa$_0$ Values of Site Response Models and kappa$_0$ Values from Other Sources

To evaluate the two damping models within the context of κ_0, the computed values in Figure 6.3 are compared with values published in the literature and those computed directly from ground motion recording computed as part of this project.

Campbell (2009) developed a linear relationship between κ_0 and the depth of sediments (H_{sed}) for selected site profiles in CENA:

$$\kappa_0(\mathrm{s}) = 0.005 + 6.05\mathrm{x}10^{-5} * H_{sed}(m) \qquad \text{eq. 6.3}$$

The κ_0 values from eq. 6.3 are compared with those computed for the 10 representative seed profiles for the different damping models in Figure 6.3. The κ_0 values derived from the Campbell (2009) damping model (Figure 6.3a) agree well with the range from eq. 6.3, although the scatter is large and at larger depths the κ_0 values of the models are mostly smaller than those predicted by eq. 6.3. It should be noted that some of the favorable agreement is due to the fact that eq. 6.3 was derived as part of the same study that recommended the Q-Vs relationship (i.e., Campbell (2009)). The κ_0 values derived from the Darendeli (2001) damping model (Figure 6.3b) agree well with eq. 6.3 at depths less than 100 m, but these values are significantly smaller than those predicted by eq. 6.3 at larger depths. This result is due to the small depth dependence in κ_0 that is produced by the Darendeli (2001) D_{min} model. Based on the results in Figure 6.3, the damping model derived from Q-Vs Model 1 of Campbell (2009) is considered most appropriate for the analyses in this study.

Table 6.1. General properties of the representative seed V_S profiles.

Sites	V_{S30} (m/s)	PI	Unit Weight (kN/m^3)	OCR
Soft	148	15	19	1.5
Ynals+ON	252	20	18.5	1.3
Ynm	240	15	19	1.5
Bin 300-500	383	15	19	1.5
RRrm+OG	391	10	19	3
RRs	356	24	19.4	3
RS+YGdto+Ygm	333	15	18.9	1.3
Scaled 400	411	15	19	1.5
Scaled 500	513	15	19	1.5
Scaled 600	616	15	19	1.5

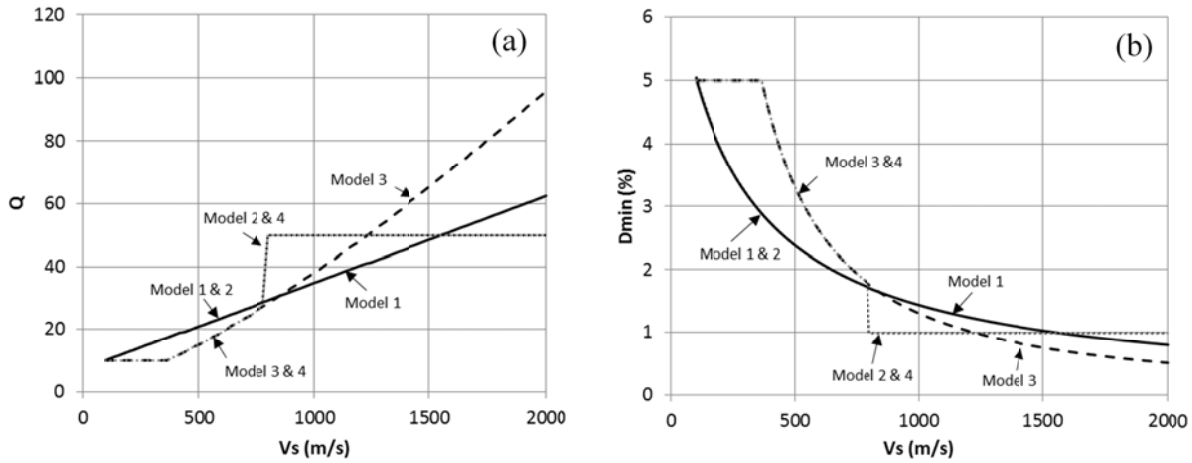

Figure 6.1. Attenuation (Q) models from Campbell (2009) in terms of (a) Q vs. V_s; (b) D_{min} vs. V_s.

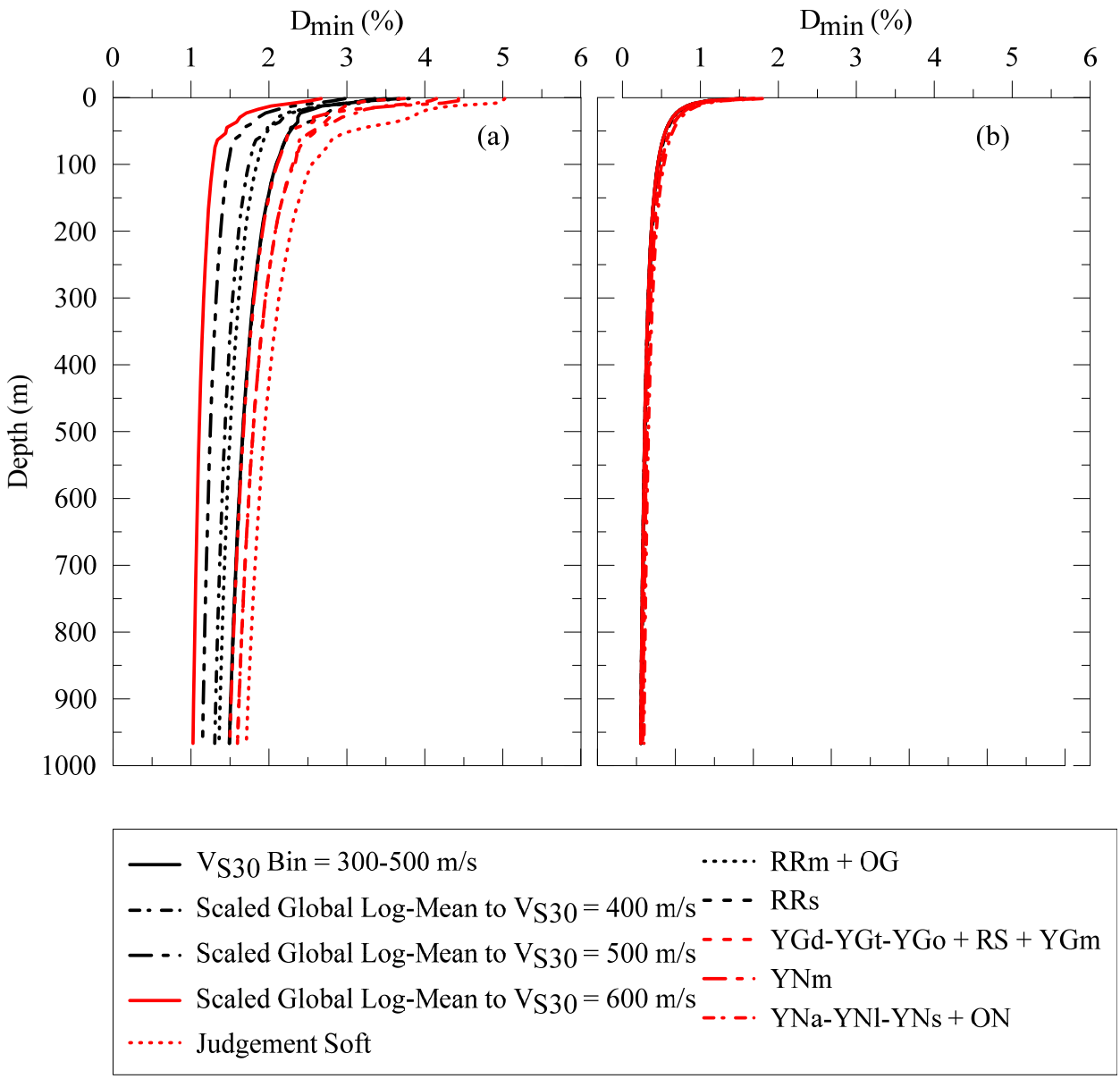

Figure 6.2. D_{min} vs. Depth from (a) Campbell (2009) Q − V_s Model 1; (b) Darendeli (2001) D_{min} model.

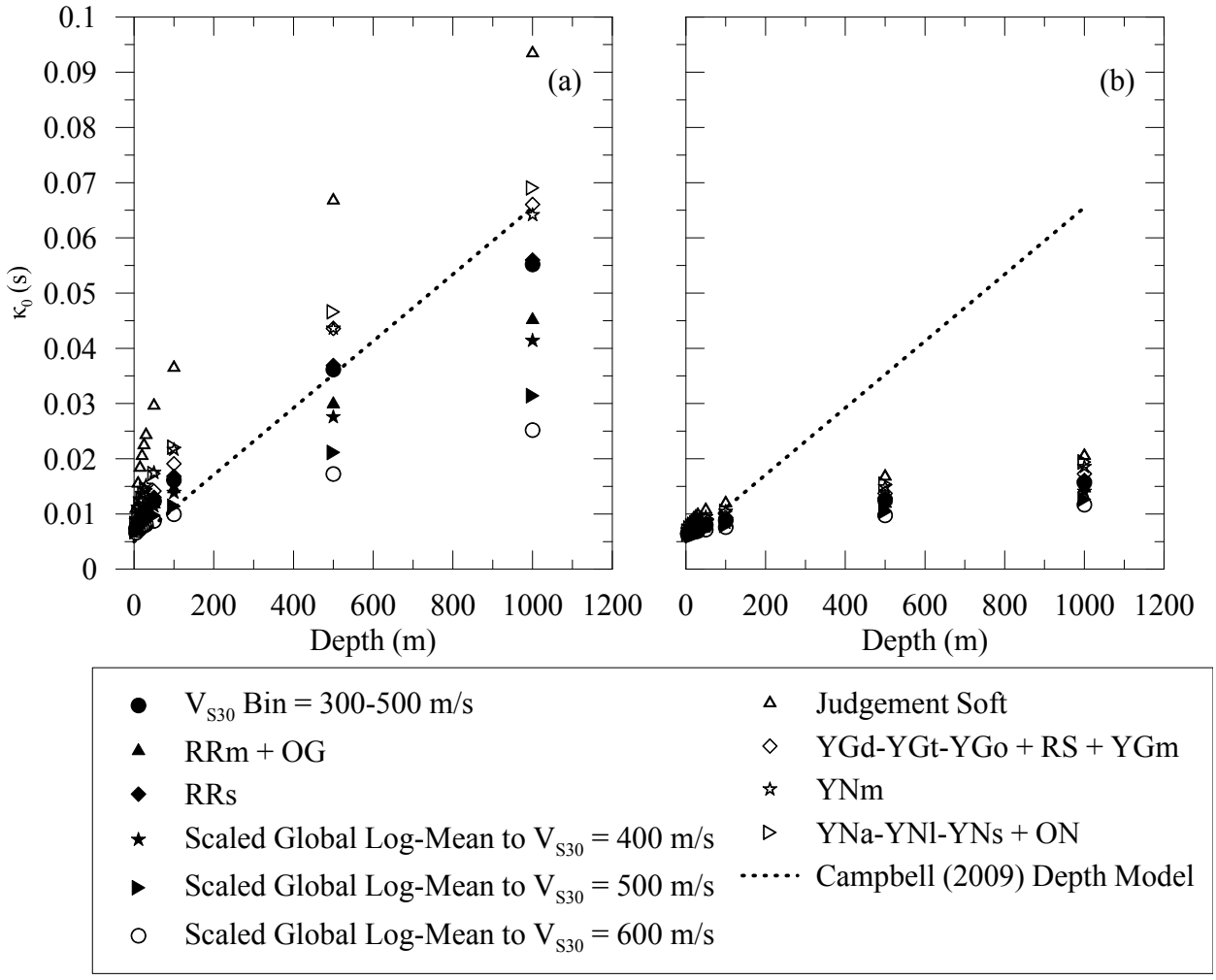

Figure 6.3. Comparison of Campbell (2009) κ_0 – depth model with κ_0 values for 10 baseline Vs models and damping from (a) Campbell (2009) Q-Vs Model 1 and (b) Darendeli (2009) D_{min} model.

Chapter 7. Nonlinear Soil and Weathered Rock Behavior

7.1 Introduction

Modulus reduction (G/G_{max}) and damping curves as a function of strain greatly affect calculated site amplification. Therefore, it is important that the modulus reduction and damping curves used as inputs for the site response analyses in this study reflect the range of site conditions and nonlinear behaviors in CENA, and that the constitutive soil model used in analysis be able to produce realistic soil behavior.

Constitutive models for use in 1-D seismic site response analyses must accurately capture initial shear modulus at small strains, shear strength of soil at large strains, and have flexible control of nonlinear soil at intermediate strains. Commonly used soil models either do not capture both large- and small-strain soil behavior or are not usable in site response analyses. Failure to capture either the large or small strain behavior of soil can lead to both under- and over- estimation of site amplification. The GQ/H model proposed by Groholski et al. (2016) is a model derived from the bivariate quadratic equation to both accurately capture initial soil stiffness and large-strain shear soil strength behavior.

Current site response analysis calculations involve solving equations of motion and require shear strain-controlled soil models, commonly known as Kondner and Zelasko (1963) derived models after the original formulation. Modifications to the Kondner and Zelasko derived models over time have typically included improvements in capturing small-strain shear behavior (such as in the model of Matasovic (1993), the MKZ model) or have included terms to capture additional effects on the shear strength behavior of the soil (such as the formulation of Hashash and Park (2001) to include the effects of confining pressure). These models have typically improved or preserved shear-strain behavior in the region most commonly of interest to engineers at the expense of being unable to capture shear strength response of soil at large strains.

Models that can capture both small-strain soil behavior and large-strain shear strength behavior by combining hysteretic curves such as the Yee et al. (2013) have been proposed. These models typically include a model curve similar to the MKZ model for low shear strains, a hyperbolic model curve asymptotic to a prescribed shear strength for large shear strains, and a transition

function between that weights each model curve to ensure smooth behavior. These models, while typically successful in capturing shear stress behavior at both large and small shear strains, are particularly difficult to implement in 1-D site response analysis codes because they lack rules for hysteretic unload-reload behavior.

The GQ/H soil model uses a smooth hyperbolic curve to control the shear stress-strain behavior of a soil for use in 1-D site response analysis. The functional form is asymptotic to a prescribed shear strength and includes model coefficients to provide control of soil nonlinearity.

G/G_{max} and damping curves used in this study are generated from Darendeli (2001) using material properties collected from sites in CENA as described in Section 7.2. The shear strength of the nonlinear curves is prescribed as a function of depth and V_S as described in Section 7.3 to address the need for both high and low V_S material to have defined shear strength. The GQ/H hyperbolic model is fit to the G/G_{max} and damping curves following the procedure in section 7.4. To account for the uncertainty and variability in nonlinear material behavior in CENA, nonlinear curves are randomized using a model based on the uncertainty ranges in Darendeli (2001) in Section 7.5.

7.2 Selection of CENA Soil Properties

An effort was undertaken to collect G/G_{max} and damping curves for sites in CENA. However, because of a lack of diversity in the geologic conditions and material properties of the collected dynamic curves, characteristic site properties were determined for use with correlation-based procedures for generating dynamic curves such as the formulations presented by Darendeli (2001). To characterize nonlinear material behavior from Darendeli (2001), soil characteristics needed are: mean stress, plasticity index (PI), overconsolidation ratio (OCR), number of cycles (N), and frequency of cycles (f). For site response analyses, N and f are typically equal to 10 and 1, respectively and the values have little impact on the shape of empirical nonlinear curves.

Material property information from a small selection of geotechnical design reports at sites in CENA was collected. Table 7.2 shows a summary of the collected data and sources for the data are given in Table 7.3. Sites were selected to provide coverage of the geologic classifications given in Kottke et al. (2012). Material properties used for empirical generation of nonlinear

curves are shown in Table 7.2. Differences between the site characteristics shown in Table 7.2 and Table 7.1 are the result of judgement decisions about the relative properties between geologic classifications and the combination of geologic classifications used with representative seed V_S profiles. Figure 7.1 shows a comparison of the PI and friction angles selected for this study to other clays. The mean stress for use in empirical correlations is calculated from the friction angle of the selected material through the at-rest coefficient of lateral earth pressure, K_0, through Jakey's equation (Jaky 1948) shown in eq. 4

$$K_0 = (1 - \sin\phi) \times OCR^{\sin\phi} \qquad \text{eq. 7.1}$$

where ϕ is the material friction angle. The selected material friction angle is also used in the GQ/H model to influence soil strength. Material properties assigned to representative seed V_S profiles as shown in Figure 3.1 and detailed in Table 7.1.

7.3 Strength Control of Nonlinear Curves

Randomized G/G_{max} nonlinear material behavior can result in unrealistic shear stress-strain behavior. V_S, density, and G/G_{max} as a function of strain behavior of soil imply a shear stress-strain response of a material. The maximum observed implied shear stress from the G/G_{max} curve between 0 % shear strain and a limiting upper value (typically 10 % shear strain) is known as the implied shear strength of the soil layer and is calculated by:

$$\tau_{implied} = \rho \cdot {V_S}^2 \cdot \frac{G}{G_{max}} \cdot \gamma \qquad \text{eq. 7.2}$$

where ρ is the soil density, and γ is the shear strain.

The strength-controlled GQ/H model places an asymptote on implied shear stress as shown in Figure 7.2. This model is preferable to the commonly used MKZ model (Matasovic (1993) after Kondner and Zelasko(1963)) because the MKZ model does not allow for control of large-strain soil strength as can be seen in Figure 7.2. However, one of the limitations of the GQ/H model is its inability to fit soil behavior with incompatible V_S, G/G_{max} curve, and model shear strength. If the implied shear strength of a nonlinear curve is significantly different than the prescribed model shear strength asymptote, the GQ/H model is unable to fit the nonlinear curves. This can

occur in material with high V_S and low target shear strength when using Darendeli (2001) or other empirical correlations that do not consider V_S or shear strength.

The nonlinear curves in Darendeli (2001) include confining stress as an input parameter and therefore change as a function of depth. Curves from Darendeli (2001) are not V_S dependent, so to capture the connection between implied shear strength and V_S, a model for soil strength is needed that is both a function of confining stress and V_S. A strength model dependent only on confining stress using the friction angles shown in Table 7.1 is insufficient, as in the context of randomization it implies that a layer with a V_S typical of a soft soil has the same shear strength as a layer with a rock-like V_S if they occur at the same confining pressure. For shallow material, it is also often insufficient to describe strength with just a friction angle for use in site response. Fitting to the strength of material with confining stresses near the surface with just a friction angle generates overly soft layer response.

To account for these strength considerations in a parametric study of site response analyses with randomized G/G_{max} curves and V_S that may not be compatible, a strength model is used as a function of friction angle and V_S-based cohesion. The strength increase of material as a function of depth is described by the friction angle with a small amount of cohesion based on the V_S as described by

$$c_{V_S} = \rho \cdot {V_S}^2 \cdot 0.80 \cdot 0.1\% \geq 10\ kPa \qquad \text{eq. 7.3}$$

where c_{V_S} is the cohesion component of the shear strength. This formulation is based on the equation for implied shear strength (eq. 7.2). This equation assumes that the material being modeled has a strength equal to the shear stress developed at 0.1% shear strain for a linear material with 20 % lower shear modulus than the model soil layer under consideration.

The total shear strength of the material is described by

$$\tau_{target,implied} = c_{V_S} + \sigma_v' \tan(\phi) \qquad \text{eq. 7.4}$$

This model is shown as a function of depth in Figure 7.3 for soil with a friction angle of 30°. The "equivalent implied friction angle" shows the total soil strength relative to overburden is calculated by

$$\tan(\varphi_{cohesionless}) = \frac{\tau_{target,implied}}{\sigma'_v} \qquad \text{eq. 7.5}$$

Where σ'_v is the effective vertical stress, and $\varphi_{cohesionless}$ is the cohesionless friction angle. This model introduces a small increase in soil strength for sites with low V_S, keeping the material strength largely dependent on confining pressure. For a soil with V_S = 300 m/s at 10 m and 19 kN/m^3 unit weight, about 50% of the strength of the material will come from the V_S-based cohesion, and half from the confining pressure. For materials with high V_S values, only a small portion of the material strength will come from confining pressure, and the majority of the strength will come from the V_S. The role of this strength is to provide a realistic upper bound to the hyperbolic GQ/H model that is dependent on V_S, G/G_{max} and the implied shear strength. However, as discussed in Section 7.4 the GQ/H model is primarily fit to the G/G_{max} curve in the range of 0.001 to 0.1 percent shear strain. The onset of nonlinearity in a site response analysis is sensitive to this region which is more influenced by the G/G_{max} curves from Darendeli (2001) than the V_S-based cohesion.

7.4 GQ/H Fitting Procedure

The GQ/H model requires a selection of a range of strains for fitting G/G_{max} and damping curves. It is recommended in Groholski et al. (2016) that the damping curve be fit over the entire strain range of interest, and that the G/G_{max} curve be fit to the small-strain range of the nonlinear curve up to 0.1 % shear strain. The GQ/H model will always be asymptotic to a maximum shear strength, and Groholski et al. (2016) recommends that the fitting bound of the curves reach a threshold of 95 % of the asymptotic shear strength at 10 % shear strain (i.e. the implied shear strength at 10 % shear strain should be 95 % of the asymptotic shear strength). These recommendations are not applicable for all possible combinations of G/G_{max} curves and V_S combinations, and a modified fitting routine was required for use in this study to generate reasonably-shaped G/G_{max} curves for the randomized soil profile layers.

The shear strength given in eq. 7.4 is the desired soil strength for strains up to 10 %, the target implied shear strength. To produce reasonable fits to the randomized soil curves with the GQ/H model, the GQ/H asymptotic shear strength is set to be higher than the target implied shear strength by the following procedure:

1. Fit the randomized G/G_{max} curve to GQ/H parameters with the model asymptotic shear strength equal to the target implied shear strength from eq. 7.4 and no threshold for the implied shear strength of the resulting fit.
2. Fit the randomized G/G_{max} curve to GQ/H parameters with the model asymptotic shear strength $\tau'_{asymptote}$ as given by:

$$\tau'_{asymptote} = \frac{\tau_{target,implied}}{\left(\frac{\tau_{target,implied}}{\tau'_{implied}}\right)} \qquad \text{eq. 7.6}$$

where $\tau'_{implied}$ is the implied shear strength from the first stage of fitting. The minimum threshold of shear strength for the second stage of fitting, δ, is given by:

$$\delta = \frac{\tau_{target,implied}}{\tau'_{asymptote}} \times 100\ \% \qquad \text{eq. 7.7}$$

This procedure ensures that the implied shear strength at 10% is always greater than or equal to the target shear strength. This procedure is shown visually in Figure 7.5 for a soil layer with V_{S30} = 500 m/s, 50 m depth, γ = 19.0 kN/m^3, PI = 15 %, and OCR = 1.5 for the mean and +/- 1 σ G/G_{max} and damping curves from Darendeli (2001)

Parameters of the GQ/H model must be defined such that the resulting behavior does not violate any of the model's boundary conditions for numerical stability (Groholski et al. 2016). The fits of the G/G_{max} to the GQ/H model in the above steps were done over several ranges of shear strains as given in Table 7.4 to ensure that the GQ/H fits were valid under the model constrains. Each range of shear strains were fit until a valid set of parameters for the GQ/H model was produced. The majority of nonlinear curves fit using this procedure are successful fit with the first range of shear strains, 0.001 to 0.1 % shear strain.

An example of the GQ/H fits to randomized soil curves for the YNm representative seed V_S profile is shown in Figure 7.4 for the V_S randomizations of the 100 m deep YNm representative seed V_S profile with 30 m thick weathered rock zone shown in Figure 5.24. Figure 7.4 shows the GQ/H fits to randomized curves at 5 m and 50 m depth within the 100 m soil region of the representative seed V_S profile, and at 110 m depth within the weathered rock zone of the YNm profile. The strength of the material in the weathered rock zone at 110 m depth is significantly higher than the strength of the soil material above 100 m depth because of the V_S-dependent strength model.

7.5 Nonlinear Curve Randomization Methodology

Darendeli (2001) proposes not only empirical correlations for the development of G/G_{max} and damping curves, but also the standard deviation of the curves generated. The standard deviation model of Darendeli (2001) can be used as a means of randomization of the curves. For each randomized V_S profile, there are three randomized nonlinear curves following a procedure similar to the one used in the equivalent-linear site response program STRATA (Kottke and Rathje 2011).

The STRATA randomization model generates two normally distributed random ε values for each soil layer, ε_G and ε_D, where ε_G describes the distance of the G/G_{max} curve from the mean, and ε_D describes the distance of the damping curve from the mean. ε_D for a specific soil layer is negatively correlated to ε_G by a factor of -0.5 in the STRATA model. Values of ε between adjacent layers can also be correlated in the STRATA model.

Three realizations of nonlinear material behavior are produced for each randomized V_S profile using the uncertainty of the G/G_{max} and damping curves in Darendeli (2001). Randomized nonlinear curves are perfectly correlated as a function of depth, and G/G_{max} curve is perfectly negatively correlated with the Damping curve. This perfect correlation results in a soil profile having a consistently higher or lower G/G_{max} curve as a function of depth, and ensure that if a G/G_{max} curve for a layer is systematically high, the corresponding damping curve will be lower. A G/G_{max} curve that is systematically high results in a material that has less strain softening than the mean curve of Darendeli (2001) and will therefore produce less hysteretic damping. Perfect

negative correlation between the G/G_{max} and damping curves helps ensure that this behavior is preserved when fitting to a hyperbolic model.

One of the three realizations of nonlinear material behavior is produced using the mean G/G_{max} and damping curves calculated from Darendeli (2001). The other two randomizations for the G/G_{max} curve at a site are perfectly negatively correlated. For a single realization of the V_S profile, there will be one soil profile with material behavior defined by the mean Darendeli (2001) G/G_{max} and damping curves, one soil profile with material behavior that has a systematically high G/G_{max} curve, and one soil profile with material behavior that has an equally systematically low G/G_{max} curve. All three realizations of soil stiffness at a site are functions of a single normally distributed random number, ε. One realization uses the mean Darendeli (2001) curve, one realization has a stiffer behavior than the mean curve ($+\varepsilon$), and one realization has softer behavior than the mean curve ($-\varepsilon$).

Generated ε values are constrained to $1.5\times\sigma$, where σ is the standard deviation from Darendeli (2001). Damping values generated are constrained to be > 0.0 and G/G_{max} values are constrained between 0 and 1. If a value for the nonlinear curves would be generated above or below its constraints, the limiting value is used.

Table 7.1: Selected soil properties for use in parametric study.

Material	PI (%)	Unit Weight (kN/m^3)	OCR	Friction Angle (φ°)	Associated Characteristic V_S Profiles		
General	15	19	1.5	25	Scaled Global	V_{S30}-Binned	Judgement Soft
Weathered Rock Zone	5	21	3	40	Weathered Rock Zone		
Young Glaciated	15	18.9	1.3	30	YGd-YGt-YGo + RS + YGm		
Old Glaciated	20	18.6	3	30	RRm + OG		
Young Nonglaciated	20	18.5	1.3	30	YNa-YNl-YNs + ON	YNm	
Old Nonglaciated	30	19	2	30	YNa-YNl-YNs + ON		
Residual Soil from Sedimentary Rock	24	19.4	3	25	RRs		
Residual Soil from Metamorphic Rock	10	19	3	25	RRm + OG		
Residual Soil	30	19.3	3	25	YGd-YGt-YGo + RS + YGm		

Table 7.2: Summary of soil property data collected for CENA sites.

Geologic Class	PI (%)			Overburden (pcf)			Data Source
	Mean	Range	# of data	Mean	Range	# of data	
OGm	19	0-52	28	118.7	104.4-127.2	6	1, 13
OGo							
OGt							
YGm	10	1-23	163	133.8	106.4-145.4	27	2, 3
YGo	17	9-30	21	120.1	111.3-125.4	12	17, 18
YGt							
YGd							
ONa	28	2-91	81	120	100.7-134.9	72	4, 5
ONc							
ONl							
ONm							
YNc	17	8-34	4	125.9	123.9-127.3	3	6, 15
YNm	37	9-59	42	123.2	98.32-141.25	57	7
YNa	18	4-34	16	111.1	86.02-136.28	36	8, 9
YNl							
YNs							
RRm	10	1-26	250	117.5	117.5	1	10, 16
RRs	20	6-44	10	123.7	115.7-130.8	10	11
RSs	27	4-47	15	122.6	116.96-130.1	3	12, 14

Table 7.3: Sources for data presented in Table 7.2.

Data Source	Geotechnical Design Report
1	HNTB Corporation. "T.H. 52 ORONOCO DESIGN-BUILD ORONOCO, MINNESOTA", 2005
2	Northeast Ohio Regional Sewer District. "Euclid creek tunnel", 2010
3	Parsons Brinckerhoff. "Rochester Intermodal Transportation Center Improvement Geotechnical Investigation Preliminary Design Phase Monroe County, New York", 2013
4	HVJ ASSOCIATES, Inc. "PART 1 GEOTECHNICAL INVESTIGATION BATTLESHIP TEXAS DRY BERTH", 2011
5	HVJ ASSOCIATES, Inc. "GREEN WATER TREATMENT DECOMMISSIONING AUSTIN, TEXAS ",2007
6	BBC&M Engineering, Inc. "Muddy Creek East Branch Interceptor – West Half Hamilton County, Ohio", 2007
7	Fugro Consultants, Inc." Pegasus Project, Phace One I-30 Bridge Over the Trinity River Dallas, Texas", 2009
8	ISG & Associates, Inc. "Geotechnical Engineering Report Council Bluffs, Iowa", 2008
9	TTL, "Geotechnical Exploration Buffalo Wild Wings Restaurant Des Moines, Iowa", 2013
10	Florecnce & Hutcheson."I-85/I-385 Interchange Improvements Greenville County, SC", 2013
11	S&ME, Inc. “Louisville-Southern Indiana Ohio River Bridges Project Vertical Borings Jefferson County, Kentucky", 2012
12	HBC/Terracon, "Geotechnical Engineering Report Classic BMW Dealership Spring Creek Parkway and North Dallas Tollway Plano, Texas", 2004
13	Terracon. "Geotechnical Engineering report proposed lift station south maple street SE of south 4th street west branch, Iowa", 2012
14	Schnabel, "Geotechnical report 1000 Mosby street Richmond, VA", 2010
15	Michael Baker Jr., Inc. ,"PRE-FINAL GEOTECHNICAL ENGINEERING REPORT LOWER HILL REDEVELOPMENT PROJECT PITTSBURGH, ALLEGHENY COUNTY, PENNSYLVANIA" , 2012
16	S&ME, "Proposed Building Sites Hunter Industrial Park Laurens, South Carolina", 2008
17	Haley & Aldrich, Inc. "SUPPLEMENTAL GEOTECHNICAL DATA REPORT PROPOSED SIBLEY POND BRIDGE REPLACEMENT MAINE DOT PIN 15618.00 CANAAN / PITTSFIELD,
18	MaineDOT "BRIDGE PROGRAM GEOTECHNICAL SECTION AUGUSTA, MAINE", 2010

Table 7.4: GQ/H Strain Fitting Ranges for G/G_{max} curves.

Randomization	Iteration	Min Bound Strain (%)	Max Bound Strain (%)
G/G_{max} $\varepsilon > 0$	1	0.001	0.1
G/G_{max} $\varepsilon > 0$	2	0.01	0.1
G/G_{max} $\varepsilon > 0$	3	0.03	0.1
G/G_{max} $\varepsilon > 0$	4	0.003	0.03
G/G_{max} $\varepsilon > 0$	5	0.003	0.01
G/G_{max} $\varepsilon = 0$	1	0.001	0.1
G/G_{max} $\varepsilon = 0$	2	0.001	0.03
G/G_{max} $\varepsilon = 0$	3	0.0001	0.01
G/G_{max} $\varepsilon = 0$	4	0.003	0.03
G/G_{max} $\varepsilon = 0$	5	0.008	0.03
G/G_{max} $\varepsilon < 0$	1	0.001	0.1
G/G_{max} $\varepsilon < 0$	2	0.0001	0.003
G/G_{max} $\varepsilon < 0$	3	0.001	0.01
G/G_{max} $\varepsilon < 0$	4	0.001	0.003
G/G_{max} $\varepsilon < 0$	5	0.003	0.03

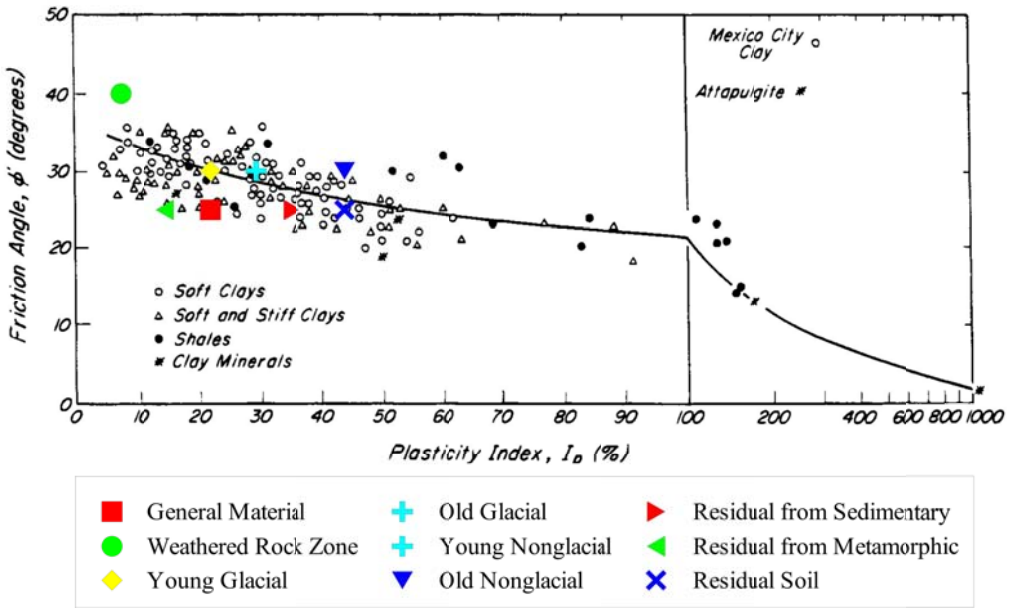

Figure 7.1: Comparison of material properties for this study compared to Figure 19.7 of Terzaghi et al. (1996).

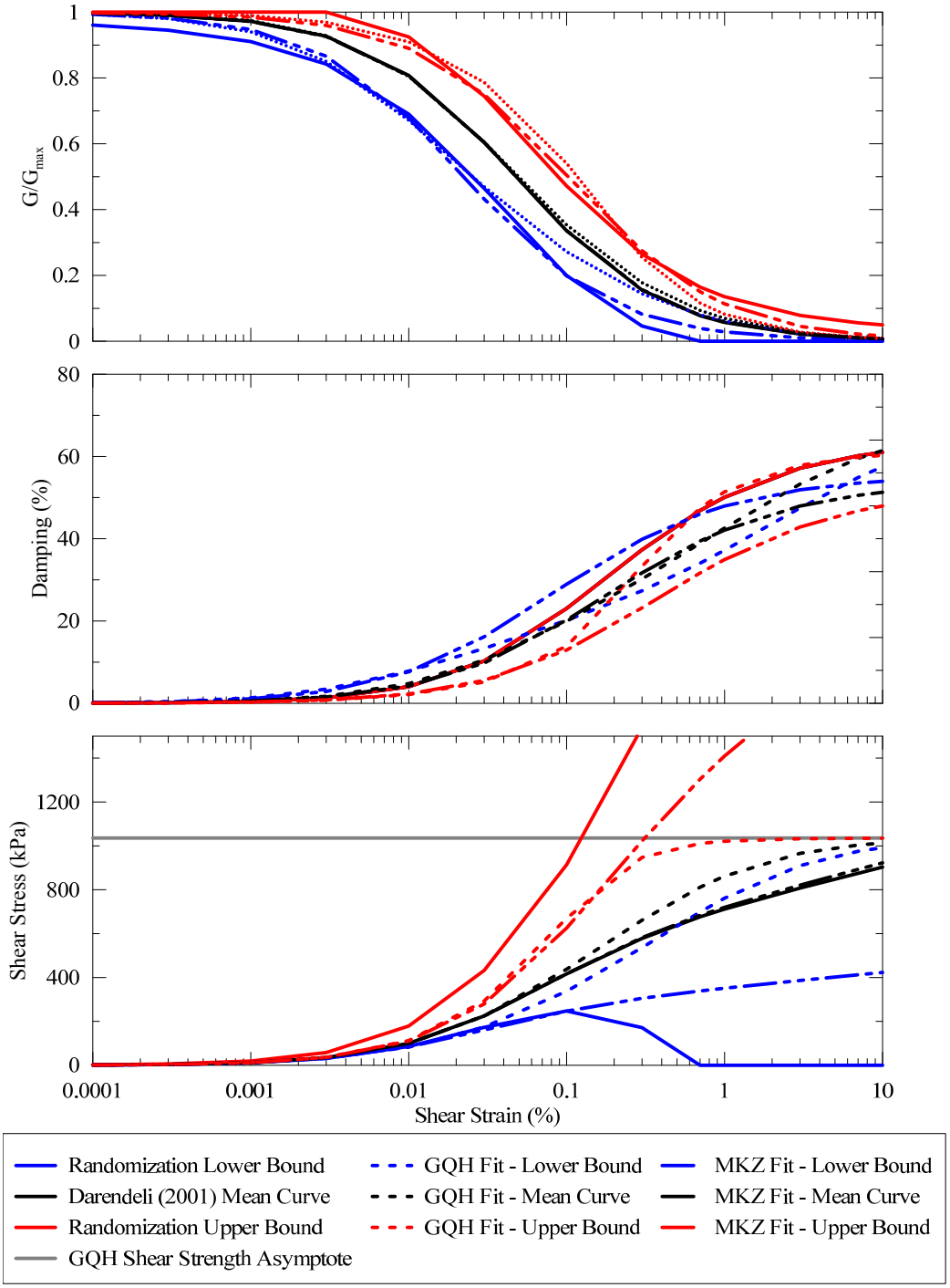

Figure 7.2: Dynamic Curves generated with Darendeli (2001) for a soil layer 5 m deep with PI = 10%, φ = 25°, σ'_v = 95 kPa, and V_S = 800 m/s. MKZ and GQ/H fits shown for GQ/H asymptote strength of 1035 kPa.

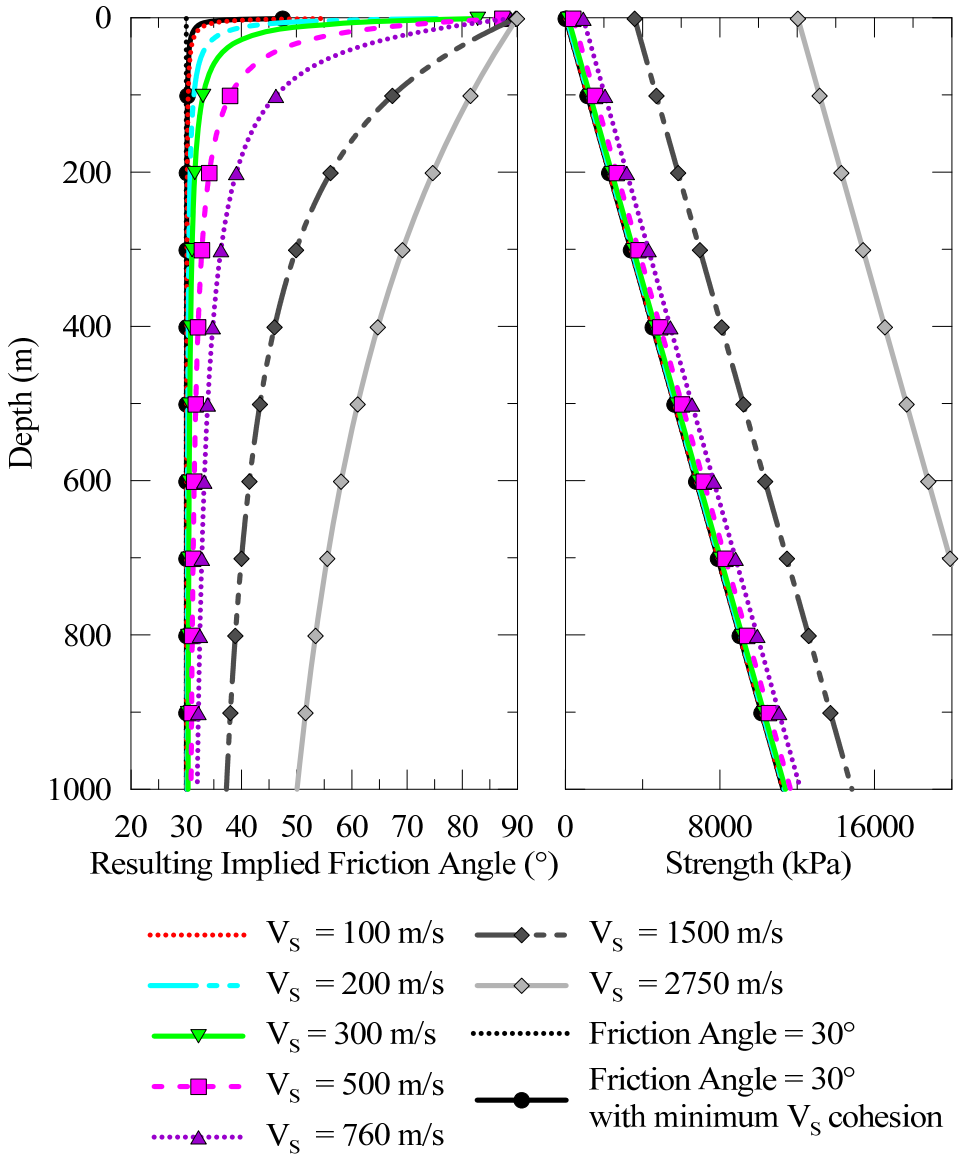

Figure 7.3: Proposed Vs-based cohesion model for implied shear strength as a function of depth for a soil with a friction angle of 30° and unit weight of 19 kPa.

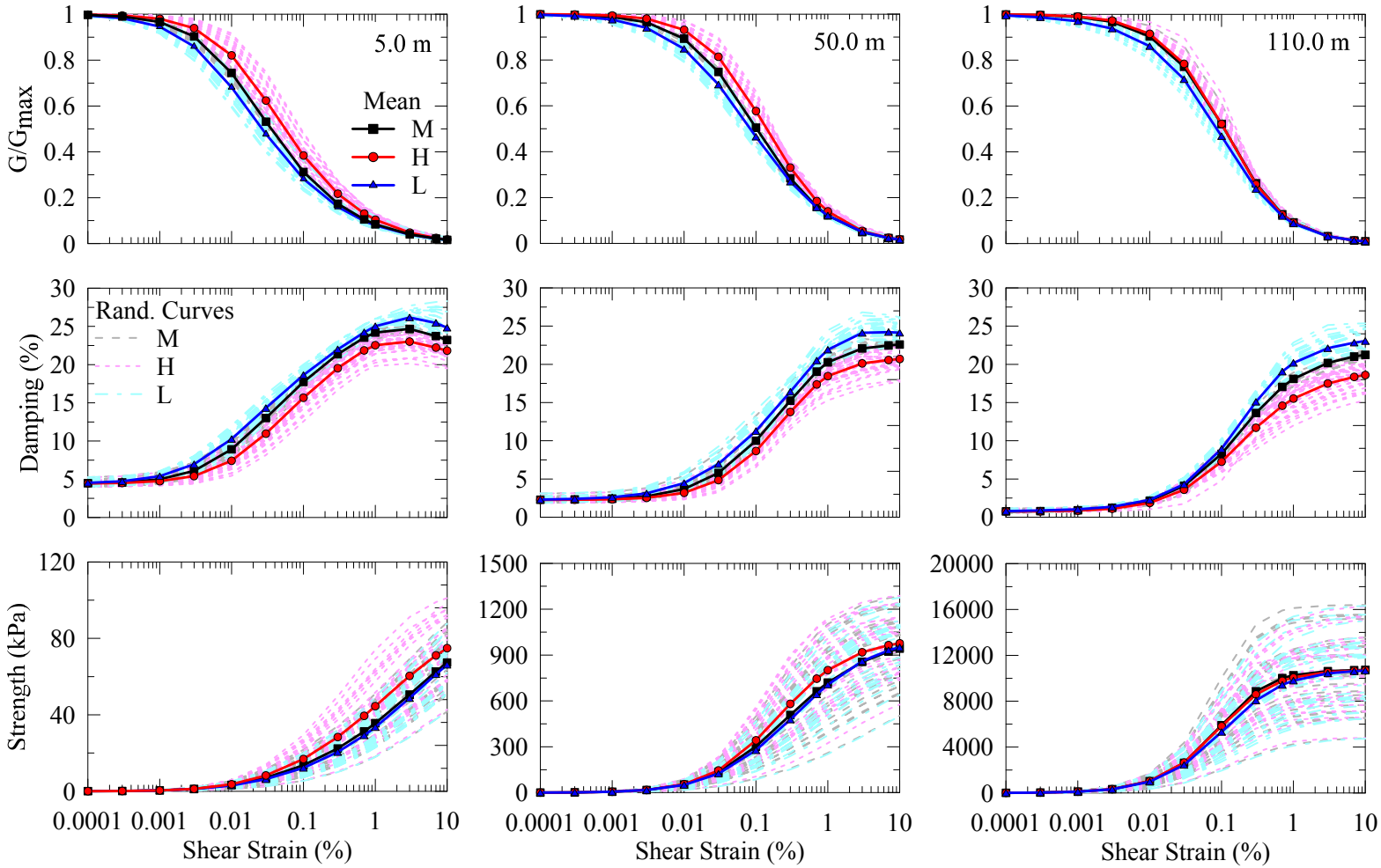

Figure 7.4: GQ/H model fits to randomized G/G_{max}, damping, and implied shear strength for the 100 m soil depth YNm representative seed V_S profile with 30 m thick weathered rock zone for positive ε_G (H), negative ε_G (L), and Darendeli (2001) mean (M) at 5 m, 50 m, and 110 m depth.

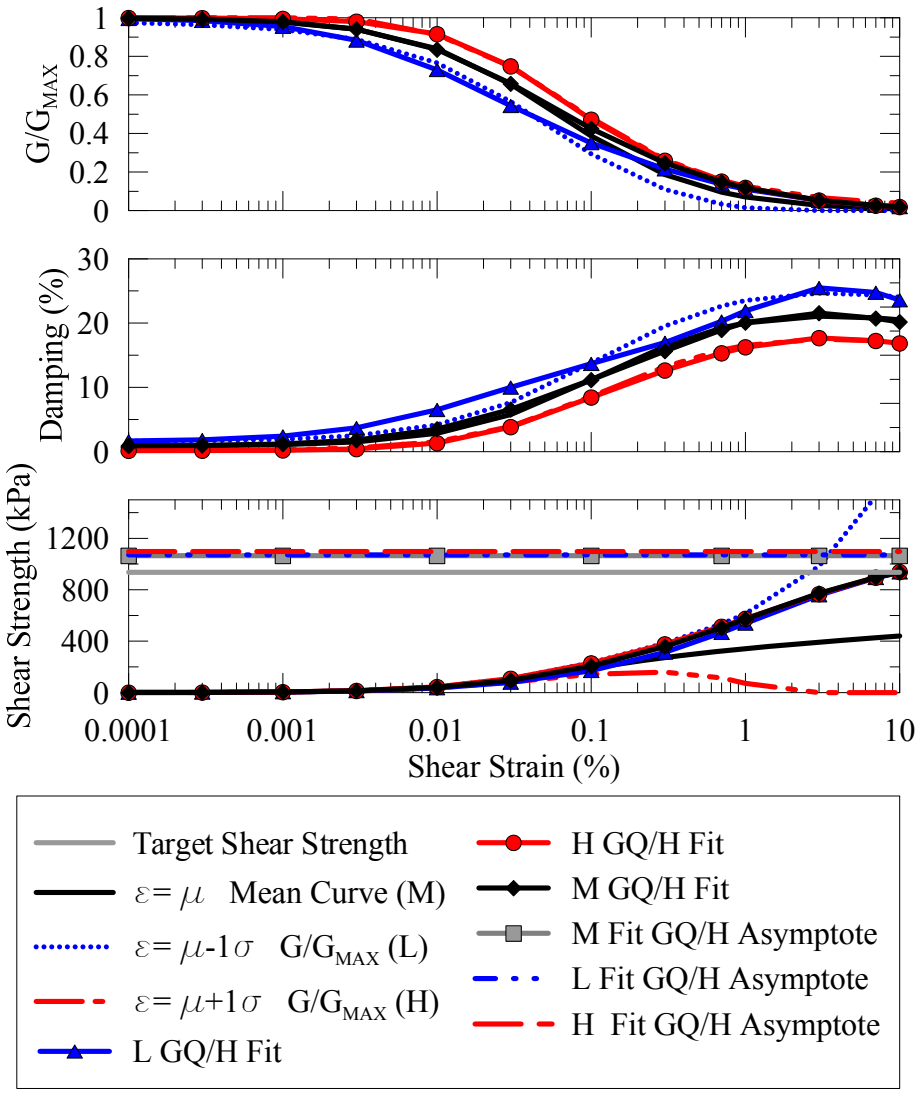

Figure 7.5: GQ/H Fitting Procedure for a soil layer with V_{S30} = 500 m/s, 50 m depth, γ = 19.0 kN/m^3, PI = 15 %, and OCR = 1.5 for the mean and +/- 1 σ G/G_{max} and damping curves from Darendeli (2001).

Chapter 8. Simulation Evaluation and Dataset

8.1 Introduction

This study uses automated generation of 70,650 unique site profiles for use in 1,747,278 site response analysis as detailed in Chapter 3, Chapter 4, Chapter 5, Chapter 6, and Chapter 7. The site response analyses developed in this study are calculated with the software DEEPSOIL V6.1 (Hashash et al. 2015b) and the results are used in the development of site amplification functions. These simulations are evaluated as a dataset in three ways: (1) the data produced and included in the database of simulations is presented Section 8.2, (2) the density of site response data for several engineering parameters is presented in Section 8.3, and (3) the response of a single site is evaluated to determine that the profile is responding as expected to ground motions of differing intensity for the LE, EL and NL analysis calculations in Section 8.4.

8.2 Simulation Database

Conducting these simulations takes approximately 11.5 days of computation time on 4 business-grade servers able to perform 96 analyses simultaneously (one analysis per computational core, and four servers with 32, 32, 24, and 8 computational cores). With the previous version of DEEPSOIL V5.1 (Hashash et al. 2011), the estimated time to perform the site response analyses in this study is estimated to be almost four months of computational time with these resources.

The complete site response simulations performed for this study are made available in database format. The database of site response simulations is about 2.9 Tb uncompressed and will be made available to researchers. The data from the simulations is the most relevant data for the development of ergodic site amplification functions in Chapter 9 and Chapter 10. The data from this study is represented visually in Figure 8.1. For each site profile and bedrock ground motion combination, simulation results at the ground surface and as a function of depth of the LE, EL, and NL analyses are provided.

To aid in the calculation of amplification functions, separate databases of information derived for each soil column (i.e. V_{S30}, soil column natural period) and information for each bedrock ground motion (i.e. PGA, PGV, PSA, time step) are also extracted. All site profile and bedrock ground

motion data provided in the supplementary databases can be calculated from the simulation inputs in the database of simulation results, but are provided for ease-of-access.

Both the time history information directly from the site response analysis and the spectral response derived from the acceleration time history are available at the ground surface as shown in Figure 8.1. The time history information provided for the top of the soil column surface layer is the acceleration, and Arias intensity (I_a). The stress and strain time history is provided for the midpoint of the top layer of the analysis. Time history information is provided for each time step in the input ground motion. The RS and FAS spectral responses of the site profile are provided at the ground surface. The 5% damped frequency domain RS is provided for 430 periods between 0.001 s and 10 s. The FAS is provided for N/2-1 evenly spaced frequencies from the Nyquist (inclusive) of the bedrock ground motion to 0 Hz (exclusive) where N is the smallest power of 2 greater than the number of points in the bedrock ground motion.

The maximum profile response as a function of depth is provided at the midpoint or boundary of each layer as shown in Figure 8.1. At each layer boundary as a function of depth, the PGA, maximum displacement, and peak AI of the site profile during analysis is provided. At each layer midpoint as a function of depth, the effective stress, and maximum strain and stress experienced by the layer during the analysis is provided.

8.3 Data Coverage

The dataset resulting from this study is significantly larger than that of previous studies. The density of data is shown visually in Figure 8.2 for several important engineering site response parameters, highlighting features of site amplification captured in this study. Figure 8.2a shows the ln(amplification) (i.e. the natural log of the ratio of surface response to outcrop ground response of a parameter) of the PGA as a function of V_{S30} from LE analyses which do not show the effect of site nonlinearity. The corresponding surface amplification of the PGA from the NL analyses is shown in Figure 8.2b. Nonlinear site amplification from intensity of the outcrop ground motion captured by this study is represented by the difference between Figures 8a and 8b. The distribution of ground motion PGA intensity as a function of site V_{S30} is shown in Figure 8.2c. Ground motion intensities are fairly evenly distributed across V_{S30}, suggesting limited bias in the capturing of nonlinear site amplification from the distribution of ground motion intensities.

A notable feature of the site response simulations presented in this study is the natural-period dependent site amplification shown in Figure 8.2d showing the amplification of the LE site response analyses at 0.1 s PSA of the 5% damped RS as a function of site natural period. There is a cluster of analyses that form a peak in the amplification near where the site natural period equals the RS period shown ($T_{nat} = T_{OSC}$). This cluster of analyses suggests that sites with natural periods near the RS oscillator period, there is an increase in amplification, and site profile resonance effects are observed.

8.4 Evaluation of Site Behavior

Simulation results from this parametric study are used in aggregate form to develop ergodic site amplification models for use in engineering and seismology. This section presents a sample of site amplification results from a site to verify that the procedurally-generated site amplification analyses in DEEPSOIL behave as expected on a site-specific basis. The site under consideration is a realization of the RS+YGdto+YGm V_S profile with Young Glaciated material as shown in Table 7.1. The V_S profile is from the 10 m depth bin and has 30 m of soil material above weathered rock and has a V_{S30} of 608 m/s and site natural period of 0.212 s. The nonlinear curves for this profile have + ε_G as described in Section 7.5. This profile was simulated with the ground motions shown in Table 8.1 ranging from 0.02 g to 2.24 g PGA. The response spectra and PGA and strain as a function of depth for the profile to the ground motions in Table 8.1 are shown in Figure 8.1 and Figure 8.2.

The simulation results presented in suggest that the procedurally-generated soil columns are behaving as expected at all levels of shaking. The relative behaviors of the NL, LE, and EL analyses, the soil column strain and PGA response as a function of depth and bedrock motion intensity, and amplification at the natural period of the soil column for weak motion shaking all demonstrate typical amplification behaviors as described below.

The site profile under investigation has 30 m of weathered rock between the 3000 m/s bedrock half-space condition and the 10 m soil profile. In the figures showing the strain and PGA response as a function of depth, the differences between the LE, EL and NL analyses are most pronounced in the lower V_S soil material than the higher V_S weathered rock material, as expected.

The LE analyses are representative of the small-strain response of the soil column, and for very low levels of bedrock motion intensity, the LE analyses will converge with both the EL and NL analyses for a sufficiently high profile layer resolution. At higher levels of shaking, the EL and NL analyses will begin to diverge from the LE analyses, and at very high levels of shaking the EL and NL analyses will diverge from each other. The V_S of the soil column and bedrock motion intensity both contribute to the divergence of the EL and NL site response analyses (Kim et al. 2015), and for softer site (lower V_{S30}) more divergence is expected for a bedrock motion intensity measure. For the weakest ground motion, Smsimm6.5_M6.5R87.7, there is good agreement in the spectral response for ground motions with very low levels of shaking (i. e. low PGA) between the LE analyses and the EL and NL analyses. At higher levels of shaking, the LE, EL, and NL analyses all begin to diverge and are largest at the highest levels of shaking.

The simulations show amplification around the site natural period of the site profile. There is a relative peak in the natural period of the site around 0.2 s in each of the surface response spectra. For the EL and NL analyses at higher levels of shaking, there is less noticeable amplification in the EL and NL analyses near the natural site period than for the LE analysis. As shaking intensifies at a site and the soil begins to strain, its stiffness decreases, changing the natural period of the site as a function of time. It is expected that for more intense shaking, the amplification near the natural period of the site will decrease.

Table 8.1: Ground motion properties for select analysis results.

Motion	PGA (g)	PGV (m/s)	Duration (s)	M_W.	Distance (km)	Motion Source	Figures
Nrcm55Rab_B-Kod270	0.1809	0.0466	18.495	5.5	0-50	NUREG	Figure 8.3 (a), (b), (c)
Nrcm55Rc_1125S08L	0.1336	0.0461	29.65	5.5	50-100	NUREG	Figure 8.3 (d), (e), (f)
Nrcm55Rc_1125S20L	0.1477	0.0377	20.645	5.5	50-100	NUREG	Figure 8.3 (g), (h), (i)
Nrcm65Rb_L-Bpl070	0.1950	0.0673	25.95	6.5	10-50	NUREG	Figure 8.3 (j), (k), (l)
Nrcm75Ra_Lcn345	2.2490	0.3694	48.12	7.5	0-10	NUREG	Figure 8.4 (a), (b), (c)
Nrcm75Rd_Tap060-N	0.0910	0.0876	64.995	7.5	100-200	NUREG	Figure 8.4 (d), (e), (f)
Smsimm5.5_M5.5R12	0.2700	0.0620	65.532	5.5	12	SMSIM	Figure 8.4 (g), (h), (i)
Smsimm6.5_M6.5R87.7	0.0204	0.0133	131.068	6.5	87.7	SMSIM	Figure 8.4 (j), (k), (l)

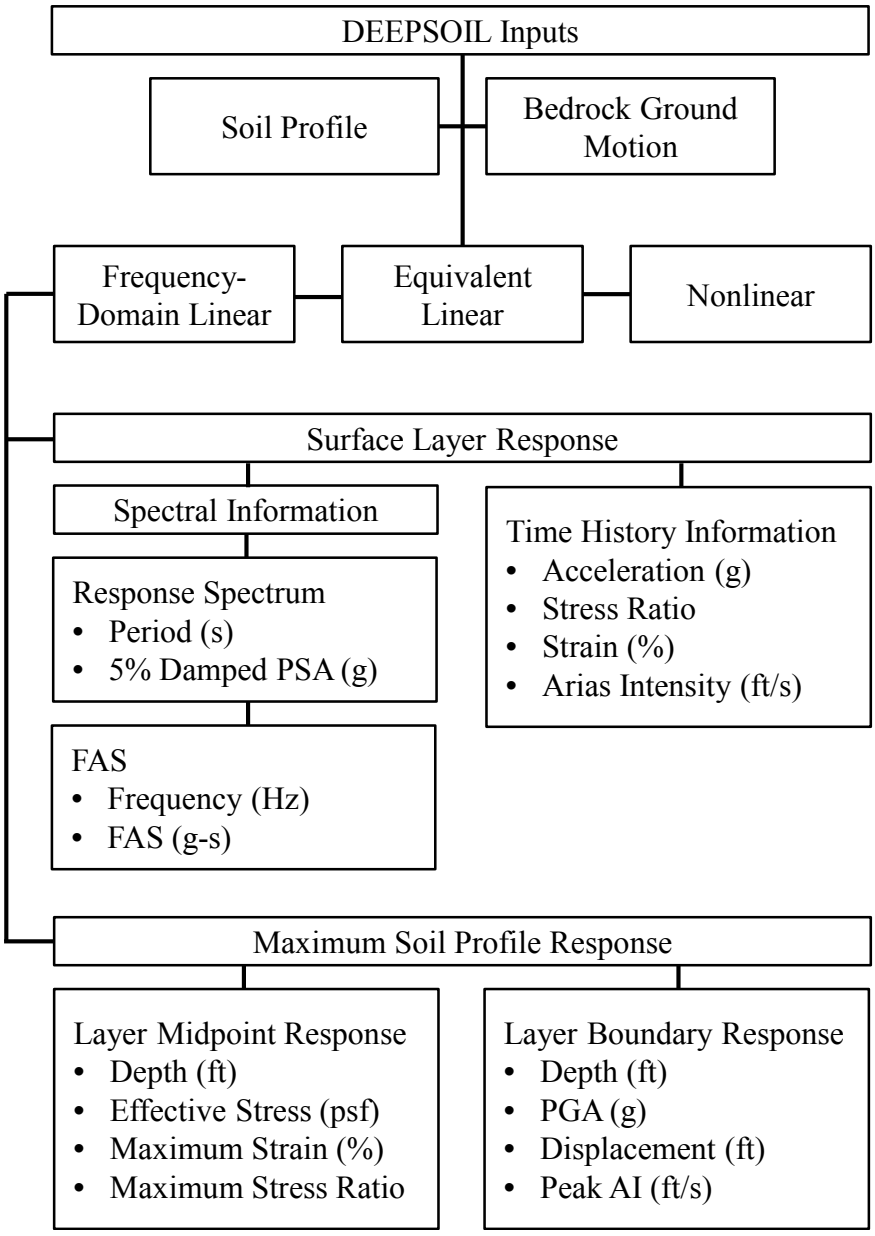

Figure 8.1: Data contained in simulation database for each site profile and rock outcrop ground motion combination.

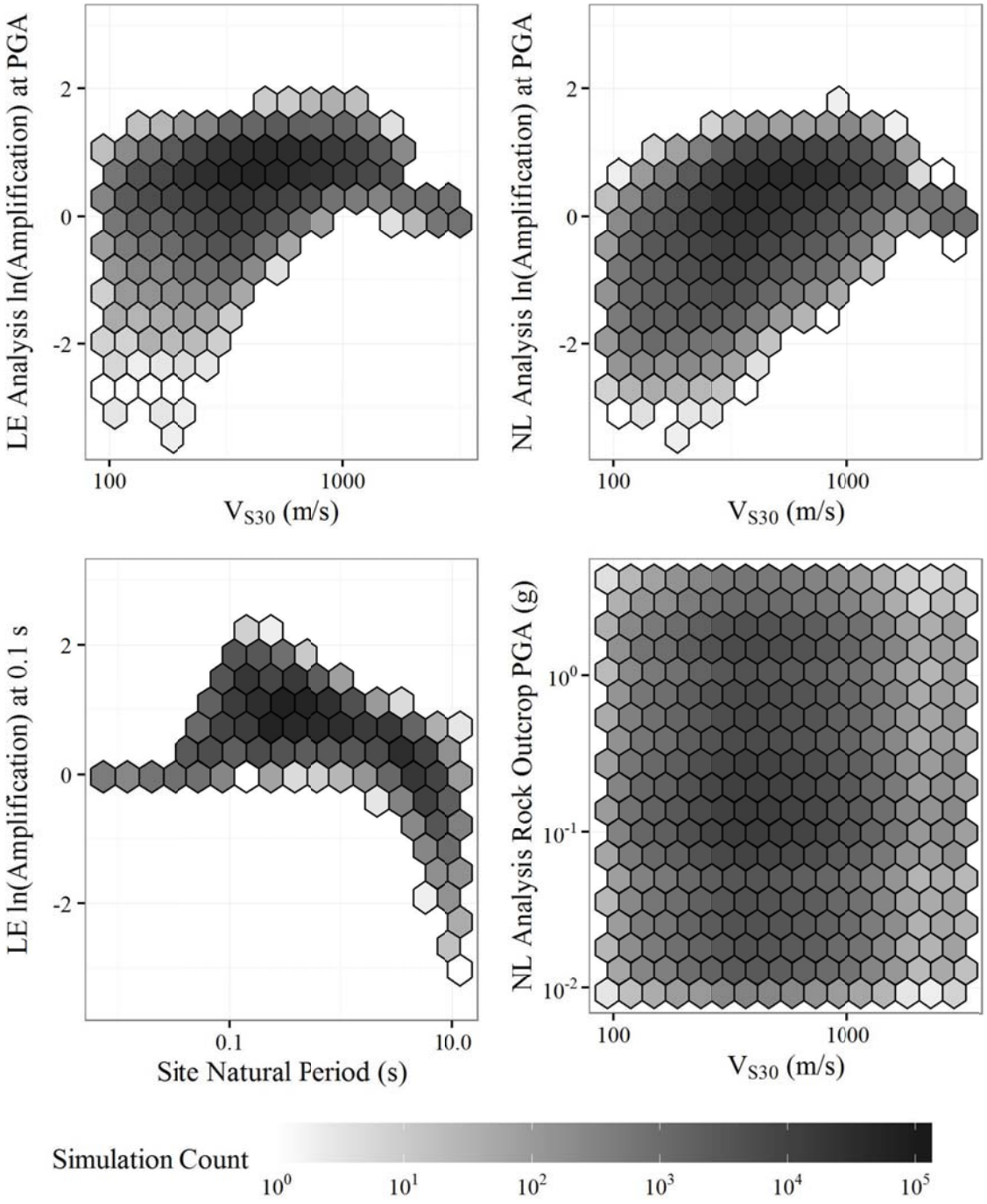

Figure 8.2: Density of 1-D site response analysis data as a function of V_{S30} for (a) PGA amplification of LE analyses, (b) PGA amplification of NL analyses, and (c) Rock outcrop PGA, and (d) amplification at 0.1 s PSA of the RS as a function of site natural period.

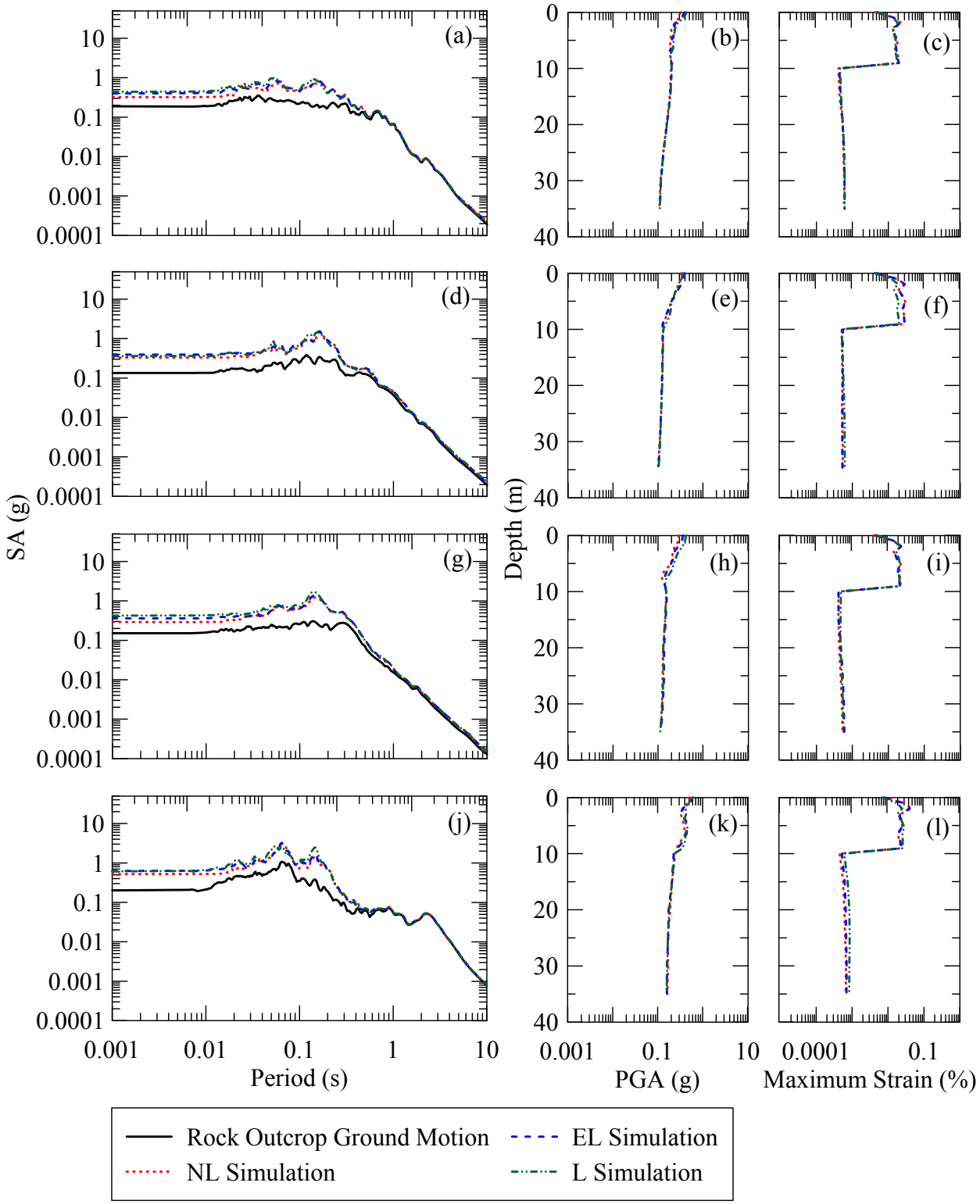

Figure 8.3. Plots of Motions and simulations. See Table 8.1 for plot descriptions.

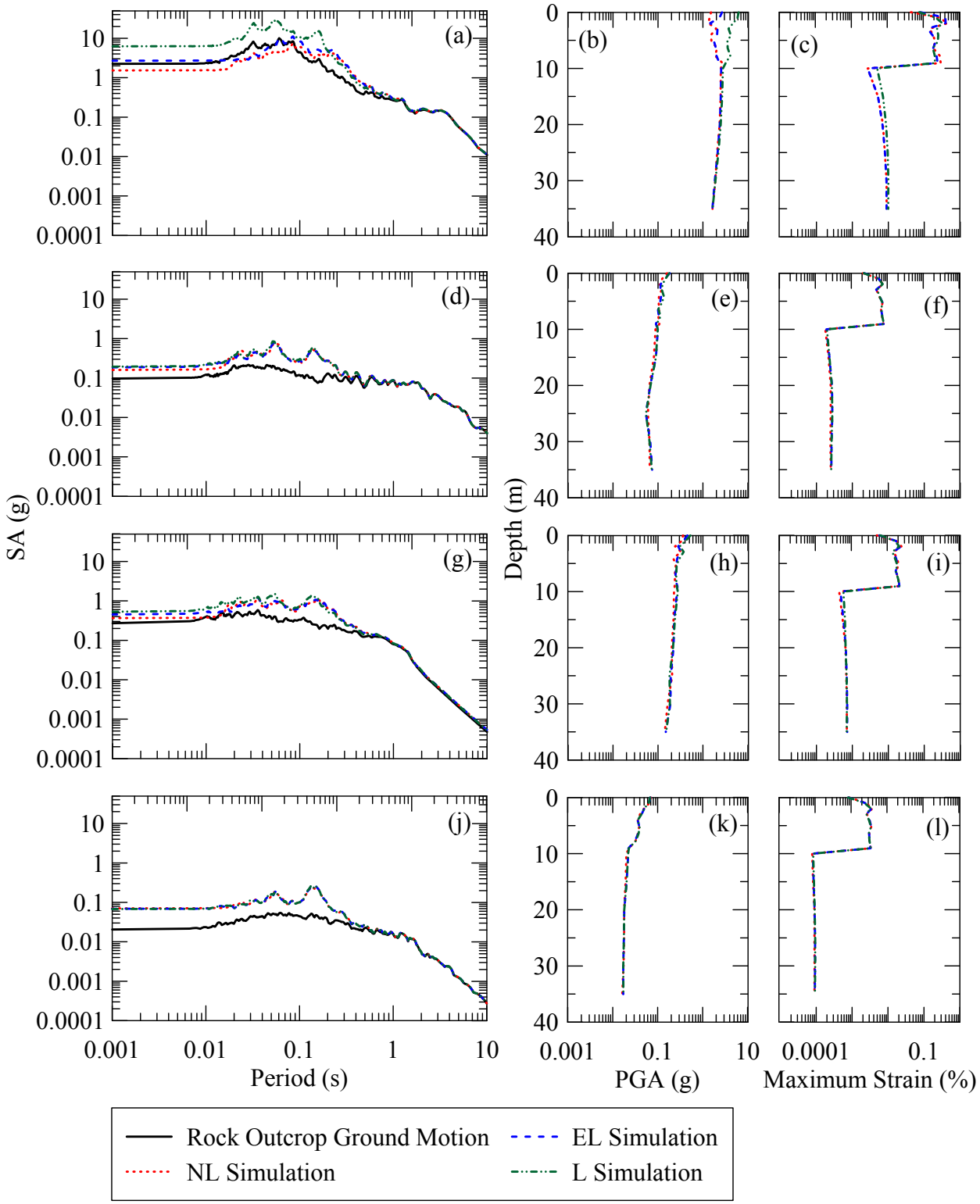

Figure 8.4. Plots of Motions and simulations. See Table 8.1 for plot descriptions.

Chapter 9. Response Spectrum Site Amplification Models

This section presents a modular linear and nonlinear RS site amplification factors and models resulting from the parametric study of site response simulations. The modular functional form is selected to provide options for model users to produce estimates of site response using available data. The linear site amplification in the response spectrum has up to three model terms for V_{S30}, depth of soil, and site natural period as shown in eq. 9.1.

$$F_{lin} = f(V_{S30}) + f(Z_{Soil}) + f(T_{nat}) \quad \text{eq. 9.1}$$

where Z_{soil} is the depth of soil, and T_{nat} is the site natural period. The expanded response spectral amplification model with nonlinearity is given in eq. 9.2.

$$F_{S,B} = F_{lin} + F_{nl} = f(V_{S30}) + f(Z_{Soil}) + f(T_{nat}) + f(NL) \quad \text{eq. 9.2}$$

where the nonlinear amplification component is represented as a function of soil stiffness and ground motion intensity characteristics, *f(NL)*.The RS amplification model components in eq. 9.2 are regressed from simulations and several sets of coefficients are provided for the component. Components of the RS amplification model are evaluated both simultaneously and independently for model use cases where data to evaluate the full model may not be available. For example, in the development of GMM's for projects such as NGA-East where the only site term known is V_{S30}, an amplification model from that requires inputs of depth to weathered rock or site natural period is only usable with additional assumptions about the site character. In contrasting cases, estimation of site amplification for sites in which the full V_S profile is known can be improved by including model effects beyond V_{S30} such as depth to weathered rock or site natural period. Table 9.1 shows the amplification coefficient models to be derived from the simulation dataset. Model terms shown in Table 9.1 can be combined to form complete site amplification models as shown in Table 9.2.

Models L1-L5 shown in Table 9.2 are intensity-independent linear site amplification models and are derived from linear elastic simulations. Model L1 is a site amplification model dependent only on V_{S30}. Models L2 and L3 are amplification models with coefficients for Z_{soil} and T_{nat} respectively calculated after the effects of V_{S30} have been removed through the regression of the

L1 coefficients as shown in Table 9.1. The Z_{soil} and T_{nat} terms in models L2 and L3, respectively, are therefore usable with alternative V_{S30}-based amplification models from other authors. Linear models L4 and L5 are amplification models with simultaneously-regressed model terms for V_{S30} and Z_{soil} (L4) and V_{S30} and T_{nat} (L5), respectively.

Models for nonlinear site amplification are represented in Table 9.2 for two different ground motion intensity measures, PGA and SA, and for two different methods of calculation. Models of the form L+N are site amplification models with independently calculated linear and nonlinear components of site amplification. The L amplification terms are calculated from the linear elastic site response simulation as shown in Table 9.1. The N amplification terms are regressed from the difference between the NL GQ/H site response simulation and the LE site response simulation. The K models, K1 and K2, are site amplification models with simultaneously calculated linear and nonlinear components of site amplification. The K amplification model terms are regressed simultaneously from the NL GQ/H site response simulations. The N1 and K1 models use period-dependent spectral acceleration (SA) of the bedrock motion and N2 and K2 models use the period-independent peak ground acceleration (PGA) of the bedrock motion as the intensity measure for nonlinear site effects.

The derivations of each of the terms for the models described in Table 9.1 are detailed below.

9.1 V_{S30} Scaling

V_{S30} is a parameter commonly used in site amplification as discussed in Chapter 2 and is used as a parameter for linear site amplification to build on previous knowledge and provide an amplification function compatible with the current state of practice. The site amplification term developed as a function of V_{S30} takes a slightly different form than the traditional linear-with-$\ln(V_{S30})$ amplification models used in CENA. The simulation data as a function of V_{S30} has a changing shape as a function of period that the V_{S30} functional form is designed to capture as shown in Figure 9.1.

Figure 9.1 shows the LE site amplification data as a function of V_{S30} at four response spectral periods 0.01 s (a), 0.1 s (b), 0.3 s (c), and 1.0 s (d) that show the change in behavior of site amplification. At all periods as shown in Figure 9.1, the mean site ln(amplification) converges to

0 for the V_{S30} = 3000 m/s reference condition. At longer periods shown in Figure 9.1(c) and Figure 9.1(d), there is a flat region from 3000 m/s to below 1000 m/s V_{S30} where there is little to no observed mean amplification and ln(amp) ≈ 0. The region of 0 ln(amp) at each period transitions into a region of V_{S30} where ln(amp) increases steadily. At short periods, as seen in Figure 9.1(a) and Figure 9.1(b) site amplification increases immediately as V_{S30} decreases from the 3000 m/s reference condition in the V_{S30} range of 3000 m/s to 2500 m/s for 0.01 s, and 3000 m/s to 1000 m/s for 0.1 s. At 0.3 s and 1.0 s period, the increase in mean amplification occurs at V_{S30} values below 1000 m/s to about 300 m/s for 0.3 s and to below 200 m/s for 1.0 s period. Below the region of increasing amplification with decreasing V_{S30}, there is a region where the mean amplification decreases as V_{S30} decreases down to the minimum V_{S30} of sites included in the simulation dataset. This region is below 2500 m/s for 0.01 s, below 700 m/s for 0.1 s, below 500 m/s for 0.3 s and is not well defined for 1.0 s. The relative peak in mean amplification in Figure 9.1(b) is due to site resonance effects and are described in Section 9.3.

The functional form of the V_{S30} scaling component, $f(V_{S30})$, of the linear site amplification models shown in Table 9.2 is given in eq. 9.3 to capture the observed simulation behavior.

$$f(V_{S30}) = \begin{cases} V_c < V_{S30} & 0 \\ V_L < V_{S30} < V_c & c_1 \ln\left(\frac{V_{S30}}{V_c}\right) \\ V_{S30} < V_L & c_1 \ln\left(\frac{V_{S30}}{V_c}\right) + c_2 \ln\left(\frac{V_{S30}}{V_L}\right) + c_3 \ln\left(\frac{V_{S30}}{V_L}\right)^2 \end{cases} \quad \text{eq. 9.3}$$

where coefficients c_1, c_2 and c_3 describe the period-dependent V_{S30} scaling in the model, V_c is a limiting velocity above which ground motions show no amplification relative to the 3000 m/s bedrock condition, and V_L is a limiting velocity below which amplification does not scale linearly with the log of V_{S30}. The V_{S30} scaling model component given in eq. 9.3 has three regions of behavior defined by V_{S30}, a departure from commonly used V_{S30} scaling functions for the WUS such as in Walling et al.(2008) and Seyhan and Stewart (2014) and for CENA as in the models presented in Table 2.2.

Above the V_c limiting velocity, there is no dependency of site amplification on V_{S30}. V_c as presented in eq. 9.3 maintains the same definition as in equation 2 of Seyhan and Stewart (2014). Above V_c there is negligible change in the site amplification relative to the 3000 m/s reference rock condition. Between V_c and V_L, the site amplification scales linearly with the log of V_{S30}. Linearly increasing site amplification as a function of V_{S30} is commonly seen in amplification functions in the WUS and other regions. Below V_L the V_{S30} scaling term has a curved region. In the region $V_{S30} < V_L$, the c_1 and c_2 terms ensure a continuous function of V_{S30}, and the c_3 term determines the degree of curvature. At longer periods, the magnitude of c_3 decreases, and the site amplification becomes more linear with the log of V_{S30}.

The V_{S30} scaling given in eq. 9.3 and regressed for the linear elastic simulation data, model $f(V_{S30})$ in eq. 9.3, is shown for several response spectral periods in Figure 9.2. Coefficients for the $f(V_{S30})$ site amplification coefficients are shown graphically in Figure 9.4 through Figure 9.7 and provided in tabular form in APPENDIX A. Model residuals are shown in APPENDIX B.

9.2 Depth Effects

Site profile depth to weathered rock has opposing effects on the linear site response simulation data at low and high periods. At low periods, amplification from deeper site profiles is lower than shallow profiles, and at high periods, amplification from deeper sites is higher than shallow profiles. These effects are seen in the simulation data and shown for response spectral periods 0.01 s and 10 s in Figure 9.8 and Figure 9.9, respectively. Figure 9.8 shows the linear elastic site response amplification as a function of V_{S30} for each depth bin of soil as outlined in the parametric study described in Chapter 3. For the sites with the greatest depth of soil horizons, 500 m and 1000 m, the site amplification is lower than for more shallow sites. The shape of the site amplification as a function of V_{S30} is similar for the deeper sites as for the shallow sites, but has been translated down to lower values of amplification. In the linear elastic simulations, the lower amplification for the deeper sites at high frequency is a result of the small strain damping, D_{min} damping out high frequency ground motion content over a greater depth of soil than for shallow sites.

The effect of soil depth at 10.0 s is shown in Figure 9.9 for the linear elastic simulations. The sites with the greatest depth of soil horizons, 500 and 1000 m, show higher amplification than for

more shallow sites. As for the depth effects at high frequency seen in Figure 9.8, the shape of the amplification as a function of V_{S30} is similar for the deep and shallow sites, however the magnitude is increased for deeper sites

The functional form adopted to capture the effects of depth on the linear site amplification is selected to capture the increase in amplification due to depth at long periods and decrease in amplification at short periods while reducing total model error and not introducing bias in model residuals and preserving the shape of the amplification as a function of V_{S30}. The effects of soil column depth, $f(Z_{Soil})$, of site amplification for the models shown in Table 9.2 is given in eq. 9.4.

$$f(Z_{Soil}) = \begin{cases} Z < 30 & 0 \\ Z \geq 30 & c_4(Z - 30\ m)^2 \end{cases} \qquad \text{eq. 9.4}$$

where c_4 describes the period-dependent depth effects, and Z is the soil depth to weathered rock in meters.

The depth effects of site amplification given in eq. 9.4 provide a correction for sites deeper than 30 m. At low periods, c_4 is negative and represents a decrease in the amplitude of ground motion at a site due to the damping of a very deep soil column. At longer periods, c_4 becomes positive and represents an increase in the amplitude of ground motions for deeper sites due to resonance effects. The 30 m limitation on the range of applicability is included for two reasons. First, there are not significant effects due to depth on site amplification for shallow sites. Second, the depth-dependent amplification model form is usable only with a V_{S30} scaling model. V_{S30} is calculated for the top 30 m of a site, and if weathered rock is included in the top 30 m (i.e. $Z < 30$ m) the V_{S30} value will be influenced by the depth to weathered rock.

The L2 amplification model presented in Table 9.2 is shown in Figure 9.10 with the L1 model for periods of 0.01 s (a), 0.1 s (b), 0.3 s (c) and 1.0 s (d) for sites with 500 and 1000 m depth. The L2 amplification model is computed by regressing the residuals of the L1 amplification model to determine the c_4 coefficient in eq. 9.4 and is an improvement of the L1 amplification model to include the effects of depth. The L4 amplification model in Table 9.2 is similar to the L2 amplification model but includes the effects of V_{S30} regressed simultaneously as the depth effects

and features slightly different V_{S30} scaling coefficients. Figure 9.10 shows agreement with the depth-dependent trends in amplification shown in Figure 9.8 and Figure 9.9 with an increase in amplification for longer periods (Figure 9.10(d)) and a decrease in amplification at lower periods (Figure 9.10(a-c))The regressed c_4 coefficient is shown in Figure 9.13 and Figure 9.14 which reveals the trend of the depth effects in the L2 and L4 models, respectively. For negative values of c_4, there will be lower amplification at deeper sites, and for positive values of $c_4$there will be higher amplification at deeper sites.

Model L2 and L4 in Table 9.2 include effects of depth on linear site amplification and model estimations for the L2 and L4 modelsare shown graphically for several response spectral periods in Figure 9.11 and Figure 9.12, respectively, for all simulations conducted in the parametric study. Model coefficients for models L2 and L4 are provided in tabular form in APPENDIX A. Model residuals are shown in APPENDIX B.

9.3 Natural Period Effects

After removing the effects of V_{S30} scaling in the linear site amplification, a residuals analysis showed two distinct trends in the site amplification with respect to site natural period, T_{nat}. The residuals of the L1 amplification model for nine response spectral periods of interest are shown in Figure 9.15 as a function of the ratio of the response spectral period (the natural period of the oscillator used in the calculation of the response spectrum, T_{OSC}) to T_{nat}. The normalization of the X-axis of Figure 9.15 is used so the oscillator periods most strongly amplified by site natural periods when $T_{OSC} \approx T_{nat}$ occur at $T_{OSC}/T_{nat} \approx 1.0$. Two distinct effects are seen in the shape of the residuals in Figure 9.15. The first effect is a series of peaks between $T_{OSC}/T_{nat} = 0.2$ and $T_{OSC}/T_{nat} = 2$. The series of peaks in the residuals show the effects of site natural period modes of resonance, with the peak near $T_{OSC}/T_{nat} \approx 1.0$ being the most dominant first mode of resonance. The second effect is a decrease in amplification for $T_{OSC}/T_{nat} < 0.2$. This decrease in amplification corresponds to sites with high T_{nat} (deep sites), and reflects a decrease in the linear amplification of higher response spectral periods for these sites due to small strain damping in the soil profile. The model for the effects of site natural period is designed to capture these two trends.

The effects of the site natural period, $f(T_{nat})$, on site amplification for models shown in Table 9.2 is given in eq. 9.5.

$$T_{nat} = \begin{cases} T_{OSC} < 0.01 & c_6 T_{nat} \\ T_{OSC} \geq 0.01 & c_5 R + c_6 T_{nat} \end{cases} \quad \text{eq. 9.5}$$

where c_5 and c_6 are coefficients that describe the period dependent natural period effects, T_{OSC} is the response spectrum frequency under consideration, T_{nat} is the soil column natural frequency, and R is given by eq. 9.6.

$$R = \frac{2}{\sqrt{3\alpha}\pi^{\frac{1}{4}}}\left(1 - \frac{(\beta)^2}{\alpha^2}\right)\exp\left(\frac{(\beta)^2}{2\alpha^2}\right) \quad \text{eq. 9.6}$$

where α is a regression coefficient and β is given eq. 9.7.

$$\beta = \ln\left(\frac{T_{OSC}}{T_{nat}}\right) - \ln(0.81) \quad \text{eq. 9.7}$$

The c_5 component of site amplification model term shown in eq. 9.5 is an amplification term that takes the functional form of a Riker wavelet (commonly called the "Mexican Hat" wavelet) to capture the effects of the first mode of site resonance. The c_6 component of the amplification model term shown in eq. 9.5 is amplification linear with T_{nat} to capture the effects of soil damping for deep sites. The c_6 coefficient is a regression parameter evaluated at each response spectral period. The location that these site effect terms affect the model residuals is shown in Figure 9.15.

For response spectral periods near the site natural period ($T_{OSC} = T_{nat}$), the resonance effects of the first mode of amplification are captured in the site amplification model using the c_5 Riker Wavelet component of the site amplification component of eq. 9.6. The Riker wavelet function used in eq. 9.6 has three main components: peak amplitude, peak width, and peak location, described by model coefficients c_5, α, and β, respectively in eq. 9.6 and eq. 9.7. The effect of these coefficients on a characteristic Riker Wavelet is shown in Figure 9.16. Coefficients c_5 and α are regression parameters evaluated at each response spectral period. The Riker wavelet natural

period effect on amplification is not observed for very low periods ($T_{OSC} < 1.0$) as seen in Figure 9.15 and so is not included for this range in eq. 9.5.

The parameter β is evaluated as a difference of ratios: T_{OSC} / T_{nat} for the site and response spectral period under consideration, and $T_{OSC} / T_{nat} = 0.81$. The β term of eq. 9.7 moves the peak of the first natural mode of amplification to $T_{OSC} / T_{nat} = 0.81$. The value of $T_{OSC} / T_{nat} = 0.81$ was determined as the mean value of the location of the first peak of the residuals as shown in Figure 9.15 and is stable at the site periods of interest for geotechnical engineering.

The L3 amplification model is useful for comparison to the L1 amplification model as a function of V_{S30}. The effects of the natural period terms of the linear site amplification on the L1 V_{S30}-based amplification (i.e. the L3 amplification model) are shown in Figure 9.17 for four periods, 0.01 s (a), 0.1 s (b), 0.3 s (c), and 1.0 s (d). The L3 amplification model as described in Table 9.2 is a modification to the L1 amplification model created from regressing the natural period effects of site amplification after accounting for the V_{S30} scaling effects. The L5 amplification model will have a slightly different shape than the L3 amplification model as it has different terms for the linear V_{S30} effects. Figure 9.17 shows the natural period model effects using T_{nat} in the natural period model as a function of V_{S30} by $T_{nat} = V_{S30}/4H$ for three values of H: 30 m, 100 m, and 500 m. The selection of the values of H are representative of different depths to bedrock for soil profiles. In Figure 9.17(a) and Figure 9.17(d) the effects of the c_6 linear with T_{nat} amplification model term are most visible in the low V_{S30} range. The amplification model shows increase in site amplification at for deep sites (H = 500 m) at long periods and a decrease in site amplification for shallow sites (H = 30 m) at short period. The depth effects captured by the c_6 amplification term are similar to those captured by the depth-dependent linear amplification function in the L2 and L4 linear models. In Figure 9.17(b) and Figure 9.17(c) the first natural mode of the shallow sites (H = 30 m) captured by the c_5 Riker wavelet amplification is seen near V_{S30} values of 1000 m/s and 300 m/s, respectively. The effects of the T_{nat} linear amplification model terms on the range of simulation data captured can be seen by comparing Figure 9.18 and to Figure 9.2.

Models L3 and L5 in Table 9.2 include the effects of T_{nat} on linear site amplification and are shown graphically for several response spectral periods in Figure 9.18 and Figure 9.19,

respectively. Model coefficients for models f(T_{nat}) are shown graphically in Figure 9.20 through Figure 9.23 and provided in tabular form in APPENDIX A. Model residuals are shown in APPENDIX B.

9.4 Nonlinear Site Effects

The nonlinear site amplification, $f(NL)$, shown in Table 9.2 is given by eq. 9.8 and eq. 9.9, modified from Chiou and Youngs (2008) and Seyhan and Stewart (2014)

$$f(NL) = \begin{cases} f_2 \ln\left(\frac{I_r + f_3}{f_3}\right) & V_{S30} < V_c \\ 0 & V_{S30} \geq V_c \end{cases} \quad \text{eq. 9.8}$$

where f_2 and f_3 describe the nonlinear site effects and I_r is an intensity measure of the 3000 m/s bedrock condition ground motion that drives site nonlinearity. In the N1 and K1 models, I_r is the rock outcrop SA at the period of interest, and in the N2 and K2 models, I_r is the rock outcrop PGA. The f_2 coefficient is given as a function of V_{S30} in eq. 9.9.

$$f_2 = f_4\left[\exp\left\{f_5\left(\min\left(V_{S30}, V_{ref}\right) - 360\right)\right\} - \exp\left\{f_5\left(V_{ref} - 360\right)\right\}\right] \quad \text{eq. 9.9}$$

where f_4 and f_5 are coefficients that describe the effect of V_{S30} on the nonlinear site effects, V_{ref} is the reference rock condition of 3000 m/s, and V_c is a velocity condition where site amplification relative to the reference rock condition of 3000 m/s is not observed and maintains the same definition as in the V_{S30} scaling linear amplification model coefficient in eq. 9.3. For the N1 and N2 models, V_c as regressed in the L1 site amplification model is used, for the K1 and K2 models, V_c is regressed simultaneously with the nonlinear amplification coefficients.

The functional forms for the nonlinear site amplification given in eq. 9.8 and eq. 9.9have two departures from the functional form proposed in Chiou and Youngs (2008) and adapted in Seyhan and Stewart (2014): the removal of an intercept in eq. 9.8 and the adjustment of V_{ref} in eq. 9.9 to the CENA reference rock condition of 3000 m/s described in Hashash et al. (2014a) from the 1130 m/s in Chiou and Youngs (2008) and 760 m/s Seyhan and Stewart (2014) reference conditions. The form of eq. 9.8 given in Chiou and Youngs (2008) and Seyhan and Stewart (2014) nonlinear amplification model form is given in eq. 9.10 as:

$$f(NL) = \begin{cases} f_1 + f_2 \ln\left(\frac{I_r + f_3}{f_3}\right) & V_{S30} < V_c \\ 0 & V_{S30} \geq V_c \end{cases} \quad \text{eq. 9.10}$$

where f_1 is the model intercept coefficient.

The change in eq. 9.8 used in previous studies to eq. 9.10 used in this study is the removal of the f_1 intercept. In the simulation data of this study, direct comparisons are possible between linear and nonlinear site response analyses, and the simulations will converge for very low levels of earthquake intensity. In previous sets of simulations such as Seyhan and Stewart (2014), nonlinear site amplification is typically regressed as amplification as a function of ground motion intensity, where there is no observation of simultaneous linear and nonlinear site response for strong shaking To interpret the nonlinear amplification effects, the f_1 intercept describes the difference between the modeled and observed site amplification at the site (i.e. the residual in the site linear amplification. In this study, the nonlinear site amplification effects can be modeled independently of the linear site amplification model by direct comparison of the linear amplification from the LE site response analysis and the NL site response analysis, and the f_1 intercept term is not needed. The parametric study tree as shown in Figure 3.1 has one of each LE, EL and NL site response analyses conducted for each profile and motion combination. The LE simulations in this study represent the bounding case of site amplification where there is no soil nonlinearity, and are therefore independent of earthquake magnitude and represent linear site amplification. The nonlinear simulations include the effects of soil nonlinearity and the total amplification at the ground surface includes the effects of both linear and nonlinear site amplification. By comparing the LE analysis results to the NL analysis results, the nonlinear site amplification can be directly evaluated.

Two kinds of site amplification models with nonlinear site effects are provided, L+N type and K type, shown in Table 9.1 and Table 9.2.The L+N model type uses linear amplification evaluated from LE analyses (i.e. the L models), and nonlinear amplification model terms evaluated from the difference between NL analyses and the corresponding LE analyses. Figure 9.24 (a) and (b) show the fitting of the N1 and N2 model coefficients, respectively, to simulation data at 0.1 s. Figure 9.25 and Figure 9.26 show the N1 and N2 nonlinear site amplification term. Figure 9.31 and Figure 9.32 show the estimated K1 and K2 site amplification and simulated GQ/H nonlinear

site response for all simulations in this parametric study as a function of V_{S30}, respectively. The coefficients for the *f(NL)* amplification are shown graphically in Figure 9.27 through Figure 9.30 and provided in tabular form in APPENDIX A. Model residuals are shown in APPENDIX B.

9.5 Response Spectral Model Coefficients and Bounds

Coefficients for the amplification models were developed through nonlinear regression model with bounds using the 'port' algorithm of a nonlinear least-squared solver in R (R Core Team 2015). Regression bounds were selected to provide stable model behavior between response spectral periods. Coefficients for each model at each period were regressed independently, and no smoothing between periods was performed after coefficient fitting. Coefficients for 115 RS periods from 0.001 s to 10 s response spectral periods for each site amplification model are available in APPENDIX A, and the model residuals are available in APPENDIX B. The periods selected for calculation are the same periods used in the NGA-East site database (Goulet et al. 2014).

Figure 9.3 through Figure 9.7 shows the regressed linear amplification coefficients and fitting bounds for $f(V_{S30})$ for the L1, L4, L5, K1, and K2 coefficient models. Reparameterization during regression was needed to simultaneously constrain the coefficients V_c and V_L. V_L was reparameterized into the coefficient *diff* as shown in eq. 9.11 as a function of V_c.

$$V_L = \frac{V_c}{10^{diff}} \qquad \text{eq. 9.11}$$

V_L must be less than V_c and cannot be constrained with fixed values unless the maximum allowable value for V_L is less than the minimum allowable value of V_c. The regression coefficient *diff* can be constrained with values that are unaffected by V_c. Two different bounds are used for $f(V_{S30})$ fitting: one set of upper and lower bounds for the L1 coefficient model and one set for the L4, L5, K1, and K2 coefficient models based on the results of the L1 model fits.

The functional form selected for $f(V_{S30})$ is more complicated than models such as the Seyhan and Stewart (2014) model which has only two fitting coefficients, the value of V_c and the slope of the linear scaling with $\ln(V_{S30})$. The functional form for the V_{S30} scaling presented in this study can have combinations of parameters that produce similar amplification shapes,

particularly when factors other than V_{S30} are considered as for the L4, L5, K1, and K2 coefficient models. A trade off occurs when the curved region of the site amplification for V_{S30} values less than V_L is very gradual and approximates a region of linear with ln(V_{S30}) amplification and can be seen in the L1 amplification model shown in Figure 9.2 at 0.3 s and 0.6 s. The region of the amplification of both periods above $V_c \approx 1000$ m/s is flat and there is no increase in amplification with V_{S30}. Between V_{S30} values of 1000 m/s and 300 m/s, the binned mean of the simulation data. is similar in magnitude and shape between 0.3 s and 0.6 s and tends to increase nearly linearly with ln(V_{S30}) between V_{S30} values of 300 m/s and 1000 m/s . However, this linear region of V_{S30} amplification is captured by different components of the V_{S30} scaling between the two response spectral periods. For the L1 model at 0.3 s, V_L = 730 m/s and for 0.6 s V_L = 250 m/s. At 0.3 s, the amplification between 300 m/s and 1000 m/s V_{S30} is both above and below V_L, and the amplification is captured by both the straight and curved region of amplification in eq. 9.3. At 0.6 s, the amplification between 300 m/s and 1000 m/s V_{S30} is entirely above V_L, and the amplification is captured by only the straight region of amplification in eq. 9.3. At 0.3 s, the curvature of the amplification below V_L is gradual, and results in an approximately linear response between 300 m/s and 1000 m/s despite the very different V_L values of each of the periods. The coefficient bounds for the regression of the V_{S30} scaling amplification terms are chosen to minimize cases where similar shapes of V_{S30} amplification of adjacent periods are achieved and coefficients between adjacent periods are stable.

Figure 9.13 through Figure 9.14 shows the regressed linear amplification coefficient and fitting bounds for $f(Z_{Soil})$ for the L2 coefficient model. Positive values of c_4 indicate an increase in amplification as a function of depth while negative values indicate a decrease in amplification as a function of depth. Figure 9.13 shows similar trends in the depth effects of amplification for the L2 and L4 coefficient models as expected.

Figure 9.20 through Figure 9.23 shows the regressed linear amplification coefficients and fitting bounds for $f(T_{nat})$ for the L3, L5, K1, and K2 coefficient models. The c_5 and c_6 coefficients in the $f(T_{nat})$ amplification model linearly scale the Riker wavelet and amplification with T_{nat}, respectively, and the α coefficient modifies the width of the Riker wavelet. The c_6 coefficient has a similar effect on site amplification as the c_4 coefficient in the $f(Z_{Soil})$ amplification term. At low periods, the negative c_6 term causes a reduction in amplification for very soft or deep sites

with high natural period, and at higher periods, the positive c_6 term causes a relative increase in amplification for those sites.

9.6 Site Correction from 760 m/s to 3000 m/s

The site response analyses conducted in this parametric study are used to develop period-dependent coefficients of average amplification of sites with V_{S30} near 760 m/s relative to the 3000 m/s CENA bedrock condition. Figure 9.33 shows two models derived from linear elastic site response analyses that describe the amplification of sites with V_{S30} near 760 m/s. The models are period-dependent and are provided in tabular form in APPENDIX A.

The depth-independent coefficients shown in Figure 9.33 are calculated from the log average amplification of all linear elastic simulations for soil profiles with V_{S30} between 700 and 800 m/s. The depth-dependent coefficients shown in Figure 9.33 are calculated from the log average amplification of all linear elastic simulations for soil profiles withV_{S30} between 700 and 800 m/s for each depth bin considered in the parametric study tree in Figure 3.1. These coefficients represent the amplification for sites with a V_{S30} near 760 m/s relative to a 3000 m/s bedrock condition at some known depth. The calculated V_{S30} of all profiles used in these analyses includes soil material, weathered rock, and 3000 m/s bedrock material. A depth-independent model is also calculated for all profiles with V_{S30} between 700 m/s and 800 m/s.

The 760/3000 model presented in this study can serve as a way to correct site amplification models developed for a 760 m/s site condition to a 3000 m/s site condition or vice versa through the use of eq. 9.12.

$$ln(amp)_{760} = ln(amp)_{3000} - C_{760-3000} \qquad \text{eq. 9.12}$$

where $\ln(amp)_{760}$ is the site amplification relative to a 760 m/s reference condition, $\ln(amp)_{3000}$ is the site amplification relative to a 3000 m/s reference condition, and $C_{760\text{-}3000}$ is the mean amplification of sites with V_{S30} near 760 m/s relative to a 3000 m/s reference condition (i.e. the 760 to 3000 m/s correction provided in APPENDIX A).

A comparison of this site correction to other models is shown in Figure 9.34. The depth-dependent site amplification models for the 5 m, 30 m, and 1000 m and depth-independent

models are shown with the 760/3000 corrections from Yenier and Atkinson (2015) for 10 km and 100 km earthquake distance, for the FAS and M6 for 10 and 100 km earthquake distances from Boore and Campbell (2016) (which supersedes previous models by the lead author), and Graizer (2015). The models developed in this study and the models by Boore and Campbell (2016) show a relative peak in amplification near 0.1 s. The models of Yenier and Atkinson (2015) and Graizer (2015), which reflect shapes commonly used in GMM development, do not show this relative peak. The behavior of the Yenier and Atkinson (2015) models resembles the behavior of the 1000 m deep 760/3000 m/s model developed in this study.

9.7 Site-Specific Comparison of Amplification Model to Simulation Data

Regression coefficients and amplification models developed up to this point have been evaluated on the period-independent performance in capturing the ergodic site amplification behavior across all sites used in the parametric study and reducing trends observed in residuals. This section will compare the shape of the site amplification and response spectra from the regressed amplification models to computed site amplification for a single soil profile and motion combination and show that the individual site amplification behaviors are preserved in the amplification models. The amplification from the simulation for the soil profile will be compared to all similar analyses in the parametric study. An analysis is considered to have similar if it has V_{S30} and T_{nat} within 20%, the same depth to weathered rock, and a bedrock motion PGA within 30%.

The site response analysis under investigation is a randomization of the RS+YGdto+YGm characteristic V_S profile with 25 m of soil material above the 30 m gradient weathered rock zone model and negative $\varepsilon_{G/Gmax}$ from the nonlinear curve randomization. The soil profile has a V_{S30} of 377 m/s with T_{nat} of 0.36 s. This profile is paired with rock outcrop ground motion from NUREG (McGuire et al. 2001) 55Rab_B-KOD180 for an M 5.5 earthquake at 0-50 km distance and has a PGA of 0.4 g. The computed LE site amplification of the soil profile is shown in Figure 9.35(a) and the NL site amplification is shown in Figure 9.35(b). The computed LE response spectrum of the soil profile is shown in Figure 9.36 (a) and the NL response spectrum is shown in Figure 9.36 (b). There are 2676 similar simulations to the conditions represented by this soil profile.

The linear site amplification from the LE analysis is shown in Figure 9.35(a) and is compared to the L1, and L5 linear amplification functions and the linear response of similar soil sites. The L1 and L5 amplification models are shown as the preferred linear amplification models. The L5 models shows an increase in site amplification near the T_{nat} of the site, and lower amplification at the longer periods. Both the L1 and L5 model capture the observed trends in this site and for the similar simulations, but the L5 models shows the capability to capture the site response through the natural period effects.

The nonlinear site amplification from the NL analysis is shown in Figure 9.35(b) and is compared to the L1+N2, L5+N2, and K2 nonlinear amplification functions and the nonlinear response of similar soil sites. The simulation is for a bedrock ground motion with PGA of 0.4 g and nonlinear effects are expected and can be observed by the lower site amplification in the nonlinear amplification when compared to the linear amplification at high frequencies. Similar to the linear amplification in Figure 9.35(a), the L5+N2 amplification model does a better job of capturing the peak site amplification at T_{nat} of the soil column. The K2 and L5+N2 nonlinear amplification models are extremely similar at all periods.

The response spectra for these simulations are shown in Figure 9.36. The response spectra calculated for the site amplification models is computed as the product of the rock outcrop ground motion response spectra and the model amplification. Trends visible in Figure 9.35 between the amplification models are also observed in the response spectra. As seen in the rock outcrop ground motion in Figure 9.36, there is a relatively large amount of frequency content near 0.01 s. This feature does not result in large differences between the linear amplification model estimations and LE site response analysis, but is likely the cause of the differences between the NL analysis and nonlinear amplification models between 0.02 and 0.1 s.

9.8 Response of Shallow Sites

This study features simulations with a fine resolution of shallow bedrock depths to investigate site amplification behavior for shallow sites. As discussed in Section 2.2, the possibility of 3000 m/s reference rock in CENA near the ground surface or large, deep impedance contrasts creates a situation where a single value V_{S30} could represent a large number of possible site conditions. The amplification models developed above are developed from the entire simulation dataset of

both shallow and deep sites. This section evaluates differences in maximum achieved strain behavior for shallow sites compared to deeper sites and the efficacy of the RS amplification models in Table 9.1 in capturing the simulated amplification behavior of shallow sites. For the purposes of this evaluation, a site is considered shallow if it has weathered rock within 30 m or less from the ground surface.

9.8.1 Depth of Maximum Achieved Strain

The site V_S profiles used in simulations in this study feature monotonically increasing profiles, so the lowest values of V_S will be at the ground surface. The parametric study is developed such that the soil region of shallow profiles is truncated by a weathered rock zone at a selected range of depths and the top portion of the V_S profiles remain unchanged from a shallow site condition for deeper sites. For example, V_S profile of a site truncated to a weathered rock zone at 500 m has a similar profile truncated to a weathered rock zone at 30 m where the V_S in the top 30 m of each of these sites is identical. The variable depth to rock does not cause significant changes in the number of simulations with large strains for each soil column depth in NL site response analyses. The nonlinear amplification functions developed in this study are developed from NL simulations where the maximum shear strain achieved anywhere in the soil profile is less than 1 %. Figure 9.37 shows the distribution of these profiles as a function of soil depth bin (DB, depth to weathered rock zone). The total number of NL simulations with shear strains greater than 1 % is n = 33,916, 5.8% of the total number of NL simulations. As shown in Figure 9.37 these simulations are evenly distributed across all soil depth bins to weathered rock with the exception of the 0 m depth bin. The 0 m depth bin is the condition with high V_S weathered rock material near the ground surface, so lower strains in the NL site response analyses are expected for this V_S profile condition than the profile conditions with soil near the ground surface. Figure 9.37 suggests that the removal of simulations with NL shear strains greater than 1 % does not produce a depth bias the of the nonlinear amplification functions.

Across all NL analyses, the maximum achieved shear strain in the majority of simulations occurs in the top of the V_S profile near the ground surface. Figure 9.38 shows the location of maximum achieved shear strain in the NL site response analyses used in development of the nonlinear amplification functions (i.e. analyses with NL shear strains less than 1 %). Figure 9.38(a) shows

the distribution of maximum achieved strain location for all profiles in this study at all depths. The majority of maximum strains occur in the top 50 m. There is a bias to this plot as there are a disproportionate amount of simulations with soil depths less than or equal to 50 m (simulations with soil thicknesses 5, 10, 15, 20 25, 30, and 50 m) when compared to simulations with depths greater than 50 m (simulations with soil thicknesses 100, 500, and 1000 m, for a ratio of 7 shallower to 3 deeper). Even with this bias, there are very few NL simulations with maximum achieved shear strains occurring below 50 m. Figure 9.38(b) shows the same data as Figure 9.38(a), but rescaled to remove the data in the top 50 m and show the deeper data. There are simulations with peak maximum achieved strains below 50 m, but as seen in Figure 9.38(b), the number is significantly smaller than the number of simulations with maximum achieved strains in the top 50 m of the soil profile.

The behavior of the value of the maximum achieved strain in the NL site response analyses as a function of depth is shown in Figure 9.39. In Figure 9.39 the binned mean of the maximum value of strain is shown as a function of depth. The data in Figure 9.39 has a density of distribution as a function of depth as shown i of data in Figure 9.38. The binned values of maximum shear strain shown in Figure 9.39 do not show any trend with depth. The average values of the maximum shear strain achieved in the soil profiles appears to be independent of the depth that the maximum shear strain occurs for the analyses conducted in this study.

9.8.2 Linear Amplification Model Applicability to Shallow Sites

The linear and nonlinear RS amplification models developed in this chapter are derived from the dataset resulting from all simulations. The distribution of simulations as a function of depth are not necessarily representative of the relative distribution of site depths across CENA. The range of depths chosen for the simulations are representative of the range of site depths that could be expected in CENA, but the relative number of simulations with soil column depths less than 30 m is not necessarily representative of the fraction of sites in CENA with depths to weathered rock less than 30 m.

The effect of the relative distribution of sites as a function of depth is primarily a factor in the derivation of the L1 V_{S30}-based amplification model and its applicability to shallow sites. The L2 and L4 amplification models include a depth correction term for sites deeper than 30 m, so the

effect of these deeper sites on the amplification of the shallow sites is reduced. The L3 and L5 amplification models have model effects for site natural period which includes the effect of depth to weathered rock in the calculation. This section evaluates how well the L1 and L5 linear amplification models capture the site response of shallow simulations. The L1 model predictions with LE simulation results for seven response spectral periods for soil horizons of 5 m, 15 m, and 30 m are shown in Figure 9.40, Figure 9.41, Figure 9.42, respectively. The L5 model predictions with LE simulation results for seven response spectral periods for soil horizons of 5 m, 15 m, and 30 m are shown in Figure 9.43, Figure 9.44, Figure 9.45, respectively.

The L1 amplification model at 5 m depth shown in Figure 9.40 fails to capture the shape of the simulation data in two main ways. At high frequencies (Figure 9.40(a) and Figure 9.40(b), 0.001 s and 0.1 s, respectively) the amplification model under-predicts the amplification for high V_{S30} sites above 500 m/s. For intermediate periods (Figure 9.40(c) and Figure 9.40(d), 0.1 s and 0.2 s, respectively) the L1 amplification model falls in the range of amplification in the simulations, but fails to capture the strong peaks in the amplification data due to site period resonance seen near V_{S30} values of 800 m/s at 0.1 s in Figure 9.40(c), and near V_{S30} values of 500 m/s at 0.2 s in Figure 9.40(d). At periods longer than 0.6 s shown in Figure 9.40(e-g), the L1 amplification model tends to more accurately capture the magnitude and shape of the mean of the LE simulation than the shorter periods.

The L1 model estimated amplification for sites deeper than 5 m shown in Figure 9.41 and Figure 9.42 for 15 m and 30 m soil column depths, respectively has similar characteristics as the estimations for 5 m soil column depth in Figure 9.40. The under-prediction of site amplification at high frequencies for the L1 model occurs at all values of V_{S30} for the soil horizon depth of 15 m and for low values of V_{S30} for the soil horizon depth of 30 m. At the 15 m soil horizon depth the L1 amplification model fails to capture the resonance effects at 0.1 s and 0.2 s not of just the first mode at 800 m/s and 500 m/s, respectively, but of a second mode of site amplification that occurs near 350 m/s at 0.1 s and 200 m/s at 0.2 s. At 30 m depth and 0.1 s period, the first mode of site resonance seen at 5 m and 15 m depth is not observed in the simulation data, and the L1 amplification model under-predicts the amplification behavior below around 300 m/s V_{S30}. At periods 1.0 s and greater, the L1 amplification model slightly over-predicts the site amplification

below 500 m/s for both the 15 m and 30 m soil horizon depths. This over-prediction is more noticeable at 1.0 s than 10.0 s.

The L5 amplification model includes terms to capture the site natural period effects which are not included in the L1 amplification model. The additional model terms in the L5 amplification model are included to capture features of the amplification due to resonance effects such as the first mode of amplification. The coefficients of the V_{S30} and T_{nat} model terms are regressed simultaneously in the L5 amplification model and differences in the coefficients of the V_{S30} scaling behavior between the L1 and L5 amplification models are therefore expected.

The effects of the L5 model are most visibly seen in sites with 5 m depth at periods 0.1 s and 0.2 s, Figure 9.43(c) and Figure 9.43(d), respectively. At these periods, the resonance term of the L5 amplification model (the c_5 term in eq. 9.5) creates a hump in the shape of the amplification near the first natural mode of amplification of the sites. At 0.1 s, the $c_5$amplification term increases the magnitude of the estimate of amplification near the V_{S30} range most affected by resonance effects in the simulation data. However, the magnitude of c c_{56} model term is not large enough to capture the full height of the peak in the simulation data due to resonance. At 0.2 s in Figure 9.43(d), the L5 amplification does a better job capturing both the shape and range of the simulation data than at 0.1 s. The estimates of the L5 amplification model for 5 m depth at 0.001 s and 0.01 s in Figure 9.43(a) and Figure 9.43(b), respectively, is similar to the L1 amplification model shown in Figure 9.40. At periods greater than 0.2 s in Figure 9.43, the estimate of the L5 amplification model is closer to the simulation data than the L1 amplification model at the corresponding periods shown in Figure 9.40.

At short periods of 0.001 and 0.01 s for depths of 15 m and 30 m the L5 amplification model does not have the same biases in estimated amplification as the L1 amplification model. The underestimation of the L1 amplification model at these periods in Figure 9.41(a) and (b) and in Figure 9.42(a) and (b) underestimate the amplification at low V_{S30}. The L5 amplification model produces a better fit of the amplification across the entire range of V_{S30} values as shown in Figure 9.44(a) and (b) and in Figure 9.45(a) and (b). This improvement of behavior comes from the c_6 model term in eq. 9.5 which produces higher amplification for sites with low natural periods for short RS period response.

In Figure 9.44(b) and (c) and Figure 9.45(c) and (d) the simulation data shows multiple peaks in the site amplification. For these periods, the peak occurring at the highest V_{S30} is the peak corresponding to the first natural mode of amplification. The L5 amplificaion model only includes a term to capture the first mode of amplification occurring at $T_{nat}/T_{OSC} = 0.81$ as outlined above. The L5 amplification model is not calibrated for these higher order peaks and does not reproduce the higher order peaks, shown for example in Figure 9.44(d) near $V_{S30} = 200$ m/s. At longer periods of 0.6, 1.0 and 10.0 s for depths of 15 m and 30 m the L5 amplification model shows improvements over the L1 amplification model in capturing both the shape and magnitude of amplification.

The L5 amplification model provides improvements to the L1 amplification model in capturing amplification behavior of shallow sites. At low periods, the c_5 term of the L5 amplification model increases the amplification of shallow sites with low V_{S30} and removes bias in the amplification present at shallow sites with the L1 amplification model. At intermediate periods where resonance effects are present in the site amplification, the L5 model reproduces peaks in amplification that approximates the height and location of the peak in the simulated amplification. At long periods, the L5 amplification model shows improvements over the L1 amplification model in the shape and magnitude of amplification.

Even with these improvements, the L5 amplification model still fails to capture some features of shallow sites amplification including the magnitude of resonance peaks and higher order modes of amplification. Natural period resonance peaks produced by the L5 amplification model do not capture the full height of the peaks seen due to resonance in the site amplification data for some shallow sites. The height of the resonance peak in the L5 amplification model is c_5 model term and is regressed as a constant for each response spectral period. Shallow sites where the resonance effects may be expected to be stronger than deep sites are not given any additional special consideration, and the peak height produced by the L5 amplification model is influenced equally by shallow and deep sites. Additionally, the resonance peaks produced by the L5 amplification model are calibrated to the location of the first mode of amplification. While the L5 amplification model is able to capture the first mode of site resonance, the model has not been expanded to other natural modes of amplification which can be seen in the amplification for shallow sites.

9.9 Comparison of Site Amplification Models to Published Models

This study presents a suite of site amplification models that feature functional forms that depart from established literature, particularly in the interpretation of V_{S30} scaling effects, and have a reference V_S condition of 3000 m/s. Despite these differences the models presented in this study have similar trends in amplification as established amplification models in literature. This section presents the amplification models produced from the CENA simulations. Two sets of comparisons to established models are presented. One set comparing the predicted site amplification as a function of period for sites of varying V_{S30}, and the second comparing the site amplification functions at periods of 0.2 s and 1.0 s as a function of V_{S30}. The spectral periods of 0.2 and 1.0 s are chosen as periods of primary interest for use in building codes (BSSC 2015).

9.9.1 Comparison Period-dependent Amplification

The amplification produced by the L1 amplification model presented in this study is compared to other linear amplification models in the WUS and CENA in Figure 9.46 for sites with V_{S30} of 200 m/s, 400 m/s, and 760 m/s as a function of period. The literature models chosen for comparison are the Boore et al. (2014) (abbreviated as BSSA14), Al Noman and Cramer (2015), and Graizer (2015). The BSSA14 and Al Noman and Cramer (2015) models use linear V_{S30} scaling for a 760 m/s reference condition, with the BSSA14 model derived for active crustal regions, and the Al Noman and Cramer (2015) model derived for CENA conditions. Both models have been adjusted to a 3000 m/s reference condition using eq. 9.12 and the 760/3000 correction procedure described in this report. The Graizer (2015) amplification model uses similar but not strictly linear V_{S30} scaling and is developed for a hard rock reference condition so is not corrected to a 3000 m/s condition as the other models.

At all levels of V_{S30} shown, the Al Noman and Cramer (2015) model shape is strongly influenced by the 760/3000 correction. For a V_{S30} of 760 m/s the BSSA14, Al Noman and Cramer (2015), and L1 amplification model converge to the 760/3000 correction, but the L1 amplification model and BSSA14 amplification model show departures from this shape for V_{S30} values of 200 and 400 m/s. The Graizer (2015) amplification model has a similar shape to the 760/3000 m/s amplification at a V_{S30} of 760 m/s, but lacks the relative peak in amplification at 0.1 s.

The L1 amplification model shows the largest departure from the other amplification models at 200 m/s where it produces lower, negative amplification for short periods. The likely cause of this is the damping of the relatively large amount of high frequency content present in the rock outcrop ground motions used in this study not present in other regions. The linear V_{S30} scaling of the BSSA14, Al Noman and Cramer (2015), and Graizer (2015) do not feature functional forms that can capture any de-amplification at low V_S values. For the higher V_{S30} of 400 m/s, the de-amplification effects of the L1 model are less pronounced, and it falls within the same range of behavior as the other literature models.

A comparison of the N2 amplification model with PGA-driven site nonlinearity is compared to the nonlinearity of the BSSA14 model corrected to a 3000 m/s condition in Figure 9.47. The L1+N2 and BSSA14 site amplification for a site with V_{S30} of 300 m/s for rock outcrop PGA values of 0 g, 0.1 g, 0.5 g, and 1.0 g is shown in Figure 9.47(a). The amplification corresponding to a 0 g PGA rock outcrop condition is considered as the linear site amplification condition of the site (e.g. the site amplification is not dependent on the intensity of the rock outcrop ground motion). The nonlinear site amplification for the N2 and BSSA14 models for the same site conditions is shown Figure 9.47(b). When nonlinearity is added to the L1 site amplification model as seen in Figure 9.47(a), the negative amplification at higher periods is greatly increased, while the BSSA14 model does not result in any negative amplification even for strong shaking. The N2 amplification model shows more site nonlinearity than the BSSA14 model and consistently stronger nonlinear effects at short periods than long periods. The BSSA14 model has the strongest nonlinear effects between 0.1 s and 1.0 s and less nonlinear effects at shorter periods.

9.9.2 Comparison of Amplification Functions at 0.2 s and 1.0 s

The amplification models in this study produce similar amplification behaviors as other established models at spectral periods of 0.2 s and 1.0s. The response of the site amplification models at these periods is of particular importance for the BSSC (2015) NEHRP site coefficients used in US building code design.

Linear site amplification as a function of V_{S30} is shown for several models at periods of 0.2 s and 1.0 s in Figure 9.48(a) and (b) respectively. The models shown are two models from CENA

and two models from the WUS. The CENA models shown are: the L1 amplification model developed in this study, the amplification factors for 30 m deep sites in the Mississippi Embayment with rock outcrop intensity less than 0.25 g fromMoon et al. (2016). The WUS models shown are: the 2015 NEHRP site amplification coefficients (BSSC 2015) for rock outcrop intensity less than 0.25 g, and the Seyhan and Stewart (2014) linear amplification model. The Seyhan and Stewart (2014) model and the NEHRP coefficients were corrected from a760 m/s reference condition to a 3000 m/s condition using the procedure in Section 9.6. In Figure 9.48(a). the amplification models have similar responses between V_{S30} values of 300 m/s and 1000 m/s, but deviate at both higher and lower V_{S30}. The L1 amplification model is the only model that estimates no amplification (e.g. ln(amp) = 0) at very high V_{S30}. The adjustment of the Seyhan and Stewart (2014) and NEHRP coefficients to a 3000 m/s reference condition causes the models to overestimate site response at high V_{S30}. At low V_{S30}, the L1 amplification model decreases at low V_{S30} while the Western models continue increasing. The L1 model's decrease in amplification at low V_{S30} produces values similar to the amplification coefficients from Moon et al. (2016). At 1.0 s all models show similar trends with V_{S30} with the CENA models producing lower amplification than the WUS models.

The depth dependency of the same amplification functions as a function of site depth is shown for RS periods of 0.2 s and 1.0 s in Figure 9.49 and Figure 9.50, respectively. The WUS models shown do not have depth dependency and are presented as vertical lines. Moon et al. (2016) presented amplification coefficients as a function of depth at discrete intervals. The L2 amplification model shown in the figures is used to show the effects of including depth to the V_{S30} model shown in Figure 9.48. Depth-dependent amplification is shown for four values of V_{S30} corresponding to NEHRP site classes (BSSC 2015): Site class B (a), Site class C (b), Site class D (c), and Site Class E (d). In Figure 9.49, both CENA models show a decrease in amplification with increasing site depth. The L2 model is more similar to the WUS models than the Moon et al. (2016) model at the ground surface, but at depth the CENA models begin to converge. In Figure 9.50 both CENA models show an increase in amplification with increasing site depth. A notable difference between the Moon et al. (2016) and L2 amplification model is the rate of increase in surface amplification. The Moon et al. (2016) model increases rapidly at

depths less than 200 m, then remains fairly constant at greater depth. The L2 model increases continuously as a function of depth.

A comparison of the nonlinearity of the site amplification models described above is shown as a function of rock outcrop PGA and V_{S30} in Figure 9.51. The NEHRP and Moon et al. (2016) models do not explicitly include nonlinear amplification. For these models, the nonlinear amplification is shown as the difference between amplification at any value of PGA and the amplification of the lowest value of PGA in the model. The N2 amplification model (PGA-driven nonlinearity) and the Seyhan and Stewart (2014) have continuous functions for nonlinear amplification. At 0.2 s in Figure 9.51(a), the N2 and Seyhan and Stewart (2014) amplification models have very similar levels of site nonlinearity which is larger than the nonlinearity of the NEHRP and Moon et al. (2016) coefficients. At 1.0 s in Figure 9.51(b), all amplification models have a similar amount of nonlinearity between 0.1 g and 0.8 g rock outcrop PGA.

The linear amplification models presented in this study show similar behaviors to previous models when evaluated as a function of V_{S30}, depth, and site nonlinearity.

9.10 Response Spectral Site Amplification Model Error Evaluation

The linear and nonlinear site amplification modes developed in this study are modular functions intended to be usable with different amounts of site information. If site natural period or depth to weathered rock are available, more advanced model forms for linear (L models) amplification can be used. The nonlinear site amplification models (L+N models and K models) are provided for two different drivers of nonlinearity: PSA and PGA. Of the suite of models provided, only the L5+N1 and K1 models and L5+N2 and K2 models are derived for the same site and motion information (V_{S30}, T_{nat}, and either PSA or PGA, respectively). The relative total error between the models is used to make recommendations for model use.

The sum of squares error for the linear models L1-L5 is shown in Figure 9.52. The error is not normalized to the number of degrees of freedom of each of the models and is calculated from the difference between the LE simulations and estimated response from the regressed linear amplification models. The L1 model which only uses V_{S30} as a parameter has the highest error of all other linear models. The effect on total error of adding depth to weathered rock (Z) and T_{nat} to

the regressed L1 V_{S30} model is shown in the L2 and L3 lines, respectively in Figure 9.52. In the range from 0.2 to 0.7 s there is little dependency of the soil column depth on amplification in the L2 model. Above this period range the reduction in model error comes from the increase in site amplification for deeper sites, and below this range, the reduction in model error comes from the reduction in site amplification for deeper sites. The L3 model shows a decrease in model error by including the effects of T_{nat} at all periods from the L1 model. Below 0.1 s the L2 model has lower error than the L3 model, but the L3 model has lower total error at higher periods.

The effect on total error of simultaneously regressing Z and T_{nat} with V_{S30} is shown in the L4 and L5 lines, respectively, in Figure 9.52. The L4 and L5 models show improvement in total error from the L2 and L3 models, respectively. The model coefficients for the L4 and L5 models are regressed simultaneously instead of sequentially, so improvement in total error at each period is expected. At 3 s, the L5 model has higher error than the L3 model as a result of the resolution of regression coefficient convergence. For frequencies in the range from 0.2 to 0.7 s, the L4 model shows little improvement to the L1 model in capturing site amplification. Above and below this period range, the L4 model has lower total error than the L1 and L2 models. The L5 model has the lowest total error of all models. The L5 model has lower total error at periods below 0.2 s than all other models. Above 0.2 s, the L5 model has similar total error to the L3 model, but still has lower total error than the L1, L2, and L4 models.

The effects of regressing additional linear models including the effects of V_{S30}, Z, and T_{nat} were additionally evaluated. No significant improvement for the amplification models as a function of V_{S30}, Z, and T_{nat} were observed over the models as a function of just V_{S30} and T_{nat}. The functional form for the T_{nat}-dependent amplification includes not just effects around the natural period (the Riker wavelet component) but also a component of site amplification that scales linearly with T_{nat}. The linear component of the T_{nat} functional form is sufficient to capture the depth-dependent site amplification effects. For model usage, if the V_S profile is available for a site so the depth to weathered rock is known, then the natural period of the site can also be calculated or reasonably estimated from the V_S and depth information. Model coefficients for the combined Z and T_{nat} models are not provided.

The sum of squares error for the purely nonlinear components of the site amplification models (N component of amplification) is shown in Figure 9.53. The sum of squared error is calculated by comparing the difference between the NL and LE analyses and the regressed N models. The difference between PSA and PGA as the driver of nonlinearity for the N1 and N2 models, respectively, has little effect on the error on the nonlinear component of amplification.

The sum of squares error for the nonlinear amplification models (L+N and K amplification models) is shown in Figure 9.54 and Figure 9.55. Figure 9.55(a) shows the nonlinear amplification models using PSA as the driver of nonlinearity (L+N2 and K2 models) and Figure 9.55(b) shows the nonlinear amplification models using PGA as the driver of nonlinearity. The sum of squares error is calculated from the difference between the NL simulation data and the regressed amplification models. The L+N nonlinear amplification models demonstrate similar trends as the L linear amplification models. The models with the highest error are the models where the linear component is dependent only V_{S30} and the linear component of models with the lowest error are dependent on V_{S30} and T_{nat} with T_{nat} being more effective than Z when regressed simultaneously with V_{S30}. The similarity in the error of the N1 and N2 amplification models shown in Figure 9.53 is evidenced in Figure 9.55 by the similarity between of the L+N amplification models in Figure 9.55(a) and Figure 9.55(b), respectively. The error of the K nonlinear amplification models shown in Figure 9.54 is lower than any of the L+N nonlinear amplification models. The linear and nonlinear model coefficients of the K models are regressed simultaneously, and, as expected, have the lowest total error of all nonlinear amplification models. The K2 model using PGA as the driver of nonlinearity has lower total error than the K1 nonlinear amplification model using PSA as the driver of nonlinearity.

The preferred models for use in modeling linear site amplification are the L1 and L5 amplification models. When only V_{S30} is available, the L1 amplification model is the only usable model presented in this study. When site natural period is available, the L5 amplification model provides significant improvement to the estimation of site amplification. When the V_{S30} scaling effects from a different amplification model are used, the L2 and L3 site amplification model terms for depth and T_{nat}, respectively, should be used. There is no preference between the N1 and N2 amplification models for nonlinear amplification, and the models produce similar results when PSA or PGA is used as the driver of nonlinearity.

The K1 and K2 models produce the lowest total error for estimating the nonlinear site amplification, the model results are very similar to the L5+N models, and it is preferred to maintain the independence of the linear and nonlinear site amplification model terms.

9.11 Applicability Range of Response Spectral Models

The site amplification models developed in this study are developed from 1-D site response analyses and are fundamentally limited in the types and ranges of site effects that are captured. Limitations on the site response analyses come from the assumptions required to perform the site response calculation (assumptions of 1-D amplification), and the limitations of the models and inputs to the calculation scheme. The amplification functions provided in this study are for the base-case site amplification absent of multidimensional and basin effects, and as such, the site amplification is denoted as ($F_{S,B}$) in eq. 9.2. The 1-D assumption of the site response begins to break down for that result in generating high shear strains within the soil profile during site response analysis. Limitations on the applicability range of the site amplification models in this study come from judgements of the efficacy of 1-D site response simulations to produce realistic site responses. The amplification models are limited by an intensity measure (PGA), a soil profile stiffness measure (V_{S30}) and a metric that estimates shear strain levels that will be generated within the soil profile.

The first bound of applicability of the site amplification functions presented in this study is the limit on ground motion intensity. The response spectral models presented in Table 9.2 are applicable for rock outcrop PGA values < 1.0 g. Ground motion intensities greater than PGA = 1.0 are uncommon and represent extreme earthquake conditions. For these extreme conditions, the assumption of 1-D site response begins to break down as higher-dimension effects such as surface waves and basin effects become pronounced in the site response.

The second bound of applicability of the site amplification functions presented in this study is the limit on profile stiffness. The response spectral models presented in Table 9.2 are applicable for sites with V_{S30} < 200 m/s. Sites with V_{S30} values less than 200 m/s require detailed modeling of the soil V_S structure and shear stress-strain behavior to accurately describe site behavior. The bound of 200 m/s is similar to the boundary of V_{S30} = 180 m/s between NEHRP (BSSC 2009) site classes D and E. Sites with lower V_{S30} than 200 m/s generally feature at least one region of

soft soil that requires detailed modeling to accurately capture nonlinear soil behavior. The shape of the V_S profile for these soft sites also becomes important, as even small impedance contrasts in layers of V_S become crucial to capture with site response analyses as strains can concentrate and layer interfaces and produce base-isolation behavior within the soil profile.

The third and final bound of applicability of the site amplification functions presented in this study is a limit on estimated peak shear strain within the soil profile at any point during shaking. The relationship between shear strain index $I_y = PGV/V_{S30}$ and maximum shear strain within the soil profile in a nonlinear site response analysis investigated by Kim et al. (2015) shows a relationship that can be used to estimate an I_y value that corresponds to a maximum strain in site response. A comparison of the I_y and maximum shear strain values in NL analyses from Kim et al. (2015) and this study are shown in Figure 9.56. The shear strain index is evaluated from the PGV of the rock outcrop ground motion and the V_{S30} of the soil profile under consideration and can be evaluated to produce an estimate of shear strain without the need to conduct a site specific nonlinear site response analysis. The I_y applicability limit of the site amplification functions is based on a range of I_y of analyses that produce shear strains near 1%. The 1% shear strain bound is selected as a way of representing a priori the analyses used in the development of the nonlinear amplification functions.

For all nonlinear amplification models, the simulations used were the GQ/H analyses with maximum strains resulting from the site response analysis in any soil layer being less than 1% shear strain. For the GQ/H analyses with shear strains larger than 1%, the N model terms are regressed without effects from the corresponding linear elastic simulation. The K models are regressed from only NL analyses with maximum shear strains of less than 1%. I_y as a function of maximum strain in the NL analyses of all simulations conducted in this study is shown in Figure 9.57 with the data binned by I_y and maximum strain and ± 1 standard deviation error bars. The data in Figure 9.57 binned by I_y in the range of 0.1 % I_y to 0.2 % I_y at + 1 standard deviation (the right horizontal error bars in Figure 9.57) is close to the bound of 1 % NL analysis shear strain used in regression of the nonlinear site amplification models. The I_y range of 0.1 % < I_y < 0.2 % is the upper bound of applicability of the I_y of applicability of the site amplification models presented in this study. The simulations conducted in this study that fall within or above the limiting I_y range are shown graphically in Figure 9.58 and Figure 9.59. Figure 9.58 shows the

count and distribution of simulations used in regression of the nonlinear amplification terms and the subset of that data within the limiting upper bound range of I_y. Of the simulations used in regression, 12.8 % have Of the simulations used in regression, 12.8 % have I_y greater than 0.1 % and 3 % have I_y greater than 0.2 %. The distribution of simulations as a function of V_{S30} and PGV used in regression of the nonlinear amplification terms and the associated I_y range is shown in Figure 9.59. Figure 9.59 shows that there is still coverage of data in the low V_S range that does not also have high enough PGV to exclude those sites from the bounds of applicability of this study.

Table 9.1: Amplification coefficient models.

Amplification Component	Simulation Data	Component Subscript	Component Model Terms
V_{S30}	$\ln(amp)_{LE}$	L1	$f(V_{S30})_{L1}$
Z_{Soil} (after V_{S30})		L2	$f(V_{S30})_{L1} + f(Z_{soil})_{L2}$
T_{nat} (after V_{S30})		L3	$f(V_{S30})_{L1} + f(T_{nat})_{L3}$
$V_{S30} + Z_{Soil}$ (simultaneous)		L4	$f(V_{S30})_{L4} + f(Z_{soil})_{L4}$
$V_{S30} + T_{nat}$ (simultaneous)		L5	$f(V_{S30})_{L5} + f(T_{nat})_{L5}$
NL (PSA)	$\ln(amp)_{GQ/H} - \ln(amp)_{LE}$	N1	$f(NL)_{N1}$
NL (PGA)		N2	$f(NL)_{N2}$
$V_{S30} + T_{nat}$ + NL(PSA) (simultaneous)	$\ln(amp)_{GQ/H}$	K1	$f(V_{S30})_{K1} + f(T_{nat})_{K1} + F(NL)_{K1}$
$V_{S30} + T_{nat}$ + NL(PSA) (simultaneous)		K2	$f(V_{S30})_{K2} + f(T_{nat})_{K2} + F(NL)_{K2}$

Table 9.2: Response Spectral Amplification Models from simulations.

Amplification Model	Model Terms	Amplification Type
L1	$f(V_{S30})_{L1}$	Linear
L2	$f(V_{S30})_{L1} + f(Z_{soil})_{L2}$	Linear
L3	$f(V_{S30})_{L1} + f(T_{Nat})_{L3}$	Linear
L4	$f(V_{S30})_{L4} + f(Z_{soil})_{L4}$	Linear
L5	$f(V_{S30})_{L5} + f(T_{Nat})_{L5}$	Linear
L1 + N1	$f(V_{S30})_{L1} + f(NL)_{N1}$	Nonlinear (PSA)
L2 + N1	$f(V_{S30})_{L1} + f(Z_{soil})_{L2} + f(NL)_{N1}$	Nonlinear (PSA)
L3 + N1	$f(V_{S30})_{L1} + f(T_{Nat})_{L3} + f(NL)_{N1}$	Nonlinear (PSA)
L4 + N1	$f(V_{S30})_{L4} + f(Z_{soil})_{L4} + f(NL)_{N1}$	Nonlinear (PSA)
L5 + N1	$f(V_{S30})_{L5} + f(T_{Nat})_{L5} + f(NL)_{N1}$	Nonlinear (PSA)
L1 + N2	$f(V_{S30})_{L1} + f(NL)_{N2}$	Nonlinear (PGA)
L2 + N2	$f(V_{S30})_{L1} + f(Z_{soil})_{L2} + f(NL)_{N2}$	Nonlinear (PGA)
L3 + N2	$f(V_{S30})_{L1} + f(T_{Nat})_{L3} + f(NL)_{N2}$	Nonlinear (PGA)
L4 + N2	$f(V_{S30})_{L4} + f(Z_{soil})_{L4} + f(NL)_{N2}$	Nonlinear (PGA)
L5 + N2	$f(V_{S30})_{L5} + f(T_{Nat})_{L5} + f(NL)_{N2}$	Nonlinear (PGA)
K1	$f(V_{S30})_{K1} + f(T_{Nat})_{K1} + f(NL)_{K1}$	Nonlinear (PSA)
K2	$f(V_{S30})_{K2} + f(T_{Nat})_{K2} + f(NL)_{K2}$	Nonlinear (PGA)

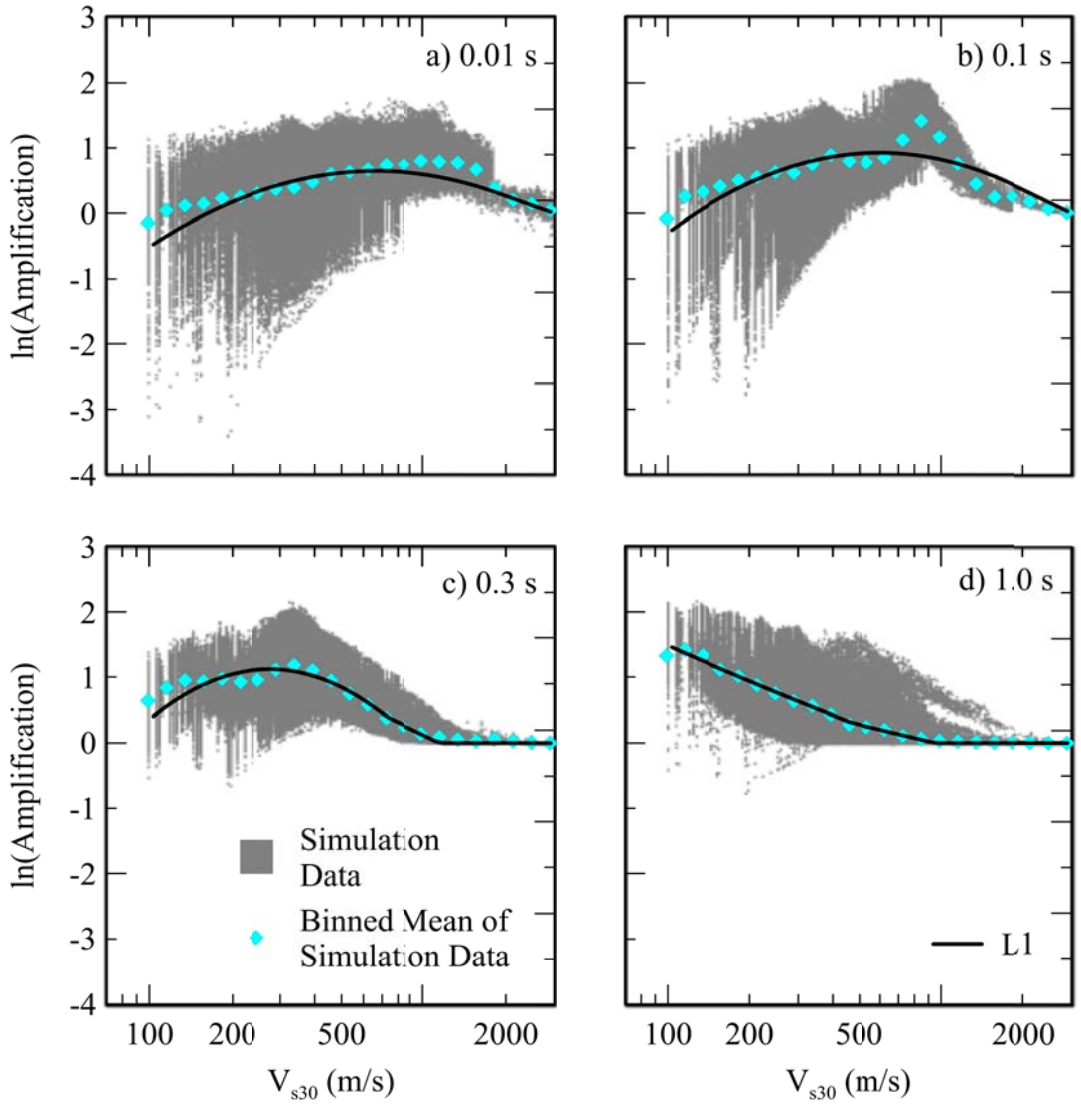

Figure 9.1: LE Simulation data and L1 amplification model at response spectral periods 0.01 s (a), 0.1 s (b), 0.3 s (c), and 1.0 s (d).

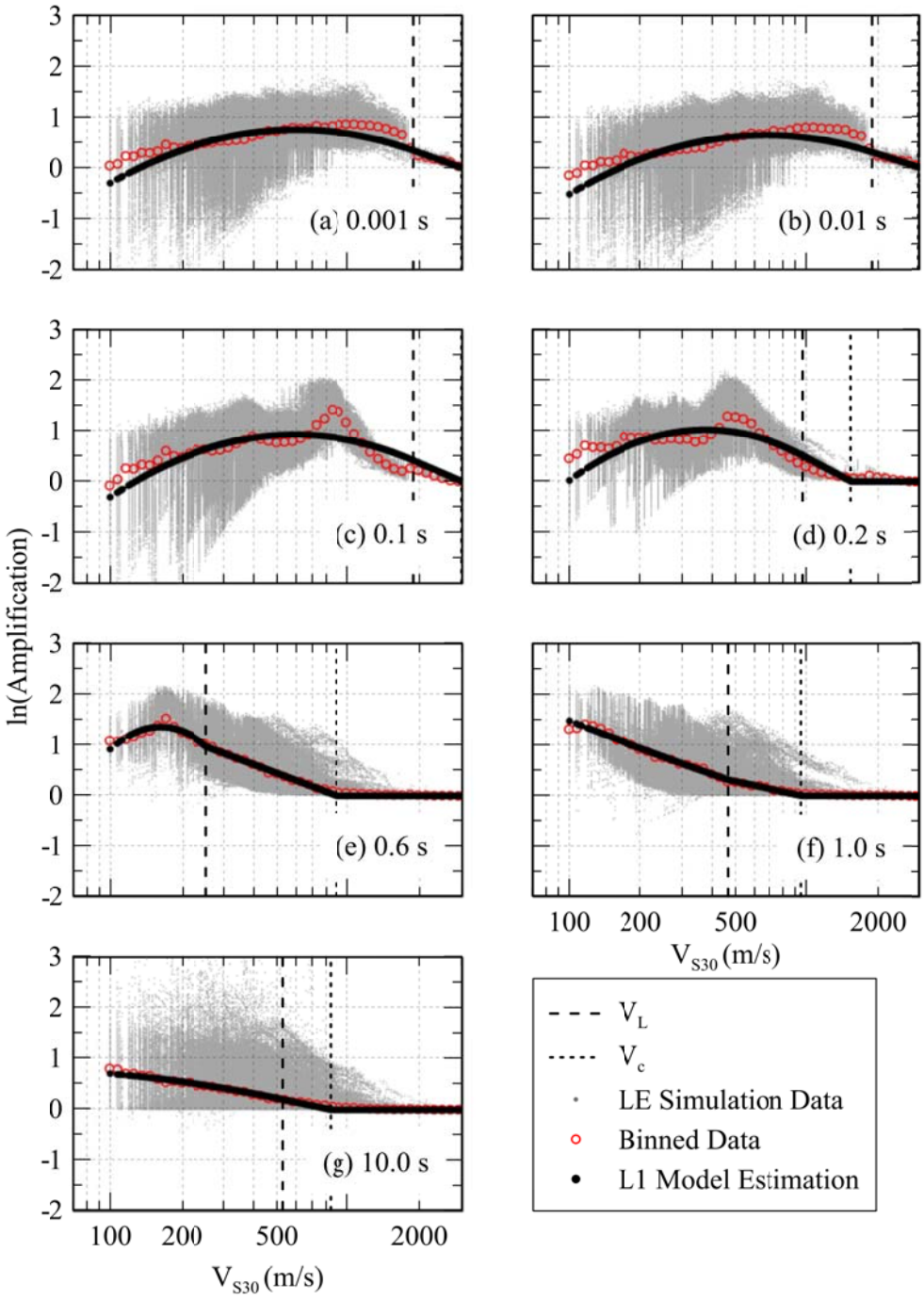

Figure 9.2: L1 Site Amplification Function for response spectral periods 0.001, 0.01, 0.1, 0.2, 0.3, 0.6, 1 and 10 s.

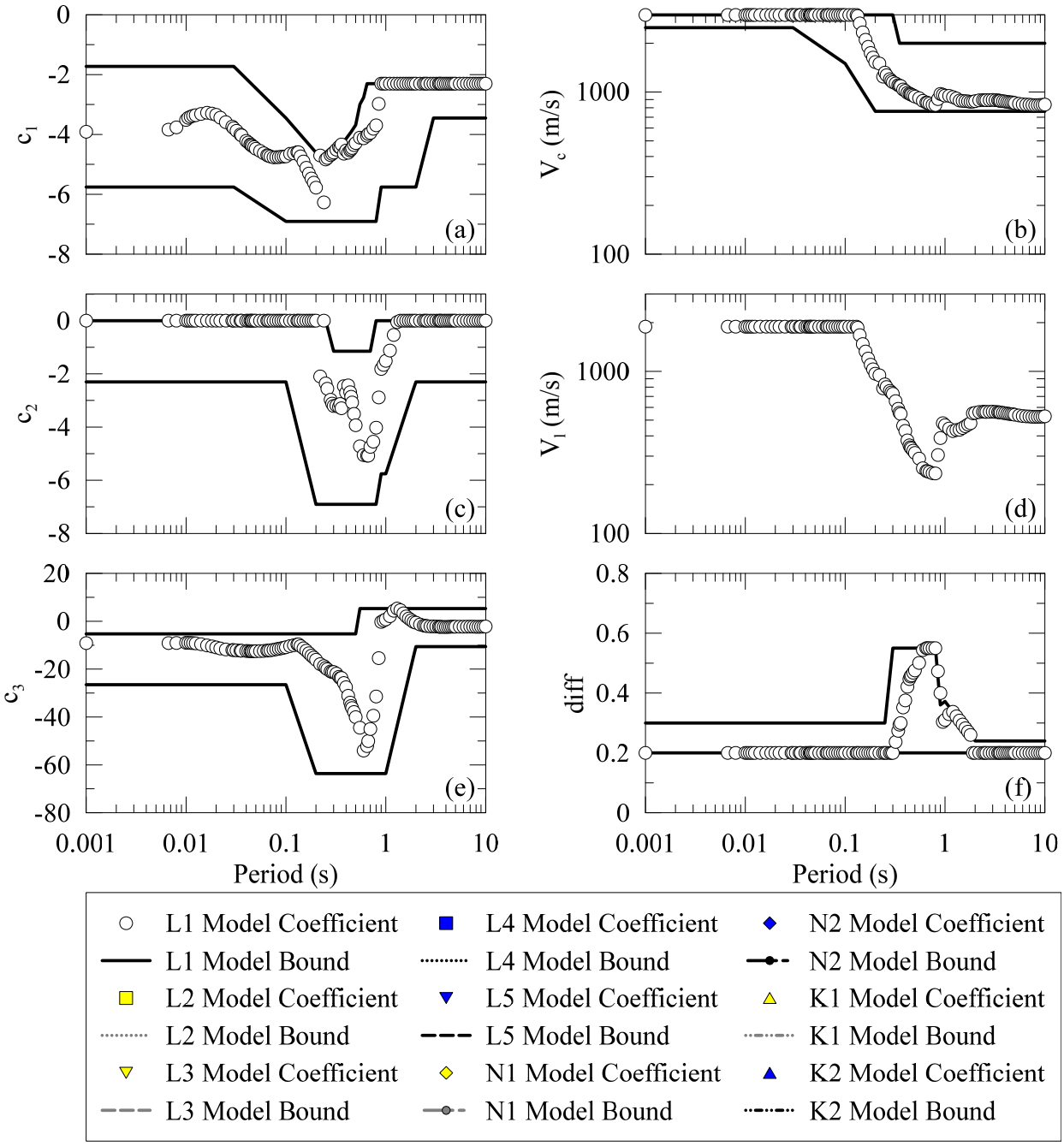

Figure 9.3 L1 model coefficients and bounds for $f(V_{S30})$ c_1 (a), c_2 (c), c_3 (e), V_c (b), V_1 (d), and *diff* (f).

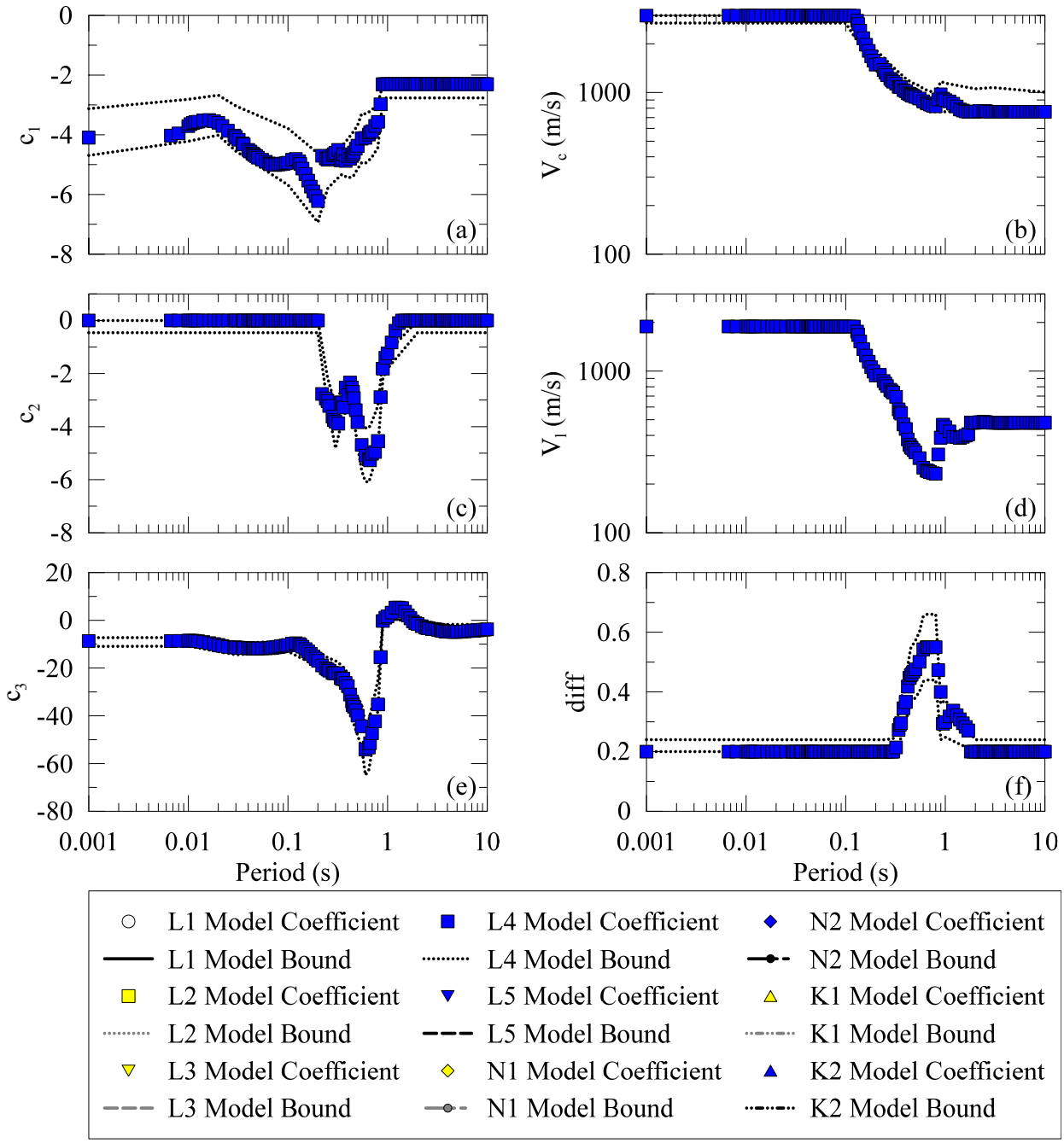

Figure 9.4: L4 model coefficients and bounds for *f(V$_{S30}$)* c_1 (a), c_2 (c), c_3 (e), V_c (b), V_1 (d), and *diff* (f).

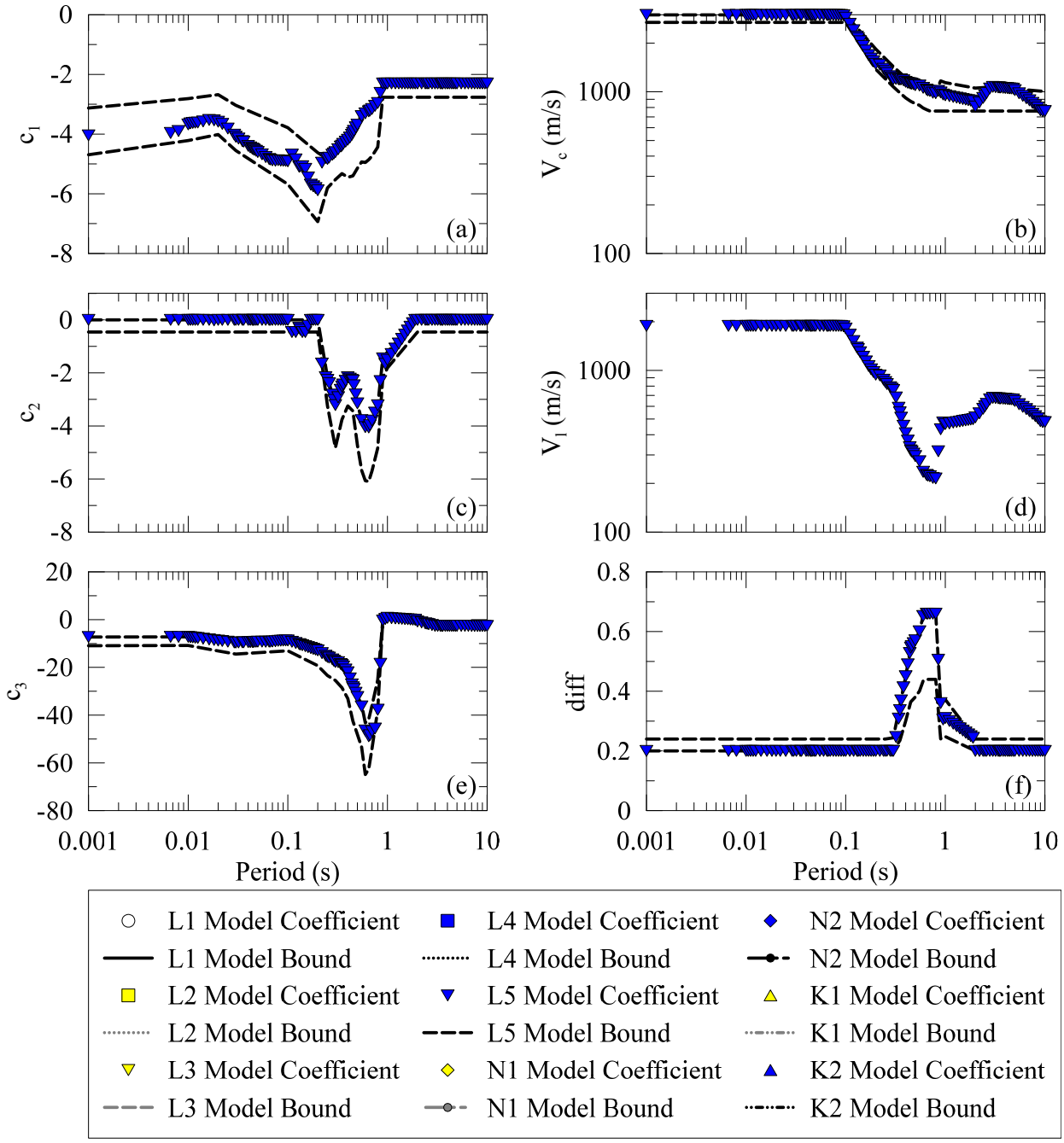

Figure 9.5 L5 model coefficients and bounds for *f(V$_{S30}$)* c_1 (a), c_2 (c), c_3 (e), V_c (b), V_1 (d), and *diff* (f).

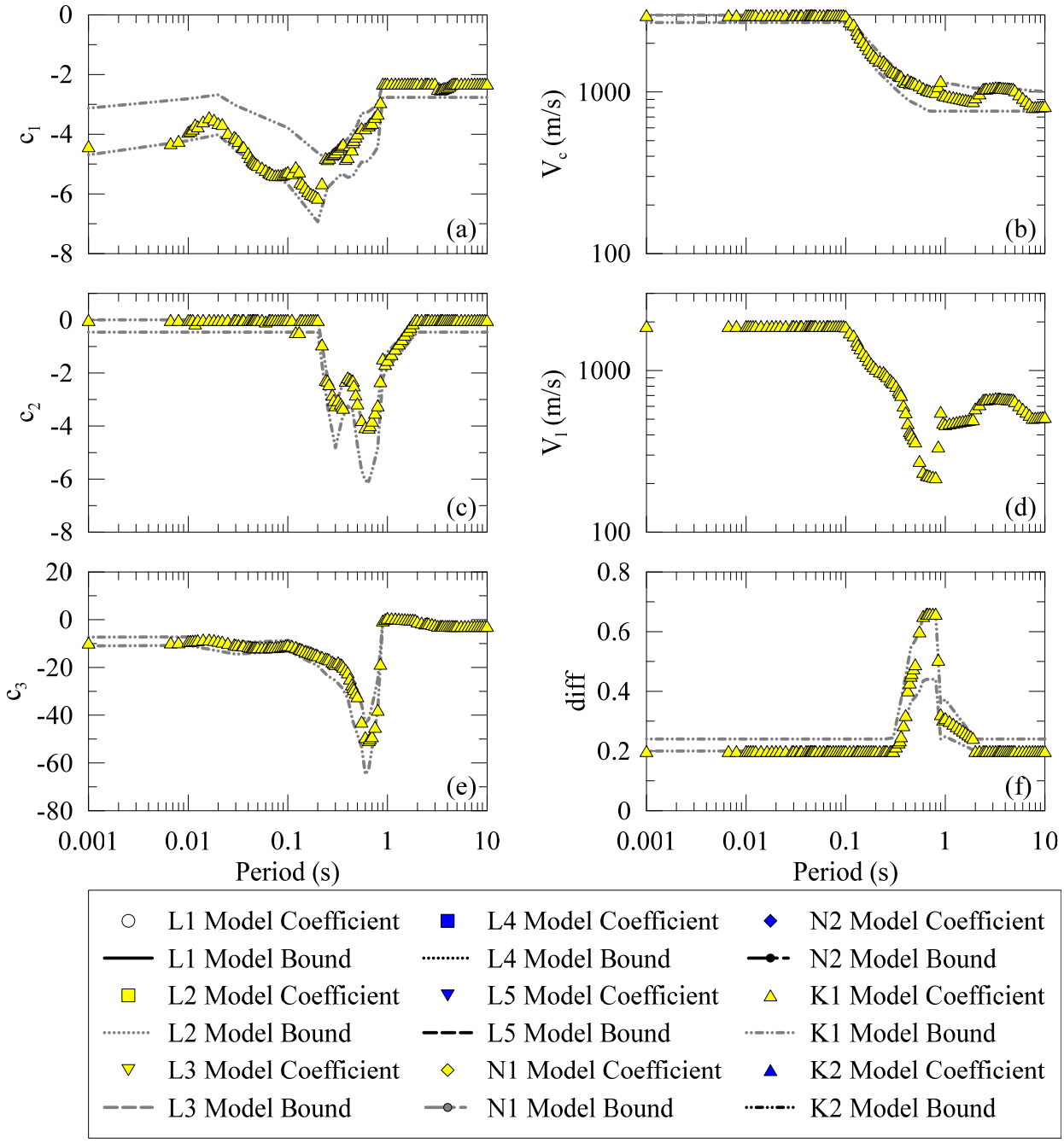

Figure 9.6 K1 model coefficients and bounds for $f(V_{S30})$ c_1 (a), c_2 (c), c_3 (e), V_c (b), V_1 (d), and *diff* (f).

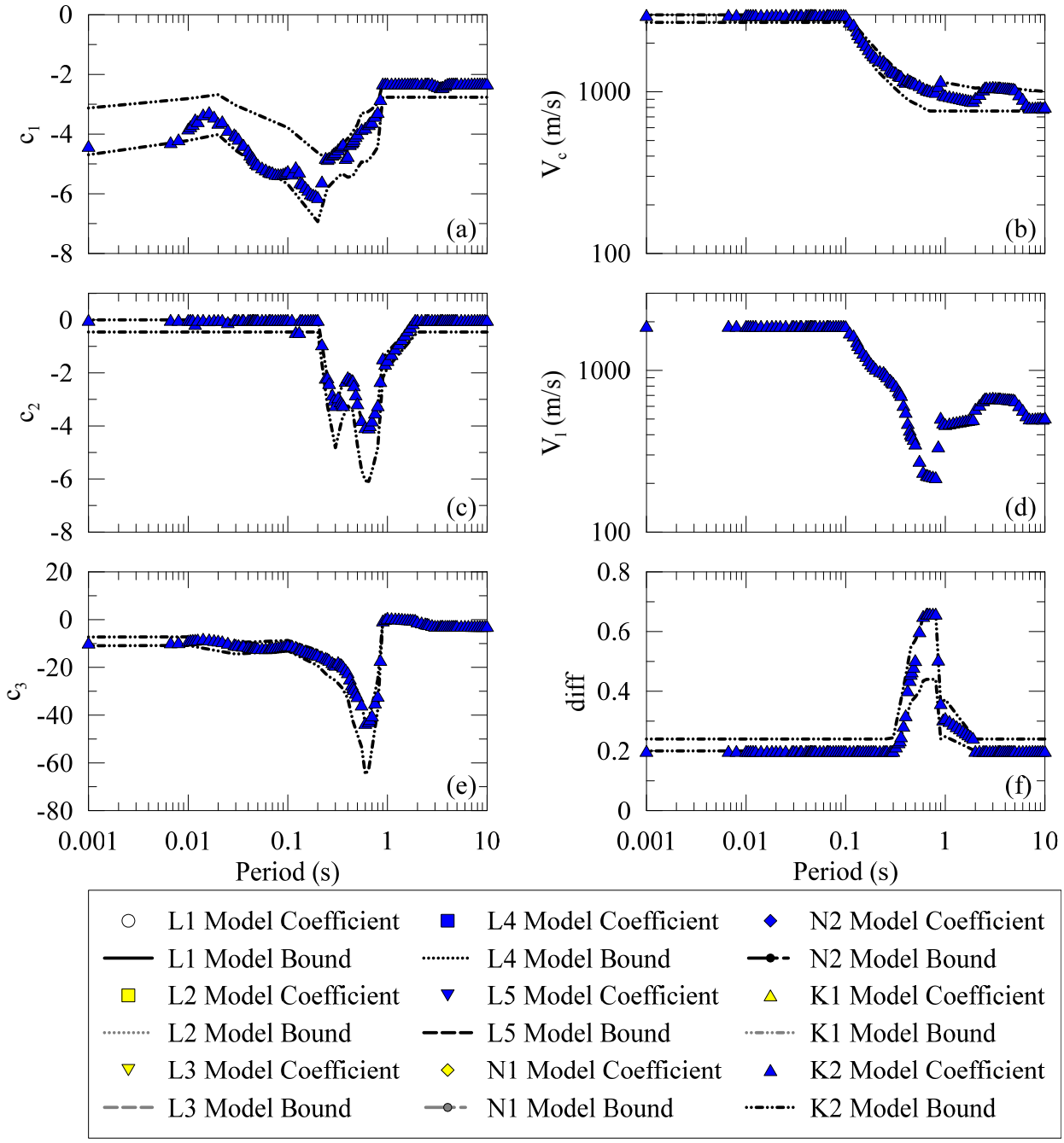

Figure 9.7 K2 model coefficients and bounds for *f(V$_{S30}$)* c_1 (a), c_2 (c), c_3 (e), V_c (b), V_1 (d), and *diff* (f).

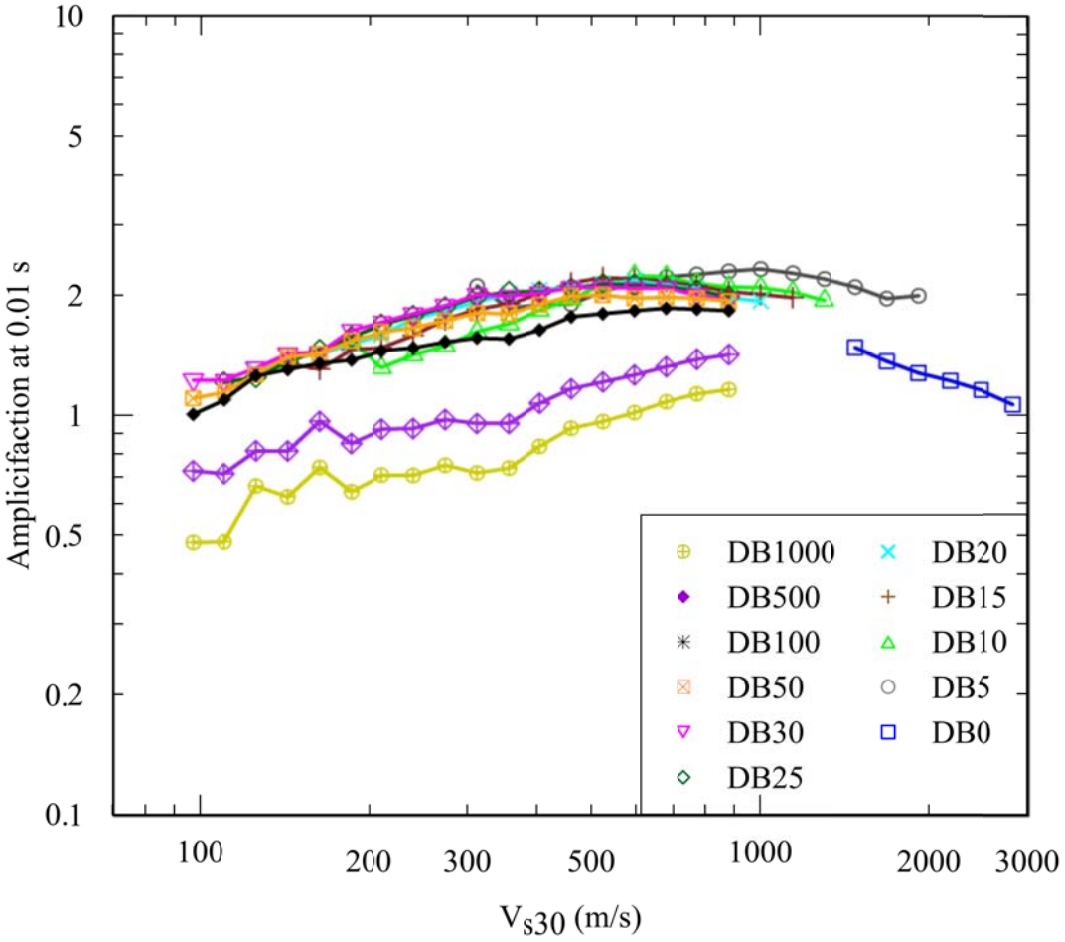

Figure 9.8: Amplification of linear elastic simulations as a function of V_{S30} for depth bins in the parametric study for 0.01 s response spectral period.

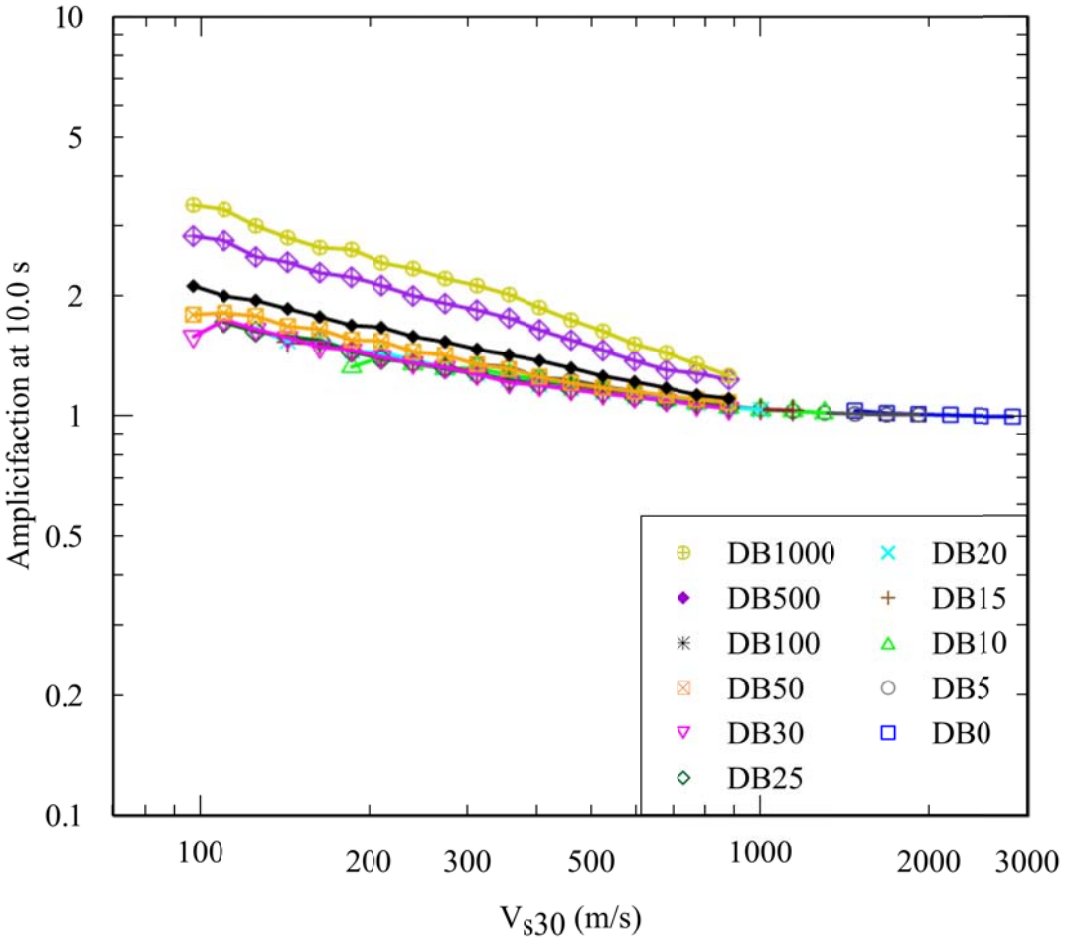

Figure 9.9:Amplification of linear elastic simulations as a function of VS30 for depth bins in the parametric study for 10.0 s response spectral period.

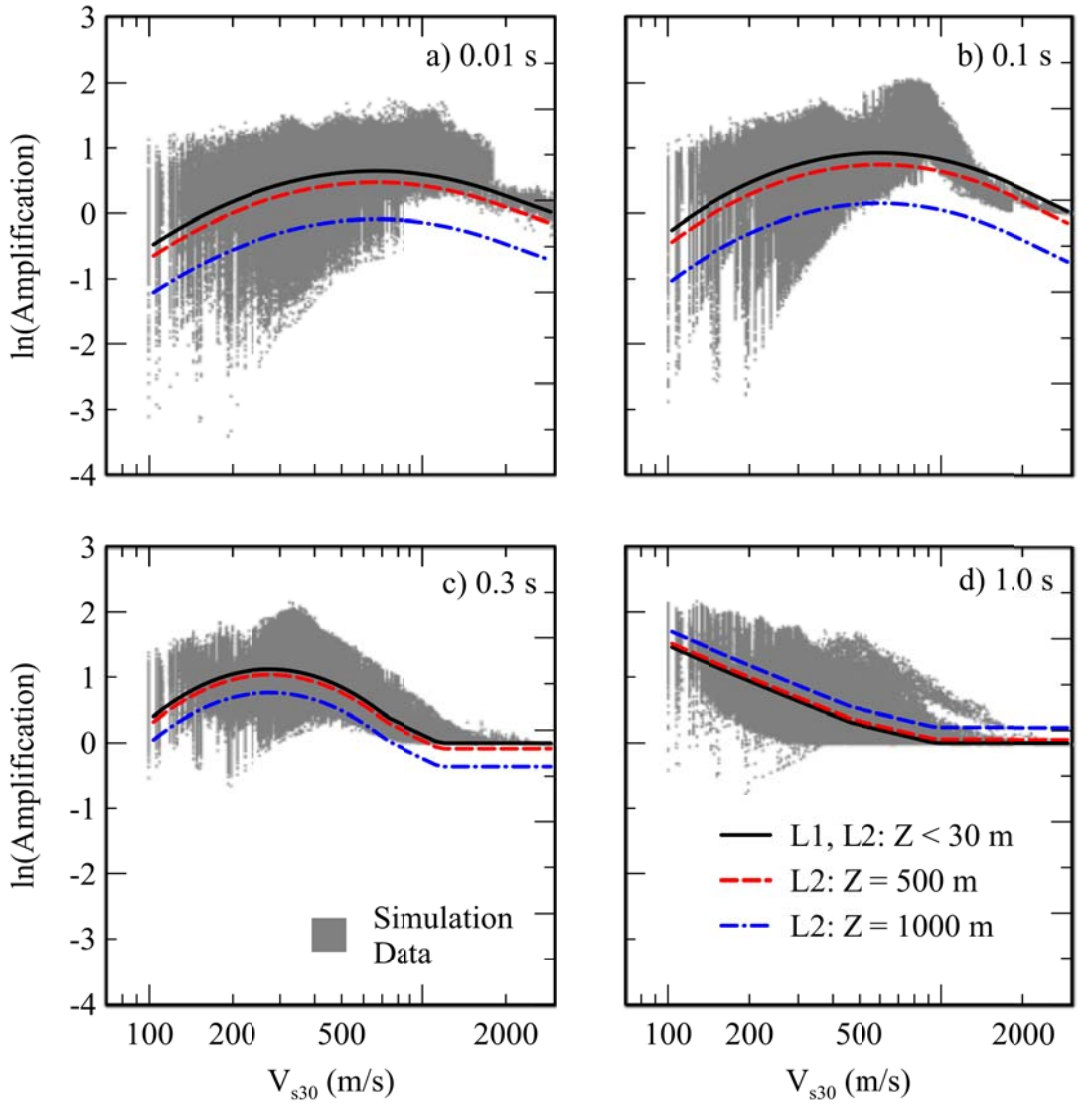

Figure 9.10: L2 Amplification model depth effects for response spectral periods of 0.01 s (a), 0.1 s (b), 0.3 s (c), and 1.0 s (d).

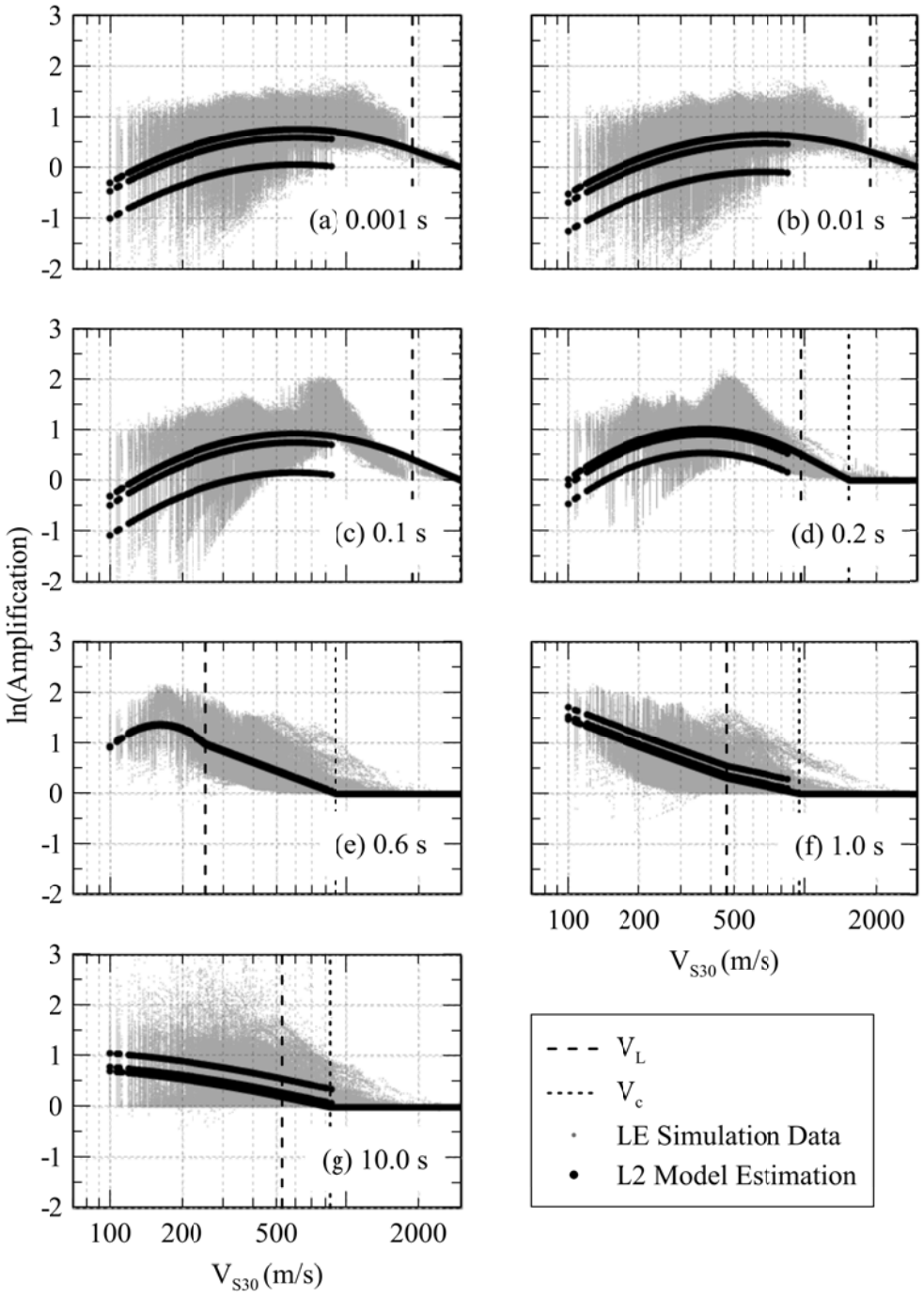

Figure 9.11: L2 Site Amplification Function for response spectral periods 0.001, 0.01, 0.1, 0.2, 0.3, 0.6, 1 and 10 s.

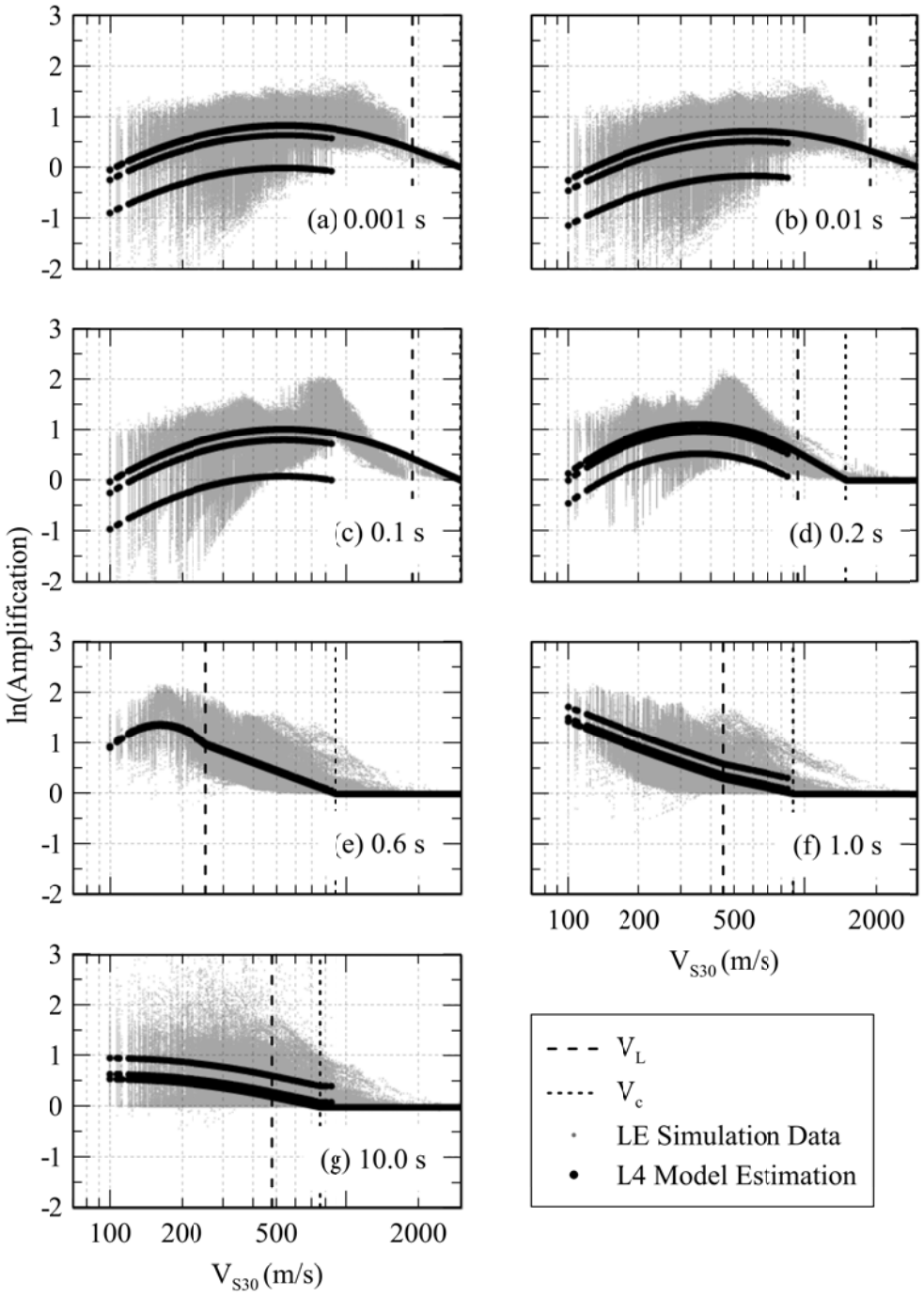

Figure 9.12 L2 Site Amplification Function for response spectral periods 0.001, 0.01, 0.1, 0.2, 0.3, 0.6, 1 and 10 s.

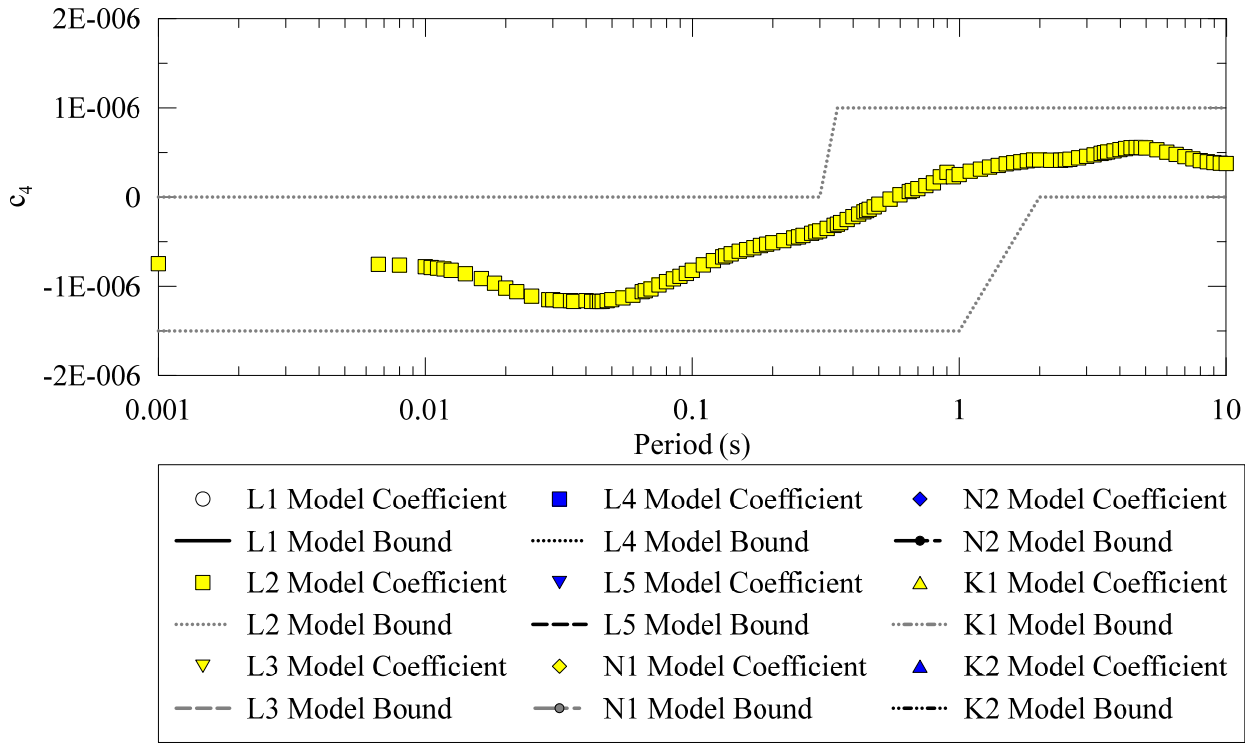

Figure 9.13: Response Spectral Coefficients for f(Z) for L2 Model.

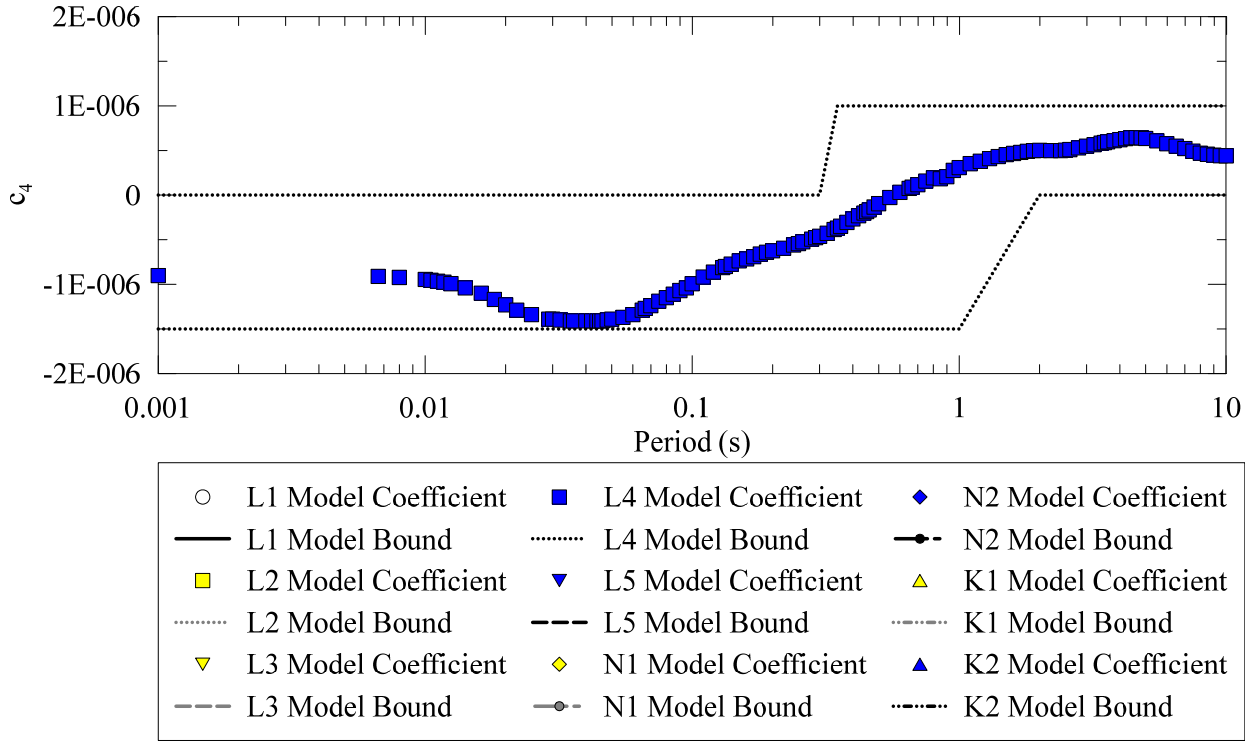

Figure 9.14 Response Spectral Coefficients for f(Z) for L4 Model.

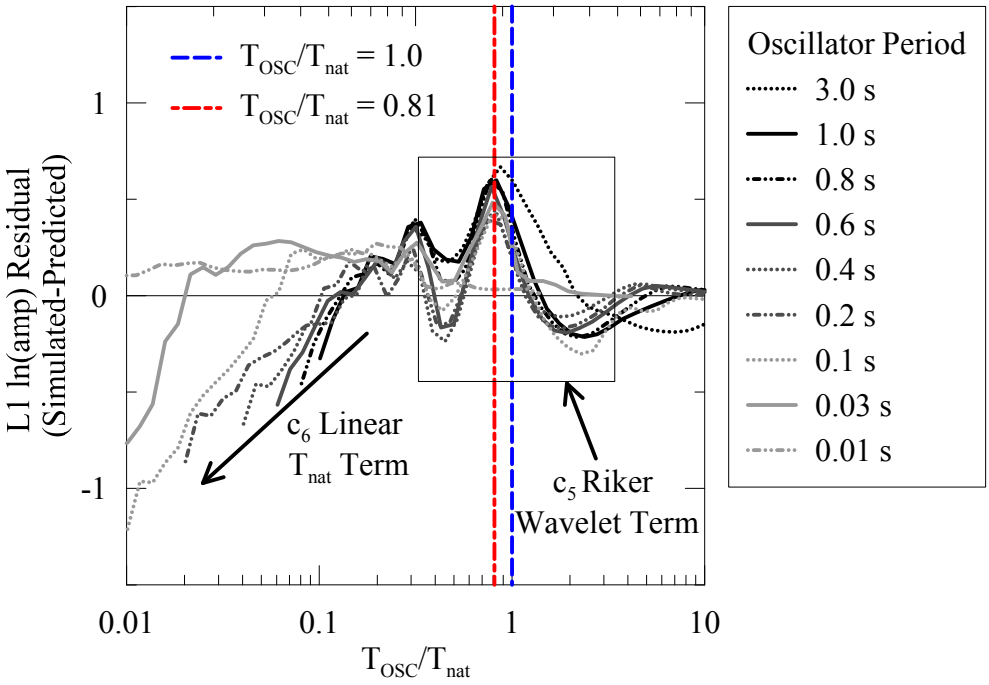

Figure 9.15: Natural Period Residuals after VS30 scaling for periods 0.001 s to 10 s.

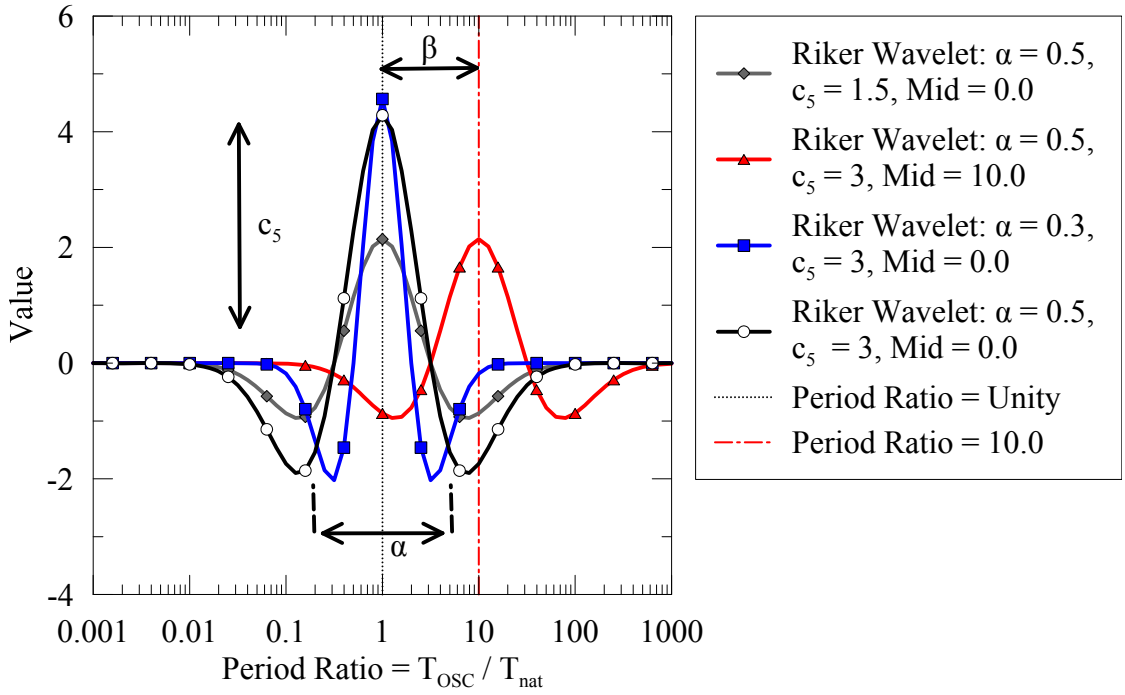

Figure 9.16: Riker wavelet coefficient effects.

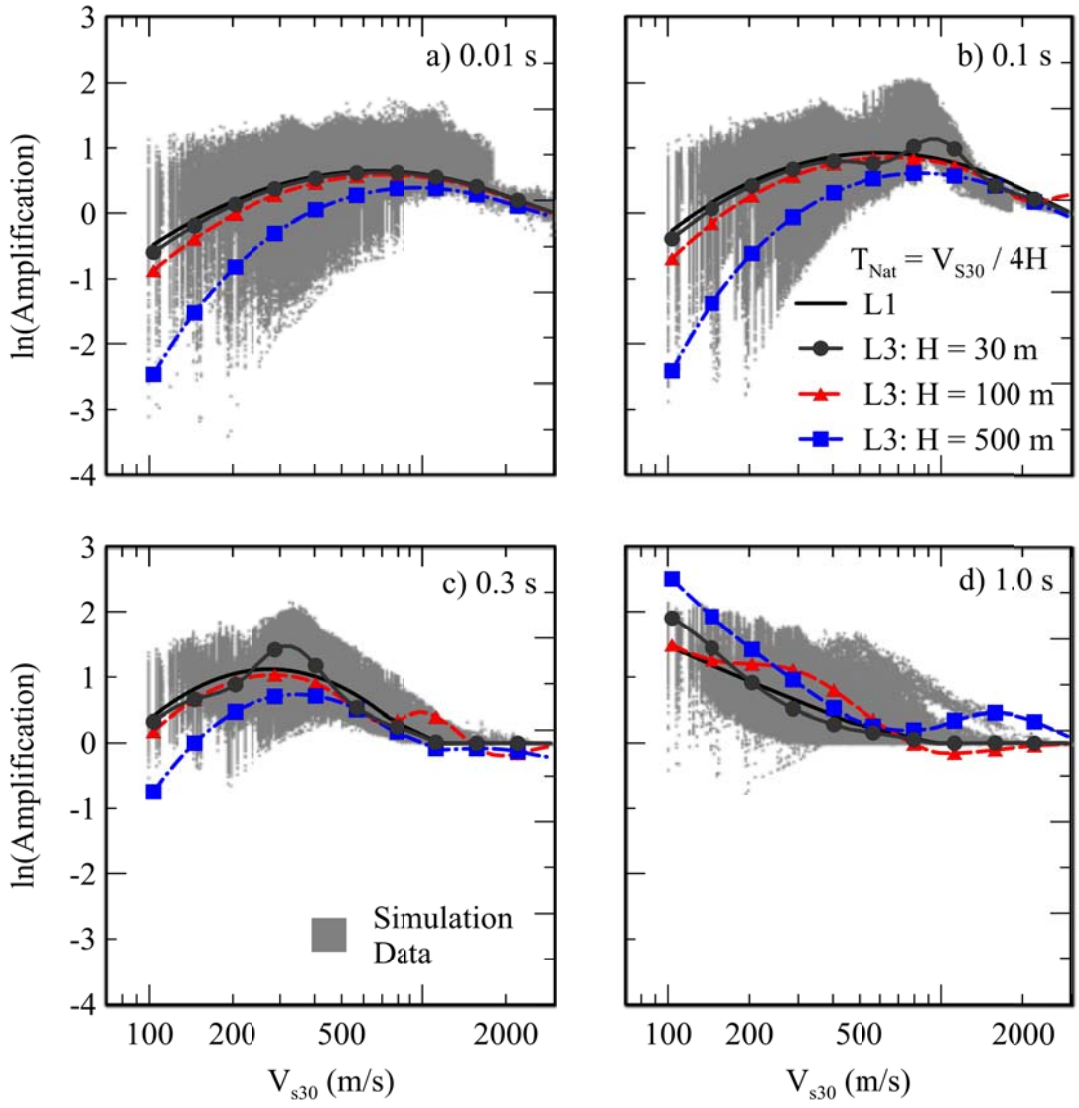

Figure 9.17: L3 Amplification model T_{nat} effects for response spectral periods of 0.01 s (a), 0.1 s (b), 0.3 s (c), and 1.0 s (d).

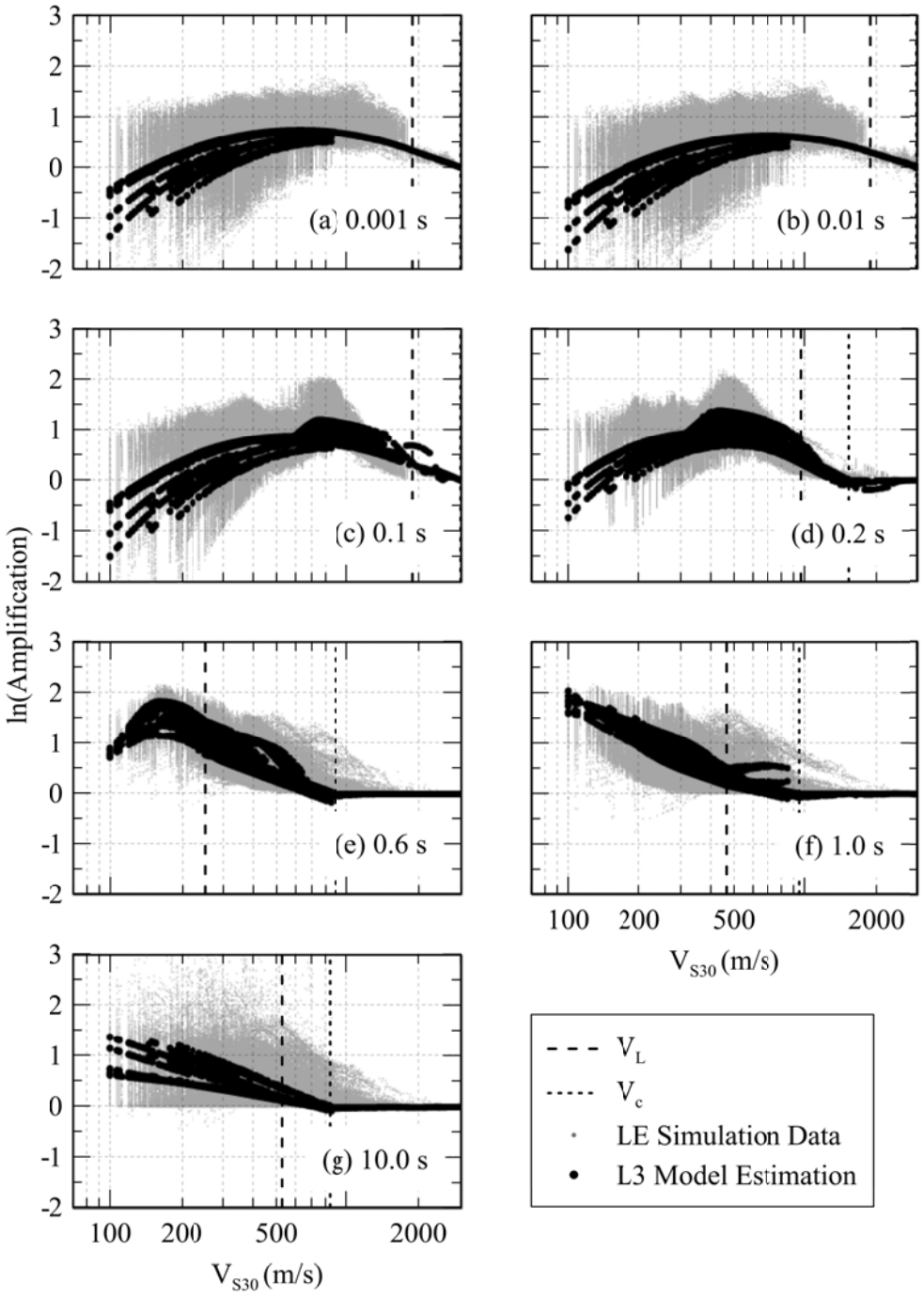

Figure 9.18: L3 Site Amplification Function for response spectral periods 0.001, 0.01, 0.1, 0.2, 0.3, 0.6, 1 and 10 s.

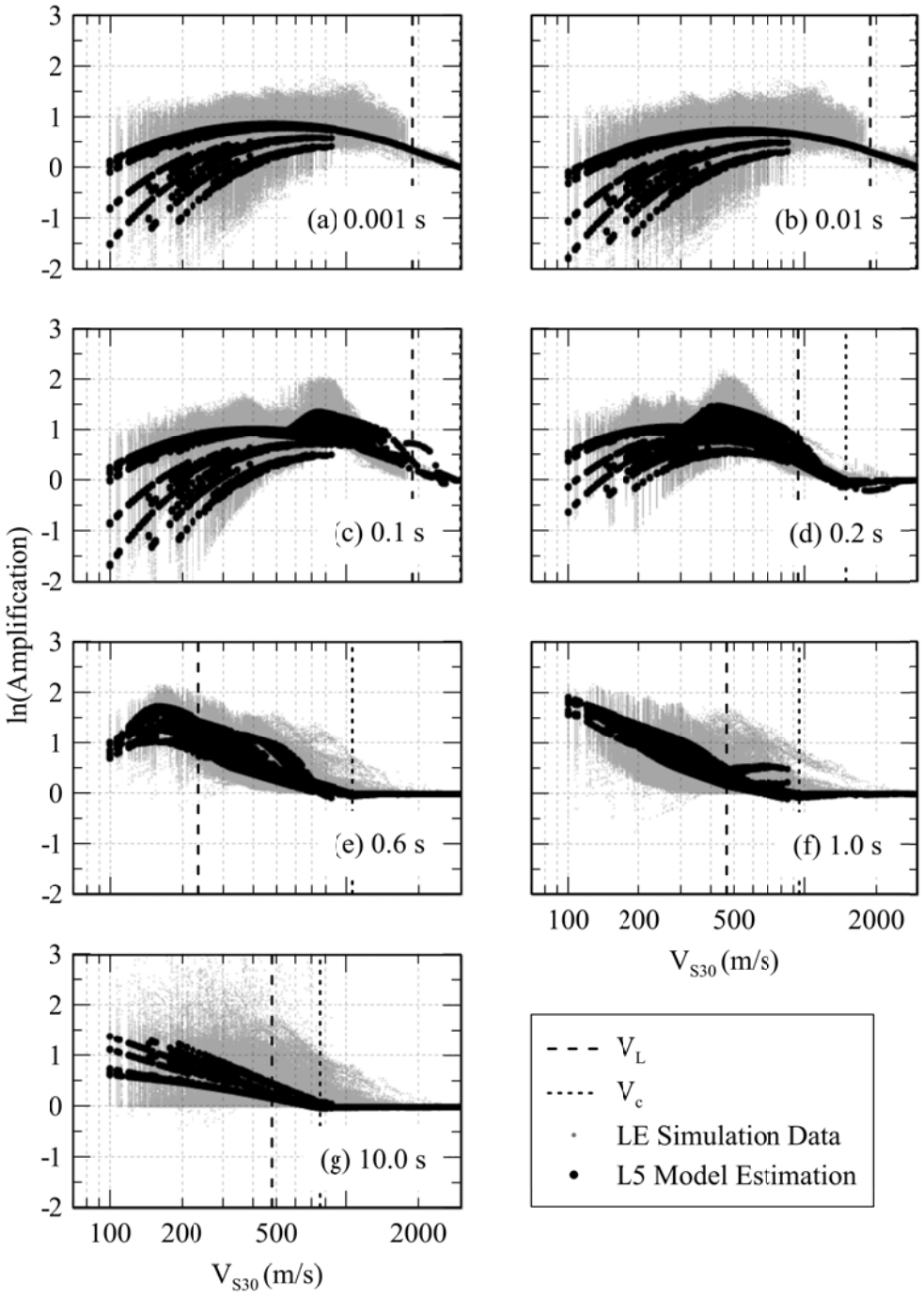

Figure 9.19: L5 Site Amplification Function for response spectral periods 0.001, 0.01, 0.1, 0.2, 0.3, 0.6, 1 and 10 s.

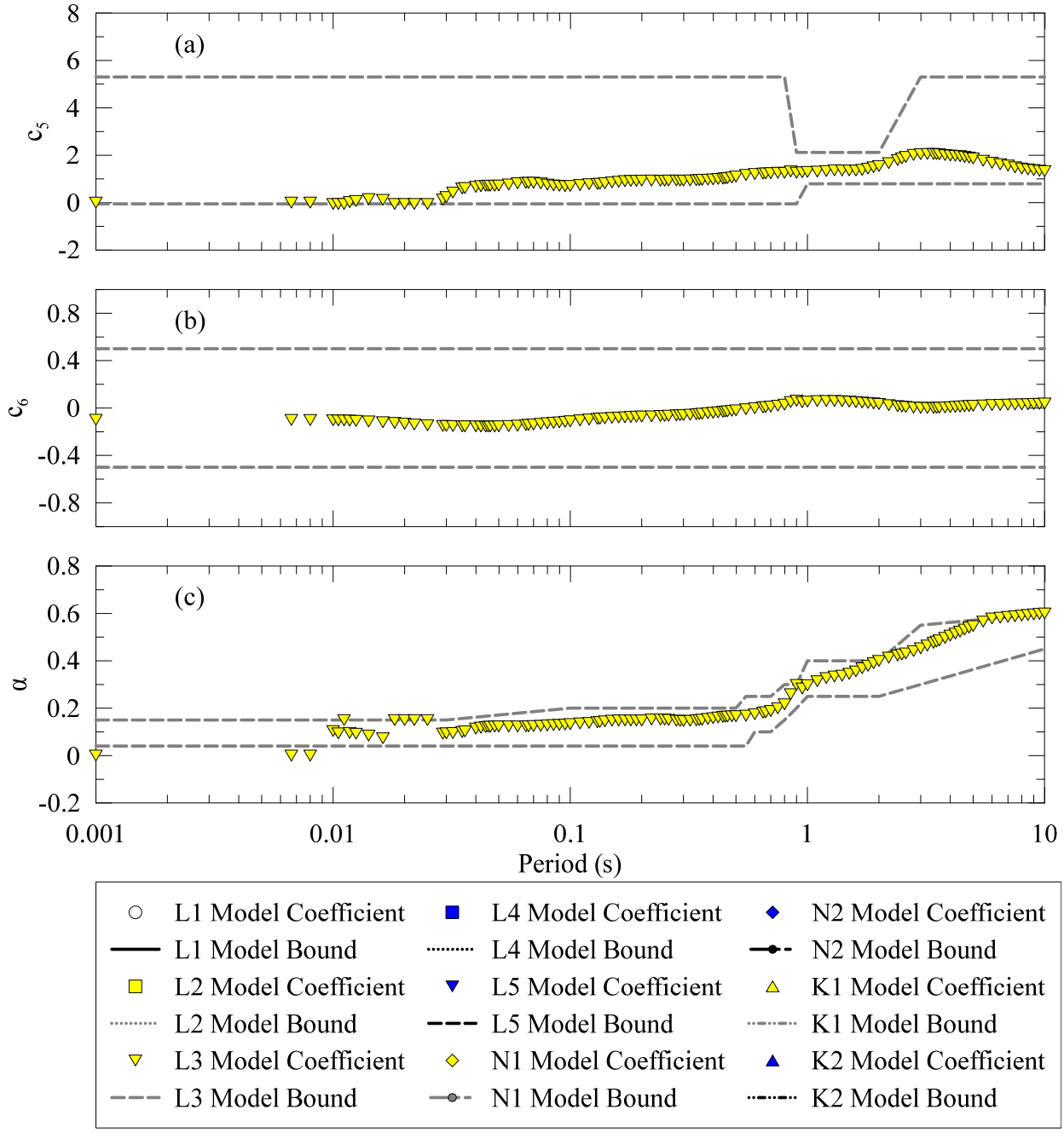

Figure 9.20: L3 model coefficients and bounds for $f(T_{nat})$ c_5 (a), c_6 (b), α (c).

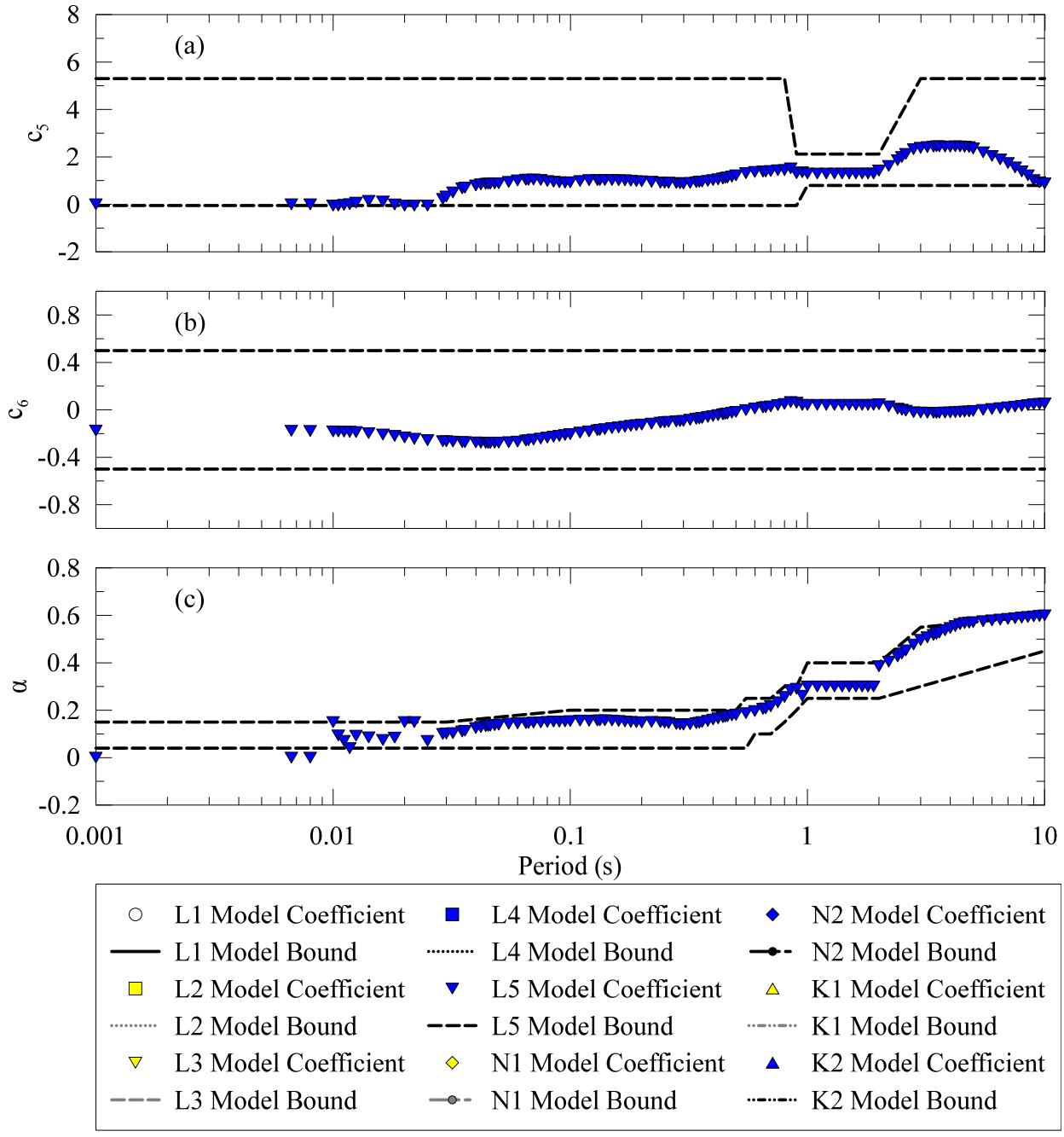

Figure 9.21 L5 model coefficients and bounds for $f(T_{nat})$ c_5 (a), c_6 (b), α (c).

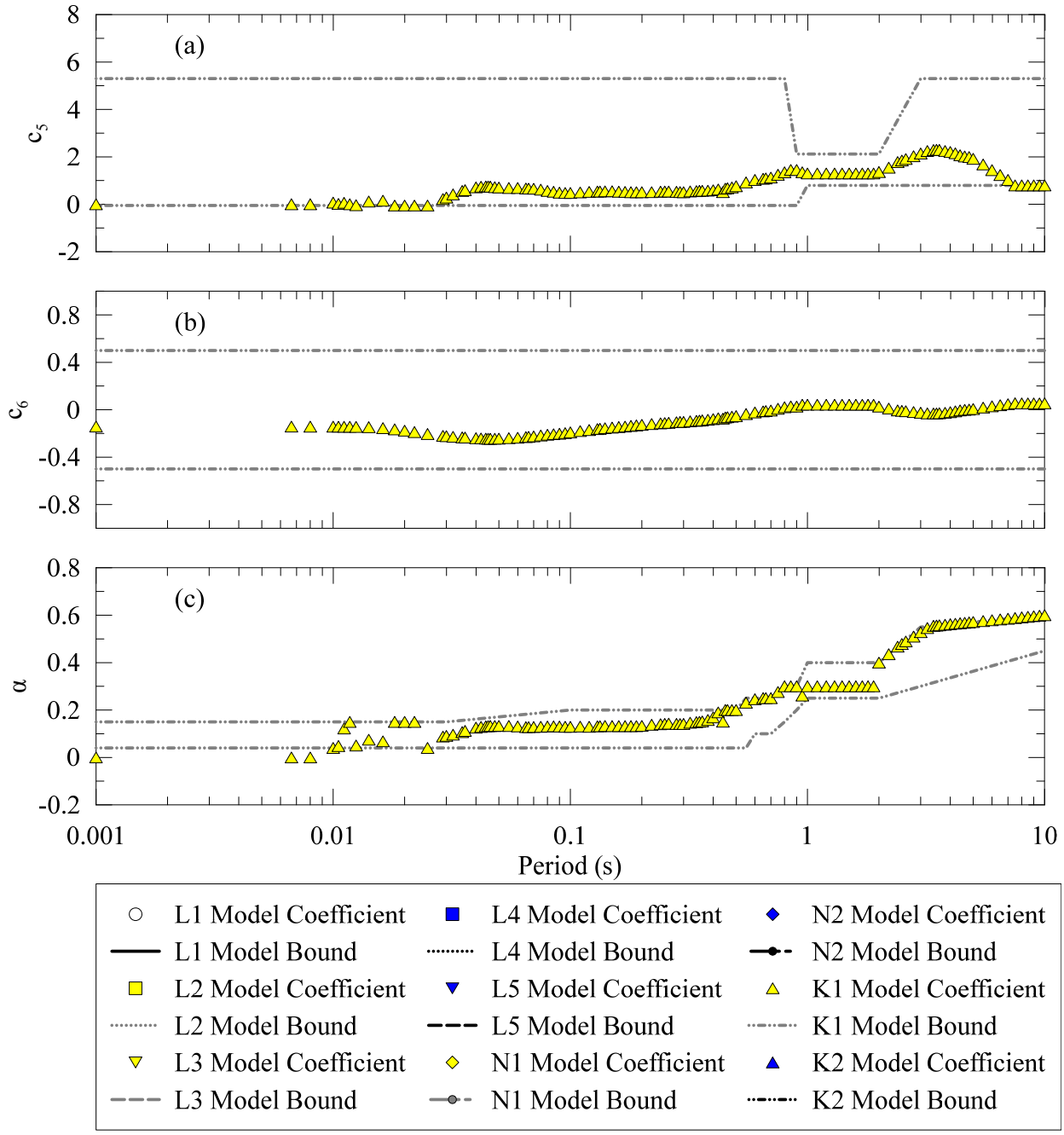

Figure 9.22 K1 model coefficients and bounds for $f(T_{nat})$ c_5 (a), c_6 (b), α (c).

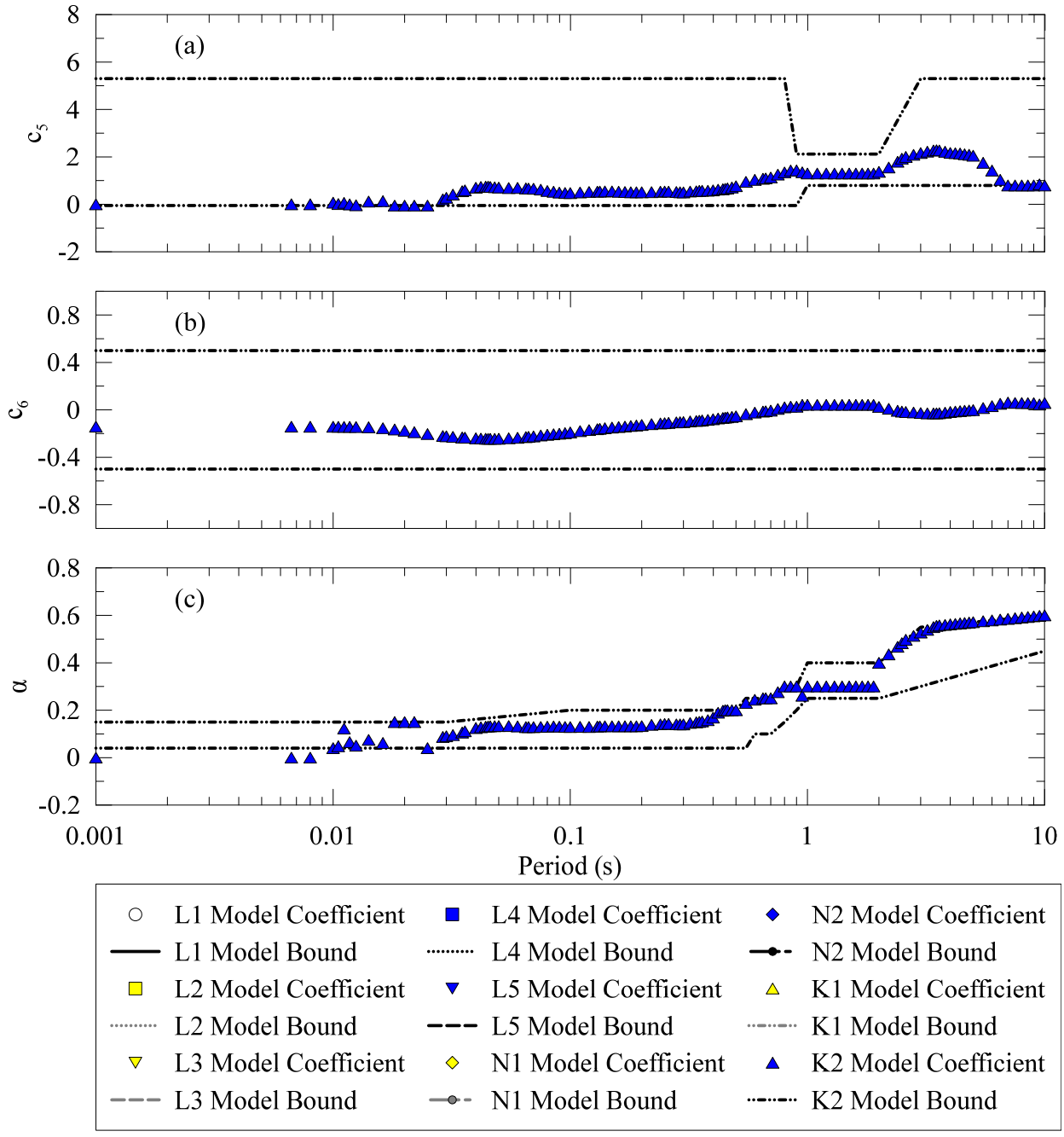

Figure 9.23 K2 model coefficients and bounds for $f(T_{nat})$ c_5 (a), c_6 (b), α (c).

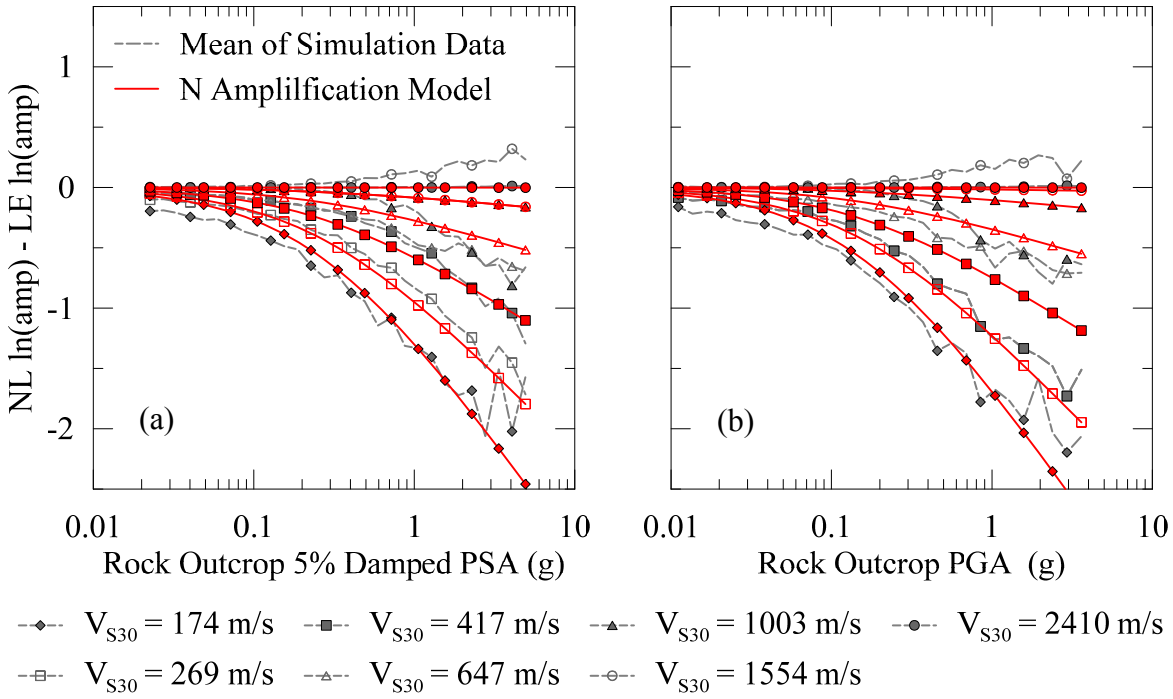

Figure 9.24: Nonlinear site amplification at 0.1 s as a function of PSA (N1) (a) and PGA (N2) (b).

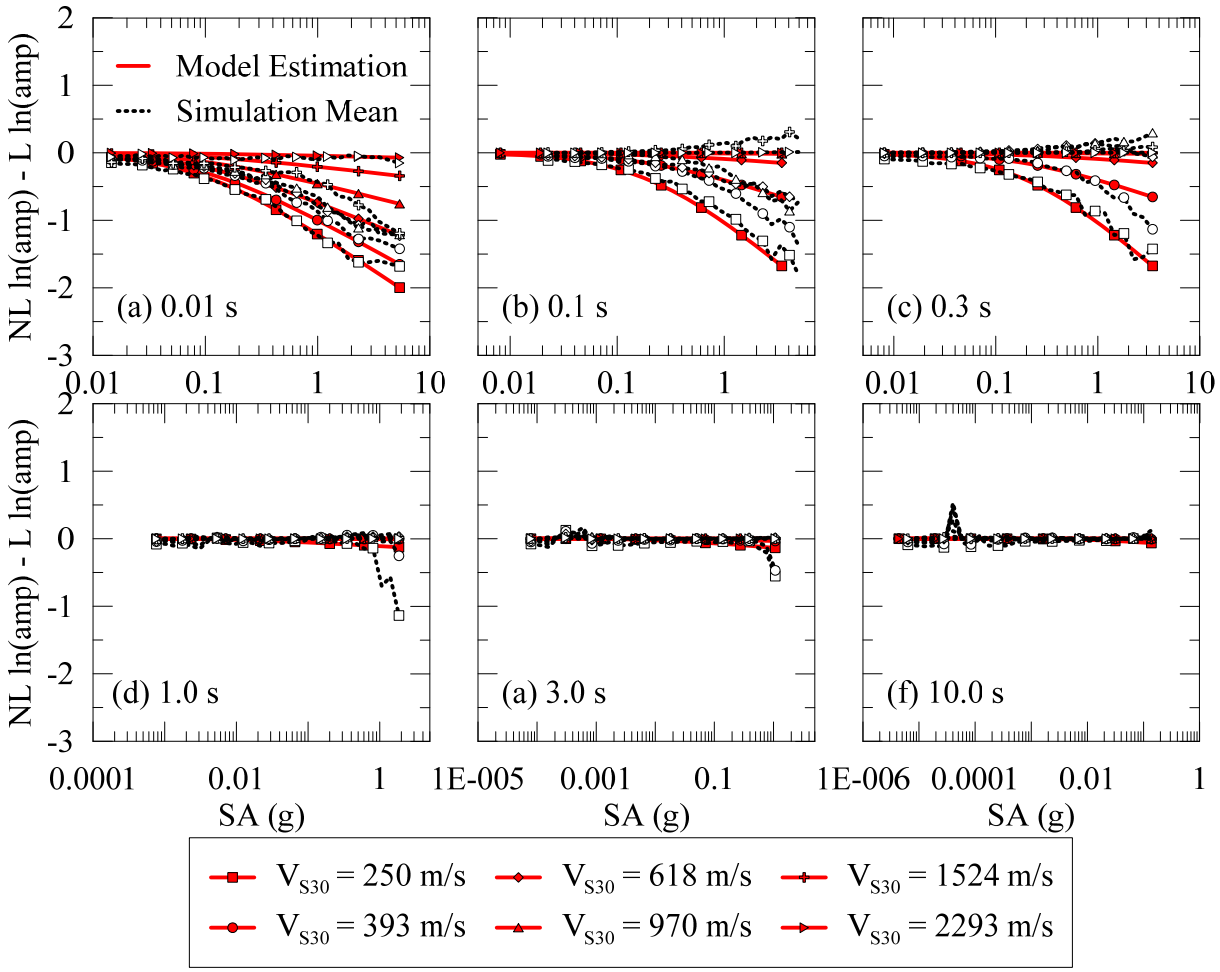

Figure 9.25: N1 RS Nonlinear site amplification model and binned mean of simulation data for response spectral periods (a) 0.01 s, (b) 0.1 s, (c) 0.3 s, (d) 1.0 s, (e) 3.0 s, and (f) 10.0 s.

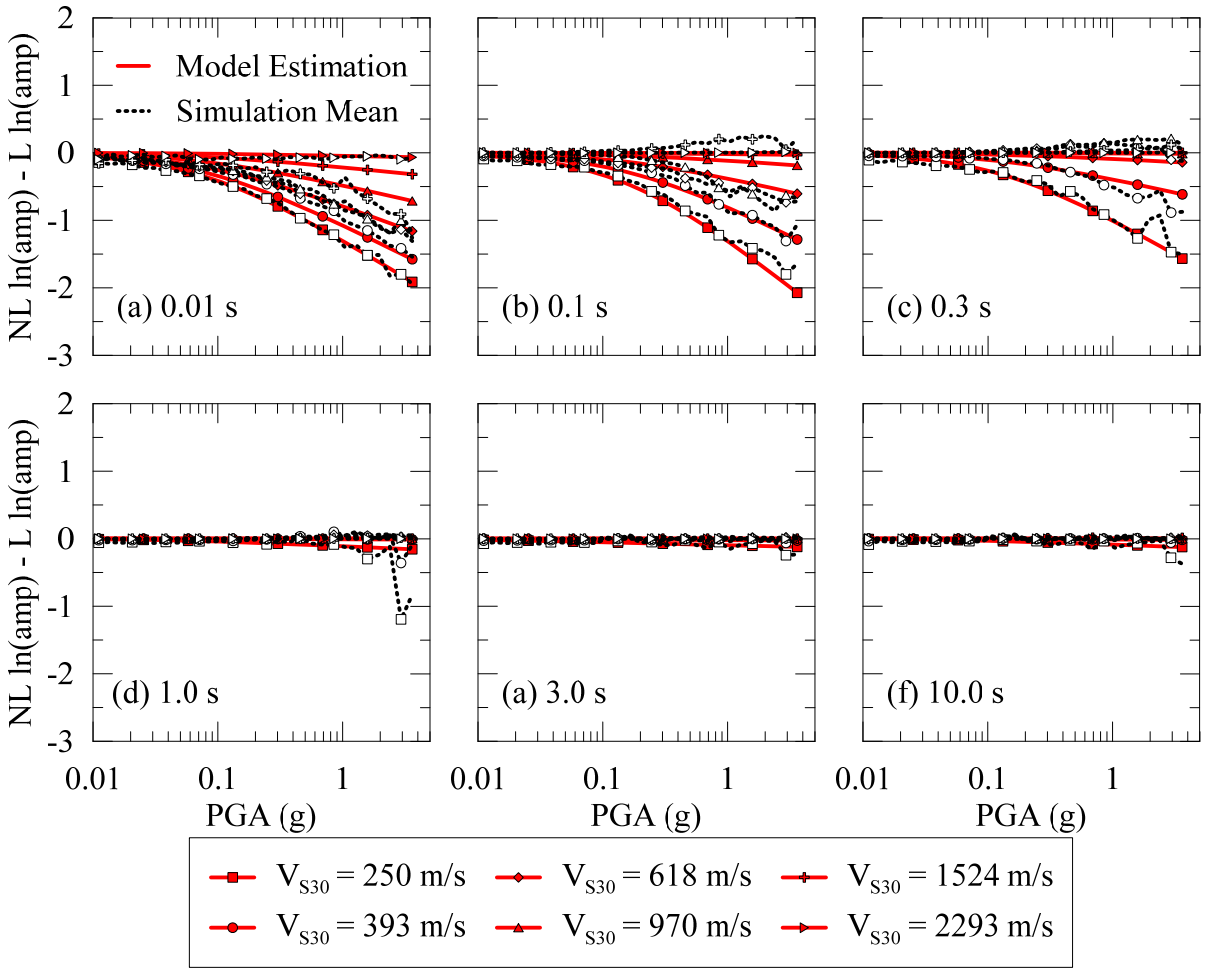

Figure 9.26: N2 Nonlinear RS site amplification model and binned mean of simulation data for response spectral periods (a) 0.01 s, (b) 0.1 s, (c) 0.3 s, (d) 1.0 s, (e) 3.0 s, and (f) 10.0 s.

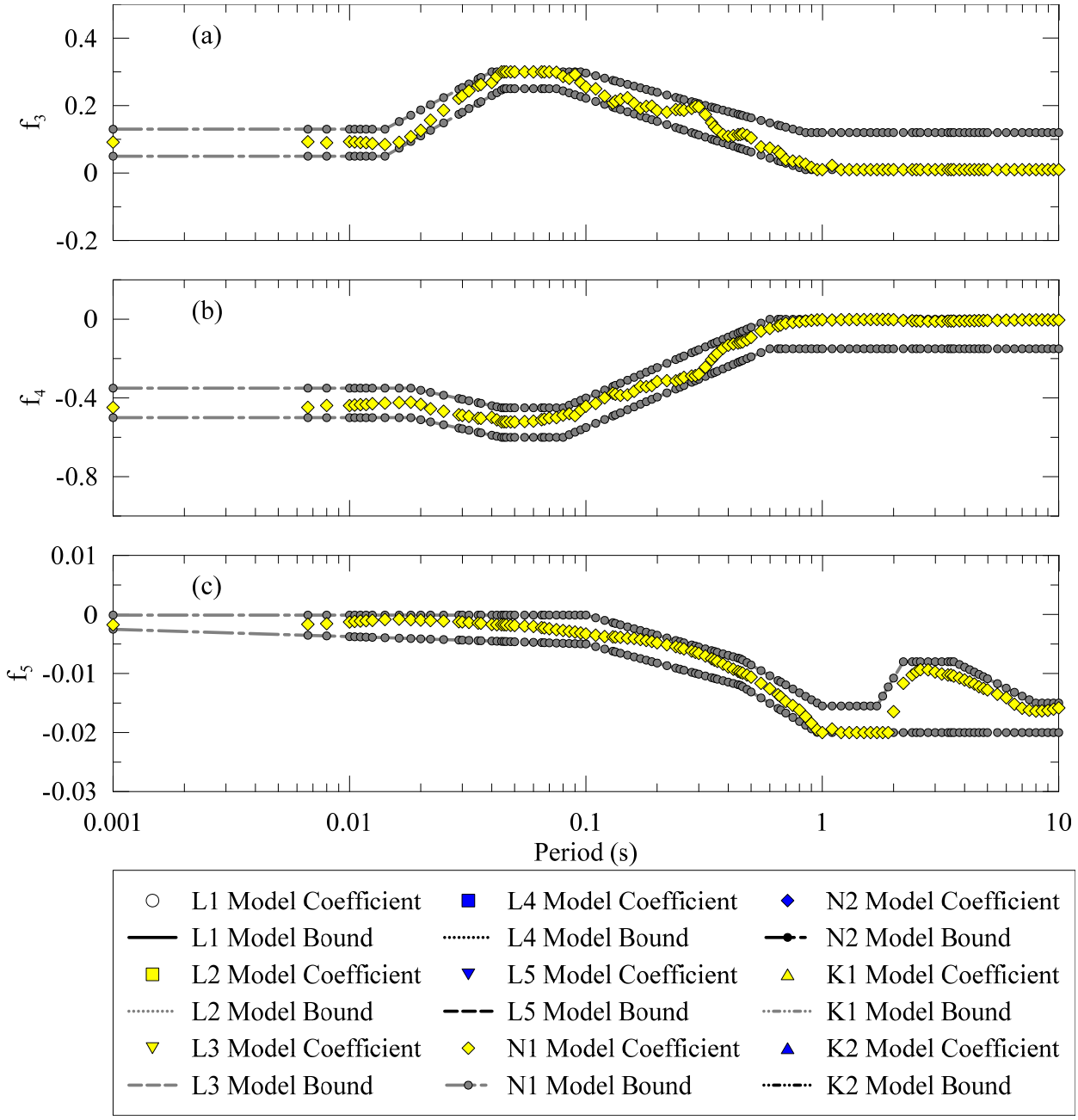

Figure 9.27: N1 model coefficients and bounds for *f(NL)* f_3 (a), f_4 (b), f_5 (c).

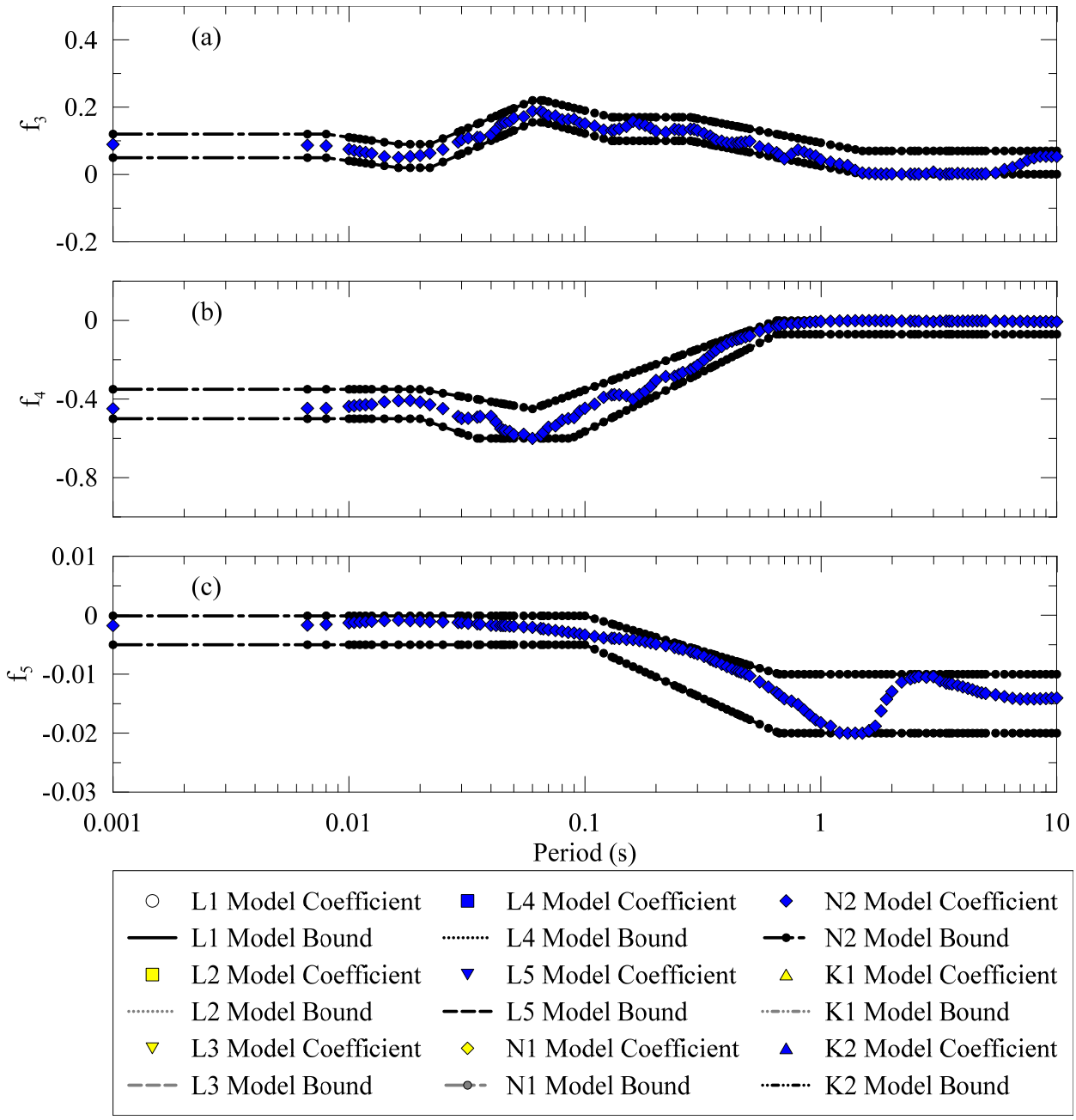

Figure 9.28 N2 model coefficients and bounds for *f(NL)* f_3 (a), f_4 (b), f_5 (c).

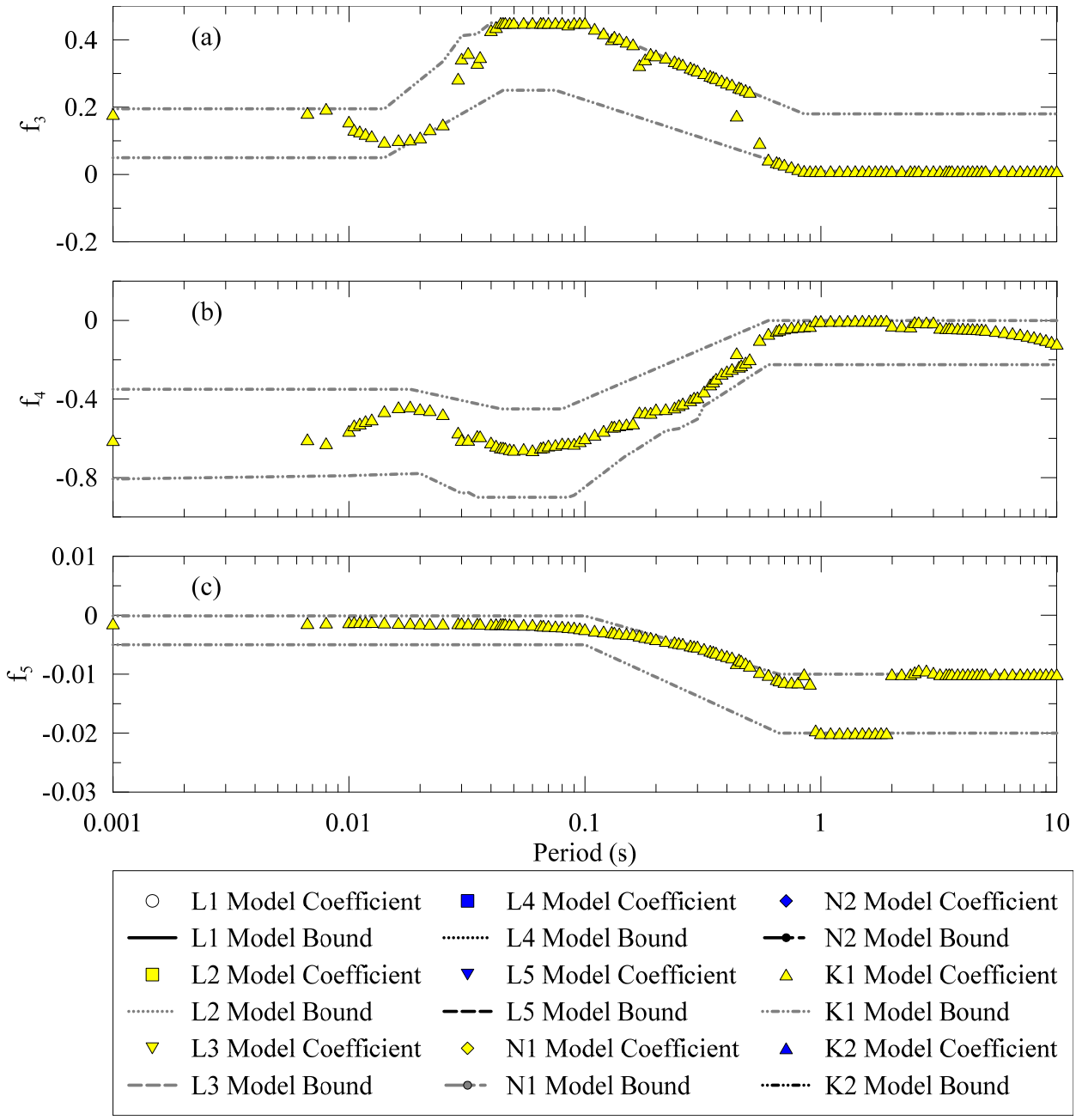

Figure 9.29 K1 model coefficients and bounds for f(NL) f3 (a), f4 (b), f5 (c).

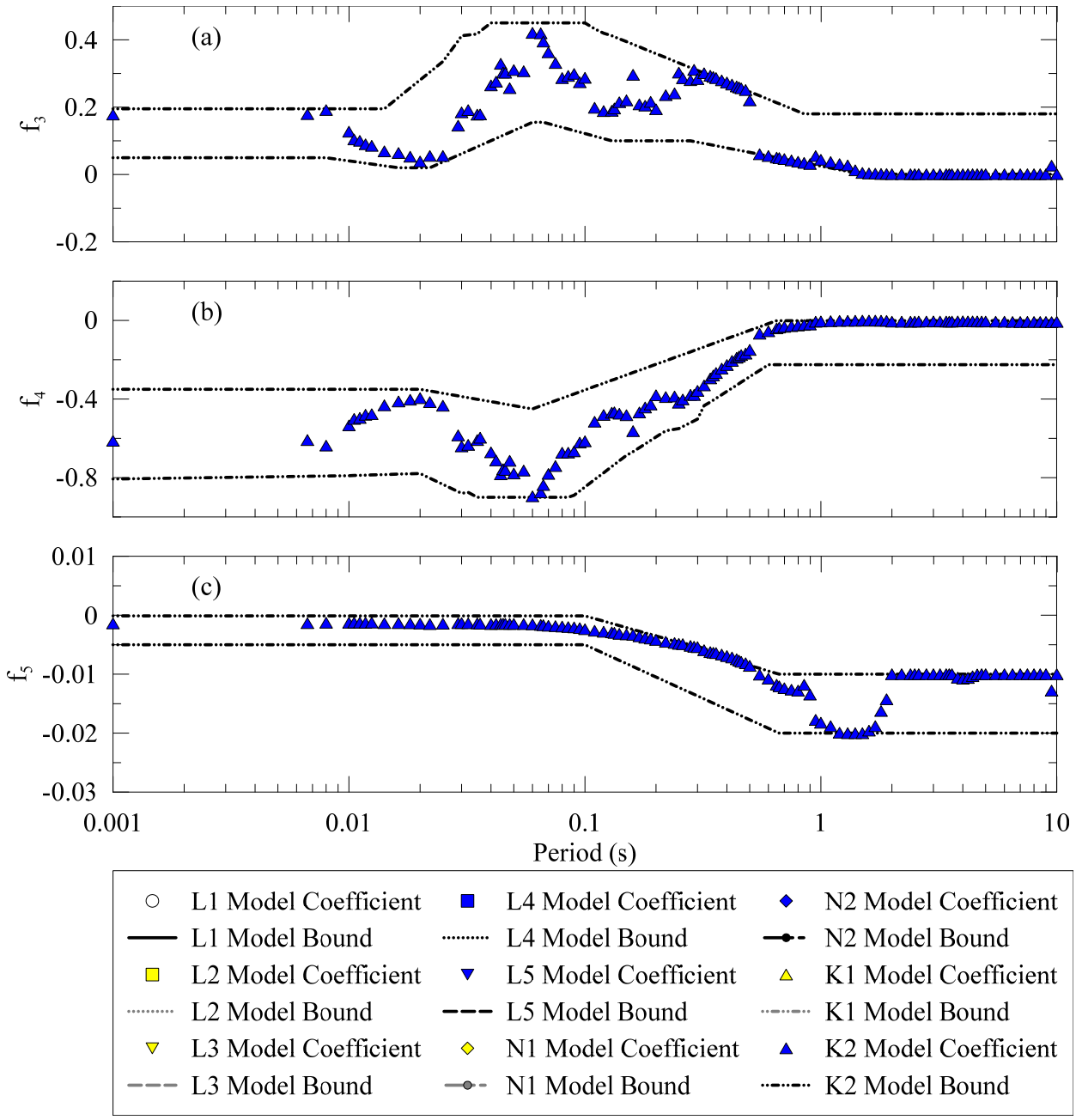

Figure 9.30 K2 model coefficients and bounds for *f(NL)* f_3 (a), f_4 (b), f_5 (c).

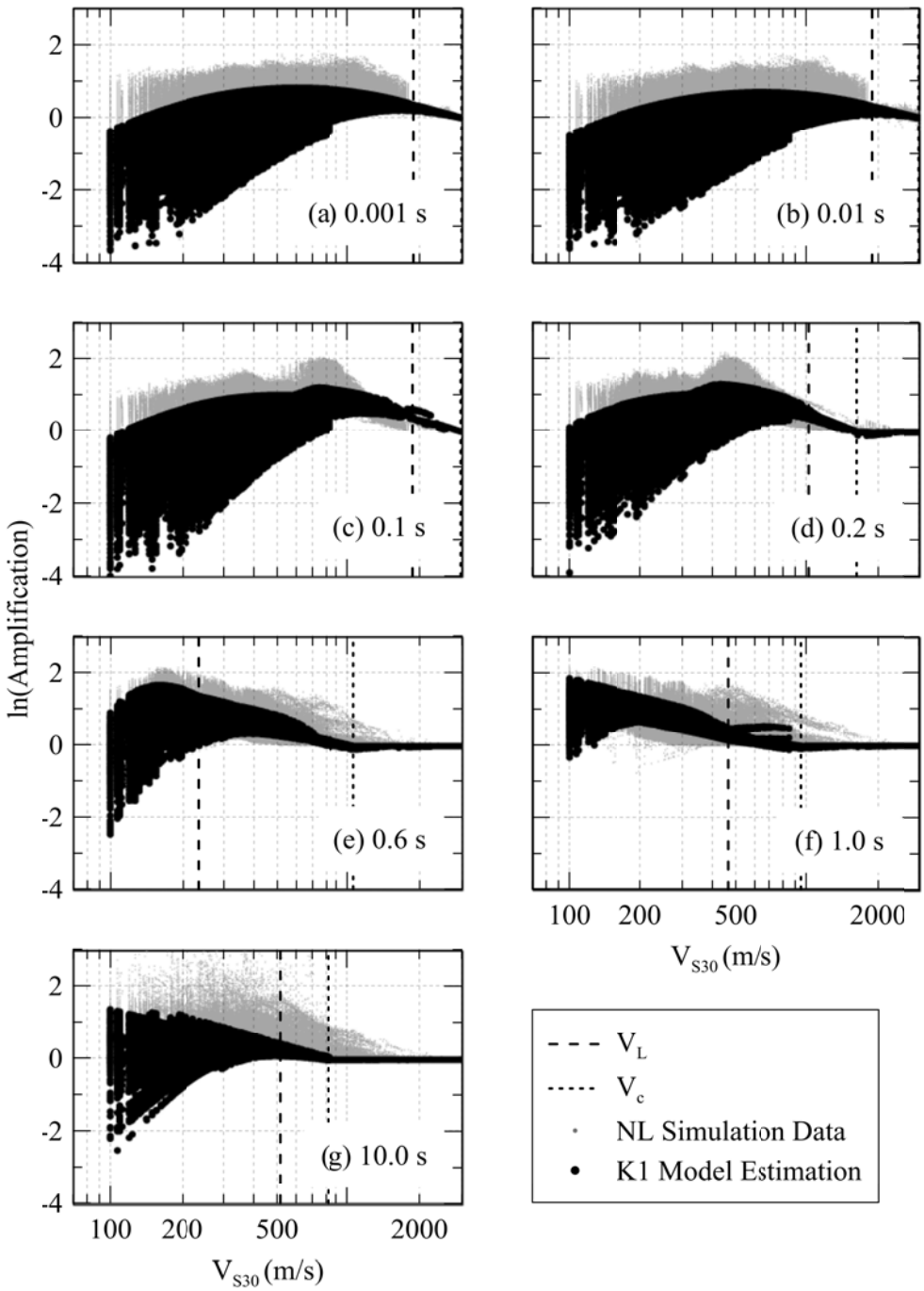

Figure 9.31: K1 site amplification model for response spectral periods 0.001, 0.01, 0.1, 0.2, 0.3, 0.6, 1 and 10 s.

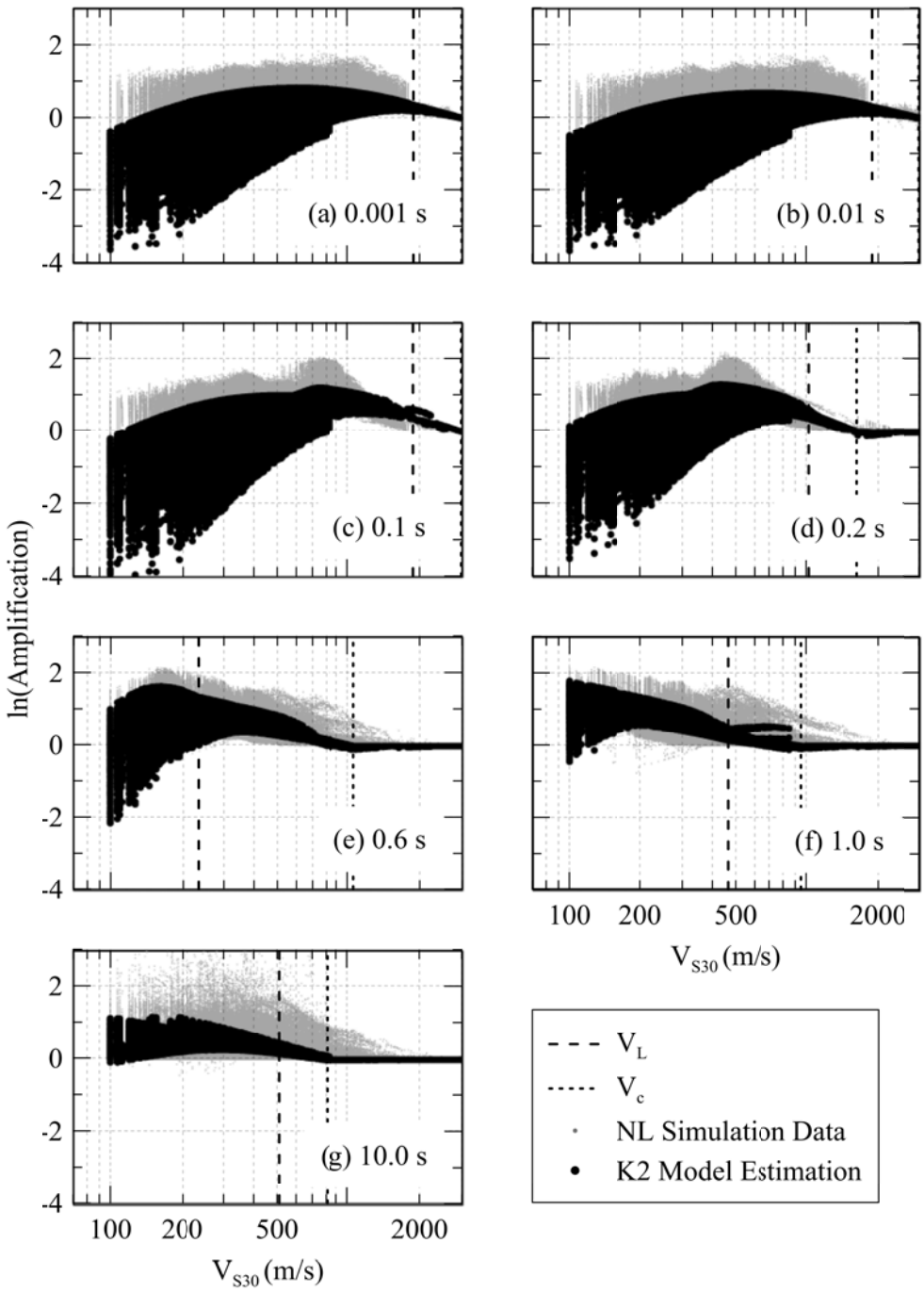

Figure 9.32: K2 site amplification model for response spectral periods 0.001, 0.01, 0.1, 0.2, 0.3, 0.6, 1 and 10 s.

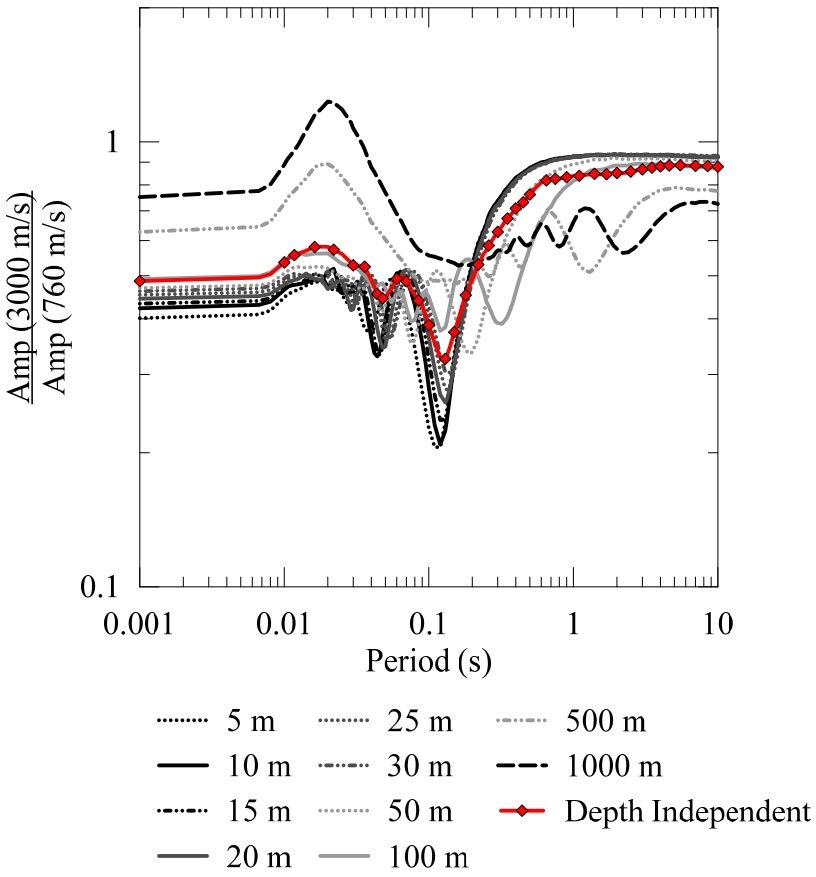

Figure 9.33: Ratio of site amplification at a 3000 m/s V_{S30} condition to amplification at a 760 m/s condition as a function of period. Shown as $1/C_{760\text{-}3000}$ for $C_{760\text{-}3000}$ as given in eq. 9.12.

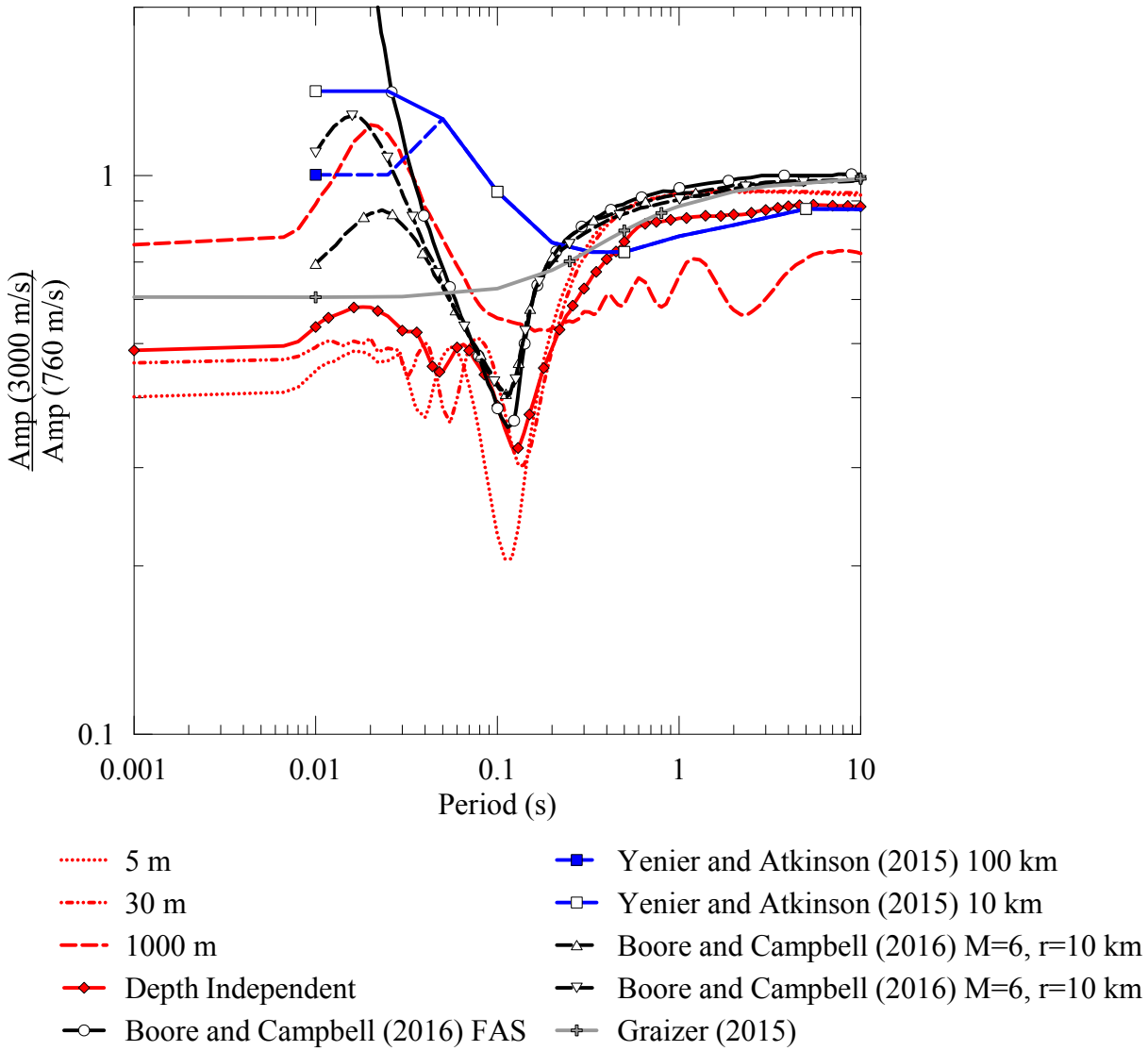

Figure 9.34: $C_{760\text{-}3000}$ from simulations for 5 m, 30 m and 1000 m depth and depth-independent $C_{760\text{-}3000}$ from this study shown with the $C_{760\text{-}3000}$ from Boore and Campbell (2016) for the FAS and M_W 6 earthquake at 10 and 100 km, and Yenier and Atkinson (2015) for 100 and 10 km. Figure adapted from Boore and Campbell (2016).

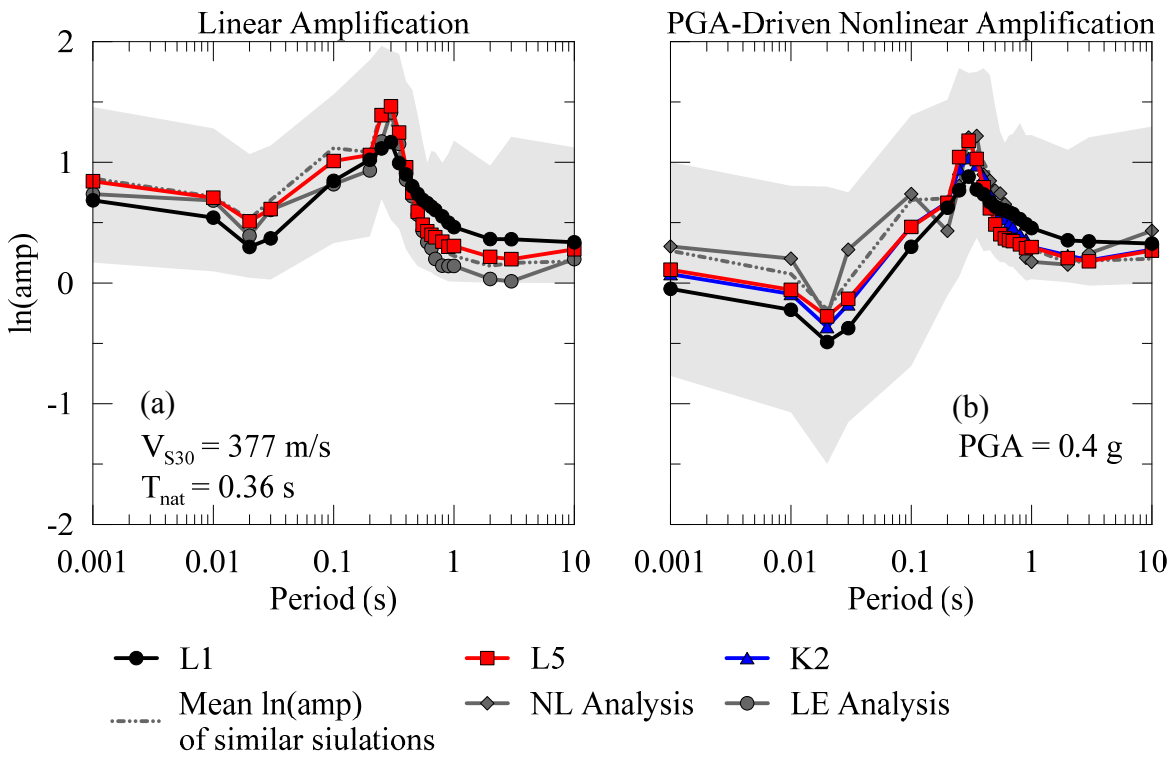

Figure 9.35: LE site amplification for a site with V_{S30} of 377 m/s, T_{nat} of 0.36 m/s, and PGA of 0.4 g with L1 and L5 model estimations with the mean of similar simulations (a) and NL site amplification for the same site with L1+N2, L5+N2, and K2 model estimations and the mean of similar simulations. Similar sites are defined as sites with the same depth, and within 20% V_{S30} and T_{nat}, and with rock outcrop PGA's within 30%. The shaded region in each plot denotes the range between the maximum and minimum values of amplification of the similar simulations.

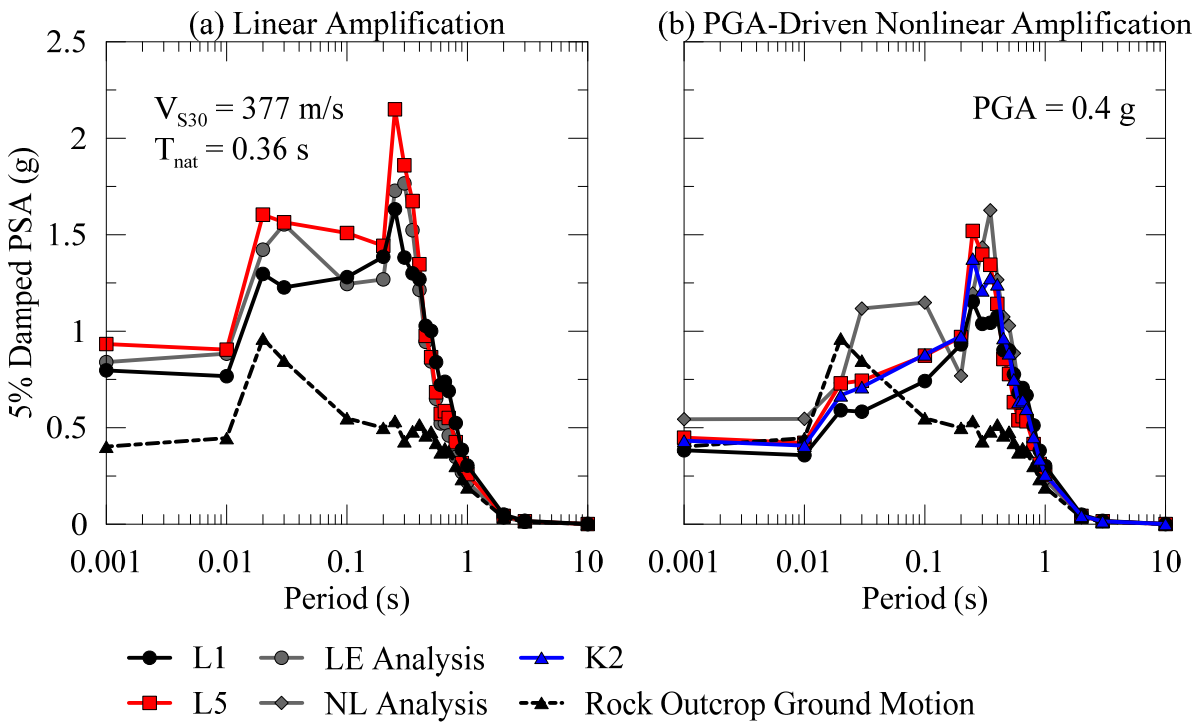

Figure 9.36: LE response spectra for a site with V_{S30} of 377 m/s, T_{nat} of 0.36 m/s, and PGA of 0.4 g with L1 and L5 model estimations and rock outcrop ground motion (a) and NL response spectra for the same site with L1+N2, L5+N2, and K2 model estimations and rock outcrop ground motion.

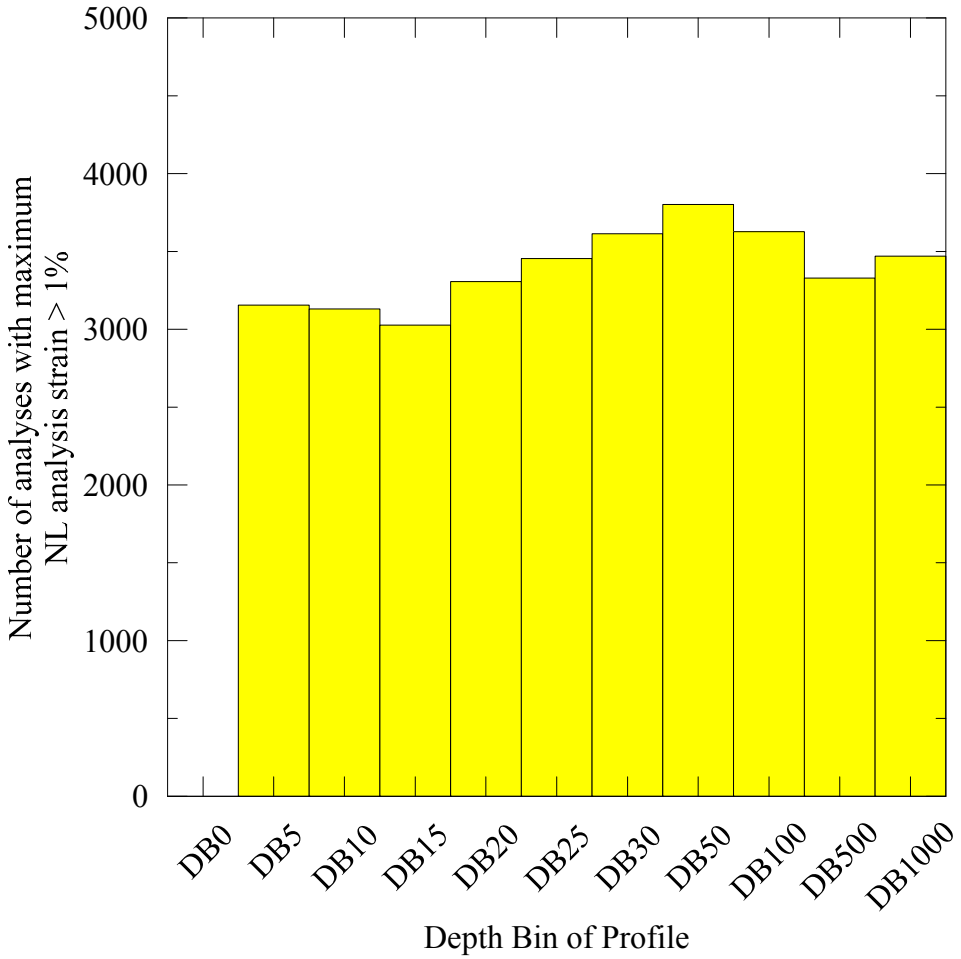

Figure 9.37 Count of NL simulations with maximum strain greater than 1% for each simulation depth bin.

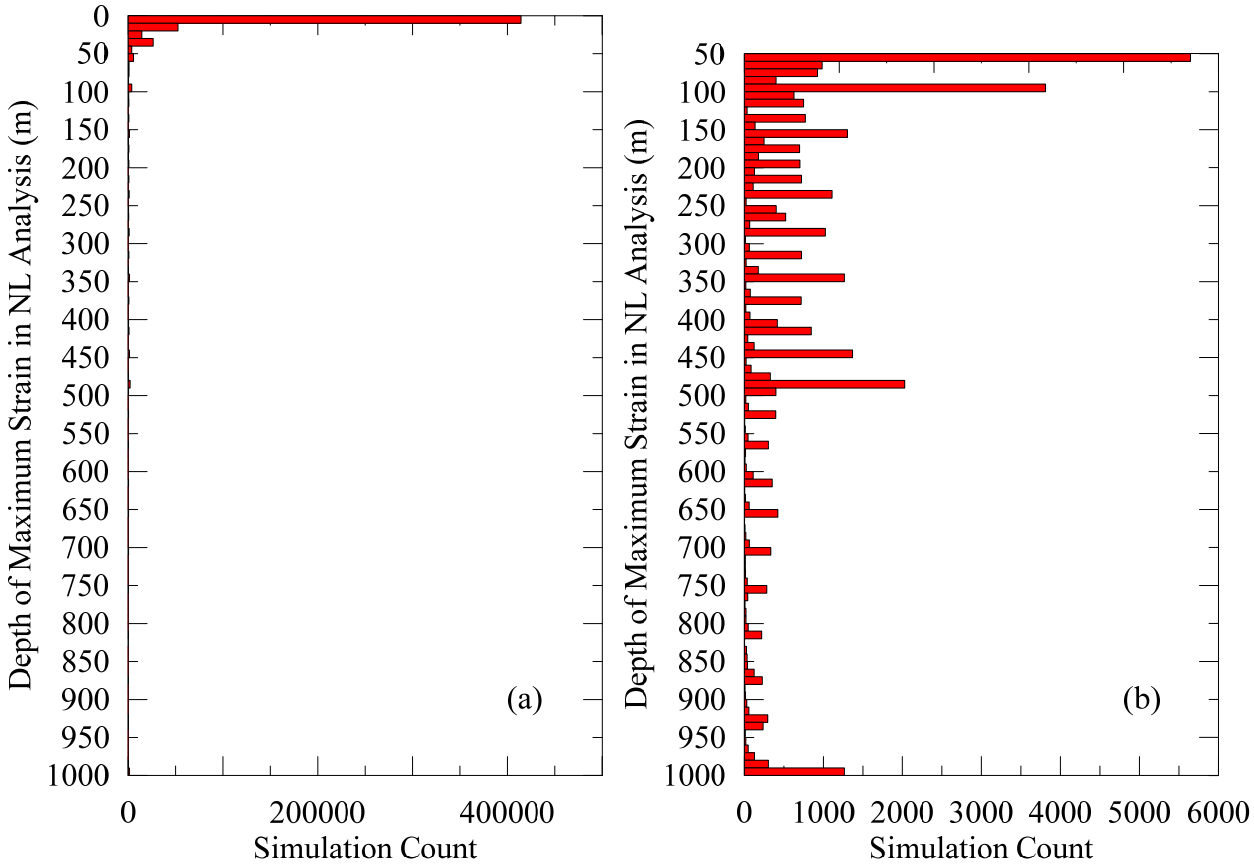

Figure 9.38 Count of location of maximum strain location as a function of depth for all NL simulations between 0 and 1000 m (a) and 50 and 1000 m (b).

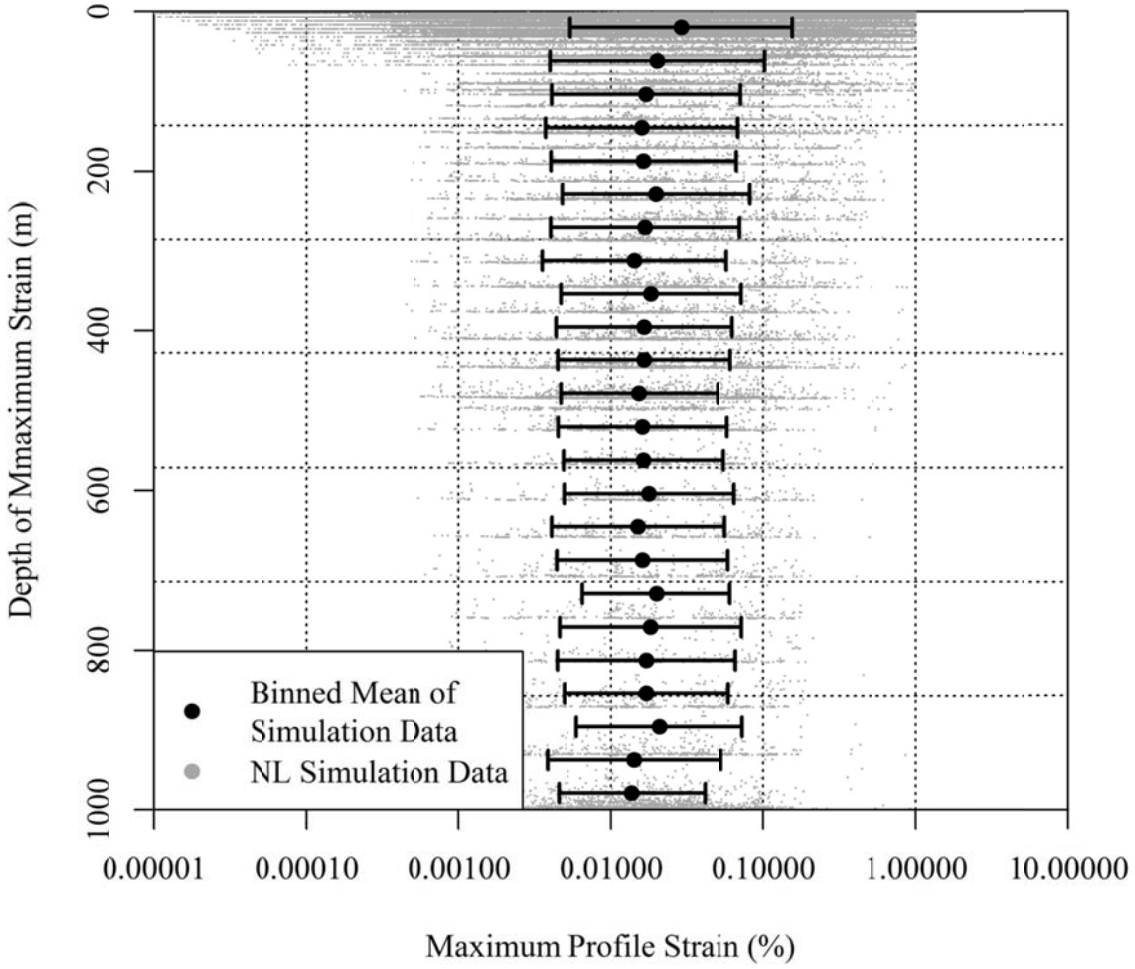

Figure 9.39 Maximum achieved shear strain in NL site response analyses with binned log mean as a function of depth. Error bars show ± 1 log standard deviation from the binned mean.

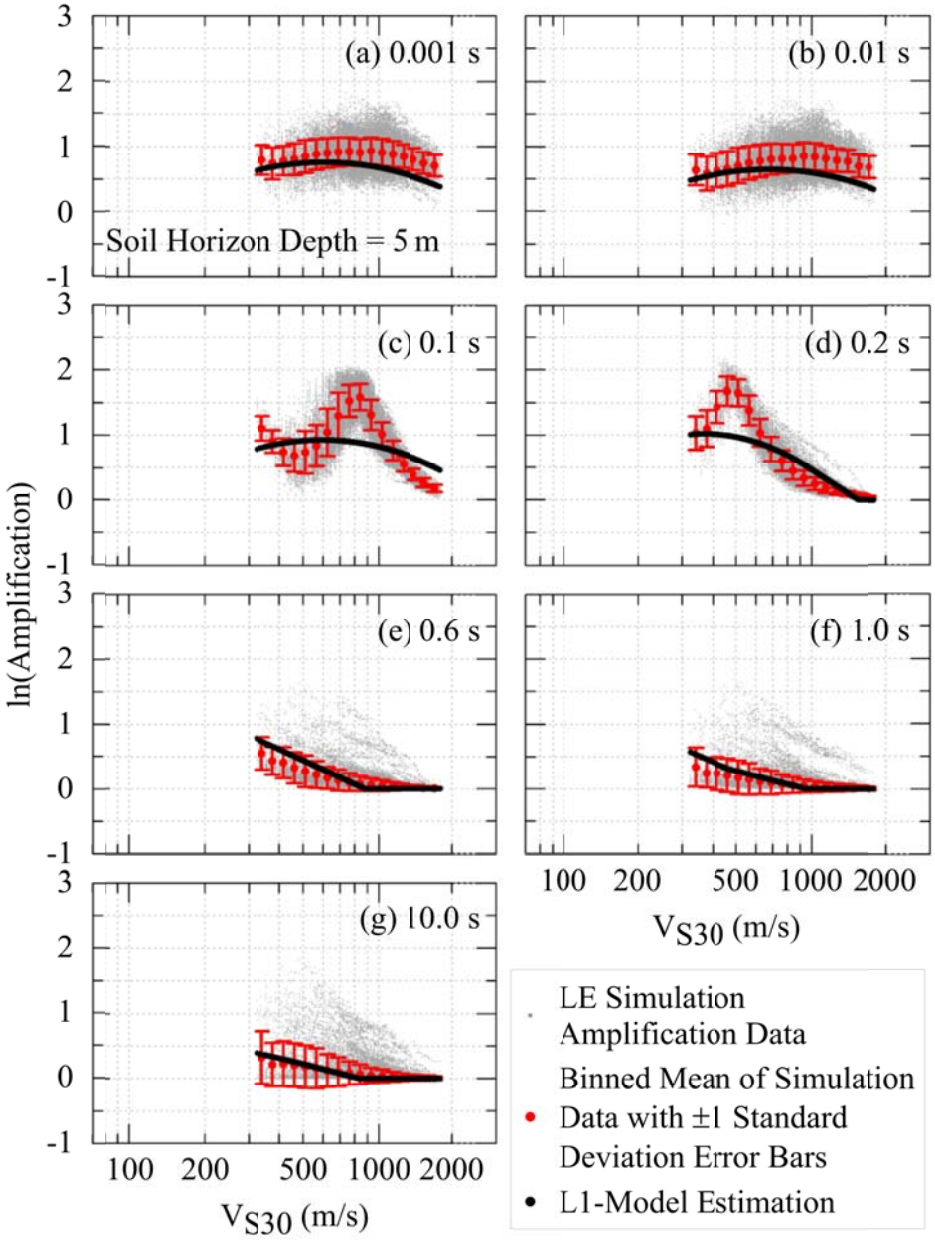

Figure 9.40 LE amplification data from sites with soil horizon thickness 5 m (5 m depth bin) for response spectral periods 0.001 s (a), 0.01s (b) , 0.1 s (c), 0.3 s (d), 0.6 s (e), 1.0 s (f), and 10.0 s (g) with the L1 linear amplification model estimation for those sites.

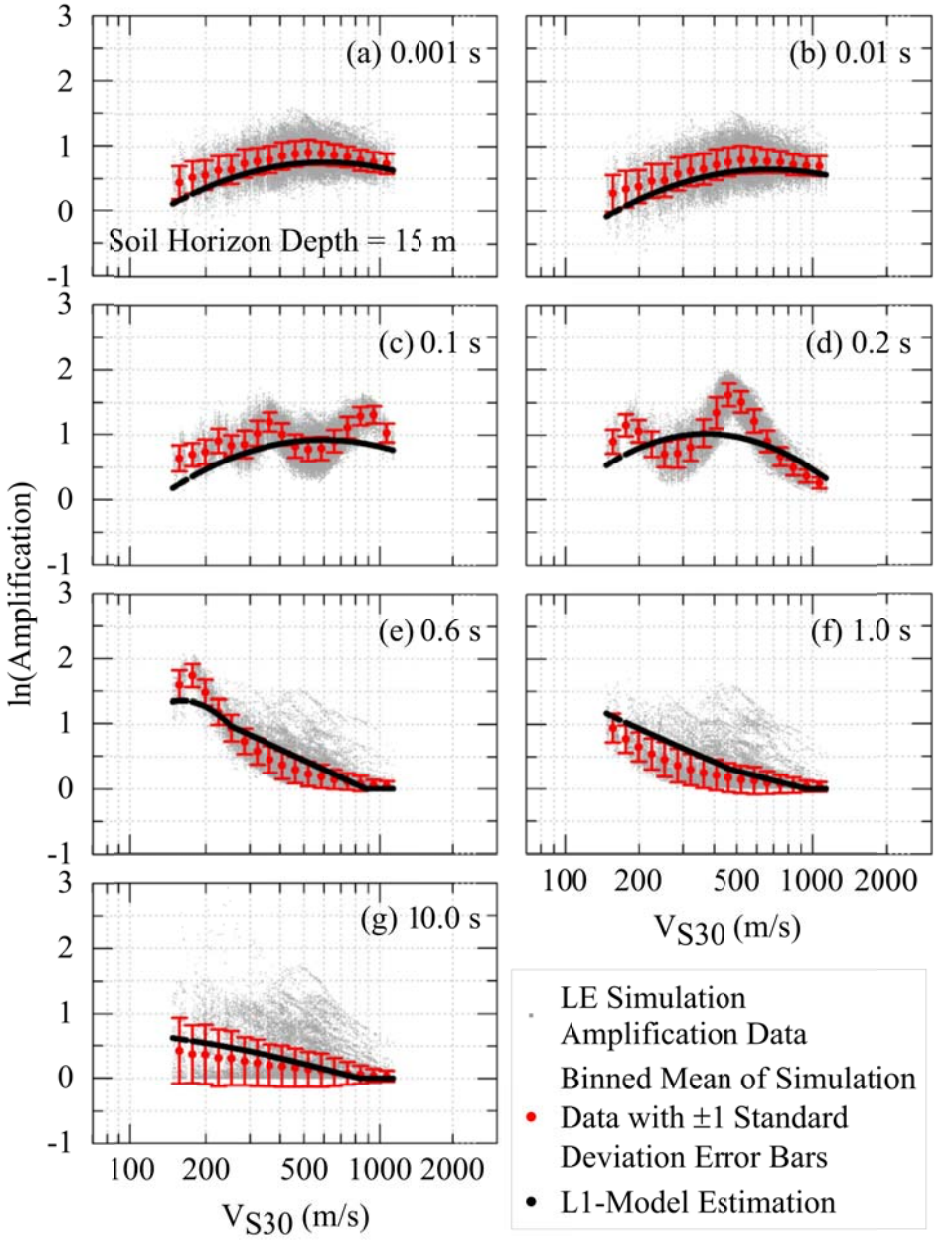

Figure 9.41 LE amplification data from sites with soil horizon thickness 15 m (15 m depth bin) for response spectral periods 0.001 s (a), 0.01s (b) , 0.1 s (c), 0.3 s (d), 0.6 s (e), 1.0 s (f), and 10.0 s (g) with the L1 linear amplification model estimation for those sites.

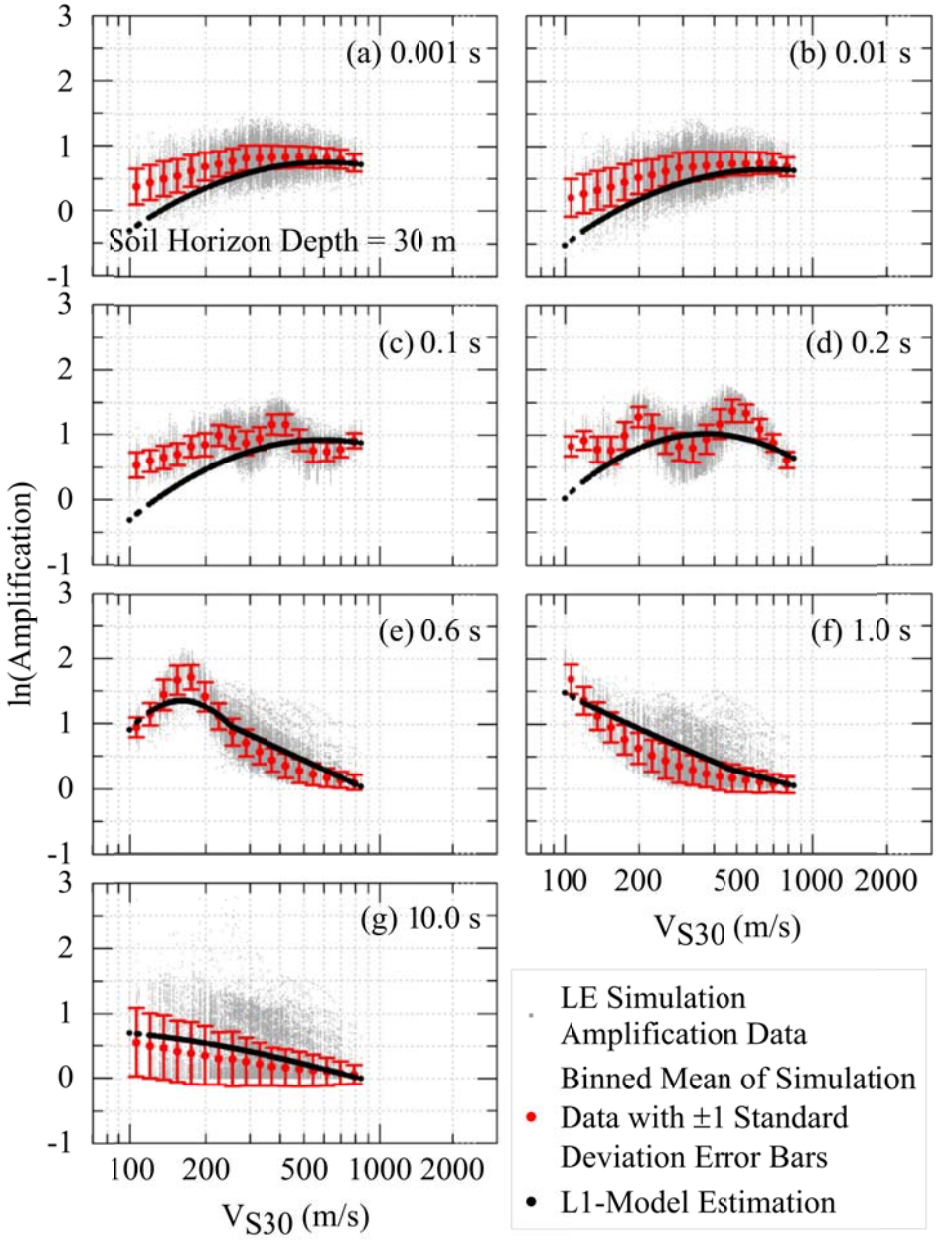

Figure 9.42 LE amplification data from sites with soil horizon thickness 30 m (30 m depth bin) for response spectral periods 0.001 s (a), 0.01s (b) , 0.1 s (c), 0.3 s (d), 0.6 s (e), 1.0 s (f), and 10.0 s (g) with the L1 linear amplification model estimation for those sites.

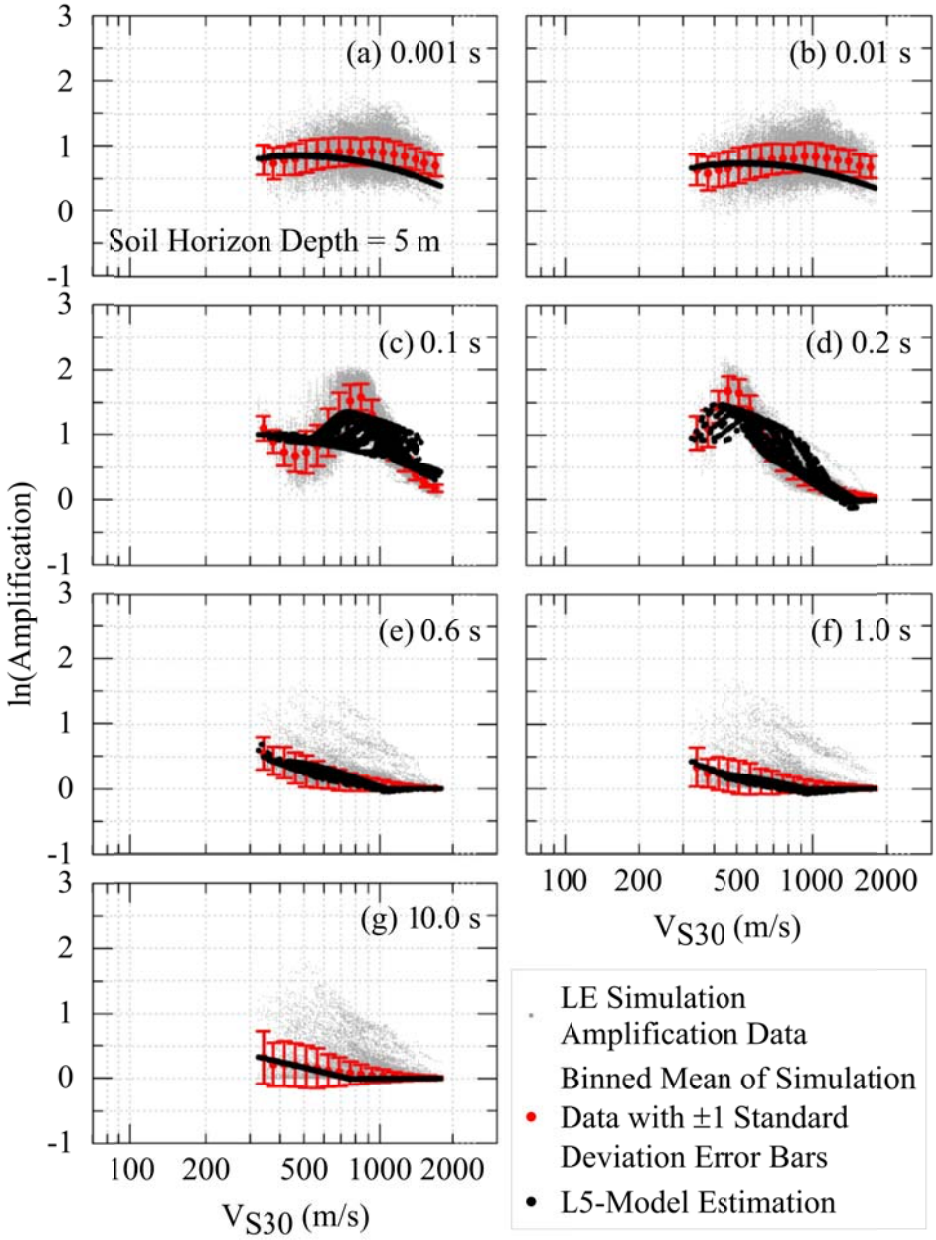

Figure 9.43 LE amplification data from sites with soil horizon thickness 5 m (5 m depth bin) for response spectral periods 0.001 s (a), 0.01s (b) , 0.1 s (c), 0.3 s (d), 0.6 s (e), 1.0 s (f), and 10.0 s (g) with the L5 linear amplification model estimation for those sites.

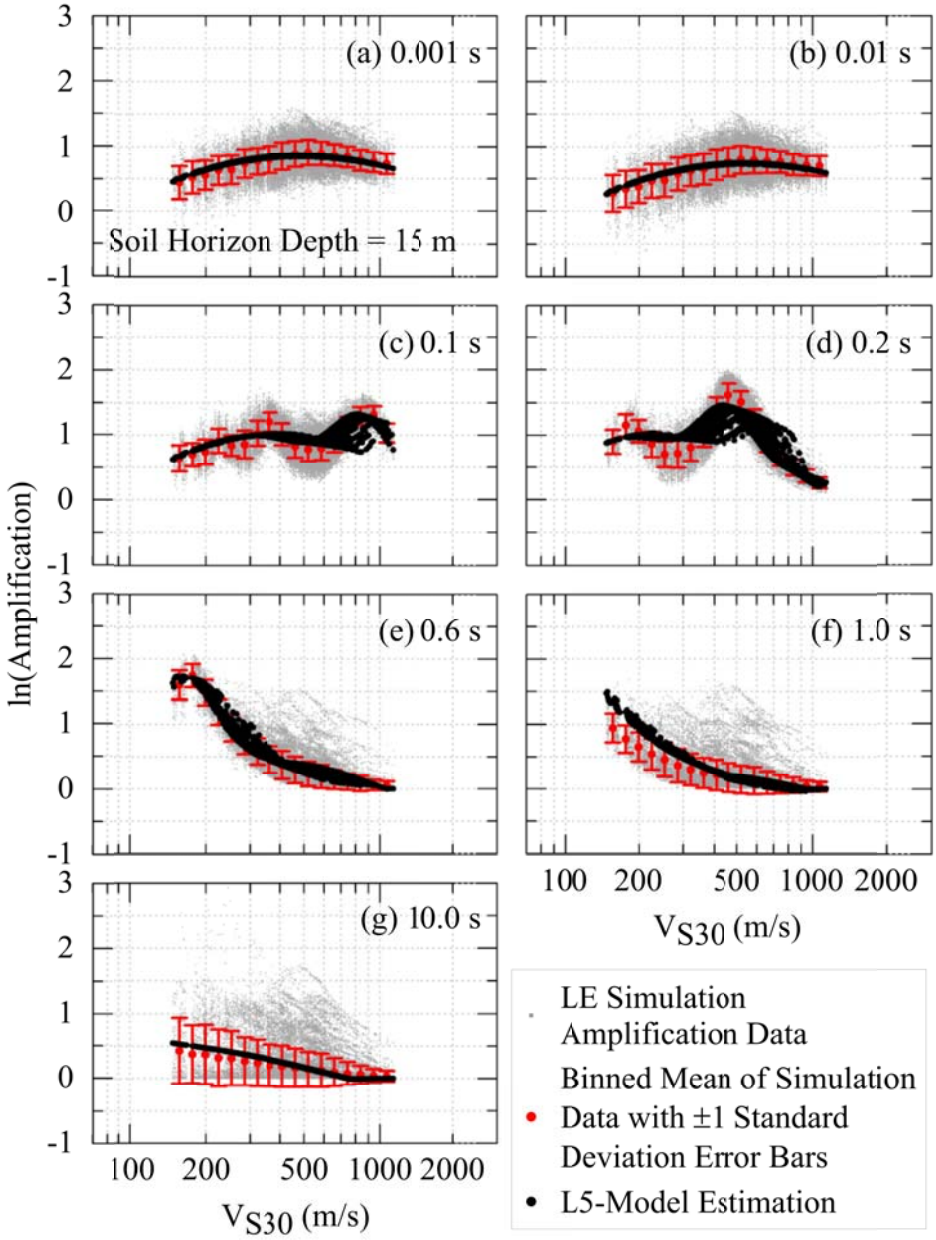

Figure 9.44 LE amplification data from sites with soil horizon thickness 15 m (15 m depth bin) for response spectral periods 0.001 s (a), 0.01s (b) , 0.1 s (c), 0.3 s (d), 0.6 s (e), 1.0 s (f), and 10.0 s (g) with the L5 linear amplification model estimation for those sites.

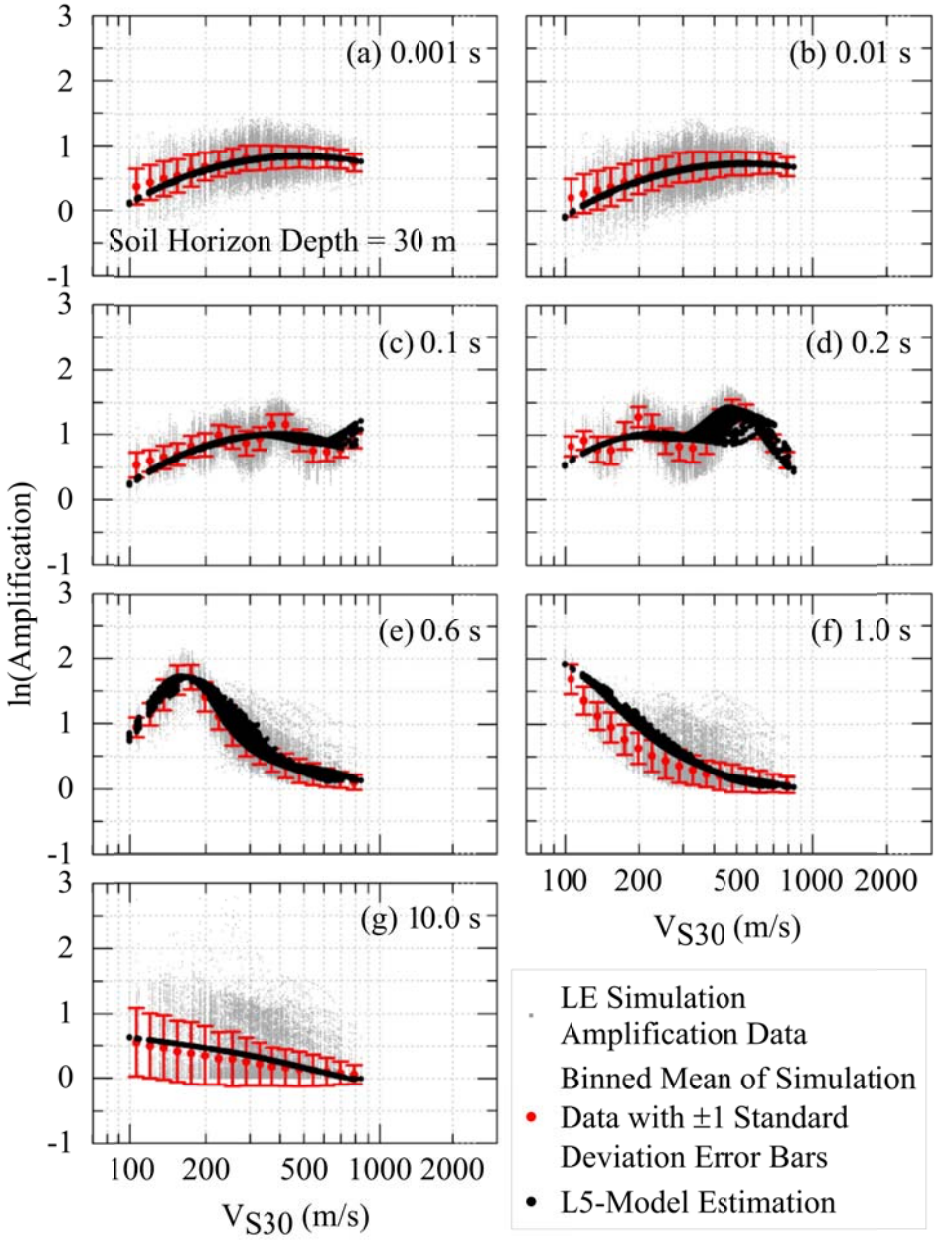

Figure 9.45 LE amplification data from sites with soil horizon thickness 30 m (30 m depth bin) for response spectral periods 0.001 s (a), 0.01s (b) , 0.1 s (c), 0.3 s (d), 0.6 s (e), 1.0 s (f), and 10.0 s (g) with the L5 linear amplification model estimation for those sites.

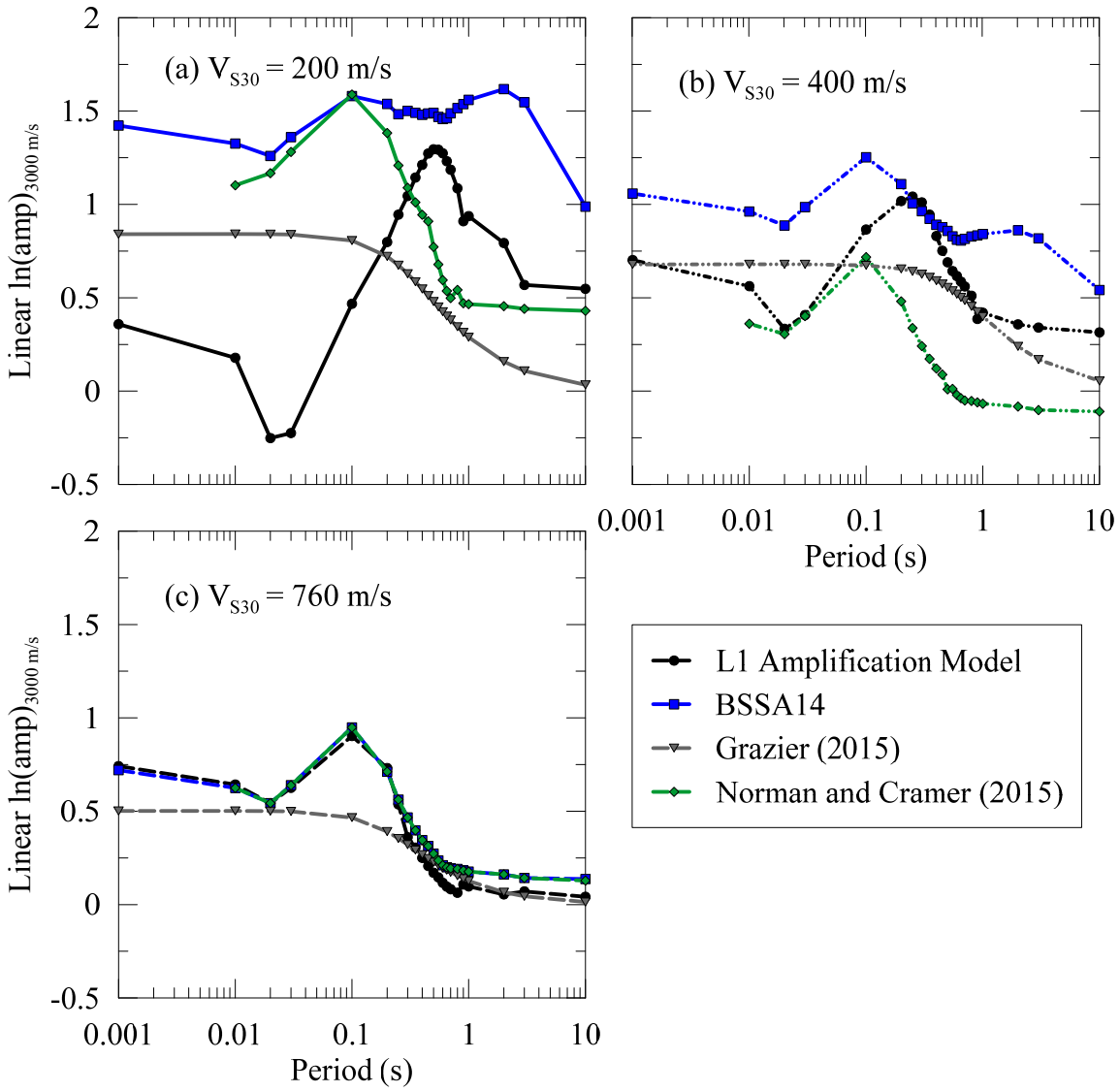

Figure 9.46: Comparison of V_{S30} linear amplification models relative to 3000 m/s. The BSSA14, and Al Noman and Cramer (2015) models have been corrected to a 3000 m/s condition using the $C_{760\text{-}3000}$ presented in this study.

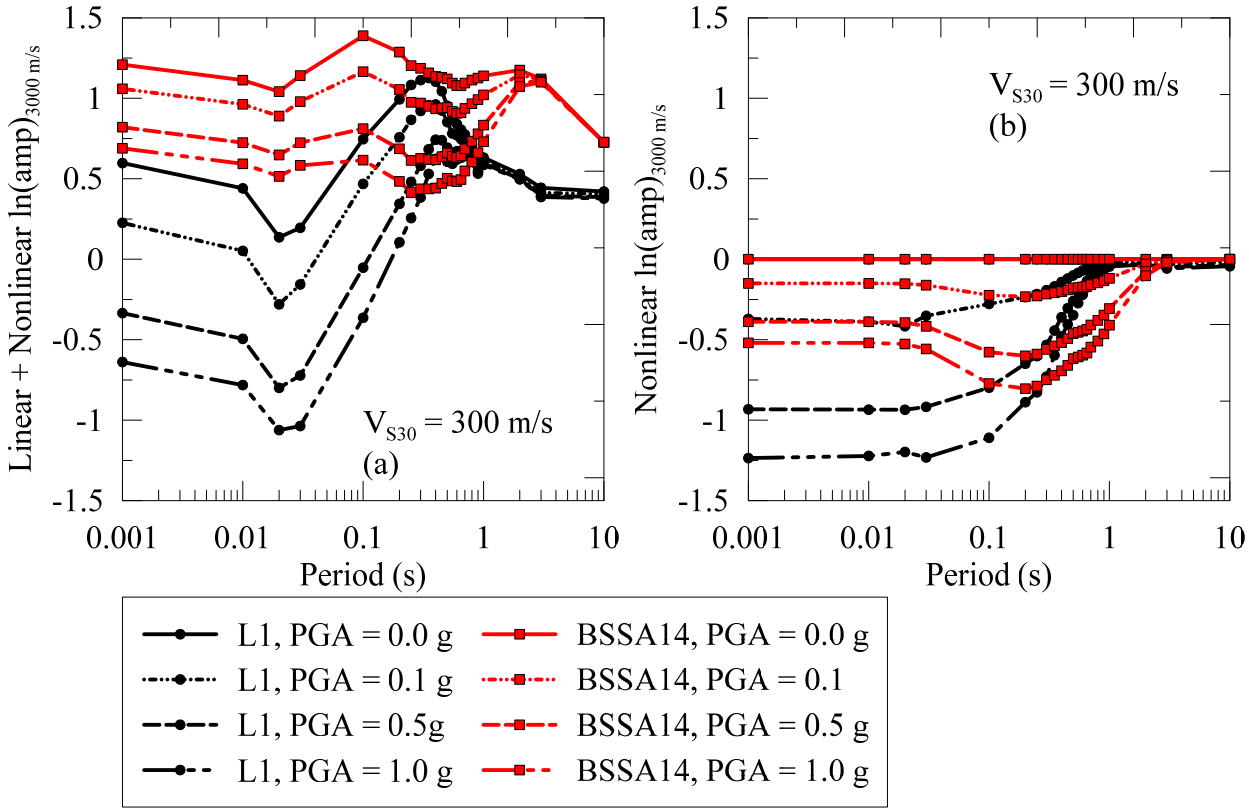

Figure 9.47: Comparison of site nonlinearity of models relative to 3000 m/s for a V_{S30} = 300 m/s site condition. The BSSA14 model has been corrected to a 3000 m/s condition using $C_{760\text{-}3000}$ as presented in this study.

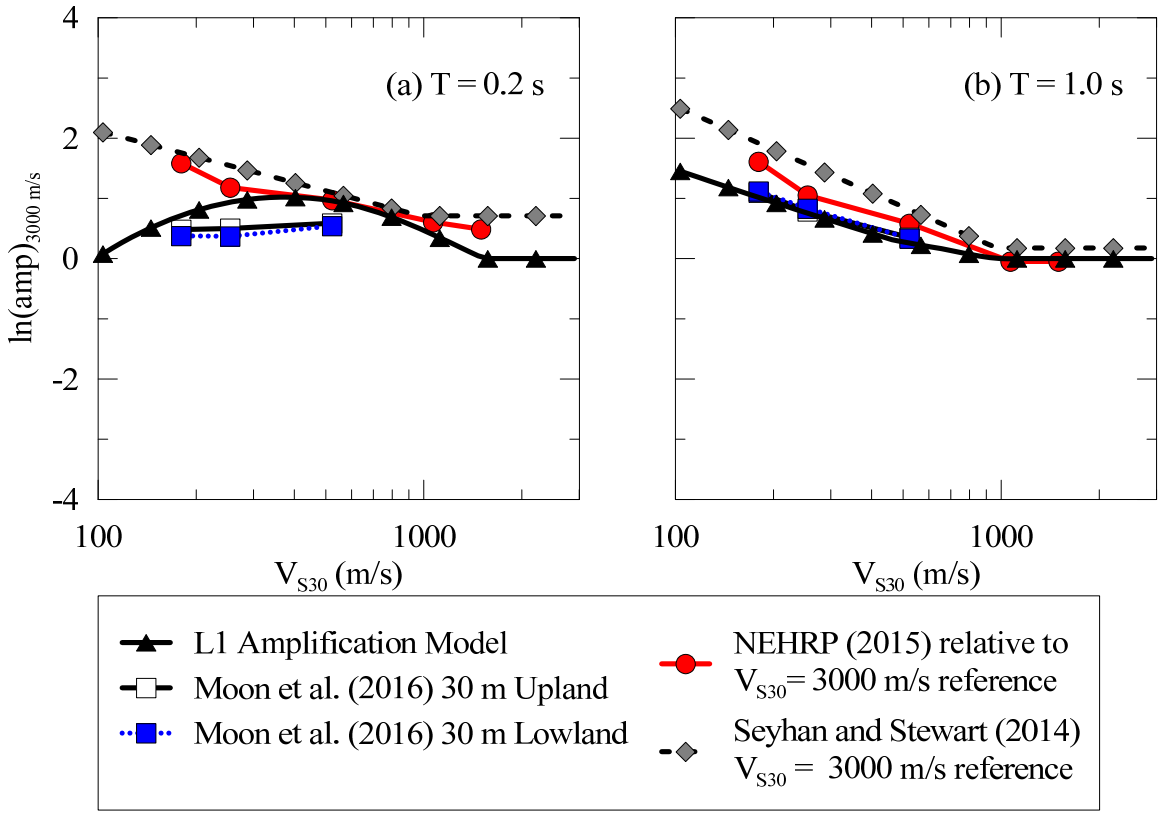

Figure 9.48 Comparison of site amplification models with natural log of site amplification relative to a 3000 m/s reference condition shown as a function of V_{S30} for response spectral periods 0.2 s (a) and 1.0 s (b). The NEHRP (2015) and amplification model has been corrected from a 760 m/s reference condition to a 3000 m/s reference condition using the 760/3000 relationship presented in this study.

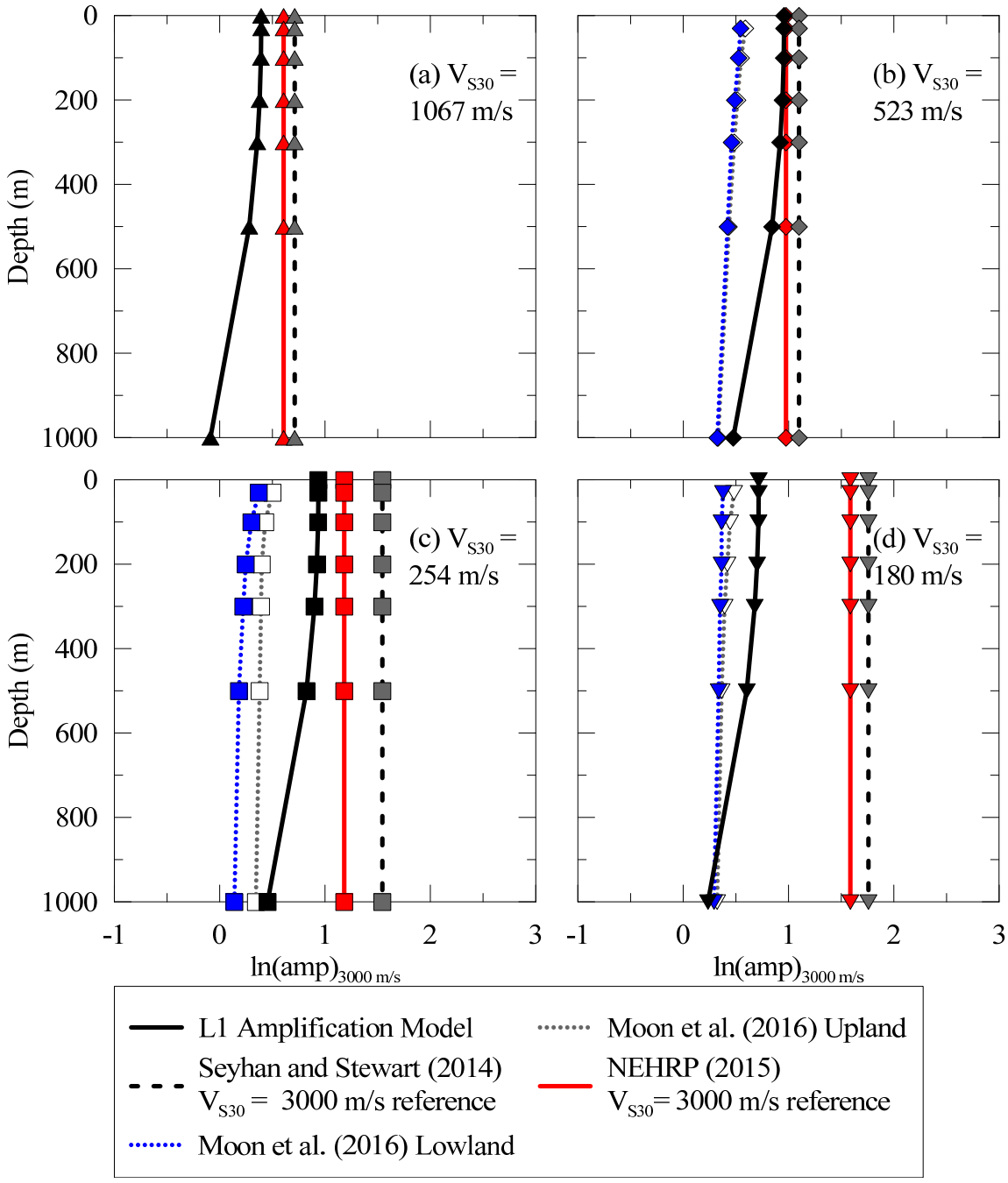

Figure 9.49 Comparison of depth dependency of site amplification models for response spectral period of 0.2 s. Amplification relative to a 3000 m/s reference condition shown as a function of depth for sites with V_{S30} = 1067 m/s (a), V_{S30} = 523 m/s (b), V_{S30} = 254 m/s (c), and V_{S30} = 180 m/s (d).

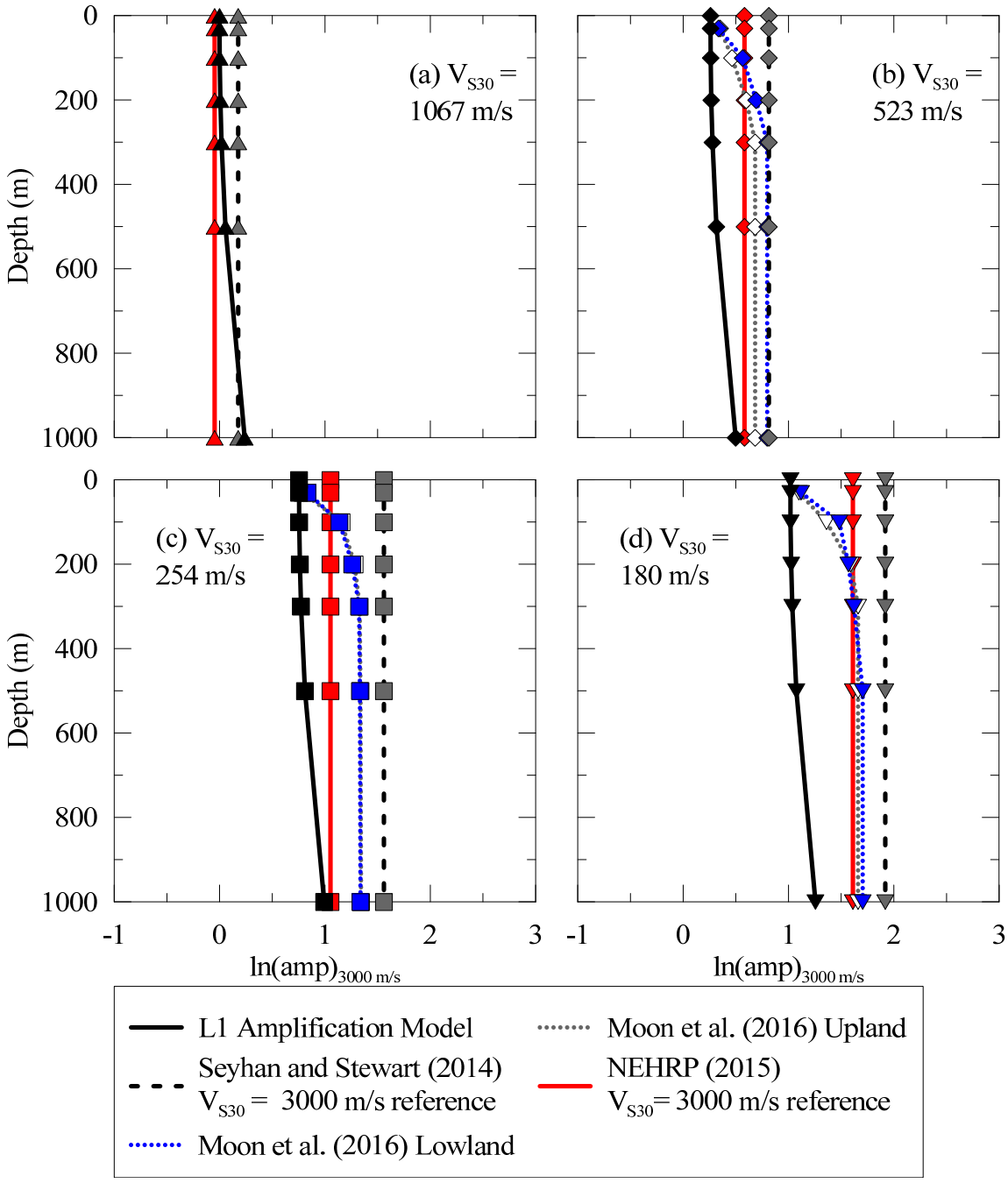

Figure 9.50 Comparison of depth dependency of site amplification models for response spectral period of 1.0 s. Amplification relative to a 3000 m/s reference condition shown as a function of depth for sites with V_{S30} = 1067 m/s (a), V_{S30} = 523 m/s (b), V_{S30} = 254 m/s (c), and V_{S30} = 180 m/s (d).

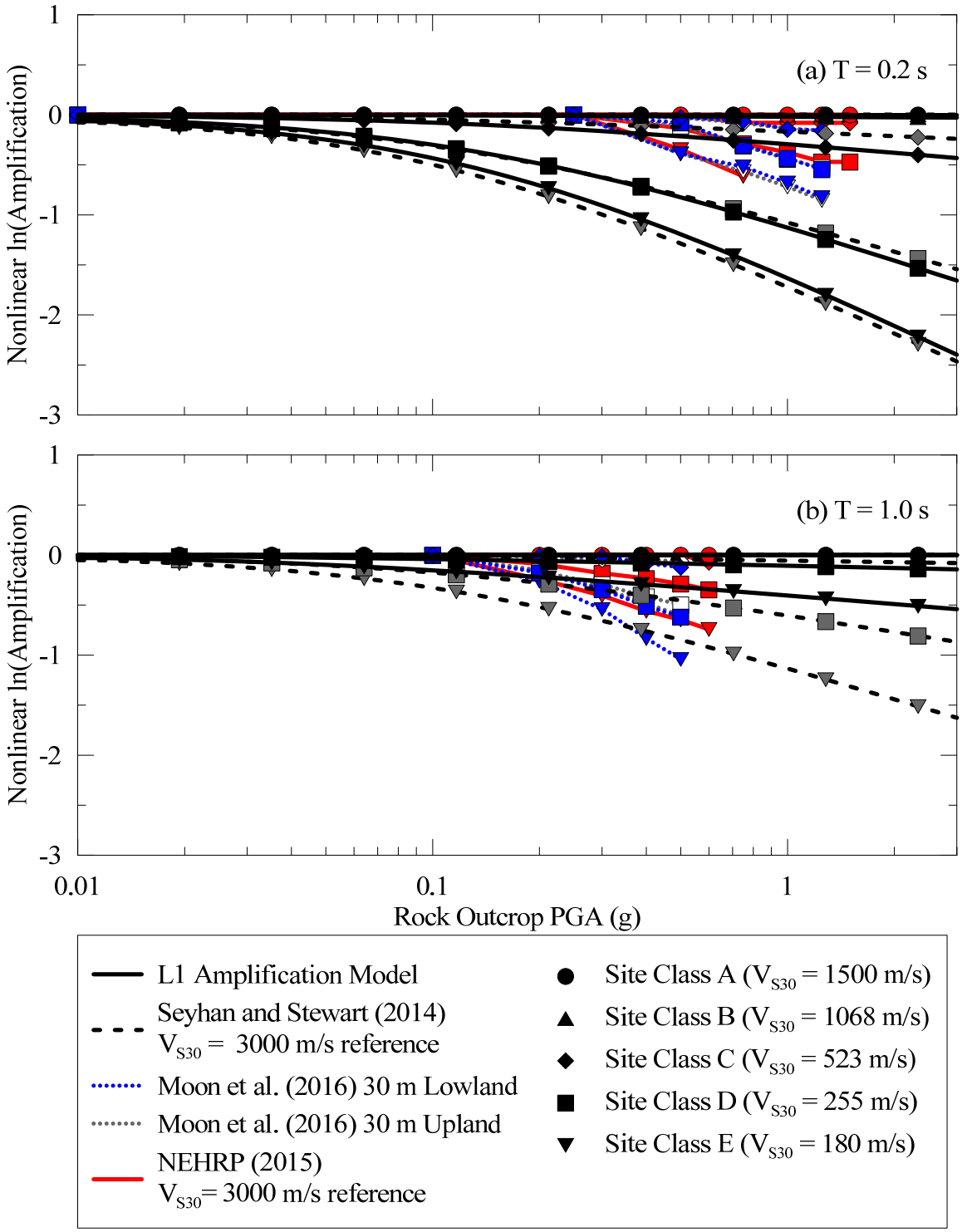

Figure 9.51 Comparison of nonlinearity of ln(amplification) of site amplification models for spectral periods of T = 0.2 s (a) and T = 1.0 s (b).

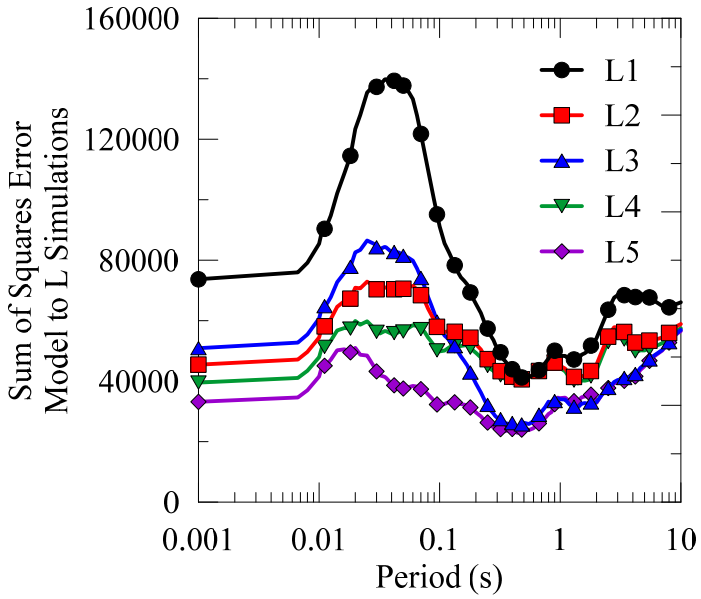

Figure 9.52: Total sum of squares error for linear site amplification models.

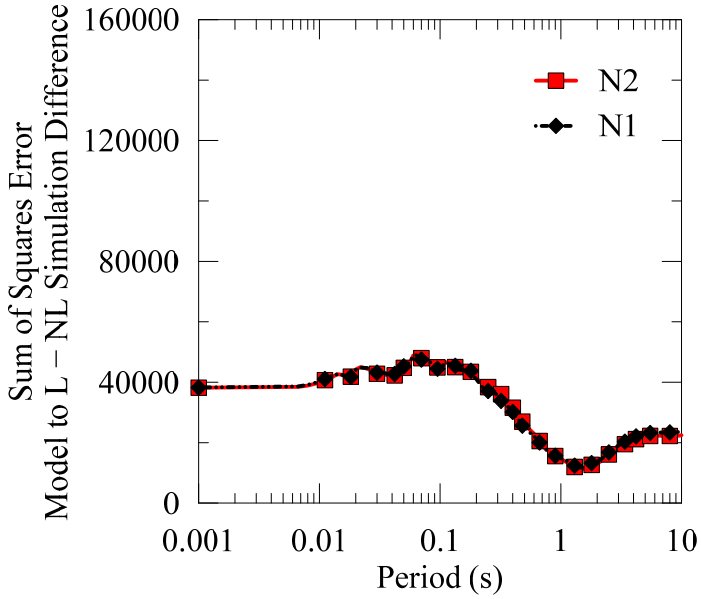

Figure 9.53: Sum of squares error for nonlinear site amplification terms (N-Terms).

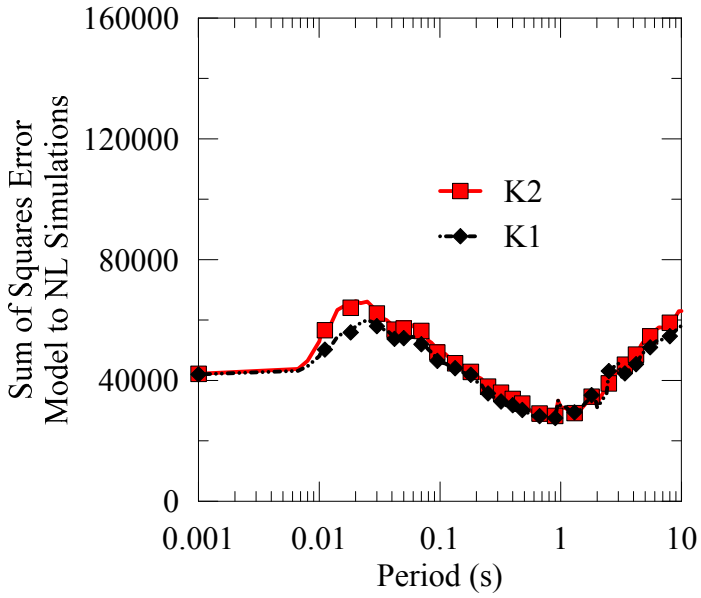

Figure 9.54: Sum of Squares error for K amplification models.

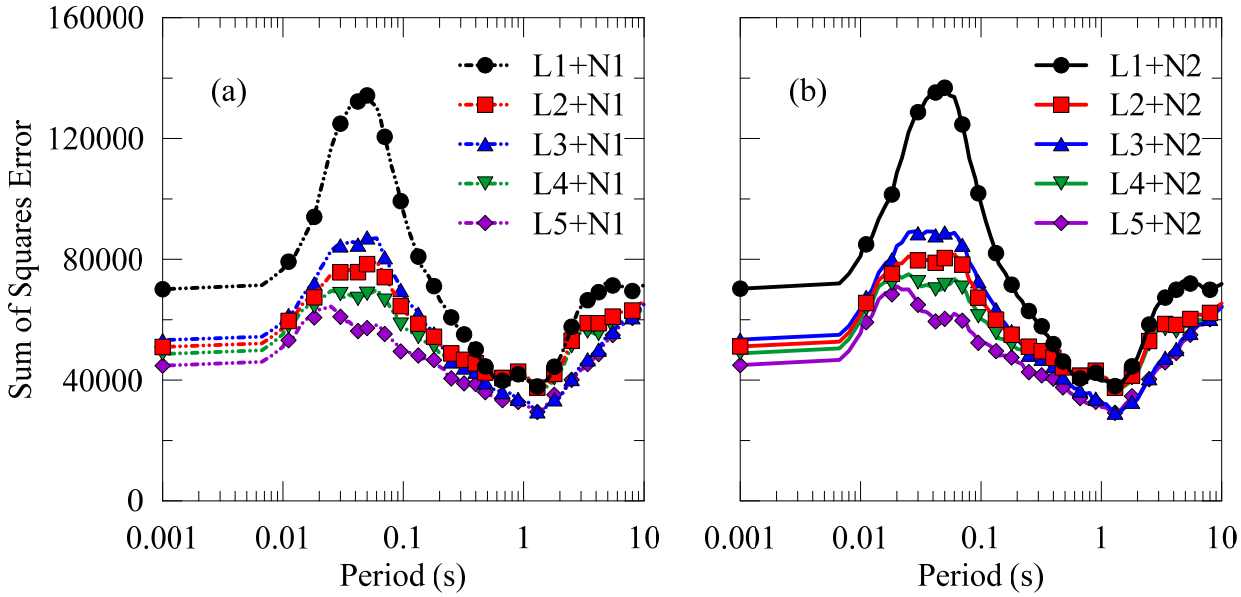

Figure 9.55: Total sum of squares error for L+N- and K-type nonlinear site amplification models with PSA as the driver of nonlinearity (a) and PGA as the driver of nonlinearity (b).

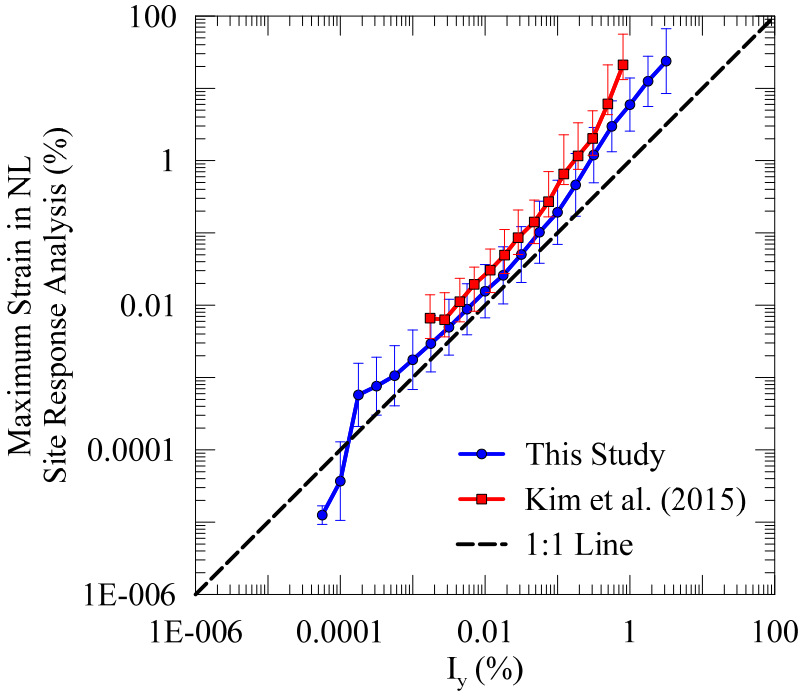

Figure 9.56 Comparison of maximum shear strain in NL site response analyses in this study and in Kim et al. (2015).

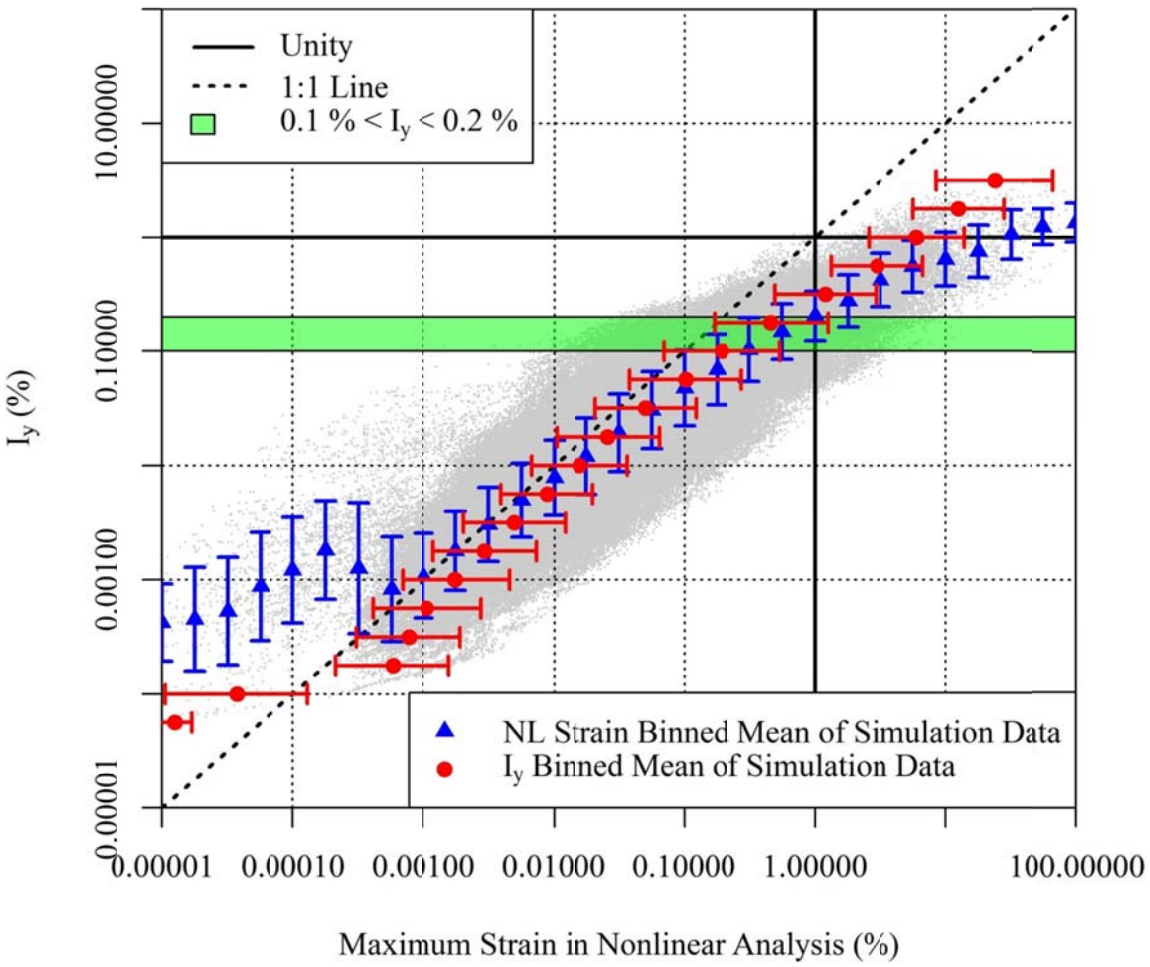

Figure 9.57 Strain index I_y as a function of maximum strainin NL analysis with site amplification I_y applicability limit of 0.1 % to 0.2 %.

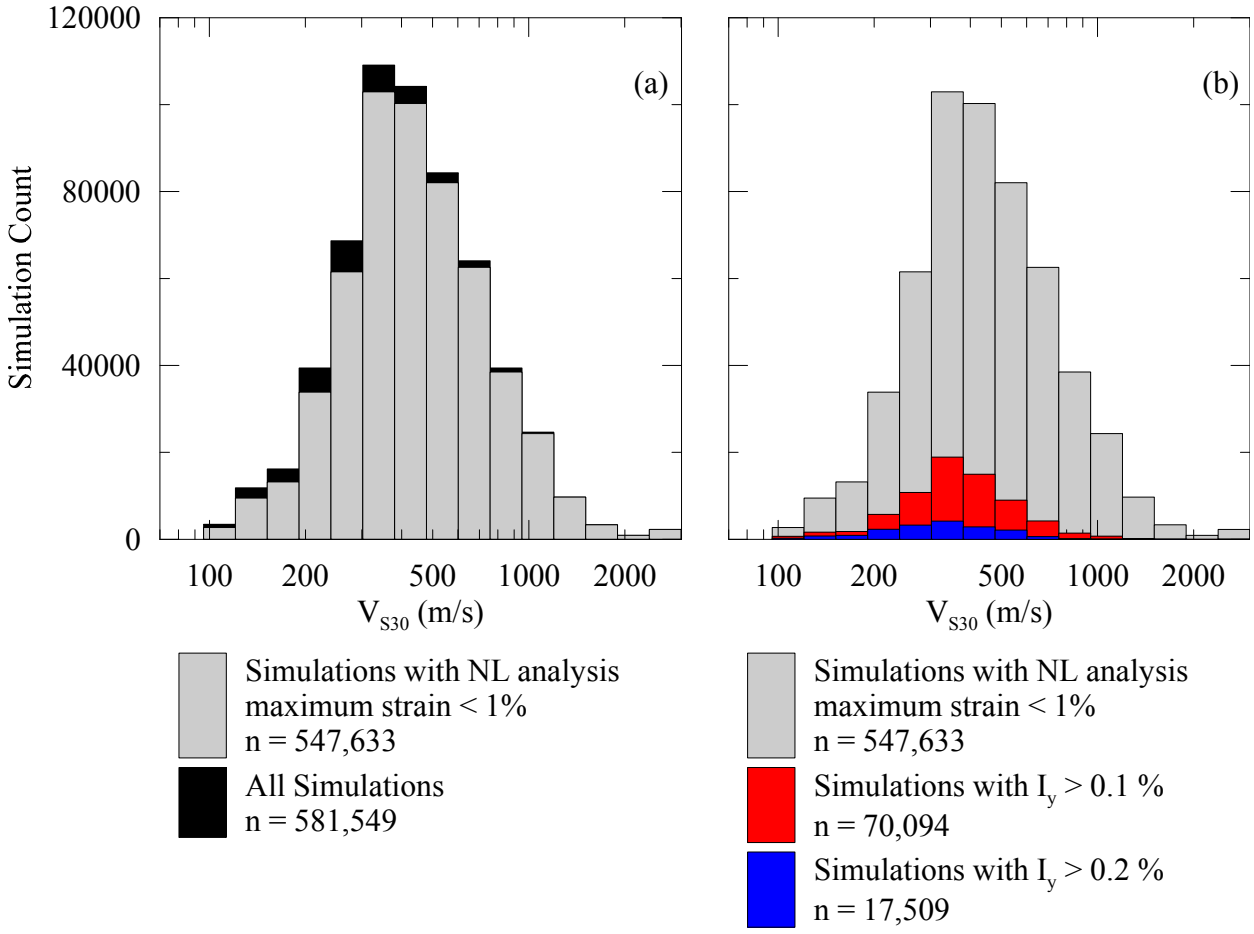

Figure 9.58 Distribution of all NL simulations and NL simulations with maximum strain less than 1 % as a function of V_{S30} (a) and the subsets of NL simulations maximum strain less than 1% with I_y greater than 0.1 % and greater than 0.2 % (b).

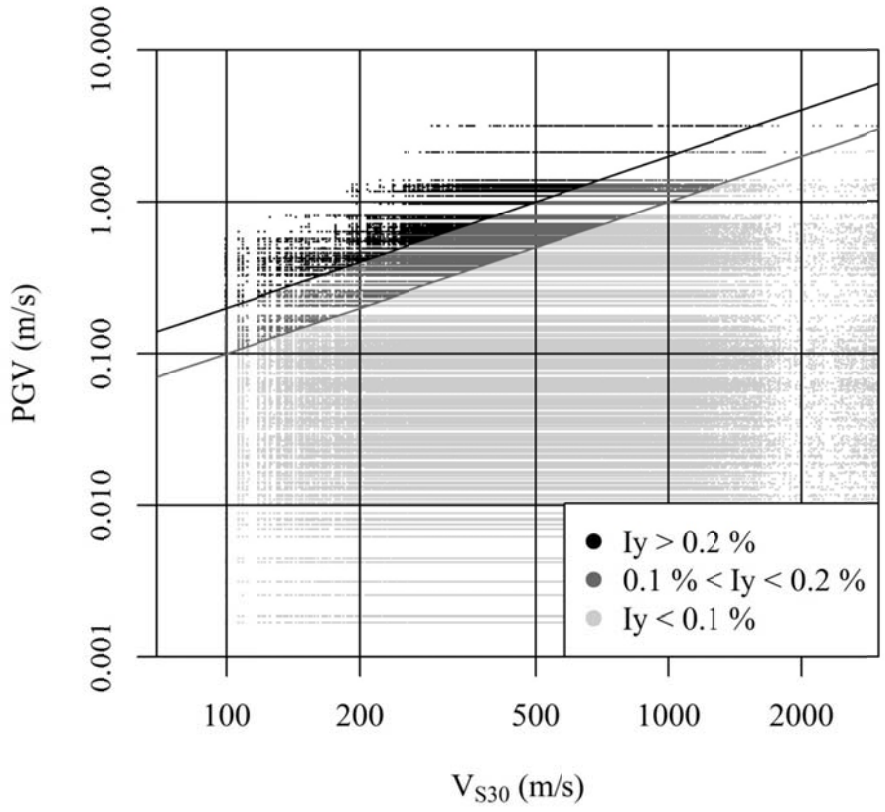

Figure 9.59 Ranges of I_y in terms of PGV and V_{S30} of simulations used in model regression with bounds shown for I_y values of 0.1 % and 0.2 %.

Chapter 10. Fourier Amplitude Spectrum Site Amplification Models

This section presents a site amplification form for the FAS for CENA. Similar to the RS amplification model presented in the FAS site amplification model follows the form given in eq. 10.1.

$$\ln(amp)_{FAS} = E_{S,B} = E_{lin} + E_{nl} \quad \text{eq. 10.1}$$

where $E_{S,B}$ is the FAS site amplification absent of multidimensional and basin effects, and is the sum of a linear amplification component (E_{lin}) and a nonlinear site amplification component (E_{nl}). This functional form is analogous to the functional form of the RS amplification model presented in eq. 2.1.

10.1 Linear Fourier Amplitude Spectrum Amplification Model

The linear site amplification component of the FAS, E_{lin}, for any site is the site-specific transfer function. Unlike the response spectrum, the linear component of amplification for the FAS can be directly computed for a V_S profile. The site transfer function can also be developed from field recordings of ground motions. In the response spectral amplification, the linear amplification for any period is affected by the frequency content of the surrounding periods and derivation of an ergodic site amplification function requires simulation with many rock outcrop ground motion conditions to capture the interdependency of frequencies in the RS. In the FAS, the transfer function at any frequency depends only on that frequency. When the transfer function is known for a site, either through calculation from a V_S profile or field recordings of ground motion, it is recommended that E_{lin} be set equal to the transfer function for the site.

For the development of GMM's as in Hollenback et al. (2015), there may be sites with ground motion stations in which the full V_S profile or ground motion recordings are unavailable, and a more general V_{S30}-based FAS amplification model may be desired. When the site specific transfer function or full V_S profile is not available, E_{lin} can be estimated as a function of V_{S30} and depth.

E_{lin} cannot be characterized with simple V_{S30} scaling terms in the same way as F_{lin}, the linear site amplification for the response spectrum given in eq. 9.3. The linear FAS amplification at 10 Hz as a function of V_{S30} for all linear elastic site response simulations at six different depths is shown in Figure 10.1. Figure 10.1 highlights the difficulty in applying generalized ergodic scaling functions to the linear elastic FAS data. The shape and amplitude of the site amplification as a function of V_{S30} in the FAS is far more sensitive to depth than the RS.

Values of the linear FAS amplification binned by V_{S30} and depth are provided as an approximation of E_{lin} in APPENDIX B. The values provided are the ratio of the smoothed FAS surface response to the smoothed FAS of the rock outcrop ground motion for 30 V_{S30} values evenly distributed between 90 m/s and 3000 m/s for soil column depths of 0 m (i.e. weathered rock-like material at the ground surface), 5 m, 10 m, 15 m, 20 m, 25 m, 30 m, 50 m, 100 m, 500 m, and 1000 m. Figure 10.1 shows the linear amplification model for a frequency of 10 Hz. The FAS amplification is smoothed using a log-rectangle smoother as described in Goulet et al. (2014). In the absence of a site-specific V_S profile to compute E_{lin}, it is recommended that the tabular form of the model be used.

10.1.1 Effect of V_S Layer Thickness Randomization on Linear Amplification

The randomized V_S profiles used in this study do not have any variability in V_S unit thicknesses, and all randomized V_S profiles are geometrically scaled profiles of the 13 representative seed V_S profiles as discussed in Chapter 5. The characteristic V_S profiles are all extended to depth with the same model. When combined with the depth extension, the V_S randomization procedure results in all randomized profiles having a very similar shape. A small subset of additional V_S profiles were generated with layer thickness randomization to determine the effect that the similar V_S shapes in the parametric study had on the observed linear amplification of the FAS.

A supplementary set of 38,727 LE analyses that included layer thickness randomization were conducted to determine the effects of variable V_S layer thickness on the shape of the linear amplification of the FAS. A version of the parametric study tree shown in Figure 3.1 for linear elastic analyses using 50 V_S realizations with layer thickness randomization instead of 30 realizations without layer thickness randomization and no study levels of nonlinear curve were generated using the Toro (1995) randomization model. The assumed parameters for the V_S

randomization were ρ = 1.0 and $\sigma_{ln(V)}$ = 0.2, assuming perfect layer correlation of V_S as for the rest of the simulations presented in this study. The assumed parameters for the layer thickness randomization were a = 1.98, b = 10.86, c = -0.5, and randomized layers were constrained to have a minimum thickness of 0.5 m and maximum thickness of 200 m. Each randomized soil profile was randomly paired with a single ground motion evenly sampled from the entire suite of ground motions.

The results of the subset of analyses with layer thickness randomization is compared to the results without layer thickness randomization in Figure 10.3. When the amplification in the FAS is plotted against V_{S30}, there is more variability in the shape of the amplification when V_S layer thickness is randomized than when it is not. The variability in the amplification of the randomized profiles is very limited, suggesting that it may be reasonable to develop ergodic site amplification functions from wavelets in future studies. The bias introduced in this study by not randomizing V_S layer thickness has no effect on the recommendation to use a linear transfer function as the linear site amplification term in the FAS site amplification model.

10.2 Nonlinear FAS Site Amplification Model

The shape of site nonlinearity in the FAS is very similar to the RS. Figure 10.4 shows the difference between the site amplification of the LE site response analyses and the NL site response analyses at 10 Hz in the FAS (a) and at an oscillator period of 0.1 s (10 Hz) in the RS (b). The same general trends, decreasing nonlinear amplification with increasing V_{S30} and increasing nonlinear amplification with increasing rock outcrop PGA are observed in both the FAS and RS.

The nonlinear site amplification function for the FAS, E_{nl}, therefore uses the same functional form as the response spectral nonlinear site amplification and is reproduced in eq. 10.2 and 10.3 based on the nonlinear site amplification function in Seyhan and Stewart (2014).

$$E_{nl} = f_2 \ln\left(\frac{I_r + f_3}{f_3}\right) \qquad \text{eq. 10.2}$$

where f_2 and f_3 describe the nonlinear site effects and I_r is PGA, the intensity measure of the 3000 m/s bedrock condition ground motion that drives site nonlinearity. The f_2 coefficient is given as a function of V_{S30} in eq. 9.9.

$$f_2 = f_4\left[\exp\left\{f_5\left(\min\left(V_{S30}, V_{ref}\right) - 360\right)\right\} - \exp\left\{f_5\left(V_{ref} - 360\right)\right\}\right] \qquad \text{eq. 10.3}$$

where f_4 and f_5 describe the effect of V_{S30} on the nonlinear site effects, and V_{ref} is the reference rock condition of 3000 m/s. The coefficients of eq. 10 are regressed from the difference between the ratio of smoothed surface response to rock outcrop motion of the LE and NL site response analyses. Coefficients for the nonlinear site amplification model for the FAS are presented in APPENDIX A. The nonlinear FAS amplification model is depicted visually at select frequencies in Figure 10.10. At low frequencies, little nonlinearity in the FAS is observed, with generally more nonlinearity at higher frequencies. Between 10.0 Hz and 33.3 Hz, the nonlinear amplification data becomes mores scattered at sites with low V_{S30}, and the nonlinear amplification model begins to deviate from the observed nonlinear amplification.

The EL site response analysis data was considered for use in the derivation of the nonlinear FAS site amplification, but was ultimately not considered due to the classic overdamping of the high frequency present in EL site response analyses. More details on the use of EL analyses in the development of the nonlinear FAS site amplification are provided in Section 10.2.1.

10.2.1 Selection of Simulation Data for FAS Nonlinear Site Amplification

The work presented in this section (10.2.1) was developed in collaboration with E. Rathje and B. Xu of the University of Texas at Austin as a part of the collaboration with the NGA-East Geotechnical Working Group.

NL site response analyses were used to develop the nonlinear FAS amplification model coefficients given in APPENDIX A. However, analyses with either the EL or NL calculation methods could be used to develop a model for FAS site nonlinearity. Nonlinear GQ/H site response analyses were preferred over the EL site response analyses for development of the nonlinear FAS amplification model because of a more realistic surface high frequency

attenuation (e.g. κ_{surf}) behavior and less significant overdamping of the high frequency ranges in the FAS that occurs in EL analyses.

An investigation by Rathje and Xu (2015, Personal Communication) investigated recordings in the NGA-West2 Database (Ancheta et al. 2013) of soft sites with strong ground motions to observe the effect of strong shaking on surface κ. Sites with V_{S30} less than 210 m/s with large PGA and PGV of recorded motions were investigated. Stations and events used in this analysis are available in Table 10.1. The κ of the surface response was compared to the rock outcrop κ to evaluate the Δκ on the surface recording that can be attributed to the site response using eq. 10.4.

$$\Delta\kappa = \kappa_{\text{Surface}} - \kappa_{\text{Outcrop}} \qquad \text{eq. 10.4}$$

The κ of the surface response (total κ) was calculated from the shape of the recording FAS. The κ of the bedrock motion κ_Q was estimated from

$$\kappa_Q = \frac{1}{Q\beta}R \qquad \text{eq. 10.5}$$

where β is bedrock V_S, Q is attenuation, and R is distance. Estimations for κ_Q of sites were made assuming β= 3500 m/s, Q = 1500, and both epicenteral distance, and closest distance as R, $\kappa_{Q,epi}$ and $\kappa_{Q,ClstD}$, respectively. Table 10.2 presents κ values for the sites and motions presented in Table 10.1. Two κ values were evaluated from the shape of the FAS of the surface recording, κ_1 and κ_2 and averaged (avg. κ) in Table 10.2 to reduce the uncertainty in the subjectivity in selecting a frequency range for the calculation of κ. The columns of Table 10.2 "avg. κ-κ_Q(epi) (s)" and "avg. κ-κ_Q(ClstD) (s)" are the difference between the averaged κ from surface recordings and $\kappa_{Q,epi}$ or $\kappa_{Q,ClstD}$ and represent estimates of Δκ for the site. Estimates of Δκ from Tables 10 and Table 10.2 are shown graphically in Figure 10.6(a) for $\kappa_{Q,\ ClstD}$ and in Figure 10.6 (b) for $\kappa_{Q,\ epi}$. For these calculations, the site Δκ has a maximum value of about 0.1 s.

A comparison between the parametric study simulations and the Δκ values shown in Figure 10.6 can be made for the EL site response analyses. The strain-compatible V_S profile from the EL

analysis can be integrated for each model soil layer as an approximation of Δκ due to the site as in eq. 10.6.

$$\Delta\kappa = \int \frac{2 \cdot D}{V_S} dz \qquad \text{eq. 10.6}$$

where D and V_S are the strain-compatible damping ratio and shear wave velocity, respectively for a soil layer at depth z.

A comparison between simulation EL analyses and the sites presented in Table 10.1 for a similar range of I_y, calculated as $I_y = (PGV/V_{S30})$, can be made to determine the applicability of using EL analyses to determine the coefficients for the FAS nonlinear site amplification model. Kim et al. (2015) found that I_y was a strong indicator of differences between the FAS from a NL site response analysis and the FAS from an EL site response analysis and was a proxy for use in estimating soil nonlinearity. Sites and simulations with a similar I_y should have similar amounts of site nonlinearity. The Δκ as calculated by eq. 10.6 from the strain compatible V_S profiles of simulations with an expected I_y of 0.3-0.5% is shown in Figure 10.7. These analyses have the similar I_y as the sites presented in Table 10.1. Note that in Table 10.1, there is no bedrock ground motion recording, and I_y is calculated as (PGV_{Surf}/V_{S30}), while in Kim et al.(2015) I_y is calculated as $PGV_{outcrop}/V_{S30}$. However, in Figure 10.7, the majority of simulations have a strain compatible Δκ well above the maximum observed 0.1 s from ground motion recordings in Figure 10.6. The large values of Δκ observed in the recordings is likely due to overdamping of high frequencies present in EL site response analyses that becomes more pronounced during strong shaking.

The nonlinear GQ/H simulations do not exhibit as much high frequency attenuation as the EL site response analyses. Two typical FAS for nonlinear site response analyses are shown in Figure 10.8. Figure 10.8(a) shows the FAS of the input motion and surface responses of the LE, EL, and NL GQ/H site response analyses. The surface κ estimated from the strain-compatible profile from the EL analysis is about 0.1 s which corresponds to the upper bound of $\kappa_{surface}$ from ground motion recordings. Lines showing the slope of the FAS corresponding to κ = 0.05 s and κ = 0.1 s are also shown for comparison. In this analysis and many others, the surface κ estimated from integration of the strain-compatible EL profile matches well with the κ as inferred from the

surface FAS as shown in Figure 10.8(a). The surface FAS from the NL analysis shown in Figure 10.8(a) has a lower slope than the EL analysis.

Figure 10.8(b) shows a site response analysis where the surface κ estimated from the strain-compatible profile from the EL analysis is about 0.28 s which is well beyond the upper bound of observed $\kappa_{surface}$ from ground motion recordings. In this figure, the classic overdamping of high frequency from the EL analyses is clearly visible. The slope of the NL surface FAS in Figure 10.8(b) is similar to the slope of the NL surface FAS shown in Figure 10.8(a).

Nonlinear GQ/H site response analyses preserve shape of FAS at high frequencies better than EL analyses which tend to overdamp high frequency site response and thus, NL analyses are used in the development of the nonlinear FAS site amplification function model coefficients.

It should be noted that for NL analyses, there is no strain-compatible soil profile analogous to that which is produced by an EL analysis, and eq. 10.6 is not appropriate for use with the results of a NL analysis. The process of fitting a slope to the FAS and inferring a value of κ is subjective and difficult to automate. This study provides no way to estimate surface κ from the results of a particular NL site response analysis.

The shape of the FAS from a NL analysis better captures κ behavior than EL analyses, but is subject to additional constrains on the range of usable frequencies. The upper bound of the usable frequency of a NL analysis is either the $f_{max} = V_S/4H$ of a soil profile where H is model layer thickness or the Nyquist frequency of the rock outcrop ground motion. All soil profiles in this study are subdivided to have $f_{max} \geq 50$ Hz, and motions are selected to have Nyquist frequencies ≥ 100 Hz. Above f_{max}, the shape of the FAS from a NL analysis becomes less reliable. Figure 10.9 shows the ratio of smoothed surface FAS to rock outcrop FAS for an NL, EL, and LE site response analysis of a site with V_{S30} = 550 m/s and rock outcrop ground motion with PGA = 0.05. Above f_{max} the behavior of the FAS ratio of the NL analysis shows a sharp decrease. The lower bound of usable frequency in an NL analysis comes from the lack of constraint on low frequency ground motion content. In a NL site response analysis, there is no way to enforce behavior of low frequency amplification of the FAS, and the amplification behavior can deviate significantly from the LE or EL site response analysis. This low frequency

behavior is not observable in the RS. Figure 10.9 shows a judgement-based lower bound of the usable frequency range of 0.1 Hz.

10.2.2 Applicable Frequency Range of Nonlinear FAS Amplification Model

NL site response analyses preserve high frequency ground motion content at high frequencies than EL site response analyses. However, there are fundamental limitations to the applicable range of frequencies appropriate for use in site amplification from NL site response analyses. The upper range of applicable frequencies is bounded by f_{max}, and the lower range of frequencies results from the lack of a low-frequency constraint on NL site response analyses.

The highest usable frequency that can be produced by a NL site response analyses is limited by the minimum $f_{max}= V_S/4H$ of the soil profile where H is model layer thickness and V_S is the shear wave velocity of that layer. The model resolution of V_S and soil layer thickness provides an upper frequency bound to the range of frequencies usable for development of site amplification in the FAS. In time-domain linear site response analyses, f_{max} serves as a box filter on the surface FAS and an abrupt drop in FAS at f_{max} occurs. In time-domain nonlinear site response analyses, the FAS above f_{max} does not have a consistent shape and the site amplification is unconstrained. In the parametric study for this investigation, the f_{max} of all soil profiles is greater than or equal to 50 Hz. Instabilities in the shape of the FAS start to become evident near f_{max} and the upper bound of frequencies provided for the nonlinear FAS site amplification is 33.3 Hz.

Low frequencies of a time-domain site response analysis are not preserved as discussed in Section 10.2. The lower bound of frequencies provided for the nonlinear FAS site amplification is 0.1 Hz. The nonlinear FAS site amplification below 0.1 Hz is unity. For the same reasons given for the RS above, the FAS amplification model is only valid for sites with $V_{S30} > 200$ m/s and ground motions with PGA values < 1.0 g. For conditions with softer sites or higher intensity ground motion, a site-specific analysis is recommended.

Table 10.1: Recordings used in Kappa Calculations for Large Strain Motions.

	Station Name	EQ Name	PGA (g)	PGV (m/s)	Vs30 (m/s)	EpiD (km)	HypD (km)	ClstD (km)	M	Hyp Depth (km)	I_y $\frac{PGV_{Surf}}{V_{S30}}$
1	NIG018	Chuetsu-oki	0.63	97.7	198	19.2	21.2	10.8	6.8	9.0	0.49
2	Christchurch Resthaven	Christchurch, New Zealand	0.52	69.5	141	7.6	9.7	5.1	6.2	6.0	0.49
3	Kashiwazaki NPP, Service Hall Array 2.4 m depth	Chuetsu-oki	0.39	97.1	201	13.6	16.3	11.0	6.8	9.0	0.48
4	Pages Road Pumping Station	Christchurch, New Zealand	0.65	89.2	206	4.9	7.7	2.0	6.2	6.0	0.43
5	El Centro Array #6	Imperial Valley-06	0.45	87.8	203	27.5	29.2	1.4	6.5	10.0	0.43
6	El Centro Array #7	Imperial Valley-06	0.44	82.7	211	27.6	29.4	0.6	6.5	10.0	0.39
7	El Centro Array #5	Imperial Valley-06	0.41	78.3	206	27.8	29.5	4.0	6.5	10.0	0.38
8	El Centro Array #4	Imperial Valley-06	0.38	79.1	209	27.1	28.9	7.1	6.5	10.0	0.38
9	Parkfield - Fault Zone 1	Parkfield-02, CA	0.64	67.3	178	8.4	11.7	2.5	6.0	8.1	0.38
10	Port Island (0 m)	Kobe, Japan	0.32	73.1	198	19.3	26.3	3.3	6.9	17.9	0.37
11	Christchurch Resthaven	Darfield, New Zealand	0.26	50.4	141	48.3	49.5	19.5	7.0	10.9	0.36
12	El Centro Array #12	El Mayor-Cucapah	0.33	68.5	197	58.0	58.3	11.3	7.2	5.5	0.35
13	Shirley Library	Christchurch, New Zealand	0.34	69.8	207	8.0	10.0	5.6	6.2	6.0	0.34
14	APEEL 2 - Redwood City	Loma Prieta	0.24	43.9	133	63.5	65.9	43.2	6.9	17.5	0.33
15	TTR008	Tottori, Japan	0.39	44.7	139	16.5	20.7	6.9	6.6	12.5	0.32
16	Christchurch Cathedral College	Christchurch, New Zealand	0.41	63.2	198	5.8	8.3	3.3	6.2	6.0	0.32
17	Foster City - APEEL 1	Loma Prieta	0.28	36.9	116	64.0	66.4	43.9	6.9	17.5	0.32
18	Christchurch Hospital	Christchurch, New Zealand	0.38	59.4	194	7.4	9.5	4.9	6.2	6.0	0.31
19	El Centro Array #11	El Mayor-Cucapah	0.50	59.8	196	59.0	59.2	16.2	7.2	5.5	0.3
20	El Centro Differential Array	Imperial Valley-06	0.44	57.8	202	27.2	29.0	5.1	6.5	10.0	0.29

Table 10.2: κ estimates from selected NGA-West2 Recordings. See text for column header description.

	Station Name	EQ Name	Usable freq. range (Hz)		linear range to calculate κ (Hz)		κ_1 (s)	κ_2 (s)	avg. κ (s)	κ_Q(epi) (s)	κ_Q (ClstD) (s)	avg. κ-κ_Q(epi) (s)	avg. κ-κ_Q(ClstD) (s)
1	NIG018	Chuetsu-oki	0.125	30	2	26	0.043	0.048	0.045	0.004	0.002	0.041	0.043
2	Christchurch Resthaven	Christchurch, New Zealand	0.100	35	3	20	0.046	0.054	0.050	0.001	0.001	0.049	0.049
3	Kashiwazaki NPP, Service Hall Array 2.4 m depth	Chuetsu-oki	0.100	30	3	25	0.037	0.034	0.036	0.003	0.002	0.033	0.034
4	Pages Road Pumping Station	Christchurch, New Zealand	0.100	80	5	20	0.053	0.038	0.045	0.001	0.000	0.044	0.045
5	El Centro Array #6	Imperial Valley-06	0.063	40	4	20	0.022	0.017	0.019	0.005	0.000	0.014	0.019
6	El Centro Array #7	Imperial Valley-06	0.075	40	4	20	0.044	0.041	0.042	0.005	0.000	0.037	0.042
7	El Centro Array #5	Imperial Valley-06	0.050	40	4	20	0.037	0.013	0.025	0.005	0.001	0.020	0.024
8	El Centro Array #4	Imperial Valley-06	0.063	40	3	15	0.061	0.044	0.052	0.005	0.001	0.047	0.051
9	Parkfield - Fault Zone 1	Parkfield-02, CA	0.188	30	5	22	0.062	0.054	0.058	0.002	0.000	0.056	0.057
10	Port Island (0 m)	Kobe, Japan	0.15	33	3	25	0.037	0.046	0.042	0.004	0.001	0.038	0.041
11	Christchurch Resthaven	Darfield, New Zealand	0.063	40	3	25	0.044	0.047	0.045	0.009	0.004	0.036	0.042
12	El Centro Array #12	El Mayor-Cucapah	0.050	80	5	25	0.053	0.052	0.053	0.011	0.002	0.042	0.051
13	Shirley Library	Christchurch, New Zealand	0.075	65	4	25	0.031	0.039	0.035	0.002	0.001	0.034	0.034
14	APEEL 2 - Redwood City	Loma Prieta	0.075	22	3	15	0.096	0.094	0.095	0.012	0.008	0.083	0.087
15	TTR008	Tottori, Japan	0.015	30	4	14	0.049	0.040	0.045	0.003	0.001	0.041	0.043
16	Christchurch Cathedral College	Christchurch, New Zealand	0.050	80	4	17	0.040	0.059	0.050	0.001	0.001	0.049	0.049
17	Foster City - APEEL 1	Loma Prieta	0.150	18	4	17	0.112	0.108	0.110	0.012	0.008	0.098	0.102
18	Christchurch Hospital	Christchurch, New Zealand	0.063	50	4	36	0.026	0.024	0.025	0.001	0.001	0.024	0.024
19	El Centro Array #11	El Mayor-Cucapah	0.075	60	4	20	0.070	0.075	0.072	0.011	0.003	0.061	0.069
20	El Centro Differential Array	Imperial Valley-06	0.029	40	9	19	0.064	0.090	0.077	0.005	0.001	0.072	0.076

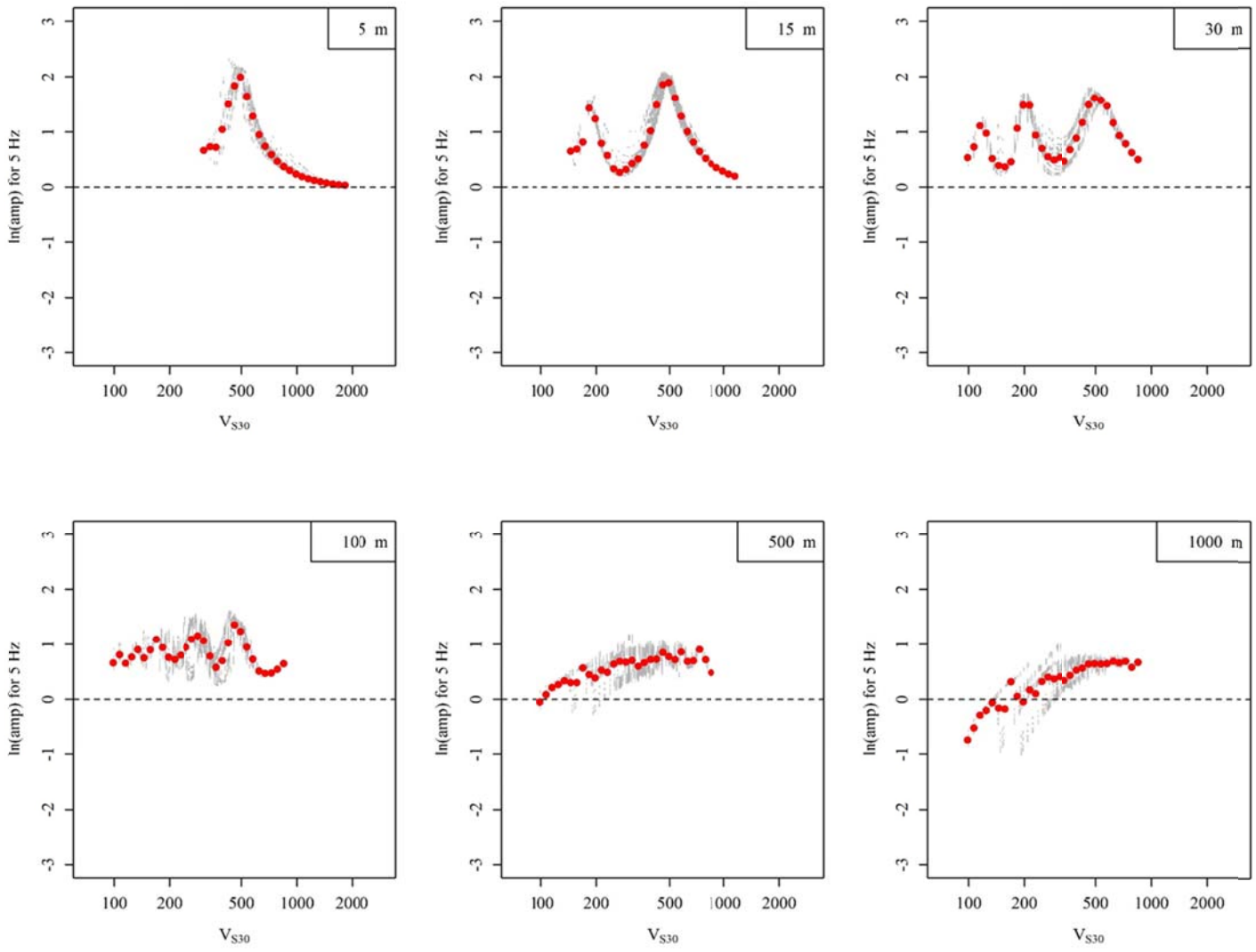

Figure 10.1: FAS Amplification at 10 Hz simulation data and binned data as a function of V_{S30} for simulations of soil depths of 5 m, 15 m, 30 m, 100 m, 500 m and 1000 m depth.

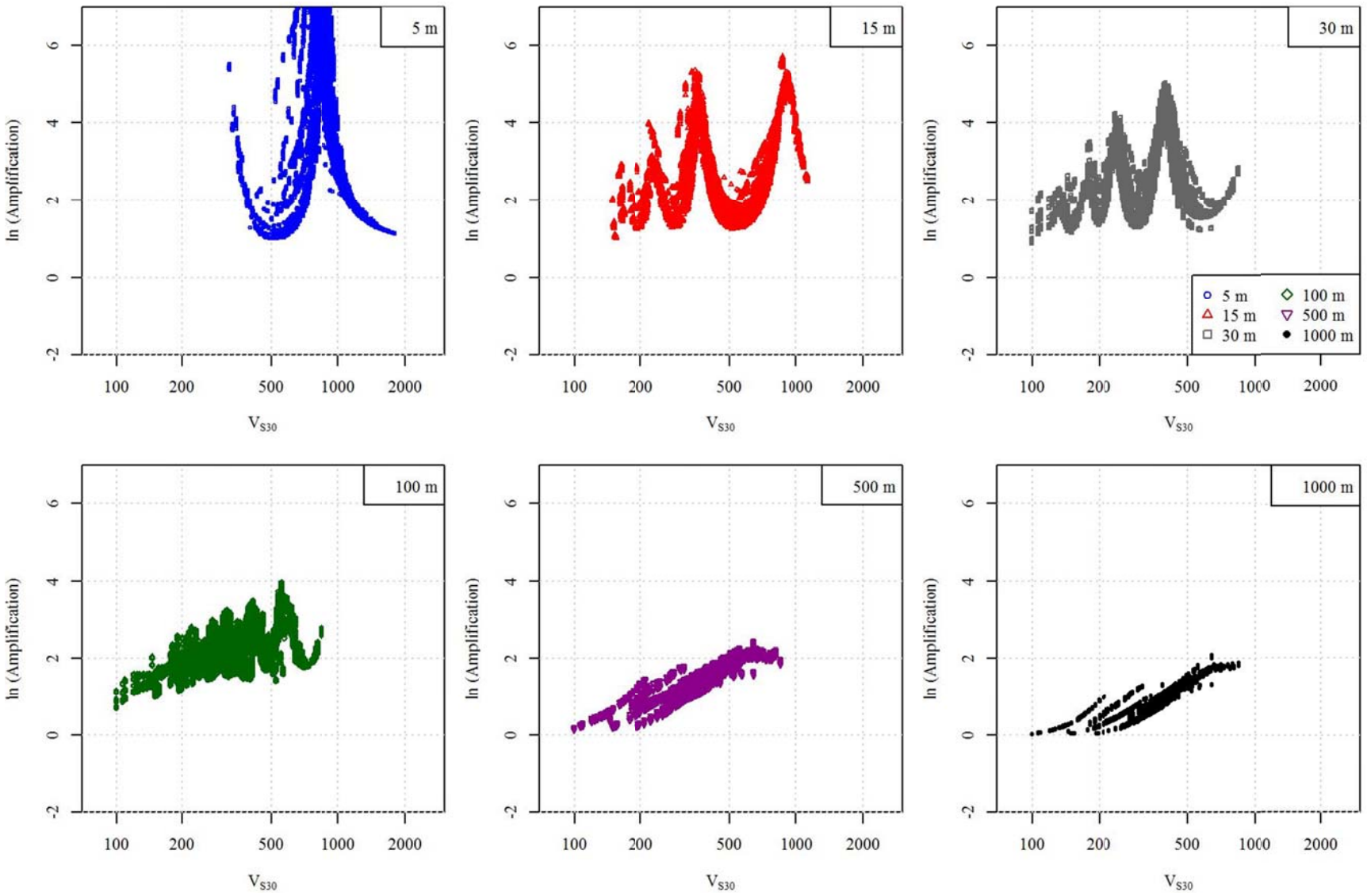

Figure 10.2: FAS linear site amplification as calculated from linear elastic site response analyses.

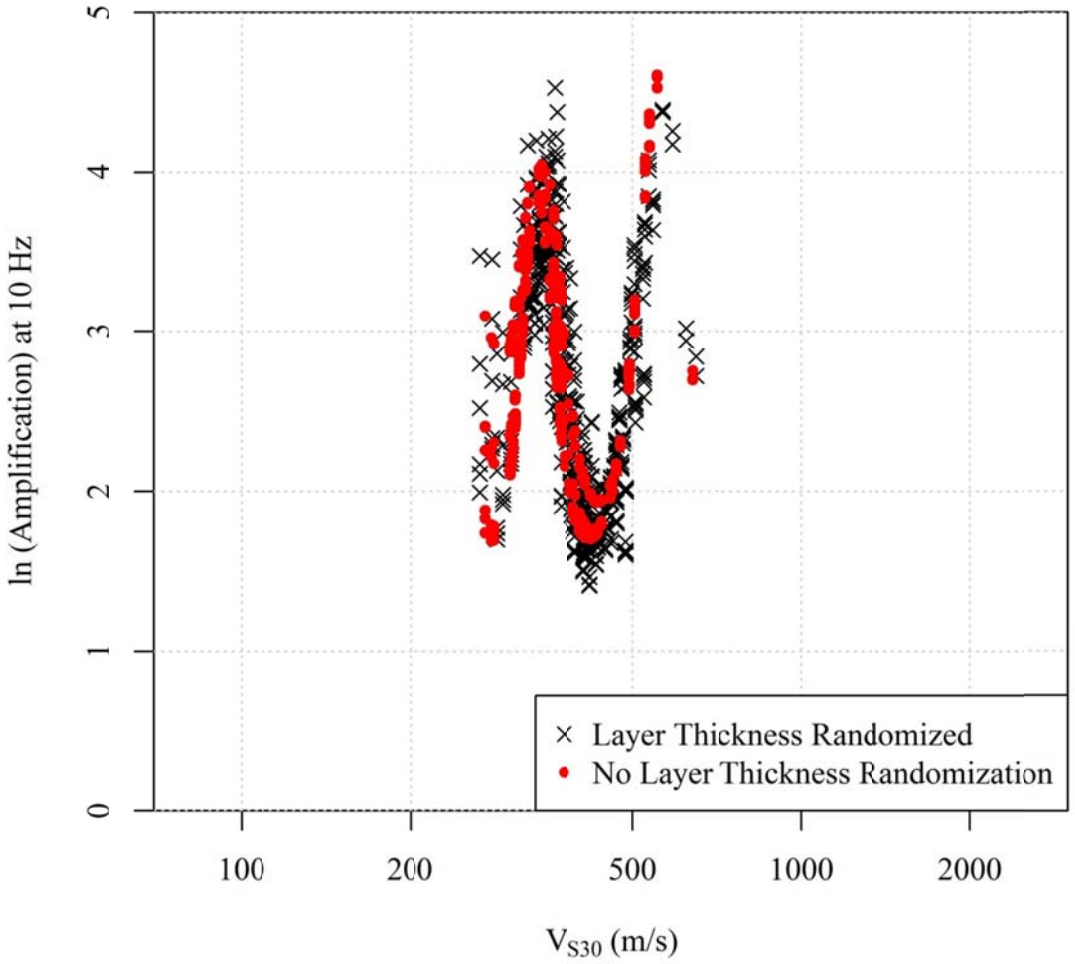

Figure 10.3: FAS amplification for the RRm+OG characteristic V_S profile at 50 m depth for 30 random realizations without layer thickness randomization, and 50 realizations with layer thickness randomization.

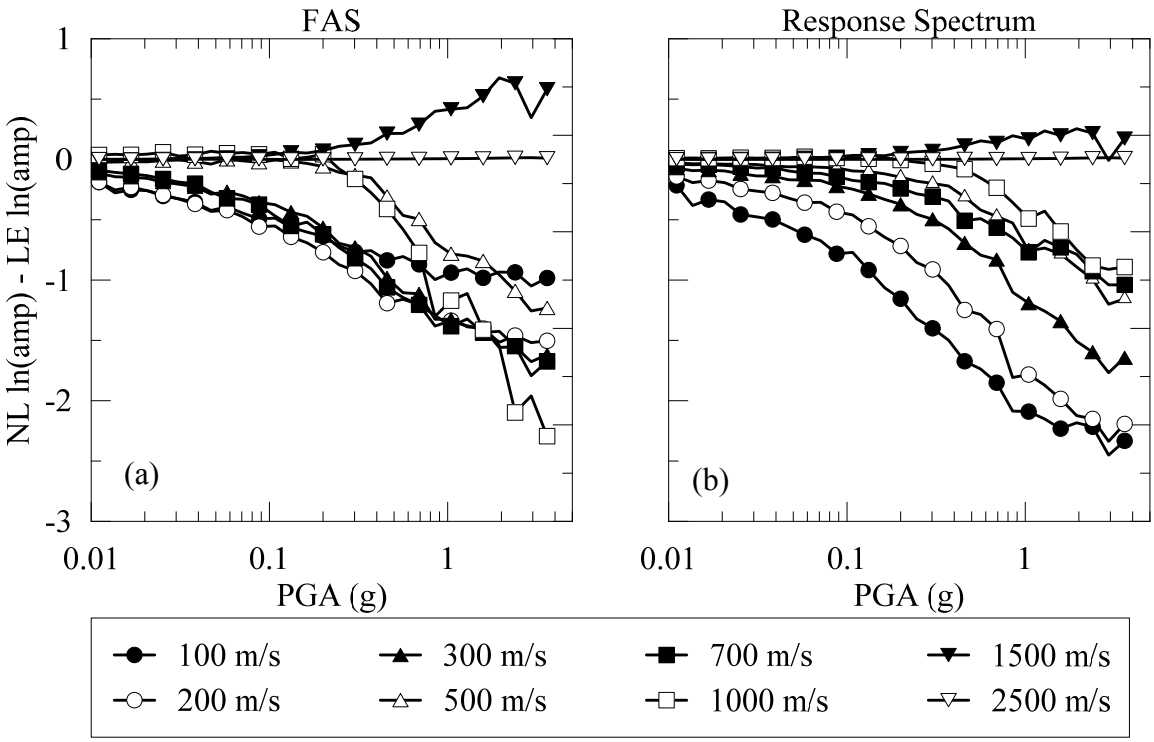

Figure 10.4: Nonlinear site amplification from simulations at 10 Hz for the FAS (a) and RS (b).

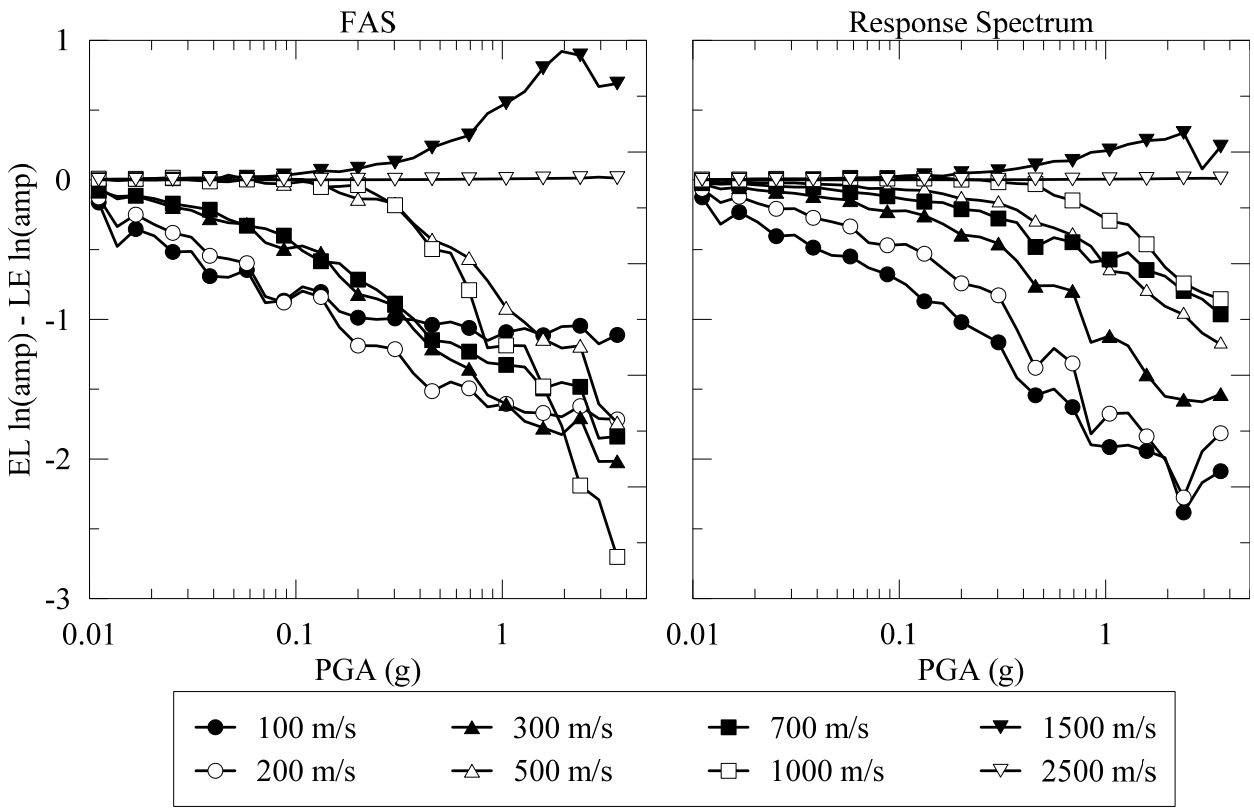

Figure 10.5: Nonlinear Site Amplification from EL Site Response analyses at 10 Hz.

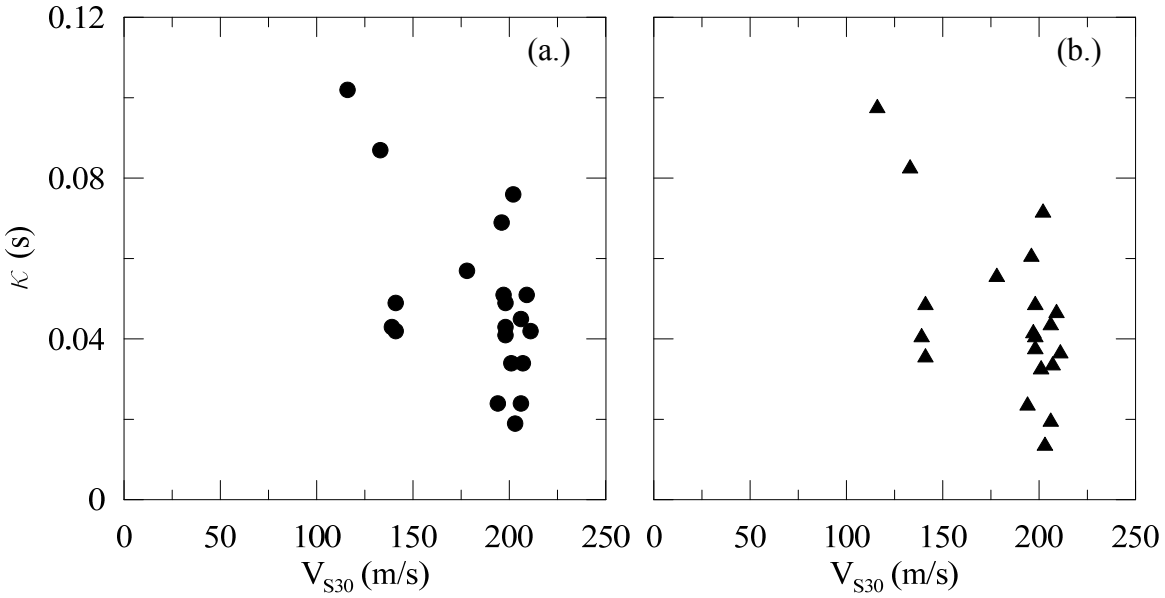

Figure 10.6: Surface kappa estimates from ground motion stations for (a) $\kappa_{Q,\ ClstD}$, and (b) $\kappa_{Q,\ epi}$.

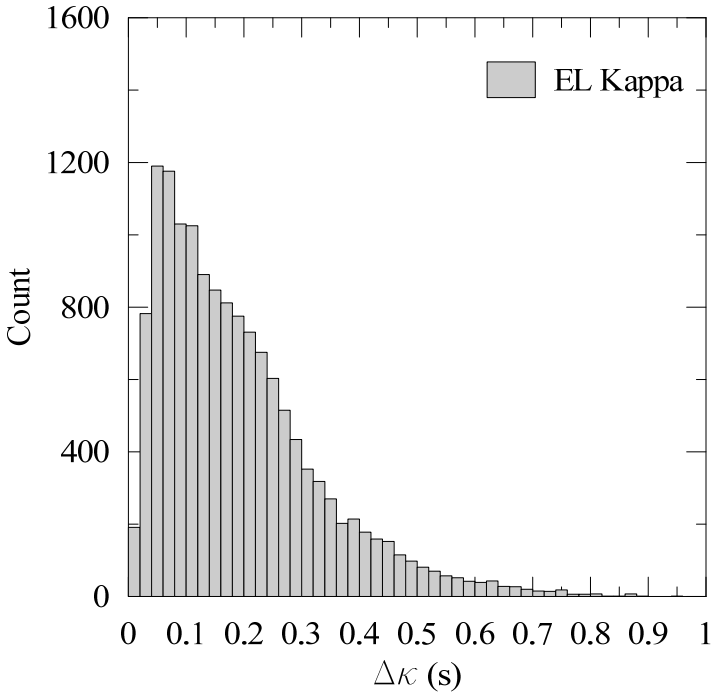

Figure 10.7: Estimated Surface kappa from strain-compatible V_S profiles of EL analyses of analyses with I_y from 0.3 to 0.5%.

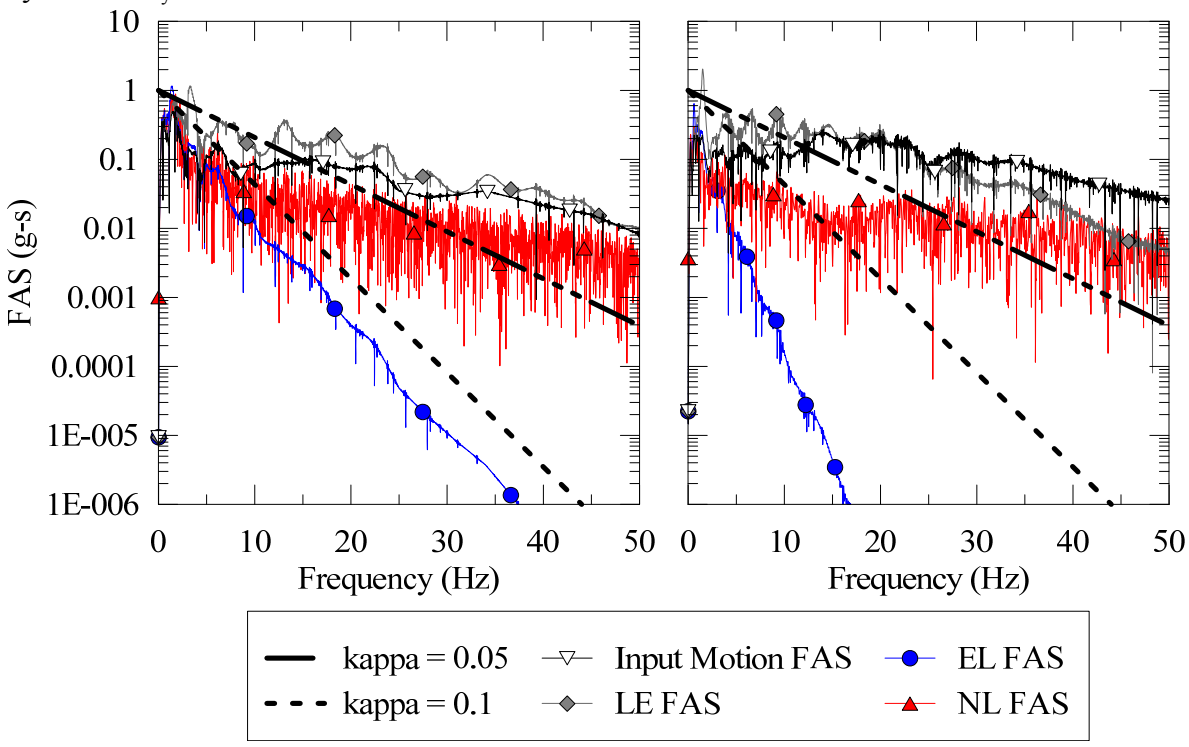

Figure 10.8: FAS for EL, NL, and LE site response analyses for a site with delta kappa as calculated from the strain equivalent EL profile of (a) 0.1 s and (b) 0.28 s.

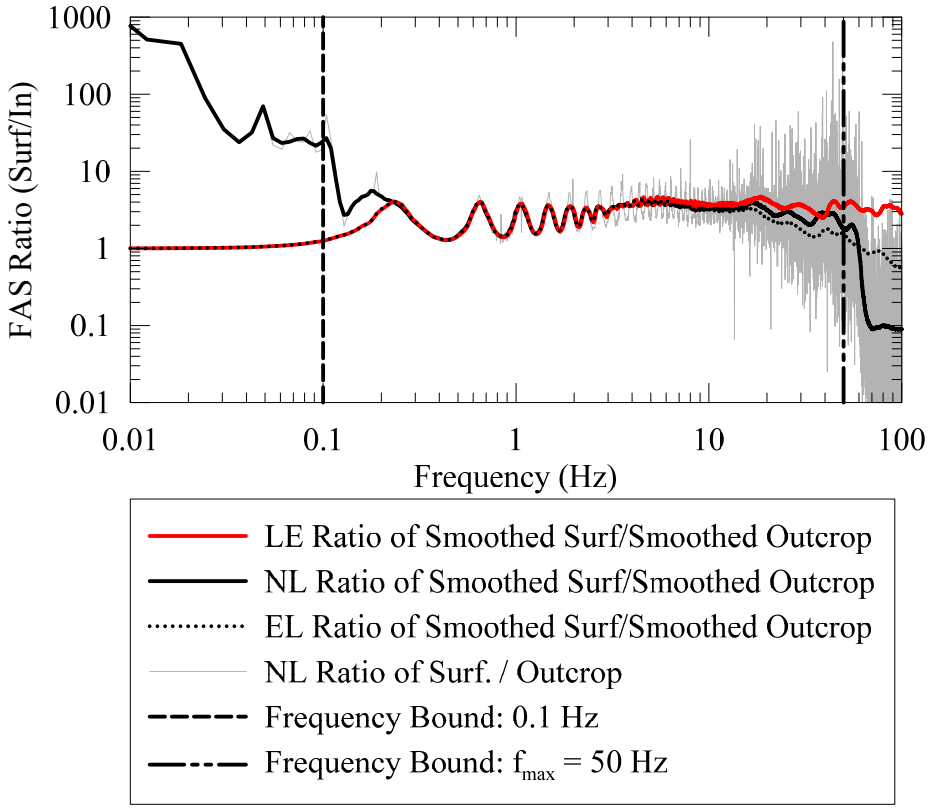

Figure 10.9: Comparison of smoothed and unsmoothed FAS amplification for a LE, NL, and EL simulation of a soil profile with V_{S30} of 550 m/s and depth of 20 m for a motion generated with SMSIM for M7.5 earthquake at 106 km distance.

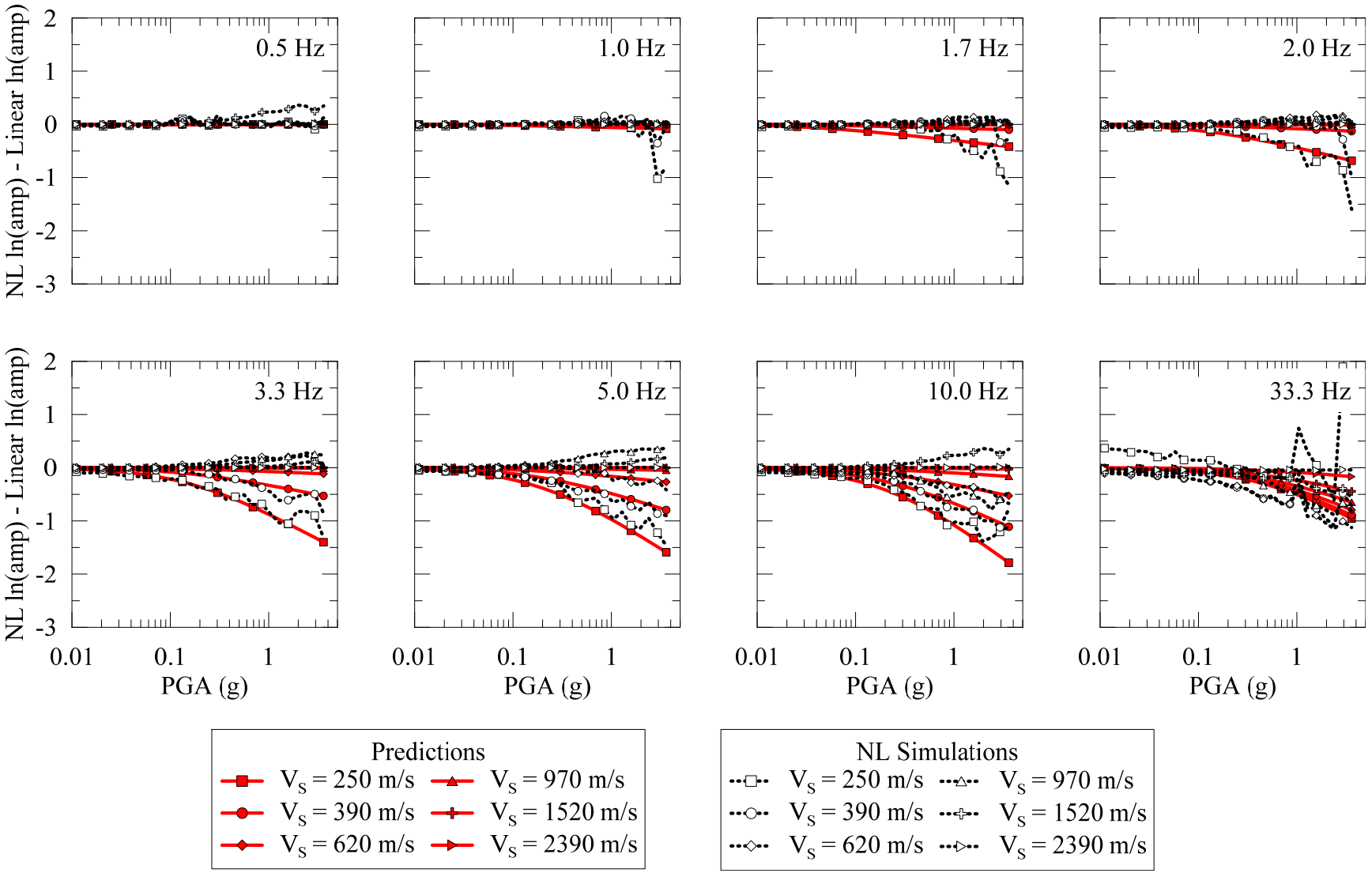

Figure 10.10: Nonlinear FAS amplification model at 0.5 Hz, 1.0 Hz, 1.7 Hz, 2.0 Hz, 3.3 Hz, 5.0 Hz, 10.0 Hz, and 33.3 Hz with site nonlinearity driven by PGA.

Chapter 11. Conclusions and Recommendations for Future Research

11.1 Conclusions

The lack of ground motion recordings and seismic site properties severely limits the empirical characterization of site amplification in CENA for GMM development and engineering design. This study characterizes the site amplification in CENA through the use of site response simulations. The contribution of this research to the field of geotechnical engineering can be summarized as follows:

(1) A database of site response simulations representative of CENA site conditions is developed. A database of 1,747,278 site response analyses, 582,426 of each LE, EL and NL analyses corresponding to 70,650 unique site profiles is produced and is the largest database of site response simulations in geotechnical engineering. In this study, the simulation dataset is used to develop site amplification functions for the RS and FAS. The dataset provides dense data as a function of V_{S30} and will be made available to researchers. Future studies that can be facilitated by this simulation dataset are discussed in Section 11.2.2.

(2) Modular linear and nonlinear site amplification functions for the RS are developed. The linear RS amplification functions feature model terms as a function of V_{S30}, as dictated by the current state of practice, but the inclusion of model terms for T_{nat} (or Z_{Soil} which serves as a proxy for T_{nat}) is shown to greatly improve the capability to estimate site amplification. The modular form of the RS model allows it to be integrated into empirical amplification functions developed for CENA. The density of the V_{S30} data used in the development of the linear amplification model reveals shapes of the V_{S30} scaling that are not seen empirical data notably that site amplification does not increase linearly with the log of V_{S30} for soft sites. The nonlinear amplification model developed in this study is the first developed for CENA conditions without influence from WUS data, and is made available in terms of both PGA and PSA for use in GMM development.

(3) A site amplification model for the FAS is developed with linear and nonlinear components. No previous nonlinear amplification model has been developed for the FAS,

and the linear amplification model used by others may be inadequate in capturing site resonance and depth effects. Simulations reveal that nonlinear amplification behavior in the FAS is very similar to the RS.

(4) A depth-based correction from 760 m/s to 3000 m/s is developed from simulations. The correction from 760 m/s to 3000 m/s (and vice-versa) is of importance for the development of seismic hazard maps in CENA. The 760/3000 correction developed in this study reveals the depth-dependency of bedrock on the correction, and a relative peak in the correction near 0.1 s PSA not present in models by others.

These contributions to the field of geotechnical engineering advance the state of practice and provide a foundation for future studies. The amplification models developed for the RS and FAS immediately contribute to the development of GMM's for CENA and are ready to be integrated into models by others. The database of site response simulations produced from this study provides a rich database to geotechnical engineers and seismologists.

11.2 Recommendations for Future Research

The simulation results from this parametric study provide a rich dataset future applications and extensions. Simplifying assumptions where used in the generation of the parametric study and refinement of the study inputs can be refined and improved to provide better estimates of site response. The dataset resulting from the simulations presented in this thesis can serve as a quality dataset for further site amplification modeling.

11.2.1 Site Response Simulations

The number of site response simulations conducted in this study required simplifying assumptions to be made while developing site profiles. Removal and improvement of some of these constraints will allow for improvement when conducting similar studies.

Some of the most notable simplifying assumptions used in the generation of the parametric study inputs are the selection of soil properties and the randomization scheme. Soil properties for each geologic class were selected from a limited literature review and review of a small number of geotechnical site reports. The soil properties presented in section are not a comprehensive review

of regional material properties, and could be improved. However, the contribution of the nonlinear soil properties to the behavior of the site amplification is expected to be minimal relative to the improvements of site amplification from changing other aspects of the parametric study.

The soil strength model used in this study was largely introduced as a modeling constraint to provide a consistent strength model to capture soil strengths for both very high V_S and very low V_S material that could exist at any depth from 0-1000 m. A more realistic model for soil strength as a function of V_S may improve estimates of nonlinearity in the soil response. The current study mitigates some of the effects of an incomplete strength model by removing analyses with resulting shear strains of > 1 % from the data and only fitting the GQ/H model to the small strain range of the G/G_{max} curve that controls the onset of nonlinearity.

For low-intensity shaking, the nonlinear and equivalent linear site response analyses for very soft sites does not converge with the linear analyses as shown by the nonlinear amplification for low PGA in Figure 9.24. This is likely due to a lack of sufficiently low intensity ground motion inputs and not due to calculation errors in DEEPSOIL. Sites with very low V_{S30} in this study are consistently very soft from the ground surface to the top of bedrock and are expected to be highly nonlinear. Ground motions with PGA values less than 0.01 are recommended to be included in future studies to ensure conversion of the nonlinear and linear amplification calculations.

The randomization methodology used in this thesis could be improved in several ways, leading to more diversity and perhaps better characterization of site amplification. The notable changes that could be made to the randomization procedure fall broadly into three categories: V_S randomization, nonlinear curve randomization, and including randomization into currently discrete input variables.

Simplifying assumptions were used in the randomization of the characteristic V_S profiles. The parameters for the Toro (1995) randomization scheme (no layer thickness randomization, and perfect correlation of V_S layers) selected ensure that all randomized V_S profiles are geometrically scaled from of one of the characteristic V_S profiles. While this methodology ensures very well behaved V_S and strength behavior, it does contribute to a lack of diversity in the V_S data, which

could limit the range of amplification behaviors observed in the dataset. Including the effects of reversals has been shown to systematically reduce site amplification (Pehlivan et al. 2015), but the current randomized V_S profiles lack varying impedance contrasts and profiles that feature depth ranges of relatively stiff or relatively soft material compared to the representative seed V_S profiles. The lack of diversity in the current V_S profiles may have an effect on the regional site amplification model proposed, but it also hinders the possibility of investigating other parameters of the V_S profiles that may contribute to amplification behavior such as various shape- or gradient-based parameters.

Another notable property that could have been included in the V_S randomization was the reference rock and half-space condition of 3000 m/s. The reference rock condition from Hashash et al. (2014a) has a confidence bound of $\pm$831 m/s and observed approximately log-normal distribution. To better reflect the real CENA bedrock condition, it would be appropriate to vary the bedrock shear wave velocity. Introducing this variability will likely most noticeably affect the amplification for the high V_{S30} sites. The lack of the randomization of the reference rock condition contributes to the divergence of the weathered rock zone V_S region of randomized V_S profiles from the weathered rock zone models, and this may be improved with reference rock randomization.

The randomization scheme for the nonlinear G/G_{max} and damping curves could also be improved. The current procedure adopted from STRATA (Kottke and Rathje 2011) has not been extensively verified or compared to the variability of real soils beyond what is presented in Darendeli (2001). Alternatively, while the current randomization scheme ensures good coverage of possible G/G_{max} and damping behavior, the input soil properties could be randomized as inputs to the randomization scheme. The G/G_{max} and damping curves of Darendeli (2001) are less sensitive to the mean soil input properties than they are to the G/G_{max} randomization, but both effects could be included in future studies.

The effect of including variability in the G/G_{max} and damping randomization as a function of depth has also not been studied. In this study, perfect correlation (ρ=1.0) was assumed for the random variable used to assign nonlinear behavior to soil layers to avoid the possibility of adjacent layers having dramatic differences in strain-softening behavior and possible resulting

strain concentrations. Both the effects of randomizing the input soil properties and inter-layer correlation of randomized soil properties are expected to have a minimal effect on the nonlinear site amplification term $F_{(NL)}$, but would allow for a more complete interpretation of the effects of soil behavior on nonlinear amplification.

There is currently no randomization of small strain damping in this study. The connection of the small-strain damping to the V_S profile successfully captures expected surface κ behavior, but inferences about the effect of small strain damping on the linear site amplification in this study are limited by this connection.

The final component that could be included in the randomization methodology of this or a similar study is the conversion of the currently discrete parametric study inputs depth and weathered rock zone model from discrete selections to continuous random variables. A continuous distribution of depth would provide better constraint on the functional form of linear depth-dependent amplification as well as better resolution of amplification behavior in the high V_{S30} range. The current dataset has a noticeable 'break' in amplification behavior around 2000 m/s V_{S30} because of the difference in amplification behavior for the 0 m depth surface rock sites with the weathered rock zone at the ground surface, and the 5 m sites with 5 m of soil material between the weathered rock zone and the ground surface. Including a range of soil depths between 0 m and 5 m would provide better resolution of the amplification in the high-V_{S30} range.

The current procedure for assignment of weathered rock zone velocities could also be improved in future work. The constraints on the weathered rock zone behavior do not provide a wide range of impedance contrasts, including the site condition where the soil material smoothly transitions the 3000 m/s reference rock without a strong impedance contrast.

11.2.2 Simulation Dataset

Changing any one of the inputs to the parametric study will require a new set of site response analyses, regressions and modeling of site amplification. However, the current parametric study dataset as it currently exists can be used as a foundation for future work in the development of site amplification models.

The most immediate work that can be completed with this dataset are amplification functions for PGV and PGD, and a variance model for site amplification in CENA. Amplification for PGV and PGD are currently not evaluated, but have application in engineering design and GMM development. Additionally, the results of this parametric study provide an unprecedented opportunity to evaluate and constrain the uncertainty and variability in site amplification as a function of many parameters including soil nonlinearity.

Having a dense dataset of analyses of any kind also lends itself to use with machine learning and other advanced data science algorithms to process and make inferences about the nature of the dataset. A database such as the one produced in this study could be used to develop amplification models or other estimates of site response through these techniques instead of traditional regression methods.

11.2.3 Site Amplification Models

The L5 linear amplification model is shown to produce the lowest error across RS periods, but still fails to the magnitude of resonance peaks and higher order modes of amplification for shallow sites as discussed in Section 9.8.2. The model can be improved with additional additive terms to capture higher order modes of amplification similar to the c_5 term in the model for the first mode of amplification in this study. The height of the resonance peaks can be improved by including site natural period in the model term for the Riker wavelet. The shallowest sites in this study tend to have the largest natural period amplification effects, so the c_5 amplification term in eq. 9.5 could be modified to have the functional form $f(T_{nat}) \times c_5 R$ which may be able to reproduce the larger peaks for shallow sites and smaller peaks for deeper sites.

Nonlinear amplification in the current model is determined exclusively from nonlinear site response analyses. The EL site response analyses are used only to constrain the selection of data for the nonlinear FAS site amplification model. The EL analyses may be included in the modeling of site amplification in future studies to inform the variability or constraints of nonlinear site amplification or constrain nonlinear amplification. However there are considerations to including the equivalent linear analyses that must be addressed such as which analyses are appropriate based on the criteria in (Kim et al. 2015) for comparison to the

nonlinear simulations and classic overdamping of the high frequency presenting unrealistic κ_0 values.

The nonlinear amplification terms for the RS and FAS may be improved further by changing the formulation or calculation of the parameters. A V_{S30}-dependent f_3 term may provide a better estimate of nonlinearity at soft sites. The nonlinear amplification is also being calculated as a single function across all sites and analyses. When empirical data is available for a particular site, nonlinear amplification can be calculated either from observed strong motions or simulations. Each randomized soil profile used in this parametric study is analyzed for 7-9 ground motions of varying intensity. The nonlinear parameters f_3, f_4, and f_5 can be calculated for individual sites which may provide more complex functions for nonlinear amplification or better estimates of each parameter. If this method is to be explored further, supplementary analyses may be required to ensure an evenly distributed range of ground motion intensities at each site. The effect and appropriateness of the 360 value in the formulation originally proposed by Chiou and Youngs (2008) (eq. 9.9 of this document) on amplification in CENA has not been explored.

Smoothing amplification coefficients and reformulation of model terms to remove multicollinearity may improve the quality of the amplification model presented. The coefficients presented in this study are independently regressed and period-independent. There are several approaches that could be used to provide more stable model fits including inter-period correlation of coefficients or functional forms as functions of period to the regressed coefficients. The overall model variance under these procedures may be increased, but more stable regression coefficients may be more physically meaningful. The current model also has several parameters that are strongly correlated used in separate model terms such as V_{S30} and site natural period. The current model is formulated under the assumption that variable amounts of data may be available at any site, and parameters such as V_{S30} can be evaluated independently of depth to reference rock or site period, but no consideration is given for the relationship between these terms or the resulting interaction between amplification terms short of regressing the model terms separately or together.

Linear and nonlinear FAS site amplification has not been as extensively studied or derived from simulations as site amplification of the RS, and many opportunities exist to build on the work

presented in this thesis. The linear FAS site amplification in this study is not captured by functions in the same way as the RS, and functional forms can be developed for the linear FAS data. Evaluation of the simulation-based amplification data suggests that depth-dependent wavelet-based functions may be able to capture the observed linear FAS amplification behavior. These functions will have the same limitations of ergodic RS site amplification function models in that V_{S30} alone will be insufficient to capture the site amplification behavior. The nonlinear FAS site amplification model in this study has not been extensively calibrated to observed $\Delta\kappa$ behavior from site nonlinearity. EL analyses are shown in this study to be inadequate in capturing observed $\Delta\kappa$ behavior. The classic high-frequency overdamping behavior of EL analyses generate $\Delta\kappa$ values much larger than in observed recordings. Nonlinear site response analyses may be able to better capture $\Delta\kappa$ behavior.

References

Aboye, S. A., R. D. Andrus, N. Ravichandran, A. H. Bhuiyan and N. Harman (2015). "Seismic Site Factors and Design Response Spectra Based on Conditions in Charleston, South Carolina." Earthquake Spectra 31(2): 723-744.

Abrahamson, N. A. and W. J. Silva (1997). "Empirical response spectral attenuation relations for shallow crustal earthquakes." Seismological Research Letters 68(1): 94-109.

Al Noman, M. N. and C. H. Cramer (2015). Empirical Ground-Motion Prediction Equations for Eastern North America. NGA-East: Median Ground-Motion Models for the Central and Eastern North America Region. Berkeley, CA, Pacific Earthquake Engineering Research Center: 193-212.

Ancheta, T. D., R. B. Darragh, J. P. Stewart, E. Seyhan, W. J. Silva, B. S. J. Chiou, K. E. Wooddell, R. W. Graves, A. R. Kottke, D. M. Boore, T. Kishida and J. L. Donahue (2013). PEER NGA-West2 Database, Pacific Earthquake Engineering Research Center: 172.

Anderson, J. G. and S. E. Hough (1984). "A model for the shape of the Fourier amplitude spectrum of acceleration at high frequencies." Bulletin of the Seismological Society of America 74(5): 1969-1993.

Anderson, N., G. Chen, S. Kociu, R. Luna, T. Thitimakorn, A. Malovichko, D. Malovichko and D. Shylakov (2003). Vertical shear-wave velocity profiles gnerated from spectral analysis of surface waves: field examples, Missouri Department of Transportation.

Anderson, N., d. Hoffman, W. Liu, R. Luna, R. Stephesnson and T. Thitimakorn (2005). Comprehensive shear-wave velocity study in the polar bluff area, southeast Missouri, RDT 05-006, Missouri Department of Transportation: 197 pages.

Anderson, N. and T. Thitimakorn (2004). A 2-D MASW shear-wave velocity profile along a test segment of interstate I-70, St. Louis, Missouri, RDT 04-012, Missouri Department of Transportation: 34 pages.

Andrus, R. D., C. D. Fairbanks, J. Zhang, W. M. Camp Iii, T. J. Casey, T. J. Cleary and W. B. Wright (2006). "Shear-wave velocity and seismic response of near-surface sediments in Charleston, South Carolina." Bulletin of the Seismological Society of America 96(5): 1897-1914.

Ashland, F. X. and N. G. McDonald (2003). Interim Map Showing Shear-Wave-Velocity Characteristics of Engineering Geologic Units in the Salt Lake Cit, Utah, Metropolitan Area.

Assimaki, D. and W. Li (2012). "Site- and ground motion-dependent nonlinear effects in seismological model predictions." Soil Dynamics and Earthquake Engineering 32(1): 143-151.

Atkinson, G. and D. Boore (2006). "Earthquake ground-motion prediction equations for eastern North America." Bulletin of the Seismological Society of America 96(6): 2181-2205.

Atkinson, G. M. (2008). "Ground-Motion Prediction Equations for Eastern North America from a Referenced Empirical Approach: Implications for Epistemic Uncertainty." Bulletin of the Seismological Society of America 98(3): 1304-1318.

Atkinson, G. M. and D. M. Boore (2011). "Modifications to Existing Ground-Motion Prediction Equations in Light of New Data." Bulletin of the Seismological Society of America 101(3): 1121-1135.

Bauer, R. A. (2004). Central U.S. Shear-wave velocity database with accompanying geological/geotechnical information of nonlithified geologic materials, External Grant Award Number 04-HQ-GR-0074, U.S. Geological Survey.

Beresnev, I. A. and G. M. Atkinson (1997). "Shear-wave velocity survey of seismographic sites in eastern Canada: Calibration of empirical regression method of estimating site response." Seismological Research Letters 68(6): 981-987.

Boore, D. (2015a). Adjusting Ground-Motion Intensity Measures to a Reference Site for which V_{S30} = 3000 m/sec. Berkeley, CA, Pacific Earthquake Engineering Research Center: 85.

Boore, D. and K. Campbell (2016). "Adjusting central and eastern North America ground-motion intensity measures between sites with different reference-rock site conditions." Bull. Seismol. Soc. Am. In Review.

Boore, D. M. (1983). "Stochastic simulation of high-frequency ground motions based on seismological models of the radiated spectra." Bulletin of the Seismological Society of America 73(6): 1865-1894.

Boore, D. M. (2003). "Prediction of ground motion using the stochastic method." Pure and Applied Geophysics 160: 635-676.

Boore, D. M. (2005). SMSIM Fortran programs for simulating ground motions from earthquakes, version 2.3. A revision of U.S.Geol.Surv.Open-File Rept. 96-80-A.

Boore, D. M. (2015b). Point-Source Stochastic-Method Simulations of Ground Motions for the PEER NGA-East Project. NGA-East: Median Ground-Motion Models for the Central and Eastern North America Region. Berkeley, CA, Pacific Earthquake Engineering Research Center: 11-49.

Boore, D. M., W. B. Joyner and T. E. Fumal (1997). "Equations for estimating horizontal response spectra and peak acceleration from western North American earthquakes: A summary of recent work." Seismological Research Letters 68(1): 128-153.

Boore, D. M., J. P. Stewart, E. Seyhan and G. M. Atkinson (2014). "NGA-West2 Equations for Predicting PGA, PGV, and 5% Damped PSA for Shallow Crustal Earthquakes." Earthquake Spectra 30(3): 1057-1085.

Bora, S. S., F. Scherbaum, N. Kuehn and P. Stafford (2014). "Fourier spectral- and duration models for the generation of response spectra adjustable to different source-, propagation-, and site conditions." Bulletin of Earthquake Engineering 12(1): 467-493.

Bozorgnia, Y. and K. W. Campbell (2015). "Vertical Ground Motion Model for PGA, PGV, and Linear Response Spectra Using the NGA-West2 Database." Earthquake Spectra 0(0).

Brandenberg, S. J., N. Bellana and T. Shantz (2010). " Shear wave velocity as function of standard penetration test resistance and vertical effective stress at California bridge sites." Soil Dynamics and Earthquake Engineering 30(10).

BSSC (2009). NEHRP recommended seismic provisions for for new buildings and other structures (FEMA P-750), 2009 edition. Washington, D.C., Building Seismic Safety Commission, National Institute of Building Sciences.

BSSC (2015). NEHRP Recommended Seismic Provisions for New Buildings and Other Structures (FEMA P-1050-1). Washington, DC, Building Seismic Safety Commission, National Institute of Building Sciences.

Calvert Cliffs 3 Nuclear Project LLC. UniStar Nuclear Operating Services LLC (2011). Calvert Cliffs, Unit 3: Combined Licensing Agreement: Final Safety Analysis Report, Revision 8, http://www.nrc.gov/reactors/new-reactors/col/calvert-cliffs/documents.html.

Campbell, K. W. (2003). "Prediction of Strong Ground Motion Using the Hybrid Empirical Method and Its Use in the Development of Ground-Motion (Attenuation) Relations in Eastern North America." Bulletin of the Seismological Society of America 93(3): 1012-1033.

Campbell, K. W. (2009). "Estimates of Shear-Wave Q and κ0 for unconsolidated and semiconsolidated sediments in Eastern North America." Bulletin of the Seismological Society of America 99(4): 2365-2392.

Chiou, B. S. J. and R. R. Youngs (2008). NGA model for average horizontal component of peak ground motion and response spectra, Pacific Engineering Research Center.

Choi, W. K. (2008). Dynamic properties of ash-flow tuffs., Unversity of Texas, Austin.

Choi, Y. and J. P. Stewart (2005). "Nonlinear site amplification as function of 30 m shear wave velocity." Earthquake spectra 21 (1): 1-30.

Dames and Moore (1974). Site parameter sutdy: Gassar seismic design for General Atomic Company. Report No. 2395-001-02. San Franciso, CA.

Darendeli, M. B. (2001). Development of a new family of normalized modulus reduction and material damping curves Ph. D., University of Texas at Austin.

Darragh, R. B., N. Abrahamson, W. J. Silva and N. Gregor (2015). Development of Hard Rock Ground-Motion Models for Region 2 of Central and Eastern North America. NGA-East:

Median Ground-Motion Models for the Central and Eastern North America Region. Berkeley, CA, Pacific Earthquake Engineering Research Center: 51-69.

Detroit Edison Company (2010). Fermi Unit 3, Combined License Application, Part 2: Final Safety Analysis Report, Revision 2, http://www.nrc.gov/reactors/new-reactors/col/fermi/documents.html.

Dickenson, S. E. (1994). Dynamic response of soft and deep cohesive soils during the Loma Prieta Earthquake of October 17, 1989. 9504791 Ph.D., University of California, Berkeley.

Dominion Virginia Power (2009). North Anna Unit 3, Combined License Application, Part 2: Final Safety Analysis Report, Revision 3, http://www.nrc.gov/reactors/new-reactors/col/north-anna/documents.html.

Douglas, J., H. Bungum and F. Scherbaum (2006). "GROUND-MOTION PREDICTION EQUATIONS FOR SOUTHERN SPAIN AND SOUTHERN NORWAY OBTAINED USING THE COMPOSITE MODEL PERSPECTIVE." Journal of Earthquake Engineering 10(1): 33-72.

Duke Energy (2010). William States Lee III Nuclear Station Units 1 and 2, Combined License Application, Part 2: Final Safety Analysis Report, Revision 3, http://www.nrc.gov/reactors/new-reactors/col/lee/documents.html.

Entergy Operations Florida Inc. (2011). Grand Gulf, Unit 3: Combined Licensing Agreement: Final Safety Analysis Report, Revision 0, http://www.nrc.gov/reactors/new-reactors/col/grand-gulf/documents.html.

Entergy Operations Inc (2008). River Bend Station 3, Combined License Application, Part 2: Final Safety Analysis Report, Revision 0, http://www.nrc.gov/reactors/new-reactors/col/river-bend/documents.html.

Exelon Generation Company (2006). Clinton, Early Site Planning Application: Part 2, Site Safety Analysis Report, Revision 0, http://www.nrc.gov/reactors/new-reactors/esp/clinton.html.

Exelon Nuclear Texas Holdings LLC (2008). Victoria County Station Units 1 and 2, Combined License Application, Part 2: Final Safety Analysis Report, Revision 0, http://www.nrc.gov/reactors/new-reactors/col/victoria/documents.html.

FEMA (1997). NEHRP recommended provisions for seismic regulations for new buildings and other structures, Part I: 337p.

Florida Power and Light Company (2010). Turkey Point Units 6 and 7, Combined License Application, Part 2: Final Safety Analysis Report, Revision 3, http://www.nrc.gov/reactors/new-reactors/col/turkey-point/documents.html.

Frankel, A., C. Mueller, D. Perkins, T. Barnhard, E. Leyendecker, E. Safak, S. Hanson, N. Dickman and M. Hopper (1996). National seismic hazard maps: Documentation June 1996, US Geological Survey: 69 p.

Frankel, A. D. (2015). Ground-Motion Predictions for Eastern North American Earthquakes Using Hybrid Broadband Seismograms from Finite-Fault Simulations with Constant Stress-Drop Scaling. NGA-East: Median Ground-Motion Models for the Central and Eastern North America Region. Berkeley, CA, Pacific Earthquake Engineering Research Center: 149-163.

Frankel, A. M., C. Perkins, D. Barnhard, T. Leyendecker, E. Safak, E. Hanson, S. Dickman, N. Hopper, M (1996). National seismic hazard maps: Documentation June 1996, US Geological Survey: 69 p.

Fullerton, D. S., C. A. Bush and J. N. Pennell (2003). Map of surficial deposits and materials in the eastern and central United States (east of 102 degrees West longitude). IMAP.

Fulton, R. J. (1995). Surficial materials of Canada, Natural Resources Canada: 1880A.

Fumal, T. E. (1978). Correlations between seismic wave velocities and physical properties of near-surface geologic materials in the southern San Francisco Bay region, California. Open-File Report.

Ge, J., J. Pujol, S. Pezeshk and S. Stovall (2007). "Determination of shallow shear-wave velocity at Mississippi embayment sites using vertical seismic profiling data." Bulletin of the Seismological Society of America 97(2): 614-623.

Gomberg, J., B. Waldron, E. Schweig, H. Hwang, A. Webbers, R. VanArsdale, K. Tucker, R. Williams, R. Street, P. Mayne, W. Stephenson, J. Odum, C. Cramer, R. Updike, S. Hutson and M. Bradley (2003). "Lithology and shear-wave velocity in Memphis, Tennessee." Bulletin of the Seismological Society of America 93(3): 986-997.

Goulet, C. A., T. Kishida, T. D. Ancheta, C. H. Cramer, R. B. Darragh, W. J. Silva, Y. M. A. Hashash, J. A. Harmon, J. P. Stewart, K. E. Wooddell and R. R. Youngs (2014). PEER NGA-East Database, Pacific Earthquake Engineering Research Center: 124.

Graizer, V. (2015). Ground-Motion Prediction Equations for the Centeral and Eastern United States. NGA-East: Median Ground-Motion Models for the Central and Eastern North America Region. Berkeley, CA, Pacific Earthquake Engineering Research Center: 213-249.

Groholski, D. R., Y. M. A. Hashash, B. Kim, M. Musgrove, J. Harmon and J. P. Stewart (2016). "Simplified Model for Small-Strain Nonlinearity and Strength in 1D Seismic Site Response Analysis." Journal of Geotechnical and Geoenvironmental Engineering 0(0): 04016042.

Hamilton, E. L. (1976). "Shear-wave velocity versus depth in marine sediments; a review." Geophysics 41(5): 985-996.

Hardin, B. O. and V. P. Drnevich (1972). "Shear modulus and damping in soils: Design equations and curves." Journal of Soil Mechanics and Foundations 98(SM7): 289-324.

Hashash, Y. M. A., S. Dashti, M. I. Romero, M. Ghayoomi and M. Musgrove (2015a). "Evaluation of 1-D seismic site response modeling of sand using centrifuge experiments." Soil Dynamics and Earthquake Engineering 78: 19-31.

Hashash, Y. M. A., D. Groholski, M. Musgrove, D. Park, C. Phillips and C.-C. Tsai (2011). DEEPSOIL V5.0, Manual and Tutorial. Urbana, IL, Board of Trustees of University of Illinois at Urbana-Champaign.

Hashash, Y. M. A., A. R. Kottke, J. P. Stewart, K. W. Campbell, B. Kim, C. Moss, S. Nikolaou, E. M. Rathje and W. J. Silva (2014a). "Reference Rock Site Condition for Central and Eastern North America." Bulletin of the Seismological Society of America 104(2): 684-701.

Hashash, Y. M. A., A. R. Kottke, J. P. Stewart, K. W. Campbell, B. Kim, C. Moss, S. Nikolau, E. M. Rathje and W. J. Silva (2014b). "Reference rock site condition for central and eastern North America." Bulletin of the Seismological Society of America 104(2): 684-701.

Hashash, Y. M. A., M. I. Musgrove, J. A. Harmon, D. Groholski, C. A. Phillips and D. Park (2015b). DEEPSOIL V6.1, User Manual. Urbana, IL, Board of Trustees of University of Illinois at Urbana-Champaign.

Hashash, Y. M. A., M. I. Musgrove, J. A. Harmon, D. R. Groholski, C. A. Phillips and D. Park (2015c). DEEPSOIL 6.0, User Manual: 116.

Hashash, Y. M. A. and D. Park (2001). "Non-linear one-dimensional seismic ground motion propagation in the Mississippi embayment." Engineering Geology 62(1-3): 185-206.

Hashash, Y. M. A., C. Phillips and D. R. Groholski (2010). Recent advances in non-linear site response analysis. Fifth International Conference in Recent Advances in Geotechnical Eartqhuake Engineering and Soil Dynamics. San Diego, CA. CD-Volume: OSP 4.

Hassani, B. and G. A. Atkinson (2015). Reference Empirical Ground-Motion Model for Eastern North America. NGA-East: Median Ground-Motion Models for the Central and Eastern North America Region. Berkeley, CA, Pacific Earthquake Engineering Research Center: 251-272.

Hassani, B. and G. M. Atkinson (2016). "Site-Effects Model for Central and Eastern North America Based on Peak Frequency." Bulletin of the Seismological Society of America.

Herrmann, R. B. and D. J. Crossley (2008). Shear-wave velocity determination for metropolitan St. Louis Focal Mechanism, USGS Grant 05HQGR0046, U.S. Geological Survey: 44 pages.

Hoar, R. J. and I. Kenneth H. Stokoe (1982). In situ seismic wave velocities and dynamic analysis for CFH compressor foundations, Kenneth E. Tand & Associates: 99 pages.

Hoffman, D., N. Anderson and D. Rogers (2008). St. Louis metro area shear-wave velocity testing, External Grant Award Number: 06HQGR0026, U.S. Geological Survey: 24 pages.

Hollenback, J., N. Kuehn, C. A. Goulet and N. Abrahamson (2015). PEER NGA-East Median Ground-Motion Models. NGA-East: Median Ground-Motion Models for the Central and Eastern North America Region. Berkeley, CA, Pacific Earthquake Engineering Research Center: 274-309.

Hough, S. E. and J. G. Anderson (1988). "High-frequency spectra observed at Anza, California: implications for Q structure (USA)." Bulletin - Seismological Society of America 78(2): 692-707.

Jaky, J. (1948). "Pressure in silos." ICSMFE, London 1: 103-107.

Jaume, S. C. (2006). "Shear wave velocity profiles via seismic cone penetration test and refraction microtremor techniques at ANSS strong motion sites in Charleston, South Carolina." Seismological Research Letters 77(6): 771-779.

Jeon, S. Y. (2008). Dynamic and cyclic properties in shear of tuff specimens from Yucca Mountain, Nevada, University of Texas, Austin.

Kaka, S. I. (2005). Development of Ontario ShakeMaps. Doctor of Philosophy, Carleton University.

Kamai, R., N. A. Abrahamson and W. J. Silva (2014). "Nonlinear Horizontal Site Amplification for Constraining the NGA-West2 GMPEs." Earthquake Spectra 30(3): 1223-1240.

Kayen, R. E., B. A. Carkin, S. C. Corbett, A. S. Zangwill, L. Lai and I. Etstevez (2013). Seismic-Shear Wave Velocity and Ground Motion Amplification Factors for 50 Sites Affected by the Mineral, Virginia M5.8 Earthquake of 23 August 2011, U.S. Geological Survey.

Kim, B., Y. M. A. Hashash, J. P. Stewart, E. M. Rathje, J. A. Harmon, M. I. Musgrove, K. W. Campbell and W. J. Silva (2015). "Relative Differences between Nonlinear and Equivalent-Linear 1D Site Response Analyses." Earthquake Spectra 0(0): null.

Kokusho, T., Y. Yoshida and Y. Esashi (1982). "Dynamic properties of soft clay for wide strain range." Soils Found. 22(4): 1–18.

Kondner, R. L. and J. S. Zelasko (1963). Hyperbolic stress-strain formulation of sands. Second pan American Conference on Soil Mechanics and Foundation Engineering, Sao Paulo, Brazil.

Kottke, A. R., Y. M. A. Hashash, J. P. Stewart, C. J. Moss, S. Nikolaou, E. M. Rathje, W. J. Silva and K. W. Campbell (2012). Development of Geologic Site Classes for Seismic

Site Amplification for Central And Eastern North America. 15th World Conference on Earthquake Engineering, Lisbon, Portugal.

Kottke, A. R. and E. M. Rathje (2011). Draft of Technical Manual for Strata.

Kramer, S. L. (1996). Geotechnical earthquake engineering. Upper Saddle River, N.J., Prentice Hall.

Lester, A. P. (2005). An examination of site response in Columbia, South Carolina: sensitivity of site response to rock input motion and the utility of Vs30, Virginia Polytechnic Institute and State University.

Lew, M. and K. Campbell (1985). Relationships Between Shear Wave Velocity and Depth of Overburden. Proceedings of Measurement and Use of Shear Wave Velocity for Evaluating Dynamic Soil Properties, Denver, Colo, American Societv of Civil Engineers.

Liu, H. P., Y. Hu, J. Dorman, T. S. Chang and J. M. Chiu (1997). "Upper Mississippi embayment shallow seismic velocities measured in situ." Engineering Geology 46(3-4): 313-330.

Luminant Generation Company LLC (2009). Comanche Peak Nuclear Plants 3 and 4, Combined License Application, Part 2: Final Safety Analysis Report, Revision 1, http://www.nrc.gov/reactors/new-reactors/col/comanche-peak/documents.html.

Marcuson, W. F. and H. E. Wahls (1972). "Time effects on dynamic shear modulus of clays." J. Soil Mech. and Found. Div. 98(12): 1359-1373.

Matasovic, N. (1993). Seismic response of composite horizontally-layered soil deposits Ph.D. Thesis, University of California, Los Angeles.

McGuire, R. K., W. J. Silva and C. J. Costantino (2001). Technical Basis for Revision of Regulatory Guidance on Design Ground Motions: Hazard- and Risk-consistent Ground Motion Spectra Guidelines (NUREG/CR-6728). R. M. Kenneally.

Menq, F. Y. (2003). Dynamic Properties of Sandy and Gravelly Soils Ph.D, University of Texas at Austin.

Mohanan, N., C. Fairbanks, R. Andrus, W. Camp, T. Cleary, T. Casey and W. Wright (2006). Electronic files of shear-wave velocity and cone penetration test measurements from the greater Charleston area, South Carolina, USGS Award Number 05HQGR0037, United States Geological Survey: 19 pages.

Moon, S.-w., Y. M. A. Hashash and D. Park (2016). "USGS hazard map compatible depth-dependent seismic site coefficients for the Upper Mississippi Embayment." KSCE Journal of Civil Engineering: 1-12.

Moos, D. and M. D. Zoback (1983). "In situ studies of velocity in fractured crystalline rocks." Journal of Geophysical Research 88(B3): 2345-2358.

Navidi, S. (2012). Development of Site Amplification Model for Use in Ground Motion Prediction Equations. Doctor of Philosophy, The University of Texas at Austin.

Nikolaou, P., S, P. Go, JE, C. Beyzaei, C. Moss and P. Deming, PW (2012). Geo-Seismic Design in the Eastern United States. Geotechnical Engineering State of the Art and Practice: 828-854.

Nine Mile Point Nuclear Project LLC and UniStar Nuclear Operating Services LLC (2011). Nine Mile Point, Unit 3: Combined Licensing Agreement: Final Safety Analysis Report, Revision 1, http://www.nrc.gov/reactors/new-reactors/col/nine-mile-point/documents.html.

Odum, J. K., R. A. Williams, W. J. Stephensen and D. M. Worley (2003). Near-surface S-wave and P-wave seismic velocitities of primary geological formations on the Piedmont and Atlantic coastal plain of South Carolina, USA, Open-File report 03-043, U.S. Geological Survey: 14 pages.

Ohio Geological Survey (2011). Seismic refraction analyses of shallow subsurface geologic materials (http://www.dnr.state.oh.us/OhioGeologicalSurvey/SurficialGeology/tabid/7124/Default.aspx).

Ohta, Y. and N. Goto (1978). "Empirical shear wave velocity equations in terms of characteristic soil indexes." Earthquake Engineering & Structural Dynamics 6(2): 167-187.

Olson, S. M. and Y. M. A. Hashash (2009). Geotechnical seismic engineering New 1-70 Mississippi River Bridge St. Louis, Missouri to St. Clair County, Illiois, HNTB Corporation: 296 pages.

Parker, G., J. A. Harmon, J. P. Stewart, Y. M. A. Hashash, A. R. Kottke, E. M. Rathje, W. J. Silva and K. Campbell (2017). "Proxy-Based VS30 Estimation in Central and Eastern North America " Bulletin of the Seismological Society of America Accepted.

PEER (2015). NGA-East: Median Ground-Motion Models for the Central and Eastern North America Region. Berkeley, CA: 351.

Pehlivan, M., Y. M. A. Hashash, H. J., E. M. Rathje, J. P. Stewart, W. J. Silva, K. Campbell and S. Nikolaou (2015). Influence of shear wave velocity reversals on one-dimensional site response of spatially varied profiles 6th International Conference on Earthquake Geotechnical Engineering. Christchurch, New Zealand.

Petersen, M. D., A. D. Frankel, S. C. Harmsen, C. S. Mueller, K. M. Haller, R. L. Wheeler, R. L. Wesson, Y. Zeng, O. S. Boyd, D. M. Perkins, N. Luco, E. H. Field, C. J. Wills and K. S. Rukstales (2008). Documentation for the 2008 Update of the United States National Seismic Hazard Maps. Open-File Rept. 2008-1128, U.S. Geol. Surv. .

Petersen, M. D., M. P. Moschetti, P. M. Powers, C. S. Mueller, K. M. Haller, A. D. Frankel, Zeng, Yuehua, Rezaeian, Sanaz, S. C. Harmsen, O. S. Boyd, Field, Ned, Chen, Rui, K. S.

Rukstales, Luco, Nico, R. L. Wheeler, R. A. Williams and A. H. Olsen (2014). Documentation for the 2014 update of the United States national seismic hazard maps, United States Geological Survey.

Pezeshk, S., A. Zandieh, K. Campbell and B. Tavakoli (2015). Ground-Motion Prediction Equations for CENA Using the Hybrid Empirical Method in Conjunction With NGA-West2 Empirical Ground-Motion Models. NGA-East: Median Ground-Motion Models for the Central and Eastern North America Region. Berkeley, CA, Pacific Earthquake Engineering Research Center: 119-147.

Pezeshk, S., A. Zandieh and B. Tavakoli (2011). "Hybrid Empirical Ground-Motion Prediction Equations for Eastern North America Using NGA Models and Updated Seismological Parameters." Bulletin of the Seismological Society of America 101(4): 1859-1870.

Progress Energy Carolinas, I. (2011). Progress Energy Harris Nuclear Units 2 & 3, Combined License Application, Part 2: Final Safety Analysis Report, Revision 3, http://www.nrc.gov/reactors/new-reactors/col/harris/documents.html.

Progress Energy Florida Inc. (2011). Levy County, Units 1 and 2: Combined Licensing Agreement: Final Safety Analysis Report, Revision 2, http://www.nrc.gov/reactors/new-reactors/col/levy/documents.html.

PSEG Power, L., and PSEG Nuclear, LLC (2011). PSEG Site, Early Site Planning Application: Part 2, Site Safety Analysis Report, Revision 0, http://www.nrc.gov/reactors/new-reactors/esp/pseg.html.

Raghu Kanth, S. T. G. and R. N. Iyengar (2007). "Estimation of seismic spectral acceleration in Peninsular India." Journal of Earth System Science 116(3): 199-214.

Read, K., H. El Naggar and D. Eaton (2008). "Site-response spectra for POLARIS station sites in southern Ontario and Quebec." Seismological Research Letters 79(6): 776-784.

Romero, S. M. and G. J. Rix (2001). Ground motion amplification in the Upper Mississippi Embayment. Atlanta, National Science Foundation Mid America Center.

Rosenblad, B. L. (2006). Deep shear-wave velocity profiles of Mississippi embayment sediments determined from surface wave measurements, USGS Award Number: 06HQGR0131, U.S. Geological Survey: 23 pages.

Salomone, L. A., J. F. Hamel and R. P. Kassawara (2012). EPRI (2004, 2006) Ground-Motion Model (GMM) review project: Shear wave velocity measurements at seismic recording stations. Draft Report. EP-P43952/C19088. Palo Alto, California, EPRI.

Santagata, M. and Y. I. Kang (2007). "Effects of geologic time on the initial stiffness of clays." Engineering Geology 89(1-2): 98-111.

Schneider, J. A., P. W. Mayne and G. J. Rix (2001). "Geotechnical site characterization in the greater Memphis area using cone penetration tests." Engineering Geology 62(1-3): 169-184.

Seed, H. B. and I. M. Idriss (1970). Soil moduli and damping factors for dynamic response analyses. Berkeley, College of Engineering University of California Berkeley.

Seyhan, E. and J. Stewart (2014). "Semi-Empirical Nonlinear Site Amplification from NGA-West2 Data and Simulations." Earthquake spectra 30(3): 1241-1256.

Shahjouei, A. and S. Pezeshk (2015). Hybrid Empirical Ground-Motion Model for Central and Eastern North America Using Hybrid Broadband Simulations and NGA-West2 GMPEs. NGA-East: Median Ground-Motion Models for the Central and Eastern North America Region. Berkeley, CA, Pacific Earthquake Engineering Research Center: 165-192.

Silva, W., N. Gregor and R. Darragh (2002a). Development of hard rock attenuation relations for central and eastern North America, internal report from Pacific Engineering.

Silva, W. J., S. Li, R. B. Darragh and N. Gregor (1999). Surface Geology Based Strong Motion Amplification Factors for the San Francisco Bay and Los Angeles Areas. PEARL Report. El Cerrito, CA, PG&E, CEC, Caltrans.

Silva, W. N., N. Gregor and R. Darragh (2002b). Development of regional hard-rock attenuation relations for central and eastern North America. El Cerrito, California., Pacific Engineering and Analysis.

Somerville, P., N. Collins, N. Abrahamson, R. Graves and C. Saikia (2001). Ground motion attenuation relations for the central and eastern United States, Final report to U.S. Geol. Survey, June 30, 2001, URS Group, Inc., Pasadena CA, USA.

Somerville, P., R. W. Graves, N. Collins, S. G. Song and S. Ni (2009). Source and Ground Motion Models for Australian Earthquakes, Geoscience Australia.

South Carolina Electric & Gas (2011). V. C. Summer Nuclear Station Units 2 & 3, Combined License Application, Part 2: Final Safety Analysis Report, Revision 5, http://www.nrc.gov/reactors/new-reactors/col/summer/documents.html.

Southern Nuclear Operating Company (2008). Vogtle Units 3 and 4, Combined License Application, Part 2: Final Safety Analysis Report, Revision 3, http://www.nrc.gov/reactors/new-reactors/col/vogtle.html

Stewart, J., A. O. L. Kwok, Y. Hashash, N. Matasovic, R. Pyke, Z. wang and Z. Yang (2008). Benchmarking of Nonlinear Geotechnical Ground Response Analysis Procedures, University of California, Berkeley.

Stewart, J. P., J. Douglas, M. B. Javanbarg, C. Di Alessandro, Y. Bozorgnia, N. Abrahamson, D. M. Boore, K. W. Campbell, E. Delavaud, M. Erdik and P. J. Stafford (2013). GEM-

PEER Task 3 Project: Selection of a Global Set of Ground Motion Prediction Equations, Pacific Earthquake Engineering Research Center.

Stokoe II, K. H. (1983). in situ seismic wave velociites Pinopolis West dam, Part 1: Crosshole seismic testing, South Carolina Public Service Authority: 188 pages.

Stokoe II, K. H., J. A. Bay and M. D. Fuhriman (1992). Crosshole seismic measurements Savnnah River site replacement tritium facility, Bechtel Incorporated.

Stokoe II, K. H., J. A. Bay, B. L. Rosenblad, S.-K. Hwang and M. R. Twede (1994). In situ seismic and dynamic laboratory measurements of geotechnical materials at Queensboro Bridge and Roosevelt Island, Steinman, Boynton, Gronquist and Birdsall.

Stokoe II, K. H., S. H. H. Lee and T. S. H. Ni (1985). In situ seismic wave velocities and foundation vibration measurements, Converse Consultants.

Stokoe II, K. H., Y.-J. Mok, J. Bay and R. Lopez (1989). In situ seismic wave velocities: Cheveron Styrene Expansion, St. James, Louisiana, Dames & Moore: 29 pages.

Stokoe II, K. H. and Y. J. Mok (1987). In situ seismic wave velocities: S. R. Bertron Power Plant, Houston, Texas, Ulrich Engineers: 90 pages.

Stokoe II, K. H., S. Nazarian and E. Turner (1983). In situ seismic wave velocities by crosshole and surface wave methods, Southwestern Laboratories, Inc: 81 pages.

Stokoe II, K. H. and E. turner (1983). In situ seismic wave velocities, Southwestern Laboratories, Inc.

STP Nuclear Operating Company (2011). South Texas Project Units 3 & 4, Combined License Application, Part 2: Final Safety Analysis Report, Revision 5, http://www.nrc.gov/reactors/new-reactors/col/south-texas-project/documents.html.

Street, R., E. Woolery, Z. Wang and J. Harris (1995). "A short note on shear-wave velocities and other site conditions at selected strong-motion stations in the New Madrid seismic zone." Seismological Research Letters 66(1): 56-63.

Sykora, D. W. and J. J. Davis (1993). Site-specific earthquake response analysis for Portsmouth Gaseous Diffusion Plant, Portsmouth, Ohio, U.S. Army Corps of Engineers: 113 pages.

Sykora, D. W. and K. H. Stokoe (1983). Correlations of in situ measurements in sands of shear wave velocity, soil characteristics, and site conditions. Geotechnical engineering report, University of Texas at Austin. Geotechnical Engineering Center.

Tavakoli, B. and S. Pezeshk (2005). "Empirical-stochastic ground-motion prediction for eastern North America." Bulletin of the Seismological Society of America 95(6): 2283-2296.

Tennessee Valley Authority (2009). Bellefonte Nuclear Plants 3 & 4, Combined License Application, Part 2: Final Safety Analysis Report, Revision 1, http://www.nrc.gov/reactors/new-reactors/col/bellefonte/documents.html.

Terzaghi, K., R. B. Peck and G. Mesri (1996). Soil Mechanics in Engineering Practice. New York, Wiley.

Toro, G. R. (1995). Probablistic models of site velocity profiles for generic and sitespecific ground-motion amplification studies. Upton, New York, Brookhaven National Laboratory.

Toro, G. R., N. A. Abrahamson and J. F. Schneider (1997). "Model of strong ground motions from earthquakes in central and eastern North America: Best estimates and uncertainties." Seismological Research Letters 68(1): 41-57.

Union Electric Company (2009). Callaway Plant Unit 2, Combined License Application, Part 2: Final Safety Analysis Report, Revision 2, http://www.nrc.gov/reactors/new-reactors/col/callaway/documents.html.

UniStar Nuclear Services LLC (2010). Bell Bend Nuclear Power Plant, Combined License Application, Part 2: Final Safety Analysis Report, Revision 2, http://www.nrc.gov/reactors/new-reactors/col/bell-bend/documents.html.

Walling, M., W. Silva and N. Abrahamson (2008). "Nonlinear Site Amplification Factors for Constraining the NGA Models." Earthquake spectra 24(1): 243-255.

Wilder, B. D. (2007). SASW Testing in the Salt Lake Valley, UT Master of Science, The University of Texas at Austin.

Wills, C. J. and K. B. Clahan (2006). "Developing a Map of Geologically Defined Site-Condition Categories for California." Bulletin of the Seismological Society of America 96(4 A): 1483-1501.

Woolery, E. W. and Z. Wang (2005). Seismic velocity measurements at expanded seismic network sites, UK/KRCEE Doc#: P8.3 2005, U.S. Department of Energy.

Xia, J., R. D. Miller, C. B. Park, J. A. Hunter, J. B. Harris and J. Ivanov (2002). "Comparing shear-wave velocity profiles inverted from multichannel surface wave with borehole measurements." Soil Dynamics and Earthquake Engineering 22(3): 181-190.

Yamada, S., M. Hyodo, R. Orense and S. V. Dinesh (2008). "Initial Shear Modulus of Remolded Sand-Clay Mixtures." Journal of geotechnical and geoenvironmental engineering 134(7): 960-971.

Yee, E., J. P. Stewart and K. Tokimatsu (2013). "Elastic and Large-Strain Nonlinear Seismic Site Response from Analysis of Vertical Array Recordings." Journal of Geotechnical and Geoenvironmental Engineering 139(10): 1789-1801.

Yenier, E. and G. A. Atkinson (2015). Regionally-Adjustable Generic Ground-Motion Prediction Equation Based on Equivalent Point-Source Simulations: Application to Central and Eastern North America. NGA-East: Median Ground-Motion Models for the Central and Eastern North America Region. Berkeley, CA, Pacific Earthquake Engineering Research Center: 85-118.

Zen, K., H. Yamazaki and Y. Umehara (1987). Experimental study on dynamic properties of soils for use in seismic response analysis. Rep. of Port and Harbour Research Institute. Yokosuka, Japan, Port and Harbour Research Institute. 26.

APPENDIX A Model Coefficients and Tables

This appendix presents coefficients for the amplification models developed in this study. Table A.1 provides a summary of table numbers for the RS amplification models and nonlinear FAS amplification model. Table A.2 provides a summary of table numbers for the linear FAS amplification model. The linear FAS amplification model is presented as ln(amp) values for 30 V_{S30} values as a function of depth at 112 frequencies. One table of ln(amp) values per frequency is provided.

Table A.1: Tables for coefficients of RS linear and nonlinear amplification models and FAS nonlinear amplification model.

Coefficient Model	Table
L1	Table A.3
L2	
L3	
L4	Table A.4
L5	Table A.5
N1	Table A.6
N2	
K1	Table A.7
K2	Table A.8
Nonlinear FAS	Table A.9

Table A.2: Tables of FAS linear amplification look-up tables for 112 frequencies.

Frequency (Hz)	Table	Frequency (Hz)	Table	Frequency (Hz)	Table	Frequency (Hz)	Table
0.1	Table A.10	0.526	Table A.38	2.778	Table A.66	14.286	Table A.94
0.105	Table A.11	0.556	Table A.39	2.857	Table A.67	15.0	Table A.95
0.111	Table A.12	0.588	Table A.40	2.941	Table A.68	15.385	Table A.96
0.118	Table A.13	0.625	Table A.41	3.125	Table A.69	16.667	Table A.97
0.125	Table A.14	0.667	Table A.42	3.333	Table A.70	18.182	Table A.98
0.133	Table A.15	0.714	Table A.43	3.448	Table A.71	20.0	Table A.99
0.143	Table A.16	0.769	Table A.44	3.571	Table A.72	20.833	Table A.100
0.154	Table A.17	0.833	Table A.45	3.846	Table A.73	21.739	Table A.101
0.167	Table A.18	0.909	Table A.46	4.0	Table A.74	22.222	Table A.102
0.182	Table A.19	1.0	Table A.47	4.167	Table A.75	22.727	Table A.103
0.2	Table A.20	1.053	Table A.48	4.545	Table A.76	23.810	Table A.104
0.208	Table A.21	1.111	Table A.49	5.0	Table A.77	25.0	Table A.105
0.217	Table A.22	1.176	Table A.50	5.263	Table A.78	27.778	Table A.106
0.227	Table A.23	1.25	Table A.51	5.556	Table A.79	28.571	Table A.107
0.238	Table A.24	1.333	Table A.52	5.882	Table A.80	31.25	Table A.108
0.25	Table A.25	1.429	Table A.53	6.250	Table A.81	33.333	Table A.109
0.263	Table A.26	1.5	Table A.54	6.667	Table A.82	34.483	Table A.110
0.278	Table A.27	1.538	Table A.55	7.143	Table A.83	40.0	Table A.111
0.286	Table A.28	1.667	Table A.56	7.5	Table A.84	45.455	Table A.112
0.294	Table A.29	1.818	Table A.57	7.692	Table A.85	50.0	Table A.113
0.313	Table A.30	2.0	Table A.58	8.333	Table A.86	54.999	Table A.114
0.333	Table A.31	2.083	Table A.59	9.091	Table A.87	61.660	Table A.115
0.357	Table A.32	2.174	Table A.60	10.0	Table A.88	70.796	Table A.116
0.385	Table A.33	2.222	Table A.61	10.526	Table A.89	80.0	Table A.117
0.4	Table A.34	2.273	Table A.62	11.111	Table A.90	85.114	Table A.118
0.417	Table A.35	2.381	Table A.63	11.765	Table A.91	90.001	Table A.119
0.455	Table A.36	2.5	Table A.64	12.5	Table A.92	95.003	Table A.120
0.5	Table A.37	2.632	Table A.65	13.333	Table A.93	100.0	Table A.121

Table A.3: Model coefficients for models L1, L2, and L3.

Model:	L1					L2	L3		
Period (s)	c_1	c_2	c_3	V_c (m/s)	V_L (m/s)	c_4	c_5	c_6	α
0.0010	-1.698	0.000	-1.722	2990	1887	-7.46E-07	0.000	-0.099	0.000
0.0067	-1.668	0.000	-1.721	2990	1887	-7.54E-07	0.000	-0.100	0.000
0.0080	-1.634	0.000	-1.714	2990	1887	-7.62E-07	0.000	-0.101	0.000
0.0100	-1.526	0.000	-1.700	2990	1887	-7.81E-07	-0.010	-0.103	0.104
0.0105	-1.496	0.000	-1.701	2990	1887	-7.89E-07	-0.010	-0.104	0.094
0.0111	-1.480	0.000	-1.710	2990	1887	-7.97E-07	-0.010	-0.105	0.150
0.0117	-1.467	0.000	-1.722	2990	1887	-8.06E-07	0.004	-0.106	0.096
0.0125	-1.458	0.000	-1.741	2990	1887	-8.21E-07	0.013	-0.108	0.092
0.0141	-1.440	0.000	-1.810	2990	1887	-8.59E-07	0.028	-0.113	0.085
0.0162	-1.422	0.000	-1.904	2990	1887	-9.13E-07	0.022	-0.119	0.073
0.0182	-1.435	0.000	-1.982	2990	1887	-9.65E-07	-0.010	-0.126	0.150
0.0200	-1.453	0.000	-2.061	2990	1887	-1.02E-06	-0.010	-0.133	0.150
0.0220	-1.494	0.000	-2.146	2990	1887	-1.06E-06	-0.010	-0.139	0.150
0.0250	-1.559	0.000	-2.224	2990	1887	-1.11E-06	-0.010	-0.145	0.150
0.0290	-1.624	0.000	-2.267	2990	1887	-1.15E-06	0.025	-0.151	0.093
0.0300	-1.647	0.000	-2.272	2990	1887	-1.15E-06	0.045	-0.151	0.094
0.0320	-1.685	0.000	-2.292	2990	1887	-1.16E-06	0.080	-0.153	0.095
0.0350	-1.738	0.000	-2.316	2990	1887	-1.16E-06	0.113	-0.154	0.100
0.0360	-1.751	0.000	-2.321	2990	1887	-1.17E-06	0.116	-0.155	0.102
0.0400	-1.830	0.000	-2.342	2990	1887	-1.16E-06	0.126	-0.155	0.114
0.0420	-1.854	0.000	-2.345	2990	1887	-1.17E-06	0.131	-0.155	0.118
0.0440	-1.883	0.000	-2.359	2990	1887	-1.17E-06	0.134	-0.156	0.121
0.0450	-1.890	0.000	-2.361	2990	1887	-1.17E-06	0.135	-0.156	0.121
0.0460	-1.905	0.000	-2.366	2990	1887	-1.17E-06	0.135	-0.156	0.122
0.0480	-1.922	0.000	-2.359	2990	1887	-1.16E-06	0.135	-0.155	0.123
0.0500	-1.945	0.000	-2.361	2990	1887	-1.15E-06	0.136	-0.154	0.123
0.0550	-1.977	0.000	-2.352	2990	1887	-1.13E-06	0.144	-0.152	0.123
0.0600	-2.011	0.000	-2.338	2990	1887	-1.10E-06	0.154	-0.149	0.123
0.0650	-2.038	0.000	-2.313	2990	1887	-1.06E-06	0.158	-0.144	0.123
0.0667	-2.046	0.000	-2.306	2990	1887	-1.05E-06	0.158	-0.142	0.124
0.0700	-2.058	0.000	-2.287	2990	1887	-1.03E-06	0.158	-0.138	0.125
0.0750	-2.069	0.000	-2.251	2990	1887	-9.85E-07	0.154	-0.133	0.126
0.0800	-2.067	0.000	-2.205	2990	1887	-9.48E-07	0.144	-0.128	0.127
0.0850	-2.067	0.000	-2.167	2990	1887	-9.17E-07	0.137	-0.124	0.129
0.0900	-2.060	0.000	-2.129	2990	1887	-8.88E-07	0.134	-0.121	0.130
0.0950	-2.058	0.000	-2.091	2990	1887	-8.56E-07	0.131	-0.116	0.131

Table A.3 Continued.

Model:	L1					L2	L3		
Period (s)	c_1	c_2	c_3	V_c (m/s)	V_L (m/s)	c_4	c_5	c_6	α
0.1000	-2.055	0.000	-2.049	2990	1887	-8.21E-07	0.133	-0.112	0.133
0.1100	-2.018	0.000	-1.956	2990	1887	-7.60E-07	0.140	-0.104	0.136
0.1200	-2.011	0.000	-1.890	2990	1887	-7.13E-07	0.147	-0.097	0.138
0.1300	-1.994	0.000	-1.824	2990	1887	-6.70E-07	0.149	-0.091	0.141
0.1333	-1.996	0.000	-1.823	2946	1859	-6.58E-07	0.150	-0.090	0.142
0.1400	-2.055	0.000	-1.956	2652	1673	-6.36E-07	0.154	-0.087	0.145
0.1500	-2.130	0.000	-2.134	2335	1474	-6.07E-07	0.161	-0.083	0.148
0.1600	-2.221	0.000	-2.318	2102	1326	-5.88E-07	0.166	-0.080	0.148
0.1700	-2.305	0.000	-2.520	1902	1200	-5.68E-07	0.172	-0.078	0.149
0.1800	-2.377	0.000	-2.710	1743	1100	-5.43E-07	0.173	-0.075	0.149
0.1900	-2.437	0.000	-2.864	1632	1030	-5.27E-07	0.174	-0.073	0.149
0.2000	-2.509	0.000	-3.033	1533	967	-5.12E-07	0.175	-0.072	0.149
0.2200	-2.043	-0.911	-3.378	1499	946	-4.88E-07	0.176	-0.070	0.153
0.2400	-2.723	0.000	-3.532	1245	786	-4.58E-07	0.174	-0.067	0.152
0.2500	-2.100	-1.025	-3.679	1318	832	-4.46E-07	0.175	-0.066	0.153
0.2600	-2.078	-1.111	-3.780	1269	801	-4.30E-07	0.176	-0.065	0.151
0.2800	-2.038	-1.291	-3.953	1202	758	-4.05E-07	0.177	-0.062	0.147
0.2900	-2.019	-1.354	-4.002	1174	741	-3.92E-07	0.176	-0.061	0.147
0.3000	-2.000	-1.393	-4.001	1152	727	-3.79E-07	0.176	-0.059	0.146
0.3200	-1.958	-1.387	-4.130	1131	656	-3.51E-07	0.177	-0.056	0.147
0.3400	-1.919	-1.409	-4.375	1104	588	-3.17E-07	0.178	-0.052	0.149
0.3500	-1.927	-1.361	-4.479	1094	556	-3.03E-07	0.180	-0.051	0.150
0.3600	-1.883	-1.430	-4.470	1089	546	-2.86E-07	0.181	-0.049	0.151
0.3800	-2.017	-1.070	-4.868	1037	461	-2.51E-07	0.183	-0.044	0.155
0.4000	-1.971	-1.175	-5.196	1018	429	-2.19E-07	0.185	-0.040	0.158
0.4200	-2.002	-1.057	-5.872	990	375	-1.90E-07	0.188	-0.036	0.161
0.4400	-1.971	-1.168	-6.412	979	350	-1.65E-07	0.191	-0.032	0.163
0.4500	-1.955	-1.243	-6.676	970	340	-1.51E-07	0.193	-0.030	0.164
0.4600	-1.934	-1.336	-6.839	963	335	-1.37E-07	0.195	-0.028	0.165
0.4800	-1.891	-1.523	-7.153	953	324	-1.10E-07	0.200	-0.024	0.166
0.5000	-1.862	-1.708	-7.556	939	314	-7.89E-08	0.208	-0.019	0.167
0.5500	-1.784	-2.051	-8.389	917	290	-2.28E-08	0.221	-0.010	0.169
0.6000	-1.792	-2.195	-10.193	883	252	2.55E-08	0.228	-0.002	0.175
0.6500	-1.758	-2.204	-9.840	862	243	6.19E-08	0.231	0.005	0.181
0.6667	-1.730	-2.204	-9.441	859	242	7.39E-08	0.233	0.008	0.183
0.7000	-1.715	-2.061	-8.490	849	239	9.52E-08	0.235	0.012	0.188

Table A.3 Continued.

Model:	L1					L2	L3		
Period (s)	c_1	c_2	c_3	V_c (m/s)	V_L (m/s)	c_4	c_5	c_6	α
0. 7500	-1.655	-1.976	-7.444	835	235	1.29E-07	0.238	0.020	0.200
0.8000	-1.604	-1.748	-5.931	832	235	1.59E-07	0.237	0.028	0.217
0.8500	-1.293	-1.254	-2.906	905	305	2.28E-07	0.249	0.051	0.259
0.9000	-1.000	-0.789	-0.053	974	388	2.77E-07	0.238	0.062	0.298
0.9500	-1.000	-0.723	0.054	963	479	2.28E-07	0.242	0.050	0.283
1.0000	-1.000	-0.657	0.142	951	466	2.53E-07	0.245	0.055	0.297
1.1000	-1.000	-0.488	0.397	947	444	2.90E-07	0.247	0.059	0.314
1.2000	-1.000	-0.233	0.824	931	428	3.13E-07	0.251	0.060	0.327
1.3000	-1.000	-0.025	1.000	913	435	3.37E-07	0.258	0.060	0.334
1.4000	-1.000	0.000	0.874	887	436	3.55E-07	0.257	0.058	0.337
1.5000	-1.000	0.000	0.622	882	447	3.73E-07	0.257	0.055	0.345
1.6000	-1.000	0.000	0.381	879	458	3.85E-07	0.256	0.051	0.355
1.7000	-1.000	0.000	0.213	876	469	3.95E-07	0.261	0.046	0.369
1.8000	-1.000	0.000	0.076	871	479	4.07E-07	0.271	0.043	0.379
1.9000	-1.000	0.000	-0.057	873	551	3.29E-07	0.282	0.039	0.390
2.0000	-1.000	0.000	-0.117	879	555	3.37E-07	0.292	0.034	0.400
2.2000	-1.000	0.000	-0.255	889	561	4.13E-07	0.315	0.025	0.413
2.4000	-1.000	0.000	-0.343	893	563	4.13E-07	0.339	0.016	0.422
2.5000	-1.000	0.000	-0.362	892	563	4.18E-07	0.352	0.012	0.427
2.6000	-1.000	0.000	-0.380	891	562	4.24E-07	0.364	0.009	0.431
2.8000	-1.000	0.000	-0.404	892	563	4.40E-07	0.380	0.004	0.441
3.0000	-1.000	0.000	-0.403	894	564	4.57E-07	0.386	0.002	0.453
3.2000	-1.000	0.000	-0.420	891	562	4.73E-07	0.387	0.001	0.464
3.4000	-1.000	0.000	-0.436	889	561	4.90E-07	0.388	0.001	0.476
3.5000	-1.000	0.000	-0.441	885	558	4.98E-07	0.387	0.002	0.481
3.6000	-1.000	0.000	-0.441	883	557	5.06E-07	0.385	0.003	0.486
3.8000	-1.000	0.000	-0.451	879	555	5.18E-07	0.378	0.005	0.497
4.0000	-1.000	0.000	-0.451	875	552	5.32E-07	0.375	0.007	0.507
4.2000	-1.000	0.000	-0.447	870	549	5.44E-07	0.373	0.010	0.515
4.4000	-1.000	0.000	-0.436	867	547	5.54E-07	0.370	0.012	0.523
4.6000	-1.000	0.000	-0.433	864	545	5.56E-07	0.364	0.015	0.532
4.8000	-1.000	0.000	-0.428	862	544	5.56E-07	0.359	0.017	0.540
5.0000	-1.000	0.000	-0.429	856	540	5.51E-07	0.352	0.019	0.546
5.5000	-1.000	0.000	-0.430	847	535	5.30E-07	0.334	0.022	0.566
6.0000	-1.000	0.000	-0.433	840	530	5.03E-07	0.317	0.025	0.579
6.5000	-1.000	0.000	-0.429	837	528	4.78E-07	0.306	0.027	0.582

Table A.3 Continued.

Model:	L1					L2	L3		
Period (s)	c_1	c_2	c_3	V_c (m/s)	V_L (m/s)	c_4	c_5	c_6	α
7.0000	-1.000	0.000	-0.424	835	527	4.54E-07	0.296	0.028	0.585
7.5000	-1.000	0.000	-0.429	832	525	4.28E-07	0.281	0.029	0.588
8.0000	-1.000	0.000	-0.437	830	524	4.09E-07	0.271	0.031	0.591
8.5000	-1.000	0.000	-0.440	831	525	3.96E-07	0.265	0.032	0.593
9.0000	-1.000	0.000	-0.434	833	525	3.87E-07	0.259	0.034	0.596
9.5000	-1.000	0.000	-0.427	834	526	3.80E-07	0.254	0.036	0.598
10.0000	-1.000	0.000	-0.415	837	528	3.77E-07	0.251	0.038	0.600

Table A.4: L4 model Coefficients.

Period (s)	c_1	c_2	c_3	c_4	V_c (m/s)	V_L (m/s)
0.0010	-1.779	0.000	-1.638	-9.02E-07	2990	1887
0.0067	-1.749	0.000	-1.635	-9.12E-07	2990	1887
0.0080	-1.717	0.000	-1.628	-9.23E-07	2990	1887
0.0100	-1.611	0.000	-1.611	-9.45E-07	2990	1887
0.0105	-1.582	0.000	-1.611	-9.55E-07	2990	1887
0.0111	-1.567	0.000	-1.620	-9.65E-07	2990	1887
0.0117	-1.554	0.000	-1.630	-9.76E-07	2990	1887
0.0125	-1.547	0.000	-1.648	-9.93E-07	2990	1887
0.0141	-1.533	0.000	-1.713	-1.04E-06	2990	1887
0.0162	-1.522	0.000	-1.801	-1.10E-06	2990	1887
0.0182	-1.540	0.000	-1.873	-1.17E-06	2990	1887
0.0200	-1.563	0.000	-1.946	-1.23E-06	2990	1887
0.0220	-1.609	0.000	-2.026	-1.29E-06	2990	1887
0.0250	-1.680	0.000	-2.098	-1.34E-06	2990	1887
0.0290	-1.748	0.000	-2.137	-1.39E-06	2990	1887
0.0300	-1.771	0.000	-2.142	-1.39E-06	2990	1887
0.0320	-1.810	0.000	-2.161	-1.40E-06	2990	1887
0.0350	-1.864	0.000	-2.184	-1.41E-06	2990	1887
0.0360	-1.878	0.000	-2.189	-1.41E-06	2990	1887
0.0400	-1.957	0.000	-2.210	-1.41E-06	2990	1887
0.0420	-1.981	0.000	-2.213	-1.41E-06	2990	1887
0.0440	-2.010	0.000	-2.227	-1.41E-06	2990	1887
0.0450	-2.017	0.000	-2.229	-1.41E-06	2990	1887
0.0460	-2.032	0.000	-2.234	-1.41E-06	2990	1887
0.0480	-2.047	0.000	-2.228	-1.40E-06	2990	1887
0.0500	-2.070	0.000	-2.231	-1.39E-06	2990	1887
0.0550	-2.100	0.000	-2.224	-1.37E-06	2990	1887
0.0600	-2.131	0.000	-2.214	-1.34E-06	2990	1887
0.0650	-2.154	0.000	-2.193	-1.29E-06	2990	1887
0.0667	-2.161	0.000	-2.187	-1.27E-06	2990	1887
0.0700	-2.169	0.000	-2.171	-1.24E-06	2990	1887
0.0750	-2.177	0.000	-2.139	-1.19E-06	2990	1887
0.0800	-2.170	0.000	-2.098	-1.15E-06	2990	1887
0.0850	-2.166	0.000	-2.063	-1.11E-06	2990	1887
0.0900	-2.157	0.000	-2.029	-1.07E-06	2990	1887
0.0950	-2.151	0.000	-1.994	-1.04E-06	2990	1887
0.1000	-2.144	0.000	-1.956	-9.94E-07	2990	1887
0.1100	-2.101	0.000	-1.870	-9.19E-07	2990	1887

Table A.4 Continued.

Period (s)	c_1	c_2	c_3	c_4	V_c (m/s)	V_L (m/s)
0.1200	-2.088	0.000	-1.809	-8.63E-07	2990	1887
0.1300	-2.127	0.000	-1.874	-8.13E-07	2784	1757
0.1333	-2.161	0.000	-1.945	-8.00E-07	2649	1672
0.1400	-2.229	0.000	-2.090	-7.74E-07	2415	1524
0.1500	-2.308	0.000	-2.271	-7.38E-07	2167	1367
0.1600	-2.404	0.000	-2.461	-7.16E-07	1977	1247
0.1700	-2.491	0.000	-2.668	-6.91E-07	1810	1142
0.1800	-2.564	0.000	-2.860	-6.61E-07	1674	1057
0.1900	-2.628	0.000	-3.024	-6.41E-07	1576	994
0.2000	-2.703	0.000	-3.200	-6.24E-07	1487	938
0.2200	-2.043	-1.203	-3.572	-5.95E-07	1499	946
0.2400	-2.082	-1.275	-3.784	-5.59E-07	1377	869
0.2500	-2.100	-1.320	-3.885	-5.44E-07	1326	837
0.2600	-2.078	-1.399	-3.978	-5.24E-07	1280	808
0.2800	-2.038	-1.573	-4.153	-4.94E-07	1214	766
0.2900	-2.019	-1.629	-4.197	-4.78E-07	1187	749
0.3000	-2.000	-1.656	-4.181	-4.62E-07	1166	736
0.3200	-1.958	-1.689	-4.189	-4.28E-07	1134	693
0.3400	-2.110	-1.341	-4.559	-3.86E-07	1085	579
0.3500	-2.083	-1.341	-4.634	-3.69E-07	1081	554
0.3600	-2.022	-1.425	-4.613	-3.49E-07	1079	546
0.3800	-2.117	-1.099	-4.948	-3.06E-07	1036	468
0.4000	-2.045	-1.223	-5.199	-2.67E-07	1020	439
0.4200	-2.087	-1.015	-5.868	-2.32E-07	989	378
0.4400	-2.047	-1.098	-6.412	-2.01E-07	978	350
0.4500	-2.025	-1.170	-6.680	-1.85E-07	969	339
0.4600	-1.995	-1.272	-6.827	-1.67E-07	963	334
0.4800	-1.939	-1.469	-7.124	-1.34E-07	953	324
0.5000	-1.896	-1.666	-7.525	-9.62E-08	939	314
0.5500	-1.793	-2.037	-8.380	-2.78E-08	918	289
0.6000	-1.783	-2.214	-10.210	3.11E-08	882	253
0.6500	-1.735	-2.273	-10.050	7.54E-08	859	242
0.6667	-1.704	-2.289	-9.704	9.01E-08	855	241
0.7000	-1.685	-2.181	-8.921	1.16E-07	843	237
0.7500	-1.607	-2.153	-7.985	1.57E-07	828	233
0.8000	-1.550	-1.973	-6.645	1.94E-07	822	232
0.8500	-1.293	-1.254	-2.906	1.83E-07	905	305
0.9000	-1.000	-0.789	-0.053	2.06E-07	974	388

Table A.4 Continued.

Period (s)	c_1	c_2	c_3	c_4	V_c (m/s)	V_L (m/s)
0.9500	-1.000	-0.610	0.203	2.77E-07	916	466
1.0000	-1.000	-0.539	0.309	3.08E-07	897	450
1.1000	-1.000	-0.360	0.609	3.52E-07	881	424
1.2000	-1.000	-0.167	1.000	3.79E-07	853	392
1.3000	-1.000	-0.041	1.000	4.08E-07	820	390
1.4000	-1.000	0.000	0.975	4.32E-07	785	386
1.5000	-1.000	0.000	0.680	4.53E-07	774	392
1.6000	-1.000	0.000	0.384	4.67E-07	765	399
1.7000	-1.000	0.000	0.158	4.78E-07	760	407
1.8000	-1.000	0.000	-0.092	4.91E-07	760	480
1.9000	-1.000	0.000	-0.223	4.99E-07	760	480
2.0000	-1.000	0.000	-0.288	5.01E-07	760	480
2.2000	-1.000	0.000	-0.461	4.98E-07	767	484
2.4000	-1.000	0.000	-0.578	4.98E-07	769	485
2.5000	-1.000	0.000	-0.608	5.04E-07	767	484
2.6000	-1.000	0.000	-0.637	5.10E-07	764	482
2.8000	-1.000	0.000	-0.683	5.29E-07	761	480
3.0000	-1.000	0.000	-0.701	5.49E-07	760	480
3.2000	-1.000	0.000	-0.751	5.65E-07	760	480
3.4000	-1.000	0.000	-0.797	5.82E-07	760	480
3.5000	-1.000	0.000	-0.818	5.89E-07	760	480
3.6000	-1.000	0.000	-0.833	5.97E-07	760	480
3.8000	-1.000	0.000	-0.867	6.09E-07	760	480
4.0000	-1.000	0.000	-0.889	6.21E-07	760	480
4.2000	-1.000	0.000	-0.908	6.33E-07	760	480
4.4000	-1.000	0.000	-0.911	6.42E-07	760	480
4.6000	-1.000	0.000	-0.914	6.43E-07	760	480
4.8000	-1.000	0.000	-0.911	6.42E-07	760	480
5.0000	-1.000	0.000	-0.915	6.35E-07	760	480
5.5000	-1.000	0.000	-0.904	6.08E-07	760	480
6.0000	-1.000	0.000	-0.885	5.76E-07	760	480
6.5000	-1.000	0.000	-0.854	5.48E-07	760	480
7.0000	-1.000	0.000	-0.821	5.22E-07	760	480
7.5000	-1.000	0.000	-0.801	4.92E-07	760	480
8.0000	-1.000	0.000	-0.790	4.70E-07	760	480
8.5000	-1.000	0.000	-0.775	4.58E-07	760	480
9.0000	-1.000	0.000	-0.754	4.48E-07	760	480
9.5000	-1.000	0.000	-0.736	4.41E-07	760	480

Table A.4 Continued.

Period (s)	c_1	c_2	c_3	c_4	V_c (m/s)	V_L (m/s)
10.0000	-1.000	0.000	-0.712	4.40E-07	760	480

Table A.5: L5 Model Coefficients.

Period (s)	c_1	c_2	c_3	c_5	c_6	V_c (m/s)	V_L (m/s)	α
0.0010	-1.7560	0.0000	-1.3778	0.0000	-0.1747	1887	2990	0.0000
0.0067	-1.7207	0.0000	-1.3628	0.0000	-0.1767	1887	2990	0.0000
0.0080	-1.6925	0.0000	-1.3614	0.0000	-0.1782	1887	2990	0.0000
0.0100	-1.5970	0.0000	-1.3596	-0.0100	-0.1814	1887	2990	0.1500
0.0105	-1.5804	0.0000	-1.3810	-0.0100	-0.1824	1887	2990	0.0935
0.0111	-1.5737	0.0000	-1.4036	-0.0039	-0.1835	1887	2990	0.0705
0.0117	-1.5697	0.0000	-1.4269	0.0016	-0.1850	1887	2990	0.0400
0.0125	-1.5688	0.0000	-1.4528	0.0135	-0.1878	1887	2990	0.0927
0.0141	-1.5522	0.0000	-1.5039	0.0279	-0.1960	1887	2990	0.0855
0.0162	-1.5316	0.0000	-1.5616	0.0222	-0.2079	1887	2990	0.0746
0.0182	-1.5369	-0.0091	-1.6093	-0.0008	-0.2199	1887	2990	0.0847
0.0200	-1.5571	0.0000	-1.6491	-0.0100	-0.2324	1887	2990	0.1500
0.0220	-1.5886	0.0000	-1.6888	-0.0100	-0.2437	1887	2990	0.1500
0.0250	-1.6568	0.0000	-1.7420	-0.0100	-0.2554	1887	2990	0.0708
0.0290	-1.7460	0.0000	-1.8038	0.0428	-0.2644	1887	2990	0.0998
0.0300	-1.7749	0.0000	-1.8180	0.0622	-0.2648	1887	2990	0.1018
0.0320	-1.8002	0.0000	-1.8084	0.0947	-0.2676	1887	2990	0.1034
0.0350	-1.8381	0.0000	-1.7950	0.1275	-0.2717	1887	2990	0.1104
0.0360	-1.8470	0.0000	-1.7909	0.1329	-0.2724	1887	2990	0.1134
0.0400	-1.9087	0.0000	-1.7752	0.1501	-0.2742	1887	2990	0.1250
0.0420	-1.9296	0.0000	-1.7679	0.1586	-0.2760	1887	2990	0.1293
0.0440	-1.9492	0.0000	-1.7610	0.1633	-0.2778	1887	2990	0.1327
0.0450	-1.9543	0.0000	-1.7577	0.1645	-0.2783	1887	2990	0.1340
0.0460	-1.9655	0.0000	-1.7544	0.1648	-0.2784	1887	2990	0.1349
0.0480	-1.9807	0.0000	-1.7481	0.1661	-0.2774	1887	2990	0.1373
0.0500	-1.9983	0.0000	-1.7420	0.1677	-0.2762	1887	2990	0.1390
0.0550	-2.0317	0.0000	-1.7401	0.1781	-0.2727	1887	2990	0.1430
0.0600	-2.0704	0.0000	-1.7452	0.1904	-0.2675	1887	2990	0.1447
0.0650	-2.0990	0.0000	-1.7403	0.1955	-0.2592	1887	2990	0.1456
0.0667	-2.1074	0.0000	-1.7395	0.1954	-0.2561	1887	2990	0.1463
0.0700	-2.1186	0.0000	-1.7311	0.1976	-0.2508	1887	2990	0.1479
0.0750	-2.1253	0.0000	-1.7075	0.1939	-0.2421	1887	2990	0.1489
0.0800	-2.1172	0.0000	-1.6721	0.1852	-0.2340	1887	2990	0.1509
0.0850	-2.1238	0.0000	-1.6631	0.1797	-0.2267	1887	2990	0.1525
0.0900	-2.1243	0.0000	-1.6546	0.1759	-0.2197	1887	2990	0.1524
0.0950	-2.1278	0.0000	-1.6465	0.1724	-0.2121	1876	2974	0.1526
0.1000	-2.1330	0.0000	-1.6389	0.1752	-0.2051	1817	2880	0.1544
0.1100	-2.0353	-0.2000	-1.7472	0.1852	-0.1920	1665	2638	0.1564
0.1200	-2.1046	-0.2000	-1.8461	0.1924	-0.1817	1519	2407	0.1558
0.1300	-2.2120	-0.1298	-1.9370	0.1937	-0.1718	1385	2195	0.1568

Table A.5 Continued.

Period (s)	c_1	c_2	c_3	c_5	c_6	V_c (m/s)	V_L (m/s)	α
0.1333	-2.2059	-0.1601	-1.9658	0.1933	-0.1690	1354	2147	0.1569
0.1400	-2.2052	-0.2000	-2.0212	0.1930	-0.1628	1296	2054	0.1574
0.1500	-2.2414	-0.2000	-2.0996	0.1931	-0.1543	1214	1924	0.1567
0.1600	-2.3683	-0.0966	-2.1729	0.1912	-0.1484	1137	1802	0.1545
0.1700	-2.4725	0.0000	-2.2418	0.1910	-0.1419	1065	1688	0.1526
0.1800	-2.4962	0.0000	-2.3068	0.1878	-0.1345	1015	1609	0.1509
0.1900	-2.5219	0.0000	-2.3682	0.1842	-0.1290	977	1548	0.1497
0.2000	-2.5544	0.0000	-2.4265	0.1830	-0.1243	941	1492	0.1487
0.2200	-2.1530	-0.7158	-2.6476	0.1794	-0.1162	930	1474	0.1509
0.2400	-2.0830	-0.9367	-2.8495	0.1730	-0.1079	876	1389	0.1496
0.2500	-2.1000	-0.9821	-2.9443	0.1713	-0.1048	848	1344	0.1483
0.2600	-2.0785	-1.0374	-2.9994	0.1716	-0.1006	823	1305	0.1465
0.2800	-2.0378	-1.2229	-3.1451	0.1696	-0.0978	788	1248	0.1417
0.2900	-2.0186	-1.3110	-3.2479	0.1672	-0.0953	771	1221	0.1405
0.3000	-2.0000	-1.3961	-3.3419	0.1651	-0.0933	756	1199	0.1392
0.3200	-1.9581	-1.2675	-3.3608	0.1705	-0.0836	681	1201	0.1412
0.3400	-1.9188	-1.1466	-3.5115	0.1756	-0.0756	587	1195	0.1451
0.3500	-1.9053	-1.0889	-3.5836	0.1790	-0.0721	550	1195	0.1471
0.3600	-1.8789	-1.0574	-3.7046	0.1817	-0.0685	510	1195	0.1503
0.3800	-1.8466	-0.9971	-3.9367	0.1862	-0.0600	455	1178	0.1551
0.4000	-1.8183	-0.9399	-4.1570	0.1930	-0.0522	409	1154	0.1606
0.4200	-1.7869	-0.9626	-4.6474	0.1989	-0.0448	368	1137	0.1658
0.4400	-1.7475	-0.9842	-5.1150	0.2054	-0.0381	335	1130	0.1704
0.4500	-1.7192	-0.9946	-5.3409	0.2102	-0.0343	320	1127	0.1730
0.4600	-1.6894	-1.0721	-5.4877	0.2135	-0.0307	315	1122	0.1748
0.4800	-1.6391	-1.2223	-5.7720	0.2206	-0.0241	306	1113	0.1781
0.5000	-1.6000	-1.3663	-6.1138	0.2303	-0.0174	295	1099	0.1802
0.5500	-1.4755	-1.6409	-6.8557	0.2476	-0.0021	274	1094	0.1876
0.6000	-1.4355	-1.7561	-8.7579	0.2574	0.0116	236	1059	0.1968
0.6500	-1.4061	-1.7632	-9.2207	0.2609	0.0204	226	1032	0.2059
0.6667	-1.3945	-1.7241	-9.1309	0.2621	0.0233	223	1020	0.2079
0.7000	-1.3722	-1.6487	-8.8175	0.2653	0.0296	221	1012	0.2169
0.7500	-1.3264	-1.5192	-8.6017	0.2709	0.0401	216	988	0.2335
0.8000	-1.2835	-1.3981	-7.1177	0.2724	0.0501	215	982	0.2561
0.8500	-1.1376	-1.0033	-3.4869	0.2863	0.0660	316	1014	0.2846
0.9000	-1.0000	-0.6312	-0.0637	0.2476	0.0597	432	991	0.2906
0.9500	-1.0000	-0.7212	0.0470	0.2548	0.0420	476	962	0.2611
1.0000	-1.0000	-0.6569	0.1420	0.2448	0.0420	466	951	0.3000
1.1000	-1.0000	-0.5594	0.1190	0.2448	0.0420	471	940	0.3000
1.2000	-1.0000	-0.4703	0.0979	0.2448	0.0420	475	930	0.3000

Table A.5 Continued.

Period (s)	c_1	c_2	c_3	c_5	c_6	V_c (m/s)	V_L (m/s)	α
1.3000	-1.0000	-0.3884	0.0786	0.2448	0.0420	480	920	0.3000
1.4000	-1.0000	-0.3126	0.0606	0.2448	0.0420	484	912	0.3000
1.5000	-1.0000	-0.2419	0.0440	0.2448	0.0420	487	904	0.3000
1.6000	-1.0000	-0.1759	0.0284	0.2448	0.0420	491	896	0.3000
1.7000	-1.0000	-0.1138	0.0137	0.2448	0.0420	494	889	0.3000
1.8000	-1.0000	-0.0553	-0.0001	0.2448	0.0420	497	883	0.3000
1.9000	-1.0000	0.0000	-0.0132	0.2448	0.0420	500	876	0.3000
2.0000	-1.0000	0.0000	-0.1402	0.2680	0.0473	512	811	0.3853
2.2000	-1.0000	0.0000	-0.2210	0.3056	0.0290	543	860	0.4049
2.4000	-1.0000	0.0000	-0.2948	0.3512	0.0101	579	918	0.4264
2.5000	-1.0000	0.0000	-0.3294	0.3762	0.0012	599	950	0.4392
2.6000	-1.0000	0.0000	-0.3627	0.4005	-0.0074	621	984	0.4521
2.8000	-1.0000	0.0000	-0.4256	0.4385	-0.0201	662	1049	0.4771
3.0000	-1.0000	0.0000	-0.4841	0.4495	-0.0224	677	1073	0.4966
3.2000	-1.0000	0.0000	-0.4848	0.4553	-0.0242	675	1070	0.5074
3.4000	-1.0000	0.0000	-0.4856	0.4592	-0.0247	673	1066	0.5174
3.5000	-1.0000	0.0000	-0.4859	0.4614	-0.0250	672	1064	0.5224
3.6000	-1.0000	0.0000	-0.4862	0.4614	-0.0244	671	1063	0.5275
3.8000	-1.0000	0.0000	-0.4869	0.4593	-0.0232	669	1060	0.5374
4.0000	-1.0000	0.0000	-0.4875	0.4594	-0.0215	667	1057	0.5466
4.2000	-1.0000	0.0000	-0.4880	0.4614	-0.0197	665	1054	0.5546
4.4000	-1.0000	0.0000	-0.4886	0.4609	-0.0171	663	1051	0.5632
4.6000	-1.0000	0.0000	-0.4891	0.4579	-0.0151	662	1049	0.5678
4.8000	-1.0000	0.0000	-0.4896	0.4556	-0.0132	660	1046	0.5695
5.0000	-1.0000	0.0000	-0.4901	0.4444	-0.0094	647	1025	0.5712
5.5000	-1.0000	0.0000	-0.4912	0.4143	-0.0005	618	980	0.5752
6.0000	-1.0000	0.0000	-0.4922	0.3849	0.0070	595	943	0.5788
6.5000	-1.0000	0.0000	-0.4932	0.3578	0.0139	577	914	0.5821
7.0000	-1.0000	0.0000	-0.4940	0.3284	0.0209	559	886	0.5852
7.5000	-1.0000	0.0000	-0.4948	0.2936	0.0272	539	855	0.5881
8.0000	-1.0000	0.0000	-0.4956	0.2618	0.0333	521	826	0.5907
8.5000	-1.0000	0.0000	-0.4963	0.2307	0.0399	505	800	0.5933
9.0000	-1.0000	0.0000	-0.4970	0.1929	0.0475	485	769	0.5956
9.5000	-1.0000	0.0000	-0.4976	0.1753	0.0508	480	760	0.5979
10.0000	-1.0000	0.0000	-0.4982	0.1662	0.0531	480	760	0.6000

Table A.6: N1 and N2 Model Coefficients.

Model	N1			N2		
Period (s)	f_3	f_4	f_5	f_3	f_4	f_5
0.0010	0.0916	-0.4482	-0.0018	0.0894	-0.4489	-0.0018
0.0067	0.0928	-0.4480	-0.0017	0.0869	-0.4470	-0.0017
0.0080	0.0898	-0.4379	-0.0016	0.0850	-0.4474	-0.0016
0.0100	0.0932	-0.4387	-0.0013	0.0752	-0.4375	-0.0013
0.0105	0.0920	-0.4361	-0.0012	0.0712	-0.4340	-0.0012
0.0111	0.0905	-0.4339	-0.0011	0.0681	-0.4311	-0.0011
0.0117	0.0902	-0.4336	-0.0011	0.0654	-0.4291	-0.0011
0.0125	0.0875	-0.4292	-0.0010	0.0624	-0.4273	-0.0010
0.0141	0.0846	-0.4260	-0.0009	0.0528	-0.4141	-0.0009
0.0162	0.0913	-0.4233	-0.0008	0.0501	-0.4083	-0.0008
0.0182	0.1078	-0.4216	-0.0009	0.0534	-0.4069	-0.0009
0.0200	0.1265	-0.4325	-0.0009	0.0566	-0.4151	-0.0010
0.0220	0.1567	-0.4551	-0.0010	0.0637	-0.4284	-0.0011
0.0250	0.1861	-0.4677	-0.0011	0.0744	-0.4483	-0.0011
0.0290	0.2217	-0.4851	-0.0012	0.0964	-0.4881	-0.0012
0.0300	0.2289	-0.4885	-0.0013	0.1036	-0.4987	-0.0013
0.0320	0.2434	-0.4934	-0.0014	0.1088	-0.4976	-0.0014
0.0350	0.2596	-0.5028	-0.0015	0.1101	-0.4921	-0.0015
0.0360	0.2627	-0.5033	-0.0015	0.1101	-0.4887	-0.0015
0.0400	0.2682	-0.4982	-0.0017	0.1184	-0.4873	-0.0017
0.0420	0.2862	-0.5109	-0.0017	0.1336	-0.5177	-0.0017
0.0440	0.3000	-0.5218	-0.0017	0.1500	-0.5504	-0.0017
0.0450	0.3000	-0.5210	-0.0017	0.1537	-0.5579	-0.0017
0.0460	0.3000	-0.5215	-0.0018	0.1546	-0.5601	-0.0018
0.0480	0.3000	-0.5216	-0.0018	0.1574	-0.5646	-0.0018
0.0500	0.3000	-0.5218	-0.0019	0.1678	-0.5807	-0.0019
0.0550	0.3000	-0.5198	-0.0020	0.1711	-0.5790	-0.0020
0.0600	0.3000	-0.5177	-0.0020	0.1884	-0.6000	-0.0021
0.0650	0.3000	-0.5103	-0.0022	0.1878	-0.5853	-0.0022
0.0667	0.3000	-0.5070	-0.0023	0.1834	-0.5702	-0.0023
0.0700	0.3000	-0.5014	-0.0024	0.1744	-0.5428	-0.0024
0.0750	0.2986	-0.4999	-0.0026	0.1739	-0.5365	-0.0026
0.0800	0.2865	-0.4871	-0.0027	0.1625	-0.5067	-0.0027
0.0850	0.2805	-0.4799	-0.0029	0.1633	-0.4993	-0.0029
0.0900	0.2920	-0.4896	-0.0030	0.1641	-0.4943	-0.0030
0.0950	0.2680	-0.4611	-0.0031	0.1529	-0.4621	-0.0032
0.1000	0.2546	-0.4415	-0.0033	0.1508	-0.4466	-0.0033
0.1100	0.2498	-0.4280	-0.0035	0.1436	-0.4261	-0.0036
0.1200	0.2280	-0.3993	-0.0037	0.1321	-0.3911	-0.0038

Table A.6 Continued.

Model	N1			N2		
Period (s)	f_3	f_4	f_5	f_3	f_4	f_5
0.1300	0.2077	-0.3761	-0.0038	0.1308	-0.3788	-0.0039
0.1333	0.2130	-0.3807	-0.0038	0.1322	-0.3775	-0.0039
0.1400	0.2182	-0.3866	-0.0039	0.1356	-0.3786	-0.0040
0.1500	0.2232	-0.3838	-0.0040	0.1427	-0.3826	-0.0041
0.1600	0.2062	-0.3662	-0.0040	0.1579	-0.4016	-0.0041
0.1700	0.1913	-0.3410	-0.0042	0.1504	-0.3775	-0.0043
0.1800	0.1976	-0.3427	-0.0044	0.1462	-0.3601	-0.0045
0.1900	0.1984	-0.3371	-0.0046	0.1385	-0.3352	-0.0047
0.2000	0.1850	-0.3163	-0.0048	0.1282	-0.3048	-0.0049
0.2200	0.1806	-0.3120	-0.0051	0.1254	-0.2849	-0.0052
0.2400	0.1880	-0.3129	-0.0054	0.1343	-0.2843	-0.0055
0.2500	0.1881	-0.3055	-0.0056	0.1329	-0.2751	-0.0056
0.2600	0.1861	-0.2956	-0.0058	0.1304	-0.2643	-0.0058
0.2800	0.1918	-0.2881	-0.0062	0.1347	-0.2502	-0.0062
0.2900	0.1977	-0.2865	-0.0064	0.1346	-0.2404	-0.0064
0.3000	0.1964	-0.2790	-0.0066	0.1307	-0.2283	-0.0065
0.3200	0.1733	-0.2437	-0.0070	0.1217	-0.2008	-0.0070
0.3400	0.1492	-0.2052	-0.0075	0.1144	-0.1750	-0.0075
0.3500	0.1368	-0.1872	-0.0077	0.1064	-0.1605	-0.0077
0.3600	0.1283	-0.1732	-0.0080	0.1023	-0.1499	-0.0079
0.3800	0.1139	-0.1477	-0.0084	0.0992	-0.1326	-0.0083
0.4000	0.1087	-0.1320	-0.0089	0.0941	-0.1159	-0.0087
0.4200	0.1110	-0.1256	-0.0093	0.0938	-0.1054	-0.0091
0.4400	0.1139	-0.1207	-0.0096	0.0936	-0.0968	-0.0094
0.4500	0.1141	-0.1172	-0.0098	0.0932	-0.0927	-0.0096
0.4600	0.1166	-0.1153	-0.0099	0.0961	-0.0908	-0.0097
0.4800	0.1121	-0.1046	-0.0103	0.0965	-0.0839	-0.0100
0.5000	0.1044	-0.0922	-0.0106	0.0989	-0.0779	-0.0103
0.5500	0.0776	-0.0597	-0.0117	0.0820	-0.0537	-0.0113
0.6000	0.0738	-0.0466	-0.0126	0.0759	-0.0401	-0.0122
0.6500	0.0643	-0.0340	-0.0136	0.0652	-0.0286	-0.0131
0.6667	0.0564	-0.0292	-0.0139	0.0584	-0.0247	-0.0134
0.7000	0.0397	-0.0202	-0.0147	0.0463	-0.0181	-0.0142
0.7500	0.0355	-0.0162	-0.0154	0.0610	-0.0178	-0.0146
0.8000	0.0336	-0.0128	-0.0162	0.0736	-0.0159	-0.0151
0.8500	0.0264	-0.0085	-0.0173	0.0668	-0.0114	-0.0161
0.9000	0.0171	-0.0052	-0.0185	0.0603	-0.0084	-0.0169
0.9500	0.0100	-0.0031	-0.0195	0.0548	-0.0063	-0.0177
1.0000	0.0100	-0.0027	-0.0200	0.0437	-0.0048	-0.0182

Table A.6 Continued.

Model	N1			N2		
Period (s)	f_3	f_4	f_5	f_3	f_4	f_5
1.1000	0.0227	-0.0039	-0.0194	0.0370	-0.0035	-0.0188
1.2000	0.0100	-0.0021	-0.0200	0.0310	-0.0022	-0.0199
1.3000	0.0100	-0.0019	-0.0200	0.0270	-0.0018	-0.0200
1.4000	0.0100	-0.0017	-0.0200	0.0124	-0.0012	-0.0200
1.5000	0.0100	-0.0015	-0.0200	0.0048	-0.0009	-0.0200
1.6000	0.0100	-0.0014	-0.0200	0.0032	-0.0008	-0.0196
1.7000	0.0100	-0.0013	-0.0200	0.0025	-0.0008	-0.0188
1.8000	0.0100	-0.0012	-0.0200	0.0015	-0.0012	-0.0162
1.9000	0.0100	-0.0011	-0.0200	0.0017	-0.0019	-0.0142
2.0000	0.0100	-0.0023	-0.0165	0.0016	-0.0024	-0.0130
2.2000	0.0100	-0.0056	-0.0117	0.0010	-0.0029	-0.0113
2.4000	0.0100	-0.0075	-0.0103	0.0013	-0.0033	-0.0108
2.5000	0.0100	-0.0085	-0.0097	0.0014	-0.0036	-0.0106
2.6000	0.0100	-0.0093	-0.0093	0.0012	-0.0036	-0.0104
2.8000	0.0100	-0.0099	-0.0094	0.0021	-0.0041	-0.0105
3.0000	0.0100	-0.0100	-0.0097	0.0075	-0.0063	-0.0104
3.2000	0.0100	-0.0095	-0.0101	0.0010	-0.0033	-0.0111
3.4000	0.0100	-0.0090	-0.0103	0.0015	-0.0032	-0.0115
3.5000	0.0100	-0.0091	-0.0102	0.0019	-0.0034	-0.0116
3.6000	0.0100	-0.0090	-0.0104	0.0024	-0.0036	-0.0117
3.8000	0.0100	-0.0085	-0.0107	0.0035	-0.0038	-0.0119
4.0000	0.0100	-0.0080	-0.0111	0.0027	-0.0033	-0.0122
4.2000	0.0100	-0.0077	-0.0114	0.0019	-0.0029	-0.0124
4.4000	0.0100	-0.0073	-0.0118	0.0016	-0.0027	-0.0126
4.6000	0.0100	-0.0066	-0.0122	0.0015	-0.0024	-0.0130
4.8000	0.0100	-0.0063	-0.0125	0.0019	-0.0024	-0.0132
5.0000	0.0100	-0.0061	-0.0128	0.0024	-0.0026	-0.0133
5.5000	0.0100	-0.0054	-0.0135	0.0048	-0.0029	-0.0135
6.0000	0.0100	-0.0048	-0.0141	0.0150	-0.0039	-0.0138
6.5000	0.0100	-0.0038	-0.0152	0.0212	-0.0041	-0.0141
7.0000	0.0100	-0.0032	-0.0159	0.0304	-0.0046	-0.0142
7.5000	0.0100	-0.0031	-0.0162	0.0422	-0.0054	-0.0142
8.0000	0.0100	-0.0031	-0.0164	0.0492	-0.0058	-0.0142
8.5000	0.0100	-0.0032	-0.0163	0.0543	-0.0061	-0.0142
9.0000	0.0100	-0.0034	-0.0163	0.0543	-0.0062	-0.0141
9.5000	0.0100	-0.0038	-0.0160	0.0542	-0.0063	-0.0141
10.0000	0.0100	-0.0042	-0.0158	0.0533	-0.0063	-0.0140

Table A.7: K1 Model Coefficients.

Period (s)	c_1	c_2	c_3	c_5	c_6	V_c (m/s)	V_L (m/s)	f_3	f_4	f_5	α
0.0010	-1.9113	0.0000	-1.8142	0.0000	-0.1414	1887	2990	0.180	-0.609	-0.001	0.0000
0.0067	-1.8663	0.0000	-1.7953	0.0000	-0.1420	1887	2990	0.183	-0.605	-0.001	0.0000
0.0080	-1.8334	0.0000	-1.7901	0.0000	-0.1423	1887	2990	0.195	-0.624	-0.001	0.0000
0.0100	-1.7010	0.0000	-1.6896	0.0134	-0.1429	1887	2990	0.157	-0.562	-0.001	0.0400
0.0105	-1.6837	0.0000	-1.6672	0.0027	-0.1432	1887	2990	0.133	-0.533	-0.001	0.0482
0.0111	-1.6555	0.0000	-1.6463	0.0115	-0.1435	1887	2990	0.128	-0.524	-0.001	0.1224
0.0117	-1.5949	-0.0603	-1.6411	0.0003	-0.1438	1887	2990	0.121	-0.512	-0.001	0.1500
0.0125	-1.6218	0.0000	-1.6202	-0.0073	-0.1447	1887	2990	0.114	-0.504	-0.001	0.0503
0.0141	-1.5500	0.0000	-1.5627	0.0219	-0.1473	1887	2990	0.097	-0.462	-0.001	0.0748
0.0162	-1.4898	0.0000	-1.5616	0.0283	-0.1551	1887	2990	0.102	-0.441	-0.001	0.0680
0.0182	-1.5245	0.0000	-1.6093	-0.0100	-0.1657	1887	2990	0.104	-0.438	-0.001	0.1500
0.0200	-1.5751	0.0000	-1.6702	-0.0100	-0.1764	1887	2990	0.110	-0.451	-0.001	0.1500
0.0220	-1.5882	0.0000	-1.7291	-0.0100	-0.1886	1887	2990	0.135	-0.456	-0.001	0.1500
0.0250	-1.7200	0.0000	-1.8376	-0.0100	-0.2044	1887	2990	0.149	-0.477	-0.001	0.0400
0.0290	-1.7746	0.0000	-1.9511	0.0416	-0.2202	1887	2990	0.285	-0.570	-0.001	0.0881
0.0300	-1.7938	0.0000	-1.9795	0.0534	-0.2229	1887	2990	0.344	-0.608	-0.001	0.0910
0.0320	-1.8349	0.0000	-1.9989	0.0782	-0.2282	1887	2990	0.361	-0.607	-0.001	0.0961
0.0350	-1.9226	0.0000	-2.0397	0.1059	-0.2339	1887	2990	0.332	-0.588	-0.001	0.1069
0.0360	-1.9220	0.0000	-2.0372	0.1118	-0.2350	1887	2990	0.349	-0.589	-0.001	0.1121
0.0400	-2.0093	0.0000	-2.1001	0.1341	-0.2407	1887	2990	0.429	-0.621	-0.002	0.1256
0.0420	-2.0684	0.0000	-2.1381	0.1396	-0.2422	1887	2990	0.437	-0.637	-0.002	0.1285
0.0440	-2.1131	0.0000	-2.1689	0.1420	-0.2442	1887	2990	0.450	-0.646	-0.001	0.1312
0.0450	-2.1272	0.0000	-2.1766	0.1416	-0.2448	1887	2990	0.450	-0.647	-0.001	0.1321
0.0460	-2.1491	0.0000	-2.1889	0.1400	-0.2448	1887	2990	0.450	-0.649	-0.001	0.1327
0.0480	-2.1673	0.0000	-2.1768	0.1360	-0.2445	1887	2990	0.450	-0.655	-0.002	0.1329
0.0500	-2.1839	0.0000	-2.1633	0.1331	-0.2439	1887	2990	0.450	-0.658	-0.002	0.1331
0.0550	-2.2227	0.0000	-2.1739	0.1290	-0.2400	1887	2990	0.450	-0.654	-0.002	0.1327
0.0600	-2.2581	-0.0265	-2.1947	0.1293	-0.2363	1887	2990	0.450	-0.660	-0.002	0.1307

Table A.7 Continued.

Period (s)	c_1	c_2	c_3	c_5	c_6	V_c (m/s)	V_L (m/s)	f_3	f_4	f_5	α
0.0650	-2.2907	-0.0005	-2.1681	0.1254	-0.2306	1887	2990	0.450	-0.648	-0.002	0.1278
0.0667	-2.3010	0.0000	-2.1683	0.1243	-0.2286	1887	2990	0.450	-0.645	-0.002	0.1279
0.0700	-2.3208	0.0000	-2.1754	0.1235	-0.2247	1887	2990	0.450	-0.637	-0.002	0.1284
0.0750	-2.3335	0.0000	-2.1659	0.1166	-0.2171	1887	2990	0.450	-0.633	-0.002	0.1291
0.0800	-2.3295	0.0000	-2.1408	0.1059	-0.2113	1887	2990	0.450	-0.626	-0.002	0.1303
0.0850	-2.3341	0.0000	-2.1168	0.0996	-0.2064	1887	2990	0.445	-0.626	-0.002	0.1312
0.0900	-2.3225	0.0000	-2.0828	0.0924	-0.2021	1887	2990	0.450	-0.628	-0.002	0.1304
0.0950	-2.2999	0.0000	-2.0328	0.0898	-0.1971	1887	2990	0.450	-0.614	-0.002	0.1294
0.1000	-2.2854	0.0000	-2.0005	0.0895	-0.1912	1870	2963	0.450	-0.599	-0.002	0.1291
0.1100	-2.3032	0.0000	-2.0539	0.0942	-0.1800	1720	2725	0.433	-0.581	-0.003	0.1300
0.1200	-2.2141	-0.2000	-2.1506	0.0986	-0.1715	1650	2615	0.419	-0.562	-0.003	0.1294
0.1300	-2.2801	-0.2000	-2.2821	0.1010	-0.1635	1521	2410	0.401	-0.540	-0.003	0.1312
0.1333	-2.4333	0.0000	-2.3104	0.1011	-0.1608	1441	2284	0.409	-0.540	-0.003	0.1317
0.1400	-2.4558	0.0000	-2.3681	0.1027	-0.1558	1371	2173	0.403	-0.533	-0.003	0.1326
0.1500	-2.5122	0.0000	-2.4776	0.1029	-0.1505	1289	2042	0.394	-0.529	-0.003	0.1323
0.1600	-2.5645	0.0000	-2.5586	0.1002	-0.1462	1229	1948	0.386	-0.524	-0.003	0.1323
0.1700	-2.6038	0.0000	-2.6226	0.0985	-0.1419	1161	1839	0.325	-0.468	-0.003	0.1323
0.1800	-2.6182	0.0000	-2.6867	0.0960	-0.1370	1105	1751	0.342	-0.468	-0.004	0.1322
0.1900	-2.6384	0.0000	-2.7546	0.0958	-0.1326	1064	1686	0.358	-0.470	-0.004	0.1321
0.2000	-2.6615	0.0000	-2.8131	0.0954	-0.1278	1025	1625	0.354	-0.452	-0.004	0.1329
0.2200	-2.4502	-0.4008	-2.9446	0.0962	-0.1208	988	1565	0.347	-0.451	-0.004	0.1380
0.2400	-2.0830	-0.9837	-3.0496	0.0999	-0.1148	979	1552	0.336	-0.443	-0.005	0.1404
0.2500	-2.1000	-0.9910	-3.0833	0.1013	-0.1127	951	1507	0.331	-0.431	-0.005	0.1416
0.2600	-2.0785	-1.0516	-3.1377	0.1010	-0.1101	923	1463	0.326	-0.422	-0.005	0.1426
0.2800	-2.0378	-1.2229	-3.3062	0.0987	-0.1051	879	1393	0.317	-0.406	-0.005	0.1414
0.2900	-2.0186	-1.3110	-3.4209	0.0970	-0.1036	858	1360	0.313	-0.393	-0.005	0.1411
0.3000	-2.0000	-1.3961	-3.5063	0.0960	-0.1027	843	1336	0.309	-0.391	-0.005	0.1414
0.3200	-1.9581	-1.3131	-3.3608	0.1023	-0.0975	802	1316	0.301	-0.361	-0.006	0.1466

Table A.7 Continued.

Period (s)	c_1	c_2	c_3	c_5	c_6	V_c (m/s)	V_L (m/s)	f_3	f_4	f_5	α
0.3400	-1.9188	-1.3697	-3.5115	0.1046	-0.0935	752	1274	0.293	-0.325	-0.006	0.1490
0.3500	-1.9000	-1.4067	-3.5836	0.1065	-0.0918	733	1261	0.290	-0.311	-0.006	0.1503
0.3600	-1.8789	-1.4389	-3.7046	0.1072	-0.0899	705	1252	0.286	-0.296	-0.006	0.1521
0.3800	-2.0979	-0.9971	-3.9367	0.1082	-0.0845	608	1174	0.279	-0.271	-0.007	0.1580
0.4000	-2.0693	-0.9399	-4.1570	0.1112	-0.0793	552	1153	0.273	-0.259	-0.007	0.1689
0.4200	-1.8969	-0.9626	-4.6474	0.1172	-0.0725	473	1195	0.267	-0.247	-0.007	0.1900
0.4400	-1.9604	-0.9842	-5.1150	0.0968	-0.0753	423	1135	0.175	-0.167	-0.008	0.1509
0.4500	-1.8523	-0.9946	-5.3409	0.1242	-0.0653	411	1164	0.259	-0.235	-0.008	0.2000
0.4600	-1.8202	-1.0721	-5.4877	0.1269	-0.0630	400	1156	0.256	-0.228	-0.008	0.2000
0.4800	-1.7730	-1.2223	-5.7720	0.1340	-0.0588	380	1141	0.251	-0.214	-0.008	0.2000
0.5000	-1.7282	-1.3663	-6.0447	0.1432	-0.0542	364	1126	0.246	-0.197	-0.009	0.2000
0.5500	-1.6478	-1.6409	-8.0519	0.1739	-0.0367	276	1101	0.094	-0.099	-0.010	0.2312
0.6000	-1.6512	-1.7561	-9.2755	0.1936	-0.0231	236	1059	0.044	-0.068	-0.010	0.2455
0.6500	-1.6084	-1.7632	-9.5141	0.2025	-0.0143	226	1034	0.037	-0.052	-0.011	0.2500
0.6667	-1.5829	-1.7241	-9.3736	0.2054	-0.0115	225	1029	0.034	-0.047	-0.011	0.2500
0.7000	-1.5715	-1.6487	-9.2105	0.2124	-0.0068	223	1019	0.029	-0.041	-0.011	0.2500
0.7500	-1.4844	-1.5192	-8.4710	0.2347	0.0078	221	1008	0.022	-0.036	-0.011	0.2758
0.8000	-1.4395	-1.3981	-7.1177	0.2540	0.0208	219	999	0.016	-0.032	-0.011	0.3000
0.8500	-1.2696	-1.0033	-3.4869	0.2730	0.0278	339	1086	0.011	-0.030	-0.010	0.3000
0.9000	-1.0000	-0.6312	-0.0637	0.2729	0.0265	555	1169	0.010	-0.028	-0.012	0.3000
0.9500	-1.0000	-0.7212	0.0470	0.2548	0.0420	476	962	0.010	-0.003	-0.020	0.2611
1.0000	-1.0000	-0.6569	0.1420	0.2448	0.0420	466	951	0.010	-0.003	-0.020	0.3000
1.1000	-1.0000	-0.5594	0.1190	0.2448	0.0420	471	940	0.010	-0.002	-0.020	0.3000
1.2000	-1.0000	-0.4703	0.0979	0.2448	0.0420	475	930	0.010	-0.002	-0.020	0.3000
1.3000	-1.0000	-0.3884	0.0786	0.2448	0.0420	480	920	0.010	-0.002	-0.020	0.3000
1.4000	-1.0000	-0.3126	0.0606	0.2448	0.0420	484	912	0.010	-0.002	-0.020	0.3000
1.5000	-1.0000	-0.2419	0.0440	0.2448	0.0420	487	904	0.010	-0.002	-0.020	0.3000
1.6000	-1.0000	-0.1759	0.0284	0.2448	0.0420	491	896	0.010	-0.001	-0.020	0.3000

Table A.7 Continued.

Period (s)	c_1	c_2	c_3	c_5	c_6	V_c (m/s)	V_L (m/s)	f_3	f_4	f_5	α
1.7000	-1.0000	-0.1138	0.0137	0.2448	0.0420	494	889	0.010	-0.001	-0.020	0.3000
1.8000	-1.0000	-0.0553	-0.0001	0.2448	0.0420	497	883	0.010	-0.001	-0.020	0.3000
1.9000	-1.0000	0.0000	-0.0132	0.2448	0.0420	500	876	0.010	-0.001	-0.020	0.3000
2.0000	-1.0000	0.0000	-0.1402	0.2566	0.0259	584	925	0.010	-0.026	-0.010	0.4000
2.2000	-1.0000	0.0000	-0.2210	0.2908	0.0101	618	980	0.010	-0.029	-0.010	0.4353
2.4000	-1.0000	0.0000	-0.2948	0.3355	-0.0060	659	1045	0.010	-0.031	-0.010	0.4674
2.5000	-1.0000	0.0000	-0.2558	0.3480	-0.0095	661	1048	0.010	-0.008	-0.010	0.4786
2.6000	-1.0000	0.0000	-0.2876	0.3600	-0.0129	664	1052	0.010	-0.009	-0.009	0.4893
2.8000	-1.0000	0.0000	-0.3476	0.3826	-0.0193	668	1058	0.010	-0.010	-0.009	0.5096
3.0000	-1.0000	0.0000	-0.4034	0.4036	-0.0252	669	1060	0.010	-0.010	-0.010	0.5284
3.2000	-1.0772	0.0000	-0.4848	0.4233	-0.0308	675	1070	0.010	-0.038	-0.010	0.5461
3.4000	-1.0841	0.0000	-0.4856	0.4311	-0.0314	673	1066	0.010	-0.039	-0.010	0.5552
3.5000	-1.0826	0.0000	-0.4859	0.4338	-0.0314	672	1064	0.010	-0.039	-0.010	0.5564
3.6000	-1.0776	0.0000	-0.4862	0.4321	-0.0300	671	1063	0.010	-0.039	-0.010	0.5576
3.8000	-1.0664	0.0000	-0.4869	0.4241	-0.0259	669	1060	0.010	-0.041	-0.010	0.5598
4.0000	-1.0533	0.0000	-0.4875	0.4160	-0.0207	667	1057	0.010	-0.041	-0.010	0.5619
4.2000	-1.0328	0.0000	-0.4880	0.4055	-0.0138	665	1054	0.010	-0.042	-0.010	0.5640
4.4000	-1.0080	0.0000	-0.4886	0.3895	-0.0055	663	1051	0.010	-0.043	-0.010	0.5659
4.6000	-1.0000	0.0000	-0.4891	0.3798	-0.0011	662	1049	0.010	-0.044	-0.010	0.5678
4.8000	-1.0000	0.0000	-0.4896	0.3755	0.0012	660	1046	0.010	-0.046	-0.010	0.5695
5.0000	-1.0000	0.0000	-0.4901	0.3614	0.0056	646	1024	0.010	-0.048	-0.010	0.5712
5.5000	-1.0000	0.0000	-0.4912	0.3166	0.0181	610	966	0.010	-0.053	-0.010	0.5752
6.0000	-1.0000	0.0000	-0.4922	0.2717	0.0289	580	919	0.010	-0.059	-0.010	0.5788
6.5000	-1.0000	0.0000	-0.4932	0.2325	0.0381	555	880	0.010	-0.064	-0.010	0.5821
7.0000	-1.0000	0.0000	-0.4940	0.1931	0.0468	533	844	0.010	-0.070	-0.010	0.5852
7.5000	-1.0000	0.0000	-0.4948	0.1500	0.0545	509	807	0.010	-0.078	-0.010	0.5881
8.0000	-1.0000	0.0000	-0.4956	0.1500	0.0531	510	809	0.010	-0.084	-0.010	0.5907
8.5000	-1.0000	0.0000	-0.4963	0.1500	0.0528	512	811	0.010	-0.092	-0.010	0.5933

Table A.7 Continued.

Period (s)	c_1	c_2	c_3	c_5	c_6	V_c (m/s)	V_L (m/s)	f_3	f_4	f_5	α
9.0000	-1.0000	0.0000	-0.4970	0.1500	0.0527	514	814	0.010	-0.099	-0.010	0.5956
9.5000	-1.0000	0.0000	-0.4976	0.1500	0.0530	515	816	0.010	-0.108	-0.010	0.5979
10.0000	-1.0000	0.0000	-0.4982	0.1500	0.0538	516	818	0.010	-0.118	-0.010	0.6000

Table A.8: K2 Model Coefficients.

Period (s)	c_1	c_2	c_3	c_5	c_6	V_C (m/s)	V_L (m/s)	f_3	f_4	f_5	α
0.0010	-1.9077	0.0000	-1.8127	0.0000	-0.1414	1887	2990	1887	2990	0.00	0.0000
0.0067	-1.8546	0.0000	-1.7906	0.0000	-0.1420	1887	2990	1887	2990	0.00	0.0000
0.0080	-1.8133	0.0000	-1.7794	0.0000	-0.1423	1887	2990	1887	2990	0.00	0.0000
0.0100	-1.6554	0.0000	-1.6537	0.0133	-0.1429	1887	2990	1887	2990	0.00	0.0400
0.0105	-1.6225	0.0000	-1.6201	0.0026	-0.1432	1887	2990	1887	2990	0.00	0.0480
0.0111	-1.5906	0.0000	-1.5994	0.0115	-0.1435	1887	2990	1887	2990	0.00	0.1226
0.0117	-1.5223	-0.0679	-1.5901	-0.0009	-0.1439	1887	2990	1887	2990	0.00	0.0653
0.0125	-1.5493	0.0000	-1.5701	-0.0072	-0.1449	1887	2990	1887	2990	0.00	0.0503
0.0141	-1.4517	0.0000	-1.5039	0.0220	-0.1475	1887	2990	1887	2990	0.00	0.0748
0.0162	-1.4175	-0.0071	-1.5616	0.0252	-0.1548	1887	2990	1887	2990	0.00	0.0618
0.0182	-1.4820	0.0000	-1.6093	-0.0100	-0.1654	1887	2990	1887	2990	0.00	0.1500
0.0200	-1.5719	0.0000	-1.6491	-0.0100	-0.1764	1887	2990	1887	2990	0.00	0.1500
0.0220	-1.5499	0.0000	-1.7059	-0.0100	-0.1886	1887	2990	1887	2990	0.00	0.1500
0.0250	-1.6762	-0.0378	-1.8286	-0.0100	-0.2042	1887	2990	1887	2990	0.00	0.0400
0.0290	-1.7394	0.0000	-1.9593	0.0399	-0.2202	1887	2990	1887	2990	0.00	0.0874
0.0300	-1.7595	0.0000	-1.9861	0.0519	-0.2228	1887	2990	1887	2990	0.00	0.0903
0.0320	-1.8041	0.0000	-2.0086	0.0770	-0.2281	1887	2990	1887	2990	0.00	0.0954
0.0350	-1.8895	0.0000	-2.0546	0.1046	-0.2338	1887	2990	1887	2990	0.00	0.1058
0.0360	-1.8938	0.0000	-2.0523	0.1106	-0.2350	1887	2990	1887	2990	0.00	0.1111
0.0400	-1.9720	0.0000	-2.1208	0.1322	-0.2406	1887	2990	1887	2990	0.00	0.1247
0.0420	-2.0351	0.0000	-2.1568	0.1379	-0.2420	1887	2990	1887	2990	0.00	0.1277
0.0440	-2.0691	0.0000	-2.1877	0.1404	-0.2437	1887	2990	1887	2990	0.00	0.1306
0.0450	-2.0899	0.0000	-2.1947	0.1402	-0.2444	1887	2990	1887	2990	0.00	0.1316
0.0460	-2.1125	0.0000	-2.2066	0.1387	-0.2445	1887	2990	1887	2990	0.00	0.1323
0.0480	-2.1586	0.0000	-2.2129	0.1352	-0.2444	1887	2990	1887	2990	0.00	0.1327
0.0500	-2.1788	0.0000	-2.2334	0.1330	-0.2436	1887	2990	1887	2990	0.00	0.1335
0.0550	-2.2227	0.0000	-2.2471	0.1295	-0.2397	1887	2990	1887	2990	0.00	0.1333
0.0600	-2.2512	0.0000	-2.2600	0.1301	-0.2358	1887	2990	1887	2990	0.00	0.1315

Table A.8 Continued.

Period (s)	c_1	c_2	c_3	c_5	c_6	V_C (m/s)	V_L (m/s)	f_3	f_4	f_5	α
0.0650	-2.2796	0.0000	-2.2470	0.1262	-0.2302	1887	2990	1887	2990	0.00	0.1288
0.0667	-2.2903	0.0000	-2.2384	0.1249	-0.2282	1887	2990	1887	2990	0.00	0.1287
0.0700	-2.2938	0.0000	-2.2055	0.1237	-0.2243	1887	2990	1887	2990	0.00	0.1288
0.0750	-2.3165	0.0000	-2.1923	0.1168	-0.2166	1887	2990	1887	2990	0.00	0.1295
0.0800	-2.3201	0.0000	-2.1581	0.1061	-0.2107	1887	2990	1887	2990	0.00	0.1305
0.0850	-2.3217	0.0000	-2.1336	0.0998	-0.2059	1887	2990	1887	2990	0.00	0.1314
0.0900	-2.3120	0.0000	-2.1075	0.0928	-0.2018	1887	2990	1887	2990	0.00	0.1307
0.0950	-2.2978	0.0000	-2.0527	0.0899	-0.1968	1887	2990	1887	2990	0.00	0.1295
0.1000	-2.2745	0.0000	-2.0060	0.0895	-0.1907	1877	2976	1877	2976	0.00	0.1290
0.1100	-2.3112	0.0000	-2.0503	0.0940	-0.1793	1714	2717	1714	2717	0.00	0.1299
0.1200	-2.2183	-0.2000	-2.1403	0.0983	-0.1707	1644	2606	1644	2606	0.00	0.1293
0.1300	-2.2864	-0.2000	-2.2712	0.1006	-0.1630	1513	2399	1513	2399	0.00	0.1310
0.1333	-2.4382	0.0000	-2.2996	0.1008	-0.1604	1436	2276	1436	2276	0.00	0.1315
0.1400	-2.4550	0.0000	-2.3643	0.1024	-0.1551	1368	2169	1368	2169	0.00	0.1325
0.1500	-2.5074	0.0000	-2.4720	0.1026	-0.1496	1286	2039	1286	2039	0.00	0.1322
0.1600	-2.5476	0.0000	-2.5593	0.1000	-0.1453	1229	1948	1229	1948	0.00	0.1323
0.1700	-2.6018	0.0000	-2.6036	0.0981	-0.1410	1158	1835	1158	1835	0.00	0.1321
0.1800	-2.6173	0.0000	-2.6614	0.0957	-0.1363	1103	1748	1103	1748	0.00	0.1320
0.1900	-2.6302	0.0000	-2.7297	0.0957	-0.1319	1064	1686	1064	1686	0.00	0.1320
0.2000	-2.6531	0.0000	-2.7721	0.0953	-0.1273	1025	1625	1025	1625	0.00	0.1329
0.2200	-2.4266	-0.4008	-2.9126	0.0966	-0.1205	991	1570	991	1570	0.00	0.1381
0.2400	-2.0830	-0.9489	-3.0113	0.1002	-0.1147	979	1552	979	1552	0.00	0.1405
0.2500	-2.1000	-0.9416	-3.0738	0.1018	-0.1126	951	1507	951	1507	0.00	0.1419
0.2600	-2.0785	-1.0368	-3.1762	0.1006	-0.1103	921	1459	921	1459	0.00	0.1421
0.2800	-2.0378	-1.2229	-3.3595	0.0978	-0.1055	876	1388	876	1388	-0.01	0.1406
0.2900	-2.0186	-1.3110	-3.5045	0.0958	-0.1042	854	1354	854	1354	-0.01	0.1400
0.3000	-2.0000	-1.3961	-3.5674	0.0947	-0.1034	839	1329	839	1329	-0.01	0.1403
0.3200	-1.9581	-1.2675	-3.3608	0.1018	-0.0977	800	1312	800	1312	-0.01	0.1463

Table A.8 Continued.

Period (s)	c_1	c_2	c_3	c_5	c_6	V_C (m/s)	V_L (m/s)	f_3	f_4	f_5	α
0.3400	-1.9188	-1.3328	-3.5115	0.1039	-0.0935	750	1270	750	1270	-0.01	0.1487
0.3500	-1.9000	-1.3669	-3.5836	0.1062	-0.0917	732	1259	732	1259	-0.01	0.1504
0.3600	-1.8789	-1.3961	-3.7046	0.1075	-0.0898	705	1252	705	1252	-0.01	0.1526
0.3800	-2.0841	-0.9971	-3.9367	0.1083	-0.0845	611	1176	611	1176	-0.01	0.1581
0. 4000	-2.0558	-0.9399	-4.1570	0.1110	-0.0795	553	1154	553	1154	-0.01	0.1687
0.4200	-1.8821	-0.9626	-4.6474	0.1168	-0.0730	473	1198	473	1198	-0.01	0.1895
0.4400	-1.8568	-0.9842	-5.1150	0.1194	-0.0685	429	1175	429	1175	-0.01	0.1978
0.4500	-1.8359	-0.9946	-5.3409	0.1232	-0.0660	405	1164	405	1164	-0.01	0.2000
0.4600	-1.8062	-1.0721	-5.4877	0.1260	-0.0636	395	1156	395	1156	-0.01	0.2000
0.4800	-1.7661	-1.2223	-5.7720	0.1334	-0.0594	376	1141	376	1141	-0.01	0.2000
0.5000	-1.7298	-1.3663	-6.0447	0.1439	-0.0547	352	1126	352	1126	-0.01	0.2000
0.5500	-1.6633	-1.6409	-6.7116	0.1788	-0.0367	276	1101	276	1101	-0.01	0.2313
0.6000	-1.6440	-1.7561	-8.1547	0.1946	-0.0235	236	1059	236	1059	-0.01	0.2440
0.6500	-1.5931	-1.7632	-8.0195	0.2032	-0.0146	226	1034	226	1034	-0.01	0.2500
0.6667	-1.5673	-1.7241	-7.8592	0.2060	-0.0118	225	1029	225	1029	-0.01	0.2500
0.7000	-1.5590	-1.6487	-7.5614	0.2136	-0.0070	223	1019	223	1019	-0.01	0.2500
0.7500	-1.4712	-1.5192	-6.5529	0.2361	0.0078	221	1008	221	1008	-0.01	0.2758
0.8000	-1.4152	-1.3981	-6.0251	0.2536	0.0206	219	999	219	999	-0.01	0.3000
0.8500	-1.2258	-1.0033	-3.1844	0.2686	0.0271	339	1086	339	1086	-0.01	0.3000
0.9000	-1.0000	-0.6312	-0.0637	0.2691	0.0260	510	1169	510	1169	-0.01	0.3000
0.9500	-1.0000	-0.7212	0.0470	0.2548	0.0420	476	962	476	962	-0.02	0.2611
1.0000	-1.0000	-0.6569	0.1420	0.2448	0.0420	466	951	466	951	-0.02	0.3000
1.1000	-1.0000	-0.5594	0.1190	0.2448	0.0420	471	940	471	940	-0.02	0.3000
1.2000	-1.0000	-0.4703	0.0979	0.2448	0.0420	475	930	475	930	-0.02	0.3000
1.3000	-1.0000	-0.3884	0.0786	0.2448	0.0420	480	920	480	920	-0.02	0.3000
1.4000	-1.0000	-0.3126	0.0606	0.2448	0.0420	484	912	484	912	-0.02	0.3000
1.5000	-1.0000	-0.2419	0.0440	0.2448	0.0420	487	904	487	904	-0.02	0.3000
1.6000	-1.0000	-0.1759	0.0284	0.2448	0.0420	491	896	491	896	-0.02	0.3000

Table A.8 Continued.

Period (s)	c_1	c_2	c_3	c_5	c_6	V_C (m/s)	V_L (m/s)	f_3	f_4	f_5	α
1.7000	-1.0000	-0.1138	0.0137	0.2448	0.0420	494	889	494	889	-0.02	0.3000
1.8000	-1.0000	-0.0553	-0.0001	0.2448	0.0420	497	883	497	883	-0.02	0.3000
1.9000	-1.0000	0.0000	-0.0132	0.2448	0.0420	500	876	500	876	-0.01	0.3000
2.0000	-1.0000	0.0000	-0.1402	0.2580	0.0251	579	917	579	917	-0.01	0.4000
2.2000	-1.0000	0.0000	-0.2210	0.2926	0.0089	613	971	613	971	-0.01	0.4353
2.4000	-1.0000	0.0000	-0.2948	0.3385	-0.0079	653	1035	653	1035	-0.01	0.4674
2.5000	-1.0000	0.0000	-0.3294	0.3631	-0.0152	672	1065	672	1065	-0.01	0.4826
2.6000	-1.0000	0.0000	-0.3627	0.3765	-0.0184	673	1067	673	1067	-0.01	0.4971
2.8000	-1.0000	0.0000	-0.4256	0.3937	-0.0225	675	1070	675	1070	-0.01	0.5135
3.0000	-1.0239	0.0000	-0.4841	0.4079	-0.0268	677	1073	677	1073	-0.01	0.5272
3.2000	-1.0405	0.0000	-0.4848	0.4187	-0.0297	675	1070	675	1070	-0.01	0.5388
3.4000	-1.0561	0.0000	-0.4856	0.4281	-0.0306	673	1066	673	1066	-0.01	0.5505
3.5000	-1.0546	0.0000	-0.4859	0.4301	-0.0300	672	1064	672	1064	-0.01	0.5558
3.6000	-1.0505	0.0000	-0.4862	0.4285	-0.0285	671	1063	671	1063	-0.01	0.5576
3.8000	-1.0244	0.0000	-0.4869	0.4182	-0.0237	669	1060	669	1060	-0.01	0.5598
4.0000	-1.0059	0.0000	-0.4875	0.4089	-0.0181	667	1057	667	1057	-0.01	0.5619
4.2000	-1.0000	0.0000	-0.4880	0.4068	-0.0144	665	1054	665	1054	-0.01	0.5640
4.4000	-1.0000	0.0000	-0.4886	0.4041	-0.0107	663	1051	663	1051	-0.01	0.5659
4.6000	-1.0000	0.0000	-0.4891	0.3981	-0.0074	662	1049	662	1049	-0.01	0.5678
4.8000	-1.0000	0.0000	-0.4896	0.3941	-0.0050	660	1046	660	1046	-0.01	0.5695
5.0000	-1.0000	0.0000	-0.4901	0.3869	-0.0023	654	1036	654	1036	-0.01	0.5712
5.5000	-1.0000	0.0000	-0.4912	0.3300	0.0148	609	966	609	966	-0.01	0.5752
6.0000	-1.0000	0.0000	-0.4922	0.2681	0.0313	570	904	570	904	-0.01	0.5788
6.5000	-1.0000	0.0000	-0.4932	0.1945	0.0505	528	837	528	837	-0.01	0.5821
7.0000	-1.0000	0.0000	-0.4940	0.1500	0.0612	504	800	504	800	-0.01	0.5852
7.5000	-1.0000	0.0000	-0.4948	0.1500	0.0581	504	798	504	798	-0.01	0.5881
8.0000	-1.0000	0.0000	-0.4956	0.1500	0.0574	505	800	505	800	-0.01	0.5907
8.5000	-1.0000	0.0000	-0.4963	0.1500	0.0572	506	803	506	803	-0.01	0.5933

Table A.8 Continued.

Period (s)	c_1	c_2	c_3	c_5	c_6	V_C (m/s)	V_L (m/s)	f_3	f_4	f_5	α
9.0000	-1.0000	0.0000	-0.4970	0.1500	0.0569	508	806	508	806	-0.01	0.5956
9.5000	-1.0000	0.0000	-0.4976	0.1591	0.0453	502	796	502	796	-0.01	0.5979
10.0000	-1.0000	0.0000	-0.4982	0.1500	0.0580	511	809	511	809	-0.01	0.6000

\

Table A.9: FAS Nonlinear Amplification coefficients.

Frequency	f_3	f_4	f_5
0.1000	1.0000	-1.00E-04	-1.00E-04
0.1053	1.0000	-1.00E-04	-1.00E-04
0.1111	1.0000	-1.00E-04	-1.00E-04
0.1176	1.0000	-1.00E-04	-1.00E-04
0.1250	1.0000	-1.00E-04	-1.00E-04
0.1333	1.0000	-1.00E-04	-1.00E-04
0.1429	1.0000	-1.00E-04	-1.00E-04
0.1538	1.0000	-1.00E-04	-1.00E-04
0.1667	1.0000	-1.00E-04	-1.00E-04
0.1818	1.0000	-1.00E-04	-1.00E-04
0.2000	1.0000	-1.00E-04	-1.00E-04
0.2083	1.0000	-1.00E-04	-1.00E-04
0.2174	1.0000	-1.00E-04	-1.00E-04
0.2273	1.0000	-1.00E-04	-1.00E-04
0.2381	1.0000	-1.00E-04	-1.00E-04
0.2500	1.0000	-1.00E-04	-1.00E-04
0.2632	1.0000	-1.00E-04	-1.00E-04
0.2778	1.0000	-1.00E-04	-1.00E-04
0.2857	1.0000	-1.00E-04	-1.00E-04
0.2941	1.0000	-1.00E-04	-1.00E-04
0.3125	1.0000	-1.00E-04	-1.00E-04
0.3333	1.0000	-1.00E-04	-1.00E-04
0.3571	1.0000	-1.00E-04	-1.00E-04
0.3846	1.0000	-1.00E-04	-1.00E-04
0.4000	1.0000	-1.00E-04	-1.00E-04
0.4167	1.0000	-1.00E-04	-1.00E-04
0.4545	1.0000	-1.00E-04	-1.00E-04
0.5000	1.0000	-1.00E-04	-1.00E-04
0.5263	1.0000	-1.00E-04	-1.00E-04
0.5556	1.0000	-1.00E-04	-1.00E-04
0.5882	1.0000	-1.00E-04	-1.00E-04
0.6250	1.0000	-1.00E-04	-1.00E-04
0.6667	1.0000	-1.00E-04	-1.00E-04
0.7143	1.0000	-1.00E-04	-1.00E-04
0.7692	1.0000	-1.00E-04	-1.00E-04
0.8333	1.0000	-0.0082	-0.0200
0.9091	0.1491	-0.0030	-0.0200
1.0000	0.0522	-0.0022	-0.0200
1.0526	0.0532	-0.0024	-0.0200
1.1111	0.0818	-0.0035	-0.0200
1.1765	0.1057	-0.0045	-0.0200

Table A.9 Continued.

Frequency	f_3	f_4	f_5
1.2500	0.0994	-0.0048	-0.0200
1.3333	0.0981	-0.0063	-0.0193
1.4286	0.0530	-0.0067	-0.0181
1.5000	0.0481	-0.0087	-0.0170
1.5385	0.0561	-0.0110	-0.0163
1.6667	0.0395	-0.0309	-0.0100
1.8182	0.1070	-0.0366	-0.0130
2.0000	0.1296	-0.0564	-0.0117
2.0833	0.1403	-0.0658	-0.0112
2.1739	0.1306	-0.0684	-0.0110
2.2222	0.1329	-0.0755	-0.0106
2.2727	0.1504	-0.0885	-0.0103
2.3810	0.1516	-0.0996	-0.0099
2.5000	0.1450	-0.1065	-0.0096
2.6316	0.1439	-0.1264	-0.0090
2.7778	0.1715	-0.1577	-0.0085
2.8571	0.1723	-0.1672	-0.0082
2.9412	0.1571	-0.1595	-0.0081
3.1250	0.1397	-0.1694	-0.0075
3.3333	0.1611	-0.2107	-0.0068
3.4483	0.1903	-0.2479	-0.0065
3.5714	0.1893	-0.2599	-0.0063
3.8462	0.1968	-0.2794	-0.0060
4.0000	0.1867	-0.2703	-0.0058
4.1667	0.2106	-0.3039	-0.0055
4.5455	0.2023	-0.3012	-0.0051
5.0000	0.1892	-0.3118	-0.0049
5.2632	0.1972	-0.3388	-0.0046
5.5556	0.2279	-0.3943	-0.0045
5.8824	0.2457	-0.4300	-0.0044
6.2500	0.2471	-0.4284	-0.0043
6.6667	0.1898	-0.3580	-0.0044
7.1429	0.1705	-0.3406	-0.0044
7.5000	0.1739	-0.3519	-0.0043
7.6923	0.1664	-0.3456	-0.0042
8.3333	0.1601	-0.3504	-0.0040
9.0909	0.1989	-0.4178	-0.0036
10.0000	0.2079	-0.4268	-0.0033
10.5263	0.2093	-0.4369	-0.0031
11.1111	0.2186	-0.4694	-0.0028
11.7647	0.2336	-0.5003	-0.0026

Table A.9 Continued.

Frequency	f_3	f_4	f_5
12.5000	0.2334	-0.5032	-0.0023
13.3333	0.2425	-0.5127	-0.0022
14.2857	0.2595	-0.5368	-0.0018
14.9999	0.2627	-0.5587	-0.0016
15.3846	0.2707	-0.5784	-0.0015
16.6667	0.2527	-0.5568	-0.0014
18.1818	0.2421	-0.5458	-0.0011
20.0000	0.2766	-0.6276	-0.0008
20.8333	0.2938	-0.6981	-0.0006
21.7391	0.2818	-0.8361	-0.0004
22.2222	0.2851	-1.0000	-0.0003
22.7273	0.2704	-1.0000	-0.0002
23.8095	0.2520	-1.0000	-0.0002
25.0000	0.2383	-1.0000	-0.0002
27.7778	0.2668	-1.0000	-0.0002
28.5714	0.2896	-1.0000	-0.0002
31.2500	0.3819	-1.0000	-0.0002
33.3333	0.4655	-1.0000	-0.0002

Table A.10: FAS Linear Amp. Look-up Table for 0.100 Hz.

V_{S30} (m/s)	Soil Depth (m)										
	0	5	10	15	20	25	30	50	100	500	1000
95.6	NA	NA	NA	NA	NA	NA	0.01306	0.02287	0.04225	0.35644	1.2251
107.9	NA	NA	NA	NA	NA	0.01042	0.01115	0.01947	0.03616	0.29747	0.98087
121.8	NA	NA	NA	NA	0.00809	0.0089	0.00859	0.01497	0.02768	0.22423	0.68814
137.4	NA	NA	NA	NA	0.00692	0.00681	0.00675	0.01172	0.0222	0.18741	0.57896
155.1	NA	NA	NA	0.00547	0.0053	0.0054	0.0055	0.00999	0.02131	0.22253	0.7828
175	NA	NA	NA	0.00425	0.00424	0.00423	0.0041	0.00716	0.01442	0.1357	0.42024
197.5	NA	NA	0.00357	0.00342	0.00331	0.00318	0.00333	0.0063	0.01521	0.17729	0.60195
222.9	NA	NA	0.0029	0.00271	0.00256	0.00256	0.00269	0.00509	0.0123	0.1442	0.4574
251.5	NA	NA	0.00221	0.00207	0.00201	0.002	0.00206	0.00405	0.01043	0.12589	0.39904
283.9	NA	NA	0.00173	0.00157	0.00159	0.00155	0.00166	0.00342	0.00928	0.11677	0.36906
320.4	NA	0.00109	0.00131	0.00122	0.00119	0.00122	0.00133	0.00278	0.00779	0.10213	0.323
361.5	NA	0.00092	0.00099	0.00092	0.00093	0.00099	0.00102	0.00223	0.00646	0.08499	0.26403
408	NA	0.0007	0.00075	0.0007	0.00073	0.00075	0.00077	0.00163	0.0046	0.06134	0.19006
460.4	NA	0.00055	0.00055	0.00054	0.00055	0.00058	0.00059	0.00123	0.00337	0.04598	0.14465
519.6	NA	0.0004	0.00041	0.00039	0.00043	0.00044	0.00047	0.00097	0.00266	0.03684	0.11605
586.4	NA	0.0003	0.00029	0.0003	0.00033	0.00034	0.00035	0.00073	0.00196	0.02753	0.08752
661.8	NA	0.00021	0.00021	0.00023	0.00024	0.00025	0.00026	0.00053	0.00141	0.01998	0.06314
746.8	NA	0.00015	0.00016	0.00017	0.00017	0.00019	0.00019	0.00039	0.00103	0.01476	0.04694
842.8	NA	0.0001	0.00012	0.00012	0.00014	0.00013	0.00015	0.00031	0.0008	0.01142	0.03572
951.1	NA	0.00006	0.00008	0.00009	0.0001	0.00011	NA	NA	NA	NA	NA
1073.4	NA	0.00004	0.00006	0.00006	NA	NA	NA	NA	NA	NA	NA
1211.4	NA	0.00003	0.00004	NA	NA	NA	NA	NA	NA	NA	NA
1367.1	0.00003	0.00002	0.00003	NA	NA	NA	NA	NA	NA	NA	NA
1542.8	0.00003	0.00001	NA	NA	NA	NA	NA	NA	NA	NA	NA
1741.1	0.00001	0.00001	NA	NA	NA	NA	NA	NA	NA	NA	NA
1964.8	-0.00001	NA	NA	NA	NA	NA	NA	NA	NA	NA	NA
2217.4	-0.00003	NA	NA	NA	NA	NA	NA	NA	NA	NA	NA
2502.4	-0.00002	NA	NA	NA	NA	NA	NA	NA	NA	NA	NA
2824	-0.00001	NA	NA	NA	NA	NA	NA	NA	NA	NA	NA

Table A.11: FAS Linear Amp. Look-up Table for 0.105 Hz.

V_{S30} (m/s)	Soil Depth (m)										
	0	5	10	15	20	25	30	50	100	500	1000
95.6	NA	NA	NA	NA	NA	NA	0.0148	0.02592	0.04808	0.4111	1.46068
107.9	NA	NA	NA	NA	NA	0.01181	0.01266	0.02206	0.04098	0.34107	1.16498
121.8	NA	NA	NA	NA	0.00916	0.0101	0.00973	0.01699	0.03139	0.25661	0.80511
137.4	NA	NA	NA	NA	0.00783	0.00772	0.00766	0.01329	0.02515	0.21405	0.67335
155.1	NA	NA	NA	0.0062	0.00601	0.00613	0.00623	0.01134	0.02416	0.25505	0.91835
175	NA	NA	NA	0.00483	0.00481	0.0048	0.00465	0.00811	0.01636	0.15458	0.48683
197.5	NA	NA	0.00404	0.00387	0.00376	0.00361	0.00378	0.00715	0.01724	0.20273	0.70098
222.9	NA	NA	0.00329	0.00307	0.0029	0.0029	0.00305	0.00577	0.01395	0.16454	0.52932
251.5	NA	NA	0.00251	0.00235	0.00228	0.00227	0.00234	0.00459	0.01183	0.14338	0.46111
283.9	NA	NA	0.00196	0.00179	0.0018	0.00176	0.00189	0.00388	0.01052	0.13299	0.42519
320.4	NA	0.00124	0.00149	0.00138	0.00136	0.00139	0.00151	0.00316	0.00883	0.11617	0.37098
361.5	NA	0.00105	0.00112	0.00104	0.00105	0.00112	0.00116	0.00254	0.00733	0.09663	0.30203
408	NA	0.00079	0.00085	0.0008	0.00084	0.00085	0.00088	0.00185	0.00522	0.06967	0.21658
460.4	NA	0.00062	0.00062	0.00061	0.00063	0.00066	0.00068	0.00139	0.00382	0.0522	0.16469
519.6	NA	0.00045	0.00046	0.00045	0.00048	0.0005	0.00054	0.0011	0.00302	0.04182	0.13198
586.4	NA	0.00034	0.00033	0.00035	0.00037	0.00039	0.00041	0.00084	0.00223	0.03126	0.09943
661.8	NA	0.00024	0.00024	0.00026	0.00028	0.00029	0.0003	0.00061	0.00161	0.02266	0.07165
746.8	NA	0.00017	0.00018	0.00019	0.0002	0.00022	0.00022	0.00045	0.00117	0.01676	0.05332
842.8	NA	0.00012	0.00014	0.00014	0.00016	0.00015	0.00017	0.00035	0.00091	0.01301	0.04057
951.1	NA	0.00007	0.00009	0.0001	0.00011	0.00013	NA	NA	NA	NA	NA
1073.4	NA	0.00005	0.00007	0.00007	NA	NA	NA	NA	NA	NA	NA
1211.4	NA	0.00003	0.00005	NA	NA	NA	NA	NA	NA	NA	NA
1367.1	0.00004	0.00002	0.00004	NA	NA	NA	NA	NA	NA	NA	NA
1542.8	0.00003	0.00001	NA	NA	NA	NA	NA	NA	NA	NA	NA
1741.1	0.00002	0.00001	NA	NA	NA	NA	NA	NA	NA	NA	NA
1964.8	-0.00001	NA	NA	NA	NA	NA	NA	NA	NA	NA	NA
2217.4	-0.00003	NA	NA	NA	NA	NA	NA	NA	NA	NA	NA
2502.4	-0.00002	NA	NA	NA	NA	NA	NA	NA	NA	NA	NA
2824	-0.00001	NA	NA	NA	NA	NA	NA	NA	NA	NA	NA

Table A.12: FAS Linear Amp. Look-up Table for 0.111 Hz.

V_{S30} (m/s)	Soil Depth (m)										
	0	5	10	15	20	25	30	50	100	500	1000
95.6	NA	NA	NA	NA	NA	NA	0.01664	0.02905	0.05419	0.46919	1.66224
107.9	NA	NA	NA	NA	NA	0.01324	0.01423	0.02478	0.046	0.38768	1.36277
121.8	NA	NA	NA	NA	0.01028	0.01136	0.0109	0.01905	0.03532	0.29013	0.93399
137.4	NA	NA	NA	NA	0.00878	0.00869	0.0086	0.01493	0.0282	0.24196	0.7743
155.1	NA	NA	NA	0.00696	0.00676	0.00687	0.00698	0.01272	0.02709	0.28983	1.03556
175	NA	NA	NA	0.00543	0.00539	0.00538	0.00521	0.00911	0.01836	0.17459	0.55863
197.5	NA	NA	0.00453	0.00435	0.00422	0.00405	0.00424	0.00803	0.01936	0.22963	0.79499
222.9	NA	NA	0.00369	0.00345	0.00325	0.00326	0.00343	0.00648	0.01566	0.18587	0.60721
251.5	NA	NA	0.00282	0.00264	0.00256	0.00255	0.00263	0.00515	0.01329	0.16172	0.52843
283.9	NA	NA	0.0022	0.00201	0.00203	0.00198	0.00212	0.00436	0.01182	0.15001	0.4854
320.4	NA	0.00139	0.00167	0.00155	0.00153	0.00156	0.00169	0.00355	0.00992	0.13089	0.42225
361.5	NA	0.00118	0.00126	0.00117	0.00118	0.00126	0.0013	0.00285	0.00823	0.10879	0.34232
408	NA	0.00089	0.00095	0.0009	0.00094	0.00096	0.00099	0.00208	0.00586	0.07839	0.24461
460.4	NA	0.0007	0.0007	0.00069	0.00071	0.00074	0.00076	0.00157	0.00429	0.05873	0.18572
519.6	NA	0.00051	0.00052	0.0005	0.00055	0.00056	0.0006	0.00124	0.0034	0.04702	0.14866
586.4	NA	0.00039	0.00038	0.00039	0.00042	0.00044	0.00046	0.00094	0.00252	0.03514	0.11191
661.8	NA	0.00028	0.00027	0.0003	0.00031	0.00033	0.00034	0.00069	0.00181	0.02544	0.08055
746.8	NA	0.00019	0.00021	0.00022	0.00023	0.00025	0.00025	0.00051	0.00132	0.01884	0.05998
842.8	NA	0.00013	0.00015	0.00016	0.00018	0.00017	0.0002	0.0004	0.00103	0.01463	0.04559
951.1	NA	0.00009	0.00011	0.00012	0.00013	0.00015	NA	NA	NA	NA	NA
1073.4	NA	0.00006	0.00007	0.00008	NA	NA	NA	NA	NA	NA	NA
1211.4	NA	0.00004	0.00005	NA	NA	NA	NA	NA	NA	NA	NA
1367.1	0.00005	0.00002	0.00004	NA	NA	NA	NA	NA	NA	NA	NA
1542.8	0.00004	0.00001	NA	NA	NA	NA	NA	NA	NA	NA	NA
1741.1	0.00002	0.00001	NA	NA	NA	NA	NA	NA	NA	NA	NA
1964.8	-0.00001	NA	NA	NA	NA	NA	NA	NA	NA	NA	NA
2217.4	-0.00002	NA	NA	NA	NA	NA	NA	NA	NA	NA	NA
2502.4	-0.00002	NA	NA	NA	NA	NA	NA	NA	NA	NA	NA
2824	-0.00001	NA	NA	NA	NA	NA	NA	NA	NA	NA	NA

Table A.13: FAS Linear Amp. Look-up Table for 0.118 Hz.

V_{S30} (m/s)	Soil Depth (m)										
	0	5	10	15	20	25	30	50	100	500	1000
95.6	NA	NA	NA	NA	NA	NA	0.01817	0.03161	0.05897	0.51531	1.77788
107.9	NA	NA	NA	NA	NA	0.01449	0.01552	0.02709	0.05038	0.43065	1.51497
121.8	NA	NA	NA	NA	0.01125	0.01237	0.01189	0.02076	0.03848	0.318	1.04364
137.4	NA	NA	NA	NA	0.00961	0.00944	0.00938	0.01628	0.03082	0.26535	0.86271
155.1	NA	NA	NA	0.0076	0.00736	0.0075	0.00763	0.01388	0.0296	0.31956	1.10282
175	NA	NA	NA	0.00589	0.00587	0.00589	0.00569	0.00996	0.02003	0.19134	0.62136
197.5	NA	NA	0.00497	0.00475	0.0046	0.00442	0.00463	0.00876	0.02112	0.25242	0.86427
222.9	NA	NA	0.00402	0.00377	0.00355	0.00355	0.00374	0.00705	0.01708	0.20343	0.67251
251.5	NA	NA	0.00308	0.00288	0.0028	0.00278	0.00287	0.00563	0.01448	0.17739	0.58588
283.9	NA	NA	0.0024	0.00219	0.00221	0.00216	0.00232	0.00475	0.01289	0.1641	0.53683
320.4	NA	0.00153	0.00183	0.00169	0.00166	0.0017	0.00185	0.00387	0.01082	0.1431	0.46495
361.5	NA	0.00129	0.00137	0.00128	0.00129	0.00138	0.00142	0.00311	0.00897	0.11885	0.37606
408	NA	0.00097	0.00104	0.00098	0.00103	0.00105	0.00108	0.00227	0.00639	0.08548	0.2681
460.4	NA	0.00076	0.00076	0.00075	0.00078	0.00081	0.00083	0.00171	0.00468	0.06396	0.20279
519.6	NA	0.00056	0.00057	0.00055	0.0006	0.00061	0.00066	0.00136	0.00371	0.05121	0.16213
586.4	NA	0.00042	0.00041	0.00043	0.00046	0.00048	0.0005	0.00103	0.00274	0.03825	0.12191
661.8	NA	0.0003	0.0003	0.00033	0.00034	0.00036	0.00037	0.00075	0.00198	0.02778	0.0878
746.8	NA	0.00021	0.00023	0.00024	0.00025	0.00027	0.00027	0.00055	0.00144	0.02056	0.06527
842.8	NA	0.00015	0.00017	0.00018	0.0002	0.00019	0.00022	0.00044	0.00113	0.01589	0.04954
951.1	NA	0.00009	0.00012	0.00013	0.00014	0.00016	NA	NA	NA	NA	NA
1073.4	NA	0.00007	0.00008	0.00009	NA	NA	NA	NA	NA	NA	NA
1211.4	NA	0.00004	0.00006	NA	NA	NA	NA	NA	NA	NA	NA
1367.1	0.00006	0.00003	0.00005	NA	NA	NA	NA	NA	NA	NA	NA
1542.8	0.00005	0.00002	NA	NA	NA	NA	NA	NA	NA	NA	NA
1741.1	0.00003	0.00001	NA	NA	NA	NA	NA	NA	NA	NA	NA
1964.8	0	NA	NA	NA	NA	NA	NA	NA	NA	NA	NA
2217.4	-0.00002	NA	NA	NA	NA	NA	NA	NA	NA	NA	NA
2502.4	-0.00002	NA	NA	NA	NA	NA	NA	NA	NA	NA	NA
2824	-0.00001	NA	NA	NA	NA	NA	NA	NA	NA	NA	NA

Table A.14: FAS Linear Amp. Look-up Table for 0.125 Hz.

V_{S30} (m/s)	Soil Depth (m)										
	0	5	10	15	20	25	30	50	100	500	1000
95.6	NA	NA	NA	NA	NA	NA	0.02024	0.03528	0.06589	0.58549	1.79161
107.9	NA	NA	NA	NA	NA	0.01613	0.01723	0.03017	0.05611	0.48594	1.68476
121.8	NA	NA	NA	NA	0.01255	0.01377	0.01327	0.02315	0.04289	0.35753	1.20177
137.4	NA	NA	NA	NA	0.01069	0.01052	0.01044	0.01812	0.03433	0.29772	0.98038
155.1	NA	NA	NA	0.00845	0.0082	0.00835	0.0085	0.01547	0.03303	0.36052	1.12948
175	NA	NA	NA	0.00657	0.00654	0.00655	0.00634	0.01107	0.0223	0.21484	0.70679
197.5	NA	NA	0.00552	0.00529	0.00512	0.00492	0.00515	0.00975	0.02354	0.28437	0.9383
222.9	NA	NA	0.00449	0.0042	0.00396	0.00396	0.00416	0.00786	0.01902	0.2282	0.76421
251.5	NA	NA	0.00343	0.0032	0.00311	0.0031	0.0032	0.00627	0.01613	0.19876	0.66663
283.9	NA	NA	0.00267	0.00244	0.00246	0.00241	0.00258	0.0053	0.01436	0.18369	0.60989
320.4	NA	0.0017	0.00203	0.00189	0.00185	0.0019	0.00206	0.00431	0.01205	0.16012	0.52599
361.5	NA	0.00144	0.00153	0.00142	0.00144	0.00153	0.00159	0.00347	0.00999	0.13279	0.42356
408	NA	0.00109	0.00116	0.00109	0.00115	0.00117	0.00121	0.00254	0.00712	0.09543	0.30078
460.4	NA	0.00085	0.00085	0.00084	0.00087	0.0009	0.00093	0.00191	0.00522	0.07141	0.22697
519.6	NA	0.00062	0.00064	0.00062	0.00067	0.00069	0.00074	0.00151	0.00413	0.05712	0.18127
586.4	NA	0.00047	0.00046	0.00048	0.00052	0.00054	0.00056	0.00115	0.00306	0.04266	0.136
661.8	NA	0.00034	0.00033	0.00037	0.00038	0.0004	0.00041	0.00084	0.00221	0.03099	0.09797
746.8	NA	0.00024	0.00025	0.00027	0.00028	0.00031	0.00031	0.00062	0.00161	0.02291	0.07275
842.8	NA	0.00017	0.00019	0.0002	0.00022	0.00022	0.00024	0.00049	0.00127	0.0177	0.05523
951.1	NA	0.00011	0.00013	0.00015	0.00016	0.00018	NA	NA	NA	NA	NA
1073.4	NA	0.00007	0.00009	0.0001	NA	NA	NA	NA	NA	NA	NA
1211.4	NA	0.00005	0.00007	NA	NA	NA	NA	NA	NA	NA	NA
1367.1	0.00007	0.00003	0.00005	NA	NA	NA	NA	NA	NA	NA	NA
1542.8	0.00005	0.00002	NA	NA	NA	NA	NA	NA	NA	NA	NA
1741.1	0.00003	0.00001	NA	NA	NA	NA	NA	NA	NA	NA	NA
1964.8	0	NA	NA	NA	NA	NA	NA	NA	NA	NA	NA
2217.4	-0.00002	NA	NA	NA	NA	NA	NA	NA	NA	NA	NA
2502.4	-0.00002	NA	NA	NA	NA	NA	NA	NA	NA	NA	NA
2824	-0.00001	NA	NA	NA	NA	NA	NA	NA	NA	NA	NA

Table A.15: FAS Linear Amp. Look-up Table for 0.133 Hz.

V_{S30} (m/s)	Soil Depth (m)										
	0	5	10	15	20	25	30	50	100	500	1000
95.6	NA	NA	NA	NA	NA	NA	0.02405	0.04198	0.07837	0.72032	1.54367
107.9	NA	NA	NA	NA	NA	0.01929	0.02059	0.03594	0.06708	0.59682	1.7399
121.8	NA	NA	NA	NA	0.0149	0.01636	0.01575	0.02751	0.05108	0.43288	1.48433
137.4	NA	NA	NA	NA	0.01273	0.0125	0.01243	0.02157	0.04091	0.361	1.17895
155.1	NA	NA	NA	0.0101	0.00975	0.00993	0.01012	0.0184	0.03929	0.44331	1.07183
175	NA	NA	NA	0.00779	0.00778	0.00781	0.00756	0.01322	0.0266	0.25858	0.85864
197.5	NA	NA	0.00658	0.0063	0.0061	0.00586	0.00614	0.01161	0.02803	0.34528	1.04112
222.9	NA	NA	0.00533	0.00501	0.00471	0.00472	0.00496	0.00936	0.02264	0.275	0.92908
251.5	NA	NA	0.00408	0.00382	0.00371	0.00369	0.00381	0.00747	0.01922	0.23978	0.81555
283.9	NA	NA	0.00318	0.0029	0.00293	0.00287	0.00308	0.00631	0.0171	0.22121	0.75332
320.4	NA	0.00204	0.00242	0.00225	0.00221	0.00226	0.00246	0.00513	0.01435	0.19216	0.64377
361.5	NA	0.00172	0.00183	0.0017	0.00172	0.00183	0.00189	0.00413	0.0119	0.15908	0.5152
408	NA	0.00129	0.00139	0.00131	0.00137	0.0014	0.00144	0.00303	0.00849	0.11408	0.3632
460.4	NA	0.00102	0.00102	0.00101	0.00104	0.00108	0.00111	0.00228	0.00622	0.08518	0.2724
519.6	NA	0.00075	0.00077	0.00074	0.0008	0.00082	0.00088	0.00181	0.00493	0.06809	0.21698
586.4	NA	0.00057	0.00056	0.00058	0.00062	0.00064	0.00067	0.00138	0.00365	0.05084	0.16249
661.8	NA	0.00041	0.0004	0.00044	0.00046	0.00048	0.0005	0.00101	0.00264	0.03693	0.11692
746.8	NA	0.00029	0.00031	0.00032	0.00034	0.00037	0.00037	0.00075	0.00193	0.02736	0.08664
842.8	NA	0.0002	0.00023	0.00024	0.00027	0.00026	0.00029	0.00059	0.00152	0.02112	0.06562
951.1	NA	0.00013	0.00016	0.00018	0.00019	0.00022	NA	NA	NA	NA	NA
1073.4	NA	0.00009	0.00011	0.00013	NA	NA	NA	NA	NA	NA	NA
1211.4	NA	0.00006	0.00008	NA	NA	NA	NA	NA	NA	NA	NA
1367.1	0.00009	0.00004	0.00006	NA	NA	NA	NA	NA	NA	NA	NA
1542.8	0.00007	0.00002	NA	NA	NA	NA	NA	NA	NA	NA	NA
1741.1	0.00005	0.00002	NA	NA	NA	NA	NA	NA	NA	NA	NA
1964.8	0.00001	NA	NA	NA	NA	NA	NA	NA	NA	NA	NA
2217.4	-0.00002	NA	NA	NA	NA	NA	NA	NA	NA	NA	NA
2502.4	-0.00003	NA	NA	NA	NA	NA	NA	NA	NA	NA	NA
2824	-0.00001	NA	NA	NA	NA	NA	NA	NA	NA	NA	NA

Table A.16: FAS Linear Amp. Look-up Table for 0.143 Hz.

V_{S30} (m/s)	Soil Depth (m)										
	0	5	10	15	20	25	30	50	100	500	1000
95.6	NA	NA	NA	NA	NA	NA	0.02698	0.04736	0.08838	0.83932	1.29563
107.9	NA	NA	NA	NA	NA	0.02151	0.02307	0.04027	0.07515	0.67972	1.59241
121.8	NA	NA	NA	NA	0.01671	0.01843	0.01772	0.03098	0.05759	0.49517	1.63499
137.4	NA	NA	NA	NA	0.01424	0.01409	0.01397	0.02426	0.04592	0.41069	1.30909
155.1	NA	NA	NA	0.0113	0.01095	0.01116	0.01135	0.02066	0.04414	0.50793	1.01547
175	NA	NA	NA	0.0088	0.00874	0.00875	0.00848	0.01479	0.02985	0.29376	0.95385
197.5	NA	NA	0.00735	0.00707	0.00686	0.00658	0.00689	0.01303	0.0315	0.39504	1.10581
222.9	NA	NA	0.00599	0.0056	0.00529	0.00529	0.00557	0.01053	0.02545	0.31271	1.05047
251.5	NA	NA	0.00459	0.00429	0.00416	0.00415	0.00429	0.00838	0.0216	0.27161	0.91219
283.9	NA	NA	0.00358	0.00326	0.0033	0.00323	0.00346	0.00709	0.01921	0.2505	0.86654
320.4	NA	0.00227	0.00272	0.00253	0.00249	0.00254	0.00276	0.00578	0.01612	0.21727	0.74019
361.5	NA	0.00192	0.00205	0.00191	0.00193	0.00206	0.00213	0.00465	0.01338	0.17957	0.58816
408	NA	0.00146	0.00156	0.00147	0.00154	0.00158	0.00162	0.0034	0.00954	0.12869	0.41176
460.4	NA	0.00115	0.00115	0.00113	0.00117	0.00122	0.00125	0.00256	0.007	0.09609	0.30878
519.6	NA	0.00084	0.00086	0.00083	0.0009	0.00093	0.001	0.00204	0.00555	0.07678	0.24541
586.4	NA	0.00064	0.00063	0.00065	0.0007	0.00072	0.00076	0.00155	0.00412	0.05734	0.18345
661.8	NA	0.00046	0.00045	0.0005	0.00052	0.00055	0.00056	0.00114	0.00297	0.04151	0.13168
746.8	NA	0.00033	0.00035	0.00037	0.00038	0.00042	0.00042	0.00084	0.00218	0.03072	0.09747
842.8	NA	0.00023	0.00026	0.00027	0.0003	0.0003	0.00033	0.00067	0.00171	0.02383	0.07401
951.1	NA	0.00015	0.00018	0.0002	0.00021	0.00025	NA	NA	NA	NA	NA
1073.4	NA	0.00011	0.00013	0.00014	NA	NA	NA	NA	NA	NA	NA
1211.4	NA	0.00007	0.0001	NA	NA	NA	NA	NA	NA	NA	NA
1367.1	0.0001	0.00004	0.00007	NA	NA	NA	NA	NA	NA	NA	NA
1542.8	0.00009	0.00003	NA	NA	NA	NA	NA	NA	NA	NA	NA
1741.1	0.00006	0.00002	NA	NA	NA	NA	NA	NA	NA	NA	NA
1964.8	0.00001	NA	NA	NA	NA	NA	NA	NA	NA	NA	NA
2217.4	-0.00002	NA	NA	NA	NA	NA	NA	NA	NA	NA	NA
2502.4	-0.00003	NA	NA	NA	NA	NA	NA	NA	NA	NA	NA
2824	-0.00002	NA	NA	NA	NA	NA	NA	NA	NA	NA	NA

Table A.17: FAS Linear Amp. Look-up Table for 0.154 Hz.

V_{S30} (m/s)	Soil Depth (m)										
	0	5	10	15	20	25	30	50	100	500	1000
95.6	NA	NA	NA	NA	NA	NA	0.0315	0.05508	0.10299	1.02189	0.99048
107.9	NA	NA	NA	NA	NA	0.0251	0.02686	0.04702	0.08784	0.82392	1.28145
121.8	NA	NA	NA	NA	0.01945	0.02144	0.02061	0.03604	0.06699	0.59021	1.6663
137.4	NA	NA	NA	NA	0.01662	0.01636	0.01625	0.02824	0.05357	0.48791	1.46329
155.1	NA	NA	NA	0.01317	0.01275	0.01298	0.0132	0.02405	0.05144	0.61458	0.97812
175	NA	NA	NA	0.0102	0.01017	0.01019	0.00987	0.01724	0.03478	0.34718	1.05682
197.5	NA	NA	0.00859	0.00823	0.00798	0.00766	0.00802	0.01517	0.03669	0.4729	1.17288
222.9	NA	NA	0.00697	0.00654	0.00616	0.00616	0.00649	0.01225	0.02963	0.36957	1.21937
251.5	NA	NA	0.00534	0.00499	0.00485	0.00483	0.00499	0.00976	0.02515	0.32104	1.01801
283.9	NA	NA	0.00416	0.0038	0.00384	0.00376	0.00403	0.00825	0.02236	0.29522	1.02829
320.4	NA	0.00266	0.00317	0.00295	0.0029	0.00296	0.00322	0.00672	0.01877	0.25533	0.88643
361.5	NA	0.00225	0.00239	0.00223	0.00225	0.0024	0.00248	0.00541	0.01558	0.21055	0.70088
408	NA	0.0017	0.00182	0.00171	0.0018	0.00184	0.00189	0.00396	0.01111	0.15042	0.4866
460.4	NA	0.00134	0.00134	0.00132	0.00137	0.00142	0.00146	0.00299	0.00815	0.11205	0.36269
519.6	NA	0.00098	0.00101	0.00097	0.00105	0.00108	0.00116	0.00238	0.00646	0.08947	0.28739
586.4	NA	0.00075	0.00073	0.00076	0.00082	0.00085	0.00089	0.00181	0.00479	0.06674	0.21422
661.8	NA	0.00054	0.00053	0.00058	0.00061	0.00064	0.00066	0.00133	0.00347	0.04837	0.15343
746.8	NA	0.00039	0.00041	0.00043	0.00045	0.00049	0.00049	0.00099	0.00254	0.03579	0.1134
842.8	NA	0.00027	0.0003	0.00032	0.00035	0.00035	0.00039	0.00078	0.002	0.02769	0.08588
951.1	NA	0.00018	0.00022	0.00024	0.00025	0.00029	NA	NA	NA	NA	NA
1073.4	NA	0.00013	0.00015	0.00017	NA	NA	NA	NA	NA	NA	NA
1211.4	NA	0.00009	0.00011	NA	NA	NA	NA	NA	NA	NA	NA
1367.1	0.00012	0.00005	0.00009	NA	NA	NA	NA	NA	NA	NA	NA
1542.8	0.00011	0.00003	NA	NA	NA	NA	NA	NA	NA	NA	NA
1741.1	0.00008	0.00002	NA	NA	NA	NA	NA	NA	NA	NA	NA
1964.8	0.00002	NA	NA	NA	NA	NA	NA	NA	NA	NA	NA
2217.4	-0.00002	NA	NA	NA	NA	NA	NA	NA	NA	NA	NA
2502.4	-0.00003	NA	NA	NA	NA	NA	NA	NA	NA	NA	NA
2824	-0.00002	NA	NA	NA	NA	NA	NA	NA	NA	NA	NA

Table A.18: FAS Linear Amp. Look-up Table for 0.167 Hz.

V_{S30} (m/s)	Soil Depth (m)										
	0	5	10	15	20	25	30	50	100	500	1000
95.6	NA	NA	NA	NA	NA	NA	0.03739	0.06549	0.1227	1.31195	0.75239
107.9	NA	NA	NA	NA	NA	0.02979	0.03187	0.05571	0.1043	1.03501	0.97902
121.8	NA	NA	NA	NA	0.0231	0.02547	0.02453	0.04285	0.07972	0.72884	1.43727
137.4	NA	NA	NA	NA	0.0197	0.01945	0.01929	0.03352	0.06365	0.59832	1.49714
155.1	NA	NA	NA	0.01561	0.01512	0.01541	0.01567	0.02854	0.06117	0.77484	0.99322
175	NA	NA	NA	0.01208	0.01206	0.01209	0.01169	0.02046	0.04131	0.42241	1.13664
197.5	NA	NA	0.01018	0.00976	0.00946	0.00908	0.00951	0.01798	0.0436	0.58708	1.17051
222.9	NA	NA	0.00828	0.00775	0.0073	0.00731	0.00769	0.01452	0.03519	0.44973	1.36352
251.5	NA	NA	0.00633	0.00592	0.00575	0.00574	0.00592	0.01157	0.02984	0.3902	1.10958
283.9	NA	NA	0.00494	0.0045	0.00456	0.00446	0.00478	0.00979	0.02654	0.35716	1.16766
320.4	NA	0.00315	0.00376	0.00349	0.00344	0.00352	0.00382	0.00798	0.02227	0.3074	1.07776
361.5	NA	0.00266	0.00284	0.00265	0.00267	0.00285	0.00295	0.00642	0.01849	0.25268	0.85811
408	NA	0.00202	0.00216	0.00204	0.00214	0.00219	0.00225	0.00471	0.01318	0.17971	0.59025
460.4	NA	0.00159	0.00159	0.00157	0.00162	0.00169	0.00174	0.00355	0.00967	0.13364	0.43656
519.6	NA	0.00117	0.0012	0.00116	0.00125	0.00129	0.00139	0.00282	0.00767	0.10658	0.34439
586.4	NA	0.00089	0.00087	0.00091	0.00097	0.00101	0.00106	0.00216	0.0057	0.07939	0.25561
661.8	NA	0.00064	0.00063	0.00069	0.00073	0.00076	0.00079	0.00158	0.00413	0.05746	0.18257
746.8	NA	0.00046	0.00048	0.00051	0.00054	0.00059	0.00059	0.00118	0.00303	0.04255	0.13481
842.8	NA	0.00033	0.00037	0.00038	0.00042	0.00042	0.00047	0.00094	0.00239	0.03294	0.10229
951.1	NA	0.00022	0.00026	0.00028	0.0003	0.00035	NA	NA	NA	NA	NA
1073.4	NA	0.00015	0.00019	0.0002	NA	NA	NA	NA	NA	NA	NA
1211.4	NA	0.00011	0.00014	NA	NA	NA	NA	NA	NA	NA	NA
1367.1	0.00015	0.00007	0.0001	NA	NA	NA	NA	NA	NA	NA	NA
1542.8	0.00013	0.00004	NA	NA	NA	NA	NA	NA	NA	NA	NA
1741.1	0.0001	0.00003	NA	NA	NA	NA	NA	NA	NA	NA	NA
1964.8	0.00003	NA	NA	NA	NA	NA	NA	NA	NA	NA	NA
2217.4	-0.00002	NA	NA	NA	NA	NA	NA	NA	NA	NA	NA
2502.4	-0.00003	NA	NA	NA	NA	NA	NA	NA	NA	NA	NA
2824	-0.00002	NA	NA	NA	NA	NA	NA	NA	NA	NA	NA

Table A.19: FAS Linear Amp. Look-up Table for 0.182 Hz.

V_{S30} (m/s)	Soil Depth (m)										
	0	5	10	15	20	25	30	50	100	500	1000
95.6	NA	NA	NA	NA	NA	NA	0.04563	0.08021	0.15083	1.72641	0.54933
107.9	NA	NA	NA	NA	NA	0.03643	0.03893	0.06831	0.12816	1.37941	0.6956
121.8	NA	NA	NA	NA	0.0283	0.03106	0.02987	0.05225	0.09767	0.93795	1.07081
137.4	NA	NA	NA	NA	0.02406	0.02368	0.02356	0.04095	0.07786	0.76351	1.32025
155.1	NA	NA	NA	0.01905	0.01847	0.0188	0.01915	0.03493	0.07492	1.00727	1.00675
175	NA	NA	NA	0.01478	0.01473	0.01478	0.01429	0.025	0.05047	0.53371	1.18345
197.5	NA	NA	0.01245	0.01191	0.01155	0.0111	0.01162	0.02197	0.05335	0.7521	1.07574
222.9	NA	NA	0.01009	0.00947	0.00892	0.00893	0.0094	0.01774	0.04304	0.5691	1.36967
251.5	NA	NA	0.00773	0.00724	0.00703	0.00701	0.00723	0.01415	0.0365	0.49251	1.19336
283.9	NA	NA	0.00604	0.0055	0.00557	0.00545	0.00584	0.01196	0.03247	0.44794	1.21879
320.4	NA	0.00386	0.00459	0.00428	0.0042	0.0043	0.00467	0.00975	0.02723	0.3834	1.2702
361.5	NA	0.00326	0.00348	0.00323	0.00327	0.00349	0.00361	0.00785	0.02259	0.31329	1.07002
408	NA	0.00248	0.00264	0.00249	0.00261	0.00268	0.00275	0.00576	0.01611	0.22163	0.73842
460.4	NA	0.00195	0.00195	0.00193	0.00199	0.00207	0.00213	0.00434	0.01183	0.16417	0.54265
519.6	NA	0.00143	0.00147	0.00142	0.00154	0.00158	0.0017	0.00346	0.00938	0.13073	0.42587
586.4	NA	0.0011	0.00107	0.00111	0.00119	0.00124	0.0013	0.00264	0.00697	0.0972	0.31443
661.8	NA	0.00079	0.00078	0.00085	0.00089	0.00094	0.00097	0.00194	0.00506	0.07032	0.2235
746.8	NA	0.00057	0.0006	0.00063	0.00066	0.00072	0.00072	0.00145	0.00372	0.052	0.16473
842.8	NA	0.00041	0.00045	0.00047	0.00052	0.00052	0.00058	0.00116	0.00294	0.04014	0.12461
951.1	NA	0.00027	0.00032	0.00035	0.00037	0.00043	NA	NA	NA	NA	NA
1073.4	NA	0.00019	0.00023	0.00025	NA	NA	NA	NA	NA	NA	NA
1211.4	NA	0.00013	0.00017	NA	NA	NA	NA	NA	NA	NA	NA
1367.1	0.0002	0.00008	0.00013	NA	NA	NA	NA	NA	NA	NA	NA
1542.8	0.00017	0.00005	NA	NA	NA	NA	NA	NA	NA	NA	NA
1741.1	0.00013	0.00004	NA	NA	NA	NA	NA	NA	NA	NA	NA
1964.8	0.00005	NA	NA	NA	NA	NA	NA	NA	NA	NA	NA
2217.4	-0.00001	NA	NA	NA	NA	NA	NA	NA	NA	NA	NA
2502.4	-0.00003	NA	NA	NA	NA	NA	NA	NA	NA	NA	NA
2824	-0.00002	NA	NA	NA	NA	NA	NA	NA	NA	NA	NA

Table A.20: FAS Linear Amp. Look-up Table for 0.200 Hz.

V_{S30} (m/s)	Soil Depth (m)										
	0	5	10	15	20	25	30	50	100	500	1000
95.6	NA	NA	NA	NA	NA	NA	0.0551	0.0971	0.18344	1.92568	0.44692
107.9	NA	NA	NA	NA	NA	0.04407	0.04723	0.08285	0.15591	1.7529	0.52223
121.8	NA	NA	NA	NA	0.03421	0.03757	0.03612	0.06335	0.11862	1.20969	0.78033
137.4	NA	NA	NA	NA	0.02909	0.02867	0.02849	0.04958	0.0944	0.97193	1.02203
155.1	NA	NA	NA	0.02306	0.02234	0.02275	0.02313	0.0422	0.09086	1.16914	0.94369
175	NA	NA	NA	0.01786	0.01781	0.01783	0.01727	0.03024	0.06113	0.67349	1.18312
197.5	NA	NA	0.01504	0.01441	0.01398	0.01341	0.01405	0.0266	0.06462	0.9064	0.93011
222.9	NA	NA	0.01221	0.01144	0.01078	0.0108	0.01136	0.02146	0.05207	0.71707	1.18518
251.5	NA	NA	0.00935	0.00875	0.00849	0.00847	0.00875	0.01711	0.0442	0.61943	1.20662
283.9	NA	NA	0.00729	0.00665	0.00673	0.00659	0.00707	0.01446	0.03929	0.55985	1.15454
320.4	NA	0.00469	0.00556	0.00517	0.00508	0.0052	0.00566	0.01179	0.03296	0.47512	1.31418
361.5	NA	0.00395	0.0042	0.00391	0.00396	0.00423	0.00437	0.0095	0.02735	0.38576	1.25148
408	NA	0.003	0.00319	0.00302	0.00317	0.00324	0.00333	0.00697	0.01949	0.27116	0.90676
460.4	NA	0.00236	0.00237	0.00234	0.00241	0.00251	0.00259	0.00526	0.0143	0.2	0.66696
519.6	NA	0.00174	0.00178	0.00172	0.00186	0.00192	0.00206	0.00419	0.01136	0.15892	0.52093
586.4	NA	0.00133	0.00131	0.00135	0.00145	0.00151	0.00158	0.00321	0.00845	0.11789	0.38294
661.8	NA	0.00096	0.00095	0.00103	0.00109	0.00114	0.00118	0.00236	0.00613	0.08518	0.27131
746.8	NA	0.0007	0.00073	0.00077	0.00081	0.00088	0.00088	0.00176	0.0045	0.06303	0.19941
842.8	NA	0.0005	0.00055	0.00058	0.00064	0.00063	0.00071	0.0014	0.00356	0.04868	0.15005
951.1	NA	0.00034	0.00039	0.00043	0.00045	0.00053	NA	NA	NA	NA	NA
1073.4	NA	0.00024	0.00028	0.00031	NA	NA	NA	NA	NA	NA	NA
1211.4	NA	0.00017	0.00021	NA	NA	NA	NA	NA	NA	NA	NA
1367.1	0.00025	0.00011	0.00016	NA	NA	NA	NA	NA	NA	NA	NA
1542.8	0.00022	0.00007	NA	NA	NA	NA	NA	NA	NA	NA	NA
1741.1	0.00017	0.00004	NA	NA	NA	NA	NA	NA	NA	NA	NA
1964.8	0.00007	NA	NA	NA	NA	NA	NA	NA	NA	NA	NA
2217.4	0	NA	NA	NA	NA	NA	NA	NA	NA	NA	NA
2502.4	-0.00003	NA	NA	NA	NA	NA	NA	NA	NA	NA	NA
2824	-0.00002	NA	NA	NA	NA	NA	NA	NA	NA	NA	NA

Table A.21: FAS Linear Amp. Look-up Table for 0.208 Hz.

V_{S30} (m/s)	Soil Depth (m)										
	0	5	10	15	20	25	30	50	100	500	1000
95.6	NA	NA	NA	NA	NA	NA	0.05854	0.10301	0.19544	1.8893	0.43248
107.9	NA	NA	NA	NA	NA	0.0467	0.05004	0.08806	0.16566	1.83852	0.48782
121.8	NA	NA	NA	NA	0.0363	0.03986	0.03839	0.06728	0.12593	1.31488	0.71073
137.4	NA	NA	NA	NA	0.0309	0.03039	0.03021	0.05258	0.10036	1.04744	0.93208
155.1	NA	NA	NA	0.02449	0.02367	0.02414	0.02454	0.0448	0.09656	1.18143	0.90482
175	NA	NA	NA	0.01894	0.0189	0.01891	0.01833	0.0321	0.06484	0.7245	1.16676
197.5	NA	NA	0.01597	0.01528	0.01483	0.01423	0.0149	0.02821	0.06861	0.94785	0.88312
222.9	NA	NA	0.01294	0.01215	0.01144	0.01146	0.01205	0.02275	0.0553	0.76998	1.10845
251.5	NA	NA	0.00991	0.00928	0.00901	0.00899	0.00927	0.01815	0.04689	0.66698	1.18618
283.9	NA	NA	0.00774	0.00706	0.00714	0.00699	0.0075	0.01534	0.04168	0.60093	1.12344
320.4	NA	0.00496	0.0059	0.00549	0.00539	0.00552	0.006	0.0125	0.03496	0.50848	1.28853
361.5	NA	0.00419	0.00446	0.00415	0.0042	0.00448	0.00463	0.01007	0.029	0.4118	1.2865
408	NA	0.00319	0.00339	0.0032	0.00336	0.00344	0.00354	0.00739	0.02066	0.28861	0.96218
460.4	NA	0.00251	0.00251	0.00248	0.00256	0.00266	0.00274	0.00558	0.01517	0.21269	0.70976
519.6	NA	0.00185	0.00189	0.00183	0.00198	0.00203	0.00219	0.00445	0.01204	0.16879	0.5542
586.4	NA	0.00141	0.00139	0.00144	0.00154	0.0016	0.00168	0.0034	0.00896	0.12511	0.40678
661.8	NA	0.00102	0.00101	0.0011	0.00115	0.00121	0.00125	0.0025	0.00651	0.0904	0.28784
746.8	NA	0.00075	0.00077	0.00082	0.00086	0.00093	0.00094	0.00187	0.00478	0.06684	0.21132
842.8	NA	0.00053	0.00058	0.00061	0.00068	0.00067	0.00075	0.00149	0.00378	0.05165	0.15905
951.1	NA	0.00036	0.00042	0.00046	0.00048	0.00056	NA	NA	NA	NA	NA
1073.4	NA	0.00026	0.0003	0.00033	NA	NA	NA	NA	NA	NA	NA
1211.4	NA	0.00018	0.00022	NA	NA	NA	NA	NA	NA	NA	NA
1367.1	0.00027	0.00011	0.00017	NA	NA	NA	NA	NA	NA	NA	NA
1542.8	0.00024	0.00007	NA	NA	NA	NA	NA	NA	NA	NA	NA
1741.1	0.00019	0.00005	NA	NA	NA	NA	NA	NA	NA	NA	NA
1964.8	0.00008	NA	NA	NA	NA	NA	NA	NA	NA	NA	NA
2217.4	0	NA	NA	NA	NA	NA	NA	NA	NA	NA	NA
2502.4	-0.00003	NA	NA	NA	NA	NA	NA	NA	NA	NA	NA
2824	-0.00002	NA	NA	NA	NA	NA	NA	NA	NA	NA	NA

Table A.22: FAS Linear Amp. Look-up Table for 0.217 Hz.

V_{S30} (m/s)	Soil Depth (m)										
	0	5	10	15	20	25	30	50	100	500	1000
95.6	NA	NA	NA	NA	NA	NA	0.06522	0.11489	0.2173	1.72443	0.42956
107.9	NA	NA	NA	NA	NA	0.05201	0.05566	0.09812	0.18505	1.88696	0.44471
121.8	NA	NA	NA	NA	0.04018	0.04429	0.04257	0.07471	0.14013	1.50645	0.60576
137.4	NA	NA	NA	NA	0.03431	0.03376	0.03354	0.05843	0.11169	1.18869	0.7875
155.1	NA	NA	NA	0.02725	0.02629	0.02681	0.02727	0.04982	0.10743	1.16326	0.82331
175	NA	NA	NA	0.02101	0.02099	0.02102	0.02038	0.03569	0.0722	0.8195	1.11257
197.5	NA	NA	0.01775	0.01698	0.01645	0.0158	0.01655	0.03132	0.07628	1.0147	0.80434
222.9	NA	NA	0.01436	0.01351	0.0127	0.01273	0.01338	0.02526	0.06145	0.87096	0.9657
251.5	NA	NA	0.01099	0.0103	0.01001	0.00998	0.0103	0.02017	0.05214	0.75895	1.11958
283.9	NA	NA	0.0086	0.00783	0.00793	0.00776	0.00834	0.01704	0.04634	0.68344	1.05741
320.4	NA	0.00554	0.00655	0.00609	0.00599	0.00613	0.00666	0.01388	0.03886	0.57487	1.20619
361.5	NA	0.00466	0.00495	0.00461	0.00467	0.00498	0.00515	0.01119	0.03221	0.4635	1.31052
408	NA	0.00353	0.00376	0.00356	0.00374	0.00382	0.00394	0.00821	0.02297	0.32319	1.0587
460.4	NA	0.00279	0.00279	0.00276	0.00285	0.00296	0.00305	0.0062	0.01685	0.23744	0.7913
519.6	NA	0.00205	0.00211	0.00204	0.0022	0.00226	0.00243	0.00494	0.01338	0.18801	0.61859
586.4	NA	0.00157	0.00154	0.0016	0.00171	0.00178	0.00187	0.00378	0.00995	0.13931	0.45349
661.8	NA	0.00114	0.00113	0.00122	0.00128	0.00135	0.00139	0.00279	0.00724	0.10053	0.31995
746.8	NA	0.00083	0.00086	0.00091	0.00096	0.00104	0.00104	0.00209	0.00531	0.0744	0.2347
842.8	NA	0.00059	0.00065	0.00068	0.00075	0.00075	0.00084	0.00166	0.00421	0.05734	0.17634
951.1	NA	0.0004	0.00047	0.00051	0.00054	0.00062	NA	NA	NA	NA	NA
1073.4	NA	0.00029	0.00034	0.00037	NA	NA	NA	NA	NA	NA	NA
1211.4	NA	0.0002	0.00025	NA	NA	NA	NA	NA	NA	NA	NA
1367.1	0.0003	0.00013	0.00019	NA	NA	NA	NA	NA	NA	NA	NA
1542.8	0.00027	0.00008	NA	NA	NA	NA	NA	NA	NA	NA	NA
1741.1	0.00021	0.00005	NA	NA	NA	NA	NA	NA	NA	NA	NA
1964.8	0.00009	NA	NA	NA	NA	NA	NA	NA	NA	NA	NA
2217.4	0.00001	NA	NA	NA	NA	NA	NA	NA	NA	NA	NA
2502.4	-0.00003	NA	NA	NA	NA	NA	NA	NA	NA	NA	NA
2824	-0.00002	NA	NA	NA	NA	NA	NA	NA	NA	NA	NA

Table A.23: FAS Linear Amp. Look-up Table for 0.227 Hz.

V_{S30} (m/s)	Soil Depth (m)										
	0	5	10	15	20	25	30	50	100	500	1000
95.6	NA	NA	NA	NA	NA	NA	0.07017	0.12436	0.23495	1.55391	0.44599
107.9	NA	NA	NA	NA	NA	0.05587	0.05986	0.10554	0.19916	1.8408	0.42875
121.8	NA	NA	NA	NA	0.04332	0.04772	0.04589	0.08062	0.15122	1.64293	0.54365
137.4	NA	NA	NA	NA	0.03693	0.03643	0.03613	0.06293	0.12026	1.28981	0.69994
155.1	NA	NA	NA	0.02921	0.02828	0.02885	0.02933	0.05363	0.1158	1.13307	0.77173
175	NA	NA	NA	0.02272	0.02261	0.02261	0.0219	0.0383	0.07769	0.88976	1.05557
197.5	NA	NA	0.019	0.01826	0.01769	0.01701	0.0178	0.0337	0.08223	1.06341	0.75502
222.9	NA	NA	0.01546	0.01448	0.01366	0.01368	0.01441	0.02721	0.06623	0.94731	0.86967
251.5	NA	NA	0.01185	0.01107	0.01077	0.01075	0.01109	0.02169	0.05616	0.82612	1.05528
283.9	NA	NA	0.00926	0.00844	0.00854	0.00835	0.00896	0.01834	0.04988	0.74884	1.00349
320.4	NA	0.00593	0.00704	0.00655	0.00645	0.0066	0.00717	0.01496	0.04185	0.62719	1.12866
361.5	NA	0.005	0.00533	0.00497	0.00503	0.00536	0.00555	0.01204	0.0347	0.5041	1.29401
408	NA	0.00381	0.00405	0.00383	0.00402	0.00412	0.00424	0.00884	0.02472	0.35025	1.11825
460.4	NA	0.003	0.003	0.00296	0.00307	0.00319	0.00329	0.00668	0.01816	0.25687	0.85237
519.6	NA	0.00221	0.00227	0.0022	0.00237	0.00243	0.00262	0.00532	0.01442	0.20325	0.66833
586.4	NA	0.00169	0.00166	0.00172	0.00185	0.00192	0.00202	0.00408	0.01073	0.15049	0.48982
661.8	NA	0.00123	0.00122	0.00132	0.00139	0.00146	0.0015	0.003	0.00779	0.10838	0.34472
746.8	NA	0.0009	0.00093	0.00099	0.00104	0.00112	0.00113	0.00225	0.00574	0.08002	0.25277
842.8	NA	0.00064	0.0007	0.00074	0.00081	0.00081	0.0009	0.00179	0.00454	0.06194	0.19019
951.1	NA	0.00044	0.00051	0.00055	0.00058	0.00067	NA	NA	NA	NA	NA
1073.4	NA	0.00031	0.00036	0.0004	NA	NA	NA	NA	NA	NA	NA
1211.4	NA	0.00022	0.00027	NA	NA	NA	NA	NA	NA	NA	NA
1367.1	0.00033	0.00014	0.0002	NA	NA	NA	NA	NA	NA	NA	NA
1542.8	0.0003	0.00009	NA	NA	NA	NA	NA	NA	NA	NA	NA
1741.1	0.00023	0.00006	NA	NA	NA	NA	NA	NA	NA	NA	NA
1964.8	0.0001	NA	NA	NA	NA	NA	NA	NA	NA	NA	NA
2217.4	0.00001	NA	NA	NA	NA	NA	NA	NA	NA	NA	NA
2502.4	-0.00003	NA	NA	NA	NA	NA	NA	NA	NA	NA	NA
2824	-0.00002	NA	NA	NA	NA	NA	NA	NA	NA	NA	NA

Table A.24: FAS Linear Amp. Look-up Table for 0.238 Hz.

V_{S30} (m/s)	Soil Depth (m)										
	0	5	10	15	20	25	30	50	100	500	1000
95.6	NA	NA	NA	NA	NA	NA	0.07728	0.13675	0.25963	1.33619	0.49325
107.9	NA	NA	NA	NA	NA	0.0616	0.06601	0.1164	0.2208	1.67234	0.4299
121.8	NA	NA	NA	NA	0.04763	0.05249	0.05046	0.08867	0.16684	1.77737	0.48237
137.4	NA	NA	NA	NA	0.04069	0.04	0.03976	0.0693	0.13268	1.42271	0.60555
155.1	NA	NA	NA	0.03218	0.03114	0.03172	0.03227	0.059	0.12768	1.08727	0.70832
175	NA	NA	NA	0.02494	0.02484	0.0249	0.02408	0.04222	0.08552	0.97625	0.96255
197.5	NA	NA	0.02098	0.02008	0.01945	0.01869	0.01958	0.0371	0.09064	1.12378	0.69953
222.9	NA	NA	0.017	0.01595	0.01502	0.01506	0.01585	0.02992	0.07291	1.05117	0.7524
251.5	NA	NA	0.01303	0.0122	0.01184	0.01182	0.0122	0.02386	0.06183	0.91487	0.95491
283.9	NA	NA	0.01017	0.00927	0.00939	0.00919	0.00986	0.02018	0.05494	0.84489	0.92554
320.4	NA	0.00652	0.00774	0.00721	0.00709	0.00726	0.00789	0.01645	0.04606	0.70328	1.01493
361.5	NA	0.00552	0.00586	0.00546	0.00553	0.0059	0.0061	0.01325	0.03819	0.56255	1.22998
408	NA	0.00419	0.00446	0.00422	0.00443	0.00453	0.00466	0.00973	0.02721	0.38886	1.1775
460.4	NA	0.0033	0.00331	0.00327	0.00338	0.00351	0.00362	0.00735	0.01999	0.28401	0.93055
519.6	NA	0.00243	0.0025	0.00242	0.00261	0.00268	0.00289	0.00586	0.01586	0.22444	0.73567
586.4	NA	0.00187	0.00183	0.0019	0.00203	0.00211	0.00223	0.00449	0.01181	0.16582	0.53942
661.8	NA	0.00136	0.00134	0.00145	0.00153	0.00161	0.00166	0.00331	0.00859	0.11942	0.37936
746.8	NA	0.00099	0.00103	0.00109	0.00114	0.00124	0.00124	0.00248	0.00631	0.08813	0.27767
842.8	NA	0.0007	0.00078	0.00082	0.0009	0.00089	0.001	0.00198	0.00502	0.068	0.20864
951.1	NA	0.00048	0.00056	0.00061	0.00064	0.00074	NA	NA	NA	NA	NA
1073.4	NA	0.00035	0.0004	0.00044	NA	NA	NA	NA	NA	NA	NA
1211.4	NA	0.00024	0.00029	NA	NA	NA	NA	NA	NA	NA	NA
1367.1	0.00037	0.00016	0.00022	NA	NA	NA	NA	NA	NA	NA	NA
1542.8	0.00033	0.0001	NA	NA	NA	NA	NA	NA	NA	NA	NA
1741.1	0.00027	0.00007	NA	NA	NA	NA	NA	NA	NA	NA	NA
1964.8	0.00012	NA	NA	NA	NA	NA	NA	NA	NA	NA	NA
2217.4	0.00002	NA	NA	NA	NA	NA	NA	NA	NA	NA	NA
2502.4	-0.00003	NA	NA	NA	NA	NA	NA	NA	NA	NA	NA
2824	-0.00002	NA	NA	NA	NA	NA	NA	NA	NA	NA	NA

Table A.25: FAS Linear Amp. Look-up Table for 0.250 Hz.

V_{S30} (m/s)	Soil Depth (m)										
	0	5	10	15	20	25	30	50	100	500	1000
95.6	NA	NA	NA	NA	NA	NA	0.08609	0.15233	0.29138	1.119	0.58661
107.9	NA	NA	NA	NA	NA	0.06849	0.07344	0.12944	0.24648	1.43478	0.46352
121.8	NA	NA	NA	NA	0.05296	0.05847	0.05619	0.09891	0.18647	1.81823	0.44041
137.4	NA	NA	NA	NA	0.04518	0.04452	0.04422	0.0772	0.14788	1.55582	0.52515
155.1	NA	NA	NA	0.03578	0.03465	0.03528	0.0359	0.06563	0.14228	1.05785	0.66775
175	NA	NA	NA	0.02774	0.02762	0.02765	0.02675	0.04695	0.0953	1.06708	0.84732
197.5	NA	NA	0.02329	0.02231	0.02164	0.02079	0.02178	0.04127	0.10108	1.18766	0.64836
222.9	NA	NA	0.0189	0.01772	0.01669	0.01673	0.01762	0.03328	0.08124	1.17615	0.64069
251.5	NA	NA	0.01448	0.01355	0.01316	0.01314	0.01356	0.02652	0.06879	1.00305	0.8372
283.9	NA	NA	0.0113	0.01032	0.01044	0.01022	0.01096	0.02244	0.06112	0.96299	0.82983
320.4	NA	0.00726	0.0086	0.00802	0.00789	0.00807	0.00877	0.01828	0.05122	0.8006	0.88605
361.5	NA	0.00613	0.00651	0.00607	0.00615	0.00656	0.00679	0.01473	0.04247	0.6365	1.11669
408	NA	0.00466	0.00495	0.00469	0.00492	0.00504	0.00518	0.01081	0.03026	0.43711	1.20437
460.4	NA	0.00367	0.00368	0.00363	0.00376	0.0039	0.00403	0.00817	0.02222	0.31808	1.01044
519.6	NA	0.00271	0.00278	0.00269	0.0029	0.00299	0.00321	0.00651	0.01765	0.25074	0.81345
586.4	NA	0.00208	0.00204	0.00211	0.00226	0.00235	0.00248	0.005	0.01314	0.18489	0.59931
661.8	NA	0.00151	0.00149	0.00162	0.0017	0.00179	0.00185	0.00369	0.00955	0.13294	0.4216
746.8	NA	0.00111	0.00114	0.00121	0.00127	0.00138	0.00139	0.00276	0.00703	0.09801	0.30802
842.8	NA	0.00079	0.00087	0.00091	0.001	0.001	0.00111	0.0022	0.00557	0.07561	0.23133
951.1	NA	0.00054	0.00063	0.00068	0.00072	0.00083	NA	NA	NA	NA	NA
1073.4	NA	0.00039	0.00045	0.00049	NA	NA	NA	NA	NA	NA	NA
1211.4	NA	0.00027	0.00033	NA	NA	NA	NA	NA	NA	NA	NA
1367.1	0.00041	0.00018	0.00025	NA	NA	NA	NA	NA	NA	NA	NA
1542.8	0.00037	0.00011	NA	NA	NA	NA	NA	NA	NA	NA	NA
1741.1	0.0003	0.00008	NA	NA	NA	NA	NA	NA	NA	NA	NA
1964.8	0.00014	NA	NA	NA	NA	NA	NA	NA	NA	NA	NA
2217.4	0.00003	NA	NA	NA	NA	NA	NA	NA	NA	NA	NA
2502.4	-0.00003	NA	NA	NA	NA	NA	NA	NA	NA	NA	NA
2824	-0.00002	NA	NA	NA	NA	NA	NA	NA	NA	NA	NA

Table A.26: FAS Linear Amp. Look-up Table for 0.263 Hz.

V_{S30} (m/s)	Soil Depth (m)										
	0	5	10	15	20	25	30	50	100	500	1000
95.6	NA	NA	NA	NA	NA	NA	0.0963	0.17043	0.32673	0.94014	0.75428
107.9	NA	NA	NA	NA	NA	0.07656	0.08201	0.14508	0.27768	1.20216	0.5423
121.8	NA	NA	NA	NA	0.05904	0.06517	0.06265	0.11036	0.20839	1.71117	0.42833
137.4	NA	NA	NA	NA	0.05047	0.04955	0.04929	0.08616	0.16552	1.64593	0.47176
155.1	NA	NA	NA	0.03999	0.0386	0.03933	0.04005	0.07327	0.15927	1.06277	0.66686
175	NA	NA	NA	0.03084	0.0308	0.03085	0.02987	0.05241	0.10654	1.14804	0.73893
197.5	NA	NA	0.0261	0.02489	0.0241	0.02317	0.02427	0.04604	0.11298	1.22809	0.61305
222.9	NA	NA	0.02104	0.0198	0.01862	0.01866	0.01963	0.03708	0.09063	1.31083	0.54895
251.5	NA	NA	0.01612	0.0151	0.01468	0.01464	0.01511	0.0296	0.07681	1.07624	0.72232
283.9	NA	NA	0.01259	0.01148	0.01163	0.01139	0.01222	0.02502	0.06823	1.08851	0.72923
320.4	NA	0.00816	0.0096	0.00894	0.00879	0.009	0.00978	0.02038	0.05717	0.91648	0.76264
361.5	NA	0.00683	0.00726	0.00677	0.00686	0.00732	0.00757	0.01642	0.04735	0.72483	0.97728
408	NA	0.00519	0.00552	0.00523	0.00549	0.00562	0.00579	0.01205	0.03374	0.49353	1.17692
460.4	NA	0.00409	0.0041	0.00405	0.00419	0.00435	0.00449	0.0091	0.02477	0.3573	1.0707
519.6	NA	0.00302	0.00311	0.003	0.00324	0.00333	0.00358	0.00727	0.01966	0.28078	0.89059
586.4	NA	0.00232	0.00228	0.00236	0.00252	0.00262	0.00276	0.00558	0.01463	0.20663	0.66471
661.8	NA	0.00169	0.00167	0.00181	0.0019	0.002	0.00206	0.00411	0.01065	0.14845	0.46867
746.8	NA	0.00124	0.00128	0.00136	0.00142	0.00154	0.00155	0.00308	0.00783	0.10938	0.34191
842.8	NA	0.00088	0.00097	0.00102	0.00112	0.00111	0.00124	0.00246	0.00623	0.08425	0.2566
951.1	NA	0.00061	0.0007	0.00076	0.0008	0.00092	NA	NA	NA	NA	NA
1073.4	NA	0.00043	0.0005	0.00055	NA	NA	NA	NA	NA	NA	NA
1211.4	NA	0.0003	0.00037	NA	NA	NA	NA	NA	NA	NA	NA
1367.1	0.00047	0.0002	0.00028	NA	NA	NA	NA	NA	NA	NA	NA
1542.8	0.00042	0.00013	NA	NA	NA	NA	NA	NA	NA	NA	NA
1741.1	0.00035	0.00009	NA	NA	NA	NA	NA	NA	NA	NA	NA
1964.8	0.00016	NA	NA	NA	NA	NA	NA	NA	NA	NA	NA
2217.4	0.00004	NA	NA	NA	NA	NA	NA	NA	NA	NA	NA
2502.4	-0.00002	NA	NA	NA	NA	NA	NA	NA	NA	NA	NA
2824	-0.00003	NA	NA	NA	NA	NA	NA	NA	NA	NA	NA

Table A.27: FAS Linear Amp. Look-up Table for 0.278 Hz.

V_{S30} (m/s)	Soil Depth (m)										
	0	5	10	15	20	25	30	50	100	500	1000
95.6	NA	NA	NA	NA	NA	NA	0.10811	0.19175	0.36946	0.79604	1.02143
107.9	NA	NA	NA	NA	NA	0.08598	0.092	0.16331	0.31346	1.0019	0.68549
121.8	NA	NA	NA	NA	0.0661	0.07305	0.0702	0.12372	0.23454	1.51274	0.44955
137.4	NA	NA	NA	NA	0.05668	0.05552	0.05523	0.09662	0.18606	1.64381	0.44693
155.1	NA	NA	NA	0.04485	0.04322	0.04407	0.04484	0.08216	0.17949	1.0887	0.72335
175	NA	NA	NA	0.03456	0.03448	0.03455	0.03343	0.05871	0.11952	1.21914	0.64395
197.5	NA	NA	0.02922	0.02787	0.02699	0.02591	0.02719	0.05159	0.12691	1.23416	0.60248
222.9	NA	NA	0.02354	0.02217	0.02084	0.02089	0.02198	0.04155	0.10169	1.42568	0.47431
251.5	NA	NA	0.01804	0.01693	0.01642	0.01638	0.01691	0.03315	0.08618	1.14219	0.61897
283.9	NA	NA	0.01411	0.01284	0.01303	0.01275	0.01368	0.028	0.07652	1.20059	0.6297
320.4	NA	0.00909	0.01074	0.01	0.00985	0.01007	0.01094	0.02282	0.06408	1.05191	0.64396
361.5	NA	0.00767	0.00813	0.00758	0.00768	0.0082	0.00847	0.01838	0.05307	0.83115	0.82911
408	NA	0.00582	0.00619	0.00586	0.00615	0.00629	0.00648	0.0135	0.03779	0.56122	1.09961
460.4	NA	0.00458	0.00459	0.00454	0.0047	0.00488	0.00503	0.0102	0.02773	0.40408	1.09934
519.6	NA	0.00338	0.00348	0.00337	0.00363	0.00373	0.00401	0.00814	0.02202	0.31668	0.96054
586.4	NA	0.0026	0.00255	0.00264	0.00283	0.00294	0.0031	0.00624	0.01638	0.23232	0.73575
661.8	NA	0.00189	0.00187	0.00203	0.00213	0.00225	0.00231	0.00461	0.01194	0.16651	0.52182
746.8	NA	0.00139	0.00143	0.00152	0.0016	0.00173	0.00174	0.00345	0.00878	0.1226	0.38119
842.8	NA	0.00099	0.00109	0.00114	0.00126	0.00125	0.0014	0.00276	0.00697	0.09433	0.28589
951.1	NA	0.00069	0.00079	0.00085	0.0009	0.00104	NA	NA	NA	NA	NA
1073.4	NA	0.00049	0.00057	0.00061	NA	NA	NA	NA	NA	NA	NA
1211.4	NA	0.00034	0.00042	NA	NA	NA	NA	NA	NA	NA	NA
1367.1	0.00053	0.00022	0.00031	NA	NA	NA	NA	NA	NA	NA	NA
1542.8	0.00048	0.00014	NA	NA	NA	NA	NA	NA	NA	NA	NA
1741.1	0.0004	0.0001	NA	NA	NA	NA	NA	NA	NA	NA	NA
1964.8	0.00019	NA	NA	NA	NA	NA	NA	NA	NA	NA	NA
2217.4	0.00005	NA	NA	NA	NA	NA	NA	NA	NA	NA	NA
2502.4	-0.00002	NA	NA	NA	NA	NA	NA	NA	NA	NA	NA
2824	-0.00003	NA	NA	NA	NA	NA	NA	NA	NA	NA	NA

Table A.28: FAS Linear Amp. Look-up Table for 0.286 Hz.

V_{S30} (m/s)	Soil Depth (m)										
	0	5	10	15	20	25	30	50	100	500	1000
95.6	NA	NA	NA	NA	NA	NA	0.11318	0.20111	0.38898	0.74418	1.15567
107.9	NA	NA	NA	NA	NA	0.09002	0.09637	0.17122	0.32906	0.93173	0.76289
121.8	NA	NA	NA	NA	0.0693	0.07653	0.07355	0.12976	0.24618	1.419	0.46843
137.4	NA	NA	NA	NA	0.05935	0.05821	0.05784	0.10126	0.19512	1.61553	0.44507
155.1	NA	NA	NA	0.04696	0.04525	0.04615	0.04694	0.08602	0.18843	1.10065	0.7613
175	NA	NA	NA	0.0362	0.03609	0.03618	0.03499	0.06147	0.12527	1.2446	0.6107
197.5	NA	NA	0.03054	0.02915	0.02827	0.02712	0.02847	0.05402	0.13308	1.22624	0.60513
222.9	NA	NA	0.02465	0.0232	0.02181	0.02187	0.02301	0.04351	0.10655	1.45846	0.45003
251.5	NA	NA	0.0189	0.01773	0.01719	0.01715	0.0177	0.03469	0.09029	1.16689	0.582
283.9	NA	NA	0.01477	0.01345	0.01364	0.01335	0.01432	0.02932	0.08015	1.23633	0.59163
320.4	NA	0.00949	0.01124	0.01047	0.0103	0.01054	0.01146	0.02389	0.0671	1.10865	0.59857
361.5	NA	0.00803	0.00851	0.00794	0.00804	0.00858	0.00887	0.01925	0.05558	0.87828	0.77006
408	NA	0.00609	0.00647	0.00613	0.00644	0.00659	0.00678	0.01413	0.03957	0.59116	1.05761
460.4	NA	0.0048	0.00481	0.00475	0.00492	0.00511	0.00527	0.01068	0.02902	0.42474	1.09995
519.6	NA	0.00354	0.00364	0.00353	0.0038	0.00391	0.0042	0.00852	0.02305	0.33247	0.98375
586.4	NA	0.00272	0.00267	0.00277	0.00296	0.00308	0.00325	0.00654	0.01715	0.24362	0.76429
661.8	NA	0.00198	0.00196	0.00212	0.00223	0.00235	0.00242	0.00483	0.0125	0.17447	0.54449
746.8	NA	0.00146	0.0015	0.0016	0.00168	0.00181	0.00182	0.00361	0.00919	0.12839	0.39803
842.8	NA	0.00104	0.00114	0.0012	0.00132	0.00131	0.00146	0.00289	0.0073	0.09875	0.29829
951.1	NA	0.00072	0.00083	0.00089	0.00095	0.00109	NA	NA	NA	NA	NA
1073.4	NA	0.00052	0.00059	0.00064	NA	NA	NA	NA	NA	NA	NA
1211.4	NA	0.00036	0.00044	NA	NA	NA	NA	NA	NA	NA	NA
1367.1	0.00056	0.00024	0.00033	NA	NA	NA	NA	NA	NA	NA	NA
1542.8	0.00051	0.00015	NA	NA	NA	NA	NA	NA	NA	NA	NA
1741.1	0.00042	0.0001	NA	NA	NA	NA	NA	NA	NA	NA	NA
1964.8	0.0002	NA	NA	NA	NA	NA	NA	NA	NA	NA	NA
2217.4	0.00006	NA	NA	NA	NA	NA	NA	NA	NA	NA	NA
2502.4	-0.00002	NA	NA	NA	NA	NA	NA	NA	NA	NA	NA
2824	-0.00003	NA	NA	NA	NA	NA	NA	NA	NA	NA	NA

Table A.29: FAS Linear Amp. Look-up Table for 0.294 Hz.

V_{S30} (m/s)	Soil Depth (m)										
	0	5	10	15	20	25	30	50	100	500	1000
95.6	NA	NA	NA	NA	NA	NA	0.11962	0.21369	0.41545	0.68601	1.33414
107.9	NA	NA	NA	NA	NA	0.09512	0.10197	0.18115	0.34868	0.85995	0.87888
121.8	NA	NA	NA	NA	0.07349	0.08102	0.07791	0.13778	0.26154	1.29994	0.50231
137.4	NA	NA	NA	NA	0.06263	0.06175	0.06124	0.10735	0.20678	1.55709	0.45165
155.1	NA	NA	NA	0.04958	0.04789	0.04882	0.04962	0.09101	0.19984	1.11418	0.8195
175	NA	NA	NA	0.0384	0.0382	0.03823	0.037	0.06493	0.13269	1.27231	0.57552
197.5	NA	NA	0.03216	0.03081	0.02993	0.02869	0.03011	0.05715	0.14111	1.20824	0.61297
222.9	NA	NA	0.02611	0.02448	0.02307	0.02313	0.02434	0.04609	0.11288	1.48178	0.42641
251.5	NA	NA	0.02	0.01873	0.01818	0.01816	0.01874	0.03668	0.09568	1.19692	0.54236
283.9	NA	NA	0.01563	0.01424	0.01443	0.01412	0.01515	0.03101	0.08487	1.26801	0.54903
320.4	NA	0.01001	0.01188	0.01107	0.0109	0.01115	0.01212	0.02528	0.07103	1.17824	0.54601
361.5	NA	0.00847	0.009	0.00841	0.0085	0.00907	0.00938	0.02037	0.05886	0.9401	0.70064
408	NA	0.00646	0.00685	0.00648	0.00681	0.00697	0.00717	0.01495	0.04186	0.63082	0.99898
460.4	NA	0.00507	0.00509	0.00502	0.0052	0.0054	0.00557	0.01129	0.03072	0.45223	1.08946
519.6	NA	0.00375	0.00385	0.00373	0.00402	0.00413	0.00445	0.00902	0.02441	0.35333	1.00626
586.4	NA	0.00288	0.00283	0.00293	0.00314	0.00326	0.00344	0.00692	0.01817	0.25863	0.79912
661.8	NA	0.0021	0.00208	0.00225	0.00236	0.00249	0.00257	0.00511	0.01322	0.18481	0.57327
746.8	NA	0.00155	0.00159	0.00169	0.00177	0.00192	0.00193	0.00382	0.00974	0.13575	0.41971
842.8	NA	0.0011	0.00121	0.00127	0.00139	0.00139	0.00155	0.00306	0.00771	0.10464	0.31465
951.1	NA	0.00076	0.00088	0.00095	0.001	0.00116	NA	NA	NA	NA	NA
1073.4	NA	0.00055	0.00063	0.00068	NA	NA	NA	NA	NA	NA	NA
1211.4	NA	0.00038	0.00046	NA	NA	NA	NA	NA	NA	NA	NA
1367.1	0.00059	0.00025	0.00035	NA	NA	NA	NA	NA	NA	NA	NA
1542.8	0.00054	0.00016	NA	NA	NA	NA	NA	NA	NA	NA	NA
1741.1	0.00045	0.00011	NA	NA	NA	NA	NA	NA	NA	NA	NA
1964.8	0.00022	NA	NA	NA	NA	NA	NA	NA	NA	NA	NA
2217.4	0.00006	NA	NA	NA	NA	NA	NA	NA	NA	NA	NA
2502.4	-0.00002	NA	NA	NA	NA	NA	NA	NA	NA	NA	NA
2824	-0.00003	NA	NA	NA	NA	NA	NA	NA	NA	NA	NA

Table A.30: FAS Linear Amp. Look-up Table for 0.313 Hz.

V_{S30} (m/s)	Soil Depth (m)										
	0	5	10	15	20	25	30	50	100	500	1000
95.6	NA	NA	NA	NA	NA	NA	0.15886	0.28557	0.56438	0.5421	1.50392
107.9	NA	NA	NA	NA	NA	0.12554	0.13491	0.24076	0.47167	0.6037	1.60247
121.8	NA	NA	NA	NA	0.09678	0.10672	0.10257	0.18224	0.35074	0.84366	0.88111
137.4	NA	NA	NA	NA	0.08248	0.08119	0.0806	0.14181	0.27549	1.099	0.64029
155.1	NA	NA	NA	0.06519	0.06299	0.06423	0.06525	0.12033	0.26631	1.05677	0.85499
175	NA	NA	NA	0.05043	0.05018	0.05023	0.04857	0.08549	0.17564	1.33191	0.5325
197.5	NA	NA	0.04235	0.04054	0.03928	0.0377	0.03951	0.07528	0.18737	1.03759	0.62893
222.9	NA	NA	0.03429	0.03217	0.03026	0.03034	0.03194	0.06057	0.1493	1.30675	0.42359
251.5	NA	NA	0.02625	0.02456	0.02386	0.02382	0.0246	0.04821	0.1265	1.2923	0.45891
283.9	NA	NA	0.02049	0.01867	0.01893	0.01852	0.01988	0.04074	0.11207	1.25155	0.41906
320.4	NA	0.01322	0.01559	0.01453	0.0143	0.01464	0.01591	0.03318	0.09363	1.40465	0.36354
361.5	NA	0.01111	0.01181	0.01102	0.01115	0.01192	0.01232	0.02673	0.07748	1.26234	0.43092
408	NA	0.00847	0.00898	0.00851	0.00894	0.00916	0.00942	0.01963	0.05506	0.86377	0.6794
460.4	NA	0.00665	0.00669	0.0066	0.00684	0.0071	0.00732	0.01484	0.04036	0.6116	0.89385
519.6	NA	0.00493	0.00506	0.00491	0.00528	0.00544	0.00585	0.01183	0.03206	0.47356	0.9803
586.4	NA	0.00379	0.00372	0.00385	0.00413	0.00429	0.00453	0.0091	0.02388	0.34375	0.91807
661.8	NA	0.00277	0.00274	0.00296	0.00311	0.00328	0.00339	0.00672	0.01737	0.24399	0.71081
746.8	NA	0.00204	0.0021	0.00223	0.00234	0.00253	0.00254	0.00504	0.0128	0.17868	0.53222
842.8	NA	0.00146	0.0016	0.00168	0.00184	0.00183	0.00204	0.00404	0.01017	0.13738	0.40159
951.1	NA	0.00102	0.00116	0.00125	0.00133	0.00152	NA	NA	NA	NA	NA
1073.4	NA	0.00073	0.00083	0.0009	NA	NA	NA	NA	NA	NA	NA
1211.4	NA	0.00051	0.00061	NA	NA	NA	NA	NA	NA	NA	NA
1367.1	0.00081	0.00034	0.00046	NA	NA	NA	NA	NA	NA	NA	NA
1542.8	0.00074	0.00022	NA	NA	NA	NA	NA	NA	NA	NA	NA
1741.1	0.00061	0.00015	NA	NA	NA	NA	NA	NA	NA	NA	NA
1964.8	0.00031	NA	NA	NA	NA	NA	NA	NA	NA	NA	NA
2217.4	0.00011	NA	NA	NA	NA	NA	NA	NA	NA	NA	NA
2502.4	-0.00001	NA	NA	NA	NA	NA	NA	NA	NA	NA	NA
2824	-0.00003	NA	NA	NA	NA	NA	NA	NA	NA	NA	NA

Table A.31: FAS Linear Amp. Look-up Table for 0.333 Hz.

V_{S30} (m/s)	Soil Depth (m)										
	0	5	10	15	20	25	30	50	100	500	1000
95.6	NA	NA	NA	NA	NA	NA	0.15886	0.28557	0.56438	0.5421	1.50392
107.9	NA	NA	NA	NA	NA	0.12554	0.13491	0.24076	0.47167	0.6037	1.60247
121.8	NA	NA	NA	NA	0.09678	0.10672	0.10257	0.18224	0.35074	0.84366	0.88111
137.4	NA	NA	NA	NA	0.08248	0.08119	0.0806	0.14181	0.27549	1.099	0.64029
155.1	NA	NA	NA	0.06519	0.06299	0.06423	0.06525	0.12033	0.26631	1.05677	0.85499
175	NA	NA	NA	0.05043	0.05018	0.05023	0.04857	0.08549	0.17564	1.33191	0.5325
197.5	NA	NA	0.04235	0.04054	0.03928	0.0377	0.03951	0.07528	0.18737	1.03759	0.62893
222.9	NA	NA	0.03429	0.03217	0.03026	0.03034	0.03194	0.06057	0.1493	1.30675	0.42359
251.5	NA	NA	0.02625	0.02456	0.02386	0.02382	0.0246	0.04821	0.1265	1.2923	0.45891
283.9	NA	NA	0.02049	0.01867	0.01893	0.01852	0.01988	0.04074	0.11207	1.25155	0.41906
320.4	NA	0.01322	0.01559	0.01453	0.0143	0.01464	0.01591	0.03318	0.09363	1.40465	0.36354
361.5	NA	0.01111	0.01181	0.01102	0.01115	0.01192	0.01232	0.02673	0.07748	1.26234	0.43092
408	NA	0.00847	0.00898	0.00851	0.00894	0.00916	0.00942	0.01963	0.05506	0.86377	0.6794
460.4	NA	0.00665	0.00669	0.0066	0.00684	0.0071	0.00732	0.01484	0.04036	0.6116	0.89385
519.6	NA	0.00493	0.00506	0.00491	0.00528	0.00544	0.00585	0.01183	0.03206	0.47356	0.9803
586.4	NA	0.00379	0.00372	0.00385	0.00413	0.00429	0.00453	0.0091	0.02388	0.34375	0.91807
661.8	NA	0.00277	0.00274	0.00296	0.00311	0.00328	0.00339	0.00672	0.01737	0.24399	0.71081
746.8	NA	0.00204	0.0021	0.00223	0.00234	0.00253	0.00254	0.00504	0.0128	0.17868	0.53222
842.8	NA	0.00146	0.0016	0.00168	0.00184	0.00183	0.00204	0.00404	0.01017	0.13738	0.40159
951.1	NA	0.00102	0.00116	0.00125	0.00133	0.00152	NA	NA	NA	NA	NA
1073.4	NA	0.00073	0.00083	0.0009	NA	NA	NA	NA	NA	NA	NA
1211.4	NA	0.00051	0.00061	NA	NA	NA	NA	NA	NA	NA	NA
1367.1	0.00081	0.00034	0.00046	NA	NA	NA	NA	NA	NA	NA	NA
1542.8	0.00074	0.00022	NA	NA	NA	NA	NA	NA	NA	NA	NA
1741.1	0.00061	0.00015	NA	NA	NA	NA	NA	NA	NA	NA	NA
1964.8	0.00031	NA	NA	NA	NA	NA	NA	NA	NA	NA	NA
2217.4	0.00011	NA	NA	NA	NA	NA	NA	NA	NA	NA	NA
2502.4	-0.00001	NA	NA	NA	NA	NA	NA	NA	NA	NA	NA
2824	-0.00003	NA	NA	NA	NA	NA	NA	NA	NA	NA	NA

Table A.32: FAS Linear Amp. Look-up Table for 0.357 Hz.

V_{S30} (m/s)	Soil Depth (m)										
	0	5	10	15	20	25	30	50	100	500	1000
95.6	NA	NA	NA	NA	NA	NA	0.18213	0.32951	0.65944	0.5417	1.0913
107.9	NA	NA	NA	NA	NA	0.14434	0.155	0.27786	0.54965	0.54631	1.54022
121.8	NA	NA	NA	NA	0.11085	0.12246	0.11766	0.2099	0.4059	0.70135	1.24638
137.4	NA	NA	NA	NA	0.09453	0.09306	0.0923	0.16282	0.31826	0.89296	0.80712
155.1	NA	NA	NA	0.07474	0.07224	0.07353	0.07479	0.13807	0.30806	0.93507	0.6725
175	NA	NA	NA	0.05761	0.05743	0.05751	0.05568	0.09807	0.20208	1.28415	0.58823
197.5	NA	NA	0.04847	0.04637	0.04497	0.04311	0.04523	0.08627	0.21609	0.93195	0.63775
222.9	NA	NA	0.03928	0.03679	0.03464	0.03472	0.03652	0.06934	0.17174	1.11865	0.48174
251.5	NA	NA	0.03004	0.0281	0.02729	0.02724	0.02813	0.05519	0.14534	1.24756	0.49682
283.9	NA	NA	0.02343	0.02137	0.02164	0.02118	0.02273	0.04663	0.12863	1.18117	0.4202
320.4	NA	0.01509	0.01783	0.01661	0.01635	0.01674	0.01819	0.03796	0.1074	1.37429	0.32518
361.5	NA	0.01272	0.0135	0.0126	0.01276	0.01362	0.01408	0.03058	0.08876	1.37411	0.34562
408	NA	0.00968	0.01028	0.00974	0.01023	0.01047	0.01077	0.02244	0.06303	1.00206	0.53873
460.4	NA	0.00762	0.00764	0.00755	0.00782	0.00812	0.00837	0.01696	0.04619	0.71028	0.74887
519.6	NA	0.00564	0.0058	0.00562	0.00604	0.00622	0.00669	0.01353	0.03666	0.54775	0.88612
586.4	NA	0.00434	0.00426	0.00441	0.00472	0.00491	0.00518	0.01041	0.02729	0.39576	0.91976
661.8	NA	0.00317	0.00314	0.00339	0.00356	0.00376	0.00387	0.00769	0.01988	0.28012	0.76601
746.8	NA	0.00234	0.00241	0.00255	0.00268	0.0029	0.00292	0.00577	0.01465	0.20461	0.58849
842.8	NA	0.00167	0.00183	0.00192	0.00211	0.00211	0.00234	0.00463	0.01166	0.15711	0.44929
951.1	NA	0.00117	0.00133	0.00143	0.00152	0.00175	NA	NA	NA	NA	NA
1073.4	NA	0.00084	0.00096	0.00104	NA	NA	NA	NA	NA	NA	NA
1211.4	NA	0.00059	0.0007	NA	NA	NA	NA	NA	NA	NA	NA
1367.1	0.00093	0.00039	0.00053	NA	NA	NA	NA	NA	NA	NA	NA
1542.8	0.00086	0.00025	NA	NA	NA	NA	NA	NA	NA	NA	NA
1741.1	0.00072	0.00017	NA	NA	NA	NA	NA	NA	NA	NA	NA
1964.8	0.00037	NA	NA	NA	NA	NA	NA	NA	NA	NA	NA
2217.4	0.00013	NA	NA	NA	NA	NA	NA	NA	NA	NA	NA
2502.4	-0.00001	NA	NA	NA	NA	NA	NA	NA	NA	NA	NA
2824	-0.00003	NA	NA	NA	NA	NA	NA	NA	NA	NA	NA

Table A.33: FAS Linear Amp. Look-up Table for 0.385 Hz.

V_{S30} (m/s)	Soil Depth (m)										
	0	5	10	15	20	25	30	50	100	500	1000
95.6	NA	NA	NA	NA	NA	NA	0.20937	0.38198	0.77766	0.59816	0.81226
107.9	NA	NA	NA	NA	NA	0.16542	0.17771	0.32109	0.64192	0.54084	1.17264
121.8	NA	NA	NA	NA	0.12701	0.14075	0.13477	0.24147	0.47075	0.607	1.53907
137.4	NA	NA	NA	NA	0.10832	0.10656	0.10573	0.18694	0.36803	0.73964	1.02348
155.1	NA	NA	NA	0.0856	0.08265	0.08405	0.0856	0.15856	0.35614	0.81572	0.56873
175	NA	NA	NA	0.0659	0.06565	0.06577	0.06369	0.11234	0.23242	1.16123	0.64618
197.5	NA	NA	0.05532	0.05303	0.05133	0.04928	0.05167	0.09876	0.24933	0.83615	0.72291
222.9	NA	NA	0.04486	0.04202	0.03956	0.03965	0.04175	0.07934	0.19724	0.9353	0.58342
251.5	NA	NA	0.03429	0.03207	0.03116	0.03112	0.03212	0.06309	0.16691	1.13512	0.56168
283.9	NA	NA	0.02675	0.02439	0.02471	0.02418	0.02595	0.05329	0.14757	1.08724	0.48579
320.4	NA	0.01723	0.02036	0.01897	0.01868	0.01911	0.02077	0.04338	0.1231	1.25231	0.33228
361.5	NA	0.01455	0.01542	0.01439	0.01457	0.01556	0.01608	0.03493	0.10163	1.38881	0.29873
408	NA	0.01104	0.01174	0.01111	0.01168	0.01196	0.0123	0.02562	0.07207	1.13829	0.42714
460.4	NA	0.0087	0.00873	0.00862	0.00893	0.00927	0.00956	0.01937	0.05279	0.82251	0.60909
519.6	NA	0.00644	0.00662	0.00642	0.0069	0.00711	0.00764	0.01545	0.04188	0.63326	0.76299
586.4	NA	0.00496	0.00487	0.00504	0.0054	0.00561	0.00592	0.0119	0.03116	0.45534	0.87232
661.8	NA	0.00362	0.00359	0.00387	0.00407	0.0043	0.00443	0.00878	0.02271	0.32137	0.79684
746.8	NA	0.00268	0.00275	0.00292	0.00307	0.00332	0.00333	0.0066	0.01673	0.23425	0.6389
842.8	NA	0.00191	0.00209	0.0022	0.00241	0.00241	0.00269	0.00529	0.01329	0.17923	0.49665
951.1	NA	0.00134	0.00152	0.00164	0.00174	0.002	NA	NA	NA	NA	NA
1073.4	NA	0.00096	0.0011	0.00119	NA	NA	NA	NA	NA	NA	NA
1211.4	NA	0.00068	0.00081	NA	NA	NA	NA	NA	NA	NA	NA
1367.1	0.00107	0.00045	0.00061	NA	NA	NA	NA	NA	NA	NA	NA
1542.8	0.00099	0.00029	NA	NA	NA	NA	NA	NA	NA	NA	NA
1741.1	0.00083	0.0002	NA	NA	NA	NA	NA	NA	NA	NA	NA
1964.8	0.00043	NA	NA	NA	NA	NA	NA	NA	NA	NA	NA
2217.4	0.00017	NA	NA	NA	NA	NA	NA	NA	NA	NA	NA
2502.4	0	NA	NA	NA	NA	NA	NA	NA	NA	NA	NA
2824	-0.00003	NA	NA	NA	NA	NA	NA	NA	NA	NA	NA

Table A.34: FAS Linear Amp. Look-up Table for 0.400 Hz.

V_{S30} (m/s)	Soil Depth (m)										
	0	5	10	15	20	25	30	50	100	500	1000
95.6	NA	NA	NA	NA	NA	NA	0.24718	0.45586	0.95733	0.76523	0.7131
107.9	NA	NA	NA	NA	NA	0.19561	0.20997	0.38272	0.78053	0.6	0.80109
121.8	NA	NA	NA	NA	0.14998	0.16594	0.15918	0.28676	0.56586	0.54378	1.44293
137.4	NA	NA	NA	NA	0.12749	0.12547	0.12456	0.22116	0.4388	0.60713	1.3145
155.1	NA	NA	NA	0.10058	0.09712	0.09903	0.10078	0.18718	0.42657	0.71217	0.59831
175	NA	NA	NA	0.07769	0.07729	0.07731	0.07478	0.1321	0.27537	0.96164	0.7293
197.5	NA	NA	0.06497	0.06224	0.06032	0.0579	0.06068	0.1163	0.29696	0.73088	0.83391
222.9	NA	NA	0.05265	0.04934	0.04646	0.04654	0.04904	0.09336	0.23368	0.73563	0.8075
251.5	NA	NA	0.04026	0.03765	0.03658	0.03654	0.03772	0.07422	0.19745	0.95217	0.60854
283.9	NA	NA	0.03144	0.02861	0.02901	0.0284	0.03048	0.06263	0.17442	0.94157	0.65225
320.4	NA	0.02014	0.02389	0.02228	0.02192	0.02243	0.02439	0.05099	0.14523	1.04741	0.40941
361.5	NA	0.017	0.01808	0.0169	0.01709	0.01826	0.01889	0.04104	0.1198	1.28088	0.29151
408	NA	0.01298	0.01377	0.01305	0.01371	0.01404	0.01444	0.03009	0.08482	1.2624	0.32513
460.4	NA	0.01021	0.01025	0.01012	0.01049	0.01089	0.01123	0.02274	0.06205	0.96996	0.45623
519.6	NA	0.00756	0.00777	0.00754	0.00811	0.00834	0.00898	0.01817	0.04924	0.75267	0.6025
586.4	NA	0.00582	0.00572	0.00592	0.00634	0.00659	0.00696	0.01397	0.03666	0.53988	0.76419
661.8	NA	0.00426	0.00423	0.00455	0.00478	0.00505	0.00521	0.01033	0.02665	0.37878	0.79397
746.8	NA	0.00316	0.00324	0.00343	0.00361	0.00391	0.00392	0.00775	0.01968	0.27508	0.6845
842.8	NA	0.00225	0.00246	0.00259	0.00284	0.00283	0.00316	0.00621	0.01563	0.21103	0.55065
951.1	NA	0.00159	0.0018	0.00193	0.00205	0.00235	NA	NA	NA	NA	NA
1073.4	NA	0.00114	0.0013	0.0014	NA	NA	NA	NA	NA	NA	NA
1211.4	NA	0.0008	0.00095	NA	NA	NA	NA	NA	NA	NA	NA
1367.1	0.00128	0.00054	0.00072	NA	NA	NA	NA	NA	NA	NA	NA
1542.8	0.00118	0.00034	NA	NA	NA	NA	NA	NA	NA	NA	NA
1741.1	0.00099	0.00023	NA	NA	NA	NA	NA	NA	NA	NA	NA
1964.8	0.00053	NA	NA	NA	NA	NA	NA	NA	NA	NA	NA
2217.4	0.00021	NA	NA	NA	NA	NA	NA	NA	NA	NA	NA
2502.4	0.00001	NA	NA	NA	NA	NA	NA	NA	NA	NA	NA
2824	-0.00003	NA	NA	NA	NA	NA	NA	NA	NA	NA	NA

Table A.35: FAS Linear Amp. Look-up Table for 0.417 Hz.

V_{S30} (m/s)	Soil Depth (m)										
	0	5	10	15	20	25	30	50	100	500	1000
95.6	NA	NA	NA	NA	NA	NA	0.24718	0.45586	0.95733	0.76523	0.7131
107.9	NA	NA	NA	NA	NA	0.19561	0.20997	0.38272	0.78053	0.6	0.80109
121.8	NA	NA	NA	NA	0.14998	0.16594	0.15918	0.28676	0.56586	0.54378	1.44293
137.4	NA	NA	NA	NA	0.12749	0.12547	0.12456	0.22116	0.4388	0.60713	1.3145
155.1	NA	NA	NA	0.10058	0.09712	0.09903	0.10078	0.18718	0.42657	0.71217	0.59831
175	NA	NA	NA	0.07769	0.07729	0.07731	0.07478	0.1321	0.27537	0.96164	0.7293
197.5	NA	NA	0.06497	0.06224	0.06032	0.0579	0.06068	0.1163	0.29696	0.73088	0.83391
222.9	NA	NA	0.05265	0.04934	0.04646	0.04654	0.04904	0.09336	0.23368	0.73563	0.8075
251.5	NA	NA	0.04026	0.03765	0.03658	0.03654	0.03772	0.07422	0.19745	0.95217	0.60854
283.9	NA	NA	0.03144	0.02861	0.02901	0.0284	0.03048	0.06263	0.17442	0.94157	0.65225
320.4	NA	0.02014	0.02389	0.02228	0.02192	0.02243	0.02439	0.05099	0.14523	1.04741	0.40941
361.5	NA	0.017	0.01808	0.0169	0.01709	0.01826	0.01889	0.04104	0.1198	1.28088	0.29151
408	NA	0.01298	0.01377	0.01305	0.01371	0.01404	0.01444	0.03009	0.08482	1.2624	0.32513
460.4	NA	0.01021	0.01025	0.01012	0.01049	0.01089	0.01123	0.02274	0.06205	0.96996	0.45623
519.6	NA	0.00756	0.00777	0.00754	0.00811	0.00834	0.00898	0.01817	0.04924	0.75267	0.6025
586.4	NA	0.00582	0.00572	0.00592	0.00634	0.00659	0.00696	0.01397	0.03666	0.53988	0.76419
661.8	NA	0.00426	0.00423	0.00455	0.00478	0.00505	0.00521	0.01033	0.02665	0.37878	0.79397
746.8	NA	0.00316	0.00324	0.00343	0.00361	0.00391	0.00392	0.00775	0.01968	0.27508	0.6845
842.8	NA	0.00225	0.00246	0.00259	0.00284	0.00283	0.00316	0.00621	0.01563	0.21103	0.55065
951.1	NA	0.00159	0.0018	0.00193	0.00205	0.00235	NA	NA	NA	NA	NA
1073.4	NA	0.00114	0.0013	0.0014	NA	NA	NA	NA	NA	NA	NA
1211.4	NA	0.0008	0.00095	NA	NA	NA	NA	NA	NA	NA	NA
1367.1	0.00128	0.00054	0.00072	NA	NA	NA	NA	NA	NA	NA	NA
1542.8	0.00118	0.00034	NA	NA	NA	NA	NA	NA	NA	NA	NA
1741.1	0.00099	0.00023	NA	NA	NA	NA	NA	NA	NA	NA	NA
1964.8	0.00053	NA	NA	NA	NA	NA	NA	NA	NA	NA	NA
2217.4	0.00021	NA	NA	NA	NA	NA	NA	NA	NA	NA	NA
2502.4	0.00001	NA	NA	NA	NA	NA	NA	NA	NA	NA	NA
2824	-0.00003	NA	NA	NA	NA	NA	NA	NA	NA	NA	NA

Table A.36: FAS Linear Amp. Look-up Table for 0.454 Hz.

V_{S30} (m/s)	Soil Depth (m)										
	0	5	10	15	20	25	30	50	100	500	1000
95.6	NA	NA	NA	NA	NA	NA	0.30059	0.5619	1.22467	1.14509	0.95831
107.9	NA	NA	NA	NA	NA	0.23585	0.25338	0.467	0.97939	0.79123	0.72352
121.8	NA	NA	NA	NA	0.18062	0.1999	0.1918	0.34747	0.69971	0.55818	0.96448
137.4	NA	NA	NA	NA	0.15318	0.15087	0.14958	0.26715	0.53666	0.53504	1.34541
155.1	NA	NA	NA	0.12042	0.11674	0.1187	0.12071	0.22539	0.52407	0.69756	0.86791
175	NA	NA	NA	0.09299	0.09249	0.09253	0.08953	0.1588	0.33343	0.75921	0.82568
197.5	NA	NA	0.07779	0.07459	0.07222	0.06929	0.07265	0.13968	0.36172	0.64482	0.87675
222.9	NA	NA	0.06316	0.05903	0.05554	0.05567	0.05869	0.11196	0.28304	0.56496	1.10492
251.5	NA	NA	0.04813	0.04498	0.04374	0.04371	0.0451	0.0889	0.23864	0.74536	0.65045
283.9	NA	NA	0.03757	0.03423	0.03466	0.03393	0.03641	0.07498	0.21039	0.76231	0.85226
320.4	NA	0.02408	0.02854	0.02659	0.02619	0.02681	0.02915	0.06101	0.17465	0.81625	0.6181
361.5	NA	0.0203	0.02159	0.0202	0.02041	0.02182	0.02257	0.04908	0.14392	1.04883	0.37005
408	NA	0.01552	0.01645	0.01559	0.01639	0.01678	0.01725	0.03598	0.10169	1.27828	0.27017
460.4	NA	0.01219	0.01226	0.01209	0.01254	0.01301	0.01342	0.0272	0.07432	1.12078	0.32831
519.6	NA	0.00905	0.00929	0.00901	0.00969	0.00997	0.01074	0.0217	0.0589	0.90055	0.44077
586.4	NA	0.00696	0.00684	0.00708	0.00758	0.00788	0.00833	0.0167	0.04383	0.64944	0.60903
661.8	NA	0.0051	0.00506	0.00545	0.00572	0.00605	0.00623	0.01235	0.03187	0.45422	0.72936
746.8	NA	0.00379	0.00387	0.00411	0.00432	0.00468	0.0047	0.00926	0.02356	0.32862	0.6979
842.8	NA	0.0027	0.00295	0.0031	0.0034	0.00339	0.00378	0.00744	0.01868	0.25148	0.59547
951.1	NA	0.00191	0.00216	0.00232	0.00246	0.00283	NA	NA	NA	NA	NA
1073.4	NA	0.00137	0.00155	0.00168	NA	NA	NA	NA	NA	NA	NA
1211.4	NA	0.00096	0.00114	NA	NA	NA	NA	NA	NA	NA	NA
1367.1	0.00154	0.00065	0.00086	NA	NA	NA	NA	NA	NA	NA	NA
1542.8	0.00144	0.00042	NA	NA	NA	NA	NA	NA	NA	NA	NA
1741.1	0.00121	0.00028	NA	NA	NA	NA	NA	NA	NA	NA	NA
1964.8	0.00065	NA	NA	NA	NA	NA	NA	NA	NA	NA	NA
2217.4	0.00027	NA	NA	NA	NA	NA	NA	NA	NA	NA	NA
2502.4	0.00002	NA	NA	NA	NA	NA	NA	NA	NA	NA	NA
2824	-0.00003	NA	NA	NA	NA	NA	NA	NA	NA	NA	NA

Table A.37: FAS Linear Amp. Look-up Table for 0.500 Hz.

V_{S30} (m/s)	Soil Depth (m)										
	0	5	10	15	20	25	30	50	100	500	1000
95.6	NA	NA	NA	NA	NA	NA	0.37466	0.71502	1.67863	1.77271	1.55562
107.9	NA	NA	NA	NA	NA	0.29247	0.31504	0.59132	1.30698	1.28132	1.1172
121.8	NA	NA	NA	NA	0.22327	0.24693	0.23693	0.43451	0.90043	0.70768	0.72375
137.4	NA	NA	NA	NA	0.18918	0.18577	0.18428	0.33192	0.68101	0.5613	0.96363
155.1	NA	NA	NA	0.14878	0.14339	0.14601	0.14853	0.27962	0.66872	0.8605	1.32746
175	NA	NA	NA	0.11438	0.11368	0.11369	0.1099	0.19609	0.41657	0.61291	0.94504
197.5	NA	NA	0.0958	0.09152	0.08855	0.08496	0.08907	0.17205	0.45654	0.6344	0.88226
222.9	NA	NA	0.07726	0.07233	0.06804	0.06821	0.07186	0.13758	0.35215	0.4468	1.07698
251.5	NA	NA	0.05899	0.05511	0.0535	0.05346	0.0552	0.10919	0.2968	0.56528	0.84695
283.9	NA	NA	0.04599	0.04184	0.04242	0.04152	0.04456	0.09196	0.26083	0.57753	0.84161
320.4	NA	0.02961	0.0349	0.03253	0.03203	0.03277	0.03565	0.07473	0.21589	0.59426	0.95929
361.5	NA	0.02487	0.02643	0.02467	0.02497	0.02669	0.0276	0.06011	0.17737	0.76664	0.61505
408	NA	0.01896	0.02012	0.01907	0.02004	0.02052	0.0211	0.04404	0.12491	1.11882	0.29688
460.4	NA	0.01491	0.01497	0.01479	0.01533	0.01591	0.01641	0.03325	0.09109	1.19448	0.24791
519.6	NA	0.01105	0.01136	0.01103	0.01184	0.01219	0.01313	0.02654	0.07212	1.05477	0.30413
586.4	NA	0.00852	0.00837	0.00866	0.00927	0.00964	0.01018	0.02041	0.05362	0.79019	0.43806
661.8	NA	0.00624	0.00619	0.00666	0.007	0.0074	0.00763	0.0151	0.039	0.55626	0.60132
746.8	NA	0.00464	0.00474	0.00503	0.0053	0.00572	0.00575	0.01134	0.02878	0.40163	0.65314
842.8	NA	0.00331	0.00362	0.00379	0.00416	0.00415	0.00463	0.00912	0.02287	0.30593	0.61024
951.1	NA	0.00234	0.00264	0.00284	0.00301	0.00344	NA	NA	NA	NA	NA
1073.4	NA	0.00169	0.00191	0.00206	NA	NA	NA	NA	NA	NA	NA
1211.4	NA	0.00118	0.0014	NA	NA	NA	NA	NA	NA	NA	NA
1367.1	0.00191	0.0008	0.00105	NA	NA	NA	NA	NA	NA	NA	NA
1542.8	0.00177	0.00052	NA	NA	NA	NA	NA	NA	NA	NA	NA
1741.1	0.00151	0.00035	NA	NA	NA	NA	NA	NA	NA	NA	NA
1964.8	0.00082	NA	NA	NA	NA	NA	NA	NA	NA	NA	NA
2217.4	0.00036	NA	NA	NA	NA	NA	NA	NA	NA	NA	NA
2502.4	0.00005	NA	NA	NA	NA	NA	NA	NA	NA	NA	NA
2824	-0.00004	NA	NA	NA	NA	NA	NA	NA	NA	NA	NA

Table A.38: FAS Linear Amp. Look-up Table for 0.526 Hz.

V_{S30} (m/s)	Soil Depth (m)										
	0	5	10	15	20	25	30	50	100	500	1000
95.6	NA	NA	NA	NA	NA	NA	0.41589	0.80712	1.94577	1.83313	1.55404
107.9	NA	NA	NA	NA	NA	0.32523	0.34946	0.6638	1.51114	1.60414	1.44428
121.8	NA	NA	NA	NA	0.24756	0.27398	0.2625	0.48459	1.02206	0.84538	0.75256
137.4	NA	NA	NA	NA	0.20899	0.20528	0.20387	0.36847	0.76432	0.62062	0.82771
155.1	NA	NA	NA	0.16406	0.15807	0.16122	0.16415	0.30973	0.75482	0.9624	1.34658
175	NA	NA	NA	0.12605	0.12532	0.12535	0.12117	0.2167	0.46358	0.57736	1.0342
197.5	NA	NA	0.10558	0.10084	0.09766	0.09362	0.09816	0.19013	0.51185	0.64825	0.83893
222.9	NA	NA	0.08512	0.07973	0.07492	0.07513	0.07917	0.1518	0.39169	0.42148	0.94167
251.5	NA	NA	0.06496	0.0607	0.05891	0.05885	0.06078	0.12038	0.32965	0.50762	0.94313
283.9	NA	NA	0.05057	0.04605	0.04668	0.04571	0.04906	0.10142	0.28924	0.50698	0.7809
320.4	NA	0.03257	0.03844	0.03581	0.03526	0.03608	0.03925	0.08239	0.23898	0.5054	1.0634
361.5	NA	0.02732	0.02909	0.02717	0.02748	0.02937	0.03038	0.06621	0.19612	0.64526	0.7898
408	NA	0.02087	0.02213	0.02098	0.02205	0.02258	0.02323	0.04848	0.13784	1.00061	0.35018
460.4	NA	0.01641	0.01648	0.01628	0.01688	0.01751	0.01807	0.03661	0.10041	1.17416	0.23584
519.6	NA	0.01215	0.01251	0.01214	0.01304	0.01343	0.01445	0.02921	0.07949	1.1042	0.25861
586.4	NA	0.00937	0.00921	0.00954	0.01021	0.01061	0.01121	0.02249	0.05907	0.85923	0.36595
661.8	NA	0.00687	0.00682	0.00734	0.0077	0.00815	0.0084	0.01663	0.04296	0.61042	0.52962
746.8	NA	0.00511	0.00522	0.00554	0.00584	0.00631	0.00633	0.0125	0.03169	0.44131	0.61104
842.8	NA	0.00365	0.00398	0.00418	0.00458	0.00457	0.0051	0.01003	0.02518	0.33608	0.60096
951.1	NA	0.00259	0.00291	0.00313	0.00332	0.0038	NA	NA	NA	NA	NA
1073.4	NA	0.00186	0.0021	0.00227	NA	NA	NA	NA	NA	NA	NA
1211.4	NA	0.00131	0.00154	NA	NA	NA	NA	NA	NA	NA	NA
1367.1	0.0021	0.00089	0.00117	NA	NA	NA	NA	NA	NA	NA	NA
1542.8	0.00196	0.00057	NA	NA	NA	NA	NA	NA	NA	NA	NA
1741.1	0.00168	0.00038	NA	NA	NA	NA	NA	NA	NA	NA	NA
1964.8	0.00092	NA	NA	NA	NA	NA	NA	NA	NA	NA	NA
2217.4	0.00041	NA	NA	NA	NA	NA	NA	NA	NA	NA	NA
2502.4	0.00006	NA	NA	NA	NA	NA	NA	NA	NA	NA	NA
2824	-0.00004	NA	NA	NA	NA	NA	NA	NA	NA	NA	NA

Table A.39: FAS Linear Amp. Look-up Table for 0.556 Hz.

V_{S30} (m/s)	Soil Depth (m)										
	0	5	10	15	20	25	30	50	100	500	1000
95.6	NA	NA	NA	NA	NA	NA	0.47234	0.93246	2.22201	1.61849	1.26546
107.9	NA	NA	NA	NA	NA	0.36689	0.39543	0.76169	1.80638	1.82604	1.59441
121.8	NA	NA	NA	NA	0.27872	0.30897	0.29544	0.55067	1.18887	1.0884	0.93291
137.4	NA	NA	NA	NA	0.2349	0.23096	0.22882	0.41635	0.87958	0.74132	0.7866
155.1	NA	NA	NA	0.18393	0.17753	0.18095	0.18406	0.34997	0.87321	0.98728	1.13282
175	NA	NA	NA	0.14123	0.1405	0.1404	0.13581	0.24342	0.52601	0.57186	1.11824
197.5	NA	NA	0.11833	0.113	0.10923	0.10476	0.10994	0.21365	0.587	0.65627	0.75756
222.9	NA	NA	0.0953	0.08927	0.08385	0.08402	0.08861	0.17032	0.44409	0.42437	0.78081
251.5	NA	NA	0.07266	0.06785	0.06594	0.06582	0.06799	0.13497	0.37312	0.47175	0.98752
283.9	NA	NA	0.05658	0.05148	0.05218	0.05111	0.05485	0.11362	0.32665	0.44813	0.739
320.4	NA	0.03634	0.04296	0.04004	0.03939	0.04033	0.04388	0.09222	0.26906	0.42172	1.04885
361.5	NA	0.03059	0.03249	0.03035	0.03072	0.03283	0.03396	0.07411	0.22055	0.52514	0.9886
408	NA	0.02328	0.02472	0.02344	0.02465	0.02524	0.02597	0.05422	0.15462	0.85316	0.45529
460.4	NA	0.01834	0.01841	0.01819	0.01886	0.01958	0.02019	0.04094	0.11253	1.10058	0.24922
519.6	NA	0.01357	0.01397	0.01357	0.01458	0.01501	0.01615	0.03267	0.08902	1.12268	0.22619
586.4	NA	0.01046	0.0103	0.01066	0.01141	0.01187	0.01254	0.02515	0.06614	0.93246	0.2953
661.8	NA	0.00768	0.00762	0.00821	0.00861	0.00912	0.00939	0.0186	0.04806	0.67653	0.44731
746.8	NA	0.00572	0.00584	0.0062	0.00653	0.00706	0.00709	0.01399	0.03543	0.49081	0.54924
842.8	NA	0.00409	0.00446	0.00468	0.00513	0.00512	0.00572	0.01123	0.02816	0.37417	0.57419
951.1	NA	0.0029	0.00326	0.0035	0.00372	0.00425	NA	NA	NA	NA	NA
1073.4	NA	0.00209	0.00235	0.00254	NA	NA	NA	NA	NA	NA	NA
1211.4	NA	0.00147	0.00173	NA	NA	NA	NA	NA	NA	NA	NA
1367.1	0.00236	0.001	0.0013	NA	NA	NA	NA	NA	NA	NA	NA
1542.8	0.00221	0.00064	NA	NA	NA	NA	NA	NA	NA	NA	NA
1741.1	0.00189	0.00043	NA	NA	NA	NA	NA	NA	NA	NA	NA
1964.8	0.00104	NA	NA	NA	NA	NA	NA	NA	NA	NA	NA
2217.4	0.00047	NA	NA	NA	NA	NA	NA	NA	NA	NA	NA
2502.4	0.00007	NA	NA	NA	NA	NA	NA	NA	NA	NA	NA
2824	-0.00004	NA	NA	NA	NA	NA	NA	NA	NA	NA	NA

Table A.40: FAS Linear Amp. Look-up Table for 0.588 Hz.

V_{S30} (m/s)	Soil Depth (m)										
	0	5	10	15	20	25	30	50	100	500	1000
95.6	NA	NA	NA	NA	NA	NA	0.54479	1.10331	2.24871	1.24129	1.01062
107.9	NA	NA	NA	NA	NA	0.42097	0.45284	0.88947	2.1377	1.69988	1.3829
121.8	NA	NA	NA	NA	0.3179	0.35205	0.33689	0.63638	1.42708	1.47051	1.31287
137.4	NA	NA	NA	NA	0.26788	0.26304	0.26061	0.47805	1.03379	0.94836	0.8416
155.1	NA	NA	NA	0.20929	0.20189	0.20554	0.20902	0.40064	1.03595	0.87538	0.81098
175	NA	NA	NA	0.16041	0.15929	0.15926	0.15383	0.27722	0.60673	0.61496	1.10368
197.5	NA	NA	0.13407	0.128	0.12379	0.11855	0.12457	0.2433	0.68565	0.65339	0.72172
222.9	NA	NA	0.10805	0.10098	0.09489	0.0951	0.10025	0.19335	0.51128	0.46397	0.64142
251.5	NA	NA	0.08224	0.07674	0.07449	0.07446	0.07688	0.15304	0.42868	0.47599	0.95668
283.9	NA	NA	0.06395	0.05821	0.05899	0.05772	0.06198	0.12862	0.37379	0.41863	0.72344
320.4	NA	0.04097	0.0485	0.04517	0.04448	0.04553	0.04955	0.10433	0.30679	0.35768	0.88448
361.5	NA	0.03454	0.03667	0.03426	0.03467	0.03707	0.03834	0.08377	0.25075	0.42177	1.09818
408	NA	0.02633	0.02791	0.02646	0.02782	0.0285	0.02931	0.06126	0.17535	0.70082	0.62743
460.4	NA	0.02069	0.02078	0.02052	0.02129	0.02209	0.02278	0.04624	0.12736	0.97688	0.30351
519.6	NA	0.01533	0.01577	0.01532	0.01645	0.01695	0.01824	0.03688	0.10063	1.08586	0.21956
586.4	NA	0.01182	0.01162	0.01203	0.01288	0.01339	0.01416	0.02838	0.07468	0.98988	0.23835
661.8	NA	0.00867	0.00861	0.00926	0.00973	0.01029	0.0106	0.021	0.05423	0.7487	0.36452
746.8	NA	0.00646	0.0066	0.007	0.00737	0.00796	0.008	0.01576	0.04002	0.54813	0.4745
842.8	NA	0.00462	0.00503	0.00528	0.00579	0.00579	0.00645	0.01265	0.0318	0.41896	0.52973
951.1	NA	0.00328	0.00369	0.00395	0.0042	0.0048	NA	NA	NA	NA	NA
1073.4	NA	0.00236	0.00266	0.00287	NA	NA	NA	NA	NA	NA	NA
1211.4	NA	0.00166	0.00196	NA	NA	NA	NA	NA	NA	NA	NA
1367.1	0.00268	0.00113	0.00147	NA	NA	NA	NA	NA	NA	NA	NA
1542.8	0.00251	0.00073	NA	NA	NA	NA	NA	NA	NA	NA	NA
1741.1	0.00215	0.00049	NA	NA	NA	NA	NA	NA	NA	NA	NA
1964.8	0.00119	NA	NA	NA	NA	NA	NA	NA	NA	NA	NA
2217.4	0.00055	NA	NA	NA	NA	NA	NA	NA	NA	NA	NA
2502.4	0.00009	NA	NA	NA	NA	NA	NA	NA	NA	NA	NA
2824	-0.00004	NA	NA	NA	NA	NA	NA	NA	NA	NA	NA

Table A.41: FAS Linear Amp. Look-up Table for 0.625 Hz.

V_{S30} (m/s)	Soil Depth (m)										
	0	5	10	15	20	25	30	50	100	500	1000
95.6	NA	NA	NA	NA	NA	NA	0.62199	1.31085	2.00822	1.03605	1.08467
107.9	NA	NA	NA	NA	NA	0.47802	0.51562	1.03818	2.2504	1.37117	1.07656
121.8	NA	NA	NA	NA	0.36028	0.39995	0.38224	0.7326	1.70701	1.74882	1.55085
137.4	NA	NA	NA	NA	0.30264	0.29745	0.29451	0.54575	1.21249	1.19033	0.99795
155.1	NA	NA	NA	0.23647	0.22768	0.23182	0.23573	0.45542	1.2201	0.75592	0.66879
175	NA	NA	NA	0.18056	0.17922	0.17922	0.17336	0.31325	0.69673	0.68102	0.98842
197.5	NA	NA	0.15055	0.14388	0.1393	0.13335	0.14001	0.27493	0.79635	0.68579	0.79557
222.9	NA	NA	0.12139	0.11346	0.10656	0.10677	0.11259	0.21798	0.58473	0.52445	0.57593
251.5	NA	NA	0.09232	0.08618	0.08362	0.08354	0.08624	0.17218	0.48971	0.5217	0.8926
283.9	NA	NA	0.0718	0.06527	0.06619	0.06477	0.06954	0.14464	0.42541	0.42827	0.71775
320.4	NA	0.04609	0.05441	0.05068	0.04988	0.05105	0.05555	0.11724	0.34763	0.32617	0.69654
361.5	NA	0.03861	0.04111	0.03842	0.03886	0.04155	0.04298	0.09405	0.28328	0.35011	1.04653
408	NA	0.02951	0.03129	0.02965	0.03116	0.03194	0.03285	0.06873	0.19738	0.5739	0.82026
460.4	NA	0.0232	0.02329	0.02299	0.02385	0.02474	0.02552	0.05181	0.14309	0.84114	0.39953
519.6	NA	0.0172	0.01767	0.01716	0.01843	0.01897	0.02043	0.04133	0.11295	1.00357	0.24436
586.4	NA	0.01324	0.01302	0.01348	0.01443	0.01501	0.01587	0.03178	0.08381	1.01093	0.20604
661.8	NA	0.00972	0.00965	0.01038	0.0109	0.01154	0.01188	0.02352	0.06081	0.81165	0.29724
746.8	NA	0.00725	0.00739	0.00784	0.00827	0.00892	0.00898	0.01767	0.04492	0.60473	0.4026
842.8	NA	0.00518	0.00564	0.00592	0.00649	0.00649	0.00723	0.0142	0.03561	0.46372	0.47766
951.1	NA	0.00368	0.00413	0.00443	0.0047	0.00539	NA	NA	NA	NA	NA
1073.4	NA	0.00265	0.00299	0.00322	NA	NA	NA	NA	NA	NA	NA
1211.4	NA	0.00187	0.00219	NA	NA	NA	NA	NA	NA	NA	NA
1367.1	0.00302	0.00127	0.00165	NA	NA	NA	NA	NA	NA	NA	NA
1542.8	0.00283	0.00082	NA	NA	NA	NA	NA	NA	NA	NA	NA
1741.1	0.00242	0.00055	NA	NA	NA	NA	NA	NA	NA	NA	NA
1964.8	0.00136	NA	NA	NA	NA	NA	NA	NA	NA	NA	NA
2217.4	0.00063	NA	NA	NA	NA	NA	NA	NA	NA	NA	NA
2502.4	0.00012	NA	NA	NA	NA	NA	NA	NA	NA	NA	NA
2824	-0.00004	NA	NA	NA	NA	NA	NA	NA	NA	NA	NA

Table A.42: FAS Linear Amp. Look-up Table for 0.667 Hz.

V_{S30} (m/s)	Soil Depth (m)										
	0	5	10	15	20	25	30	50	100	500	1000
95.6	NA	NA	NA	NA	NA	NA	0.72921	1.61864	1.63175	0.99225	1.46665
107.9	NA	NA	NA	NA	NA	0.55615	0.60355	1.25893	2.06562	1.0702	1.04346
121.8	NA	NA	NA	NA	0.41737	0.46362	0.44269	0.8654	2.05195	1.72291	1.42664
137.4	NA	NA	NA	NA	0.34948	0.34258	0.33948	0.63742	1.47324	1.48845	1.26891
155.1	NA	NA	NA	0.2722	0.26166	0.26649	0.27115	0.52991	1.43195	0.71487	0.75345
175	NA	NA	NA	0.20711	0.20576	0.20576	0.19882	0.36142	0.82022	0.75723	0.85399
197.5	NA	NA	0.17305	0.16493	0.15932	0.15268	0.16022	0.31702	0.93375	0.78341	0.91925
222.9	NA	NA	0.13891	0.12992	0.1219	0.12206	0.12875	0.25032	0.68693	0.6355	0.63091
251.5	NA	NA	0.10545	0.09844	0.09556	0.09539	0.09854	0.19752	0.57267	0.59247	0.76938
283.9	NA	NA	0.082	0.07449	0.07547	0.07392	0.07935	0.16569	0.49459	0.49441	0.7456
320.4	NA	0.0525	0.06211	0.05783	0.0569	0.05823	0.06338	0.13403	0.40198	0.32802	0.54106
361.5	NA	0.04407	0.04691	0.04379	0.04433	0.04737	0.04902	0.10748	0.32645	0.29873	0.84198
408	NA	0.03364	0.03567	0.03381	0.03552	0.0364	0.03744	0.07842	0.22653	0.45002	1.00319
460.4	NA	0.02647	0.02655	0.02621	0.02719	0.02821	0.02909	0.0591	0.16374	0.6838	0.56767
519.6	NA	0.01957	0.02014	0.01956	0.021	0.02163	0.02329	0.04712	0.12908	0.87167	0.31668
586.4	NA	0.01509	0.01484	0.01536	0.01644	0.01711	0.01808	0.03625	0.0957	0.98659	0.19717
661.8	NA	0.01108	0.011	0.01183	0.01242	0.01314	0.01355	0.02681	0.0694	0.86894	0.23637
746.8	NA	0.00827	0.00843	0.00894	0.00942	0.01018	0.01024	0.02017	0.05111	0.66945	0.32323
842.8	NA	0.00591	0.00643	0.00675	0.0074	0.0074	0.00824	0.01617	0.0407	0.51894	0.40867
951.1	NA	0.00421	0.00472	0.00505	0.00537	0.00614	NA	NA	NA	NA	NA
1073.4	NA	0.00303	0.00341	0.00368	NA	NA	NA	NA	NA	NA	NA
1211.4	NA	0.00213	0.0025	NA	NA	NA	NA	NA	NA	NA	NA
1367.1	0.00347	0.00145	0.00188	NA	NA	NA	NA	NA	NA	NA	NA
1542.8	0.00324	0.00094	NA	NA	NA	NA	NA	NA	NA	NA	NA
1741.1	0.00278	0.00063	NA	NA	NA	NA	NA	NA	NA	NA	NA
1964.8	0.00157	NA	NA	NA	NA	NA	NA	NA	NA	NA	NA
2217.4	0.00074	NA	NA	NA	NA	NA	NA	NA	NA	NA	NA
2502.4	0.00015	NA	NA	NA	NA	NA	NA	NA	NA	NA	NA
2824	-0.00003	NA	NA	NA	NA	NA	NA	NA	NA	NA	NA

Table A.43: FAS Linear Amp. Look-up Table for 0.714 Hz.

V_{S30} (m/s)	Soil Depth (m)										
	0	5	10	15	20	25	30	50	100	500	1000
95.6	NA	NA	NA	NA	NA	NA	0.88535	2.06388	1.31394	1.22674	1.49777
107.9	NA	NA	NA	NA	NA	0.66683	0.72151	1.59211	1.6587	0.99521	1.44368
121.8	NA	NA	NA	NA	0.49323	0.54961	0.52458	1.05793	2.20143	1.33572	1.07654
137.4	NA	NA	NA	NA	0.41189	0.40394	0.39981	0.76569	1.83488	1.6255	1.39581
155.1	NA	NA	NA	0.31974	0.30701	0.31261	0.31795	0.63168	1.56446	0.84922	1.03885
175	NA	NA	NA	0.24232	0.24054	0.24049	0.23201	0.42565	0.99695	0.87773	0.83317
197.5	NA	NA	0.20141	0.19238	0.18598	0.17776	0.1869	0.37297	1.06918	0.88985	0.94225
222.9	NA	NA	0.16188	0.15118	0.14169	0.14218	0.1499	0.29364	0.82822	0.87942	0.89062
251.5	NA	NA	0.12282	0.11447	0.11105	0.11095	0.11463	0.23092	0.68971	0.64025	0.60776
283.9	NA	NA	0.09527	0.08658	0.08772	0.08581	0.09222	0.19335	0.59064	0.65804	0.83661
320.4	NA	0.06079	0.07206	0.0671	0.06606	0.0676	0.0736	0.15623	0.47586	0.39662	0.50298
361.5	NA	0.05117	0.05438	0.05082	0.0514	0.05499	0.05688	0.12509	0.3846	0.2899	0.57933
408	NA	0.039	0.04136	0.03919	0.04121	0.04224	0.04343	0.09111	0.26516	0.34811	1.01252
460.4	NA	0.03063	0.03078	0.03038	0.03152	0.03271	0.03375	0.06864	0.19108	0.52613	0.80458
519.6	NA	0.02271	0.02335	0.02268	0.02435	0.02507	0.027	0.05467	0.15033	0.70613	0.47299
586.4	NA	0.0175	0.0172	0.01782	0.01907	0.01983	0.02098	0.04208	0.11124	0.89624	0.23466
661.8	NA	0.01284	0.01276	0.01372	0.01441	0.01525	0.01572	0.03112	0.08058	0.89455	0.19747
746.8	NA	0.00959	0.00978	0.01037	0.01093	0.01181	0.01186	0.02338	0.05932	0.73324	0.24789
842.8	NA	0.00686	0.00746	0.00784	0.00859	0.00859	0.00956	0.01878	0.04713	0.58231	0.33027
951.1	NA	0.00489	0.00548	0.00587	0.00623	0.00713	NA	NA	NA	NA	NA
1073.4	NA	0.00353	0.00396	0.00426	NA	NA	NA	NA	NA	NA	NA
1211.4	NA	0.00248	0.00291	NA	NA	NA	NA	NA	NA	NA	NA
1367.1	0.00403	0.00169	0.00219	NA	NA	NA	NA	NA	NA	NA	NA
1542.8	0.00379	0.00109	NA	NA	NA	NA	NA	NA	NA	NA	NA
1741.1	0.00325	0.00074	NA	NA	NA	NA	NA	NA	NA	NA	NA
1964.8	0.00184	NA	NA	NA	NA	NA	NA	NA	NA	NA	NA
2217.4	0.00088	NA	NA	NA	NA	NA	NA	NA	NA	NA	NA
2502.4	0.00018	NA	NA	NA	NA	NA	NA	NA	NA	NA	NA
2824	-0.00003	NA	NA	NA	NA	NA	NA	NA	NA	NA	NA

Table A.44: FAS Linear Amp. Look-up Table for 0.769 Hz.

V_{S30} (m/s)	Soil Depth (m)										
	0	5	10	15	20	25	30	50	100	500	1000
95.6	NA	NA	NA	NA	NA	NA	1.08182	2.276	1.09028	1.66423	1.15221
107.9	NA	NA	NA	NA	NA	0.79963	0.87033	2.02137	1.32846	1.19054	1.5236
121.8	NA	NA	NA	NA	0.58682	0.65728	0.62373	1.31119	1.97514	1.04628	1.10664
137.4	NA	NA	NA	NA	0.48602	0.47598	0.47141	0.92495	2.12117	1.41573	1.21868
155.1	NA	NA	NA	0.37517	0.36028	0.36656	0.3732	0.75661	1.58765	1.12999	1.16549
175	NA	NA	NA	0.28369	0.28134	0.28129	0.27091	0.50264	1.20728	1.04084	0.88363
197.5	NA	NA	0.23557	0.22454	0.21664	0.20707	0.21771	0.43994	1.18469	0.93213	0.83346
222.9	NA	NA	0.18848	0.17588	0.16491	0.1652	0.17444	0.344	0.99245	1.14864	1.06233
251.5	NA	NA	0.14271	0.13295	0.12893	0.12882	0.13305	0.26987	0.8322	0.67603	0.58964
283.9	NA	NA	0.11058	0.1004	0.10176	0.09955	0.10695	0.22548	0.70765	0.83941	0.83876
320.4	NA	0.07049	0.08362	0.07776	0.07653	0.07835	0.08531	0.18174	0.56428	0.5494	0.61662
361.5	NA	0.05932	0.06299	0.05885	0.05952	0.06366	0.06589	0.14534	0.45319	0.33943	0.42888
408	NA	0.0451	0.04786	0.04537	0.0477	0.04889	0.05029	0.1057	0.31015	0.28654	0.81088
460.4	NA	0.03548	0.03562	0.03514	0.03649	0.03786	0.03906	0.07952	0.22256	0.39896	0.9723
519.6	NA	0.02625	0.02701	0.02625	0.02818	0.02901	0.03123	0.06334	0.17471	0.55073	0.69647
586.4	NA	0.02024	0.0199	0.02061	0.02206	0.02294	0.02427	0.04871	0.12904	0.76668	0.32865
661.8	NA	0.01486	0.01477	0.01587	0.01666	0.01765	0.01818	0.03598	0.09335	0.86949	0.19447
746.8	NA	0.0111	0.01132	0.012	0.01265	0.01367	0.01373	0.02708	0.06873	0.77575	0.19595
842.8	NA	0.00794	0.00864	0.00907	0.00993	0.00993	0.01107	0.02174	0.05457	0.6395	0.25988
951.1	NA	0.00567	0.00634	0.00679	0.00721	0.00824	NA	NA	NA	NA	NA
1073.4	NA	0.00409	0.00458	0.00494	NA	NA	NA	NA	NA	NA	NA
1211.4	NA	0.00287	0.00337	NA	NA	NA	NA	NA	NA	NA	NA
1367.1	0.00468	0.00197	0.00253	NA	NA	NA	NA	NA	NA	NA	NA
1542.8	0.00441	0.00127	NA	NA	NA	NA	NA	NA	NA	NA	NA
1741.1	0.00379	0.00086	NA	NA	NA	NA	NA	NA	NA	NA	NA
1964.8	0.00216	NA	NA	NA	NA	NA	NA	NA	NA	NA	NA
2217.4	0.00104	NA	NA	NA	NA	NA	NA	NA	NA	NA	NA
2502.4	0.00023	NA	NA	NA	NA	NA	NA	NA	NA	NA	NA
2824	-0.00003	NA	NA	NA	NA	NA	NA	NA	NA	NA	NA

Table A.45: FAS Linear Amp. Look-up Table for 0.833 Hz.

V_{S30} (m/s)	Soil Depth (m)										
	0	5	10	15	20	25	30	50	100	500	1000
95.6	NA	NA	NA	NA	NA	NA	1.39157	1.94929	0.94324	1.60733	1.36085
107.9	NA	NA	NA	NA	NA	0.99699	1.09094	2.25287	1.08316	1.66411	1.16531
121.8	NA	NA	NA	NA	0.71577	0.80502	0.76274	1.70715	1.54615	1.02995	1.50482
137.4	NA	NA	NA	NA	0.59085	0.57681	0.56998	1.1634	2.05547	1.08065	1.07719
155.1	NA	NA	NA	0.45288	0.43301	0.44022	0.44866	0.93803	1.62244	1.46056	1.10454
175	NA	NA	NA	0.3391	0.33604	0.33583	0.32327	0.60972	1.46724	1.22422	1.07858
197.5	NA	NA	0.28134	0.26757	0.25785	0.24625	0.25912	0.5327	1.33019	0.98169	0.78726
222.9	NA	NA	0.22433	0.20912	0.19558	0.19595	0.20695	0.41234	1.20339	1.19856	0.89923
251.5	NA	NA	0.16912	0.15753	0.15258	0.15245	0.15757	0.32249	1.01361	0.82604	0.84053
283.9	NA	NA	0.13076	0.11862	0.12026	0.1177	0.12651	0.26868	0.87683	0.90651	0.67551
320.4	NA	0.08327	0.09874	0.09182	0.09038	0.09249	0.10074	0.21585	0.68845	0.81948	0.85285
361.5	NA	0.06989	0.07435	0.06941	0.07025	0.07514	0.07778	0.17224	0.54784	0.49326	0.49971
408	NA	0.05318	0.05647	0.05352	0.05625	0.05765	0.05932	0.12504	0.3711	0.27398	0.52754
460.4	NA	0.04178	0.04198	0.04144	0.04301	0.04464	0.04601	0.09389	0.26456	0.29906	0.90992
519.6	NA	0.03091	0.03183	0.03092	0.0332	0.0342	0.03681	0.07474	0.20722	0.40608	0.92209
586.4	NA	0.02384	0.02346	0.02429	0.02599	0.02703	0.02859	0.05743	0.15253	0.60699	0.51952
661.8	NA	0.01751	0.0174	0.01869	0.01963	0.02079	0.02142	0.04242	0.11025	0.78141	0.24657
746.8	NA	0.01309	0.01333	0.01414	0.01491	0.0161	0.01618	0.03186	0.08096	0.78154	0.17341
842.8	NA	0.00936	0.01018	0.01069	0.0117	0.0117	0.01302	0.02559	0.0643	0.68578	0.20275
951.1	NA	0.00669	0.00747	0.008	0.00849	0.00972	NA	NA	NA	NA	NA
1073.4	NA	0.00483	0.0054	0.00582	NA	NA	NA	NA	NA	NA	NA
1211.4	NA	0.00339	0.00397	NA	NA	NA	NA	NA	NA	NA	NA
1367.1	0.00555	0.00233	0.00299	NA	NA	NA	NA	NA	NA	NA	NA
1542.8	0.00521	0.0015	NA	NA	NA	NA	NA	NA	NA	NA	NA
1741.1	0.00449	0.00102	NA	NA	NA	NA	NA	NA	NA	NA	NA
1964.8	0.00257	NA	NA	NA	NA	NA	NA	NA	NA	NA	NA
2217.4	0.00126	NA	NA	NA	NA	NA	NA	NA	NA	NA	NA
2502.4	0.00029	NA	NA	NA	NA	NA	NA	NA	NA	NA	NA
2824	-0.00003	NA	NA	NA	NA	NA	NA	NA	NA	NA	NA

Table A.46: FAS Linear Amp. Look-up Table for 0.909 Hz.

V_{S30} (m/s)	Soil Depth (m)										
	0	5	10	15	20	25	30	50	100	500	1000
95.6	NA	NA	NA	NA	NA	NA	1.88489	1.416	0.87985	1.08748	1.30693
107.9	NA	NA	NA	NA	NA	1.30361	1.43985	1.86764	0.92717	1.53784	1.40128
121.8	NA	NA	NA	NA	0.9098	1.02609	0.96729	2.17266	1.19904	1.42167	1.35418
137.4	NA	NA	NA	NA	0.73783	0.7178	0.70958	1.53871	1.63712	1.022	1.32697
155.1	NA	NA	NA	0.55875	0.53278	0.54219	0.55267	1.21614	1.61801	1.35166	1.07743
175	NA	NA	NA	0.41479	0.41037	0.4101	0.39452	0.76038	1.77046	1.33524	1.20282
197.5	NA	NA	0.34287	0.32558	0.31315	0.29862	0.31458	0.66374	1.45982	0.96583	0.90593
222.9	NA	NA	0.27265	0.25342	0.2367	0.23701	0.25009	0.50634	1.48696	0.97388	0.69333
251.5	NA	NA	0.20443	0.19016	0.18414	0.18378	0.18998	0.39377	1.19116	1.01847	0.9712
283.9	NA	NA	0.15763	0.14281	0.1446	0.14152	0.15222	0.32646	1.10922	0.83626	0.65666
320.4	NA	0.10026	0.11874	0.11025	0.10846	0.11104	0.12104	0.26123	0.86531	1.07387	0.88274
361.5	NA	0.08387	0.08929	0.08326	0.08423	0.09015	0.09329	0.20788	0.67979	0.80529	0.79682
408	NA	0.06379	0.06767	0.06409	0.06741	0.0691	0.07111	0.15047	0.4537	0.34469	0.39741
460.4	NA	0.0501	0.05028	0.04962	0.05152	0.05346	0.05514	0.11273	0.32064	0.24586	0.59941
519.6	NA	0.03707	0.03811	0.03702	0.03975	0.04095	0.04408	0.08962	0.25007	0.29055	0.87905
586.4	NA	0.02854	0.02806	0.02907	0.03111	0.03235	0.03422	0.06883	0.18374	0.44412	0.77976
661.8	NA	0.02096	0.02083	0.02237	0.0235	0.0249	0.02564	0.05079	0.13237	0.64076	0.38583
746.8	NA	0.01567	0.01596	0.01693	0.01785	0.01927	0.01939	0.03818	0.09723	0.72875	0.20312
842.8	NA	0.01121	0.01218	0.01279	0.01401	0.01403	0.01562	0.03066	0.07718	0.6999	0.17395
951.1	NA	0.00802	0.00895	0.00958	0.01018	0.01161	NA	NA	NA	NA	NA
1073.4	NA	0.00579	0.00648	0.00697	NA	NA	NA	NA	NA	NA	NA
1211.4	NA	0.00407	0.00475	NA	NA	NA	NA	NA	NA	NA	NA
1367.1	0.00664	0.00279	0.00358	NA	NA	NA	NA	NA	NA	NA	NA
1542.8	0.00626	0.0018	NA	NA	NA	NA	NA	NA	NA	NA	NA
1741.1	0.00541	0.00122	NA	NA	NA	NA	NA	NA	NA	NA	NA
1964.8	0.00313	NA	NA	NA	NA	NA	NA	NA	NA	NA	NA
2217.4	0.00155	NA	NA	NA	NA	NA	NA	NA	NA	NA	NA
2502.4	0.00037	NA	NA	NA	NA	NA	NA	NA	NA	NA	NA
2824	-0.00002	NA	NA	NA	NA	NA	NA	NA	NA	NA	NA

Table A.47: FAS Linear Amp. Look-up Table for 1.0 Hz.

V_{S30} (m/s)	Soil Depth (m)										
	0	5	10	15	20	25	30	50	100	500	1000
95.6	NA	NA	NA	NA	NA	NA	2.2665	1.03067	0.94508	1.21232	1.17828
107.9	NA	NA	NA	NA	NA	1.80558	1.99432	1.32276	0.88162	1.05364	1.21728
121.8	NA	NA	NA	NA	1.2026	1.38144	1.2834	2.06036	0.97813	1.67951	1.26943
137.4	NA	NA	NA	NA	0.95392	0.9265	0.91301	2.01592	1.24022	1.3682	1.37209
155.1	NA	NA	NA	0.71069	0.67423	0.68506	0.69932	1.63151	1.37122	0.92176	1.01225
175	NA	NA	NA	0.5204	0.51359	0.51281	0.4915	0.9814	1.9424	1.20154	1.11041
197.5	NA	NA	0.4264	0.40475	0.38808	0.36944	0.38984	0.85504	1.48823	0.89102	0.90803
222.9	NA	NA	0.33721	0.31247	0.29149	0.29196	0.30862	0.6385	1.72833	0.75366	0.9137
251.5	NA	NA	0.25157	0.2336	0.22581	0.22556	0.23324	0.49203	1.34248	1.00871	0.74801
283.9	NA	NA	0.1933	0.17475	0.17716	0.17315	0.18643	0.4056	1.35014	0.78644	0.86162
320.4	NA	0.12175	0.14509	0.13472	0.13247	0.13563	0.14791	0.32262	1.11705	1.01118	0.61303
361.5	NA	0.1023	0.10893	0.10151	0.10268	0.10996	0.11381	0.25569	0.86931	1.08924	0.89086
408	NA	0.07761	0.08246	0.07808	0.08213	0.08417	0.0866	0.18417	0.5677	0.55758	0.56805
460.4	NA	0.06093	0.06121	0.06039	0.0627	0.06508	0.06711	0.13762	0.39677	0.27159	0.36376
519.6	NA	0.04504	0.04635	0.04502	0.04834	0.04979	0.05361	0.10922	0.30774	0.22873	0.55014
586.4	NA	0.03468	0.03411	0.03534	0.03783	0.03933	0.04162	0.08383	0.22494	0.30749	0.85225
661.8	NA	0.02548	0.02533	0.02719	0.02855	0.03025	0.03118	0.06181	0.16157	0.47782	0.62222
746.8	NA	0.01905	0.0194	0.02056	0.02169	0.02341	0.02354	0.04645	0.11832	0.61412	0.31788
842.8	NA	0.01363	0.01481	0.01555	0.01701	0.01704	0.01897	0.03727	0.09376	0.65848	0.2008
951.1	NA	0.00975	0.01088	0.01164	0.01237	0.01411	NA	NA	NA	NA	NA
1073.4	NA	0.00705	0.00787	0.00847	NA	NA	NA	NA	NA	NA	NA
1211.4	NA	0.00496	0.00577	NA	NA	NA	NA	NA	NA	NA	NA
1367.1	0.00814	0.00341	0.00435	NA	NA	NA	NA	NA	NA	NA	NA
1542.8	0.00766	0.0022	NA	NA	NA	NA	NA	NA	NA	NA	NA
1741.1	0.00663	0.00149	NA	NA	NA	NA	NA	NA	NA	NA	NA
1964.8	0.00383	NA	NA	NA	NA	NA	NA	NA	NA	NA	NA
2217.4	0.00192	NA	NA	NA	NA	NA	NA	NA	NA	NA	NA
2502.4	0.00048	NA	NA	NA	NA	NA	NA	NA	NA	NA	NA
2824	-0.00001	NA	NA	NA	NA	NA	NA	NA	NA	NA	NA

Table A.48: FAS Linear Amp. Look-up Table for 1.053 Hz.

V_{S30} (m/s)	Soil Depth (m)										
	0	5	10	15	20	25	30	50	100	500	1000
95.6	NA	NA	NA	NA	NA	NA	2.16241	0.90554	1.03463	1.44214	1.24382
107.9	NA	NA	NA	NA	NA	2.08189	2.20655	1.13858	0.90709	1.08087	1.10668
121.8	NA	NA	NA	NA	1.38463	1.60907	1.48642	1.8001	0.91934	1.48199	1.41345
137.4	NA	NA	NA	NA	1.08532	1.0512	1.03425	2.12165	1.11083	1.54471	1.24643
155.1	NA	NA	NA	0.79894	0.7562	0.76841	0.78456	1.822	1.21646	0.87439	1.12841
175	NA	NA	NA	0.57909	0.57183	0.57019	0.54625	1.11463	1.87296	1.09234	1.07851
197.5	NA	NA	0.47355	0.44847	0.42979	0.40869	0.43167	0.96792	1.47444	0.91885	0.90356
222.9	NA	NA	0.37285	0.34542	0.32159	0.32218	0.34069	0.7144	1.73761	0.69547	1.00359
251.5	NA	NA	0.27749	0.25734	0.24857	0.24826	0.25682	0.54703	1.4127	0.96669	0.70691
283.9	NA	NA	0.21266	0.19226	0.19476	0.19025	0.20482	0.44932	1.42147	0.76671	0.89072
320.4	NA	0.13358	0.15949	0.14791	0.1454	0.14883	0.1624	0.35622	1.24723	0.87407	0.58123
361.5	NA	0.11227	0.1195	0.11134	0.11257	0.12054	0.12478	0.28167	0.97727	1.10035	0.79231
408	NA	0.08513	0.09041	0.08553	0.08996	0.09223	0.09488	0.20229	0.63136	0.70254	0.71547
460.4	NA	0.06676	0.06705	0.06611	0.06866	0.07125	0.0735	0.15102	0.43869	0.32076	0.35519
519.6	NA	0.04933	0.05074	0.04927	0.0529	0.05449	0.05869	0.11972	0.33899	0.22631	0.41713
586.4	NA	0.03799	0.03733	0.03867	0.04139	0.04305	0.04554	0.09183	0.24733	0.2628	0.75806
661.8	NA	0.02789	0.02771	0.02975	0.03124	0.0331	0.03412	0.06768	0.17726	0.40909	0.72122
746.8	NA	0.02086	0.02122	0.0225	0.02374	0.02563	0.02575	0.05084	0.12956	0.55012	0.40042
842.8	NA	0.01492	0.0162	0.01701	0.01861	0.01866	0.02073	0.04076	0.10256	0.62035	0.23762
951.1	NA	0.01068	0.01191	0.01274	0.01353	0.01546	NA	NA	NA	NA	NA
1073.4	NA	0.00771	0.00862	0.00927	NA	NA	NA	NA	NA	NA	NA
1211.4	NA	0.00543	0.00632	NA	NA	NA	NA	NA	NA	NA	NA
1367.1	0.0089	0.00373	0.00475	NA	NA	NA	NA	NA	NA	NA	NA
1542.8	0.0084	0.00241	NA	NA	NA	NA	NA	NA	NA	NA	NA
1741.1	0.00727	0.00163	NA	NA	NA	NA	NA	NA	NA	NA	NA
1964.8	0.00422	NA	NA	NA	NA	NA	NA	NA	NA	NA	NA
2217.4	0.00212	NA	NA	NA	NA	NA	NA	NA	NA	NA	NA
2502.4	0.00054	NA	NA	NA	NA	NA	NA	NA	NA	NA	NA
2824	-0.00001	NA	NA	NA	NA	NA	NA	NA	NA	NA	NA

Table A.49: FAS Linear Amp. Look-up Table for 1.111 Hz.

V_{S30} (m/s)	Soil Depth (m)										
	0	5	10	15	20	25	30	50	100	500	1000
95.6	NA	NA	NA	NA	NA	NA	1.8043	0.78283	1.23929	1.43725	1.10115
107.9	NA	NA	NA	NA	NA	2.25503	2.21627	0.95314	0.99619	1.36209	1.24729
121.8	NA	NA	NA	NA	1.69625	1.96857	1.81679	1.45539	0.8832	1.14962	1.35058
137.4	NA	NA	NA	NA	1.303	1.25313	1.23428	2.04718	0.98604	1.57094	1.23246
155.1	NA	NA	NA	0.93912	0.88503	0.89863	0.9169	1.97953	1.04263	1.03344	1.25024
175	NA	NA	NA	0.67245	0.66097	0.65869	0.62902	1.33118	1.65997	1.00799	1.09232
197.5	NA	NA	0.54555	0.5153	0.49316	0.46795	0.49522	1.13571	1.42111	0.99223	0.9507
222.9	NA	NA	0.4271	0.39456	0.36701	0.36742	0.38889	0.83336	1.64617	0.70924	0.93382
251.5	NA	NA	0.31614	0.2927	0.28256	0.28218	0.29214	0.63305	1.48916	0.89154	0.79228
283.9	NA	NA	0.24143	0.21805	0.22088	0.21592	0.23255	0.51647	1.46285	0.76342	0.79836
320.4	NA	0.1516	0.18062	0.16743	0.16464	0.16858	0.18404	0.40725	1.4083	0.68568	0.67392
361.5	NA	0.12653	0.13512	0.12593	0.12731	0.13642	0.14131	0.32113	1.14399	0.99565	0.62611
408	NA	0.09618	0.1021	0.09668	0.10171	0.10431	0.10733	0.22984	0.73084	0.90264	0.86997
460.4	NA	0.07533	0.07567	0.07468	0.0776	0.08053	0.08307	0.17117	0.50279	0.43246	0.45473
519.6	NA	0.05562	0.05726	0.05566	0.05977	0.06157	0.06631	0.1356	0.38667	0.25425	0.3202
586.4	NA	0.04284	0.04216	0.04367	0.04674	0.04861	0.05145	0.10382	0.28092	0.22378	0.56653
661.8	NA	0.03144	0.03128	0.03359	0.03527	0.03741	0.03853	0.07652	0.20083	0.32794	0.77582
746.8	NA	0.02352	0.02396	0.0254	0.02679	0.02894	0.02907	0.05736	0.14673	0.46222	0.53011
842.8	NA	0.01683	0.01829	0.0192	0.02104	0.02105	0.02343	0.04607	0.11624	0.55521	0.31547
951.1	NA	0.01206	0.01345	0.01438	0.0153	0.01743	NA	NA	NA	NA	NA
1073.4	NA	0.00871	0.00973	0.01047	NA	NA	NA	NA	NA	NA	NA
1211.4	NA	0.00613	0.00714	NA	NA	NA	NA	NA	NA	NA	NA
1367.1	0.01003	0.00422	0.00536	NA	NA	NA	NA	NA	NA	NA	NA
1542.8	0.00948	0.00272	NA	NA	NA	NA	NA	NA	NA	NA	NA
1741.1	0.00824	0.00184	NA	NA	NA	NA	NA	NA	NA	NA	NA
1964.8	0.00478	NA	NA	NA	NA	NA	NA	NA	NA	NA	NA
2217.4	0.00243	NA	NA	NA	NA	NA	NA	NA	NA	NA	NA
2502.4	0.00063	NA	NA	NA	NA	NA	NA	NA	NA	NA	NA
2824	0	NA	NA	NA	NA	NA	NA	NA	NA	NA	NA

Table A.50: FAS Linear Amp. Look-up Table for 1.176 Hz.

V_{S30} (m/s)	Soil Depth (m)										
	0	5	10	15	20	25	30	50	100	500	1000
95.6	NA	NA	NA	NA	NA	NA	1.46109	0.70754	1.53017	1.13079	1.02776
107.9	NA	NA	NA	NA	NA	2.10516	1.94126	0.82204	1.15359	1.49081	1.18931
121.8	NA	NA	NA	NA	2.04395	2.21768	2.12346	1.20253	0.89487	1.06498	1.15164
137.4	NA	NA	NA	NA	1.5729	1.50353	1.47532	1.81364	0.91179	1.37106	1.35401
155.1	NA	NA	NA	1.10748	1.03456	1.05191	1.07481	1.99164	0.92574	1.32182	1.13498
175	NA	NA	NA	0.77682	0.76255	0.75889	0.72315	1.58065	1.42517	1.05453	1.19763
197.5	NA	NA	0.62615	0.58956	0.5631	0.53344	0.56487	1.29811	1.31943	1.0324	0.94485
222.9	NA	NA	0.48692	0.44877	0.41609	0.4167	0.44131	0.96833	1.49712	0.86334	0.82441
251.5	NA	NA	0.35831	0.33121	0.31947	0.31893	0.33019	0.73005	1.50519	0.77693	0.89658
283.9	NA	NA	0.27247	0.24577	0.24886	0.24332	0.26229	0.59077	1.4557	0.81402	0.68992
320.4	NA	0.17019	0.20342	0.18837	0.18516	0.18962	0.20711	0.4629	1.5161	0.5706	0.81706
361.5	NA	0.1426	0.15181	0.14139	0.14304	0.15327	0.15881	0.36346	1.30806	0.81967	0.57368
408	NA	0.1079	0.11455	0.10846	0.11412	0.11703	0.12043	0.2592	0.83983	1.04107	0.8635
460.4	NA	0.08448	0.08487	0.08371	0.08699	0.09029	0.09315	0.19242	0.57221	0.584	0.62628
519.6	NA	0.0623	0.06416	0.06237	0.06698	0.06901	0.07428	0.15222	0.4375	0.31839	0.33415
586.4	NA	0.04794	0.0472	0.04891	0.05234	0.05445	0.05763	0.11646	0.31687	0.21226	0.40243
661.8	NA	0.03518	0.03502	0.0376	0.03948	0.04187	0.04313	0.0857	0.22562	0.26775	0.71498
746.8	NA	0.02633	0.02682	0.02844	0.03	0.03238	0.03256	0.06431	0.16453	0.38306	0.63793
842.8	NA	0.01885	0.02047	0.0215	0.02354	0.02356	0.02624	0.05162	0.13008	0.4856	0.41396
951.1	NA	0.01351	0.01506	0.01609	0.01709	0.01951	NA	NA	NA	NA	NA
1073.4	NA	0.00976	0.01089	0.01172	NA	NA	NA	NA	NA	NA	NA
1211.4	NA	0.00687	0.008	NA	NA	NA	NA	NA	NA	NA	NA
1367.1	0.01128	0.00473	0.00602	NA	NA	NA	NA	NA	NA	NA	NA
1542.8	0.01062	0.00305	NA	NA	NA	NA	NA	NA	NA	NA	NA
1741.1	0.00921	0.00207	NA	NA	NA	NA	NA	NA	NA	NA	NA
1964.8	0.00538	NA	NA	NA	NA	NA	NA	NA	NA	NA	NA
2217.4	0.00275	NA	NA	NA	NA	NA	NA	NA	NA	NA	NA
2502.4	0.00072	NA	NA	NA	NA	NA	NA	NA	NA	NA	NA
2824	0.00001	NA	NA	NA	NA	NA	NA	NA	NA	NA	NA

Table A.51: FAS Linear Amp. Look-up Table for 1.250 Hz.

V_{S30} (m/s)	Soil Depth (m)										
	0	5	10	15	20	25	30	50	100	500	1000
95.6	NA	NA	NA	NA	NA	NA	1.16146	0.6652	1.87045	0.93677	1.09125
107.9	NA	NA	NA	NA	NA	1.6985	1.53308	0.72112	1.44169	1.23253	1.01644
121.8	NA	NA	NA	NA	2.23962	2.16643	2.21891	0.98434	0.97176	1.29345	1.23172
137.4	NA	NA	NA	NA	1.95471	1.87026	1.81157	1.49749	0.87892	1.13701	1.29124
155.1	NA	NA	NA	1.35596	1.25653	1.27406	1.30503	1.82947	0.84766	1.4579	1.04323
175	NA	NA	NA	0.92643	0.90347	0.8997	0.85359	1.85884	1.19545	1.2277	1.31291
197.5	NA	NA	0.73556	0.69257	0.65764	0.62172	0.66029	1.47586	1.15136	0.99632	0.89945
222.9	NA	NA	0.56851	0.52111	0.48227	0.48239	0.51184	1.15718	1.29843	1.09496	0.88539
251.5	NA	NA	0.41449	0.38231	0.36817	0.36764	0.38066	0.86355	1.43431	0.67066	0.86691
283.9	NA	NA	0.31392	0.28233	0.2859	0.27928	0.30123	0.69223	1.40015	0.88761	0.73469
320.4	NA	0.1945	0.2334	0.2158	0.212	0.21708	0.23723	0.53764	1.55971	0.55105	0.83603
361.5	NA	0.16291	0.17369	0.16155	0.16337	0.17519	0.18154	0.41957	1.46522	0.60489	0.6858
408	NA	0.12306	0.13083	0.12376	0.13018	0.13355	0.13746	0.29755	0.9852	1.06285	0.69054
460.4	NA	0.09633	0.09676	0.0954	0.09913	0.10287	0.10614	0.22025	0.66454	0.79521	0.82437
519.6	NA	0.07099	0.07308	0.07101	0.07628	0.07858	0.08462	0.17388	0.50509	0.44803	0.48689
586.4	NA	0.05461	0.05373	0.05565	0.05956	0.06198	0.0656	0.13284	0.36378	0.23339	0.29757
661.8	NA	0.04006	0.03985	0.04277	0.04493	0.04765	0.04907	0.09763	0.25798	0.22128	0.55279
746.8	NA	0.02997	0.0305	0.03235	0.03414	0.03684	0.03703	0.07316	0.18766	0.30414	0.68716
842.8	NA	0.02145	0.02328	0.02445	0.02677	0.02681	0.02986	0.05866	0.14827	0.40428	0.53393
951.1	NA	0.01537	0.01713	0.01831	0.01945	0.02217	NA	NA	NA	NA	NA
1073.4	NA	0.01111	0.01239	0.01332	NA	NA	NA	NA	NA	NA	NA
1211.4	NA	0.00782	0.00909	NA	NA	NA	NA	NA	NA	NA	NA
1367.1	0.01277	0.00539	0.00684	NA	NA	NA	NA	NA	NA	NA	NA
1542.8	0.01212	0.00348	NA	NA	NA	NA	NA	NA	NA	NA	NA
1741.1	0.01053	0.00236	NA	NA	NA	NA	NA	NA	NA	NA	NA
1964.8	0.00615	NA	NA	NA	NA	NA	NA	NA	NA	NA	NA
2217.4	0.00315	NA	NA	NA	NA	NA	NA	NA	NA	NA	NA
2502.4	0.00085	NA	NA	NA	NA	NA	NA	NA	NA	NA	NA
2824	0.00002	NA	NA	NA	NA	NA	NA	NA	NA	NA	NA

Table A.52: FAS Linear Amp. Look-up Table for 1.333 Hz.

V_{S30} (m/s)	Soil Depth (m)										
	0	5	10	15	20	25	30	50	100	500	1000
95.6	NA	NA	NA	NA	NA	NA	0.94499	0.67544	1.86626	1.20077	0.96495
107.9	NA	NA	NA	NA	NA	1.33384	1.22595	0.6705	1.80121	0.94815	1.1024
121.8	NA	NA	NA	NA	2.03872	1.80808	1.96381	0.8347	1.13081	1.48199	1.2177
137.4	NA	NA	NA	NA	2.21872	2.17067	2.08956	1.22833	0.90456	1.16838	1.17239
155.1	NA	NA	NA	1.67399	1.54247	1.561	1.59545	1.54888	0.82873	1.23473	1.14742
175	NA	NA	NA	1.11085	1.07788	1.07184	1.0114	2.00775	1.03183	1.40396	1.20534
197.5	NA	NA	0.87093	0.81388	0.77108	0.72568	0.77312	1.62806	0.9885	0.95006	0.93688
222.9	NA	NA	0.66424	0.6062	0.55828	0.55851	0.59303	1.37502	1.103	1.15712	0.96936
251.5	NA	NA	0.4792	0.44085	0.42372	0.42301	0.43835	1.02082	1.30432	0.72702	0.7795
283.9	NA	NA	0.36038	0.32365	0.3276	0.31981	0.3453	0.81276	1.29811	0.86891	0.8415
320.4	NA	0.22135	0.26683	0.24654	0.24207	0.24776	0.2711	0.62409	1.50911	0.65314	0.70162
361.5	NA	0.18548	0.1982	0.1841	0.18614	0.19967	0.20697	0.48408	1.53642	0.48049	0.78339
408	NA	0.13997	0.149	0.14072	0.14813	0.15193	0.15638	0.34097	1.14231	0.91704	0.54668
460.4	NA	0.1095	0.10992	0.10835	0.11262	0.11692	0.12059	0.25139	0.77105	0.98446	0.85023
519.6	NA	0.08053	0.08294	0.08059	0.08659	0.08919	0.09604	0.19804	0.58183	0.63735	0.72676
586.4	NA	0.06196	0.06093	0.06314	0.06757	0.07032	0.0744	0.151	0.41653	0.29734	0.31293
661.8	NA	0.04541	0.04518	0.0485	0.05093	0.05401	0.05565	0.11088	0.29415	0.20316	0.39276
746.8	NA	0.03397	0.03458	0.03668	0.0387	0.04177	0.04199	0.083	0.21352	0.24464	0.62555
842.8	NA	0.0243	0.02639	0.0277	0.03033	0.0304	0.03383	0.06652	0.16831	0.33041	0.61078
951.1	NA	0.01742	0.0194	0.02074	0.02203	0.02516	NA	NA	NA	NA	NA
1073.4	NA	0.01259	0.01404	0.01511	NA	NA	NA	NA	NA	NA	NA
1211.4	NA	0.00887	0.0103	NA	NA	NA	NA	NA	NA	NA	NA
1367.1	0.01462	0.00611	0.00774	NA	NA	NA	NA	NA	NA	NA	NA
1542.8	0.01378	0.00394	NA	NA	NA	NA	NA	NA	NA	NA	NA
1741.1	0.01196	0.00267	NA	NA	NA	NA	NA	NA	NA	NA	NA
1964.8	0.007	NA	NA	NA	NA	NA	NA	NA	NA	NA	NA
2217.4	0.00361	NA	NA	NA	NA	NA	NA	NA	NA	NA	NA
2502.4	0.00098	NA	NA	NA	NA	NA	NA	NA	NA	NA	NA
2824	0.00003	NA	NA	NA	NA	NA	NA	NA	NA	NA	NA

Table A.53: FAS Linear Amp. Look-up Table for 1.429 Hz.

V_{S30} (m/s)	Soil Depth (m)										
	0	5	10	15	20	25	30	50	100	500	1000
95.6	NA	NA	NA	NA	NA	NA	0.77497	0.75616	1.4726	1.2734	0.99719
107.9	NA	NA	NA	NA	NA	1.03632	0.96967	0.66984	1.87754	1.16158	0.99195
121.8	NA	NA	NA	NA	1.57339	1.38117	1.53877	0.72299	1.43861	1.23905	1.05425
137.4	NA	NA	NA	NA	2.0837	2.14924	2.12359	0.99466	1.01396	1.36992	1.2344
155.1	NA	NA	NA	2.0259	1.94707	1.93949	1.94089	1.2261	0.88428	1.03523	1.09018
175	NA	NA	NA	1.38398	1.33718	1.32484	1.24082	1.94793	0.9116	1.40861	1.1447
197.5	NA	NA	1.06349	0.98723	0.92859	0.8683	0.92997	1.73311	0.85253	1.01496	1.00417
222.9	NA	NA	0.79593	0.72191	0.66143	0.66177	0.70392	1.64455	0.91195	0.99242	0.91108
251.5	NA	NA	0.56592	0.51861	0.49739	0.49637	0.51498	1.21766	1.13265	0.95638	0.842
283.9	NA	NA	0.4223	0.37784	0.3826	0.3731	0.40363	0.9811	1.14789	0.7642	0.77748
320.4	NA	0.25721	0.31081	0.28654	0.28126	0.2881	0.31527	0.74251	1.35649	0.83595	0.65034
361.5	NA	0.21503	0.22995	0.21339	0.21559	0.23151	0.24001	0.57074	1.50287	0.51905	0.73424
408	NA	0.1618	0.17226	0.16271	0.17127	0.17573	0.18095	0.39819	1.31139	0.66265	0.59189
460.4	NA	0.12641	0.12693	0.12507	0.13006	0.13501	0.13929	0.29197	0.91088	1.05553	0.64811
519.6	NA	0.09291	0.09568	0.09294	0.09986	0.10285	0.11081	0.22941	0.6838	0.88515	0.85769
586.4	NA	0.07136	0.07019	0.07276	0.07788	0.08102	0.08581	0.1746	0.4862	0.43045	0.48356
661.8	NA	0.05228	0.05203	0.05586	0.05868	0.06225	0.06412	0.12795	0.34124	0.22015	0.28882
746.8	NA	0.0391	0.0398	0.04222	0.04455	0.0481	0.04833	0.09572	0.24679	0.20083	0.46731
842.8	NA	0.02797	0.03038	0.03189	0.03493	0.03498	0.03897	0.07664	0.1944	0.26046	0.59889
951.1	NA	0.02006	0.02234	0.02388	0.02536	0.02897	NA	NA	NA	NA	NA
1073.4	NA	0.0145	0.01617	0.01738	NA	NA	NA	NA	NA	NA	NA
1211.4	NA	0.01021	0.01186	NA	NA	NA	NA	NA	NA	NA	NA
1367.1	0.01681	0.00704	0.00892	NA	NA	NA	NA	NA	NA	NA	NA
1542.8	0.01585	0.00454	NA	NA	NA	NA	NA	NA	NA	NA	NA
1741.1	0.01379	0.00308	NA	NA	NA	NA	NA	NA	NA	NA	NA
1964.8	0.00809	NA	NA	NA	NA	NA	NA	NA	NA	NA	NA
2217.4	0.0042	NA	NA	NA	NA	NA	NA	NA	NA	NA	NA
2502.4	0.00116	NA	NA	NA	NA	NA	NA	NA	NA	NA	NA
2824	0.00005	NA	NA	NA	NA	NA	NA	NA	NA	NA	NA

Table A.54: FAS Linear Amp. Look-up Table for 1.5 Hz.

V_{S30} (m/s)	Soil Depth (m)										
	0	5	10	15	20	25	30	50	100	500	1000
95.6	NA	NA	NA	NA	NA	NA	0.6856	0.87878	1.1858	1.07668	0.97041
107.9	NA	NA	NA	NA	NA	0.87432	0.83241	0.71366	1.64967	1.29599	0.9965
121.8	NA	NA	NA	NA	1.28681	1.14586	1.27777	0.67758	1.71617	1.00435	1.10623
137.4	NA	NA	NA	NA	1.76002	1.88906	1.93345	0.87343	1.1651	1.39695	1.18028
155.1	NA	NA	NA	2.13187	2.16737	2.13726	2.09171	1.04105	0.98858	1.07816	1.01725
175	NA	NA	NA	1.63252	1.58639	1.56438	1.45551	1.78096	0.86518	1.26285	1.27033
197.5	NA	NA	1.24509	1.1503	1.0738	0.9989	1.07376	1.73506	0.79489	1.11796	0.96162
222.9	NA	NA	0.91823	0.825	0.75248	0.75222	0.80177	1.81151	0.8049	0.88404	0.91575
251.5	NA	NA	0.6417	0.58598	0.56082	0.55944	0.581	1.36531	1.0068	1.05866	0.90275
283.9	NA	NA	0.47552	0.4242	0.4292	0.41828	0.45293	1.12888	1.03249	0.73256	0.72933
320.4	NA	0.28696	0.34809	0.32011	0.31411	0.3218	0.35262	0.84702	1.20906	0.93082	0.74334
361.5	NA	0.23968	0.25632	0.23779	0.24019	0.25807	0.2676	0.64532	1.41582	0.66834	0.67861
408	NA	0.18009	0.19177	0.18091	0.19048	0.19553	0.20127	0.44671	1.40709	0.52096	0.71226
460.4	NA	0.14038	0.14107	0.13893	0.14447	0.14998	0.15471	0.32599	1.02349	0.95275	0.50807
519.6	NA	0.10325	0.10613	0.10312	0.1108	0.1141	0.12297	0.25533	0.77048	1.00838	0.75362
586.4	NA	0.07914	0.07782	0.08067	0.08637	0.08984	0.0952	0.1942	0.54469	0.56771	0.66828
661.8	NA	0.05795	0.05767	0.06188	0.06503	0.06895	0.07104	0.14201	0.38049	0.26342	0.29373
746.8	NA	0.04331	0.04409	0.04678	0.04937	0.05331	0.05358	0.10608	0.27409	0.18869	0.3536
842.8	NA	0.03098	0.03365	0.03534	0.03866	0.03873	0.04318	0.085	0.2156	0.22258	0.52334
951.1	NA	0.02223	0.02474	0.02644	0.02809	0.032	NA	NA	NA	NA	NA
1073.4	NA	0.01606	0.0179	0.01925	NA	NA	NA	NA	NA	NA	NA
1211.4	NA	0.01131	0.01313	NA	NA	NA	NA	NA	NA	NA	NA
1367.1	0.01866	0.00781	0.00987	NA	NA	NA	NA	NA	NA	NA	NA
1542.8	0.01761	0.00504	NA	NA	NA	NA	NA	NA	NA	NA	NA
1741.1	0.01529	0.00342	NA	NA	NA	NA	NA	NA	NA	NA	NA
1964.8	0.00899	NA	NA	NA	NA	NA	NA	NA	NA	NA	NA
2217.4	0.00467	NA	NA	NA	NA	NA	NA	NA	NA	NA	NA
2502.4	0.0013	NA	NA	NA	NA	NA	NA	NA	NA	NA	NA
2824	0.00006	NA	NA	NA	NA	NA	NA	NA	NA	NA	NA

Table A.55: FAS Linear Amp. Look-up Table for 1.538 Hz.

V_{S30} (m/s)	Soil Depth (m)										
	0	5	10	15	20	25	30	50	100	500	1000
95.6	NA	NA	NA	NA	NA	NA	0.65223	0.9623	1.08192	0.99886	0.95579
107.9	NA	NA	NA	NA	NA	0.80758	0.77656	0.75108	1.48834	1.28082	1.01027
121.8	NA	NA	NA	NA	1.16227	1.0465	1.168	0.66573	1.82254	0.97651	1.11117
137.4	NA	NA	NA	NA	1.58998	1.72526	1.80027	0.82434	1.26533	1.34634	1.13612
155.1	NA	NA	NA	2.10801	2.20294	2.17444	2.11102	0.96158	1.06256	1.10912	0.98343
175	NA	NA	NA	1.76091	1.72412	1.69305	1.57646	1.67618	0.85399	1.18308	1.28313
197.5	NA	NA	1.34999	1.24326	1.15703	1.07375	1.15551	1.71102	0.77888	1.14609	0.93605
222.9	NA	NA	0.98732	0.8825	0.80376	0.80228	0.85634	1.86557	0.76128	0.86937	0.93773
251.5	NA	NA	0.6837	0.62294	0.59566	0.59424	0.6172	1.43585	0.94553	1.06169	0.90384
283.9	NA	NA	0.50453	0.44967	0.45454	0.44292	0.47979	1.20695	0.97502	0.745	0.74051
320.4	NA	0.30261	0.36826	0.33836	0.33192	0.33996	0.37284	0.90513	1.1317	0.94271	0.77708
361.5	NA	0.25276	0.27066	0.25103	0.25341	0.27235	0.28253	0.68652	1.35726	0.75154	0.67458
408	NA	0.19001	0.20233	0.19071	0.20082	0.20619	0.21222	0.47308	1.44153	0.47808	0.76285
460.4	NA	0.14789	0.14863	0.14635	0.1522	0.15803	0.16302	0.34437	1.08101	0.86657	0.48155
519.6	NA	0.10872	0.11172	0.10858	0.11668	0.12015	0.12951	0.26937	0.81725	1.03113	0.66089
586.4	NA	0.0833	0.0819	0.0849	0.09091	0.09457	0.10018	0.20469	0.57608	0.64425	0.74322
661.8	NA	0.06099	0.06069	0.06512	0.06843	0.07257	0.07476	0.14959	0.40151	0.29516	0.32324
746.8	NA	0.04556	0.0464	0.04921	0.05195	0.05609	0.05637	0.11165	0.28915	0.18934	0.30925
842.8	NA	0.03259	0.03539	0.03716	0.04066	0.04073	0.0454	0.08948	0.22685	0.20835	0.47418
951.1	NA	0.02338	0.02602	0.02781	0.02957	0.03364	NA	NA	NA	NA	NA
1073.4	NA	0.0169	0.01883	0.02024	NA	NA	NA	NA	NA	NA	NA
1211.4	NA	0.01189	0.01381	NA	NA	NA	NA	NA	NA	NA	NA
1367.1	0.01964	0.00821	0.01037	NA	NA	NA	NA	NA	NA	NA	NA
1542.8	0.01851	0.0053	NA	NA	NA	NA	NA	NA	NA	NA	NA
1741.1	0.01609	0.0036	NA	NA	NA	NA	NA	NA	NA	NA	NA
1964.8	0.00947	NA	NA	NA	NA	NA	NA	NA	NA	NA	NA
2217.4	0.00492	NA	NA	NA	NA	NA	NA	NA	NA	NA	NA
2502.4	0.00138	NA	NA	NA	NA	NA	NA	NA	NA	NA	NA
2824	0.00007	NA	NA	NA	NA	NA	NA	NA	NA	NA	NA

Table A.56: FAS Linear Amp. Look-up Table for 1.667 Hz.

V_{S30} (m/s)	Soil Depth (m)										
	0	5	10	15	20	25	30	50	100	500	1000
95.6	NA	NA	NA	NA	NA	NA	0.59678	1.36078	0.93651	1.193	0.94515
107.9	NA	NA	NA	NA	NA	0.64486	0.65003	0.96315	1.08032	1.00992	0.97406
121.8	NA	NA	NA	NA	0.85908	0.80372	0.90233	0.68491	1.7794	1.25371	1.00783
137.4	NA	NA	NA	NA	1.1564	1.27901	1.37213	0.72347	1.66183	1.09484	1.10597
155.1	NA	NA	NA	1.7245	1.9268	1.94855	1.88435	0.77386	1.32716	1.14268	0.99362
175	NA	NA	NA	2.07889	2.11324	2.04761	1.96559	1.32371	0.88207	1.15532	1.13155
197.5	NA	NA	1.77139	1.61752	1.49136	1.36655	1.46937	1.53777	0.79543	1.05875	0.94824
222.9	NA	NA	1.26251	1.10992	0.99796	0.99529	1.06524	1.84118	0.67453	1.04826	0.95987
251.5	NA	NA	0.84389	0.76342	0.72473	0.72288	0.75259	1.63402	0.77958	0.91004	0.81789
283.9	NA	NA	0.61089	0.54167	0.54747	0.53277	0.57827	1.45289	0.80038	0.86016	0.82346
320.4	NA	0.36101	0.44149	0.40446	0.39624	0.40578	0.44585	1.12363	0.90107	0.81479	0.74132
361.5	NA	0.3008	0.3223	0.29805	0.30086	0.32373	0.33597	0.84059	1.1293	0.90612	0.70888
408	NA	0.22465	0.23967	0.22567	0.23766	0.24408	0.25147	0.56958	1.46887	0.50233	0.75493
460.4	NA	0.17467	0.17546	0.17263	0.17967	0.18663	0.1924	0.41048	1.25781	0.56732	0.60373
519.6	NA	0.12794	0.13165	0.12782	0.13748	0.14155	0.15263	0.31992	0.98173	0.88939	0.42814
586.4	NA	0.09794	0.09634	0.09989	0.10692	0.11129	0.11786	0.24191	0.68917	0.87962	0.75533
661.8	NA	0.07167	0.07131	0.07656	0.08043	0.0853	0.0879	0.17634	0.47712	0.44996	0.53438
746.8	NA	0.05352	0.05449	0.05779	0.06102	0.06586	0.06623	0.13146	0.34157	0.22765	0.2621
842.8	NA	0.03825	0.04153	0.04363	0.04778	0.04787	0.0533	0.10517	0.26795	0.18728	0.32336
951.1	NA	0.02745	0.03054	0.03265	0.03466	0.03961	NA	NA	NA	NA	NA
1073.4	NA	0.01983	0.0221	0.02375	NA	NA	NA	NA	NA	NA	NA
1211.4	NA	0.01396	0.0162	NA	NA	NA	NA	NA	NA	NA	NA
1367.1	0.02298	0.00965	0.01219	NA	NA	NA	NA	NA	NA	NA	NA
1542.8	0.02173	0.00622	NA	NA	NA	NA	NA	NA	NA	NA	NA
1741.1	0.01889	0.00422	NA	NA	NA	NA	NA	NA	NA	NA	NA
1964.8	0.01116	NA	NA	NA	NA	NA	NA	NA	NA	NA	NA
2217.4	0.00583	NA	NA	NA	NA	NA	NA	NA	NA	NA	NA
2502.4	0.00166	NA	NA	NA	NA	NA	NA	NA	NA	NA	NA
2824	0.0001	NA	NA	NA	NA	NA	NA	NA	NA	NA	NA

Table A.57: FAS Linear Amp. Look-up Table for 1.818 Hz.

V_{S30} (m/s)	Soil Depth (m)										
	0	5	10	15	20	25	30	50	100	500	1000
95.6	NA	NA	NA	NA	NA	NA	0.62705	1.71626	1.10354	1.06902	0.88274
107.9	NA	NA	NA	NA	NA	0.54617	0.59346	1.42269	0.9411	1.20565	0.97128
121.8	NA	NA	NA	NA	0.63112	0.63115	0.71255	0.82672	1.28792	1.17987	1.02865
137.4	NA	NA	NA	NA	0.83371	0.94036	1.02215	0.7045	1.82303	1.16227	1.05967
155.1	NA	NA	NA	1.2098	1.38397	1.44046	1.4189	0.65769	1.43519	1.11619	0.88365
175	NA	NA	NA	1.95003	2.05143	2.0387	2.09491	1.02037	1.04467	1.30007	1.17561
197.5	NA	NA	2.10564	2.04853	1.95378	1.80555	1.83955	1.25013	0.92691	0.9965	0.94545
222.9	NA	NA	1.67913	1.46743	1.29477	1.28836	1.38391	1.56162	0.6709	1.12462	0.93961
251.5	NA	NA	1.08223	0.96801	0.9121	0.90885	0.94821	1.71052	0.6714	0.86814	0.8954
283.9	NA	NA	0.76412	0.67029	0.67688	0.65726	0.71668	1.64652	0.64474	0.92677	0.73446
320.4	NA	0.43802	0.54279	0.49427	0.48351	0.49534	0.54576	1.4074	0.69235	0.68149	0.70606
361.5	NA	0.36436	0.39194	0.36139	0.36443	0.39283	0.40811	1.06221	0.86106	0.81415	0.69247
408	NA	0.27081	0.28956	0.27199	0.28673	0.2946	0.30352	0.70366	1.33773	0.7263	0.63525
460.4	NA	0.21	0.21088	0.20739	0.21591	0.22435	0.23139	0.50038	1.39899	0.42407	0.79555
519.6	NA	0.15326	0.15773	0.15317	0.16483	0.16972	0.18305	0.38719	1.17594	0.56738	0.5737
586.4	NA	0.1172	0.11519	0.11949	0.12799	0.13319	0.14107	0.29149	0.83783	0.93187	0.47752
661.8	NA	0.08555	0.08517	0.09148	0.09611	0.10195	0.10508	0.2117	0.57731	0.70076	0.72928
746.8	NA	0.06385	0.06504	0.06899	0.07285	0.0787	0.07907	0.15738	0.4109	0.3453	0.39914
842.8	NA	0.04562	0.04956	0.05205	0.057	0.05708	0.06353	0.1256	0.32059	0.21729	0.2553
951.1	NA	0.03273	0.03643	0.03893	0.04133	0.04721	NA	NA	NA	NA	NA
1073.4	NA	0.02365	0.02635	0.02832	NA	NA	NA	NA	NA	NA	NA
1211.4	NA	0.01665	0.01931	NA	NA	NA	NA	NA	NA	NA	NA
1367.1	0.02743	0.01151	0.01451	NA	NA	NA	NA	NA	NA	NA	NA
1542.8	0.0259	0.00743	NA	NA	NA	NA	NA	NA	NA	NA	NA
1741.1	0.02256	0.00504	NA	NA	NA	NA	NA	NA	NA	NA	NA
1964.8	0.01332	NA	NA	NA	NA	NA	NA	NA	NA	NA	NA
2217.4	0.00701	NA	NA	NA	NA	NA	NA	NA	NA	NA	NA
2502.4	0.00202	NA	NA	NA	NA	NA	NA	NA	NA	NA	NA
2824	0.00014	NA	NA	NA	NA	NA	NA	NA	NA	NA	NA

Table A.58: FAS Linear Amp. Look-up Table for 2.0 Hz.

V_{S30} (m/s)	Soil Depth (m)										
	0	5	10	15	20	25	30	50	100	500	1000
95.6	NA	NA	NA	NA	NA	NA	0.80614	1.27564	1.49819	1.04321	0.76214
107.9	NA	NA	NA	NA	NA	0.53416	0.64176	1.69873	1.18558	1.06327	0.91068
121.8	NA	NA	NA	NA	0.47563	0.53551	0.60689	1.19494	0.96879	1.13138	1.00272
137.4	NA	NA	NA	NA	0.59919	0.70096	0.77788	0.81303	1.38873	1.22536	1.03823
155.1	NA	NA	NA	0.81878	0.95877	1.02484	1.01868	0.63396	1.40839	0.9054	0.86181
175	NA	NA	NA	1.38458	1.5053	1.57306	1.72688	0.81478	1.38597	1.22421	1.08394
197.5	NA	NA	1.8328	2.01082	2.11854	2.13955	1.98507	0.94905	1.1148	1.08418	0.89142
222.9	NA	NA	2.01622	1.9415	1.75907	1.71161	1.82	1.1992	0.79728	0.94311	0.92083
251.5	NA	NA	1.46479	1.28382	1.19362	1.18789	1.23873	1.54782	0.66004	1.04527	0.85431
283.9	NA	NA	0.98936	0.85559	0.86291	0.8352	0.91473	1.65406	0.55323	0.82465	0.80575
320.4	NA	0.5431	0.684	0.61843	0.60404	0.61894	0.68463	1.64829	0.53191	0.80454	0.73629
361.5	NA	0.45091	0.48625	0.4467	0.45025	0.48632	0.50585	1.35663	0.62408	0.66458	0.7031
408	NA	0.33267	0.35632	0.3339	0.35202	0.3619	0.373	0.8927	1.07162	0.92511	0.7222
460.4	NA	0.25675	0.25792	0.25324	0.26377	0.2742	0.28269	0.62316	1.3986	0.55425	0.64018
519.6	NA	0.18651	0.19197	0.18631	0.20068	0.20667	0.22297	0.47745	1.33366	0.38369	0.79022
586.4	NA	0.14222	0.13988	0.14509	0.15542	0.16173	0.17135	0.35716	1.01376	0.67553	0.45615
661.8	NA	0.10361	0.10315	0.11081	0.11646	0.12355	0.1274	0.25789	0.70793	0.88828	0.55598
746.8	NA	0.07721	0.0787	0.08352	0.08815	0.09522	0.09574	0.19111	0.50159	0.56208	0.62993
842.8	NA	0.05515	0.0599	0.06294	0.06893	0.06908	0.07684	0.15226	0.38965	0.32654	0.38038
951.1	NA	0.03955	0.04401	0.04705	0.05001	0.05703	NA	NA	NA	NA	NA
1073.4	NA	0.02857	0.03182	0.03419	NA	NA	NA	NA	NA	NA	NA
1211.4	NA	0.02011	0.02332	NA	NA	NA	NA	NA	NA	NA	NA
1367.1	0.03325	0.01391	0.01753	NA	NA	NA	NA	NA	NA	NA	NA
1542.8	0.03131	0.00898	NA	NA	NA	NA	NA	NA	NA	NA	NA
1741.1	0.02722	0.00609	NA	NA	NA	NA	NA	NA	NA	NA	NA
1964.8	0.01611	NA	NA	NA	NA	NA	NA	NA	NA	NA	NA
2217.4	0.00852	NA	NA	NA	NA	NA	NA	NA	NA	NA	NA
2502.4	0.00249	NA	NA	NA	NA	NA	NA	NA	NA	NA	NA
2824	0.0002	NA	NA	NA	NA	NA	NA	NA	NA	NA	NA

Table A.59: FAS Linear Amp. Look-up Table for 2.083 Hz.

V_{S30} (m/s)	Soil Depth (m)										
	0	5	10	15	20	25	30	50	100	500	1000
95.6	NA	NA	NA	NA	NA	NA	0.94923	1.00441	1.45866	0.94332	0.71623
107.9	NA	NA	NA	NA	NA	0.56476	0.70858	1.53168	1.39184	1.07459	0.86739
121.8	NA	NA	NA	NA	0.43529	0.52484	0.59324	1.43057	0.94885	1.21682	1.00587
137.4	NA	NA	NA	NA	0.52846	0.6303	0.70766	0.91731	1.18259	1.14195	1.02311
155.1	NA	NA	NA	0.691	0.82391	0.89535	0.89347	0.66126	1.3556	0.94113	0.82625
175	NA	NA	NA	1.1672	1.28205	1.35345	1.50686	0.76164	1.55792	1.16798	1.06613
197.5	NA	NA	1.58212	1.7948	1.97424	2.09535	1.91045	0.84948	1.19906	1.05549	0.89211
222.9	NA	NA	2.00308	2.06598	1.97126	1.8904	1.96557	1.05869	0.89959	0.99475	0.90129
251.5	NA	NA	1.67974	1.46877	1.35502	1.34574	1.39526	1.4322	0.69744	1.02713	0.84176
283.9	NA	NA	1.11701	0.95752	0.96453	0.93159	1.02293	1.58091	0.54462	0.82455	0.7902
320.4	NA	0.59835	0.76025	0.68399	0.66758	0.68385	0.75807	1.68859	0.48713	0.87094	0.69357
361.5	NA	0.49579	0.53552	0.49101	0.49436	0.53475	0.5565	1.478	0.54549	0.68106	0.67798
408	NA	0.36401	0.39041	0.36533	0.38523	0.3963	0.40862	0.99262	0.9502	0.91236	0.74246
460.4	NA	0.28039	0.28162	0.27636	0.288	0.29937	0.30872	0.68719	1.33471	0.68178	0.57959
519.6	NA	0.20324	0.20917	0.20294	0.21868	0.22512	0.24305	0.52403	1.35998	0.39805	0.71246
586.4	NA	0.15479	0.15211	0.15787	0.1691	0.17607	0.18657	0.39048	1.08861	0.54578	0.58781
661.8	NA	0.11262	0.11212	0.12049	0.12665	0.13446	0.13849	0.28111	0.77296	0.87024	0.44415
746.8	NA	0.08389	0.0855	0.09071	0.09584	0.10353	0.10405	0.20805	0.54717	0.6685	0.65629
842.8	NA	0.05987	0.06506	0.0684	0.07492	0.07506	0.08358	0.16573	0.42454	0.40367	0.48221
951.1	NA	0.04293	0.0478	0.05108	0.05426	0.06202	NA	NA	NA	NA	NA
1073.4	NA	0.03101	0.03456	0.03712	NA	NA	NA	NA	NA	NA	NA
1211.4	NA	0.02183	0.02531	NA	NA	NA	NA	NA	NA	NA	NA
1367.1	0.03606	0.01511	0.01902	NA	NA	NA	NA	NA	NA	NA	NA
1542.8	0.03395	0.00974	NA	NA	NA	NA	NA	NA	NA	NA	NA
1741.1	0.0296	0.00661	NA	NA	NA	NA	NA	NA	NA	NA	NA
1964.8	0.01751	NA	NA	NA	NA	NA	NA	NA	NA	NA	NA
2217.4	0.00927	NA	NA	NA	NA	NA	NA	NA	NA	NA	NA
2502.4	0.00272	NA	NA	NA	NA	NA	NA	NA	NA	NA	NA
2824	0.00022	NA	NA	NA	NA	NA	NA	NA	NA	NA	NA

Table A.60: FAS Linear Amp. Look-up Table for 2.174 Hz.

V_{S30} (m/s)	Soil Depth (m)										
	0	5	10	15	20	25	30	50	100	500	1000
95.6	NA	NA	NA	NA	NA	NA	1.1715	0.77087	1.20224	0.85319	0.57789
107.9	NA	NA	NA	NA	NA	0.63126	0.82513	1.22248	1.50199	1.03784	0.78145
121.8	NA	NA	NA	NA	0.40924	0.53709	0.60296	1.64699	1.01367	1.17747	0.98022
137.4	NA	NA	NA	NA	0.46673	0.57301	0.65244	1.0881	1.02753	1.10147	1.01041
155.1	NA	NA	NA	0.5696	0.69946	0.77722	0.77951	0.7237	1.23937	1.06552	0.78837
175	NA	NA	NA	0.96637	1.07817	1.14608	1.28594	0.72608	1.7006	1.10901	1.06144
197.5	NA	NA	1.30992	1.51518	1.72504	1.91361	1.74806	0.76369	1.28298	1.01551	0.86619
222.9	NA	NA	1.86448	2.07125	2.12535	2.02478	2.02985	0.92268	1.04902	1.07139	0.88955
251.5	NA	NA	1.91492	1.70656	1.56815	1.54716	1.58212	1.29159	0.76865	0.9487	0.87667
283.9	NA	NA	1.2886	1.09088	1.09678	1.05688	1.16351	1.46311	0.56038	0.86855	0.74296
320.4	NA	0.66746	0.85804	0.76738	0.74761	0.7663	0.85156	1.67382	0.45614	0.8814	0.70346
361.5	NA	0.55061	0.59724	0.54628	0.54964	0.5953	0.62029	1.58126	0.475	0.74565	0.66071
408	NA	0.40291	0.43275	0.40411	0.42648	0.43916	0.45288	1.11625	0.8237	0.81869	0.71765
460.4	NA	0.30918	0.31071	0.30478	0.31792	0.33052	0.34085	0.76764	1.22815	0.8394	0.62363
519.6	NA	0.22373	0.23028	0.22341	0.24085	0.24789	0.26761	0.5818	1.34984	0.48698	0.57657
586.4	NA	0.17	0.1671	0.17356	0.18588	0.19356	0.20523	0.43164	1.16318	0.43968	0.71994
661.8	NA	0.12359	0.1231	0.13232	0.13907	0.14769	0.15212	0.30977	0.84998	0.7783	0.39051
746.8	NA	0.09198	0.0938	0.09954	0.10514	0.1136	0.11413	0.22879	0.60182	0.7638	0.59974
842.8	NA	0.06562	0.07132	0.07494	0.08216	0.08226	0.09164	0.18209	0.46689	0.50689	0.57673
951.1	NA	0.04705	0.0524	0.05599	0.05945	0.06786	NA	NA	NA	NA	NA
1073.4	NA	0.03398	0.03786	0.04071	NA	NA	NA	NA	NA	NA	NA
1211.4	NA	0.02391	0.02773	NA	NA	NA	NA	NA	NA	NA	NA
1367.1	0.03933	0.01654	0.02083	NA	NA	NA	NA	NA	NA	NA	NA
1542.8	0.03722	0.01067	NA	NA	NA	NA	NA	NA	NA	NA	NA
1741.1	0.03241	0.00725	NA	NA	NA	NA	NA	NA	NA	NA	NA
1964.8	0.01921	NA	NA	NA	NA	NA	NA	NA	NA	NA	NA
2217.4	0.01018	NA	NA	NA	NA	NA	NA	NA	NA	NA	NA
2502.4	0.00301	NA	NA	NA	NA	NA	NA	NA	NA	NA	NA
2824	0.00026	NA	NA	NA	NA	NA	NA	NA	NA	NA	NA

Table A.61: FAS Linear Amp. Look-up Table for 2.222 Hz.

V_{S30} (m/s)	Soil Depth (m)										
	0	5	10	15	20	25	30	50	100	500	1000
95.6	NA	NA	NA	NA	NA	NA	1.31091	0.68159	1.02181	0.82821	0.54105
107.9	NA	NA	NA	NA	NA	0.6806	0.9085	1.05978	1.47612	0.98017	0.756
121.8	NA	NA	NA	NA	0.40391	0.55436	0.61891	1.69454	1.08732	1.1308	0.96113
137.4	NA	NA	NA	NA	0.4425	0.55156	0.63286	1.20107	0.97988	1.12241	1.00695
155.1	NA	NA	NA	0.51587	0.64466	0.72631	0.73049	0.77152	1.16606	1.07897	0.79559
175	NA	NA	NA	0.87453	0.98585	1.05257	1.18624	0.71763	1.73045	1.09727	1.04829
197.5	NA	NA	1.1817	1.37514	1.58478	1.7862	1.64342	0.72924	1.31789	1.0083	0.84112
222.9	NA	NA	1.75922	2.01387	2.14442	2.05173	2.01244	0.86204	1.14078	1.08465	0.88462
251.5	NA	NA	2.0124	1.83056	1.69089	1.65674	1.67919	1.21615	0.81459	0.9101	0.87422
283.9	NA	NA	1.39226	1.17058	1.1755	1.13054	1.24584	1.39392	0.58085	0.8982	0.74397
320.4	NA	0.70787	0.91553	0.81602	0.79397	0.8141	0.90594	1.64229	0.44843	0.86091	0.71743
361.5	NA	0.58242	0.63302	0.57764	0.5812	0.63008	0.65681	1.61497	0.4456	0.77575	0.67539
408	NA	0.42506	0.4568	0.42619	0.44983	0.46328	0.47795	1.18429	0.76384	0.75569	0.69269
460.4	NA	0.32545	0.32707	0.32083	0.33475	0.34811	0.35887	0.81352	1.16409	0.91088	0.67846
519.6	NA	0.23519	0.24211	0.23483	0.25325	0.26072	0.28141	0.61435	1.32742	0.56131	0.5355
586.4	NA	0.17852	0.17552	0.18233	0.19528	0.20335	0.21561	0.45488	1.19561	0.40659	0.74911
661.8	NA	0.1297	0.1292	0.13886	0.14598	0.155	0.15972	0.32588	0.89132	0.71095	0.40452
746.8	NA	0.09646	0.09842	0.10446	0.11032	0.11919	0.11976	0.24041	0.6321	0.794	0.54428
842.8	NA	0.06883	0.07481	0.07859	0.08615	0.08629	0.09612	0.19131	0.49063	0.56292	0.60332
951.1	NA	0.04933	0.05494	0.05872	0.06241	0.07112	NA	NA	NA	NA	NA
1073.4	NA	0.03563	0.0397	0.04269	NA	NA	NA	NA	NA	NA	NA
1211.4	NA	0.02507	0.02906	NA	NA	NA	NA	NA	NA	NA	NA
1367.1	0.04131	0.01734	0.02184	NA	NA	NA	NA	NA	NA	NA	NA
1542.8	0.03901	0.01119	NA	NA	NA	NA	NA	NA	NA	NA	NA
1741.1	0.03395	0.0076	NA	NA	NA	NA	NA	NA	NA	NA	NA
1964.8	0.02014	NA	NA	NA	NA	NA	NA	NA	NA	NA	NA
2217.4	0.01069	NA	NA	NA	NA	NA	NA	NA	NA	NA	NA
2502.4	0.00316	NA	NA	NA	NA	NA	NA	NA	NA	NA	NA
2824	0.00028	NA	NA	NA	NA	NA	NA	NA	NA	NA	NA

Table A.62: FAS Linear Amp. Look-up Table for 2.273 Hz.

V_{S30} (m/s)	Soil Depth (m)										
	0	5	10	15	20	25	30	50	100	500	1000
95.6	NA	NA	NA	NA	NA	NA	1.43677	0.61852	0.87135	0.78805	0.5028
107.9	NA	NA	NA	NA	NA	0.73876	1.00189	0.93084	1.39873	0.92198	0.71024
121.8	NA	NA	NA	NA	0.40478	0.5783	0.64226	1.68095	1.18191	1.10159	0.94779
137.4	NA	NA	NA	NA	0.42529	0.53705	0.62089	1.31802	0.95751	1.16065	1.00101
155.1	NA	NA	NA	0.47115	0.59853	0.6847	0.69106	0.82861	1.09852	1.05515	0.79359
175	NA	NA	NA	0.79665	0.9087	0.97525	1.10246	0.71677	1.72399	1.09608	1.03433
197.5	NA	NA	1.07668	1.25529	1.45869	1.66135	1.5404	0.70358	1.34137	1.00757	0.82213
222.9	NA	NA	1.6442	1.9288	2.11769	2.04293	1.9638	0.8114	1.23459	1.06832	0.87493
251.5	NA	NA	2.07383	1.93432	1.8076	1.75684	1.76508	1.1464	0.86299	0.89651	0.86115
283.9	NA	NA	1.49923	1.25389	1.25667	1.20601	1.32829	1.32768	0.60857	0.91244	0.75609
320.4	NA	0.74723	0.97472	0.86541	0.84096	0.86241	0.96093	1.5995	0.44705	0.8322	0.72551
361.5	NA	0.61378	0.66907	0.60922	0.61258	0.66484	0.69337	1.63117	0.42314	0.79212	0.68496
408	NA	0.44694	0.48075	0.44805	0.47294	0.48713	0.50255	1.2482	0.71258	0.70644	0.67718
460.4	NA	0.3417	0.3433	0.33655	0.35124	0.36529	0.37656	0.85907	1.10248	0.95698	0.72814
519.6	NA	0.24652	0.25369	0.246	0.26539	0.27319	0.29489	0.64665	1.29676	0.64457	0.53438
586.4	NA	0.18692	0.18373	0.19085	0.20445	0.21287	0.22572	0.4778	1.22067	0.3924	0.74216
661.8	NA	0.13567	0.13516	0.14527	0.15272	0.16215	0.16713	0.34168	0.93006	0.64424	0.44432
746.8	NA	0.10085	0.10291	0.10924	0.11537	0.12465	0.12524	0.25164	0.66181	0.80544	0.48648
842.8	NA	0.07195	0.0782	0.08216	0.09006	0.09022	0.10053	0.2002	0.51328	0.61511	0.60707
951.1	NA	0.05156	0.0574	0.06138	0.06526	0.07435	NA	NA	NA	NA	NA
1073.4	NA	0.03724	0.04149	0.04459	NA	NA	NA	NA	NA	NA	NA
1211.4	NA	0.0262	0.03035	NA	NA	NA	NA	NA	NA	NA	NA
1367.1	0.04324	0.01812	0.02282	NA	NA	NA	NA	NA	NA	NA	NA
1542.8	0.04078	0.01169	NA	NA	NA	NA	NA	NA	NA	NA	NA
1741.1	0.03544	0.00794	NA	NA	NA	NA	NA	NA	NA	NA	NA
1964.8	0.02104	NA	NA	NA	NA	NA	NA	NA	NA	NA	NA
2217.4	0.01118	NA	NA	NA	NA	NA	NA	NA	NA	NA	NA
2502.4	0.00332	NA	NA	NA	NA	NA	NA	NA	NA	NA	NA
2824	0.00029	NA	NA	NA	NA	NA	NA	NA	NA	NA	NA

Table A.63: FAS Linear Amp. Look-up Table for 2.381 Hz.

V_{S30} (m/s)	Soil Depth (m)										
	0	5	10	15	20	25	30	50	100	500	1000
95.6	NA	NA	NA	NA	NA	NA	1.58603	0.53845	0.64148	0.6599	0.36108
107.9	NA	NA	NA	NA	NA	0.90781	1.25976	0.70691	1.08563	0.85489	0.58347
121.8	NA	NA	NA	NA	0.42592	0.65745	0.72227	1.48819	1.40477	1.09835	0.90098
137.4	NA	NA	NA	NA	0.40443	0.52408	0.61451	1.55948	0.98047	1.18533	0.98123
155.1	NA	NA	NA	0.3877	0.51609	0.61008	0.62272	0.99755	0.99211	0.96481	0.7788
175	NA	NA	NA	0.6509	0.76145	0.82939	0.94552	0.73819	1.59403	1.14624	1.00543
197.5	NA	NA	0.87156	1.02485	1.20747	1.39715	1.31575	0.66705	1.35408	0.98843	0.80638
222.9	NA	NA	1.36927	1.67553	1.93834	1.91937	1.78076	0.72093	1.42518	0.96519	0.83375
251.5	NA	NA	2.06857	2.08415	2.02778	1.93473	1.90889	0.99735	0.98232	0.95996	0.83632
283.9	NA	NA	1.74165	1.46311	1.46123	1.39181	1.52136	1.17758	0.70063	0.87987	0.76547
320.4	NA	0.8451	1.12255	0.98729	0.95721	0.9816	1.09655	1.47044	0.46389	0.76625	0.69408
361.5	NA	0.69262	0.75625	0.68551	0.68898	0.74892	0.78223	1.61824	0.38873	0.77572	0.67795
408	NA	0.49892	0.53818	0.50081	0.52865	0.54464	0.56212	1.38413	0.61272	0.6478	0.68778
460.4	NA	0.3803	0.3821	0.37413	0.39066	0.40657	0.41904	0.968	0.96589	0.95069	0.76774
519.6	NA	0.27303	0.28129	0.27265	0.29432	0.30305	0.32723	0.72516	1.20274	0.83566	0.63662
586.4	NA	0.20675	0.20325	0.21113	0.22623	0.23557	0.24981	0.53251	1.25528	0.41355	0.6344
661.8	NA	0.14974	0.14924	0.16049	0.16872	0.17918	0.18468	0.37906	1.01439	0.50471	0.58368
746.8	NA	0.11121	0.11356	0.12048	0.12736	0.13758	0.13822	0.27877	0.73057	0.77444	0.3842
842.8	NA	0.07932	0.08623	0.0907	0.09939	0.09949	0.11094	0.22093	0.56595	0.71099	0.55336
951.1	NA	0.0568	0.06328	0.06764	0.0719	0.08198	NA	NA	NA	NA	NA
1073.4	NA	0.04101	0.0457	0.04914	NA	NA	NA	NA	NA	NA	NA
1211.4	NA	0.02886	0.03345	NA	NA	NA	NA	NA	NA	NA	NA
1367.1	0.04775	0.01997	0.02515	NA	NA	NA	NA	NA	NA	NA	NA
1542.8	0.04487	0.01288	NA	NA	NA	NA	NA	NA	NA	NA	NA
1741.1	0.03903	0.00874	NA	NA	NA	NA	NA	NA	NA	NA	NA
1964.8	0.02319	NA	NA	NA	NA	NA	NA	NA	NA	NA	NA
2217.4	0.01233	NA	NA	NA	NA	NA	NA	NA	NA	NA	NA
2502.4	0.00368	NA	NA	NA	NA	NA	NA	NA	NA	NA	NA
2824	0.00034	NA	NA	NA	NA	NA	NA	NA	NA	NA	NA

Table A.64: FAS Linear Amp. Look-up Table for 2.5 Hz.

V_{S30} (m/s)	Soil Depth (m)										
	0	5	10	15	20	25	30	50	100	500	1000
95.6	NA	NA	NA	NA	NA	NA	1.48461	0.54271	0.56722	0.57815	0.27511
107.9	NA	NA	NA	NA	NA	1.1648	1.51872	0.57174	0.76115	0.75927	0.47052
121.8	NA	NA	NA	NA	0.4825	0.79583	0.8631	1.15002	1.48575	1.03824	0.81727
137.4	NA	NA	NA	NA	0.40887	0.54107	0.64211	1.67548	1.1221	1.12526	0.94932
155.1	NA	NA	NA	0.32279	0.45249	0.56006	0.5789	1.23693	0.98816	0.93401	0.75473
175	NA	NA	NA	0.52593	0.6416	0.71081	0.8194	0.80108	1.34758	1.20561	0.99119
197.5	NA	NA	0.69473	0.83203	0.9979	1.167	1.10734	0.66096	1.31437	0.95107	0.78001
222.9	NA	NA	1.09946	1.38353	1.64746	1.68268	1.53427	0.65511	1.53509	0.92611	0.80529
251.5	NA	NA	1.87011	2.05736	2.11612	2.01121	1.94641	0.86247	1.11406	1.02505	0.82193
283.9	NA	NA	1.93847	1.71451	1.70701	1.60796	1.71655	1.02358	0.83993	0.84324	0.74007
320.4	NA	0.96654	1.31438	1.14069	1.10117	1.12875	1.26236	1.30494	0.51573	0.76088	0.67894
361.5	NA	0.78649	0.86325	0.77767	0.78049	0.8505	0.88903	1.54039	0.37798	0.74175	0.63855
408	NA	0.56111	0.60696	0.56242	0.59417	0.6128	0.63264	1.50165	0.53114	0.67759	0.71509
460.4	NA	0.42533	0.42765	0.418	0.43674	0.45463	0.46854	1.09402	0.83323	0.8116	0.70133
519.6	NA	0.30414	0.31317	0.30331	0.32779	0.33746	0.36467	0.81738	1.08075	0.95592	0.74385
586.4	NA	0.22969	0.22561	0.23448	0.25138	0.26169	0.27772	0.59647	1.25152	0.5119	0.52567
661.8	NA	0.16597	0.16538	0.17798	0.18714	0.19865	0.2048	0.42239	1.09319	0.40362	0.69606
746.8	NA	0.12305	0.12571	0.13344	0.14103	0.15249	0.15318	0.30955	0.80546	0.6713	0.37758
842.8	NA	0.08768	0.09541	0.10034	0.10995	0.11011	0.12261	0.24487	0.6257	0.75252	0.44472
951.1	NA	0.06275	0.06998	0.07481	0.07954	0.09055	NA	NA	NA	NA	NA
1073.4	NA	0.04531	0.05051	0.05431	NA	NA	NA	NA	NA	NA	NA
1211.4	NA	0.03188	0.03698	NA	NA	NA	NA	NA	NA	NA	NA
1367.1	0.05262	0.02206	0.02775	NA	NA	NA	NA	NA	NA	NA	NA
1542.8	0.04955	0.01424	NA	NA	NA	NA	NA	NA	NA	NA	NA
1741.1	0.04309	0.00966	NA	NA	NA	NA	NA	NA	NA	NA	NA
1964.8	0.02562	NA	NA	NA	NA	NA	NA	NA	NA	NA	NA
2217.4	0.01365	NA	NA	NA	NA	NA	NA	NA	NA	NA	NA
2502.4	0.00409	NA	NA	NA	NA	NA	NA	NA	NA	NA	NA
2824	0.00039	NA	NA	NA	NA	NA	NA	NA	NA	NA	NA

Table A.65: FAS Linear Amp. Look-up Table for 2.632 Hz.

V_{S30} (m/s)	Soil Depth (m)										
	0	5	10	15	20	25	30	50	100	500	1000
95.6	NA	NA	NA	NA	NA	NA	1.14624	0.653	0.6764	0.5276	0.19137
107.9	NA	NA	NA	NA	NA	1.45246	1.56341	0.52663	0.59065	0.62451	0.367
121.8	NA	NA	NA	NA	0.58334	1.01045	1.08456	0.84382	1.30369	0.92296	0.71619
137.4	NA	NA	NA	NA	0.44591	0.59642	0.71214	1.55276	1.33586	1.07479	0.89565
155.1	NA	NA	NA	0.27855	0.41232	0.53747	0.56305	1.47634	1.08427	0.99239	0.73732
175	NA	NA	NA	0.42437	0.54611	0.6187	0.72279	0.91875	1.11512	1.1285	0.97593
197.5	NA	NA	0.54572	0.67165	0.82901	0.97998	0.9345	0.69162	1.20999	0.93396	0.74183
222.9	NA	NA	0.87384	1.1241	1.35628	1.41157	1.28815	0.61709	1.49167	0.94957	0.77708
251.5	NA	NA	1.55866	1.84723	2.00381	1.93963	1.84914	0.75231	1.25021	0.98663	0.80849
283.9	NA	NA	2.00311	1.95843	1.93744	1.82015	1.86327	0.87763	1.00527	0.85236	0.72085
320.4	NA	1.11379	1.55938	1.3348	1.28153	1.30816	1.45654	1.12752	0.61412	0.81038	0.68584
361.5	NA	0.90092	0.99639	0.88983	0.89167	0.97437	1.01956	1.40994	0.39614	0.74345	0.64946
408	NA	0.63524	0.68919	0.63563	0.67204	0.69384	0.71641	1.57568	0.46992	0.77144	0.7102
460.4	NA	0.47815	0.48043	0.46913	0.49077	0.51096	0.52656	1.23192	0.71522	0.64902	0.6342
519.6	NA	0.34008	0.35008	0.33894	0.36661	0.37727	0.40781	0.92524	0.94773	0.91067	0.71212
586.4	NA	0.25603	0.25132	0.26146	0.28019	0.29173	0.30983	0.6715	1.20388	0.68002	0.56317
661.8	NA	0.18444	0.1839	0.19793	0.20814	0.2211	0.22787	0.47252	1.15442	0.36792	0.66998
746.8	NA	0.13654	0.13961	0.14818	0.15665	0.16941	0.17004	0.34485	0.8844	0.53628	0.47369
842.8	NA	0.09723	0.10583	0.11128	0.122	0.12215	0.13618	0.2724	0.69209	0.7153	0.36223
951.1	NA	0.06955	0.07756	0.08294	0.08818	0.10041	NA	NA	NA	NA	NA
1073.4	NA	0.0502	0.05598	0.06019	NA	NA	NA	NA	NA	NA	NA
1211.4	NA	0.03531	0.04095	NA	NA	NA	NA	NA	NA	NA	NA
1367.1	0.05815	0.02443	0.0307	NA	NA	NA	NA	NA	NA	NA	NA
1542.8	0.05486	0.01577	NA	NA	NA	NA	NA	NA	NA	NA	NA
1741.1	0.04761	0.0107	NA	NA	NA	NA	NA	NA	NA	NA	NA
1964.8	0.02837	NA	NA	NA	NA	NA	NA	NA	NA	NA	NA
2217.4	0.01514	NA	NA	NA	NA	NA	NA	NA	NA	NA	NA
2502.4	0.00456	NA	NA	NA	NA	NA	NA	NA	NA	NA	NA
2824	0.00045	NA	NA	NA	NA	NA	NA	NA	NA	NA	NA

Table A.66: FAS Linear Amp. Look-up Table for 2.778 Hz.

V_{S30} (m/s)	Soil Depth (m)										
	0	5	10	15	20	25	30	50	100	500	1000
95.6	NA	NA	NA	NA	NA	NA	0.7793	0.90162	0.95329	0.46513	0.10897
107.9	NA	NA	NA	NA	NA	1.54769	1.32501	0.58213	0.60605	0.57149	0.25037
121.8	NA	NA	NA	NA	0.7493	1.31109	1.3757	0.63813	0.94338	0.84696	0.59567
137.4	NA	NA	NA	NA	0.52598	0.70595	0.84509	1.2379	1.45881	1.03027	0.8154
155.1	NA	NA	NA	0.2573	0.39931	0.54691	0.58163	1.59784	1.17605	0.97639	0.70575
175	NA	NA	NA	0.34168	0.47244	0.55135	0.65302	1.11844	0.96753	1.05272	0.95903
197.5	NA	NA	0.42041	0.5355	0.68629	0.82655	0.79316	0.77171	1.07501	0.94935	0.71452
222.9	NA	NA	0.67902	0.90448	1.10499	1.16138	1.06765	0.6107	1.30084	0.94727	0.74233
251.5	NA	NA	1.23869	1.5375	1.72956	1.73227	1.63624	0.668	1.35455	0.88878	0.7723
283.9	NA	NA	1.89733	2.08972	2.05947	1.96432	1.90201	0.74636	1.17579	0.89846	0.71553
320.4	NA	1.30493	1.84728	1.58515	1.51325	1.5214	1.66443	0.95185	0.7746	0.83839	0.6646
361.5	NA	1.04706	1.16837	1.03324	1.03202	1.13062	1.18268	1.23949	0.45284	0.77012	0.64169
408	NA	0.72664	0.79135	0.7262	0.76821	0.79395	0.81979	1.58394	0.43115	0.84599	0.68546
460.4	NA	0.54224	0.54498	0.53079	0.55588	0.57907	0.59645	1.37232	0.6127	0.59716	0.71168
519.6	NA	0.38289	0.39432	0.38144	0.4131	0.4249	0.45956	1.05384	0.81363	0.72894	0.61505
586.4	NA	0.28718	0.28184	0.29337	0.31446	0.32755	0.34784	0.76179	1.11437	0.85665	0.69355
661.8	NA	0.20629	0.20568	0.2215	0.233	0.2476	0.25513	0.53252	1.1852	0.41927	0.5445
746.8	NA	0.1524	0.15596	0.16555	0.175	0.18924	0.19002	0.38663	0.96483	0.41604	0.61013
842.8	NA	0.10844	0.11806	0.12417	0.13622	0.13631	0.15203	0.3049	0.76551	0.60931	0.38072
951.1	NA	0.07751	0.08645	0.0925	0.09831	0.11234	NA	NA	NA	NA	NA
1073.4	NA	0.05592	0.06238	0.06708	NA	NA	NA	NA	NA	NA	NA
1211.4	NA	0.03932	0.0456	NA	NA	NA	NA	NA	NA	NA	NA
1367.1	0.06484	0.02721	0.03419	NA	NA	NA	NA	NA	NA	NA	NA
1542.8	0.06103	0.01755	NA	NA	NA	NA	NA	NA	NA	NA	NA
1741.1	0.053	0.01192	NA	NA	NA	NA	NA	NA	NA	NA	NA
1964.8	0.03152	NA	NA	NA	NA	NA	NA	NA	NA	NA	NA
2217.4	0.01686	NA	NA	NA	NA	NA	NA	NA	NA	NA	NA
2502.4	0.00511	NA	NA	NA	NA	NA	NA	NA	NA	NA	NA
2824	0.00052	NA	NA	NA	NA	NA	NA	NA	NA	NA	NA

Table A.67: FAS Linear Amp. Look-up Table for 2.857 Hz.

V_{S30} (m/s)	Soil Depth (m)										
	0	5	10	15	20	25	30	50	100	500	1000
95.6	NA	NA	NA	NA	NA	NA	0.63554	1.05887	1.0521	0.44027	0.0944
107.9	NA	NA	NA	NA	NA	1.47666	1.13017	0.65937	0.69369	0.54553	0.22469
121.8	NA	NA	NA	NA	0.86995	1.45068	1.49617	0.5748	0.78071	0.79297	0.53181
137.4	NA	NA	NA	NA	0.58726	0.78677	0.94328	1.0614	1.41953	0.98487	0.76274
155.1	NA	NA	NA	0.25725	0.40504	0.56727	0.60736	1.57312	1.1964	0.94474	0.67526
175	NA	NA	NA	0.30904	0.44596	0.529	0.63015	1.25442	0.93949	1.08192	0.9441
197.5	NA	NA	0.36598	0.4777	0.62615	0.76276	0.73473	0.83556	1.01573	0.94583	0.69814
222.9	NA	NA	0.59652	0.80987	0.998	1.05481	0.97387	0.62195	1.17816	0.91761	0.7252
251.5	NA	NA	1.09767	1.37957	1.57125	1.59962	1.51003	0.63794	1.37209	0.87487	0.75967
283.9	NA	NA	1.79554	2.07177	2.04636	1.98138	1.86571	0.69086	1.24647	0.88572	0.69997
320.4	NA	1.42279	1.97018	1.72711	1.64315	1.62995	1.75505	0.87186	0.87544	0.82907	0.6504
361.5	NA	1.13562	1.27301	1.11794	1.11488	1.22147	1.27533	1.14835	0.49974	0.76504	0.62768
408	NA	0.77891	0.8513	0.77818	0.82338	0.85141	0.87927	1.55798	0.42252	0.85617	0.68941
460.4	NA	0.5789	0.58164	0.5657	0.59267	0.6176	0.6358	1.43569	0.57004	0.63099	0.74966
519.6	NA	0.40683	0.41905	0.40517	0.43912	0.45156	0.48854	1.12429	0.75192	0.63582	0.61952
586.4	NA	0.30454	0.29878	0.31109	0.3334	0.34737	0.36884	0.81185	1.05901	0.90597	0.72662
661.8	NA	0.21845	0.21773	0.23449	0.24672	0.26224	0.27018	0.566	1.18423	0.48249	0.50595
746.8	NA	0.16113	0.16495	0.17512	0.18512	0.20022	0.20104	0.41	1.00096	0.37674	0.64568
842.8	NA	0.11457	0.12477	0.13122	0.14402	0.14414	0.16055	0.32247	0.80391	0.5464	0.43397
951.1	NA	0.08186	0.09132	0.09775	0.10387	0.11879	NA	NA	NA	NA	NA
1073.4	NA	0.05905	0.06589	0.07088	NA	NA	NA	NA	NA	NA	NA
1211.4	NA	0.04151	0.04816	NA	NA	NA	NA	NA	NA	NA	NA
1367.1	0.06845	0.02873	0.03608	NA	NA	NA	NA	NA	NA	NA	NA
1542.8	0.06436	0.01853	NA	NA	NA	NA	NA	NA	NA	NA	NA
1741.1	0.05591	0.01258	NA	NA	NA	NA	NA	NA	NA	NA	NA
1964.8	0.03325	NA	NA	NA	NA	NA	NA	NA	NA	NA	NA
2217.4	0.0178	NA	NA	NA	NA	NA	NA	NA	NA	NA	NA
2502.4	0.00541	NA	NA	NA	NA	NA	NA	NA	NA	NA	NA
2824	0.00055	NA	NA	NA	NA	NA	NA	NA	NA	NA	NA

Table A.68: FAS Linear Amp. Look-up Table for 2.941 Hz.

V_{S30} (m/s)	Soil Depth (m)										
	0	5	10	15	20	25	30	50	100	500	1000
95.6	NA	NA	NA	NA	NA	NA	0.50612	1.19332	1.07741	0.42906	0.05334
107.9	NA	NA	NA	NA	NA	1.31647	0.91349	0.78601	0.84544	0.51208	0.17787
121.8	NA	NA	NA	NA	1.0334	1.53617	1.55927	0.53438	0.65598	0.71778	0.45976
137.4	NA	NA	NA	NA	0.67529	0.90421	1.07638	0.88994	1.29732	0.92525	0.70887
155.1	NA	NA	NA	0.26653	0.42222	0.60345	0.65071	1.47559	1.19728	0.89905	0.63321
175	NA	NA	NA	0.28081	0.42552	0.51377	0.61531	1.41549	0.94616	1.12612	0.93245
197.5	NA	NA	0.31239	0.42134	0.56935	0.702	0.68003	0.92894	0.96905	0.92156	0.67366
222.9	NA	NA	0.51398	0.71728	0.89315	0.95061	0.8823	0.64747	1.04241	0.89328	0.70529
251.5	NA	NA	0.9581	1.22013	1.4031	1.44719	1.36965	0.6145	1.35227	0.89865	0.74847
283.9	NA	NA	1.65955	1.98547	1.97037	1.94737	1.78524	0.63826	1.30083	0.85783	0.68223
320.4	NA	1.57294	2.05759	1.88004	1.78721	1.74099	1.82997	0.79075	0.99704	0.80233	0.64151
361.5	NA	1.24778	1.40366	1.22474	1.21793	1.33278	1.38529	1.04639	0.57012	0.74498	0.61076
408	NA	0.84354	0.92546	0.84233	0.89122	0.92228	0.95244	1.50652	0.42227	0.84144	0.69248
460.4	NA	0.62319	0.62601	0.6081	0.63758	0.66467	0.68391	1.49527	0.52934	0.7034	0.75023
519.6	NA	0.43566	0.44878	0.43376	0.47062	0.48389	0.52369	1.20489	0.6879	0.56724	0.66603
586.4	NA	0.32527	0.31908	0.33241	0.35628	0.3713	0.39432	0.8727	0.99174	0.91106	0.7136
661.8	NA	0.23289	0.23213	0.25019	0.26327	0.27986	0.28842	0.60639	1.16916	0.57944	0.51392
746.8	NA	0.17152	0.17573	0.18657	0.1973	0.21348	0.21436	0.43824	1.03654	0.35561	0.64019
842.8	NA	0.12185	0.13282	0.13971	0.15346	0.15348	0.17092	0.34431	0.84615	0.47582	0.50774
951.1	NA	0.08705	0.09717	0.10403	0.11058	0.12642	NA	NA	NA	NA	NA
1073.4	NA	0.06278	0.07009	0.07535	NA	NA	NA	NA	NA	NA	NA
1211.4	NA	0.04414	0.05125	NA	NA	NA	NA	NA	NA	NA	NA
1367.1	0.0727	0.03054	0.03836	NA	NA	NA	NA	NA	NA	NA	NA
1542.8	0.06838	0.0197	NA	NA	NA	NA	NA	NA	NA	NA	NA
1741.1	0.05932	0.01337	NA	NA	NA	NA	NA	NA	NA	NA	NA
1964.8	0.03533	NA	NA	NA	NA	NA	NA	NA	NA	NA	NA
2217.4	0.01893	NA	NA	NA	NA	NA	NA	NA	NA	NA	NA
2502.4	0.00577	NA	NA	NA	NA	NA	NA	NA	NA	NA	NA
2824	0.0006	NA	NA	NA	NA	NA	NA	NA	NA	NA	NA

Table A.69: FAS Linear Amp. Look-up Table for 3.125 Hz.

V_{S30} (m/s)	Soil Depth (m)										
	0	5	10	15	20	25	30	50	100	500	1000
95.6	NA	NA	NA	NA	NA	NA	0.33069	1.1886	0.86587	0.3978	-0.00931
107.9	NA	NA	NA	NA	NA	0.89476	0.57035	1.11483	1.07565	0.45367	0.11947
121.8	NA	NA	NA	NA	1.38725	1.42142	1.4039	0.55552	0.5926	0.61547	0.34691
137.4	NA	NA	NA	NA	0.93151	1.21389	1.37066	0.65059	0.92234	0.81921	0.56648
155.1	NA	NA	NA	0.31836	0.49633	0.72804	0.79484	1.15957	1.16138	0.85442	0.55977
175	NA	NA	NA	0.24821	0.41243	0.515	0.61965	1.65846	1.07859	1.09658	0.89393
197.5	NA	NA	0.22686	0.33144	0.48148	0.60938	0.60035	1.18398	0.93997	0.87062	0.63657
222.9	NA	NA	0.37036	0.56073	0.72087	0.7771	0.73246	0.74704	0.83236	0.89129	0.68218
251.5	NA	NA	0.7278	0.94854	1.11432	1.16368	1.11017	0.60081	1.2045	0.93306	0.7103
283.9	NA	NA	1.34916	1.66636	1.68478	1.73837	1.53617	0.56062	1.29919	0.79892	0.65805
320.4	NA	1.92829	2.0147	2.07939	2.00467	1.88668	1.85529	0.65433	1.22162	0.77085	0.6333
361.5	NA	1.52141	1.69707	1.48381	1.46029	1.57607	1.60299	0.85395	0.77203	0.70144	0.60392
408	NA	0.99843	1.10327	0.994	1.05225	1.08919	1.12297	1.34694	0.45519	0.75883	0.684
460.4	NA	0.72538	0.72945	0.70626	0.74154	0.7737	0.79502	1.55948	0.47133	0.88333	0.67086
519.6	NA	0.50174	0.51662	0.4987	0.54223	0.55756	0.60366	1.3612	0.57887	0.60202	0.72319
586.4	NA	0.37184	0.36491	0.38042	0.40823	0.42526	0.45187	1.00687	0.85217	0.76987	0.61456
661.8	NA	0.2651	0.2644	0.2853	0.30041	0.31921	0.32905	0.69742	1.09897	0.79749	0.64697
746.8	NA	0.19464	0.19981	0.21226	0.22443	0.24297	0.24389	0.5012	1.08253	0.39501	0.53542
842.8	NA	0.13817	0.15077	0.1587	0.17426	0.17434	0.19433	0.3929	0.92538	0.36889	0.60988
951.1	NA	0.09856	0.11013	0.11794	0.12541	0.14327	NA	NA	NA	NA	NA
1073.4	NA	0.07104	0.07938	0.08529	NA	NA	NA	NA	NA	NA	NA
1211.4	NA	0.04995	0.05802	NA	NA	NA	NA	NA	NA	NA	NA
1367.1	0.0821	0.03455	0.04342	NA	NA	NA	NA	NA	NA	NA	NA
1542.8	0.07721	0.02229	NA	NA	NA	NA	NA	NA	NA	NA	NA
1741.1	0.06685	0.01512	NA	NA	NA	NA	NA	NA	NA	NA	NA
1964.8	0.03987	NA	NA	NA	NA	NA	NA	NA	NA	NA	NA
2217.4	0.02144	NA	NA	NA	NA	NA	NA	NA	NA	NA	NA
2502.4	0.00656	NA	NA	NA	NA	NA	NA	NA	NA	NA	NA
2824	0.0007	NA	NA	NA	NA	NA	NA	NA	NA	NA	NA

Table A.70: FAS Linear Amp. Look-up Table for 3.333 Hz.

V_{S30} (m/s)	Soil Depth (m)										
	0	5	10	15	20	25	30	50	100	500	1000
95.6	NA	NA	NA	NA	NA	NA	0.27631	0.82272	0.60578	0.34943	-0.09916
107.9	NA	NA	NA	NA	NA	0.5583	0.35196	1.21252	0.93126	0.4377	0.05101
121.8	NA	NA	NA	NA	1.49893	0.98817	0.95675	0.75579	0.81104	0.55525	0.25707
137.4	NA	NA	NA	NA	1.31059	1.49887	1.51934	0.54537	0.6384	0.69257	0.43062
155.1	NA	NA	NA	0.43558	0.65136	0.96431	1.05927	0.82051	1.05731	0.76766	0.45167
175	NA	NA	NA	0.25382	0.44717	0.57237	0.68504	1.58149	1.31317	1.02319	0.83317
197.5	NA	NA	0.16854	0.27124	0.4276	0.55509	0.56055	1.46906	0.98827	0.85925	0.58291
222.9	NA	NA	0.25519	0.43578	0.58457	0.64302	0.6196	0.94756	0.76028	0.86742	0.64135
251.5	NA	NA	0.53346	0.7252	0.87819	0.92554	0.89025	0.64254	0.98966	0.85868	0.67254
283.9	NA	NA	1.03341	1.29214	1.33152	1.4188	1.2415	0.52268	1.14473	0.83891	0.6305
320.4	NA	2.22431	1.69595	1.98974	1.98983	1.8622	1.68825	0.55061	1.33051	0.79193	0.5997
361.5	NA	1.87583	1.96196	1.80211	1.73906	1.79856	1.75507	0.68418	1.03954	0.74938	0.5779
408	NA	1.21215	1.34924	1.19949	1.2669	1.30705	1.33443	1.14001	0.55065	0.73761	0.67209
460.4	NA	0.86018	0.86511	0.83313	0.87631	0.91442	0.93733	1.51626	0.44907	0.90072	0.72167
519.6	NA	0.58505	0.60279	0.58078	0.63297	0.64997	0.70382	1.47866	0.49535	0.81434	0.6618
586.4	NA	0.4302	0.42182	0.44021	0.47243	0.49219	0.52332	1.15793	0.71756	0.59515	0.66773
661.8	NA	0.3046	0.30401	0.3283	0.34573	0.36756	0.37888	0.80958	0.98225	0.8888	0.68504
746.8	NA	0.22286	0.22911	0.24335	0.2575	0.27893	0.27986	0.57892	1.08248	0.55775	0.48546
842.8	NA	0.15798	0.17246	0.18162	0.19935	0.19934	0.22243	0.45234	0.9905	0.34893	0.54526
951.1	NA	0.11245	0.12585	0.1348	0.14323	0.16367	NA	NA	NA	NA	NA
1073.4	NA	0.08099	0.09056	0.0974	NA	NA	NA	NA	NA	NA	NA
1211.4	NA	0.05691	0.06611	NA	NA	NA	NA	NA	NA	NA	NA
1367.1	0.0934	0.03937	0.04953	NA	NA	NA	NA	NA	NA	NA	NA
1542.8	0.08761	0.0254	NA	NA	NA	NA	NA	NA	NA	NA	NA
1741.1	0.07588	0.01723	NA	NA	NA	NA	NA	NA	NA	NA	NA
1964.8	0.04535	NA	NA	NA	NA	NA	NA	NA	NA	NA	NA
2217.4	0.0244	NA	NA	NA	NA	NA	NA	NA	NA	NA	NA
2502.4	0.00751	NA	NA	NA	NA	NA	NA	NA	NA	NA	NA
2824	0.00083	NA	NA	NA	NA	NA	NA	NA	NA	NA	NA

Table A.71: FAS Linear Amp. Look-up Table for 3.448 Hz.

V_{S30} (m/s)	Soil Depth (m)										
	0	5	10	15	20	25	30	50	100	500	1000
95.6	NA	NA	NA	NA	NA	NA	0.30413	0.64464	0.64461	0.30305	-0.15677
107.9	NA	NA	NA	NA	NA	0.44072	0.2906	1.08397	0.74525	0.38872	0.00612
121.8	NA	NA	NA	NA	1.37309	0.76403	0.73498	0.93769	0.97917	0.52073	0.21572
137.4	NA	NA	NA	NA	1.46579	1.50897	1.44811	0.55388	0.60466	0.63368	0.37388
155.1	NA	NA	NA	0.53348	0.77846	1.13553	1.24619	0.69778	0.97907	0.70279	0.3752
175	NA	NA	NA	0.27733	0.49131	0.63365	0.75291	1.39344	1.39646	1.00346	0.78874
197.5	NA	NA	0.15179	0.25433	0.41651	0.54566	0.55978	1.55686	1.03545	0.84686	0.55588
222.9	NA	NA	0.20674	0.38423	0.5287	0.58907	0.57754	1.1076	0.78874	0.86001	0.63268
251.5	NA	NA	0.44637	0.62793	0.77648	0.82263	0.79525	0.69462	0.89958	0.83428	0.6512
283.9	NA	NA	0.88878	1.12131	1.16543	1.25236	1.09882	0.52294	1.02636	0.83315	0.60183
320.4	NA	2.23323	1.48495	1.82233	1.86614	1.76691	1.54384	0.51201	1.30231	0.78659	0.59285
361.5	NA	2.04867	2.01889	1.9493	1.86108	1.86163	1.7731	0.60874	1.16435	0.75875	0.56682
408	NA	1.35067	1.50631	1.3357	1.40546	1.43925	1.45449	1.02652	0.63592	0.76864	0.66534
460.4	NA	0.94814	0.95324	0.91441	0.96286	1.00465	1.02697	1.44582	0.45599	0.82021	0.72669
519.6	NA	0.6375	0.65682	0.63205	0.68998	0.70813	0.7671	1.50492	0.46448	0.89652	0.67179
586.4	NA	0.46605	0.45695	0.4773	0.51214	0.53376	0.56777	1.23856	0.65356	0.5705	0.70674
661.8	NA	0.32873	0.32831	0.35477	0.37371	0.39733	0.4097	0.8786	0.91023	0.83324	0.63343
746.8	NA	0.24002	0.24699	0.26239	0.27779	0.30098	0.3017	0.62636	1.0591	0.67342	0.54214
842.8	NA	0.16994	0.18569	0.19566	0.21489	0.21482	0.23977	0.4885	1.01156	0.38902	0.48503
951.1	NA	0.12083	0.13539	0.14505	0.15419	0.17643	NA	NA	NA	NA	NA
1073.4	NA	0.08701	0.09735	0.10478	NA	NA	NA	NA	NA	NA	NA
1211.4	NA	0.06115	0.07104	NA	NA	NA	NA	NA	NA	NA	NA
1367.1	0.10019	0.04228	0.05325	NA	NA	NA	NA	NA	NA	NA	NA
1542.8	0.094	0.02728	NA	NA	NA	NA	NA	NA	NA	NA	NA
1741.1	0.08146	0.01849	NA	NA	NA	NA	NA	NA	NA	NA	NA
1964.8	0.04859	NA	NA	NA	NA	NA	NA	NA	NA	NA	NA
2217.4	0.02617	NA	NA	NA	NA	NA	NA	NA	NA	NA	NA
2502.4	0.00809	NA	NA	NA	NA	NA	NA	NA	NA	NA	NA
2824	0.0009	NA	NA	NA	NA	NA	NA	NA	NA	NA	NA

Table A.72: FAS Linear Amp. Look-up Table for 3.571 Hz.

V_{S30} (m/s)	Soil Depth (m)										
	0	5	10	15	20	25	30	50	100	500	1000
95.6	NA	NA	NA	NA	NA	NA	0.3843	0.5446	0.7919	0.25652	-0.21497
107.9	NA	NA	NA	NA	NA	0.36314	0.26746	0.86856	0.62367	0.36923	-0.04132
121.8	NA	NA	NA	NA	1.14976	0.58473	0.55414	1.12142	1.06994	0.49698	0.18677
137.4	NA	NA	NA	NA	1.50167	1.38964	1.27661	0.61545	0.66317	0.59701	0.31472
155.1	NA	NA	NA	0.66762	0.95062	1.31626	1.42811	0.6219	0.90823	0.65388	0.30249
175	NA	NA	NA	0.31891	0.55903	0.72439	0.85405	1.15928	1.38413	0.9565	0.73235
197.5	NA	NA	0.14634	0.24961	0.41919	0.55149	0.57585	1.55848	1.08624	0.80967	0.51328
222.9	NA	NA	0.16701	0.34204	0.48334	0.54712	0.54811	1.30153	0.86818	0.85532	0.60144
251.5	NA	NA	0.36837	0.54051	0.68731	0.73303	0.71306	0.77478	0.83958	0.84854	0.62923
283.9	NA	NA	0.7588	0.96889	1.01734	1.09926	0.96833	0.5399	0.90767	0.79012	0.59028
320.4	NA	2.12108	1.27805	1.61147	1.68787	1.62632	1.38293	0.48533	1.21353	0.76189	0.56861
361.5	NA	2.14455	1.98734	2.03542	1.93578	1.86112	1.73775	0.54337	1.24104	0.72746	0.55894
408	NA	1.5098	1.67343	1.49335	1.55859	1.57541	1.56855	0.91596	0.74813	0.8026	0.65788
460.4	NA	1.05231	1.05764	1.00974	1.06407	1.10864	1.12907	1.34795	0.47899	0.72597	0.69406
519.6	NA	0.69795	0.71903	0.69081	0.75556	0.77481	0.839	1.49784	0.44425	0.89459	0.69899
586.4	NA	0.50696	0.49674	0.51923	0.55733	0.58068	0.61788	1.31344	0.59646	0.61862	0.70628
661.8	NA	0.35589	0.35559	0.38453	0.40513	0.43105	0.44413	0.95399	0.83585	0.72458	0.59346
746.8	NA	0.25914	0.26703	0.28372	0.30044	0.32569	0.32601	0.67919	1.02005	0.77912	0.62454
842.8	NA	0.18326	0.20043	0.21124	0.23212	0.23205	0.25904	0.52792	1.01924	0.46881	0.46471
951.1	NA	0.13017	0.14593	0.15642	0.16632	0.19004	NA	NA	NA	NA	NA
1073.4	NA	0.09369	0.10488	0.11292	NA	NA	NA	NA	NA	NA	NA
1211.4	NA	0.06583	0.07651	NA	NA	NA	NA	NA	NA	NA	NA
1367.1	0.10789	0.04549	0.05727	NA	NA	NA	NA	NA	NA	NA	NA
1542.8	0.10106	0.02935	NA	NA	NA	NA	NA	NA	NA	NA	NA
1741.1	0.08748	0.01989	NA	NA	NA	NA	NA	NA	NA	NA	NA
1964.8	0.05214	NA	NA	NA	NA	NA	NA	NA	NA	NA	NA
2217.4	0.02812	NA	NA	NA	NA	NA	NA	NA	NA	NA	NA
2502.4	0.00873	NA	NA	NA	NA	NA	NA	NA	NA	NA	NA
2824	0.00099	NA	NA	NA	NA	NA	NA	NA	NA	NA	NA

Table A.73: FAS Linear Amp. Look-up Table for 3.846 Hz.

V_{S30} (m/s)	Soil Depth (m)										
	0	5	10	15	20	25	30	50	100	500	1000
95.6	NA	NA	NA	NA	NA	NA	0.72565	0.62809	0.89098	0.18705	-0.32001
107.9	NA	NA	NA	NA	NA	0.33961	0.35791	0.54598	0.77435	0.28816	-0.15245
121.8	NA	NA	NA	NA	0.71646	0.3707	0.3257	1.17182	0.87528	0.46506	0.11619
137.4	NA	NA	NA	NA	1.18433	0.92396	0.82338	0.89859	0.94732	0.53128	0.22935
155.1	NA	NA	NA	1.03971	1.36016	1.49187	1.52476	0.62729	0.82733	0.53398	0.15759
175	NA	NA	NA	0.47078	0.78495	1.01203	1.16	0.76348	1.07358	0.834	0.59937
197.5	NA	NA	0.17559	0.28372	0.47488	0.61968	0.66928	1.29191	1.13372	0.73648	0.42459
222.9	NA	NA	0.11983	0.293	0.43221	0.50467	0.53331	1.58754	1.12979	0.81757	0.54896
251.5	NA	NA	0.24476	0.40305	0.55002	0.59898	0.59225	1.02495	0.82554	0.8342	0.58399
283.9	NA	NA	0.54697	0.7241	0.78116	0.85332	0.76073	0.63471	0.74509	0.77431	0.54667
320.4	NA	1.6819	0.93046	1.21631	1.30835	1.29924	1.08405	0.47465	0.93559	0.75277	0.53734
361.5	NA	1.99985	1.69718	1.92495	1.87326	1.6732	1.53422	0.44991	1.20573	0.6894	0.5321
408	NA	1.83775	1.93828	1.80794	1.82939	1.7776	1.7071	0.72734	1.00939	0.78795	0.63627
460.4	NA	1.31596	1.31861	1.24204	1.3066	1.34822	1.35542	1.12039	0.5818	0.73905	0.69618
519.6	NA	0.84258	0.86773	0.82914	0.91042	0.93132	1.00468	1.38421	0.44308	0.71687	0.68056
586.4	NA	0.60232	0.58857	0.61605	0.66194	0.68907	0.73348	1.41093	0.51173	0.82969	0.67117
661.8	NA	0.41803	0.41739	0.45237	0.4767	0.50749	0.52251	1.1121	0.69697	0.5492	0.67824
746.8	NA	0.30217	0.31221	0.33203	0.35153	0.38136	0.38199	0.799	0.91105	0.81765	0.64293
842.8	NA	0.21318	0.23341	0.24615	0.27075	0.27049	0.30199	0.61784	0.98865	0.69535	0.57048
951.1	NA	0.15098	0.16961	0.18192	0.19335	0.22103	NA	NA	NA	NA	NA
1073.4	NA	0.10853	0.12175	0.13094	NA	NA	NA	NA	NA	NA	NA
1211.4	NA	0.0762	0.08868	NA	NA	NA	NA	NA	NA	NA	NA
1367.1	0.12472	0.05265	0.06623	NA	NA	NA	NA	NA	NA	NA	NA
1542.8	0.11641	0.03395	NA	NA	NA	NA	NA	NA	NA	NA	NA
1741.1	0.10039	0.02304	NA	NA	NA	NA	NA	NA	NA	NA	NA
1964.8	0.06007	NA	NA	NA	NA	NA	NA	NA	NA	NA	NA
2217.4	0.03246	NA	NA	NA	NA	NA	NA	NA	NA	NA	NA
2502.4	0.01012	NA	NA	NA	NA	NA	NA	NA	NA	NA	NA
2824	0.00117	NA	NA	NA	NA	NA	NA	NA	NA	NA	NA

Table A.74: FAS Linear Amp. Look-up Table for 4.000 Hz.

V_{S30} (m/s)	Soil Depth (m)										
	0	5	10	15	20	25	30	50	100	500	1000
95.6	NA	NA	NA	NA	NA	NA	0.96486	0.81776	0.77144	0.18033	-0.3738
107.9	NA	NA	NA	NA	NA	0.40571	0.49676	0.52753	0.89705	0.26924	-0.20841
121.8	NA	NA	NA	NA	0.56846	0.3279	0.27435	0.99106	0.69698	0.42843	0.0699
137.4	NA	NA	NA	NA	0.92842	0.69647	0.62393	1.06809	1.04573	0.51252	0.19637
155.1	NA	NA	NA	1.23773	1.48008	1.40014	1.37123	0.71893	0.7809	0.4784	0.1037
175	NA	NA	NA	0.59809	0.96565	1.21242	1.34571	0.63736	0.85909	0.77519	0.51082
197.5	NA	NA	0.21723	0.32991	0.53753	0.69333	0.76083	1.0784	1.11173	0.70112	0.3644
222.9	NA	NA	0.11451	0.28784	0.42808	0.50667	0.55276	1.58179	1.24021	0.78792	0.51865
251.5	NA	NA	0.1964	0.35009	0.49894	0.55011	0.55094	1.20303	0.87025	0.79941	0.56446
283.9	NA	NA	0.45825	0.62074	0.68363	0.75219	0.67615	0.72703	0.7308	0.77754	0.52668
320.4	NA	1.45651	0.7838	1.04524	1.13474	1.13787	0.95092	0.49506	0.79325	0.74656	0.51762
361.5	NA	1.77379	1.4884	1.74305	1.73743	1.50927	1.3842	0.42068	1.1045	0.71869	0.5156
408	NA	1.97405	1.98241	1.92154	1.90114	1.808	1.70863	0.64686	1.13931	0.74787	0.62875
460.4	NA	1.48991	1.49014	1.39407	1.45679	1.48484	1.47722	1.00175	0.67257	0.83684	0.69466
519.6	NA	0.93631	0.96353	0.91732	1.0092	1.02953	1.10685	1.2844	0.46694	0.67119	0.67444
586.4	NA	0.66184	0.64594	0.67664	0.72691	0.75655	0.8049	1.42196	0.48438	0.88925	0.68853
661.8	NA	0.45597	0.45539	0.4939	0.52077	0.55415	0.57072	1.1943	0.63307	0.56304	0.69829
746.8	NA	0.32816	0.33961	0.36121	0.38249	0.41516	0.41584	0.8687	0.84338	0.73457	0.59337
842.8	NA	0.23111	0.25335	0.26724	0.29403	0.29375	0.32801	0.67293	0.95083	0.78351	0.62049
951.1	NA	0.16344	0.18375	0.19727	0.20964	0.23972	NA	NA	NA	NA	NA
1073.4	NA	0.11738	0.1318	0.14182	NA	NA	NA	NA	NA	NA	NA
1211.4	NA	0.0824	0.09593	NA	NA	NA	NA	NA	NA	NA	NA
1367.1	0.13507	0.0569	0.0716	NA	NA	NA	NA	NA	NA	NA	NA
1542.8	0.12527	0.03669	NA	NA	NA	NA	NA	NA	NA	NA	NA
1741.1	0.10808	0.02489	NA	NA	NA	NA	NA	NA	NA	NA	NA
1964.8	0.06471	NA	NA	NA	NA	NA	NA	NA	NA	NA	NA
2217.4	0.035	NA	NA	NA	NA	NA	NA	NA	NA	NA	NA
2502.4	0.01096	NA	NA	NA	NA	NA	NA	NA	NA	NA	NA
2824	0.00129	NA	NA	NA	NA	NA	NA	NA	NA	NA	NA

Table A.75: FAS Linear Amp. Look-up Table for 4.167 Hz.

V_{S30} (m/s)	Soil Depth (m)										
	0	5	10	15	20	25	30	50	100	500	1000
95.6	NA	NA	NA	NA	NA	NA	1.10684	0.99301	0.64384	0.13344	-0.43166
107.9	NA	NA	NA	NA	NA	0.54956	0.72819	0.63284	0.8906	0.21699	-0.26643
121.8	NA	NA	NA	NA	0.47141	0.33793	0.27317	0.74337	0.63423	0.40204	0.01468
137.4	NA	NA	NA	NA	0.70409	0.51215	0.46192	1.16765	1.00116	0.49116	0.1577
155.1	NA	NA	NA	1.38196	1.4383	1.1859	1.10668	0.86849	0.73656	0.4356	0.01685
175	NA	NA	NA	0.77631	1.19115	1.40155	1.49674	0.55989	0.70477	0.70178	0.44121
197.5	NA	NA	0.28671	0.40728	0.63802	0.81137	0.90205	0.8638	1.03973	0.64984	0.30244
222.9	NA	NA	0.12591	0.30003	0.44325	0.53021	0.59887	1.4311	1.25924	0.75364	0.46119
251.5	NA	NA	0.15776	0.30736	0.45954	0.51458	0.52387	1.39837	0.94818	0.78602	0.52729
283.9	NA	NA	0.37817	0.52682	0.59582	0.66148	0.60186	0.87023	0.77508	0.75045	0.50273
320.4	NA	1.24672	0.64594	0.88762	0.97318	0.98469	0.82655	0.54166	0.68155	0.72264	0.49635
361.5	NA	1.50577	1.26749	1.51284	1.54561	1.32	1.2139	0.40566	0.95724	0.7173	0.50279
408	NA	2.03836	1.9265	1.95843	1.88798	1.76413	1.64921	0.57458	1.24007	0.74122	0.61415
460.4	NA	1.6916	1.68812	1.57841	1.62332	1.62091	1.59398	0.88284	0.79838	0.88154	0.67472
519.6	NA	1.05516	1.08538	1.02899	1.13338	1.1514	1.22791	1.16036	0.51588	0.72655	0.68148
586.4	NA	0.73471	0.71683	0.75166	0.80729	0.83946	0.89285	1.39416	0.4695	0.85218	0.7027
661.8	NA	0.50158	0.50157	0.54462	0.57444	0.61123	0.6293	1.27347	0.57304	0.66475	0.66956
746.8	NA	0.35929	0.37277	0.3966	0.42005	0.45635	0.45638	0.95105	0.76832	0.61403	0.56713
842.8	NA	0.25265	0.2773	0.29276	0.32232	0.32152	0.35962	0.7385	0.89486	0.79925	0.6018
951.1	NA	0.17827	0.20077	0.21564	0.22915	0.26191	NA	NA	NA	NA	NA
1073.4	NA	0.12796	0.14383	0.15479	NA	NA	NA	NA	NA	NA	NA
1211.4	NA	0.0898	0.1046	NA	NA	NA	NA	NA	NA	NA	NA
1367.1	0.14669	0.06196	0.07811	NA	NA	NA	NA	NA	NA	NA	NA
1542.8	0.13593	0.03997	NA	NA	NA	NA	NA	NA	NA	NA	NA
1741.1	0.11713	0.0271	NA	NA	NA	NA	NA	NA	NA	NA	NA
1964.8	0.07017	NA	NA	NA	NA	NA	NA	NA	NA	NA	NA
2217.4	0.03799	NA	NA	NA	NA	NA	NA	NA	NA	NA	NA
2502.4	0.01195	NA	NA	NA	NA	NA	NA	NA	NA	NA	NA
2824	0.00142	NA	NA	NA	NA	NA	NA	NA	NA	NA	NA

Table A.76: FAS Linear Amp. Look-up Table for 4.545 Hz.

V_{S30} (m/s)	Soil Depth (m)										
	0	5	10	15	20	25	30	50	100	500	1000
95.6	NA	NA	NA	NA	NA	NA	0.84039	0.86865	0.79903	0.06995	-0.56133
107.9	NA	NA	NA	NA	NA	1.0389	1.09986	1.00809	0.65526	0.16095	-0.38336
121.8	NA	NA	NA	NA	0.48596	0.5948	0.48998	0.525	0.88774	0.31979	-0.10919
137.4	NA	NA	NA	NA	0.45701	0.32706	0.31518	0.92659	0.69238	0.43262	0.0652
155.1	NA	NA	NA	1.20622	0.93517	0.67463	0.60308	1.10308	0.85561	0.34501	-0.0987
175	NA	NA	NA	1.20724	1.46288	1.38771	1.35476	0.61472	0.71255	0.58317	0.2935
197.5	NA	NA	0.54931	0.69641	0.99559	1.20724	1.31792	0.61159	0.82744	0.53795	0.15517
222.9	NA	NA	0.22185	0.39934	0.55837	0.67215	0.80974	0.92994	0.95667	0.65159	0.3373
251.5	NA	NA	0.12522	0.27022	0.43562	0.50405	0.53439	1.5223	1.13028	0.73758	0.44239
283.9	NA	NA	0.25674	0.38241	0.46865	0.53171	0.50451	1.29813	0.99886	0.71875	0.44355
320.4	NA	0.91776	0.41912	0.63263	0.71493	0.74008	0.63067	0.74693	0.67428	0.70588	0.44381
361.5	NA	1.04948	0.88387	1.08253	1.14458	0.97179	0.89804	0.44071	0.65772	0.67282	0.46707
408	NA	1.81953	1.53875	1.73191	1.59345	1.46945	1.37582	0.47744	1.20453	0.7744	0.58809
460.4	NA	1.99309	1.96266	1.91462	1.84951	1.75081	1.68563	0.68399	1.11667	0.73276	0.66036
519.6	NA	1.38137	1.41373	1.32443	1.44644	1.44104	1.4805	0.90552	0.71604	0.8414	0.66047
586.4	NA	0.92684	0.90087	0.94699	1.01505	1.04945	1.11004	1.22	0.49982	0.67775	0.68224
661.8	NA	0.61751	0.61776	0.67282	0.70995	0.75509	0.77604	1.35824	0.48856	0.87905	0.68662
746.8	NA	0.43599	0.45495	0.48429	0.51353	0.55859	0.55748	1.12562	0.62501	0.56031	0.67861
842.8	NA	0.30511	0.33604	0.35526	0.39169	0.39012	0.43591	0.89068	0.75579	0.59897	0.57885
951.1	NA	0.21415	0.24219	0.26037	0.27695	0.31749	NA	NA	NA	NA	NA
1073.4	NA	0.15346	0.17304	0.1864	NA	NA	NA	NA	NA	NA	NA
1211.4	NA	0.10762	0.1257	NA	NA	NA	NA	NA	NA	NA	NA
1367.1	0.17467	0.07417	0.09355	NA	NA	NA	NA	NA	NA	NA	NA
1542.8	0.16126	0.04784	NA	NA	NA	NA	NA	NA	NA	NA	NA
1741.1	0.13854	0.0324	NA	NA	NA	NA	NA	NA	NA	NA	NA
1964.8	0.08308	NA	NA	NA	NA	NA	NA	NA	NA	NA	NA
2217.4	0.04512	NA	NA	NA	NA	NA	NA	NA	NA	NA	NA
2502.4	0.01431	NA	NA	NA	NA	NA	NA	NA	NA	NA	NA
2824	0.00175	NA	NA	NA	NA	NA	NA	NA	NA	NA	NA

Table A.77: FAS Linear Amp. Look-up Table for 5.0 Hz.

V_{S30} (m/s)	Soil Depth (m)										
	0	5	10	15	20	25	30	50	100	500	1000
95.6	NA	NA	NA	NA	NA	NA	0.53346	0.731	0.66172	-0.05192	-0.73532
107.9	NA	NA	NA	NA	NA	0.93733	0.72822	0.78511	0.80844	0.08591	-0.52042
121.8	NA	NA	NA	NA	0.87388	1.08334	1.01363	0.87261	0.73654	0.25241	-0.22552
137.4	NA	NA	NA	NA	0.52211	0.43651	0.46652	0.58556	0.84526	0.34887	-0.05997
155.1	NA	NA	NA	0.71634	0.51313	0.39765	0.36503	0.91947	0.8468	0.26981	-0.22925
175	NA	NA	NA	1.30651	1.06402	0.83115	0.77489	0.98978	0.98354	0.50824	0.18549
197.5	NA	NA	1.05261	1.20028	1.43217	1.51156	1.48848	0.67794	0.77074	0.4204	-0.00043
222.9	NA	NA	0.48406	0.66399	0.86315	1.01967	1.24947	0.60541	0.72959	0.54833	0.19389
251.5	NA	NA	0.17902	0.32443	0.51509	0.61182	0.67526	1.07306	1.03338	0.64599	0.31952
283.9	NA	NA	0.19872	0.30575	0.41801	0.48253	0.49308	1.52003	1.10571	0.65465	0.35895
320.4	NA	0.68516	0.2525	0.45032	0.53464	0.57441	0.50889	1.17666	0.9776	0.66586	0.38239
361.5	NA	0.71094	0.58906	0.75293	0.8264	0.70338	0.65268	0.61192	0.6008	0.6605	0.42687
408	NA	1.32516	1.06994	1.28857	1.16984	1.07828	1.02626	0.46251	0.86239	0.73101	0.55372
460.4	NA	1.83801	1.77896	1.86356	1.69041	1.55692	1.48202	0.5504	1.32002	0.83639	0.63169
519.6	NA	1.77929	1.79346	1.71115	1.75189	1.68553	1.61281	0.68754	1.06876	0.71678	0.64169
586.4	NA	1.22166	1.17629	1.23556	1.30904	1.32856	1.37156	0.96066	0.64977	0.82164	0.67014
661.8	NA	0.78071	0.7814	0.85452	0.90103	0.95531	0.97588	1.26932	0.47279	0.69415	0.67032
746.8	NA	0.53976	0.56782	0.60491	0.64137	0.69825	0.69461	1.25787	0.51538	0.80849	0.61909
842.8	NA	0.37529	0.41505	0.43965	0.48545	0.48279	0.53942	1.06481	0.61187	0.54027	0.63228
951.1	NA	0.26149	0.2973	0.32025	0.34038	0.39076	NA	NA	NA	NA	NA
1073.4	NA	0.18688	0.21161	0.22826	NA	NA	NA	NA	NA	NA	NA
1211.4	NA	0.1309	0.1533	NA	NA	NA	NA	NA	NA	NA	NA
1367.1	0.21182	0.09007	0.11395	NA	NA	NA	NA	NA	NA	NA	NA
1542.8	0.1928	0.05806	NA	NA	NA	NA	NA	NA	NA	NA	NA
1741.1	0.16494	0.03933	NA	NA	NA	NA	NA	NA	NA	NA	NA
1964.8	0.09931	NA	NA	NA	NA	NA	NA	NA	NA	NA	NA
2217.4	0.05419	NA	NA	NA	NA	NA	NA	NA	NA	NA	NA
2502.4	0.01734	NA	NA	NA	NA	NA	NA	NA	NA	NA	NA
2824	0.00217	NA	NA	NA	NA	NA	NA	NA	NA	NA	NA

Table A.78: FAS Linear Amp. Look-up Table for 5.263 Hz.

V_{S30} (m/s)	Soil Depth (m)										
	0	5	10	15	20	25	30	50	100	500	1000
95.6	NA	NA	NA	NA	NA	NA	0.64388	0.85418	0.67207	-0.1443	-0.87014
107.9	NA	NA	NA	NA	NA	0.65002	0.53856	0.67787	0.7218	0.02263	-0.6045
121.8	NA	NA	NA	NA	1.08189	1.05527	1.07881	1.00153	0.68868	0.21709	-0.2881
137.4	NA	NA	NA	NA	0.72113	0.65671	0.70268	0.6364	0.89245	0.31954	-0.12491
155.1	NA	NA	NA	0.5769	0.43261	0.37929	0.36261	0.72796	0.68852	0.20422	-0.31282
175	NA	NA	NA	1.08064	0.77644	0.58156	0.54784	1.14546	0.9835	0.48107	0.14378
197.5	NA	NA	1.26289	1.3748	1.43033	1.38322	1.30175	0.83554	0.80978	0.37137	-0.08065
222.9	NA	NA	0.7169	0.90007	1.12097	1.26865	1.45836	0.57734	0.8082	0.50375	0.12464
251.5	NA	NA	0.25709	0.40571	0.61625	0.73914	0.82801	0.81311	0.88857	0.58862	0.25187
283.9	NA	NA	0.20163	0.30034	0.43169	0.49923	0.53363	1.34047	1.00962	0.62831	0.29669
320.4	NA	0.59689	0.19424	0.38699	0.47543	0.52441	0.48126	1.41475	1.12814	0.64865	0.34444
361.5	NA	0.57898	0.47268	0.62413	0.70422	0.60125	0.56061	0.7849	0.73565	0.64344	0.38996
408	NA	1.09904	0.87085	1.07528	0.98184	0.90476	0.86827	0.5	0.69773	0.7367	0.53214
460.4	NA	1.61404	1.55088	1.65435	1.4789	1.36527	1.30115	0.51539	1.24111	0.80513	0.62423
519.6	NA	1.9197	1.89312	1.86506	1.79613	1.70232	1.56826	0.60287	1.23175	0.76589	0.62213
586.4	NA	1.42534	1.36474	1.42789	1.48437	1.47749	1.48378	0.83251	0.78459	0.82208	0.65601
661.8	NA	0.89027	0.89056	0.97604	1.02677	1.08326	1.09941	1.16054	0.50324	0.66733	0.67977
746.8	NA	0.60651	0.6412	0.68323	0.72449	0.78832	0.78182	1.27215	0.4827	0.83045	0.6726
842.8	NA	0.41961	0.46536	0.49364	0.54585	0.54179	0.60595	1.14481	0.55007	0.68231	0.6257
951.1	NA	0.29098	0.33213	0.35811	0.38054	0.43694	NA	NA	NA	NA	NA
1073.4	NA	0.20756	0.23569	0.25434	NA	NA	NA	NA	NA	NA	NA
1211.4	NA	0.14532	0.17044	NA	NA	NA	NA	NA	NA	NA	NA
1367.1	0.23341	0.09987	0.12656	NA	NA	NA	NA	NA	NA	NA	NA
1542.8	0.21147	0.06438	NA	NA	NA	NA	NA	NA	NA	NA	NA
1741.1	0.18072	0.04358	NA	NA	NA	NA	NA	NA	NA	NA	NA
1964.8	0.10896	NA	NA	NA	NA	NA	NA	NA	NA	NA	NA
2217.4	0.05964	NA	NA	NA	NA	NA	NA	NA	NA	NA	NA
2502.4	0.0192	NA	NA	NA	NA	NA	NA	NA	NA	NA	NA
2824	0.00244	NA	NA	NA	NA	NA	NA	NA	NA	NA	NA

Table A.79: FAS Linear Amp. Look-up Table for 5.556 Hz.

V_{S30} (m/s)	Soil Depth (m)										
	0	5	10	15	20	25	30	50	100	500	1000
95.6	NA	NA	NA	NA	NA	NA	0.8536	0.80096	0.61188	-0.25915	-1.03643
107.9	NA	NA	NA	NA	NA	0.48597	0.55542	0.79506	0.67528	-0.06669	-0.73093
121.8	NA	NA	NA	NA	1.03509	0.77613	0.87169	0.8867	0.79709	0.17765	-0.35907
137.4	NA	NA	NA	NA	1.00982	0.95892	0.97693	0.83159	0.77447	0.27444	-0.19345
155.1	NA	NA	NA	0.54073	0.45543	0.46911	0.46636	0.61332	0.6473	0.15569	-0.40797
175	NA	NA	NA	0.78012	0.56455	0.41434	0.40108	1.10696	0.83294	0.46311	0.09348
197.5	NA	NA	1.26461	1.31024	1.19338	1.07421	0.99392	1.01125	0.85309	0.32004	-0.15889
222.9	NA	NA	0.98428	1.19863	1.39018	1.46813	1.4855	0.66742	0.91675	0.44081	0.04282
251.5	NA	NA	0.39452	0.55027	0.78947	0.95015	1.07108	0.63459	0.78442	0.53242	0.17698
283.9	NA	NA	0.23494	0.32631	0.48428	0.55775	0.624	1.02076	0.87071	0.57082	0.22989
320.4	NA	0.52318	0.15444	0.34383	0.43966	0.49979	0.48255	1.49984	1.13782	0.61204	0.29751
361.5	NA	0.46319	0.37151	0.51398	0.60251	0.51833	0.48845	1.04715	0.94839	0.63546	0.36021
408	NA	0.89387	0.69327	0.88409	0.81522	0.75017	0.72637	0.58628	0.61368	0.71728	0.50471
460.4	NA	1.35173	1.29286	1.38676	1.23514	1.14815	1.10342	0.50762	1.0306	0.74045	0.60498
519.6	NA	1.93438	1.8694	1.89699	1.70986	1.60833	1.43912	0.53709	1.28743	0.78956	0.61782
586.4	NA	1.65831	1.59174	1.64786	1.65129	1.59548	1.54422	0.71285	0.95649	0.72172	0.64717
661.8	NA	1.0341	1.03276	1.13317	1.18583	1.2355	1.23987	1.02191	0.57389	0.783	0.67351
746.8	NA	0.69009	0.73441	0.78254	0.82927	0.90195	0.8901	1.23347	0.47142	0.72109	0.66538
842.8	NA	0.47465	0.5282	0.56096	0.62079	0.61381	0.68658	1.20075	0.49937	0.81411	0.62768
951.1	NA	0.32709	0.37493	0.40474	0.43038	0.49309	NA	NA	NA	NA	NA
1073.4	NA	0.2328	0.26524	0.28614	NA	NA	NA	NA	NA	NA	NA
1211.4	NA	0.16286	0.19139	NA	NA	NA	NA	NA	NA	NA	NA
1367.1	0.26026	0.11176	0.14179	NA	NA	NA	NA	NA	NA	NA	NA
1542.8	0.23373	0.07206	NA	NA	NA	NA	NA	NA	NA	NA	NA
1741.1	0.19899	0.04873	NA	NA	NA	NA	NA	NA	NA	NA	NA
1964.8	0.12042	NA	NA	NA	NA	NA	NA	NA	NA	NA	NA
2217.4	0.06609	NA	NA	NA	NA	NA	NA	NA	NA	NA	NA
2502.4	0.02141	NA	NA	NA	NA	NA	NA	NA	NA	NA	NA
2824	0.00275	NA	NA	NA	NA	NA	NA	NA	NA	NA	NA

Table A.80: FAS Linear Amp. Look-up Table for 5.882 Hz.

V_{S30} (m/s)	Soil Depth (m)										
	0	5	10	15	20	25	30	50	100	500	1000
95.6	NA	NA	NA	NA	NA	NA	0.8303	0.57973	0.49935	-0.38972	-1.22063
107.9	NA	NA	NA	NA	NA	0.5463	0.7673	0.83773	0.66076	-0.17961	-0.89455
121.8	NA	NA	NA	NA	0.70442	0.51495	0.58995	0.69074	0.77341	0.12172	-0.44001
137.4	NA	NA	NA	NA	1.08612	1.07307	1.07066	0.97729	0.71081	0.23291	-0.26542
155.1	NA	NA	NA	0.63391	0.62174	0.70041	0.7058	0.69145	0.79111	0.09903	-0.50589
175	NA	NA	NA	0.57024	0.46586	0.35053	0.35416	0.86918	0.71508	0.40881	0.02849
197.5	NA	NA	1.00749	1.02067	0.85469	0.75449	0.7074	1.08745	0.85996	0.27895	-0.23176
222.9	NA	NA	1.14189	1.3934	1.47019	1.43653	1.25094	0.89244	0.92066	0.38233	-0.04813
251.5	NA	NA	0.61809	0.78386	1.05514	1.23064	1.35683	0.57202	0.77054	0.47698	0.09526
283.9	NA	NA	0.31196	0.39615	0.59284	0.67612	0.78506	0.73868	0.79674	0.51971	0.15565
320.4	NA	0.47174	0.14158	0.3284	0.43597	0.51013	0.52363	1.32262	0.96969	0.58231	0.23771
361.5	NA	0.368	0.2925	0.42879	0.52789	0.4626	0.44398	1.32893	1.09905	0.60614	0.32455
408	NA	0.71911	0.5446	0.72463	0.67748	0.62349	0.61139	0.74093	0.66208	0.70675	0.48794
460.4	NA	1.09247	1.0469	1.13383	1.01056	0.94629	0.92132	0.53771	0.8007	0.798	0.59029
519.6	NA	1.7844	1.71437	1.75425	1.50628	1.42232	1.25425	0.49816	1.17195	0.7378	0.59576
586.4	NA	1.84711	1.80295	1.81853	1.73579	1.62609	1.51304	0.61381	1.13003	0.72956	0.62587
661.8	NA	1.22001	1.21391	1.32794	1.37081	1.39137	1.37336	0.87802	0.69588	0.82553	0.65972
746.8	NA	0.79286	0.85044	0.90568	0.95742	1.0376	1.01676	1.14136	0.49081	0.6419	0.64446
842.8	NA	0.54102	0.60461	0.64304	0.71249	0.70265	0.78422	1.20804	0.46917	0.77095	0.64328
951.1	NA	0.36982	0.42628	0.46103	0.49024	0.56252	NA	NA	NA	NA	NA
1073.4	NA	0.26257	0.30048	0.32443	NA	NA	NA	NA	NA	NA	NA
1211.4	NA	0.18358	0.21624	NA	NA	NA	NA	NA	NA	NA	NA
1367.1	0.29164	0.12577	0.16001	NA	NA	NA	NA	NA	NA	NA	NA
1542.8	0.25794	0.08104	NA	NA	NA	NA	NA	NA	NA	NA	NA
1741.1	0.2195	0.05478	NA	NA	NA	NA	NA	NA	NA	NA	NA
1964.8	0.13318	NA	NA	NA	NA	NA	NA	NA	NA	NA	NA
2217.4	0.07346	NA	NA	NA	NA	NA	NA	NA	NA	NA	NA
2502.4	0.02399	NA	NA	NA	NA	NA	NA	NA	NA	NA	NA
2824	0.00313	NA	NA	NA	NA	NA	NA	NA	NA	NA	NA

Table A.81: FAS Linear Amp. Look-up Table for 6.250 Hz.

V_{S30} (m/s)	Soil Depth (m)										
	0	5	10	15	20	25	30	50	100	500	1000
95.6	NA	NA	NA	NA	NA	NA	0.52345	0.5761	0.44474	-0.53195	-1.43584
107.9	NA	NA	NA	NA	NA	0.7921	0.84913	0.63355	0.53542	-0.30957	-1.07743
121.8	NA	NA	NA	NA	0.41261	0.49358	0.52828	0.74479	0.68693	0.03673	-0.55679
137.4	NA	NA	NA	NA	0.81902	0.85565	0.86722	0.8873	0.79293	0.1901	-0.3429
155.1	NA	NA	NA	0.85786	0.92237	0.98637	0.98843	0.84902	0.78061	0.03254	-0.60462
175	NA	NA	NA	0.50256	0.50214	0.41292	0.43605	0.63376	0.79895	0.36326	-0.05072
197.5	NA	NA	0.67192	0.70434	0.58801	0.53729	0.52823	0.99526	0.81483	0.22783	-0.31067
222.9	NA	NA	1.07432	1.30802	1.24332	1.15127	0.8947	1.12019	0.79778	0.32622	-0.1407
251.5	NA	NA	0.94144	1.11549	1.35924	1.4496	1.5014	0.64465	0.84868	0.41892	0.00881
283.9	NA	NA	0.45371	0.53011	0.78507	0.88433	1.04538	0.57789	0.82264	0.47178	0.07536
320.4	NA	0.44152	0.1643	0.34911	0.47465	0.56725	0.62032	0.98987	0.77773	0.53413	0.17101
361.5	NA	0.29606	0.23916	0.37102	0.4844	0.43894	0.43382	1.44505	1.06046	0.58342	0.2758
408	NA	0.57431	0.42235	0.59657	0.57017	0.52609	0.52608	0.98942	0.83943	0.69464	0.45966
460.4	NA	0.86379	0.83213	0.91958	0.81996	0.77475	0.76813	0.62037	0.66727	0.77113	0.57737
519.6	NA	1.51955	1.47008	1.4888	1.25257	1.19815	1.05605	0.49337	0.93451	0.74839	0.57956
586.4	NA	1.9021	1.90396	1.83827	1.67709	1.53698	1.38499	0.53999	1.22111	0.78563	0.61408
661.8	NA	1.45262	1.44179	1.55201	1.55614	1.51254	1.46304	0.7451	0.87319	0.72658	0.64919
746.8	NA	0.92289	0.99829	1.06047	1.11482	1.19572	1.15714	1.01104	0.55146	0.73327	0.66113
842.8	NA	0.62242	0.69895	0.74477	0.8256	0.81056	0.89949	1.15532	0.46687	0.63163	0.64847
951.1	NA	0.42116	0.48871	0.52967	0.56275	0.64633	NA	NA	NA	NA	NA
1073.4	NA	0.29805	0.34296	0.37044	NA	NA	NA	NA	NA	NA	NA
1211.4	NA	0.2081	0.24596	NA	NA	NA	NA	NA	NA	NA	NA
1367.1	0.327	0.14234	0.18164	NA	NA	NA	NA	NA	NA	NA	NA
1542.8	0.2851	0.09168	NA	NA	NA	NA	NA	NA	NA	NA	NA
1741.1	0.2416	0.06193	NA	NA	NA	NA	NA	NA	NA	NA	NA
1964.8	0.14763	NA	NA	NA	NA	NA	NA	NA	NA	NA	NA
2217.4	0.08191	NA	NA	NA	NA	NA	NA	NA	NA	NA	NA
2502.4	0.027	NA	NA	NA	NA	NA	NA	NA	NA	NA	NA
2824	0.00357	NA	NA	NA	NA	NA	NA	NA	NA	NA	NA

Table A.82: FAS Linear Amp. Look-up Table for 6.667 Hz.

V_{S30} (m/s)	Soil Depth (m)										
	0	5	10	15	20	25	30	50	100	500	1000
95.6	NA	NA	NA	NA	NA	NA	0.33995	0.61334	0.32414	-0.69859	-1.66277
107.9	NA	NA	NA	NA	NA	0.82673	0.58214	0.5408	0.47118	-0.45776	-1.29486
121.8	NA	NA	NA	NA	0.35429	0.72428	0.72676	0.82711	0.67645	-0.07941	-0.72316
137.4	NA	NA	NA	NA	0.45475	0.53973	0.59969	0.73943	0.76027	0.12528	-0.43927
155.1	NA	NA	NA	1.0665	1.06746	1.05231	1.06651	0.90631	0.64405	-0.02355	-0.70692
175	NA	NA	NA	0.5933	0.71036	0.64523	0.6925	0.633	0.87443	0.30998	-0.13679
197.5	NA	NA	0.42375	0.51131	0.45317	0.44566	0.475	0.80304	0.75681	0.16856	-0.41067
222.9	NA	NA	0.79907	0.9919	0.86977	0.79204	0.59908	1.12179	0.72471	0.26084	-0.2321
251.5	NA	NA	1.22582	1.37507	1.47848	1.40066	1.32507	0.85675	0.87789	0.35365	-0.0856
283.9	NA	NA	0.70109	0.7653	1.09134	1.1998	1.35148	0.55946	0.87288	0.41225	-0.00837
320.4	NA	0.43736	0.23737	0.4211	0.57469	0.69376	0.80061	0.70467	0.7484	0.48766	0.09717
361.5	NA	0.24929	0.21591	0.34577	0.47858	0.45648	0.46931	1.25432	0.85313	0.54711	0.21511
408	NA	0.45685	0.32614	0.49825	0.49285	0.45964	0.47364	1.29054	1.07029	0.67223	0.41945
460.4	NA	0.66645	0.64945	0.74085	0.66166	0.63305	0.64399	0.78135	0.68084	0.75609	0.54982
519.6	NA	1.23766	1.19269	1.19884	1.00539	0.97854	0.87093	0.53429	0.70969	0.75242	0.56964
586.4	NA	1.78455	1.81711	1.66183	1.47807	1.34501	1.19059	0.49702	1.13989	0.7291	0.6032
661.8	NA	1.69348	1.70061	1.74562	1.67031	1.54483	1.46091	0.63061	1.08186	0.71654	0.6333
746.8	NA	1.09409	1.19508	1.25912	1.3029	1.36238	1.29622	0.86462	0.6706	0.79817	0.6386
842.8	NA	0.72613	0.82015	0.87504	0.96907	0.94376	1.03637	1.04575	0.50274	0.66466	0.63945
951.1	NA	0.48479	0.56745	0.61585	0.65417	0.75077	NA	NA	NA	NA	NA
1073.4	NA	0.34157	0.39567	0.42758	NA	NA	NA	NA	NA	NA	NA
1211.4	NA	0.23822	0.28272	NA	NA	NA	NA	NA	NA	NA	NA
1367.1	0.36906	0.1625	0.2079	NA	NA	NA	NA	NA	NA	NA	NA
1542.8	0.31525	0.10463	NA	NA	NA	NA	NA	NA	NA	NA	NA
1741.1	0.26617	0.07061	NA	NA	NA	NA	NA	NA	NA	NA	NA
1964.8	0.16412	NA	NA	NA	NA	NA	NA	NA	NA	NA	NA
2217.4	0.09176	NA	NA	NA	NA	NA	NA	NA	NA	NA	NA
2502.4	0.03058	NA	NA	NA	NA	NA	NA	NA	NA	NA	NA
2824	0.00411	NA	NA	NA	NA	NA	NA	NA	NA	NA	NA

Table A.83: FAS Linear Amp. Look-up Table for 7.143 Hz.

V_{S30} (m/s)	Soil Depth (m)										
	0	5	10	15	20	25	30	50	100	500	1000
95.6	NA	NA	NA	NA	NA	NA	0.53846	0.43767	0.29802	-0.85605	-1.87647
107.9	NA	NA	NA	NA	NA	0.51302	0.32156	0.61002	0.34868	-0.62715	-1.52835
121.8	NA	NA	NA	NA	0.59162	0.83191	0.83116	0.62037	0.55054	-0.22027	-0.92176
137.4	NA	NA	NA	NA	0.3381	0.48719	0.59777	0.7815	0.68951	0.0198	-0.58647
155.1	NA	NA	NA	0.98611	0.78697	0.77492	0.80821	0.79433	0.71042	-0.09643	-0.83177
175	NA	NA	NA	0.822	1.0017	0.96135	1.0432	0.86284	0.75339	0.25486	-0.22956
197.5	NA	NA	0.32197	0.48909	0.47977	0.51434	0.59012	0.70363	0.74566	0.09101	-0.53163
222.9	NA	NA	0.45826	0.67185	0.59272	0.54713	0.44667	0.84601	0.77797	0.19233	-0.33387
251.5	NA	NA	1.16186	1.28413	1.23232	1.06	0.92973	1.09001	0.78422	0.28521	-0.18679
283.9	NA	NA	1.04572	1.1234	1.3964	1.46546	1.46005	0.72834	0.83065	0.3438	-0.10596
320.4	NA	0.46708	0.3913	0.57566	0.7743	0.9301	1.09626	0.56973	0.88872	0.43528	0.01454
361.5	NA	0.23528	0.23521	0.36567	0.52582	0.53449	0.57408	0.88447	0.70256	0.49967	0.14405
408	NA	0.36716	0.26047	0.43382	0.45247	0.43324	0.4651	1.43072	1.13553	0.6466	0.36954
460.4	NA	0.49969	0.49941	0.59707	0.53762	0.52568	0.55413	1.05335	0.86012	0.74983	0.51656
519.6	NA	0.97703	0.93768	0.94299	0.79173	0.78676	0.71377	0.64337	0.61139	0.73577	0.5514
586.4	NA	1.53801	1.55812	1.36038	1.21063	1.10678	0.97756	0.49698	0.9059	0.73654	0.57828
661.8	NA	1.84136	1.88573	1.77514	1.61882	1.44483	1.33868	0.54386	1.2081	0.7774	0.62242
746.8	NA	1.32557	1.45638	1.49657	1.49282	1.48563	1.38937	0.72348	0.86287	0.69971	0.62947
842.8	NA	0.86323	0.98172	1.0459	1.15112	1.10725	1.18908	0.89857	0.5968	0.79055	0.63474
951.1	NA	0.56555	0.66926	0.72826	0.77052	0.88223	NA	NA	NA	NA	NA
1073.4	NA	0.39608	0.46271	0.5007	NA	NA	NA	NA	NA	NA	NA
1211.4	NA	0.27583	0.32886	NA	NA	NA	NA	NA	NA	NA	NA
1367.1	0.41875	0.18744	0.24125	NA	NA	NA	NA	NA	NA	NA	NA
1542.8	0.34771	0.12068	NA	NA	NA	NA	NA	NA	NA	NA	NA
1741.1	0.29277	0.08132	NA	NA	NA	NA	NA	NA	NA	NA	NA
1964.8	0.18289	NA	NA	NA	NA	NA	NA	NA	NA	NA	NA
2217.4	0.10331	NA	NA	NA	NA	NA	NA	NA	NA	NA	NA
2502.4	0.03491	NA	NA	NA	NA	NA	NA	NA	NA	NA	NA
2824	0.00477	NA	NA	NA	NA	NA	NA	NA	NA	NA	NA

Table A.84: FAS Linear Amp. Look-up Table for 7.5 Hz.

V_{S30} (m/s)	Soil Depth (m)										
	0	5	10	15	20	25	30	50	100	500	1000
95.6	NA	NA	NA	NA	NA	NA	0.65304	0.44252	0.27615	-0.94804	-2.02429
107.9	NA	NA	NA	NA	NA	0.37526	0.40516	0.50573	0.31402	-0.74586	-1.68389
121.8	NA	NA	NA	NA	0.81135	0.64992	0.64761	0.52299	0.49552	-0.32961	-1.07744
137.4	NA	NA	NA	NA	0.45227	0.64321	0.73306	0.79552	0.66165	-0.07499	-0.71826
155.1	NA	NA	NA	0.76983	0.49736	0.56612	0.60743	0.74438	0.69413	-0.16159	-0.93725
175	NA	NA	NA	0.98366	1.04329	1.04239	1.11066	0.98065	0.71418	0.22011	-0.29282
197.5	NA	NA	0.35202	0.59763	0.62304	0.68954	0.79181	0.75496	0.76347	0.03413	-0.626
222.9	NA	NA	0.29782	0.54175	0.50494	0.47416	0.44109	0.65359	0.78461	0.13285	-0.4168
251.5	NA	NA	0.89638	1.02776	0.95355	0.79207	0.6891	1.10346	0.73628	0.25339	-0.25402
283.9	NA	NA	1.20181	1.3487	1.4383	1.43844	1.31445	0.93745	0.78001	0.28795	-0.18148
320.4	NA	0.51616	0.57164	0.75474	0.99341	1.15873	1.3204	0.58648	0.94812	0.39317	-0.04577
361.5	NA	0.25037	0.28287	0.41563	0.6014	0.63843	0.70426	0.67555	0.75612	0.47009	0.09
408	NA	0.32438	0.23826	0.41426	0.45312	0.4461	0.49399	1.31869	1.00376	0.61813	0.32612
460.4	NA	0.40522	0.4173	0.52144	0.47656	0.47646	0.51809	1.27291	1.04527	0.72448	0.48841
519.6	NA	0.82223	0.78964	0.79822	0.67152	0.67992	0.62821	0.77322	0.65396	0.73865	0.53048
586.4	NA	1.3418	1.34095	1.14838	1.03333	0.9506	0.84425	0.53128	0.7487	0.74909	0.57228
661.8	NA	1.83387	1.87878	1.65862	1.48004	1.31209	1.2034	0.50701	1.16384	0.73563	0.60357
746.8	NA	1.50949	1.65367	1.6409	1.57553	1.49946	1.39177	0.63981	1.01349	0.67424	0.6222
842.8	NA	0.9832	1.12267	1.18968	1.29297	1.22966	1.27874	0.79737	0.70314	0.73072	0.62541
951.1	NA	0.63287	0.75527	0.82302	0.86904	0.98753	NA	NA	NA	NA	NA
1073.4	NA	0.44073	0.51846	0.56167	NA	NA	NA	NA	NA	NA	NA
1211.4	NA	0.30647	0.36696	NA	NA	NA	NA	NA	NA	NA	NA
1367.1	0.45654	0.20776	0.26837	NA	NA	NA	NA	NA	NA	NA	NA
1542.8	0.37098	0.13367	NA	NA	NA	NA	NA	NA	NA	NA	NA
1741.1	0.31097	0.09004	NA	NA	NA	NA	NA	NA	NA	NA	NA
1964.8	0.19659	NA	NA	NA	NA	NA	NA	NA	NA	NA	NA
2217.4	0.11218	NA	NA	NA	NA	NA	NA	NA	NA	NA	NA
2502.4	0.03833	NA	NA	NA	NA	NA	NA	NA	NA	NA	NA
2824	0.0053	NA	NA	NA	NA	NA	NA	NA	NA	NA	NA

Table A.85: FAS Linear Amp. Look-up Table for 7.692 Hz.

V_{S30} (m/s)	Soil Depth (m)										
	0	5	10	15	20	25	30	50	100	500	1000
95.6	NA	NA	NA	NA	NA	NA	0.63947	0.47555	0.25854	-0.99634	-2.10256
107.9	NA	NA	NA	NA	NA	0.39527	0.5082	0.43402	0.30921	-0.79886	-1.75851
121.8	NA	NA	NA	NA	0.85129	0.51638	0.50841	0.54538	0.4653	-0.38888	-1.16103
137.4	NA	NA	NA	NA	0.56937	0.73949	0.79319	0.7528	0.62571	-0.12812	-0.79052
155.1	NA	NA	NA	0.65711	0.39258	0.5131	0.55845	0.74635	0.65752	-0.2065	-0.99825
175	NA	NA	NA	1.01567	0.97442	0.99403	1.05188	0.97219	0.739	0.20426	-0.32337
197.5	NA	NA	0.40531	0.69061	0.73572	0.81744	0.91645	0.80577	0.75755	0.00218	-0.67578
222.9	NA	NA	0.25026	0.51056	0.49511	0.46998	0.47446	0.60112	0.75066	0.10777	-0.46343
251.5	NA	NA	0.73546	0.88426	0.82202	0.68021	0.59744	1.04625	0.74255	0.22455	-0.2881
283.9	NA	NA	1.21837	1.40663	1.37719	1.34325	1.18845	1.04281	0.76545	0.27134	-0.21831
320.4	NA	0.55154	0.69451	0.87498	1.12659	1.27785	1.40428	0.63484	0.93357	0.37094	-0.07945
361.5	NA	0.26762	0.32115	0.45563	0.65727	0.71158	0.79412	0.60241	0.8175	0.44575	0.06181
408	NA	0.30953	0.23553	0.4134	0.46397	0.46444	0.52216	1.20675	0.90247	0.6068	0.306
460.4	NA	0.36339	0.38249	0.49053	0.45361	0.45998	0.50876	1.36484	1.12968	0.71901	0.47235
519.6	NA	0.75164	0.72284	0.73366	0.61836	0.63343	0.59236	0.86026	0.71615	0.73539	0.52635
586.4	NA	1.24188	1.23238	1.04875	0.95067	0.87758	0.78274	0.56184	0.69029	0.73772	0.55688
661.8	NA	1.79386	1.82486	1.56629	1.38922	1.23287	1.12775	0.49669	1.09828	0.71066	0.60061
746.8	NA	1.60151	1.74284	1.69078	1.58935	1.47777	1.36985	0.60278	1.08061	0.71098	0.60349
842.8	NA	1.05463	1.20507	1.26975	1.36476	1.28903	1.31346	0.74768	0.77182	0.68165	0.62418
951.1	NA	0.67153	0.80525	0.87795	0.92462	1.04676	NA	NA	NA	NA	NA
1073.4	NA	0.46602	0.55049	0.59599	NA	NA	NA	NA	NA	NA	NA
1211.4	NA	0.32377	0.38854	NA	NA	NA	NA	NA	NA	NA	NA
1367.1	0.4772	0.21914	0.2837	NA	NA	NA	NA	NA	NA	NA	NA
1542.8	0.38261	0.141	NA	NA	NA	NA	NA	NA	NA	NA	NA
1741.1	0.31997	0.09494	NA	NA	NA	NA	NA	NA	NA	NA	NA
1964.8	0.20369	NA	NA	NA	NA	NA	NA	NA	NA	NA	NA
2217.4	0.11696	NA	NA	NA	NA	NA	NA	NA	NA	NA	NA
2502.4	0.04022	NA	NA	NA	NA	NA	NA	NA	NA	NA	NA
2824	0.0056	NA	NA	NA	NA	NA	NA	NA	NA	NA	NA

Table A.86: FAS Linear Amp. Look-up Table for 8.333 Hz.

V_{S30} (m/s)	Soil Depth (m)										
	0	5	10	15	20	25	30	50	100	500	1000
95.6	NA	NA	NA	NA	NA	NA	0.45523	0.42988	0.21694	-1.15747	-2.35858
107.9	NA	NA	NA	NA	NA	0.62194	0.62168	0.46844	0.2689	-0.94001	-1.98674
121.8	NA	NA	NA	NA	0.6483	0.38524	0.32726	0.55719	0.34213	-0.57462	-1.41178
137.4	NA	NA	NA	NA	0.84356	0.75305	0.68691	0.58037	0.50065	-0.29315	-1.02648
155.1	NA	NA	NA	0.52839	0.35076	0.62188	0.69311	0.77113	0.59313	-0.35631	-1.21718
175	NA	NA	NA	0.82662	0.56258	0.63485	0.67226	0.7714	0.78149	0.13582	-0.43399
197.5	NA	NA	0.72098	0.9914	1.05345	1.12955	1.15064	0.9078	0.67795	-0.08626	-0.82862
222.9	NA	NA	0.26361	0.58463	0.6367	0.62418	0.76004	0.71084	0.67446	0.01724	-0.60911
251.5	NA	NA	0.35337	0.55533	0.5626	0.48278	0.46303	0.75357	0.79156	0.14888	-0.4059
283.9	NA	NA	0.99867	1.22	0.97385	0.89505	0.77483	1.12799	0.78794	0.20471	-0.33011
320.4	NA	0.72146	1.13512	1.3044	1.45023	1.47361	1.38256	0.93999	0.78007	0.29426	-0.19413
361.5	NA	0.37273	0.51569	0.65996	0.92382	1.03931	1.1726	0.53992	0.92201	0.38495	-0.02943
408	NA	0.29682	0.27097	0.45653	0.55247	0.58361	0.68198	0.81142	0.71558	0.55459	0.2269
460.4	NA	0.26552	0.30843	0.43154	0.42253	0.45145	0.52597	1.38473	1.13748	0.6783	0.40833
519.6	NA	0.56593	0.55464	0.57437	0.49285	0.52755	0.51914	1.19671	1.03308	0.71463	0.48935
586.4	NA	0.95945	0.94028	0.79014	0.73577	0.6897	0.6277	0.72633	0.65043	0.73247	0.54146
661.8	NA	1.56734	1.51287	1.23547	1.09467	0.98308	0.90067	0.50836	0.81926	0.75234	0.58541
746.8	NA	1.79826	1.85203	1.67482	1.49059	1.30443	1.2187	0.52032	1.14648	0.74837	0.60342
842.8	NA	1.32018	1.50016	1.51235	1.53005	1.41766	1.33649	0.61335	1.00766	0.68664	0.61189
951.1	NA	0.81208	0.98908	1.07708	1.11637	1.23494	NA	NA	NA	NA	NA
1073.4	NA	0.55641	0.66619	0.72093	NA	NA	NA	NA	NA	NA	NA
1211.4	NA	0.38496	0.46586	NA	NA	NA	NA	NA	NA	NA	NA
1367.1	0.54088	0.25898	0.33741	NA	NA	NA	NA	NA	NA	NA	NA
1542.8	0.41801	0.1665	NA	NA	NA	NA	NA	NA	NA	NA	NA
1741.1	0.34597	0.11183	NA	NA	NA	NA	NA	NA	NA	NA	NA
1964.8	0.22588	NA	NA	NA	NA	NA	NA	NA	NA	NA	NA
2217.4	0.13246	NA	NA	NA	NA	NA	NA	NA	NA	NA	NA
2502.4	0.04665	NA	NA	NA	NA	NA	NA	NA	NA	NA	NA
2824	0.00663	NA	NA	NA	NA	NA	NA	NA	NA	NA	NA

Table A.87: FAS Linear Amp. Look-up Table for 9.091 Hz.

V_{S30} (m/s)	Soil Depth (m)										
	0	5	10	15	20	25	30	50	100	500	1000
95.6	NA	NA	NA	NA	NA	NA	0.43846	0.26181	0.08484	-1.43525	-2.75115
107.9	NA	NA	NA	NA	NA	0.45245	0.4449	0.41173	0.21683	-1.11264	-2.25815
121.8	NA	NA	NA	NA	0.58281	0.61261	0.59752	0.40628	0.31619	-0.7403	-1.64674
137.4	NA	NA	NA	NA	0.6105	0.39249	0.37585	0.57358	0.3928	-0.48639	-1.29491
155.1	NA	NA	NA	0.69507	0.71319	0.78986	0.83362	0.62754	0.49466	-0.54095	-1.48836
175	NA	NA	NA	0.49895	0.35544	0.47939	0.57833	0.76855	0.68204	0.00604	-0.6183
197.5	NA	NA	0.90963	0.88149	0.82556	0.89361	0.87688	0.82172	0.69076	-0.18723	-0.99995
222.9	NA	NA	0.54455	0.88291	1.00418	1.01932	1.12704	0.94517	0.684	-0.07312	-0.76905
251.5	NA	NA	0.20568	0.47691	0.5457	0.53281	0.59215	0.64686	0.69572	0.04373	-0.56323
283.9	NA	NA	0.60879	0.74974	0.58657	0.53948	0.52069	0.79604	0.77411	0.13279	-0.45645
320.4	NA	1.05596	1.20218	1.39585	1.26489	1.18667	0.96834	1.19631	0.76872	0.21397	-0.32494
361.5	NA	0.61133	0.90037	1.06087	1.32471	1.41034	1.47444	0.78294	0.78268	0.30654	-0.14415
408	NA	0.35049	0.40794	0.60537	0.77614	0.86172	1.01811	0.57271	0.85237	0.49209	0.13363
460.4	NA	0.21567	0.29067	0.43663	0.46836	0.5308	0.64177	0.98899	0.78934	0.62337	0.32271
519.6	NA	0.41256	0.43053	0.46635	0.42213	0.48064	0.5088	1.39371	1.16912	0.68053	0.43134
586.4	NA	0.70952	0.70263	0.58563	0.57037	0.54907	0.52137	1.04065	0.85145	0.72808	0.52526
661.8	NA	1.2677	1.13654	0.9169	0.82045	0.75285	0.69848	0.61353	0.62569	0.7265	0.57509
746.8	NA	1.76936	1.61518	1.40307	1.21944	1.03614	0.98452	0.49481	0.93686	0.7	0.59861
842.8	NA	1.636	1.77069	1.63388	1.49397	1.37977	1.20152	0.51649	1.1218	0.7078	0.59709
951.1	NA	1.01332	1.25237	1.33761	1.33373	1.37447	NA	NA	NA	NA	NA
1073.4	NA	0.68011	0.82854	0.89453	NA	NA	NA	NA	NA	NA	NA
1211.4	NA	0.46734	0.57196	NA	NA	NA	NA	NA	NA	NA	NA
1367.1	0.60734	0.31188	0.41006	NA	NA	NA	NA	NA	NA	NA	NA
1542.8	0.4537	0.20019	NA	NA	NA	NA	NA	NA	NA	NA	NA
1741.1	0.36807	0.13406	NA	NA	NA	NA	NA	NA	NA	NA	NA
1964.8	0.24901	NA	NA	NA	NA	NA	NA	NA	NA	NA	NA
2217.4	0.15058	NA	NA	NA	NA	NA	NA	NA	NA	NA	NA
2502.4	0.05465	NA	NA	NA	NA	NA	NA	NA	NA	NA	NA
2824	0.00797	NA	NA	NA	NA	NA	NA	NA	NA	NA	NA

Table A.88: FAS Linear Amp. Look-up Table for 10.0 Hz.

V_{S30} (m/s)	Soil Depth (m)										
	0	5	10	15	20	25	30	50	100	500	1000
95.6	NA	NA	NA	NA	NA	NA	0.13074	-0.00059	-0.17024	-1.86788	-3.31515
107.9	NA	NA	NA	NA	NA	0.41526	0.3877	0.20863	0.05714	-1.43781	-2.69489
121.8	NA	NA	NA	NA	0.4704	0.38926	0.48634	0.45151	0.27223	-0.89634	-1.90365
137.4	NA	NA	NA	NA	0.59774	0.52777	0.53579	0.46223	0.33576	-0.6741	-1.55556
155.1	NA	NA	NA	0.55759	0.72474	0.48911	0.45843	0.54401	0.36476	-0.77818	-1.83326
175	NA	NA	NA	0.55793	0.647	0.74187	0.8359	0.71854	0.58646	-0.18055	-0.87627
197.5	NA	NA	0.52883	0.47401	0.36783	0.52508	0.60299	0.77256	0.61428	-0.346	-1.24221
222.9	NA	NA	0.71888	0.92779	0.95329	1.04595	0.8953	0.76921	0.6578	-0.17446	-0.93862
251.5	NA	NA	0.37811	0.7529	0.875	0.9197	1.02363	0.87169	0.68535	-0.06638	-0.74819
283.9	NA	NA	0.32847	0.49255	0.47975	0.4618	0.5642	0.64945	0.7156	0.02162	-0.62612
320.4	NA	1.50589	0.68004	0.88885	0.74859	0.71917	0.60259	0.87744	0.81741	0.14079	-0.46167
361.5	NA	1.06448	1.25195	1.41354	1.41755	1.28945	1.13985	1.15143	0.75673	0.22599	-0.28196
408	NA	0.52597	0.73806	0.95062	1.20938	1.33512	1.4094	0.65645	0.92489	0.41898	0.02456
460.4	NA	0.24115	0.36476	0.54841	0.6468	0.76595	0.93039	0.62801	0.73789	0.55982	0.22571
519.6	NA	0.30208	0.36489	0.42695	0.43331	0.5236	0.59852	1.06721	0.80213	0.6254	0.35034
586.4	NA	0.50245	0.52508	0.44284	0.46644	0.47214	0.48558	1.31984	1.10684	0.69946	0.47185
661.8	NA	0.96598	0.8226	0.66118	0.60406	0.57448	0.54978	0.87296	0.70845	0.73903	0.55951
746.8	NA	1.53309	1.19941	1.04118	0.91001	0.7739	0.75198	0.5635	0.67219	0.73123	0.58042
842.8	NA	1.80021	1.70458	1.46204	1.22274	1.14966	0.96271	0.48283	0.90783	0.6983	0.59806
951.1	NA	1.30769	1.57131	1.5662	1.44783	1.32611	NA	NA	NA	NA	NA
1073.4	NA	0.85725	1.06322	1.13401	NA	NA	NA	NA	NA	NA	NA
1211.4	NA	0.58113	0.72134	NA	NA	NA	NA	NA	NA	NA	NA
1367.1	0.66188	0.38304	0.51062	NA	NA	NA	NA	NA	NA	NA	NA
1542.8	0.48742	0.24526	NA	NA	NA	NA	NA	NA	NA	NA	NA
1741.1	0.3837	0.1637	NA	NA	NA	NA	NA	NA	NA	NA	NA
1964.8	0.27163	NA	NA	NA	NA	NA	NA	NA	NA	NA	NA
2217.4	0.17078	NA	NA	NA	NA	NA	NA	NA	NA	NA	NA
2502.4	0.06462	NA	NA	NA	NA	NA	NA	NA	NA	NA	NA
2824	0.00972	NA	NA	NA	NA	NA	NA	NA	NA	NA	NA

Table A.89: FAS Linear Amp. Look-up Table for 10.526 Hz.

V_{S30} (m/s)	Soil Depth (m)										
	0	5	10	15	20	25	30	50	100	500	1000
95.6	NA	NA	NA	NA	NA	NA	0.19134	-0.12445	-0.33459	-2.08816	-3.61615
107.9	NA	NA	NA	NA	NA	0.36842	0.18926	0.06221	-0.08184	-1.6715	-2.99458
121.8	NA	NA	NA	NA	0.20452	0.37627	0.44275	0.38077	0.22462	-1.00331	-2.067
137.4	NA	NA	NA	NA	0.56012	0.59397	0.60122	0.46187	0.3157	-0.75364	-1.68601
155.1	NA	NA	NA	0.33031	0.55541	0.41253	0.39293	0.49778	0.28633	-0.91291	-2.02601
175	NA	NA	NA	0.64324	0.79225	0.74204	0.76885	0.60634	0.51101	-0.28109	-1.02068
197.5	NA	NA	0.32728	0.44452	0.3567	0.56941	0.70027	0.76981	0.57715	-0.4524	-1.39814
222.9	NA	NA	0.60551	0.74927	0.67638	0.79809	0.66132	0.70499	0.63013	-0.24798	-1.05186
251.5	NA	NA	0.60332	0.95368	1.07609	1.10972	1.15008	0.9144	0.67385	-0.12366	-0.84508
283.9	NA	NA	0.30678	0.49742	0.57395	0.57081	0.75347	0.77425	0.7147	-0.04776	-0.7308
320.4	NA	1.4829	0.42506	0.64683	0.56996	0.57866	0.53733	0.68261	0.76713	0.09389	-0.54377
361.5	NA	1.2837	1.18402	1.32018	1.20682	1.01959	0.84815	1.11255	0.77961	0.186	-0.35302
408	NA	0.68839	0.98524	1.1957	1.41274	1.47033	1.4014	0.85403	0.8127	0.3648	-0.04494
460.4	NA	0.30072	0.4607	0.67452	0.82457	0.98355	1.16177	0.56319	0.87926	0.5081	0.17342
519.6	NA	0.26937	0.36351	0.44381	0.48683	0.59921	0.70463	0.823	0.67362	0.59818	0.30196
586.4	NA	0.41811	0.4608	0.39862	0.44412	0.46643	0.50595	1.274	1.06292	0.67017	0.43268
661.8	NA	0.82038	0.69322	0.55771	0.51989	0.50984	0.50215	1.07231	0.88656	0.72682	0.54219
746.8	NA	1.37343	0.99976	0.87233	0.77012	0.66019	0.65082	0.65421	0.62013	0.71626	0.58007
842.8	NA	1.75392	1.51694	1.28193	1.04793	0.999	0.83427	0.50319	0.7479	0.72006	0.55663
951.1	NA	1.48977	1.68317	1.58136	1.40733	1.21218	NA	NA	NA	NA	NA
1073.4	NA	0.97947	1.22065	1.27627	NA	NA	NA	NA	NA	NA	NA
1211.4	NA	0.65701	0.82229	NA	NA	NA	NA	NA	NA	NA	NA
1367.1	0.67649	0.4291	0.57661	NA	NA	NA	NA	NA	NA	NA	NA
1542.8	0.5015	0.27433	NA	NA	NA	NA	NA	NA	NA	NA	NA
1741.1	0.38864	0.18265	NA	NA	NA	NA	NA	NA	NA	NA	NA
1964.8	0.28234	NA	NA	NA	NA	NA	NA	NA	NA	NA	NA
2217.4	0.18173	NA	NA	NA	NA	NA	NA	NA	NA	NA	NA
2502.4	0.07058	NA	NA	NA	NA	NA	NA	NA	NA	NA	NA
2824	0.01081	NA	NA	NA	NA	NA	NA	NA	NA	NA	NA

Table A.90: FAS Linear Amp. Look-up Table for 11.111 Hz.

V_{S30} (m/s)	Soil Depth (m)										
	0	5	10	15	20	25	30	50	100	500	1000
95.6	NA	NA	NA	NA	NA	NA	0.22622	-0.20521	-0.37742	-2.27405	-3.88994
107.9	NA	NA	NA	NA	NA	0.20605	0.15649	-0.05906	-0.25126	-1.89982	-3.30444
121.8	NA	NA	NA	NA	0.12981	0.39873	0.43081	0.27507	0.14299	-1.16963	-2.29054
137.4	NA	NA	NA	NA	0.31952	0.47575	0.53215	0.46716	0.29078	-0.839	-1.82798
155.1	NA	NA	NA	0.21919	0.54904	0.50693	0.51188	0.4523	0.24005	-1.04473	-2.21648
175	NA	NA	NA	0.58618	0.73547	0.54697	0.53165	0.56949	0.45898	-0.39141	-1.17946
197.5	NA	NA	0.28339	0.55941	0.53068	0.74876	0.85808	0.72622	0.53254	-0.56808	-1.56695
222.9	NA	NA	0.40926	0.5486	0.44004	0.57882	0.56802	0.76193	0.58949	-0.34386	-1.19444
251.5	NA	NA	0.79696	1.00213	1.0794	1.08395	1.02615	0.82107	0.63081	-0.1811	-0.94457
283.9	NA	NA	0.40276	0.61984	0.79088	0.80779	1.0197	0.92608	0.67325	-0.11632	-0.84261
320.4	NA	1.19883	0.25752	0.50235	0.48671	0.53353	0.57646	0.65722	0.73115	0.034	-0.6403
361.5	NA	1.2895	0.94062	1.04744	0.92382	0.75341	0.63162	0.89383	0.76893	0.15048	-0.42735
408	NA	0.88837	1.20446	1.37107	1.4351	1.36414	1.18423	1.07115	0.71516	0.32219	-0.11874
460.4	NA	0.40946	0.61985	0.87474	1.07954	1.24767	1.37246	0.60355	0.98569	0.48595	0.1164
519.6	NA	0.26003	0.39313	0.49585	0.58856	0.72904	0.86885	0.64397	0.72878	0.56045	0.25092
586.4	NA	0.35036	0.4179	0.37903	0.44945	0.49145	0.56271	1.08149	0.88397	0.63767	0.38443
661.8	NA	0.68772	0.58513	0.47452	0.45708	0.46764	0.47916	1.25036	1.07524	0.71425	0.51642
746.8	NA	1.19882	0.82492	0.72474	0.64903	0.56589	0.56823	0.79496	0.66168	0.74066	0.56441
842.8	NA	1.62643	1.28897	1.08449	0.87941	0.85165	0.71534	0.55993	0.63056	0.71366	0.59642
951.1	NA	1.66375	1.6922	1.49037	1.29467	1.06565	NA	NA	NA	NA	NA
1073.4	NA	1.13256	1.39805	1.40885	NA	NA	NA	NA	NA	NA	NA
1211.4	NA	0.74923	0.94494	NA	NA	NA	NA	NA	NA	NA	NA
1367.1	0.67679	0.48368	0.65638	NA	NA	NA	NA	NA	NA	NA	NA
1542.8	0.51198	0.30846	NA	NA	NA	NA	NA	NA	NA	NA	NA
1741.1	0.39114	0.20483	NA	NA	NA	NA	NA	NA	NA	NA	NA
1964.8	0.29265	NA	NA	NA	NA	NA	NA	NA	NA	NA	NA
2217.4	0.19292	NA	NA	NA	NA	NA	NA	NA	NA	NA	NA
2502.4	0.07718	NA	NA	NA	NA	NA	NA	NA	NA	NA	NA
2824	0.01208	NA	NA	NA	NA	NA	NA	NA	NA	NA	NA

Table A.91: FAS Linear Amp. Look-up Table for 11.765 Hz.

V_{S30} (m/s)	Soil Depth (m)										
	0	5	10	15	20	25	30	50	100	500	1000
95.6	NA	NA	NA	NA	NA	NA	0.15675	-0.16314	-0.38039	-2.43281	-4.14982
107.9	NA	NA	NA	NA	NA	0.1618	0.23565	-0.18119	-0.35201	-2.11192	-3.60288
121.8	NA	NA	NA	NA	0.22384	0.26018	0.26058	0.11758	0.0127	-1.40605	-2.58999
137.4	NA	NA	NA	NA	0.1188	0.37383	0.46146	0.40326	0.24541	-0.95972	-2.00854
155.1	NA	NA	NA	0.28946	0.57922	0.57569	0.60227	0.40536	0.20944	-1.16709	-2.40739
175	NA	NA	NA	0.36349	0.58783	0.36931	0.37365	0.57141	0.38918	-0.51278	-1.34672
197.5	NA	NA	0.42119	0.65605	0.749	0.84668	0.86617	0.65545	0.46311	-0.69319	-1.75128
222.9	NA	NA	0.23735	0.47141	0.39335	0.5571	0.69155	0.78616	0.55223	-0.4574	-1.36045
251.5	NA	NA	0.75074	0.81668	0.83199	0.83747	0.7465	0.71046	0.62772	-0.25509	-1.06282
283.9	NA	NA	0.61316	0.83857	1.03037	1.07778	1.16789	0.92013	0.64661	-0.18411	-0.9588
320.4	NA	0.82865	0.19399	0.46785	0.51922	0.6088	0.75462	0.81375	0.73643	-0.04253	-0.75442
361.5	NA	1.03415	0.64486	0.75074	0.68991	0.57554	0.51832	0.67592	0.75965	0.10208	-0.51307
408	NA	1.09988	1.25315	1.35526	1.22573	1.05935	0.87299	1.13642	0.73439	0.27874	-0.19286
460.4	NA	0.59441	0.86919	1.15902	1.35266	1.42527	1.3987	0.77472	0.90362	0.43277	0.04925
519.6	NA	0.28468	0.46739	0.59922	0.76448	0.93842	1.09939	0.56048	0.90957	0.52051	0.19604
586.4	NA	0.30175	0.40074	0.39087	0.49241	0.5591	0.67071	0.83585	0.71853	0.61111	0.33325
661.8	NA	0.56922	0.49743	0.41288	0.4187	0.45275	0.48762	1.28883	1.11263	0.69074	0.4772
746.8	NA	1.01446	0.67281	0.59707	0.54789	0.4927	0.50697	0.9881	0.8115	0.72083	0.55175
842.8	NA	1.44581	1.06009	0.89363	0.72579	0.71464	0.60967	0.66718	0.59604	0.71811	0.59265
951.1	NA	1.78757	1.57484	1.31199	1.1307	0.90645	NA	NA	NA	NA	NA
1073.4	NA	1.32999	1.56674	1.48818	NA	NA	NA	NA	NA	NA	NA
1211.4	NA	0.86584	1.09771	NA	NA	NA	NA	NA	NA	NA	NA
1367.1	0.6593	0.55059	0.75555	NA	NA	NA	NA	NA	NA	NA	NA
1542.8	0.51639	0.34998	NA	NA	NA	NA	NA	NA	NA	NA	NA
1741.1	0.39144	0.23138	NA	NA	NA	NA	NA	NA	NA	NA	NA
1964.8	0.30253	NA	NA	NA	NA	NA	NA	NA	NA	NA	NA
2217.4	0.20442	NA	NA	NA	NA	NA	NA	NA	NA	NA	NA
2502.4	0.08459	NA	NA	NA	NA	NA	NA	NA	NA	NA	NA
2824	0.01357	NA	NA	NA	NA	NA	NA	NA	NA	NA	NA

Table A.92: FAS Linear Amp. Look-up Table for 12.5 Hz.

V_{S30} (m/s)	Soil Depth (m)										
	0	5	10	15	20	25	30	50	100	500	1000
95.6	NA	NA	NA	NA	NA	NA	0.01664	-0.20401	-0.54993	-2.68063	-4.49507
107.9	NA	NA	NA	NA	NA	0.06702	0.19627	-0.16391	-0.3484	-2.27614	-3.86716
121.8	NA	NA	NA	NA	0.13998	0.15835	0.14268	-0.02533	-0.15912	-1.65852	-2.92111
137.4	NA	NA	NA	NA	0.19815	0.4062	0.41482	0.27555	0.1421	-1.15217	-2.26733
155.1	NA	NA	NA	0.3598	0.37697	0.46667	0.51448	0.40794	0.18517	-1.29183	-2.61235
175	NA	NA	NA	0.18921	0.56903	0.43786	0.49056	0.50232	0.35292	-0.63014	-1.51233
197.5	NA	NA	0.55659	0.51381	0.74802	0.68445	0.65192	0.60271	0.40378	-0.83353	-1.96194
222.9	NA	NA	0.25138	0.56022	0.57631	0.73347	0.87453	0.67579	0.49786	-0.57605	-1.53715
251.5	NA	NA	0.45826	0.55045	0.53722	0.58446	0.56979	0.74006	0.59636	-0.35484	-1.21685
283.9	NA	NA	0.76879	1.01196	1.05902	1.11479	1.01518	0.75437	0.65195	-0.25816	-1.07992
320.4	NA	0.54142	0.26923	0.57836	0.71263	0.83684	1.04433	0.98677	0.70618	-0.1232	-0.8818
361.5	NA	0.66039	0.41109	0.54691	0.5644	0.51577	0.53074	0.65623	0.73985	0.03405	-0.61742
408	NA	1.21187	1.04799	1.13387	0.91262	0.74605	0.62166	0.95795	0.80751	0.23872	-0.26703
460.4	NA	0.85912	1.16431	1.40388	1.44365	1.32897	1.16394	1.03043	0.71218	0.37305	-0.03003
519.6	NA	0.36027	0.61282	0.78098	1.04172	1.21522	1.31758	0.59981	0.97781	0.48122	0.1342
586.4	NA	0.27891	0.41937	0.44737	0.59018	0.68925	0.85139	0.63888	0.70484	0.55563	0.28208
661.8	NA	0.46749	0.43427	0.37856	0.41266	0.47456	0.53956	1.11675	0.92121	0.65251	0.42768
746.8	NA	0.83391	0.54496	0.49243	0.47002	0.44618	0.47466	1.17441	1.00895	0.70656	0.5255
842.8	NA	1.23993	0.85172	0.72147	0.59171	0.59653	0.52658	0.83883	0.68151	0.7226	0.56305
951.1	NA	1.79843	1.36079	1.09314	0.94746	0.75051	NA	NA	NA	NA	NA
1073.4	NA	1.5648	1.6528	1.46364	NA	NA	NA	NA	NA	NA	NA
1211.4	NA	1.01756	1.28236	NA	NA	NA	NA	NA	NA	NA	NA
1367.1	0.62173	0.63413	0.88164	NA	NA	NA	NA	NA	NA	NA	NA
1542.8	0.51236	0.40089	NA	NA	NA	NA	NA	NA	NA	NA	NA
1741.1	0.38948	0.2641	NA	NA	NA	NA	NA	NA	NA	NA	NA
1964.8	0.31168	NA	NA	NA	NA	NA	NA	NA	NA	NA	NA
2217.4	0.21618	NA	NA	NA	NA	NA	NA	NA	NA	NA	NA
2502.4	0.0929	NA	NA	NA	NA	NA	NA	NA	NA	NA	NA
2824	0.01535	NA	NA	NA	NA	NA	NA	NA	NA	NA	NA

Table A.93: FAS Linear Amp. Look-up Table for 13.333 Hz.

V_{S30} (m/s)	Soil Depth (m)										
	0	5	10	15	20	25	30	50	100	500	1000
95.6	NA	NA	NA	NA	NA	NA	-0.15844	-0.32223	-0.75414	-3.0007	-4.93112
107.9	NA	NA	NA	NA	NA	-0.07185	0.06979	-0.16211	-0.47772	-2.50238	-4.19066
121.8	NA	NA	NA	NA	0.01938	0.09712	0.22953	-0.15877	-0.2949	-1.8894	-3.24569
137.4	NA	NA	NA	NA	0.17167	0.29589	0.25124	0.11853	-0.00791	-1.41198	-2.60187
155.1	NA	NA	NA	0.25892	0.12989	0.38152	0.46739	0.37436	0.14787	-1.43907	-2.84963
175	NA	NA	NA	0.22603	0.54475	0.56816	0.637	0.4699	0.32845	-0.72797	-1.67232
197.5	NA	NA	0.46287	0.22529	0.56497	0.47286	0.50816	0.56184	0.32896	-0.9926	-2.19803
222.9	NA	NA	0.37389	0.61608	0.80781	0.85916	0.81568	0.61068	0.4443	-0.70604	-1.73193
251.5	NA	NA	0.18874	0.44796	0.44424	0.57296	0.66993	0.78499	0.53453	-0.48065	-1.40266
283.9	NA	NA	0.7008	0.9058	0.78537	0.82719	0.70983	0.69386	0.60919	-0.35002	-1.22627
320.4	NA	0.38712	0.52641	0.84738	1.01928	1.10858	1.19746	0.91501	0.67049	-0.19932	-1.01227
361.5	NA	0.38054	0.29166	0.47641	0.58073	0.61055	0.71583	0.8457	0.68897	-0.05127	-0.74598
408	NA	1.09604	0.70049	0.84088	0.65971	0.55036	0.49833	0.70141	0.79531	0.19553	-0.34829
460.4	NA	1.09532	1.30009	1.3939	1.21889	0.99408	0.82358	1.14647	0.69423	0.32406	-0.11219
519.6	NA	0.51665	0.86424	1.06442	1.33914	1.38954	1.32743	0.80288	0.79746	0.42758	0.05703
586.4	NA	0.29432	0.49046	0.5705	0.77169	0.9084	1.10415	0.55537	0.84287	0.52678	0.2271
661.8	NA	0.38593	0.40199	0.38116	0.45168	0.54872	0.65275	0.8364	0.6841	0.60991	0.37237
746.8	NA	0.67068	0.44406	0.41536	0.42228	0.43504	0.48091	1.21903	1.06539	0.68246	0.48006
842.8	NA	1.02675	0.67085	0.57538	0.4836	0.50349	0.47121	1.06437	0.89747	0.70747	0.53823
951.1	NA	1.66759	1.11284	0.87617	0.77071	0.61309	NA	NA	NA	NA	NA
1073.4	NA	1.7713	1.58411	1.32142	NA	NA	NA	NA	NA	NA	NA
1211.4	NA	1.21637	1.46655	NA	NA	NA	NA	NA	NA	NA	NA
1367.1	0.56636	0.73945	1.03825	NA	NA	NA	NA	NA	NA	NA	NA
1542.8	0.49797	0.46403	NA	NA	NA	NA	NA	NA	NA	NA	NA
1741.1	0.38493	0.30392	NA	NA	NA	NA	NA	NA	NA	NA	NA
1964.8	0.32084	NA	NA	NA	NA	NA	NA	NA	NA	NA	NA
2217.4	0.22798	NA	NA	NA	NA	NA	NA	NA	NA	NA	NA
2502.4	0.10209	NA	NA	NA	NA	NA	NA	NA	NA	NA	NA
2824	0.01744	NA	NA	NA	NA	NA	NA	NA	NA	NA	NA

Table A.94: FAS Linear Amp. Look-up Table for 14.286 Hz.

V_{S30} (m/s)	Soil Depth (m)										
	0	5	10	15	20	25	30	50	100	500	1000
95.6	NA	NA	NA	NA	NA	NA	-0.1508	-0.36767	-0.83956	-3.28829	-5.35941
107.9	NA	NA	NA	NA	NA	-0.01457	-0.12538	-0.29103	-0.70829	-2.82783	-4.63478
121.8	NA	NA	NA	NA	0.11908	-0.06618	0.1965	-0.14271	-0.29555	-2.06527	-3.52259
137.4	NA	NA	NA	NA	0.0157	0.17658	0.18287	-0.03906	-0.17941	-1.67555	-2.95475
155.1	NA	NA	NA	0.18055	0.19626	0.3882	0.45338	0.26214	0.02995	-1.65873	-3.17293
175	NA	NA	NA	0.31825	0.29714	0.47546	0.53618	0.47116	0.30378	-0.83521	-1.85095
197.5	NA	NA	0.2622	0.16605	0.55292	0.55193	0.62831	0.51401	0.26942	-1.1546	-2.44804
222.9	NA	NA	0.39775	0.45739	0.75017	0.6715	0.55223	0.59516	0.36737	-0.86703	-1.96773
251.5	NA	NA	0.19812	0.59358	0.64712	0.77659	0.88962	0.67511	0.49886	-0.61505	-1.60285
283.9	NA	NA	0.46317	0.59075	0.48918	0.54825	0.59121	0.80066	0.57359	-0.47209	-1.41528
320.4	NA	0.3964	0.79168	1.06479	1.09878	1.12685	0.98462	0.71973	0.67226	-0.28164	-1.15154
361.5	NA	0.25156	0.33953	0.58856	0.79497	0.90208	1.06178	0.94915	0.6836	-0.14652	-0.89306
408	NA	0.78134	0.42512	0.61911	0.54758	0.50808	0.53852	0.65555	0.71422	0.12772	-0.45468
460.4	NA	1.09428	1.10729	1.09739	0.84766	0.66399	0.57537	0.93474	0.84586	0.28458	-0.18903
519.6	NA	0.76243	1.17693	1.37469	1.38553	1.24355	1.05152	1.08236	0.65813	0.36847	-0.03059
586.4	NA	0.37023	0.64817	0.80423	1.06958	1.20488	1.29849	0.62922	0.91816	0.49201	0.16202
661.8	NA	0.3336	0.4127	0.43796	0.55972	0.70285	0.85428	0.61193	0.66557	0.58017	0.31461
746.8	NA	0.53183	0.37445	0.37282	0.4143	0.47371	0.54334	1.03453	0.86427	0.63412	0.42391
842.8	NA	0.82222	0.51916	0.45732	0.40653	0.44328	0.45493	1.20994	1.0723	0.67828	0.50198
951.1	NA	1.4317	0.87558	0.68169	0.61369	0.50461	NA	NA	NA	NA	NA
1073.4	NA	1.82076	1.36452	1.10144	NA	NA	NA	NA	NA	NA	NA
1211.4	NA	1.46914	1.56808	NA	NA	NA	NA	NA	NA	NA	NA
1367.1	0.49818	0.87836	1.23452	NA	NA	NA	NA	NA	NA	NA	NA
1542.8	0.47248	0.54486	NA	NA	NA	NA	NA	NA	NA	NA	NA
1741.1	0.37779	0.35387	NA	NA	NA	NA	NA	NA	NA	NA	NA
1964.8	0.32981	NA	NA	NA	NA	NA	NA	NA	NA	NA	NA
2217.4	0.24014	NA	NA	NA	NA	NA	NA	NA	NA	NA	NA
2502.4	0.11222	NA	NA	NA	NA	NA	NA	NA	NA	NA	NA
2824	0.01999	NA	NA	NA	NA	NA	NA	NA	NA	NA	NA

Table A.95: FAS Linear Amp. Look-up Table for 15.0 Hz.

V_{S30} (m/s)	Soil Depth (m)										
	0	5	10	15	20	25	30	50	100	500	1000
95.6	NA	NA	NA	NA	NA	NA	-0.16673	-0.41325	-0.92489	-3.49436	-5.67922
107.9	NA	NA	NA	NA	NA	-0.02728	-0.14481	-0.34374	-0.78106	-3.03659	-4.93816
121.8	NA	NA	NA	NA	0.10334	-0.03528	0.10355	-0.12887	-0.37358	-2.21768	-3.74333
137.4	NA	NA	NA	NA	0.08251	0.13404	0.23535	-0.09544	-0.23916	-1.82186	-3.17163
155.1	NA	NA	NA	0.22906	0.19411	0.3167	0.33915	0.14721	-0.07614	-1.87174	-3.46191
175	NA	NA	NA	0.2681	0.17941	0.39393	0.46912	0.41382	0.2611	-0.94361	-2.01336
197.5	NA	NA	0.25811	0.27574	0.57519	0.63462	0.69045	0.48668	0.23551	-1.26552	-2.62695
222.9	NA	NA	0.3195	0.29773	0.61287	0.50928	0.51127	0.53205	0.31274	-0.98804	-2.14712
251.5	NA	NA	0.3511	0.66354	0.82554	0.85406	0.87513	0.61701	0.44621	-0.71256	-1.75055
283.9	NA	NA	0.32114	0.45977	0.45328	0.5482	0.71827	0.78563	0.53836	-0.56736	-1.56034
320.4	NA	0.52819	0.76284	0.9812	0.89501	0.92928	0.75619	0.74058	0.6495	-0.35141	-1.26566
361.5	NA	0.26703	0.49457	0.78627	1.01889	1.10952	1.19887	0.84708	0.65997	-0.2082	-0.99432
408	NA	0.57263	0.32561	0.55798	0.57831	0.59419	0.69311	0.78015	0.71437	0.06466	-0.54636
460.4	NA	0.93779	0.85809	0.85575	0.64865	0.52604	0.49601	0.71799	0.83759	0.26045	-0.2434
519.6	NA	0.93909	1.29801	1.44419	1.19209	0.9957	0.80665	1.12634	0.73696	0.33219	-0.08749
586.4	NA	0.47531	0.83003	1.04466	1.27438	1.33556	1.2671	0.78665	0.8329	0.44735	0.10665
661.8	NA	0.32274	0.45504	0.52249	0.69169	0.87086	1.04211	0.53847	0.79821	0.54434	0.27631
746.8	NA	0.45431	0.34987	0.37002	0.43989	0.53967	0.62936	0.83362	0.68765	0.60485	0.381
842.8	NA	0.69626	0.43508	0.39625	0.37697	0.42665	0.47438	1.16148	1.00737	0.65975	0.46417
951.1	NA	1.24823	0.73125	0.56678	0.52361	0.44796	NA	NA	NA	NA	NA
1073.4	NA	1.72079	1.17284	0.94003	NA	NA	NA	NA	NA	NA	NA
1211.4	NA	1.6402	1.53912	NA	NA	NA	NA	NA	NA	NA	NA
1367.1	0.44898	0.99867	1.37478	NA	NA	NA	NA	NA	NA	NA	NA
1542.8	0.45111	0.61317	NA	NA	NA	NA	NA	NA	NA	NA	NA
1741.1	0.37213	0.39566	NA	NA	NA	NA	NA	NA	NA	NA	NA
1964.8	0.33575	NA	NA	NA	NA	NA	NA	NA	NA	NA	NA
2217.4	0.24862	NA	NA	NA	NA	NA	NA	NA	NA	NA	NA
2502.4	0.11958	NA	NA	NA	NA	NA	NA	NA	NA	NA	NA
2824	0.02202	NA	NA	NA	NA	NA	NA	NA	NA	NA	NA

Table A.96: FAS Linear Amp. Look-up Table for 15.385 Hz.

V_{S30} (m/s)	Soil Depth (m)										
	0	5	10	15	20	25	30	50	100	500	1000
95.6	NA	NA	NA	NA	NA	NA	-0.2097	-0.45418	-0.99074	-3.62134	-5.86561
107.9	NA	NA	NA	NA	NA	-0.06024	-0.13571	-0.34953	-0.80317	-3.13146	-5.08523
121.8	NA	NA	NA	NA	0.07865	-0.01571	0.03684	-0.16124	-0.45771	-2.32089	-3.88399
137.4	NA	NA	NA	NA	0.11421	0.08194	0.24476	-0.09849	-0.24144	-1.88519	-3.27171
155.1	NA	NA	NA	0.24535	0.13876	0.2716	0.28411	0.08116	-0.14719	-1.99181	-3.62375
175	NA	NA	NA	0.21025	0.17953	0.37763	0.47076	0.36752	0.22565	-1.01434	-2.11266
197.5	NA	NA	0.292	0.32047	0.52509	0.61775	0.66781	0.47488	0.2234	-1.32468	-2.72127
222.9	NA	NA	0.27926	0.24447	0.57815	0.48691	0.56022	0.50433	0.28855	-1.04923	-2.24091
251.5	NA	NA	0.43401	0.63508	0.85979	0.82152	0.79431	0.61863	0.42373	-0.76656	-1.83107
283.9	NA	NA	0.28292	0.4547	0.50221	0.61257	0.81057	0.73704	0.51561	-0.61647	-1.63567
320.4	NA	0.63953	0.66483	0.86827	0.75159	0.80558	0.67616	0.79595	0.63483	-0.39271	-1.33121
361.5	NA	0.31358	0.59659	0.90141	1.10876	1.16312	1.17842	0.77007	0.63973	-0.23892	-1.04476
408	NA	0.48966	0.30842	0.56354	0.63531	0.68193	0.81028	0.85871	0.72098	0.03115	-0.5958
460.4	NA	0.8365	0.73321	0.75373	0.58012	0.48862	0.48802	0.6441	0.78683	0.24181	-0.27429
519.6	NA	1.01175	1.29625	1.40341	1.05446	0.86538	0.70042	1.06895	0.79352	0.31978	-0.11489
586.4	NA	0.54961	0.94241	1.17404	1.33661	1.33844	1.19043	0.88366	0.76581	0.43428	0.07573
661.8	NA	0.32737	0.49043	0.5836	0.78053	0.97376	1.13558	0.53195	0.8737	0.54114	0.25969
746.8	NA	0.42212	0.34623	0.37852	0.46454	0.58787	0.68901	0.73822	0.63392	0.58046	0.36003
842.8	NA	0.63887	0.39984	0.37285	0.3707	0.42761	0.49554	1.0869	0.91694	0.64121	0.44686
951.1	NA	1.15662	0.66579	0.51581	0.48521	0.42762	NA	NA	NA	NA	NA
1073.4	NA	1.63703	1.07611	0.86137	NA	NA	NA	NA	NA	NA	NA
1211.4	NA	1.70752	1.49152	NA	NA	NA	NA	NA	NA	NA	NA
1367.1	0.42544	1.06797	1.43838	NA	NA	NA	NA	NA	NA	NA	NA
1542.8	0.43973	0.65184	NA	NA	NA	NA	NA	NA	NA	NA	NA
1741.1	0.36933	0.41907	NA	NA	NA	NA	NA	NA	NA	NA	NA
1964.8	0.3386	NA	NA	NA	NA	NA	NA	NA	NA	NA	NA
2217.4	0.25289	NA	NA	NA	NA	NA	NA	NA	NA	NA	NA
2502.4	0.12335	NA	NA	NA	NA	NA	NA	NA	NA	NA	NA
2824	0.02313	NA	NA	NA	NA	NA	NA	NA	NA	NA	NA

Table A.97: FAS Linear Amp. Look-up Table for 16.667 Hz.

V_{S30} (m/s)	Soil Depth (m)										
	0	5	10	15	20	25	30	50	100	500	1000
95.6	NA	NA	NA	NA	NA	NA	-0.35458	-0.62114	-1.2187	-4.08467	-6.50612
107.9	NA	NA	NA	NA	NA	-0.20856	-0.20071	-0.44047	-0.9585	-3.47608	-5.5972
121.8	NA	NA	NA	NA	-0.02705	-0.06175	-0.1331	-0.28856	-0.67377	-2.67023	-4.36114
137.4	NA	NA	NA	NA	0.07631	-0.03679	0.14742	-0.08347	-0.32233	-2.10747	-3.6068
155.1	NA	NA	NA	0.20525	0.0481	0.16572	0.23376	-0.05453	-0.34359	-2.34728	-4.12043
175	NA	NA	NA	0.15867	0.20602	0.30354	0.35267	0.20926	0.06367	-1.29555	-2.48544
197.5	NA	NA	0.30749	0.2364	0.20636	0.42206	0.55543	0.42423	0.1605	-1.53177	-3.04496
222.9	NA	NA	0.22445	0.27292	0.60565	0.62742	0.69531	0.46931	0.21903	-1.22971	-2.52524
251.5	NA	NA	0.43863	0.31337	0.6807	0.55578	0.52767	0.58107	0.34569	-0.95345	-2.10907
283.9	NA	NA	0.36832	0.61667	0.77969	0.87137	0.90575	0.62857	0.46221	-0.77794	-1.88295
320.4	NA	1.02759	0.27691	0.50057	0.45249	0.6161	0.72916	0.83436	0.58297	-0.54004	-1.56057
361.5	NA	0.61609	0.81712	1.05662	1.04402	0.97398	0.81903	0.70751	0.63012	-0.3362	-1.2085
408	NA	0.35863	0.42345	0.75968	0.96372	1.07427	1.13736	0.91337	0.66022	-0.06404	-0.74574
460.4	NA	0.53722	0.4457	0.575	0.51972	0.52784	0.62697	0.68869	0.6983	0.16132	-0.39791
519.6	NA	1.0594	1.04522	1.04076	0.66714	0.56337	0.49953	0.72398	0.8003	0.2823	-0.19429
586.4	NA	0.83374	1.25544	1.40221	1.22509	1.06458	0.8346	1.05983	0.6687	0.36832	-0.01643
661.8	NA	0.39852	0.68222	0.87647	1.12707	1.25578	1.25947	0.66244	0.88769	0.48762	0.18212
746.8	NA	0.35686	0.38084	0.45887	0.60557	0.81696	0.93983	0.54128	0.70548	0.54198	0.30434
842.8	NA	0.48999	0.32454	0.33611	0.39571	0.4795	0.62355	0.76441	0.61699	0.60072	0.38303
951.1	NA	0.90003	0.49499	0.38992	0.39908	0.40151	NA	NA	NA	NA	NA
1073.4	NA	1.32242	0.80457	0.64361	NA	NA	NA	NA	NA	NA	NA
1211.4	NA	1.75529	1.24543	NA	NA	NA	NA	NA	NA	NA	NA
1367.1	0.36136	1.31858	1.52738	NA	NA	NA	NA	NA	NA	NA	NA
1542.8	0.40594	0.79514	NA	NA	NA	NA	NA	NA	NA	NA	NA
1741.1	0.36237	0.50362	NA	NA	NA	NA	NA	NA	NA	NA	NA
1964.8	0.34677	NA	NA	NA	NA	NA	NA	NA	NA	NA	NA
2217.4	0.26603	NA	NA	NA	NA	NA	NA	NA	NA	NA	NA
2502.4	0.13517	NA	NA	NA	NA	NA	NA	NA	NA	NA	NA
2824	0.02696	NA	NA	NA	NA	NA	NA	NA	NA	NA	NA

Table A.98: FAS Linear Amp. Look-up Table for 18.182 Hz.

V_{S30} (m/s)	Soil Depth (m)										
	0	5	10	15	20	25	30	50	100	500	1000
95.6	NA	NA	NA	NA	NA	NA	-0.45134	-0.77979	-1.43399	-4.58027	-7.22307
107.9	NA	NA	NA	NA	NA	-0.28034	-0.36079	-0.62302	-1.19956	-3.96315	-6.28101
121.8	NA	NA	NA	NA	-0.15793	-0.22103	-0.12864	-0.33939	-0.77486	-2.98766	-4.83886
137.4	NA	NA	NA	NA	-0.04912	0.00073	-0.03308	-0.2145	-0.56431	-2.47042	-4.10242
155.1	NA	NA	NA	0.16768	0.12124	0.01489	0.19823	-0.08462	-0.39827	-2.61441	-4.55332
175	NA	NA	NA	0.21772	0.07756	0.1698	0.21083	0.01635	-0.12886	-1.61645	-2.91838
197.5	NA	NA	0.15371	0.15678	0.22054	0.44694	0.51089	0.29915	0.01102	-1.83869	-3.49017
222.9	NA	NA	0.2037	0.29551	0.36503	0.54781	0.54714	0.42317	0.1707	-1.43467	-2.84512
251.5	NA	NA	0.17328	0.1824	0.59235	0.56978	0.65968	0.49909	0.25777	-1.15864	-2.42535
283.9	NA	NA	0.43116	0.58122	0.75258	0.69738	0.59441	0.62911	0.37045	-0.98846	-2.19322
320.4	NA	0.8747	0.17767	0.51725	0.6185	0.8332	0.94443	0.65535	0.50824	-0.71914	-1.83609
361.5	NA	0.87822	0.58837	0.71406	0.61499	0.62579	0.59587	0.83415	0.59055	-0.46356	-1.41906
408	NA	0.44295	0.7306	1.04566	1.11661	1.12916	0.97251	0.71136	0.6604	-0.14369	-0.88818
460.4	NA	0.31567	0.36429	0.66426	0.76104	0.87754	1.02477	0.94205	0.73039	0.04874	-0.56092
519.6	NA	0.81315	0.65357	0.66937	0.48413	0.47395	0.53229	0.60544	0.70736	0.21118	-0.30681
586.4	NA	1.0363	1.2415	1.12551	0.80969	0.65383	0.53777	0.8409	0.79551	0.31942	-0.10203
661.8	NA	0.60443	1.04784	1.2672	1.31114	1.17417	0.98176	0.97552	0.63009	0.41601	0.08492
746.8	NA	0.35598	0.52304	0.66923	0.8984	1.15273	1.17905	0.55477	0.89823	0.49833	0.23509
842.8	NA	0.3813	0.30884	0.3693	0.51935	0.63984	0.87986	0.52121	0.65073	0.56592	0.32326
951.1	NA	0.67998	0.3656	0.31186	0.37022	0.45225	NA	NA	NA	NA	NA
1073.4	NA	1.00262	0.57195	0.46309	NA	NA	NA	NA	NA	NA	NA
1211.4	NA	1.521	0.93061	NA	NA	NA	NA	NA	NA	NA	NA
1367.1	0.32181	1.58089	1.36534	NA	NA	NA	NA	NA	NA	NA	NA
1542.8	0.37797	0.9982	NA	NA	NA	NA	NA	NA	NA	NA	NA
1741.1	0.36164	0.61962	NA	NA	NA	NA	NA	NA	NA	NA	NA
1964.8	0.35373	NA	NA	NA	NA	NA	NA	NA	NA	NA	NA
2217.4	0.27983	NA	NA	NA	NA	NA	NA	NA	NA	NA	NA
2502.4	0.14772	NA	NA	NA	NA	NA	NA	NA	NA	NA	NA
2824	0.03177	NA	NA	NA	NA	NA	NA	NA	NA	NA	NA

Table A.99: FAS Linear Amp. Look-up Table for 20.0 Hz.

V_{S30} (m/s)	Soil Depth (m)										
	0	5	10	15	20	25	30	50	100	500	1000
95.6	NA	NA	NA	NA	NA	NA	-0.65612	-1.07499	-1.76212	-5.21104	-8.12314
107.9	NA	NA	NA	NA	NA	-0.47303	-0.47626	-0.79716	-1.43106	-4.48204	-7.03212
121.8	NA	NA	NA	NA	-0.2528	-0.28877	-0.28423	-0.50997	-1.01241	-3.44237	-5.4821
137.4	NA	NA	NA	NA	-0.16635	-0.13511	-0.08311	-0.27707	-0.69137	-2.81486	-4.6138
155.1	NA	NA	NA	0.01975	0.02248	0.01418	0.06864	-0.12863	-0.55349	-2.97561	-5.10443
175	NA	NA	NA	0.13758	0.13378	0.11033	0.27405	0.00721	-0.18989	-1.85858	-3.29511
197.5	NA	NA	0.11112	0.20227	0.18848	0.35312	0.33318	0.12819	-0.18905	-2.2316	-4.04968
222.9	NA	NA	0.13312	0.2379	0.23576	0.42995	0.54073	0.33099	0.05613	-1.71662	-3.26395
251.5	NA	NA	0.25866	0.34717	0.52196	0.63982	0.64246	0.46069	0.189	-1.38026	-2.77489
283.9	NA	NA	0.27985	0.20714	0.5659	0.50544	0.64621	0.5081	0.27363	-1.22085	-2.54965
320.4	NA	0.37275	0.48059	0.71496	0.86948	0.84907	0.68401	0.67475	0.40891	-0.95434	-2.18164
361.5	NA	0.54597	0.25061	0.48092	0.55903	0.75908	0.9061	0.68726	0.53621	-0.633	-1.68882
408	NA	0.69193	0.75833	0.8773	0.72388	0.67954	0.60495	0.79801	0.63463	-0.25435	-1.07298
460.4	NA	0.3502	0.60949	1.01618	1.13344	1.16037	1.07911	0.79155	0.63855	-0.02786	-0.70163
519.6	NA	0.51324	0.42263	0.56612	0.62146	0.7148	0.89599	0.9053	0.71246	0.09044	-0.47815
586.4	NA	0.93082	0.86964	0.67212	0.51022	0.44966	0.47819	0.59801	0.71904	0.27246	-0.19417
661.8	NA	0.92444	1.33253	1.24734	0.96364	0.74445	0.59233	0.96163	0.74372	0.35705	-0.00768
746.8	NA	0.46288	0.86761	1.07215	1.23989	1.18893	1.05394	0.83133	0.68375	0.43436	0.14023
842.8	NA	0.336	0.39105	0.52311	0.81379	0.9582	1.16338	0.51835	0.90926	0.50824	0.25362
951.1	NA	0.50706	0.29448	0.30562	0.43261	0.63318	NA	NA	NA	NA	NA
1073.4	NA	0.72735	0.39115	0.33646	NA	NA	NA	NA	NA	NA	NA
1211.4	NA	1.14938	0.64117	NA	NA	NA	NA	NA	NA	NA	NA
1367.1	0.32632	1.65561	1.02716	NA	NA	NA	NA	NA	NA	NA	NA
1542.8	0.35359	1.28411	NA	NA	NA	NA	NA	NA	NA	NA	NA
1741.1	0.36615	0.78355	NA	NA	NA	NA	NA	NA	NA	NA	NA
1964.8	0.35783	NA	NA	NA	NA	NA	NA	NA	NA	NA	NA
2217.4	0.29305	NA	NA	NA	NA	NA	NA	NA	NA	NA	NA
2502.4	0.16062	NA	NA	NA	NA	NA	NA	NA	NA	NA	NA
2824	0.0378	NA	NA	NA	NA	NA	NA	NA	NA	NA	NA

Table A.100: FAS Linear Amp. Look-up Table for 20.833 Hz.

V_{S30} (m/s)	Soil Depth (m)										
	0	5	10	15	20	25	30	50	100	500	1000
95.6	NA	NA	NA	NA	NA	NA	-0.75932	-1.22874	-1.92426	-5.52718	-8.55652
107.9	NA	NA	NA	NA	NA	-0.5609	-0.56448	-0.91395	-1.56276	-4.73711	-7.39625
121.8	NA	NA	NA	NA	-0.32155	-0.36741	-0.35006	-0.59248	-1.11874	-3.66348	-5.78837
137.4	NA	NA	NA	NA	-0.19654	-0.20701	-0.12397	-0.32188	-0.7654	-2.97859	-4.85479
155.1	NA	NA	NA	-0.07415	-0.05287	-0.01305	-0.00658	-0.20119	-0.67111	-3.17953	-5.39488
175	NA	NA	NA	0.12958	0.11668	0.04557	0.2246	0.00264	-0.22918	-1.96659	-3.463
197.5	NA	NA	0.03755	0.16055	0.13033	0.30891	0.3055	0.07159	-0.26813	-2.39779	-4.29336
222.9	NA	NA	0.0816	0.24114	0.26977	0.43986	0.48316	0.26945	-0.02086	-1.86557	-3.47886
251.5	NA	NA	0.26652	0.29944	0.36652	0.54892	0.56204	0.42269	0.16131	-1.48948	-2.94079
283.9	NA	NA	0.27185	0.1882	0.59089	0.60641	0.72706	0.51432	0.23343	-1.31632	-2.70364
320.4	NA	0.30517	0.5125	0.60666	0.77459	0.70089	0.57073	0.60957	0.36625	-1.05932	-2.33637
361.5	NA	0.35801	0.24778	0.5562	0.69686	0.87852	0.98206	0.66659	0.49839	-0.72143	-1.82191
408	NA	0.75741	0.59652	0.70331	0.5722	0.59269	0.61699	0.8333	0.62116	-0.31436	-1.16928
460.4	NA	0.46257	0.76667	1.08783	1.10315	1.044	0.89166	0.69274	0.68656	-0.05504	-0.75585
519.6	NA	0.43308	0.42066	0.6335	0.8023	0.91676	1.05951	0.94532	0.65375	0.0454	-0.54861
586.4	NA	0.81424	0.70117	0.5572	0.47144	0.45488	0.55323	0.64048	0.69176	0.23053	-0.24972
661.8	NA	1.01791	1.28897	1.06892	0.76022	0.59067	0.49149	0.8013	0.80247	0.34632	-0.03822
746.8	NA	0.55527	1.06555	1.22717	1.25391	1.03662	0.88925	0.95193	0.59798	0.40983	0.09637
842.8	NA	0.34461	0.46966	0.6428	0.99336	1.10388	1.17156	0.613	0.84706	0.47643	0.21824
951.1	NA	0.45292	0.28844	0.33349	0.4979	0.76387	NA	NA	NA	NA	NA
1073.4	NA	0.63081	0.33491	0.30439	NA	NA	NA	NA	NA	NA	NA
1211.4	NA	1.0025	0.53931	NA	NA	NA	NA	NA	NA	NA	NA
1367.1	0.34682	1.59224	0.88436	NA	NA	NA	NA	NA	NA	NA	NA
1542.8	0.34295	1.41645	NA	NA	NA	NA	NA	NA	NA	NA	NA
1741.1	0.36619	0.86985	NA	NA	NA	NA	NA	NA	NA	NA	NA
1964.8	0.35755	NA	NA	NA	NA	NA	NA	NA	NA	NA	NA
2217.4	0.29773	NA	NA	NA	NA	NA	NA	NA	NA	NA	NA
2502.4	0.16596	NA	NA	NA	NA	NA	NA	NA	NA	NA	NA
2824	0.04068	NA	NA	NA	NA	NA	NA	NA	NA	NA	NA

Table A.101: FAS Linear Amp. Look-up Table for 21.739 Hz.

V_{S30} (m/s)	Soil Depth (m)										
	0	5	10	15	20	25	30	50	100	500	1000
95.6	NA	NA	NA	NA	NA	NA	-0.85366	-1.3648	-2.07812	-5.84769	-9.00831
107.9	NA	NA	NA	NA	NA	-0.6169	-0.65771	-1.07083	-1.73003	-5.04082	-7.81881
121.8	NA	NA	NA	NA	-0.40544	-0.48167	-0.39838	-0.66799	-1.21673	-3.88471	-6.10219
137.4	NA	NA	NA	NA	-0.25611	-0.24948	-0.1968	-0.40072	-0.87038	-3.18042	-5.14179
155.1	NA	NA	NA	-0.17771	-0.12616	-0.07297	-0.0553	-0.25653	-0.75248	-3.38341	-5.69912
175	NA	NA	NA	0.07301	0.07447	0.01428	0.16034	-0.04773	-0.32374	-2.1198	-3.68199
197.5	NA	NA	-0.02797	0.13881	0.14193	0.26003	0.2999	0.04335	-0.32738	-2.55762	-4.53958
222.9	NA	NA	0.02598	0.24805	0.22856	0.38744	0.40278	0.18518	-0.11897	-2.04015	-3.727
251.5	NA	NA	0.18629	0.21369	0.25745	0.46772	0.53423	0.3909	0.11472	-1.61723	-3.13138
283.9	NA	NA	0.28634	0.27146	0.58287	0.68667	0.70584	0.49729	0.20601	-1.42213	-2.87133
320.4	NA	0.36598	0.41056	0.39067	0.62369	0.57623	0.586	0.54089	0.32277	-1.1632	-2.49682
361.5	NA	0.26093	0.33524	0.67593	0.8418	0.90852	0.88637	0.67153	0.4557	-0.82777	-1.97533
408	NA	0.73501	0.39478	0.56529	0.52227	0.64134	0.74696	0.78481	0.59771	-0.38083	-1.27584
460.4	NA	0.59567	0.86091	1.02664	0.92364	0.82792	0.68855	0.6988	0.68761	-0.09243	-0.82307
519.6	NA	0.39468	0.49142	0.7739	1.00805	1.09032	1.10981	0.84686	0.63143	0.0087	-0.61162
586.4	NA	0.67768	0.56017	0.50054	0.49719	0.52946	0.70713	0.75533	0.6998	0.17729	-0.32529
661.8	NA	1.04837	1.13993	0.85572	0.58855	0.48072	0.43991	0.63618	0.76967	0.3308	-0.06999
746.8	NA	0.6822	1.23651	1.29292	1.14548	0.83441	0.70934	0.98948	0.62203	0.37812	0.0537
842.8	NA	0.37587	0.59009	0.80902	1.16299	1.19266	1.07453	0.76745	0.68222	0.43867	0.17623
951.1	NA	0.40947	0.30049	0.38678	0.59747	0.93152	NA	NA	NA	NA	NA
1073.4	NA	0.54246	0.2895	0.28618	NA	NA	NA	NA	NA	NA	NA
1211.4	NA	0.86256	0.44637	NA	NA	NA	NA	NA	NA	NA	NA
1367.1	0.38076	1.47661	0.74477	NA	NA	NA	NA	NA	NA	NA	NA
1542.8	0.33336	1.53838	NA	NA	NA	NA	NA	NA	NA	NA	NA
1741.1	0.36167	0.97348	NA	NA	NA	NA	NA	NA	NA	NA	NA
1964.8	0.3549	NA	NA	NA	NA	NA	NA	NA	NA	NA	NA
2217.4	0.30151	NA	NA	NA	NA	NA	NA	NA	NA	NA	NA
2502.4	0.17146	NA	NA	NA	NA	NA	NA	NA	NA	NA	NA
2824	0.0439	NA	NA	NA	NA	NA	NA	NA	NA	NA	NA

Table A.102: FAS Linear Amp. Look-up Table for 22.222 Hz.

V_{S30} (m/s)	Soil Depth (m)										
	0	5	10	15	20	25	30	50	100	500	1000
95.6	NA	NA	NA	NA	NA	NA	-0.90891	-1.42057	-2.16054	-6.0148	-9.24294
107.9	NA	NA	NA	NA	NA	-0.63339	-0.71152	-1.15202	-1.81657	-5.20315	-8.04377
121.8	NA	NA	NA	NA	-0.46903	-0.52975	-0.42183	-0.70577	-1.26645	-3.99551	-6.26386
137.4	NA	NA	NA	NA	-0.29228	-0.26112	-0.23737	-0.44315	-0.92697	-3.29116	-5.29641
155.1	NA	NA	NA	-0.232	-0.14721	-0.10904	-0.06176	-0.28292	-0.78734	-3.48226	-5.85266
175	NA	NA	NA	0.03038	0.04659	0.0192	0.12533	-0.08022	-0.378	-2.20722	-3.80415
197.5	NA	NA	-0.04962	0.13723	0.15996	0.22004	0.2899	0.03593	-0.35104	-2.63468	-4.6627
222.9	NA	NA	0.00264	0.24486	0.1873	0.34807	0.38111	0.14214	-0.16456	-2.1359	-3.86203
251.5	NA	NA	0.13238	0.1915	0.25015	0.44976	0.5441	0.37001	0.07919	-1.68788	-3.23564
283.9	NA	NA	0.28505	0.32676	0.5362	0.67887	0.65403	0.47054	0.1919	-1.48072	-2.96202
320.4	NA	0.44461	0.33221	0.28654	0.57312	0.56172	0.63504	0.53115	0.30459	-1.21426	-2.5781
361.5	NA	0.25868	0.39753	0.71606	0.87775	0.86506	0.78374	0.66324	0.42943	-0.88542	-2.05765
408	NA	0.68199	0.31495	0.53347	0.54928	0.71272	0.82964	0.74141	0.58153	-0.41729	-1.33338
460.4	NA	0.64698	0.85869	0.94865	0.80628	0.71958	0.62013	0.74196	0.67131	-0.11813	-0.86541
519.6	NA	0.39745	0.55432	0.86374	1.0836	1.13089	1.0703	0.76809	0.63427	-0.00422	-0.63844
586.4	NA	0.6086	0.50925	0.49923	0.54086	0.59883	0.8074	0.81435	0.70531	0.15026	-0.36525
661.8	NA	1.03591	1.03861	0.75696	0.52343	0.44728	0.43704	0.58112	0.72759	0.32137	-0.0892
746.8	NA	0.75424	1.28561	1.27497	1.05435	0.73382	0.62853	0.96063	0.66809	0.37261	0.03571
842.8	NA	0.40216	0.66969	0.90503	1.21727	1.19565	0.99303	0.85234	0.60006	0.4147	0.15331
951.1	NA	0.39315	0.31502	0.4253	0.66197	1.02166	NA	NA	NA	NA	NA
1073.4	NA	0.50264	0.27203	0.2838	NA	NA	NA	NA	NA	NA	NA
1211.4	NA	0.79718	0.40456	NA	NA	NA	NA	NA	NA	NA	NA
1367.1	0.40309	1.40436	0.67938	NA	NA	NA	NA	NA	NA	NA	NA
1542.8	0.33008	1.58549	NA	NA	NA	NA	NA	NA	NA	NA	NA
1741.1	0.35693	1.0316	NA	NA	NA	NA	NA	NA	NA	NA	NA
1964.8	0.35228	NA	NA	NA	NA	NA	NA	NA	NA	NA	NA
2217.4	0.30291	NA	NA	NA	NA	NA	NA	NA	NA	NA	NA
2502.4	0.17424	NA	NA	NA	NA	NA	NA	NA	NA	NA	NA
2824	0.04563	NA	NA	NA	NA	NA	NA	NA	NA	NA	NA

Table A.103: FAS Linear Amp. Look-up Table for 22.727 Hz.

V_{S30} (m/s)	Soil Depth (m)										
	0	5	10	15	20	25	30	50	100	500	1000
95.6	NA	NA	NA	NA	NA	NA	-0.95584	-1.47558	-2.24331	-6.18976	-9.49262
107.9	NA	NA	NA	NA	NA	-0.66363	-0.7613	-1.22908	-1.89935	-5.36865	-8.27521
121.8	NA	NA	NA	NA	-0.53841	-0.57087	-0.45476	-0.75001	-1.32306	-4.1137	-6.43412
137.4	NA	NA	NA	NA	-0.32901	-0.27715	-0.27398	-0.48765	-0.98288	-3.40676	-5.45774
155.1	NA	NA	NA	-0.28245	-0.16119	-0.14387	-0.07069	-0.30111	-0.81855	-3.58167	-6.00864
175	NA	NA	NA	-0.01421	0.01256	0.02291	0.09154	-0.11234	-0.43235	-2.29739	-3.93093
197.5	NA	NA	-0.06873	0.13199	0.16562	0.17432	0.27722	0.02934	-0.37343	-2.71332	-4.78886
222.9	NA	NA	-0.01813	0.23954	0.1506	0.31182	0.36722	0.10502	-0.21344	-2.23536	-4.00324
251.5	NA	NA	0.08512	0.19042	0.26883	0.44488	0.54811	0.34188	0.04037	-1.76526	-3.34894
283.9	NA	NA	0.27416	0.36664	0.46109	0.63607	0.60184	0.4445	0.16624	-1.5442	-3.05891
320.4	NA	0.53666	0.25833	0.21355	0.55638	0.58068	0.69156	0.53288	0.28525	-1.2661	-2.66264
361.5	NA	0.28698	0.45781	0.72255	0.87341	0.79035	0.66937	0.64136	0.40099	-0.94562	-2.14414
408	NA	0.60773	0.2618	0.5323	0.60815	0.79899	0.90264	0.69882	0.56333	-0.45705	-1.39456
460.4	NA	0.67729	0.81909	0.8508	0.68914	0.63227	0.5854	0.79446	0.65271	-0.14937	-0.9144
519.6	NA	0.41612	0.63086	0.95619	1.12046	1.12618	0.99132	0.69248	0.646	-0.01672	-0.66495
586.4	NA	0.54135	0.47392	0.51884	0.60921	0.69128	0.90565	0.85726	0.69453	0.12043	-0.40803
661.8	NA	1.00676	0.92907	0.66943	0.47331	0.42927	0.45169	0.55496	0.6865	0.30582	-0.11354
746.8	NA	0.83049	1.2987	1.22264	0.94945	0.64006	0.55794	0.90252	0.72098	0.35894	0.01954
842.8	NA	0.43758	0.7639	1.00178	1.23883	1.16555	0.89538	0.92733	0.5452	0.42836	0.12777
951.1	NA	0.38066	0.33649	0.47365	0.73741	1.10301	NA	NA	NA	NA	NA
1073.4	NA	0.46553	0.25848	0.28654	NA	NA	NA	NA	NA	NA	NA
1211.4	NA	0.73453	0.36602	NA	NA	NA	NA	NA	NA	NA	NA
1367.1	0.42893	1.32509	0.61661	NA	NA	NA	NA	NA	NA	NA	NA
1542.8	0.32865	1.61839	NA	NA	NA	NA	NA	NA	NA	NA	NA
1741.1	0.35029	1.09462	NA	NA	NA	NA	NA	NA	NA	NA	NA
1964.8	0.34845	NA	NA	NA	NA	NA	NA	NA	NA	NA	NA
2217.4	0.30386	NA	NA	NA	NA	NA	NA	NA	NA	NA	NA
2502.4	0.17704	NA	NA	NA	NA	NA	NA	NA	NA	NA	NA
2824	0.04743	NA	NA	NA	NA	NA	NA	NA	NA	NA	NA

Table A.104: FAS Linear Amp. Look-up Table for 23.810 Hz.

V_{S30} (m/s)	Soil Depth (m)										
	0	5	10	15	20	25	30	50	100	500	1000
95.6	NA	NA	NA	NA	NA	NA	-1.02865	-1.57411	-2.40815	-6.5616	-10.0390
107.9	NA	NA	NA	NA	NA	-0.7751	-0.86418	-1.35353	-2.06128	-5.70538	-8.74626
121.8	NA	NA	NA	NA	-0.65414	-0.6189	-0.5471	-0.87756	-1.46467	-4.3817	-6.81478
137.4	NA	NA	NA	NA	-0.43154	-0.35545	-0.33123	-0.56606	-1.0885	-3.63939	-5.78782
155.1	NA	NA	NA	-0.3602	-0.19424	-0.19943	-0.10332	-0.34953	-0.89683	-3.79528	-6.3398
175	NA	NA	NA	-0.1033	-0.06086	0.00791	0.03528	-0.14888	-0.50833	-2.46751	-4.17902
197.5	NA	NA	-0.09927	0.09051	0.14114	0.10798	0.24761	-0.00116	-0.43065	-2.88455	-5.05828
222.9	NA	NA	-0.04442	0.21919	0.12541	0.26789	0.34127	0.0708	-0.29263	-2.42786	-4.28223
251.5	NA	NA	0.05637	0.22659	0.31374	0.41684	0.48976	0.2693	-0.0502	-1.93573	-3.59656
283.9	NA	NA	0.21727	0.35745	0.29445	0.50506	0.55252	0.40795	0.11754	-1.68626	-3.27168
320.4	NA	0.64486	0.19277	0.20342	0.59921	0.6729	0.74993	0.52883	0.24308	-1.38013	-2.84516
361.5	NA	0.40972	0.51155	0.60616	0.75486	0.62001	0.51899	0.56908	0.34428	-1.06551	-2.3203
408	NA	0.44576	0.24842	0.60608	0.76522	0.93229	0.94194	0.66074	0.52185	-0.54845	-1.53118
460.4	NA	0.65303	0.64504	0.64693	0.51931	0.56568	0.63248	0.84763	0.63282	-0.21905	-1.0226
519.6	NA	0.49063	0.78584	1.08726	1.04312	0.97887	0.77195	0.63437	0.6673	-0.04801	-0.72637
586.4	NA	0.42796	0.46104	0.63016	0.80818	0.91537	1.03827	0.8608	0.62629	0.07035	-0.4846
661.8	NA	0.908	0.71868	0.53866	0.42339	0.44707	0.54263	0.60057	0.66195	0.25956	-0.17598
746.8	NA	0.97278	1.20711	1.0403	0.73706	0.49025	0.45809	0.73273	0.77536	0.35033	-0.01106
842.8	NA	0.54144	0.98015	1.16443	1.16333	1.0142	0.69437	0.99309	0.57197	0.37071	0.08434
951.1	NA	0.36999	0.404	0.60595	0.91251	1.19353	NA	NA	NA	NA	NA
1073.4	NA	0.40132	0.24486	0.30946	NA	NA	NA	NA	NA	NA	NA
1211.4	NA	0.61838	0.29897	NA	NA	NA	NA	NA	NA	NA	NA
1367.1	0.48961	1.1579	0.50143	NA	NA	NA	NA	NA	NA	NA	NA
1542.8	0.3325	1.62734	NA	NA	NA	NA	NA	NA	NA	NA	NA
1741.1	0.33224	1.23241	NA	NA	NA	NA	NA	NA	NA	NA	NA
1964.8	0.33697	NA	NA	NA	NA	NA	NA	NA	NA	NA	NA
2217.4	0.30416	NA	NA	NA	NA	NA	NA	NA	NA	NA	NA
2502.4	0.18269	NA	NA	NA	NA	NA	NA	NA	NA	NA	NA
2824	0.0513	NA	NA	NA	NA	NA	NA	NA	NA	NA	NA

Table A.105: FAS Linear Amp. Look-up Table for 25.0 Hz.

V_{S30} (m/s)	Soil Depth (m)										
	0	5	10	15	20	25	30	50	100	500	1000
95.6	NA	NA	NA	NA	NA	NA	-1.10791	-1.67258	-2.5774	-6.96028	-10.6122
107.9	NA	NA	NA	NA	NA	-0.90592	-0.95866	-1.46267	-2.23484	-6.07164	-9.26639
121.8	NA	NA	NA	NA	-0.74105	-0.69463	-0.65076	-1.04748	-1.64426	-4.7064	-7.26415
137.4	NA	NA	NA	NA	-0.57278	-0.4719	-0.39539	-0.65096	-1.19845	-3.88172	-6.13699
155.1	NA	NA	NA	-0.42438	-0.25803	-0.24019	-0.17294	-0.43623	-1.01562	-4.05645	-6.72827
175	NA	NA	NA	-0.22279	-0.12214	-0.04648	0.00579	-0.16882	-0.57007	-2.63637	-4.43505
197.5	NA	NA	-0.14648	0.00851	0.0954	0.10157	0.20917	-0.05424	-0.51487	-3.08946	-5.37141
222.9	NA	NA	-0.10708	0.18057	0.16631	0.24614	0.28137	0.05709	-0.35871	-2.60283	-4.55072
251.5	NA	NA	0.06596	0.23496	0.27711	0.34044	0.39215	0.18866	-0.15165	-2.13146	-3.87635
283.9	NA	NA	0.16647	0.26614	0.23439	0.43767	0.55376	0.36556	0.03375	-1.85375	-3.51765
320.4	NA	0.56301	0.25495	0.34225	0.60182	0.69919	0.66143	0.4727	0.19556	-1.51675	-3.05655
361.5	NA	0.53265	0.44047	0.37536	0.59588	0.54888	0.57885	0.52883	0.2911	-1.18319	-2.50198
408	NA	0.33911	0.34032	0.69892	0.85574	0.88963	0.77961	0.66715	0.47125	-0.66257	-1.6943
460.4	NA	0.53652	0.42606	0.5234	0.50494	0.67068	0.80891	0.76322	0.60855	-0.29532	-1.14103
519.6	NA	0.58953	0.86428	1.05328	0.80011	0.74137	0.5906	0.7346	0.64863	-0.09787	-0.81101
586.4	NA	0.36965	0.54295	0.83138	1.00906	1.081	1.00837	0.74586	0.60502	0.03476	-0.54671
661.8	NA	0.77108	0.54972	0.47856	0.4572	0.55804	0.72625	0.74652	0.69132	0.19597	-0.26106
746.8	NA	1.05851	0.99348	0.81181	0.55868	0.40102	0.42442	0.57752	0.71717	0.33211	-0.04649
842.8	NA	0.69996	1.179	1.2221	0.94814	0.7927	0.5244	0.89328	0.72425	0.36094	0.04899
951.1	NA	0.38365	0.51862	0.79992	1.08104	1.12843	NA	NA	NA	NA	NA
1073.4	NA	0.35109	0.25352	0.36352	NA	NA	NA	NA	NA	NA	NA
1211.4	NA	0.5126	0.24606	NA	NA	NA	NA	NA	NA	NA	NA
1367.1	0.55476	0.98844	0.39815	NA	NA	NA	NA	NA	NA	NA	NA
1542.8	0.35111	1.54842	NA	NA	NA	NA	NA	NA	NA	NA	NA
1741.1	0.31096	1.38018	NA	NA	NA	NA	NA	NA	NA	NA	NA
1964.8	0.31966	NA	NA	NA	NA	NA	NA	NA	NA	NA	NA
2217.4	0.30128	NA	NA	NA	NA	NA	NA	NA	NA	NA	NA
2502.4	0.18862	NA	NA	NA	NA	NA	NA	NA	NA	NA	NA
2824	0.05562	NA	NA	NA	NA	NA	NA	NA	NA	NA	NA

Table A.106: FAS Linear Amp. Look-up Table for 27.778 Hz.

V_{S30} (m/s)	Soil Depth (m)										
	0	5	10	15	20	25	30	50	100	500	1000
95.6	NA	NA	NA	NA	NA	NA	-1.35703	-1.95976	-3.00177	-7.8851	-11.9311
107.9	NA	NA	NA	NA	NA	-1.11293	-1.14729	-1.68235	-2.59492	-6.90003	-10.4649
121.8	NA	NA	NA	NA	-0.85182	-0.96235	-0.87978	-1.346	-2.01132	-5.43149	-8.27832
137.4	NA	NA	NA	NA	-0.74913	-0.61653	-0.58927	-0.94755	-1.52601	-4.50566	-7.02175
155.1	NA	NA	NA	-0.51005	-0.48481	-0.42054	-0.34663	-0.65226	-1.2965	-4.69515	-7.66447
175	NA	NA	NA	-0.3998	-0.22606	-0.20621	-0.1277	-0.31657	-0.76958	-3.07263	-5.08129
197.5	NA	NA	-0.25616	-0.22926	-0.06233	0.01783	0.11069	-0.1539	-0.69451	-3.56678	-6.10551
222.9	NA	NA	-0.19168	0.05168	0.11114	0.14395	0.20922	-0.01067	-0.47243	-2.96707	-5.13492
251.5	NA	NA	-0.10411	0.16933	0.22347	0.29049	0.31409	0.07064	-0.34444	-2.56995	-4.51498
283.9	NA	NA	0.11149	0.27199	0.3134	0.36755	0.40003	0.1977	-0.16298	-2.26689	-4.12138
320.4	NA	0.20559	0.21005	0.37976	0.25014	0.46677	0.54757	0.37938	0.04827	-1.85781	-3.56864
361.5	NA	0.31779	0.26373	0.27137	0.60163	0.68655	0.71359	0.47388	0.19866	-1.44701	-2.91838
408	NA	0.3987	0.51219	0.50085	0.5854	0.52716	0.53168	0.5442	0.36152	-0.9049	-2.05003
460.4	NA	0.33609	0.29692	0.69192	0.83987	0.90847	0.84096	0.65278	0.51161	-0.48361	-1.42507
519.6	NA	0.6652	0.57713	0.59079	0.45632	0.60244	0.73163	0.75031	0.59748	-0.24168	-1.03941
586.4	NA	0.49494	0.84027	1.03248	0.87613	0.79344	0.58997	0.67094	0.6335	-0.02889	-0.67513
661.8	NA	0.4952	0.45625	0.67638	0.84851	0.98608	1.01752	0.80552	0.57338	0.0907	-0.41916
746.8	NA	0.9624	0.53639	0.47944	0.41413	0.48728	0.63358	0.66016	0.65618	0.23082	-0.1848
842.8	NA	1.05667	1.12507	0.88947	0.48015	0.43496	0.39184	0.50964	0.65981	0.34309	-0.01052
951.1	NA	0.53043	0.93167	1.20577	1.05712	0.64788	NA	NA	NA	NA	NA
1073.4	NA	0.31325	0.37689	0.61854	NA	NA	NA	NA	NA	NA	NA
1211.4	NA	0.34266	0.20079	NA	NA	NA	NA	NA	NA	NA	NA
1367.1	0.61481	0.6733	0.23588	NA	NA	NA	NA	NA	NA	NA	NA
1542.8	0.43394	1.18378	NA	NA	NA	NA	NA	NA	NA	NA	NA
1741.1	0.28518	1.56174	NA	NA	NA	NA	NA	NA	NA	NA	NA
1964.8	0.27332	NA	NA	NA	NA	NA	NA	NA	NA	NA	NA
2217.4	0.28214	NA	NA	NA	NA	NA	NA	NA	NA	NA	NA
2502.4	0.20177	NA	NA	NA	NA	NA	NA	NA	NA	NA	NA
2824	0.06573	NA	NA	NA	NA	NA	NA	NA	NA	NA	NA

Table A.107: FAS Linear Amp. Look-up Table for 28.571 Hz.

V_{S30} (m/s)	Soil Depth (m)										
	0	5	10	15	20	25	30	50	100	500	1000
95.6	NA	NA	NA	NA	NA	NA	-1.41833	-2.04955	-3.12024	-8.14428	-12.3128
107.9	NA	NA	NA	NA	NA	-1.16924	-1.21797	-1.75557	-2.70538	-7.1333	-10.8000
121.8	NA	NA	NA	NA	-0.90011	-1.01322	-0.92829	-1.40451	-2.10668	-5.63251	-8.56133
137.4	NA	NA	NA	NA	-0.77096	-0.66698	-0.64629	-1.0361	-1.62091	-4.68938	-7.27815
155.1	NA	NA	NA	-0.52812	-0.56256	-0.47151	-0.38344	-0.70424	-1.36674	-4.86564	-7.92112
175	NA	NA	NA	-0.43396	-0.26408	-0.23291	-0.16905	-0.36151	-0.83231	-3.20508	-5.27067
197.5	NA	NA	-0.29226	-0.28587	-0.09019	-0.0159	0.08524	-0.17593	-0.73931	-3.69582	-6.30856
222.9	NA	NA	-0.21461	-0.01196	0.08676	0.13761	0.19691	-0.03602	-0.50868	-3.07851	-5.30934
251.5	NA	NA	-0.12631	0.16274	0.23303	0.27766	0.28552	0.06042	-0.3812	-2.66975	-4.672
283.9	NA	NA	0.05716	0.28191	0.28448	0.31055	0.37296	0.16278	-0.21592	-2.38391	-4.29271
320.4	NA	0.24527	0.14203	0.31424	0.23252	0.4492	0.55012	0.34149	0.00058	-1.96206	-3.7217
361.5	NA	0.23492	0.28734	0.35113	0.58695	0.64548	0.62653	0.45293	0.17531	-1.52358	-3.03788
408	NA	0.43407	0.47535	0.39393	0.53595	0.5507	0.60145	0.52585	0.33487	-0.96296	-2.14145
460.4	NA	0.3356	0.36451	0.7354	0.85927	0.82858	0.70869	0.67553	0.48058	-0.5453	-1.51314
519.6	NA	0.62225	0.46231	0.51578	0.4971	0.69173	0.83802	0.67493	0.58175	-0.27884	-1.10031
586.4	NA	0.5504	0.86166	0.94128	0.73718	0.6602	0.52836	0.71926	0.62288	-0.05973	-0.72583
661.8	NA	0.45411	0.50688	0.79123	0.9629	1.03775	0.96255	0.71585	0.57532	0.08244	-0.44366
746.8	NA	0.89086	0.46176	0.45173	0.44093	0.58759	0.74177	0.74067	0.66221	0.19929	-0.23408
842.8	NA	1.08909	1.00445	0.75887	0.40602	0.39254	0.41809	0.48933	0.60371	0.32703	-0.03522
951.1	NA	0.60298	1.04168	1.21562	0.95102	0.53481	NA	NA	NA	NA	NA
1073.4	NA	0.32298	0.44189	0.72525	NA	NA	NA	NA	NA	NA	NA
1211.4	NA	0.31175	0.20674	NA	NA	NA	NA	NA	NA	NA	NA
1367.1	0.59706	0.60266	0.20715	NA	NA	NA	NA	NA	NA	NA	NA
1542.8	0.45833	1.07465	NA	NA	NA	NA	NA	NA	NA	NA	NA
1741.1	0.28819	1.54809	NA	NA	NA	NA	NA	NA	NA	NA	NA
1964.8	0.26263	NA	NA	NA	NA	NA	NA	NA	NA	NA	NA
2217.4	0.27404	NA	NA	NA	NA	NA	NA	NA	NA	NA	NA
2502.4	0.20535	NA	NA	NA	NA	NA	NA	NA	NA	NA	NA
2824	0.06856	NA	NA	NA	NA	NA	NA	NA	NA	NA	NA

Table A.108: FAS Linear Amp. Look-up Table for 31.25 Hz.

V_{S30} (m/s)	Soil Depth (m)										
	0	5	10	15	20	25	30	50	100	500	1000
95.6	NA	NA	NA	NA	NA	NA	-1.68222	-2.43233	-3.56481	-9.0727	-13.6131
107.9	NA	NA	NA	NA	NA	-1.40413	-1.42829	-2.03404	-3.07638	-7.92724	-11.9351
121.8	NA	NA	NA	NA	-1.10499	-1.18229	-1.0767	-1.57776	-2.39593	-6.28791	-9.50098
137.4	NA	NA	NA	NA	-0.90839	-0.89024	-0.82394	-1.25784	-1.9091	-5.27994	-8.11298
155.1	NA	NA	NA	-0.6647	-0.72196	-0.59583	-0.53854	-0.90281	-1.633	-5.46015	-8.80158
175	NA	NA	NA	-0.50347	-0.45156	-0.34345	-0.28461	-0.50128	-1.02143	-3.63558	-5.89301
197.5	NA	NA	-0.43867	-0.40918	-0.17734	-0.10554	-0.01609	-0.28907	-0.90684	-4.14769	-7.00894
222.9	NA	NA	-0.31571	-0.19326	-0.02248	0.07536	0.11548	-0.12461	-0.66185	-3.48211	-5.92543
251.5	NA	NA	-0.17791	0.08624	0.18014	0.18313	0.24116	0.00678	-0.46249	-2.97184	-5.16514
283.9	NA	NA	-0.02659	0.19929	0.24994	0.29541	0.31563	0.08808	-0.36855	-2.74688	-4.83814
320.4	NA	0.32591	0.11459	0.34282	0.34949	0.40891	0.4032	0.22451	-0.15682	-2.3107	-4.2399
361.5	NA	0.27496	0.30297	0.41093	0.32281	0.46453	0.53333	0.38467	0.05915	-1.79933	-3.45371
408	NA	0.40577	0.30073	0.30868	0.59005	0.71003	0.70445	0.50127	0.27081	-1.15384	-2.44722
460.4	NA	0.40921	0.55185	0.52853	0.57228	0.50987	0.51099	0.55613	0.3999	-0.72838	-1.78429
519.6	NA	0.42812	0.3071	0.60976	0.81671	0.89815	0.82138	0.66788	0.51181	-0.42902	-1.3273
586.4	NA	0.61808	0.66443	0.52874	0.45995	0.54503	0.68328	0.71742	0.57935	-0.17665	-0.90781
661.8	NA	0.48103	0.7984	1.00975	0.93757	0.79477	0.58595	0.60518	0.63949	0.04629	-0.52889
746.8	NA	0.62059	0.40375	0.57707	0.74455	0.97385	0.95587	0.77783	0.56387	0.11702	-0.35644
842.8	NA	0.96039	0.59567	0.45783	0.34741	0.42685	0.69351	0.71424	0.67589	0.22066	-0.17721
951.1	NA	0.89132	1.15603	0.89521	0.57033	0.33099	NA	NA	NA	NA	NA
1073.4	NA	0.42841	0.76627	1.0815	NA	NA	NA	NA	NA	NA	NA
1211.4	NA	0.25858	0.28958	NA	NA	NA	NA	NA	NA	NA	NA
1367.1	0.46841	0.41702	0.16051	NA	NA	NA	NA	NA	NA	NA	NA
1542.8	0.50077	0.76211	NA	NA	NA	NA	NA	NA	NA	NA	NA
1741.1	0.32584	1.33295	NA	NA	NA	NA	NA	NA	NA	NA	NA
1964.8	0.24591	NA	NA	NA	NA	NA	NA	NA	NA	NA	NA
2217.4	0.24398	NA	NA	NA	NA	NA	NA	NA	NA	NA	NA
2502.4	0.21697	NA	NA	NA	NA	NA	NA	NA	NA	NA	NA
2824	0.07783	NA	NA	NA	NA	NA	NA	NA	NA	NA	NA

Table A.109: FAS Linear Amp. Look-up Table for 33.333 Hz.

V_{S30} (m/s)	Soil Depth (m)										
	0	5	10	15	20	25	30	50	100	500	1000
95.6	NA	NA	NA	NA	NA	NA	-1.9163	-2.72954	-3.93148	-9.80635	-14.6499
107.9	NA	NA	NA	NA	NA	-1.60362	-1.615	-2.3058	-3.38834	-8.56691	-12.8351
121.8	NA	NA	NA	NA	-1.26589	-1.34478	-1.22877	-1.74308	-2.63555	-6.79157	-10.2167
137.4	NA	NA	NA	NA	-1.05198	-1.01504	-0.92229	-1.37889	-2.11124	-5.72837	-8.75564
155.1	NA	NA	NA	-0.8514	-0.78117	-0.72155	-0.65296	-1.07831	-1.85514	-5.94649	-9.51438
175	NA	NA	NA	-0.56315	-0.59877	-0.46566	-0.37389	-0.64025	-1.18699	-3.9723	-6.38412
197.5	NA	NA	-0.56505	-0.46175	-0.28813	-0.17257	-0.09478	-0.38568	-1.04606	-4.51034	-7.56132
222.9	NA	NA	-0.39206	-0.28577	-0.08888	0.01994	0.03709	-0.2121	-0.7836	-3.79691	-6.40679
251.5	NA	NA	-0.2486	-0.04302	0.13123	0.14378	0.22108	-0.03803	-0.54486	-3.22877	-5.56967
283.9	NA	NA	-0.07543	0.19869	0.23322	0.25902	0.26327	0.02491	-0.45	-2.99001	-5.22486
320.4	NA	0.06765	0.05003	0.33505	0.28329	0.31614	0.38021	0.15779	-0.26114	-2.56432	-4.62583
361.5	NA	0.29098	0.20138	0.31011	0.29378	0.4604	0.55124	0.31226	-0.04641	-2.03044	-3.79794
408	NA	0.27772	0.33166	0.42768	0.48211	0.53887	0.55079	0.45095	0.21788	-1.30651	-2.68713
460.4	NA	0.37911	0.45577	0.29769	0.49826	0.61805	0.70552	0.52947	0.36984	-0.84049	-1.96854
519.6	NA	0.4019	0.43223	0.75374	0.78904	0.69906	0.54678	0.63416	0.44796	-0.56018	-1.5158
586.4	NA	0.54265	0.43217	0.46008	0.5836	0.77239	0.85442	0.63104	0.54959	-0.25135	-1.03307
661.8	NA	0.58878	0.89416	0.82783	0.62507	0.53825	0.48564	0.75305	0.59262	-0.02721	-0.64142
746.8	NA	0.4737	0.56552	0.83464	0.99213	0.95689	0.80187	0.60727	0.58493	0.09974	-0.40319
842.8	NA	0.77374	0.40694	0.39996	0.50295	0.63821	0.93927	0.83488	0.55714	0.14881	-0.2732
951.1	NA	1.05533	0.97472	0.58442	0.3918	0.3459	NA	NA	NA	NA	NA
1073.4	NA	0.59835	1.03801	1.13872	NA	NA	NA	NA	NA	NA	NA
1211.4	NA	0.27048	0.42897	NA	NA	NA	NA	NA	NA	NA	NA
1367.1	0.36495	0.31969	0.17451	NA	NA	NA	NA	NA	NA	NA	NA
1542.8	0.46315	0.57864	NA	NA	NA	NA	NA	NA	NA	NA	NA
1741.1	0.36371	1.09457	NA	NA	NA	NA	NA	NA	NA	NA	NA
1964.8	0.25478	NA	NA	NA	NA	NA	NA	NA	NA	NA	NA
2217.4	0.22373	NA	NA	NA	NA	NA	NA	NA	NA	NA	NA
2502.4	0.22521	NA	NA	NA	NA	NA	NA	NA	NA	NA	NA
2824	0.08464	NA	NA	NA	NA	NA	NA	NA	NA	NA	NA

Table A.110: FAS Linear Amp. Look-up Table for 34.483 Hz.

V_{S30} (m/s)	Soil Depth (m)										
	0	5	10	15	20	25	30	50	100	500	1000
95.6	NA	NA	NA	NA	NA	NA	-2.04094	-2.8593	-4.13387	-10.2097	-15.2243
107.9	NA	NA	NA	NA	NA	-1.69187	-1.72684	-2.46593	-3.57124	-8.93202	-13.3447
121.8	NA	NA	NA	NA	-1.37343	-1.44693	-1.30564	-1.84401	-2.76951	-7.07255	-10.6162
137.4	NA	NA	NA	NA	-1.1297	-1.07783	-0.98387	-1.44337	-2.21847	-5.97066	-9.10349
155.1	NA	NA	NA	-0.95492	-0.82954	-0.78942	-0.69123	-1.15527	-1.95376	-6.19512	-9.89058
175	NA	NA	NA	-0.60401	-0.64974	-0.51211	-0.43816	-0.73281	-1.28855	-4.16992	-6.6669
197.5	NA	NA	-0.62484	-0.47725	-0.33851	-0.22513	-0.12997	-0.43796	-1.12372	-4.71235	-7.8692
222.9	NA	NA	-0.44649	-0.30855	-0.12137	-0.01093	0.00041	-0.26185	-0.84617	-3.96698	-6.66851
251.5	NA	NA	-0.27377	-0.1223	0.09573	0.11194	0.18941	-0.07011	-0.59674	-3.37861	-5.80095
283.9	NA	NA	-0.11064	0.17853	0.20436	0.22486	0.24421	-0.00153	-0.48422	-3.11703	-5.43095
320.4	NA	-0.01397	-0.01762	0.28522	0.26495	0.30438	0.38286	0.1375	-0.3058	-2.69099	-4.82552
361.5	NA	0.2148	0.17191	0.31661	0.35654	0.42339	0.46902	0.26991	-0.10115	-2.15791	-3.98827
408	NA	0.24827	0.36293	0.45588	0.36366	0.45461	0.52494	0.43395	0.17126	-1.39576	-2.82354
460.4	NA	0.32518	0.38073	0.2793	0.55278	0.70089	0.75164	0.5477	0.34868	-0.90142	-2.07051
519.6	NA	0.41576	0.50791	0.7196	0.65999	0.57179	0.49249	0.56741	0.42616	-0.6219	-1.61058
586.4	NA	0.48515	0.35316	0.53441	0.71055	0.86884	0.83827	0.62744	0.52667	-0.29878	-1.107
661.8	NA	0.63468	0.83472	0.67256	0.49039	0.49633	0.55134	0.76817	0.58481	-0.0698	-0.70628
746.8	NA	0.44085	0.69779	0.94516	1.01004	0.81717	0.66331	0.56917	0.61432	0.09029	-0.43132
842.8	NA	0.67735	0.36258	0.43473	0.66047	0.79569	0.96899	0.77085	0.50643	0.13068	-0.30677
951.1	NA	1.08663	0.83182	0.46346	0.3487	0.4165	NA	NA	NA	NA	NA
1073.4	NA	0.72152	1.13318	1.05715	NA	NA	NA	NA	NA	NA	NA
1211.4	NA	0.29749	0.5389	NA	NA	NA	NA	NA	NA	NA	NA
1367.1	0.3289	0.28125	0.20086	NA	NA	NA	NA	NA	NA	NA	NA
1542.8	0.42129	0.49631	NA	NA	NA	NA	NA	NA	NA	NA	NA
1741.1	0.37654	0.96768	NA	NA	NA	NA	NA	NA	NA	NA	NA
1964.8	0.26547	NA	NA	NA	NA	NA	NA	NA	NA	NA	NA
2217.4	0.21571	NA	NA	NA	NA	NA	NA	NA	NA	NA	NA
2502.4	0.22929	NA	NA	NA	NA	NA	NA	NA	NA	NA	NA
2824	0.0882	NA	NA	NA	NA	NA	NA	NA	NA	NA	NA

Table A.111: FAS Linear Amp. Look-up Table for 40.000 Hz.

V_{S30} (m/s)	Soil Depth (m)										
	0	5	10	15	20	25	30	50	100	500	1000
95.6	NA	NA	NA	NA	NA	NA	-2.4648	-3.4032	-4.9554	-12.0179	-17.8424
107.9	NA	NA	NA	NA	NA	-2.07072	-2.2107	-3.00999	-4.4065	-10.6171	-15.7303
121.8	NA	NA	NA	NA	-1.69878	-1.83816	-1.71996	-2.43289	-3.45983	-8.46524	-12.5630
137.4	NA	NA	NA	NA	-1.54814	-1.4455	-1.3206	-1.84513	-2.76715	-7.1322	-10.7635
155.1	NA	NA	NA	-1.21099	-1.13657	-1.08566	-0.95489	-1.49078	-2.45774	-7.39139	-11.6753
175	NA	NA	NA	-0.99163	-0.8571	-0.77799	-0.69661	-1.08583	-1.72648	-5.0903	-7.98995
197.5	NA	NA	-0.80897	-0.66899	-0.60149	-0.45023	-0.37137	-0.75579	-1.54616	-5.71234	-9.37219
222.9	NA	NA	-0.68899	-0.42686	-0.33233	-0.19883	-0.18352	-0.50427	-1.1768	-4.81109	-7.94503
251.5	NA	NA	-0.48273	-0.34774	-0.07872	-0.01517	0.03733	-0.23494	-0.85176	-4.09082	-6.90416
283.9	NA	NA	-0.26143	-0.10091	0.07473	0.12758	0.18633	-0.08173	-0.65518	-3.72946	-6.41439
320.4	NA	0.14146	-0.12631	0.18258	0.2291	0.28071	0.27808	0.04324	-0.46446	-3.24183	-5.72281
361.5	NA	0.10759	0.03313	0.28962	0.36053	0.30146	0.32519	0.07263	-0.37641	-2.77127	-4.90145
408	NA	0.20071	0.18805	0.41343	0.40885	0.35619	0.42315	0.26973	-0.04383	-1.87842	-3.53673
460.4	NA	0.2796	0.42585	0.52068	0.27753	0.45331	0.56014	0.45635	0.21953	-1.22413	-2.5814
519.6	NA	0.39764	0.45928	0.2506	0.59659	0.71991	0.69786	0.52125	0.33497	-0.87591	-2.02772
586.4	NA	0.4048	0.55483	0.56757	0.59086	0.49785	0.53693	0.54366	0.41737	-0.54655	-1.48123
661.8	NA	0.5509	0.29764	0.57906	0.73545	0.84316	0.76993	0.61623	0.51192	-0.23693	-0.97734
746.8	NA	0.61346	0.69117	0.63113	0.44974	0.49198	0.60554	0.69703	0.56478	-0.05549	-0.66138
842.8	NA	0.44434	0.69327	0.91452	0.86716	0.75604	0.44179	0.61929	0.57744	0.08522	-0.42018
951.1	NA	0.77274	0.37912	0.39954	0.66312	1.00365	NA	NA	NA	NA	NA
1073.4	NA	1.11206	0.79767	0.43821	NA	NA	NA	NA	NA	NA	NA
1211.4	NA	0.65714	1.11866	NA	NA	NA	NA	NA	NA	NA	NA
1367.1	0.40748	0.23243	0.54174	NA	NA	NA	NA	NA	NA	NA	NA
1542.8	0.28135	0.23935	NA	NA	NA	NA	NA	NA	NA	NA	NA
1741.1	0.30095	0.50728	NA	NA	NA	NA	NA	NA	NA	NA	NA
1964.8	0.29912	NA	NA	NA	NA	NA	NA	NA	NA	NA	NA
2217.4	0.21449	NA	NA	NA	NA	NA	NA	NA	NA	NA	NA
2502.4	0.24161	NA	NA	NA	NA	NA	NA	NA	NA	NA	NA
2824	0.10281	NA	NA	NA	NA	NA	NA	NA	NA	NA	NA

Table A.112: FAS Linear Amp. Look-up Table for 45.455 Hz.

V_{S30} (m/s)	Soil Depth (m)										
	0	5	10	15	20	25	30	50	100	500	1000
95.6	NA	NA	NA	NA	NA	NA	-3.0423	-4.1615	-5.8851	-13.8973	-20.5004
107.9	NA	NA	NA	NA	NA	-2.60708	-2.6022	-3.58264	-5.14206	-12.2120	-18.0210
121.8	NA	NA	NA	NA	-2.14889	-2.21691	-2.13029	-2.87181	-4.15445	-9.82859	-14.4856
137.4	NA	NA	NA	NA	-1.81919	-1.76879	-1.68328	-2.34733	-3.37012	-8.33691	-12.4537
155.1	NA	NA	NA	-1.50395	-1.49843	-1.41586	-1.26975	-1.86959	-2.98996	-8.60394	-13.4658
175	NA	NA	NA	-1.22287	-1.13294	-1.05339	-0.91237	-1.32529	-2.10302	-5.9541	-9.2522
197.5	NA	NA	-1.05125	-1.01866	-0.80554	-0.64318	-0.57937	-1.046	-1.95147	-6.7019	-10.8591
222.9	NA	NA	-0.87389	-0.68255	-0.56701	-0.41332	-0.38143	-0.74582	-1.52447	-5.66494	-9.21971
251.5	NA	NA	-0.68692	-0.42726	-0.26638	-0.1659	-0.12256	-0.44185	-1.1418	-4.83135	-8.02712
283.9	NA	NA	-0.44285	-0.26022	-0.08118	0.01538	0.08575	-0.2174	-0.87089	-4.37355	-7.4242
320.4	NA	-0.07879	-0.23997	-0.06051	0.11852	0.24059	0.22829	-0.03154	-0.61061	-3.78327	-6.60277
361.5	NA	-0.00668	-0.0349	0.21846	0.34221	0.28901	0.28239	0.04489	-0.45816	-3.1905	-5.61468
408	NA	0.04584	0.08724	0.3816	0.39568	0.33832	0.33288	0.12938	-0.25999	-2.34982	-4.24053
460.4	NA	0.09353	0.26692	0.48318	0.41952	0.34411	0.42973	0.30076	0.03978	-1.61285	-3.15522
519.6	NA	0.27272	0.47585	0.56161	0.25131	0.49411	0.57599	0.4583	0.23922	-1.13951	-2.4467
586.4	NA	0.34268	0.54309	0.24423	0.61356	0.7262	0.6428	0.5135	0.35703	-0.74147	-1.80698
661.8	NA	0.46005	0.53308	0.58452	0.60826	0.493	0.49458	0.5104	0.42776	-0.4352	-1.27412
746.8	NA	0.64878	0.24093	0.56332	0.68977	0.82227	0.73116	0.59113	0.50403	-0.17998	-0.87023
842.8	NA	0.67375	0.73834	0.63091	0.3552	0.43913	0.72013	0.59815	0.54608	-0.03728	-0.61535
951.1	NA	0.45985	0.58256	0.92308	0.88621	0.47583	NA	NA	NA	NA	NA
1073.4	NA	0.74138	0.33302	0.3407	NA	NA	NA	NA	NA	NA	NA
1211.4	NA	1.05218	0.81434	NA	NA	NA	NA	NA	NA	NA	NA
1367.1	0.55406	0.40575	1.13511	NA	NA	NA	NA	NA	NA	NA	NA
1542.8	0.4067	0.15233	NA	NA	NA	NA	NA	NA	NA	NA	NA
1741.1	0.28536	0.25108	NA	NA	NA	NA	NA	NA	NA	NA	NA
1964.8	0.27619	NA	NA	NA	NA	NA	NA	NA	NA	NA	NA
2217.4	0.2382	NA	NA	NA	NA	NA	NA	NA	NA	NA	NA
2502.4	0.24053	NA	NA	NA	NA	NA	NA	NA	NA	NA	NA
2824	0.113	NA	NA	NA	NA	NA	NA	NA	NA	NA	NA

Table A.113: FAS Linear Amp. Look-up Table for 50.0 Hz.

V_{S30} (m/s)	Soil Depth (m)										
	0	5	10	15	20	25	30	50	100	500	1000
95.6	NA	NA	NA	NA	NA	NA	-3.5286	-4.7333	-6.6673	-15.4967	-22.7315
107.9	NA	NA	NA	NA	NA	-3.0322	-3.0575	-4.1522	-5.8602	-13.6366	-20.0148
121.8	NA	NA	NA	NA	-2.57683	-2.64531	-2.4025	-3.25823	-4.66151	-10.9124	-16.0399
137.4	NA	NA	NA	NA	-2.19404	-2.03849	-1.98052	-2.6691	-3.86899	-9.3228	-13.8483
155.1	NA	NA	NA	-1.88918	-1.68733	-1.65658	-1.5338	-2.22072	-3.43237	-9.61131	-14.9457
175	NA	NA	NA	-1.3875	-1.38865	-1.26646	-1.11819	-1.57183	-2.44173	-6.67949	-10.3015
197.5	NA	NA	-1.36304	-1.17769	-1.01155	-0.82095	-0.73793	-1.24865	-2.25817	-7.49411	-12.0653
222.9	NA	NA	-1.06052	-0.9251	-0.70246	-0.55057	-0.51529	-0.9377	-1.81406	-6.38228	-10.2934
251.5	NA	NA	-0.82601	-0.54544	-0.42217	-0.31736	-0.25988	-0.62163	-1.39461	-5.45672	-8.96822
283.9	NA	NA	-0.58187	-0.33656	-0.22448	-0.09624	-0.02384	-0.36251	-1.08707	-4.94455	-8.29738
320.4	NA	-0.31922	-0.37668	-0.16348	0.01481	0.1392	0.16627	-0.13576	-0.76645	-4.26241	-7.36001
361.5	NA	-0.18032	-0.12587	0.04191	0.24748	0.27736	0.24506	-0.00649	-0.55192	-3.5692	-6.23592
408	NA	0.0165	0.00437	0.30076	0.37398	0.31416	0.31112	0.13391	-0.28916	-2.59363	-4.67659
460.4	NA	0.07302	0.18198	0.44541	0.38899	0.31826	0.39662	0.16952	-0.15085	-1.96911	-3.67053
519.6	NA	0.25444	0.37552	0.45475	0.3794	0.44033	0.49403	0.3603	0.11632	-1.40261	-2.84232
586.4	NA	0.28989	0.52267	0.5233	0.35976	0.51266	0.55635	0.47206	0.28924	-0.90761	-2.07784
661.8	NA	0.44544	0.63829	0.23467	0.54035	0.66124	0.6985	0.53353	0.39546	-0.55751	-1.483
746.8	NA	0.51393	0.43885	0.70933	0.74198	0.47833	0.46399	0.55118	0.43819	-0.32225	-1.07862
842.8	NA	0.68771	0.3279	0.44431	0.63019	0.77868	0.73927	0.59807	0.50257	-0.13175	-0.76325
951.1	NA	0.50024	0.80907	0.77853	0.4693	0.42467	NA	NA	NA	NA	NA
1073.4	NA	0.45318	0.36362	0.68387	NA	NA	NA	NA	NA	NA	NA
1211.4	NA	0.93189	0.40526	NA	NA	NA	NA	NA	NA	NA	NA
1367.1	0.38344	0.71909	1.01227	NA	NA	NA	NA	NA	NA	NA	NA
1542.8	0.42875	0.18682	NA	NA	NA	NA	NA	NA	NA	NA	NA
1741.1	0.35851	0.13868	NA	NA	NA	NA	NA	NA	NA	NA	NA
1964.8	0.2918	NA	NA	NA	NA	NA	NA	NA	NA	NA	NA
2217.4	0.24854	NA	NA	NA	NA	NA	NA	NA	NA	NA	NA
2502.4	0.2335	NA	NA	NA	NA	NA	NA	NA	NA	NA	NA
2824	0.11848	NA	NA	NA	NA	NA	NA	NA	NA	NA	NA

Table A.114: FAS Linear Amp. Look-up Table for 54.999 Hz.

V_{S30} (m/s)	Soil Depth (m)										
	0	5	10	15	20	25	30	50	100	500	1000
95.6	NA	NA	NA	NA	NA	NA	-3.9972	-5.3654	-7.4804	-17.1742	-25.1195
107.9	NA	NA	NA	NA	NA	-3.4588	-3.521	-4.7093	-6.6132	-15.1765	-22.1795
121.8	NA	NA	NA	NA	-2.9203	-3.0431	-2.7850	-3.7777	-5.2894	-12.1650	-17.7970
137.4	NA	NA	NA	NA	-2.5884	-2.3917	-2.2623	-3.0333	-4.3672	-10.3737	-15.3528
155.1	NA	NA	NA	-2.17273	-1.9826	-1.93052	-1.83865	-2.5888	-3.93925	-10.7346	-16.5964
175	NA	NA	NA	-1.72698	-1.61895	-1.52286	-1.33902	-1.89292	-2.83221	-7.49748	-11.4793
197.5	NA	NA	-1.60862	-1.35391	-1.2523	-1.06176	-0.93462	-1.48751	-2.61157	-8.3677	-13.3896
222.9	NA	NA	-1.32	-1.08263	-0.89144	-0.70103	-0.64941	-1.1337	-2.0959	-7.12659	-11.4266
251.5	NA	NA	-0.99875	-0.7875	-0.55932	-0.46789	-0.43047	-0.82499	-1.6927	-6.17075	-10.0310
283.9	NA	NA	-0.73732	-0.43111	-0.3425	-0.23444	-0.16642	-0.54659	-1.34797	-5.59205	-9.27768
320.4	NA	-0.37458	-0.53078	-0.22947	-0.1273	0.00573	0.046	-0.28949	-0.98795	-4.83596	-8.23941
361.5	NA	-0.34978	-0.24725	-0.10699	0.10431	0.17738	0.22584	-0.06986	-0.67282	-3.99997	-6.93042
408	NA	-0.11948	-0.05165	0.14636	0.27921	0.32164	0.28071	0.08565	-0.37151	-2.91294	-5.20418
460.4	NA	-0.04795	0.06991	0.36036	0.40458	0.33013	0.33344	0.19763	-0.16275	-2.17011	-4.04658
519.6	NA	0.11229	0.26382	0.51466	0.39314	0.29428	0.39874	0.21148	-0.08284	-1.75543	-3.3407
586.4	NA	0.24514	0.45636	0.43724	0.31215	0.50536	0.55406	0.42355	0.22563	-1.10666	-2.39575
661.8	NA	0.35115	0.50397	0.42843	0.51636	0.6087	0.51885	0.48128	0.34812	-0.6923	-1.71008
746.8	NA	0.42841	0.63186	0.35424	0.50573	0.60819	0.63861	0.5092	0.41665	-0.43168	-1.26624
842.8	NA	0.48549	0.27078	0.65845	0.77204	0.6438	0.38815	0.50708	0.42834	-0.27119	-0.96466
951.1	NA	0.68904	0.58591	0.37984	0.41554	0.83089	NA	NA	NA	NA	NA
1073.4	NA	0.39275	0.69291	0.90842	NA	NA	NA	NA	NA	NA	NA
1211.4	NA	0.58063	0.25692	NA	NA	NA	NA	NA	NA	NA	NA
1367.1	0.30855	0.98972	0.47668	NA	NA	NA	NA	NA	NA	NA	NA
1542.8	0.33953	0.34862	NA	NA	NA	NA	NA	NA	NA	NA	NA
1741.1	0.30825	0.09905	NA	NA	NA	NA	NA	NA	NA	NA	NA
1964.8	0.30241	NA	NA	NA	NA	NA	NA	NA	NA	NA	NA
2217.4	0.25474	NA	NA	NA	NA	NA	NA	NA	NA	NA	NA
2502.4	0.22432	NA	NA	NA	NA	NA	NA	NA	NA	NA	NA
2824	0.12205	NA	NA	NA	NA	NA	NA	NA	NA	NA	NA

Table A.115: FAS Linear Amp. Look-up Table for 61.660 Hz.

V_{S30} (m/s)	Soil Depth (m)										
	0	5	10	15	20	25	30	50	100	500	1000
95.6	NA	NA	NA	NA	NA	NA	-4.6827	-6.2198	-8.6160	-19.4610	-28.3744
107.9	NA	NA	NA	NA	NA	-4.0786	-4.1167	-5.4843	-7.6137	-17.1906	-25.0318
121.8	NA	NA	NA	NA	-3.4773	-3.5882	-3.3086	-4.4010	-6.1334	-13.8596	-20.1588
137.4	NA	NA	NA	NA	-3.0279	-2.85375	-2.68843	-3.60218	-5.06723	-11.8101	-17.3873
155.1	NA	NA	NA	-2.60982	-2.44011	-2.31049	-2.17517	-3.00175	-4.56862	-12.1785	-18.7476
175	NA	NA	NA	-2.09066	-1.94021	-1.82701	-1.67415	-2.28926	-3.36716	-8.59971	-13.0599
197.5	NA	NA	-1.93022	-1.72515	-1.5265	-1.33074	-1.18708	-1.83247	-3.09742	-9.55192	-15.1739
222.9	NA	NA	-1.64219	-1.29746	-1.13135	-0.9542	-0.86915	-1.42521	-2.50865	-8.14574	-12.9642
251.5	NA	NA	-1.25769	-1.03532	-0.77212	-0.61911	-0.57659	-1.0525	-2.02618	-7.06004	-11.3880
283.9	NA	NA	-0.90666	-0.66533	-0.51558	-0.42106	-0.37313	-0.79461	-1.70514	-6.4691	-10.6007
320.4	NA	-0.58601	-0.70196	-0.35858	-0.27338	-0.16533	-0.11679	-0.48873	-1.2876	-5.60369	-9.41802
361.5	NA	-0.52448	-0.41717	-0.1845	-0.07033	0.03635	0.09512	-0.23309	-0.91738	-4.65573	-7.93806
408	NA	-0.29189	-0.18341	-0.0255	0.12863	0.21238	0.2385	0.00181	-0.50524	-3.36698	-5.93502
460.4	NA	-0.12619	0.01343	0.18898	0.29956	0.32289	0.31493	0.15999	-0.23908	-2.49037	-4.59374
519.6	NA	0.04644	0.1424	0.38291	0.40363	0.35988	0.31331	0.19258	-0.14281	-2.02606	-3.81065
586.4	NA	0.14884	0.33295	0.47464	0.39942	0.25052	0.4174	0.24167	-0.01211	-1.50073	-2.94588
661.8	NA	0.3145	0.51919	0.4488	0.23421	0.50275	0.58577	0.43979	0.27119	-0.8936	-2.03477
746.8	NA	0.38781	0.44288	0.35319	0.58773	0.58347	0.54108	0.48612	0.36736	-0.56953	-1.50493
842.8	NA	0.42858	0.60392	0.43898	0.47119	0.50115	0.69961	0.54628	0.413	-0.38378	-1.16472
951.1	NA	0.64224	0.25241	0.64143	0.7698	0.4307	NA	NA	NA	NA	NA
1073.4	NA	0.657	0.72625	0.45282	NA	NA	NA	NA	NA	NA	NA
1211.4	NA	0.33804	0.58899	NA	NA	NA	NA	NA	NA	NA	NA
1367.1	0.49631	0.85747	0.19049	NA	NA	NA	NA	NA	NA	NA	NA
1542.8	0.30272	0.77973	NA	NA	NA	NA	NA	NA	NA	NA	NA
1741.1	0.2627	0.17576	NA	NA	NA	NA	NA	NA	NA	NA	NA
1964.8	0.25167	NA	NA	NA	NA	NA	NA	NA	NA	NA	NA
2217.4	0.23759	NA	NA	NA	NA	NA	NA	NA	NA	NA	NA
2502.4	0.21065	NA	NA	NA	NA	NA	NA	NA	NA	NA	NA
2824	0.12418	NA	NA	NA	NA	NA	NA	NA	NA	NA	NA

Table A.116: FAS Linear Amp. Look-up Table for 70.796 Hz.

V_{S30} (m/s)	Soil Depth (m)										
	0	5	10	15	20	25	30	50	100	500	1000
95.6	NA	NA	NA	NA	NA	NA	-5.5258	-7.3547	-10.059	-22.5267	-32.7394
107.9	NA	NA	NA	NA	NA	-4.8395	-4.9022	-6.5302	-8.9573	-19.9537	-28.9393
121.8	NA	NA	NA	NA	-4.1322	-4.2928	-3.9967	-5.2892	-7.2758	-16.1226	-23.3436
137.4	NA	NA	NA	NA	-3.6787	-3.4726	-3.2781	-4.3253	-6.0332	-13.7875	-20.1758
155.1	NA	NA	NA	-3.1360	-2.9524	-2.8365	-2.6599	-3.6815	-5.4427	-14.1852	-21.7106
175	NA	NA	NA	-2.58931	-2.43326	-2.26975	-2.0682	-2.77326	-4.05135	-10.0600	-15.1770
197.5	NA	NA	-2.35494	-2.12073	-1.9115	-1.70949	-1.58144	-2.32572	-3.78098	-11.193	-17.6380
222.9	NA	NA	-2.01914	-1.70381	-1.48181	-1.28432	-1.18396	-1.81917	-3.07976	-9.55676	-15.0797
251.5	NA	NA	-1.60396	-1.28408	-1.05946	-0.90608	-0.80064	-1.35431	-2.48114	-8.25881	-13.2231
283.9	NA	NA	-1.22954	-0.95274	-0.76233	-0.58309	-0.56219	-1.06838	-2.11371	-7.59793	-12.3389
320.4	NA	-0.76277	-0.94587	-0.63127	-0.4525	-0.33254	-0.31272	-0.74404	-1.67172	-6.62779	-11.0067
361.5	NA	-0.7449	-0.61062	-0.30877	-0.20794	-0.15143	-0.09684	-0.47168	-1.27679	-5.56472	-9.33146
408	NA	-0.49082	-0.38018	-0.10791	-0.06863	0.04479	0.09223	-0.19252	-0.7754	-4.0702	-7.01418
460.4	NA	-0.33463	-0.11425	0.00196	0.12222	0.19219	0.24287	0.03278	-0.40965	-3.0057	-5.41831
519.6	NA	-0.10936	0.06736	0.21274	0.28001	0.32718	0.31206	0.15938	-0.21127	-2.37858	-4.42477
586.4	NA	0.03399	0.18898	0.3484	0.38935	0.3483	0.30438	0.19703	-0.09565	-1.81566	-3.48325
661.8	NA	0.217	0.33742	0.45691	0.40751	0.2422	0.39319	0.22101	-0.0053	-1.34737	-2.65852
746.8	NA	0.37465	0.46971	0.44673	0.23247	0.46348	0.56815	0.43168	0.29079	-0.79032	-1.86412
842.8	NA	0.4083	0.4175	0.32662	0.44243	0.59335	0.49923	0.5015	0.36375	-0.53735	-1.4334
951.1	NA	0.38032	0.53671	0.34915	0.4897	0.72654	NA	NA	NA	NA	NA
1073.4	NA	0.60961	0.18446	0.59836	NA	NA	NA	NA	NA	NA	NA
1211.4	NA	0.55315	0.69672	NA	NA	NA	NA	NA	NA	NA	NA
1367.1	0.28833	0.39809	0.56808	NA	NA	NA	NA	NA	NA	NA	NA
1542.8	0.38854	1.03949	NA	NA	NA	NA	NA	NA	NA	NA	NA
1741.1	0.27553	0.56613	NA	NA	NA	NA	NA	NA	NA	NA	NA
1964.8	0.23311	NA	NA	NA	NA	NA	NA	NA	NA	NA	NA
2217.4	0.1971	NA	NA	NA	NA	NA	NA	NA	NA	NA	NA
2502.4	0.18448	NA	NA	NA	NA	NA	NA	NA	NA	NA	NA
2824	0.12503	NA	NA	NA	NA	NA	NA	NA	NA	NA	NA

Table A.117: FAS Linear Amp. Look-up Table for 80.0 Hz.

V_{S30} (m/s)	Soil Depth (m)										
	0	5	10	15	20	25	30	50	100	500	1000
95.6	NA	NA	NA	NA	NA	NA	-6.4277	-8.5503	-11.5909	-25.6489	-37.1352
107.9	NA	NA	NA	NA	NA	-5.6450	-5.6986	-7.5728	-10.305	-22.7308	-32.8711
121.8	NA	NA	NA	NA	-4.8654	-5.0128	-4.6592	-6.1716	-8.401	-18.4045	-26.5553
137.4	NA	NA	NA	NA	-4.2974	-4.0667	-3.8715	-5.0842	-7.0201	-15.7661	-22.9784
155.1	NA	NA	NA	-3.6978	-3.5052	-3.3703	-3.1367	-4.2870	-6.2985	-16.1949	-24.6938
175	NA	NA	NA	-3.0447	-2.8877	-2.6803	-2.4942	-3.3243	-4.7481	-11.5509	-17.3293
197.5	NA	NA	-2.7886	-2.5632	-2.2843	-2.0626	-1.9012	-2.7445	-4.4116	-12.7902	-20.0673
222.9	NA	NA	-2.41628	-2.02559	-1.8133	-1.58199	-1.52964	-2.2403	-3.66071	-10.9863	-17.2209
251.5	NA	NA	-1.92913	-1.62759	-1.33063	-1.18749	-1.06061	-1.68953	-2.97847	-9.51101	-15.1135
283.9	NA	NA	-1.48733	-1.1504	-1.00871	-0.83093	-0.73386	-1.31364	-2.50714	-8.70564	-14.0582
320.4	NA	-1.09905	-1.16508	-0.83137	-0.65745	-0.49387	-0.49021	-0.99693	-2.0396	-7.65231	-12.5945
361.5	NA	-0.94368	-0.80817	-0.5389	-0.34637	-0.31641	-0.27233	-0.70311	-1.61966	-6.47196	-10.7312
408	NA	-0.66642	-0.53477	-0.2349	-0.17802	-0.11991	-0.05773	-0.3636	-1.04652	-4.77168	-8.09944
460.4	NA	-0.4981	-0.28541	-0.04508	-0.03506	0.0742	0.11875	-0.13719	-0.63025	-3.57452	-6.29832
519.6	NA	-0.22781	-0.03093	0.04547	0.14746	0.21329	0.24937	0.05059	-0.36104	-2.81857	-5.1292
586.4	NA	-0.08568	0.12489	0.2012	0.29099	0.32946	0.32731	0.19172	-0.13796	-2.08529	-3.96704
661.8	NA	0.12686	0.22604	0.35378	0.40241	0.37854	0.30815	0.22698	-0.02523	-1.54976	-3.03873
746.8	NA	0.27593	0.32983	0.46208	0.42261	0.25185	0.36753	0.22495	0.0284	-1.19352	-2.40932
842.8	NA	0.38319	0.47167	0.46817	0.26198	0.51047	0.49857	0.39846	0.26949	-0.75345	-1.76592
951.1	NA	0.4485	0.45471	0.28988	0.51547	0.44353	NA	NA	NA	NA	NA
1073.4	NA	0.29502	0.46977	0.47085	NA	NA	NA	NA	NA	NA	NA
1211.4	NA	0.64674	0.17702	NA	NA	NA	NA	NA	NA	NA	NA
1367.1	0.43724	0.32766	0.83513	NA	NA	NA	NA	NA	NA	NA	NA
1542.8	0.26308	0.51796	NA	NA	NA	NA	NA	NA	NA	NA	NA
1741.1	0.28277	1.06697	NA	NA	NA	NA	NA	NA	NA	NA	NA
1964.8	0.26229	NA	NA	NA	NA	NA	NA	NA	NA	NA	NA
2217.4	0.21096	NA	NA	NA	NA	NA	NA	NA	NA	NA	NA
2502.4	0.1627	NA	NA	NA	NA	NA	NA	NA	NA	NA	NA
2824	0.12569	NA	NA	NA	NA	NA	NA	NA	NA	NA	NA

Table A.118: FAS Linear Amp. Look-up Table for 85.114 Hz.

V_{S30} (m/s)	Soil Depth (m)										
	0	5	10	15	20	25	30	50	100	500	1000
95.6	NA	NA	NA	NA	NA	NA	-6.9115	-9.2093	-12.4304	-27.3964	-39.6149
107.9	NA	NA	NA	NA	NA	-6.0904	-6.1594	-8.1762	-11.0725	-24.2668	-35.045
121.8	NA	NA	NA	NA	-5.2481	-5.4181	-5.0300	-6.6563	-9.01831	-19.669	-28.3334
137.4	NA	NA	NA	NA	-4.6642	-4.4041	-4.1864	-5.4980	-7.55736	-16.8626	-24.5333
155.1	NA	NA	NA	-4.0263	-3.7873	-3.6528	-3.4144	-4.6528	-6.78279	-17.3021	-26.3327
175	NA	NA	NA	-3.3130	-3.1526	-2.9171	-2.7248	-3.6042	-5.13535	-12.3823	-18.5264
197.5	NA	NA	-3.0586	-2.7814	-2.4882	-2.272	-2.0993	-3.0126	-4.77567	-13.6907	-21.4257
222.9	NA	NA	-2.6257	-2.2416	-1.9962	-1.7410	-1.6830	-2.4417	-3.96389	-11.7595	-18.3903
251.5	NA	NA	-2.1092	-1.7770	-1.4929	-1.3406	-1.2280	-1.8955	-3.25861	-10.2162	-16.1753
283.9	NA	NA	-1.6519	-1.3172	-1.1239	-0.9564	-0.8522	-1.4698	-2.74833	-9.34086	-15.0330
320.4	NA	-1.2453	-1.2983	-0.9213	-0.7793	-0.6108	-0.5763	-1.1206	-2.23416	-8.2119	-13.4694
361.5	NA	-1.0949	-0.9246	-0.6534	-0.4417	-0.3859	-0.3447	-0.8087	-1.78108	-6.95048	-11.4804
408	NA	-0.7739	-0.6215	-0.3394	-0.2261	-0.183	-0.1459	-0.4718	-1.20434	-5.16758	-8.71006
460.4	NA	-0.5840	-0.3577	-0.1113	-0.0968	-0.0067	0.05944	-0.2080	-0.74589	-3.87911	-6.77824
519.6	NA	-0.3052	-0.1152	0.034	0.06802	0.16275	0.19483	-0.0255	-0.45596	-3.0775	-5.53519
586.4	NA	-0.1415	0.09803	0.11244	0.2277	0.28311	0.29489	0.14105	-0.21055	-2.28623	-4.28751
661.8	NA	0.06977	0.18134	0.31032	0.34472	0.34741	0.35233	0.25936	-0.01418	-1.63636	-3.21899
746.8	NA	0.22911	0.29867	0.40597	0.40281	0.38096	0.31263	0.1877	-0.0337	-1.3354	-2.63227
842.8	NA	0.40119	0.3738	0.41674	0.44496	0.26878	0.38353	0.26402	0.10102	-0.98416	-2.05966
951.1	NA	0.47355	0.4291	0.52365	0.23004	0.53278	NA	NA	NA	NA	NA
1073.4	NA	0.36283	0.59236	0.16849	NA	NA	NA	NA	NA	NA	NA
1211.4	NA	0.49172	0.18238	NA	NA	NA	NA	NA	NA	NA	NA
1367.1	0.33907	0.4655	0.41734	NA	NA	NA	NA	NA	NA	NA	NA
1542.8	0.33103	0.28229	NA	NA	NA	NA	NA	NA	NA	NA	NA
1741.1	0.22692	1.0203	NA	NA	NA	NA	NA	NA	NA	NA	NA
1964.8	0.27045	NA	NA	NA	NA	NA	NA	NA	NA	NA	NA
2217.4	0.21272	NA	NA	NA	NA	NA	NA	NA	NA	NA	NA
2502.4	0.15786	NA	NA	NA	NA	NA	NA	NA	NA	NA	NA
2824	0.12617	NA	NA	NA	NA	NA	NA	NA	NA	NA	NA

Table A.119: FAS Linear Amp. Look-up Table for 90.0 Hz.

V_{S30} (m/s)	Soil Depth (m)										
	0	5	10	15	20	25	30	50	100	500	1000
95.6	NA	NA	NA	NA	NA	NA	-7.3304	-9.7892	-13.1748	-29.0159	-41.9092
107.9	NA	NA	NA	NA	NA	-6.4596	-6.5942	-8.7469	-11.8040	-25.7472	-37.1330
121.8	NA	NA	NA	NA	-5.5737	-5.8164	-5.3919	-7.1235	-9.62144	-20.881	-30.0338
137.4	NA	NA	NA	NA	-5.0073	-4.7267	-4.4859	-5.9019	-8.05892	-17.9038	-26.0070
155.1	NA	NA	NA	-4.3231	-4.0707	-3.9228	-3.6834	-5.0039	-7.25811	-18.3703	-27.9162
175	NA	NA	NA	-3.5553	-3.3952	-3.1571	-2.9452	-3.8788	-5.50412	-13.1686	-19.6578
197.5	NA	NA	-3.2780	-3.0039	-2.6991	-2.4715	-2.3000	-3.2731	-5.13211	-14.5578	-22.7313
222.9	NA	NA	-2.8247	-2.4213	-2.1695	-1.9123	-1.8330	-2.6432	-4.25622	-12.4976	-19.5067
251.5	NA	NA	-2.2832	-1.9256	-1.6552	-1.4717	-1.3616	-2.0708	-3.5089	-10.8706	-17.1697
283.9	NA	NA	-1.8068	-1.4722	-1.2486	-1.0701	-0.9831	-1.6398	-2.98849	-9.9586	-15.9721
320.4	NA	-1.3020	-1.4259	-1.0369	-0.8688	-0.7269	-0.6615	-1.2334	-2.41774	-8.73696	-14.2933
361.5	NA	-1.2232	-1.0301	-0.7291	-0.5533	-0.4566	-0.3974	-0.9004	-1.92489	-7.39854	-12.1863
408	NA	-0.8625	-0.7174	-0.4379	-0.2962	-0.2358	-0.2176	-0.5688	-1.34099	-5.53359	-9.28072
460.4	NA	-0.6781	-0.4160	-0.1808	-0.1302	-0.0708	-0.0084	-0.2727	-0.85343	-4.16797	-7.23293
519.6	NA	-0.3872	-0.1913	0.02695	0.00026	0.11628	0.15018	-0.0895	-0.55066	-3.32365	-5.92228
586.4	NA	-0.2073	0.03813	0.04979	0.18975	0.24297	0.25427	0.07601	-0.27661	-2.47569	-4.59104
661.8	NA	0.00735	0.18777	0.23896	0.30731	0.33681	0.33999	0.23204	-0.05663	-1.77285	-3.44562
746.8	NA	0.21037	0.20888	0.37862	0.4153	0.36182	0.29771	0.23869	0.01077	-1.3696	-2.74179
842.8	NA	0.32112	0.33393	0.44041	0.38933	0.17824	0.3459	0.1681	-0.02799	-1.18278	-2.32524
951.1	NA	0.45075	0.45762	0.46597	0.18728	0.3906	NA	NA	NA	NA	NA
1073.4	NA	0.49241	0.51844	0.17376	NA	NA	NA	NA	NA	NA	NA
1211.4	NA	0.33761	0.39594	NA	NA	NA	NA	NA	NA	NA	NA
1367.1	0.27198	0.59888	0.108	NA	NA	NA	NA	NA	NA	NA	NA
1542.8	0.32869	0.17839	NA	NA	NA	NA	NA	NA	NA	NA	NA
1741.1	0.23668	0.77124	NA	NA	NA	NA	NA	NA	NA	NA	NA
1964.8	0.23785	NA	NA	NA	NA	NA	NA	NA	NA	NA	NA
2217.4	0.21423	NA	NA	NA	NA	NA	NA	NA	NA	NA	NA
2502.4	0.15809	NA	NA	NA	NA	NA	NA	NA	NA	NA	NA
2824	0.12665	NA	NA	NA	NA	NA	NA	NA	NA	NA	NA

Table A.120: FAS Linear Amp. Look-up Table for 95.0 Hz.

V_{S30} (m/s)	Soil Depth (m)										
	0	5	10	15	20	25	30	50	100	500	1000
95.6	NA	NA	NA	NA	NA	NA	-7.7940	-10.388	-13.9492	-30.6379	-44.2326
107.9	NA	NA	NA	NA	NA	-6.8614	-6.9818	-9.2881	-12.4881	-27.1989	-39.2136
121.8	NA	NA	NA	NA	-5.9249	-6.1652	-5.7531	-7.6042	-10.2236	-22.0841	-31.7310
137.4	NA	NA	NA	NA	-5.3123	-5.0431	-4.7932	-6.3004	-8.56551	-18.9474	-27.4867
155.1	NA	NA	NA	-4.5869	-4.3620	-4.2061	-3.9465	-5.3502	-7.73127	-19.4371	-29.5047
175	NA	NA	NA	-3.8072	-3.6349	-3.3940	-3.1651	-4.1623	-5.86888	-13.9483	-20.7863
197.5	NA	NA	-3.4780	-3.2306	-2.9102	-2.6727	-2.4933	-3.5163	-5.48387	-15.4217	-24.0403
222.9	NA	NA	-3.0239	-2.6142	-2.3441	-2.0859	-1.9897	-2.8600	-4.55212	-13.2414	-20.6258
251.5	NA	NA	-2.4574	-2.0936	-1.8007	-1.5934	-1.4811	-2.2296	-3.75277	-11.5118	-18.1514
283.9	NA	NA	-1.9581	-1.5967	-1.3803	-1.1917	-1.1177	-1.8101	-3.22691	-10.5779	-16.9151
320.4	NA	-1.4407	-1.5507	-1.1691	-0.9559	-0.8301	-0.7531	-1.3517	-2.60518	-9.26327	-15.1202
361.5	NA	-1.3039	-1.1332	-0.7982	-0.6518	-0.5394	-0.4516	-0.9848	-2.06826	-7.84014	-12.8847
408	NA	-0.9705	-0.8113	-0.5193	-0.3779	-0.2896	-0.2651	-0.6482	-1.45912	-5.881	-9.83138
460.4	NA	-0.7656	-0.4786	-0.2651	-0.1576	-0.1251	-0.0757	-0.3471	-0.96935	-4.46105	-7.69204
519.6	NA	-0.4543	-0.2496	-0.0171	-0.0503	0.06807	0.09668	-0.1439	-0.64094	-3.56333	-6.30158
586.4	NA	-0.2721	-0.0216	0.04727	0.13799	0.19828	0.22249	0.01871	-0.34277	-2.66378	-4.89279
661.8	NA	-0.0327	0.16763	0.17351	0.26744	0.30045	0.31874	0.18544	-0.11243	-1.92437	-3.68694
746.8	NA	0.15086	0.18108	0.35084	0.37002	0.35896	0.35322	0.26954	0.04022	-1.41374	-2.85827
842.8	NA	0.23603	0.33361	0.42852	0.38694	0.35639	0.25793	0.19456	-0.00736	-1.23176	-2.43913
951.1	NA	0.42246	0.43984	0.35573	0.34567	0.08277	NA	NA	NA	NA	NA
1073.4	NA	0.54422	0.4054	0.38481	NA	NA	NA	NA	NA	NA	NA
1211.4	NA	0.30186	0.55856	NA	NA	NA	NA	NA	NA	NA	NA
1367.1	0.34791	0.65175	0.0297	NA	NA	NA	NA	NA	NA	NA	NA
1542.8	0.27032	0.18561	NA	NA	NA	NA	NA	NA	NA	NA	NA
1741.1	0.25209	0.48736	NA	NA	NA	NA	NA	NA	NA	NA	NA
1964.8	0.21002	NA	NA	NA	NA	NA	NA	NA	NA	NA	NA
2217.4	0.2086	NA	NA	NA	NA	NA	NA	NA	NA	NA	NA
2502.4	0.16223	NA	NA	NA	NA	NA	NA	NA	NA	NA	NA
2824	0.12705	NA	NA	NA	NA	NA	NA	NA	NA	NA	NA

Table A.121: FAS Linear Amp. Look-up Table for 100.0 Hz.

V_{S30} (m/s)	Soil Depth (m)										
	0	5	10	15	20	25	30	50	100	500	1000
95.6	NA	NA	NA	NA	NA	NA	-8.1357	-10.859	-14.5698	-31.9951	-46.2531
107.9	NA	NA	NA	NA	NA	-7.1564	-7.2444	-9.6532	-12.9712	-28.3139	-40.9391
121.8	NA	NA	NA	NA	-6.1901	-6.3982	-6.0160	-7.9512	-10.6710	-23.0430	-33.1327
137.4	NA	NA	NA	NA	-5.5160	-5.2748	-5.0134	-6.5829	-8.93493	-19.7571	-28.6857
155.1	NA	NA	NA	-4.7677	-4.5642	-4.4077	-4.1282	-5.6023	-8.07195	-20.2687	-30.7953
175	NA	NA	NA	-4.0100	-3.8118	-3.5585	-3.3154	-4.3561	-6.12606	-14.5368	-21.6657
197.5	NA	NA	-3.6198	-3.3809	-3.0635	-2.8069	-2.6205	-3.6772	-5.72591	-16.0721	-25.0678
222.9	NA	NA	-3.1647	-2.7643	-2.4649	-2.1953	-2.0984	-3.0135	-4.76375	-13.8020	-21.5015
251.5	NA	NA	-2.5811	-2.2091	-1.8900	-1.6837	-1.5659	-2.3373	-3.92348	-11.9816	-18.9040
283.9	NA	NA	-2.0674	-1.6703	-1.4772	-1.2724	-1.2045	-1.9198	-3.3868	-11.0263	-17.6307
320.4	NA	-1.5455	-1.6351	-1.2558	-1.0256	-0.8886	-0.8160	-1.4377	-2.7362	-9.6456	-15.7460
361.5	NA	-1.3540	-1.1994	-0.8505	-0.7010	-0.5990	-0.4980	-1.0474	-2.1728	-8.15967	-13.4048
408	NA	-1.0568	-0.8766	-0.5661	-0.4359	-0.3320	-0.2920	-0.6979	-1.53484	-6.12112	-10.2217
460.4	NA	-0.8281	-0.5309	-0.3236	-0.1899	-0.1497	-0.1300	-0.4055	-1.05159	-4.67227	-8.02713
519.6	NA	-0.5025	-0.2853	-0.0524	-0.0746	0.02637	0.05817	-0.1804	-0.70118	-3.73029	-6.5709
586.4	NA	-0.3118	-0.0596	0.05319	0.10153	0.181	0.21619	-0.0057	-0.38715	-2.79343	-5.10407
661.8	NA	-0.0546	0.13041	0.12144	0.23315	0.27186	0.29687	0.14981	-0.14829	-2.02583	-3.85238
746.8	NA	0.0902	0.194	0.31286	0.33345	0.36528	0.38175	0.27856	0.02973	-1.47059	-2.96777
842.8	NA	0.21222	0.29433	0.40088	0.44262	0.45386	0.23774	0.22283	0.03444	-1.2235	-2.47173
951.1	NA	0.3992	0.40461	0.36588	0.4459	0.08426	NA	NA	NA	NA	NA
1073.4	NA	0.51677	0.35447	0.51544	NA	NA	NA	NA	NA	NA	NA
1211.4	NA	0.32595	0.56204	NA	NA	NA	NA	NA	NA	NA	NA
1367.1	0.39819	0.62385	0.07461	NA	NA	NA	NA	NA	NA	NA	NA
1542.8	0.2399	0.23727	NA	NA	NA	NA	NA	NA	NA	NA	NA
1741.1	0.238	0.31696	NA	NA	NA	NA	NA	NA	NA	NA	NA
1964.8	0.20305	NA	NA	NA	NA	NA	NA	NA	NA	NA	NA
2217.4	0.19862	NA	NA	NA	NA	NA	NA	NA	NA	NA	NA
2502.4	0.16623	NA	NA	NA	NA	NA	NA	NA	NA	NA	NA
2824	0.12714	NA	NA	NA	NA	NA	NA	NA	NA	NA	NA

APPENDIX B RS Amplification Model Residuals

Model residuals are provided for 5 linear amplification models and L2 nonlinear amplification models. The linear amplification (L models) model residuals are calculated as the difference between the ln(amp) of the LE simulations and the regressed ln(amp) as computed by the amplification model. The nonlinear amplification model residuals (L+N and K models) are calculated as the difference between the ln(amp) of the NL simulations and the regressed ln(amp) as computed by the amplification model. Model residuals are presented the linear models as a function of V_{S30}, soil depth, the ratio of oscillator period to site natural period (T_{OSC}/T_{nat}) as described in Table B.1. Model residuals for the N models are provided as a function rock outcrop PGA, and for the K models as a function of V_{S30}, soil depth, T_{OSC}/T_{nat}, and PGA as described in Table B.2. Error bars show +/- 1 log standard deviation in the residual.

Table B.1: Figures of residuals for linear amplification models.

Model	Residual	Figure
L1	V_{S30}	Figure B.1
	Z	Figure B.2
	T_{OSC}/T_{nat}	Figure B.3: Amplification model residuals as a function of T_{nat} for periods 0.001 s (a), 0.01 s (b), 0.1 s(c), 0.2 s (d), 0.6 s (e), 1.0 s (f), 10.0 s (g).
L2	V_{S30}	Figure B.4
	Z	Figure B.5
	T_{OSC}/T_{nat}	Figure B.6
L3	V_{S30}	Figure B.7
	Z	Figure B.8
	T_{OSC}/T_{nat}	Figure B.9
L4	V_{S30}	Figure B.10
	Z	Figure B.11
	T_{OSC}/T_{nat}	Figure B.12
L5	V_{S30}	Figure B.13
	Z	Figure B.14
	T_{OSC}/T_{nat}	Figure B.15

Table B.2: Figures of residuals for nonlinear amplification models.

Model	Residual	Figure
N1	V_{S30}	Figure B.16
	SA	Figure B.17
K1	V_{S30}	Figure B.20
	Z	Figure B.21
	T_{OSC}/T_{nat}	Figure B.22
	SA	Figure B.23

Model	Residual	Figure
N2	V_{S30}	Figure B.18
	PGA	Figure B.19
K2	V_{S30}	Figure B.24
	Z	Figure B.25
	T_{OSC}/T_{nat}	Figure B.26
	PGA	Figure B.27

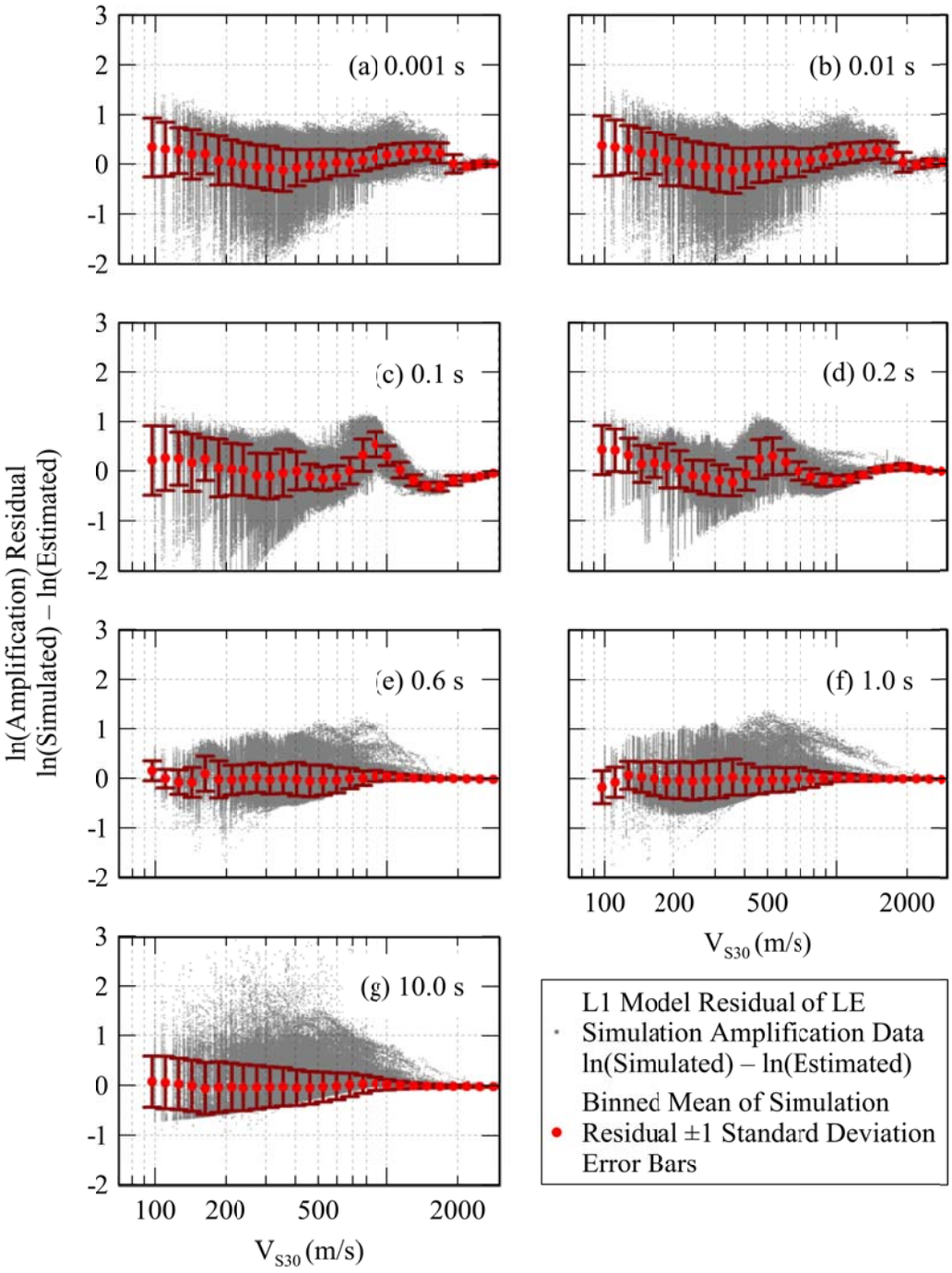

Figure B.1: L1 Amplification model residuals as a function of V_{S30} for periods 0.001 s (a), 0.01 s (b), 0.1 s(c), 0.2 s (d), 0.6 s (e), 1.0 s (f), 10.0 s (g).

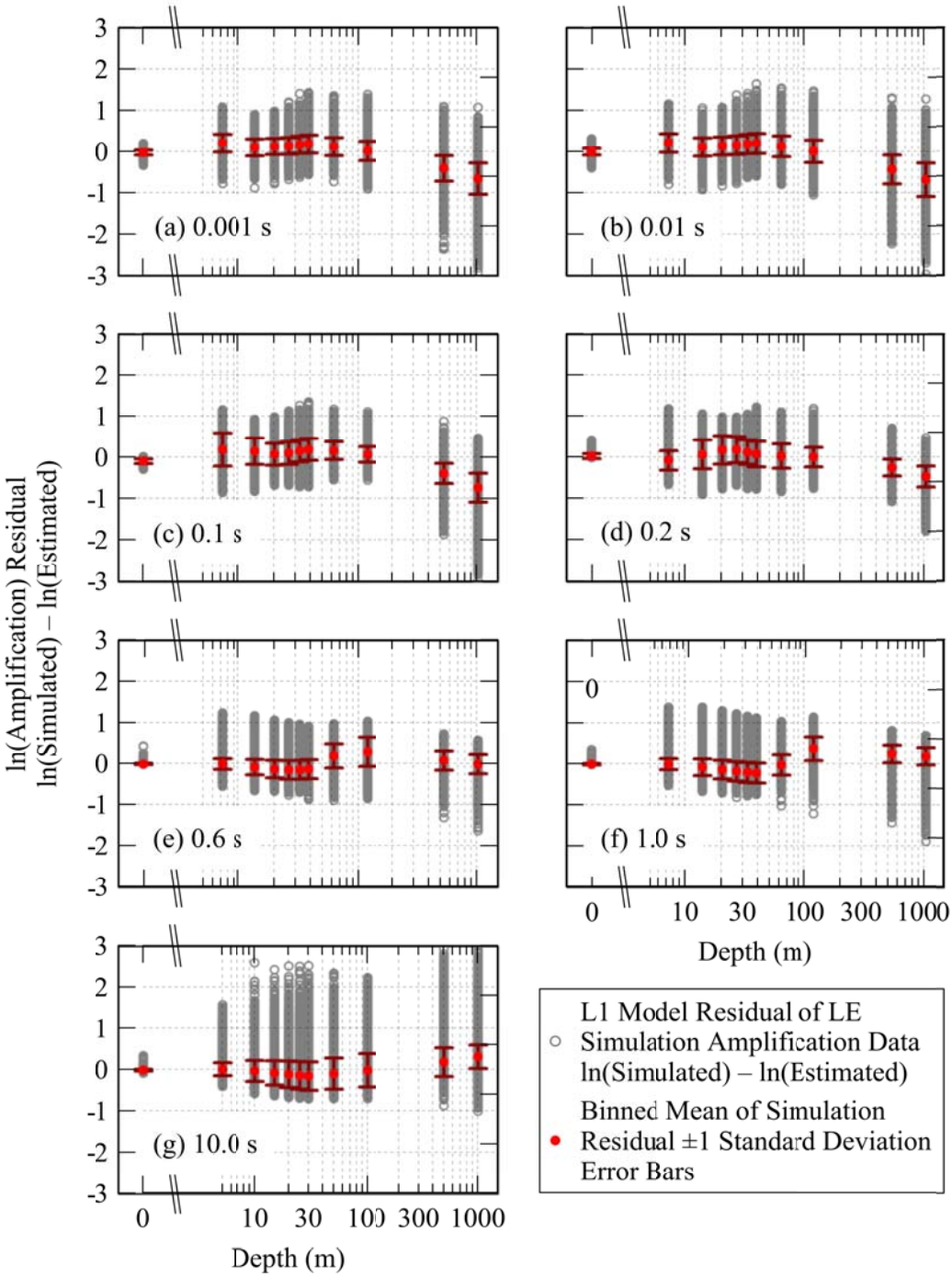

Figure B.2: L1 Amplification model residuals as a function of Z for periods 0.001 s (a), 0.01 s (b), 0.1 s(c), 0.2 s (d), 0.6 s (e), 1.0 s (f), 10.0 s (g).

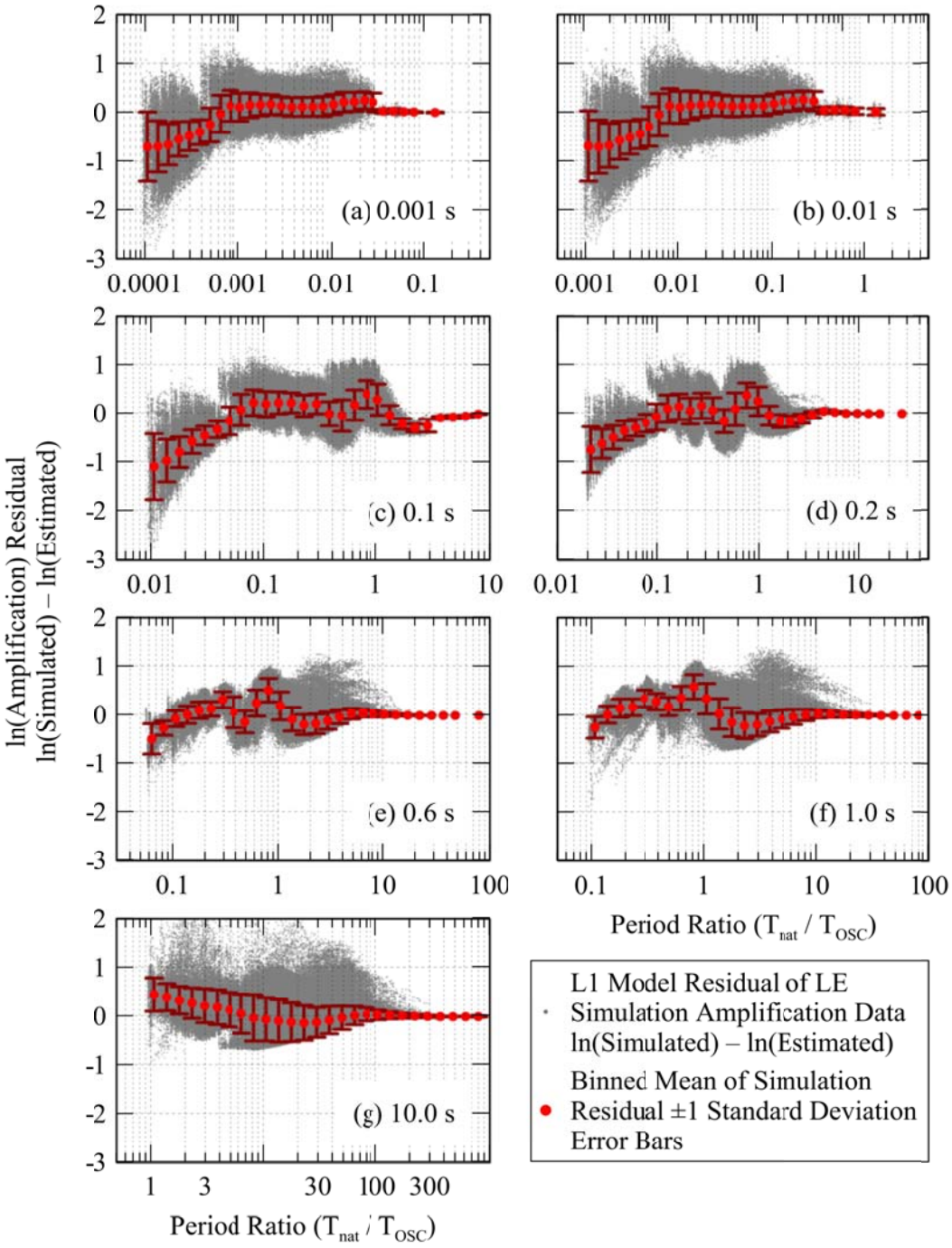

Figure B.3: Amplification model residuals as a function of T_{nat} for periods 0.001 s (a), 0.01 s (b), 0.1 s(c), 0.2 s (d), 0.6 s (e), 1.0 s (f), 10.0 s (g).

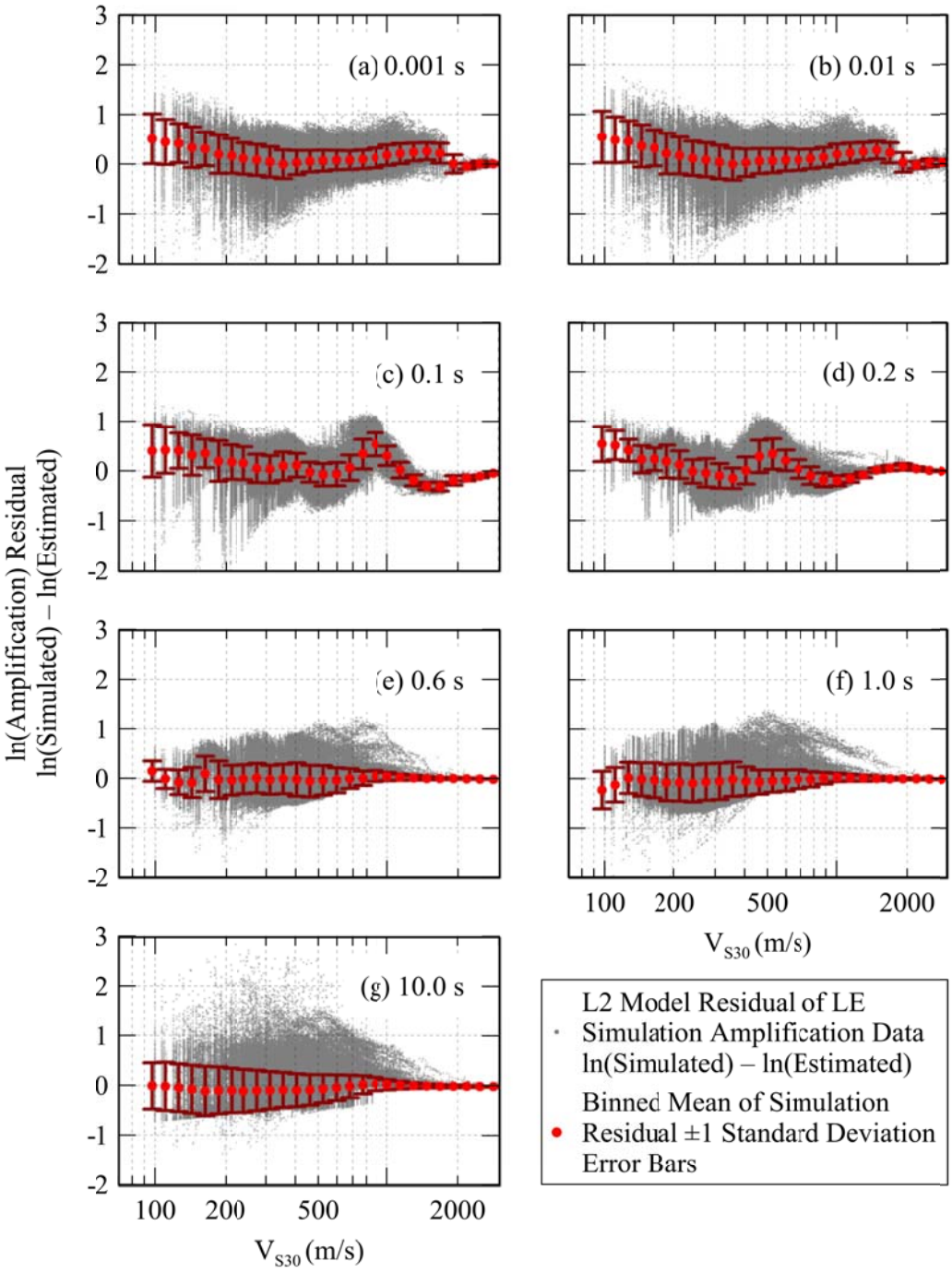

Figure B.4: L2 Amplification model residuals as a function of V_{S30} for periods 0.001 s, 0.01 s, 0.1 s, 0.2 s, 0.3 s, 0.6 s, 1.0 s, and 10.0 s

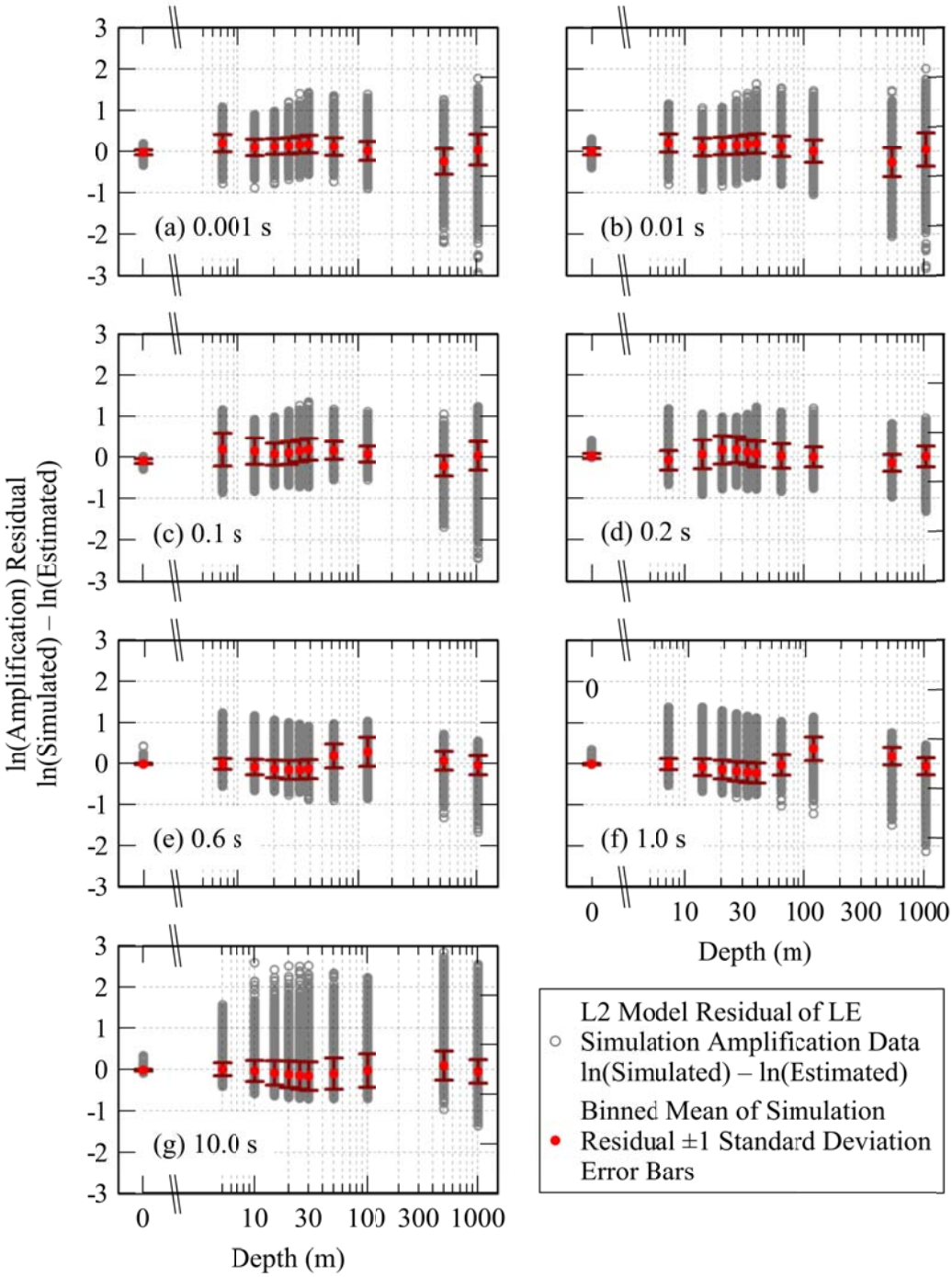

Figure B.5: L2 Amplification model residuals as a function of Z for periods 0.001 s (a), 0.01 s (b), 0.1 s(c), 0.2 s (d), 0.6 s (e), 1.0 s (f), 10.0 s (g).

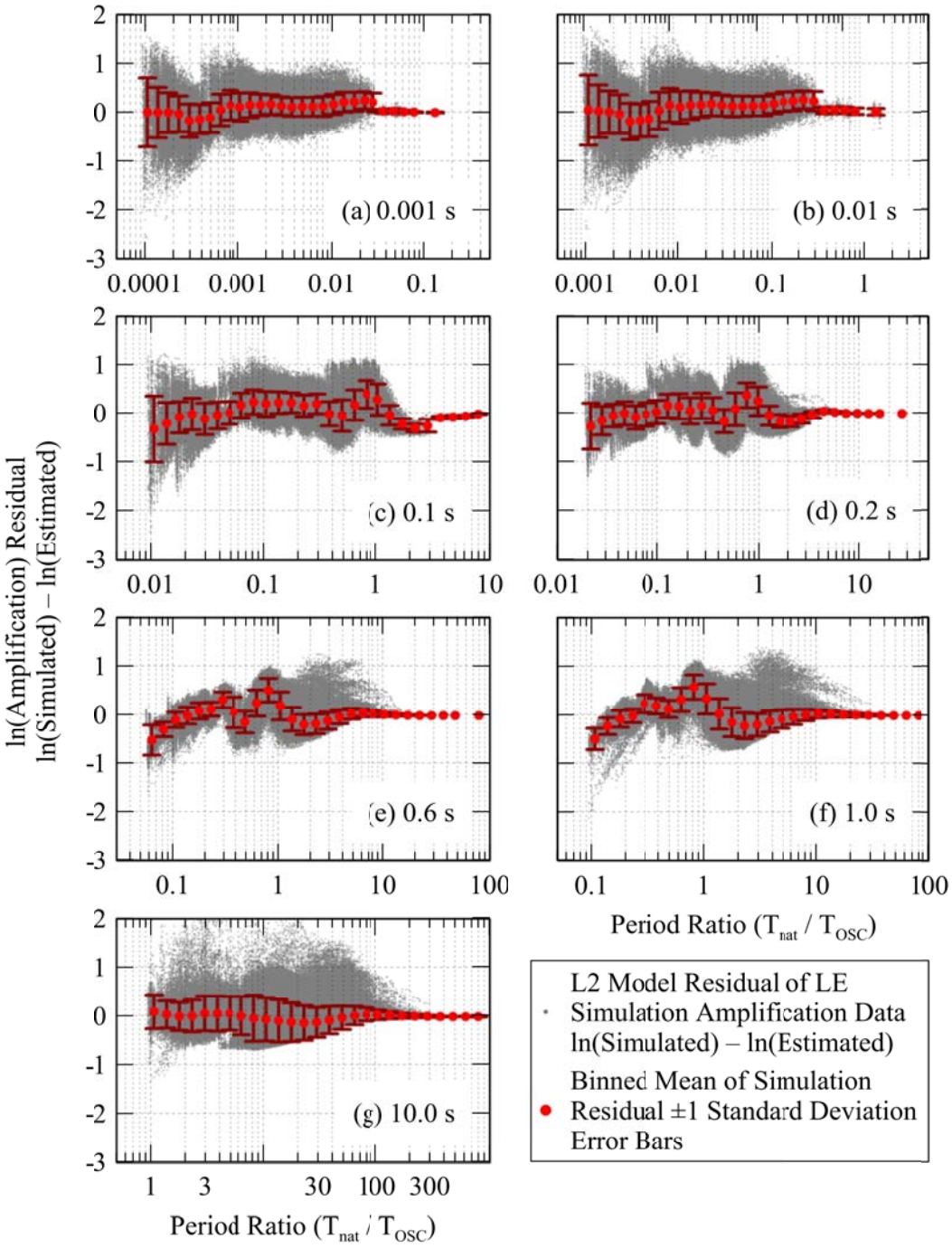

Figure B.6: L2 Amplification model residuals as a function of T_{nat} for periods 0.001 s (a), 0.01 s (b), 0.1 s(c), 0.2 s (d), 0.6 s (e), 1.0 s (f), 10.0 s (g).

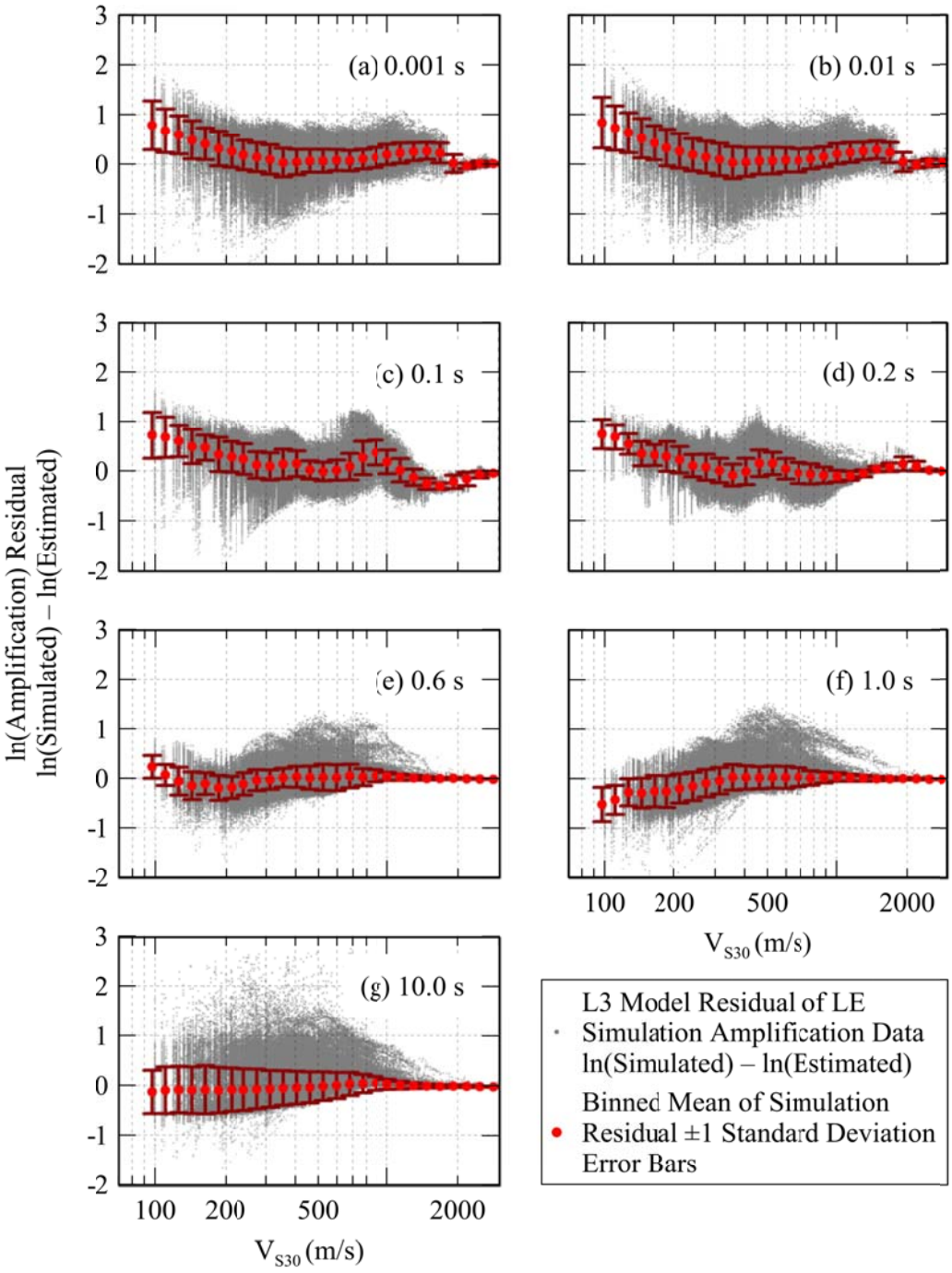

Figure B.7: L3 Amplification model residuals as a function of V_{S30} for periods 0.001 s (a), 0.01 s (b), 0.1 s(c), 0.2 s (d), 0.6 s (e), 1.0 s (f), 10.0 s (g).

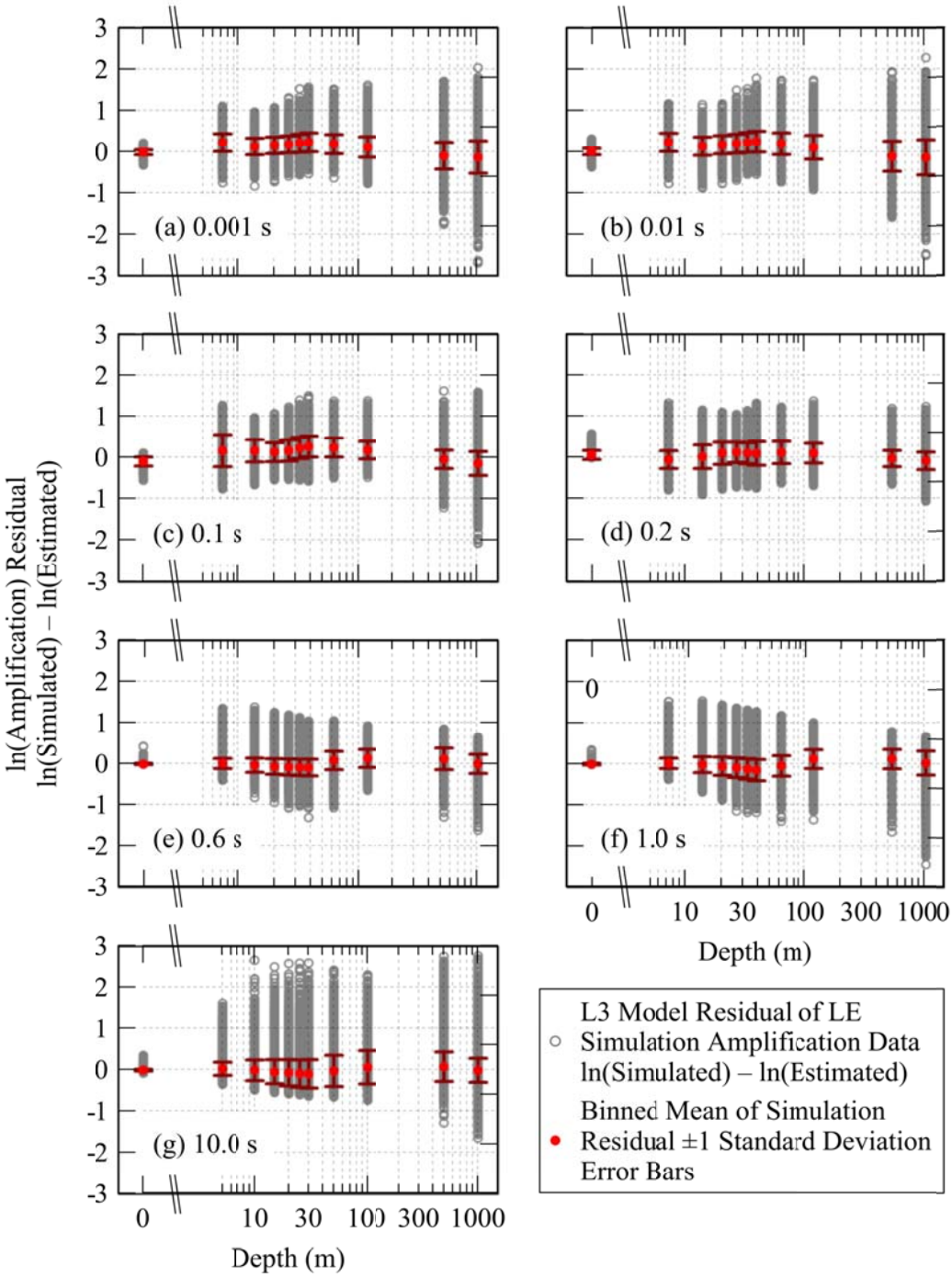

Figure B.8: L3 Amplification model residuals as a function of Z for periods 0.001 s (a), 0.01 s (b), 0.1 s(c), 0.2 s (d), 0.6 s (e), 1.0 s (f), 10.0 s (g).

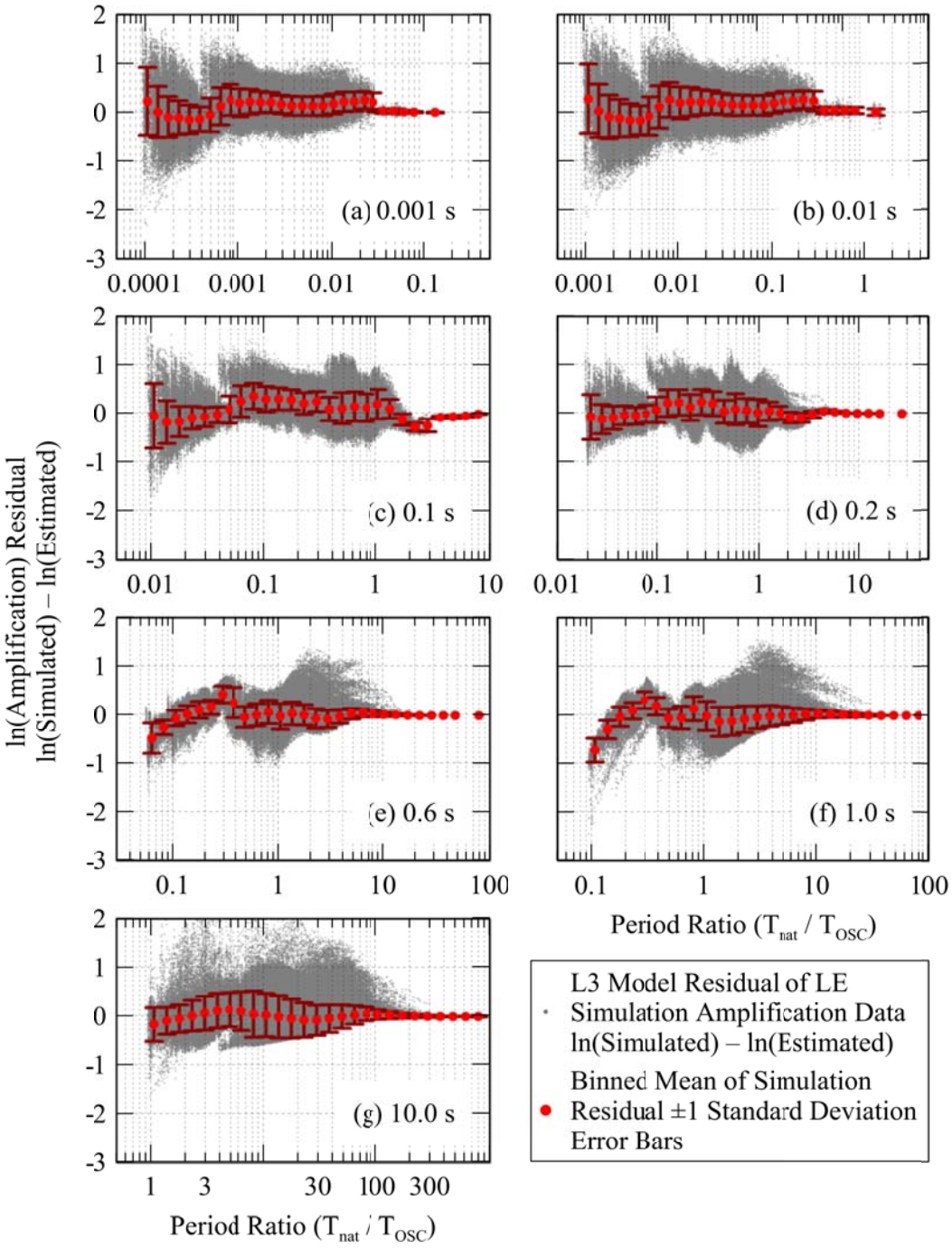

Figure B.9: L3 Amplification model residuals as a function of T_{nat} for periods 0.001 s (a), 0.01 s (b), 0.1 s(c), 0.2 s (d), 0.6 s (e), 1.0 s (f), 10.0 s (g).

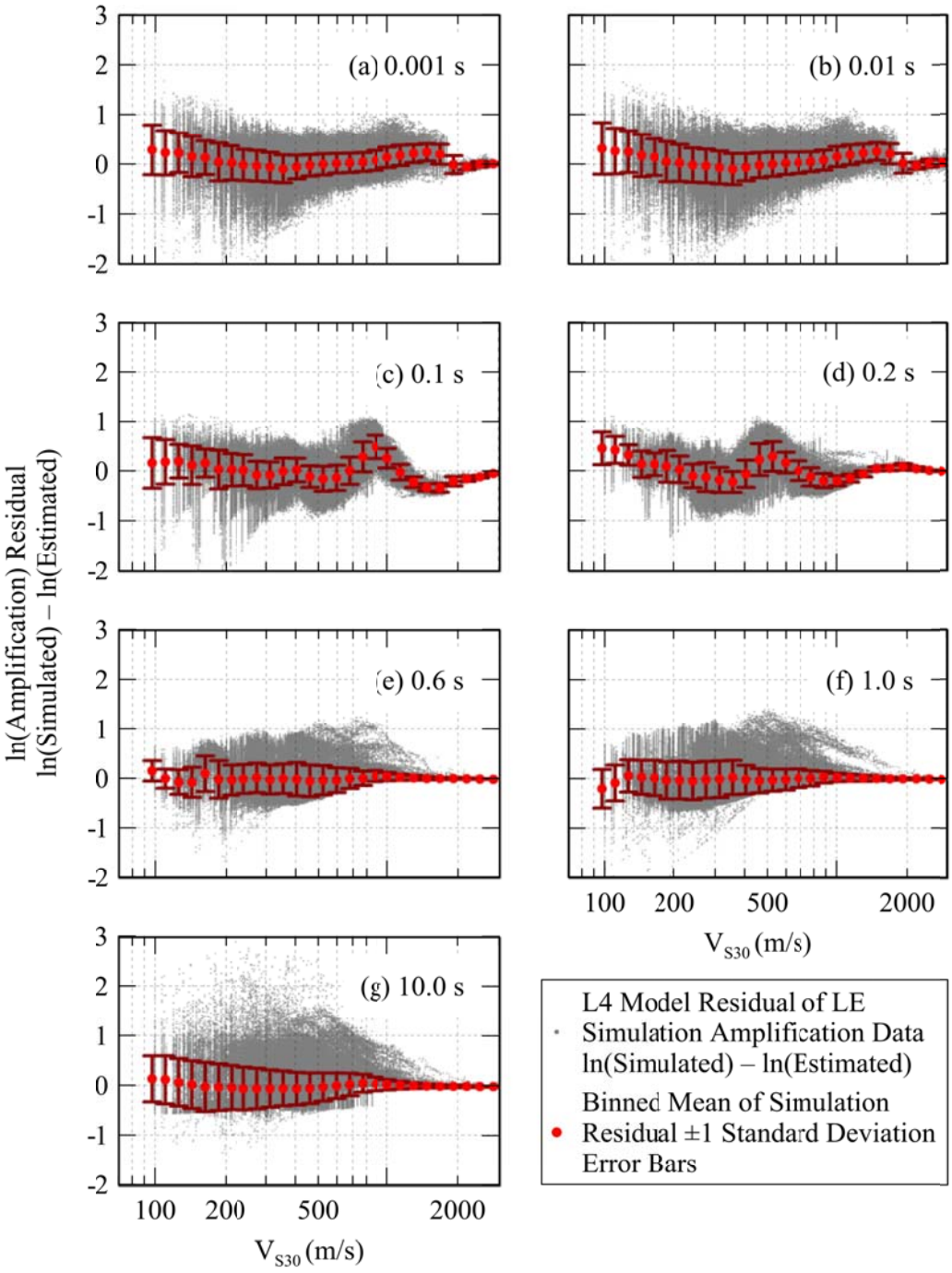

Figure B.10: L4 Amplification model residuals as a function of V_{S30} for periods 0.001 s (a), 0.01 s (b), 0.1 s(c), 0.2 s (d), 0.6 s (e), 1.0 s (f), 10.0 s (g).

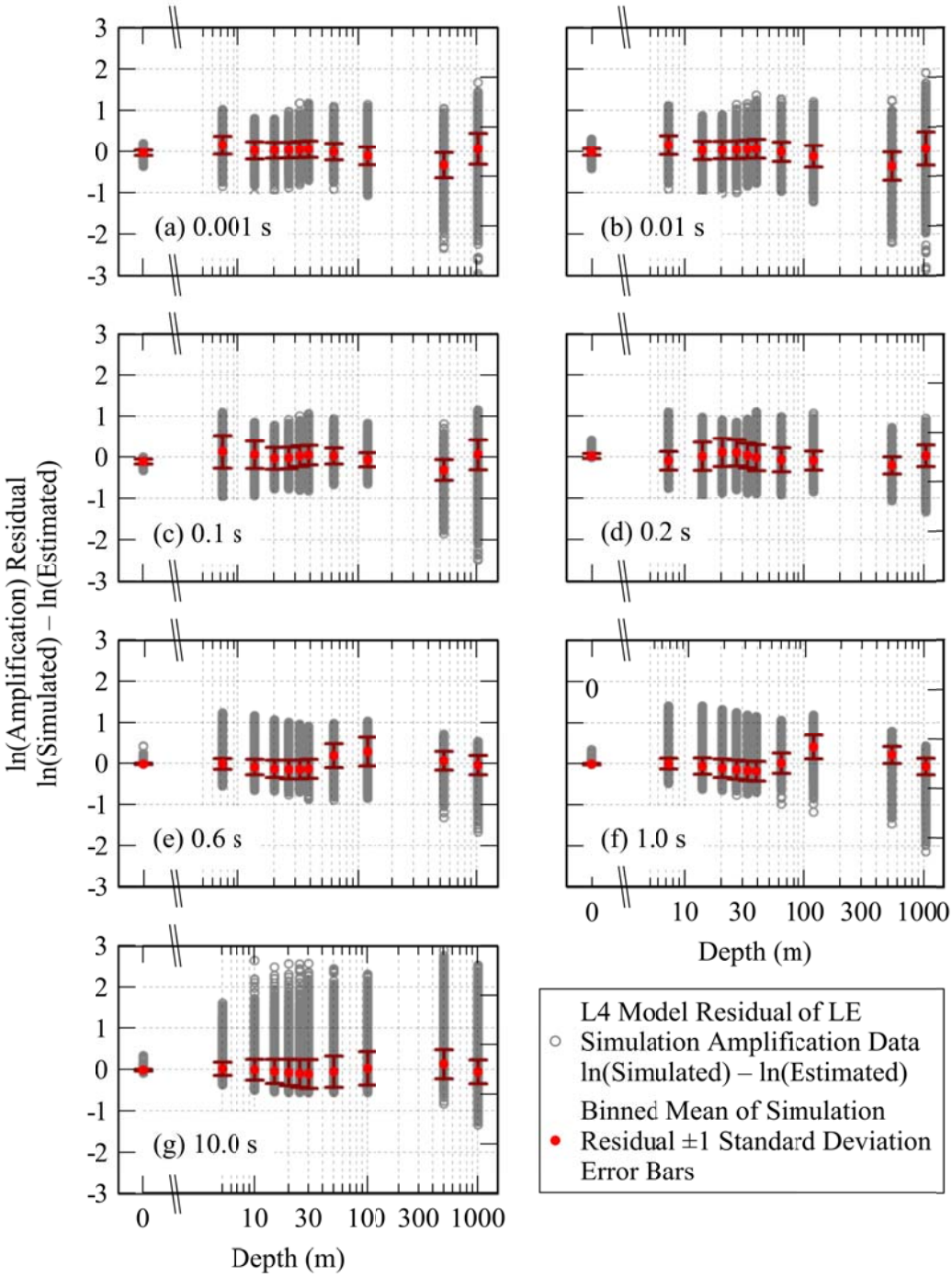

Figure B.11: L4 Amplification model residuals as a function of Z for periods 0.001 s (a), 0.01 s (b), 0.1 s(c), 0.2 s (d), 0.6 s (e), 1.0 s (f), 10.0 s (g).

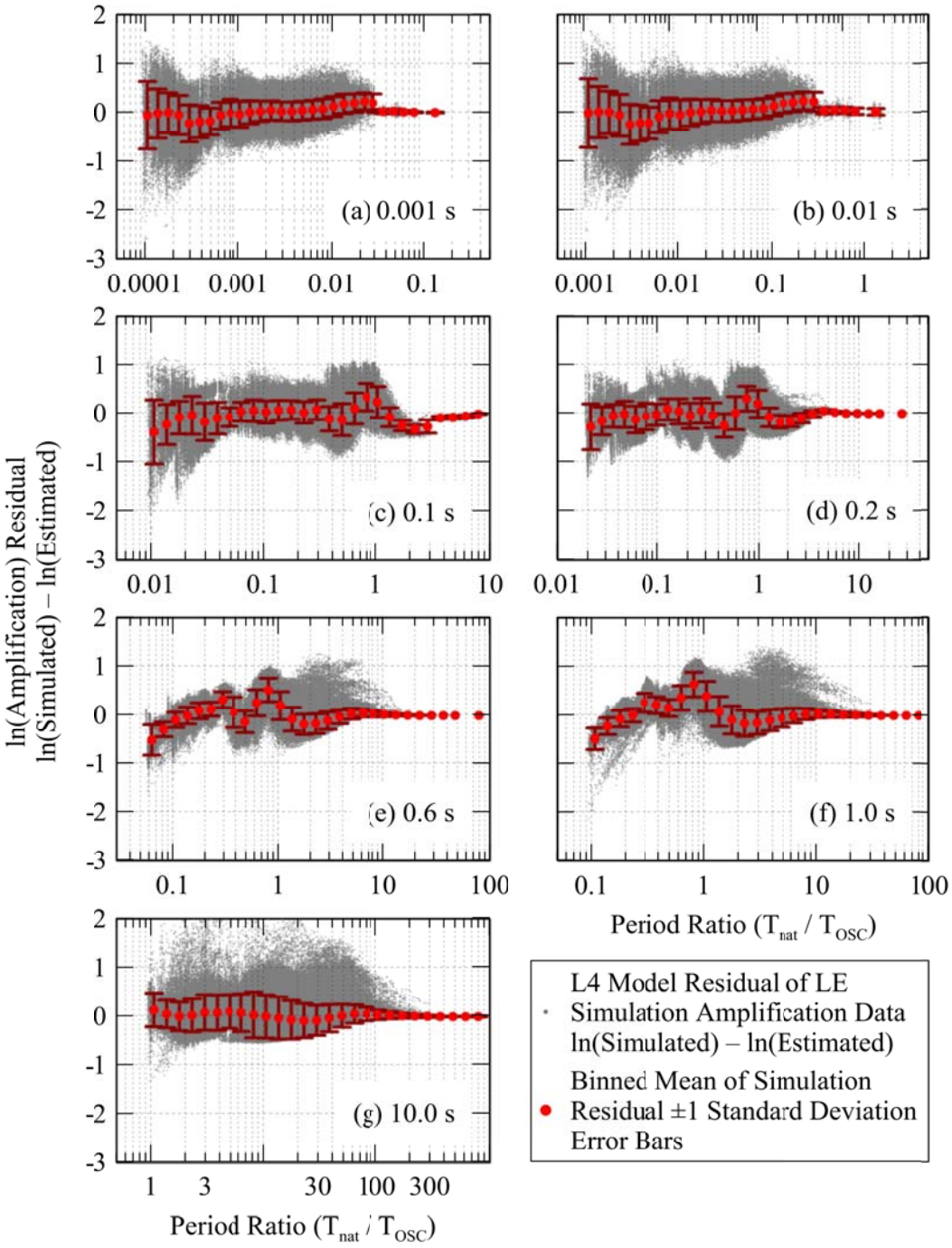

Figure B.12: L4 Amplification model residuals as a function of T_{nat} for periods 0.001 s (a), 0.01 s (b), 0.1 s(c), 0.2 s (d), 0.6 s (e), 1.0 s (f), 10.0 s (g).

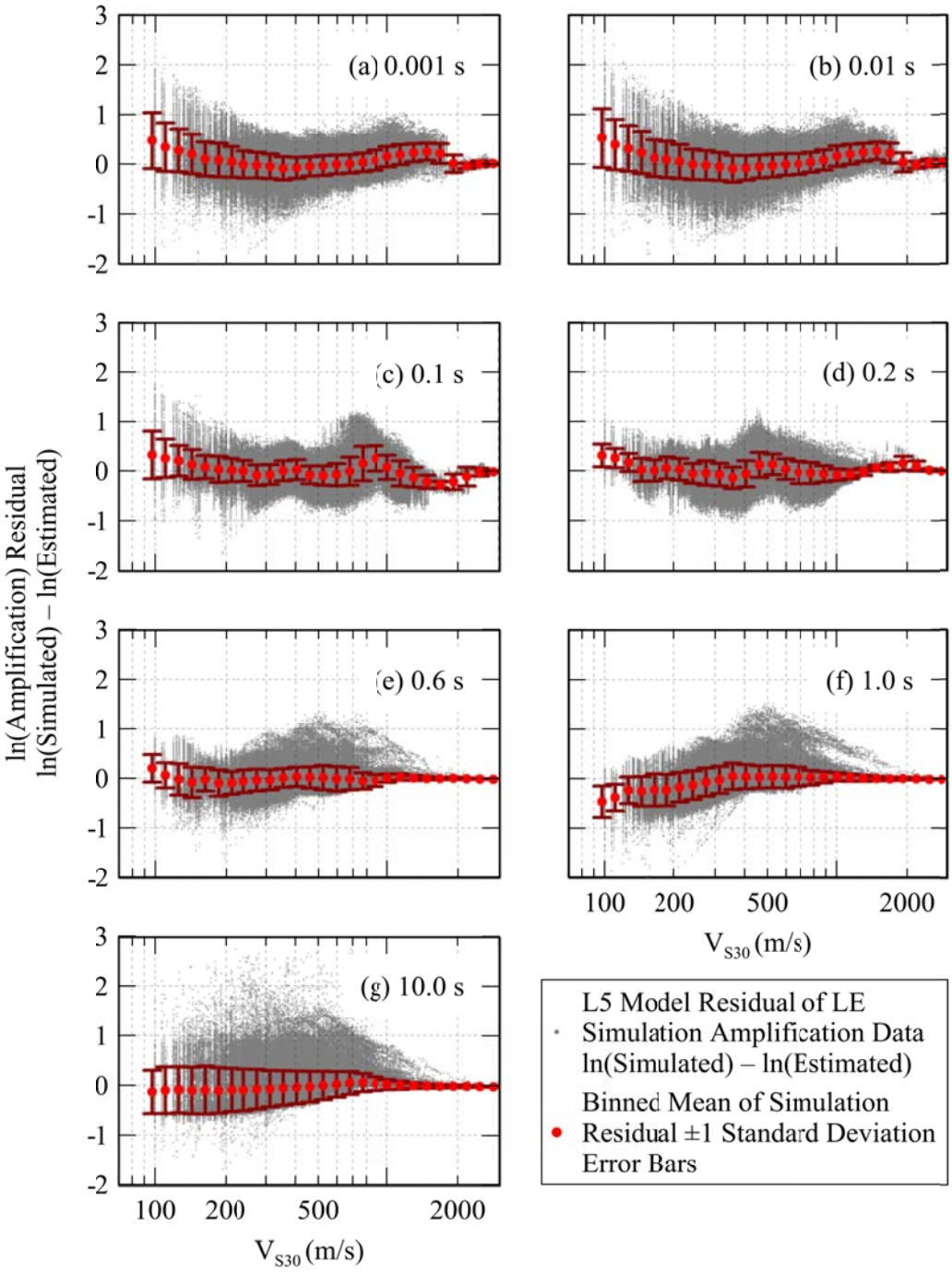

Figure B.13: L5 Amplification model residuals as a function of V_{S30} for periods 0.001 s (a), 0.01 s (b), 0.1 s(c), 0.2 s (d), 0.6 s (e), 1.0 s (f), 10.0 s (g).

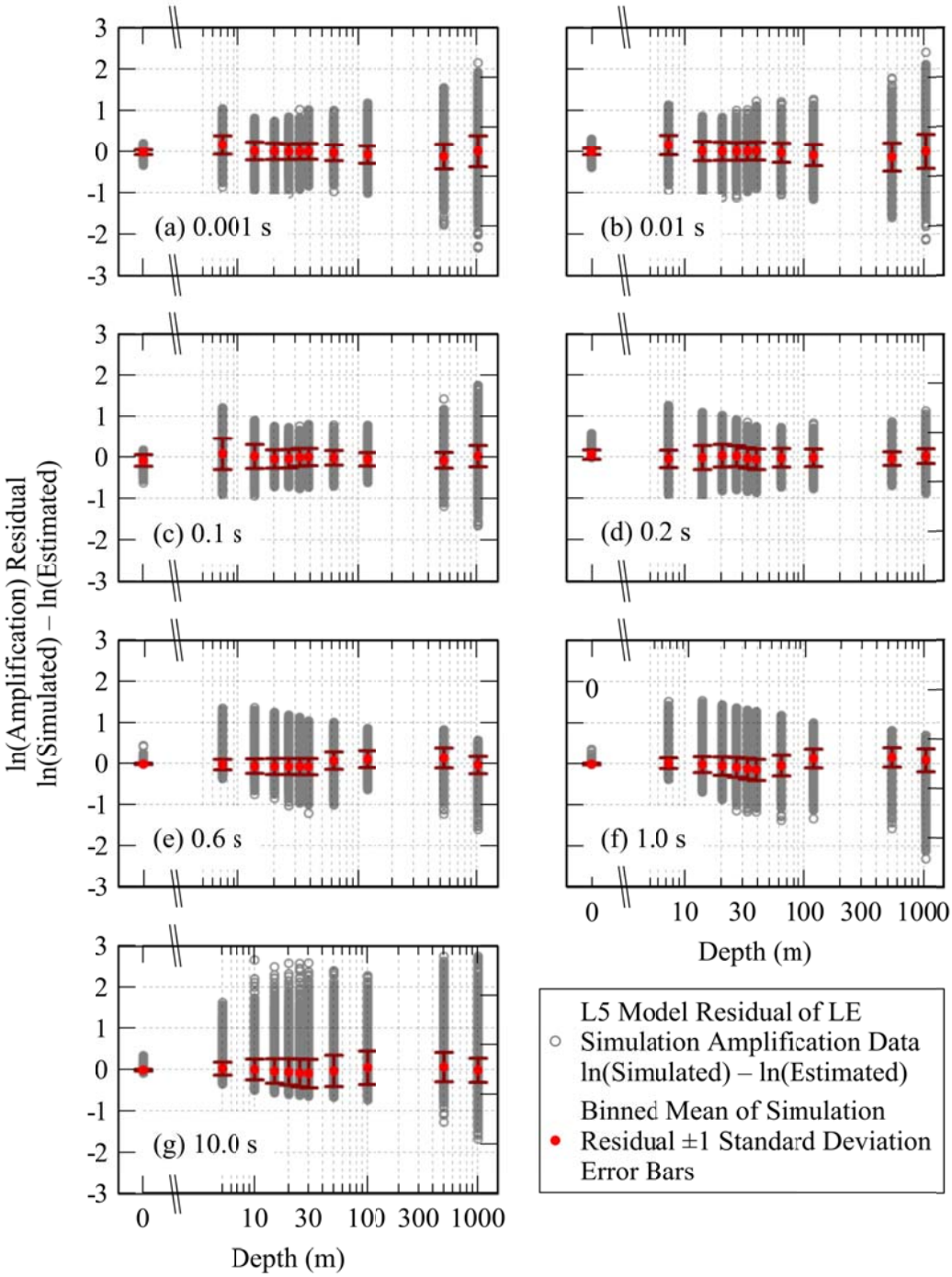

Figure B.14: L5 Amplification model residuals as a function of Z for periods 0.001 s (a), 0.01 s (b), 0.1 s(c), 0.2 s (d), 0.6 s (e), 1.0 s (f), 10.0 s (g).

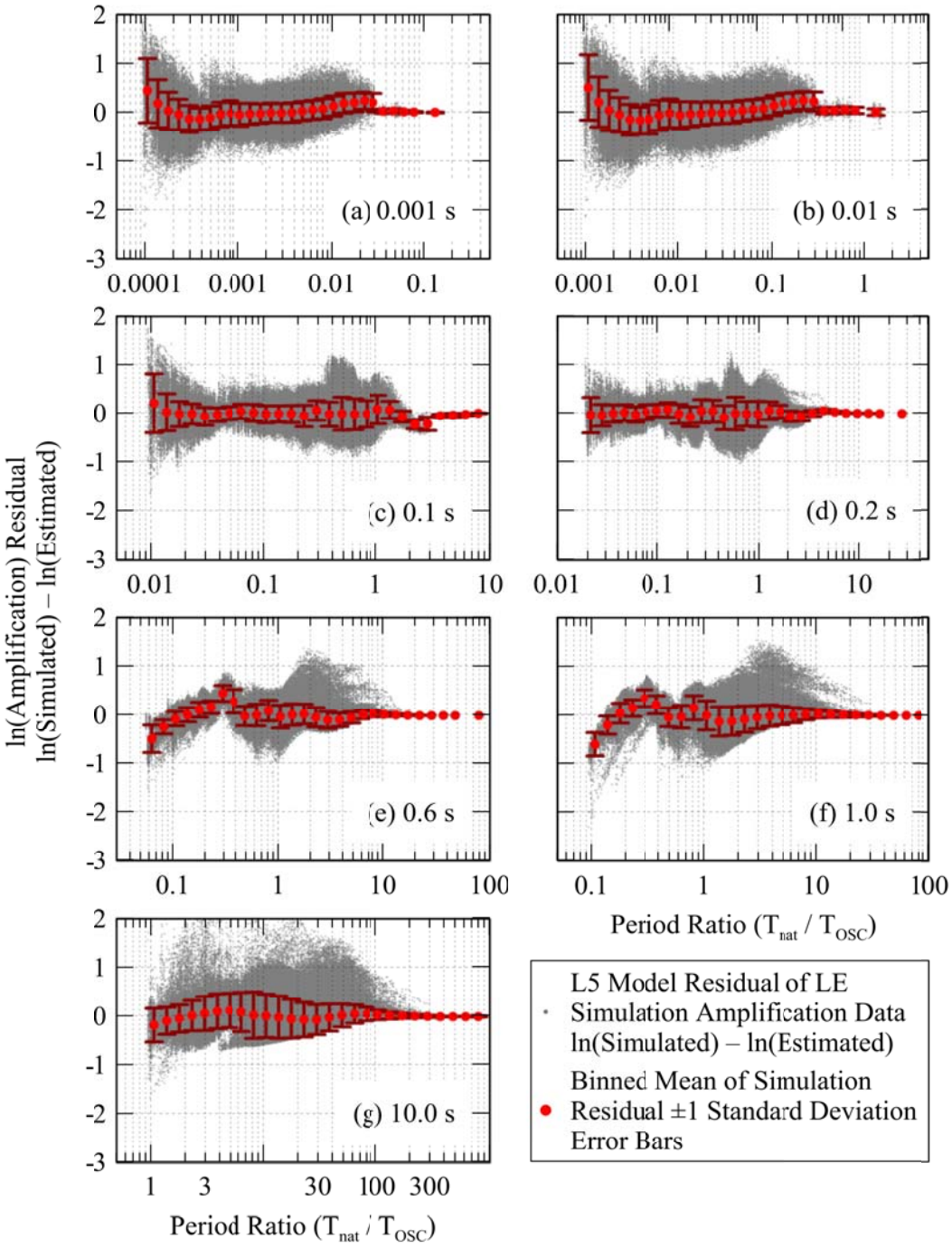

Figure B.15: L5 Amplification model residuals as a function of T_{nat} for periods 0.001 s (a), 0.01 s (b), 0.1 s(c), 0.2 s (d), 0.6 s (e), 1.0 s (f), 10.0 s (g).

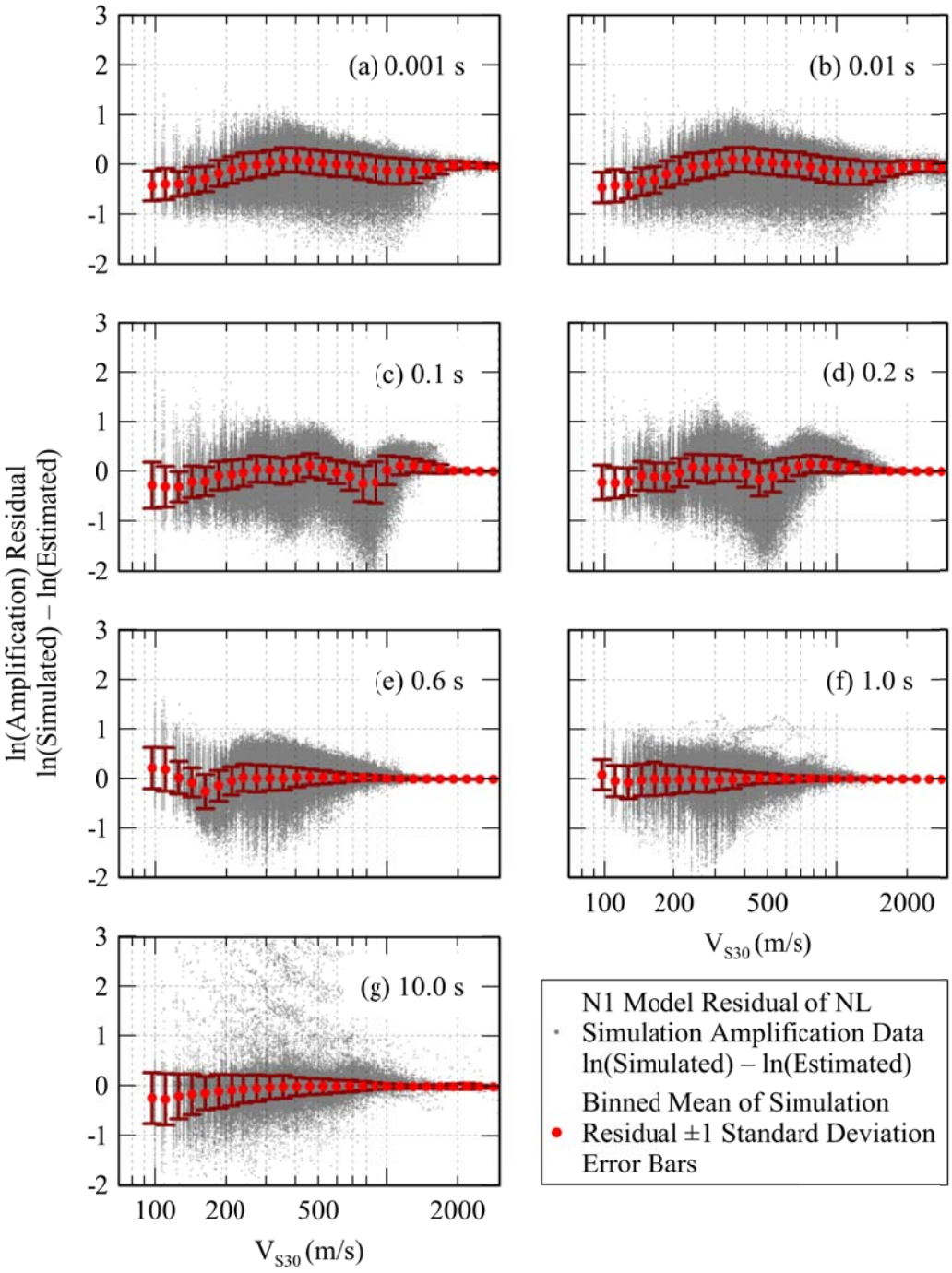

Figure B.16 N1 V_{S30} residuals for 0.001 s (a), 0.01 s (b), 0.1 s(c), 0.2 s (d), 0.6 s (e), 1.0 s (f), 10.0 s (g).

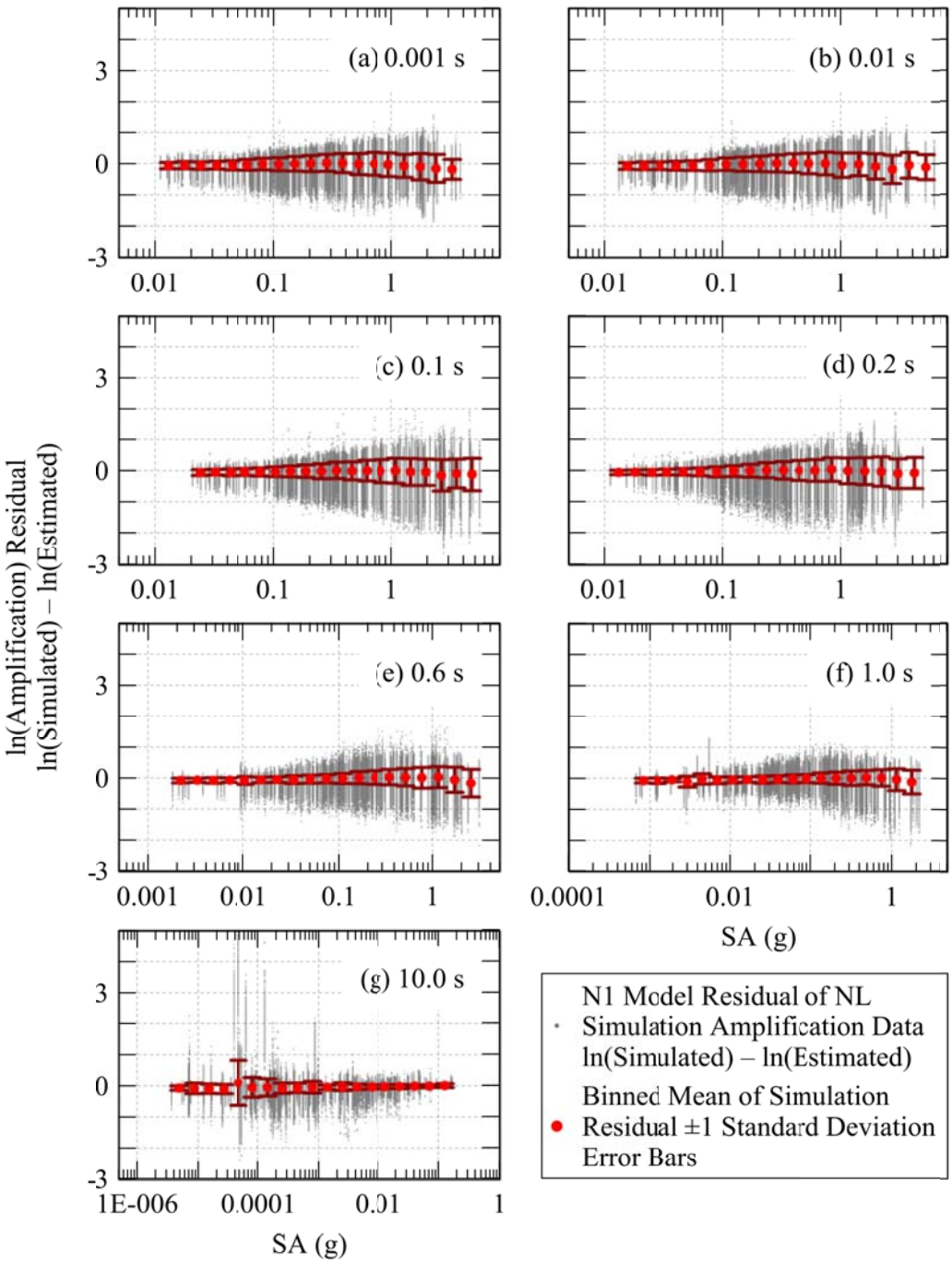

Figure B.17 N1 SA residuals for 0.001 s (a), 0.01 s (b), 0.1 s(c), 0.2 s (d), 0.6 s (e), 1.0 s (f), 10.0 s (g).

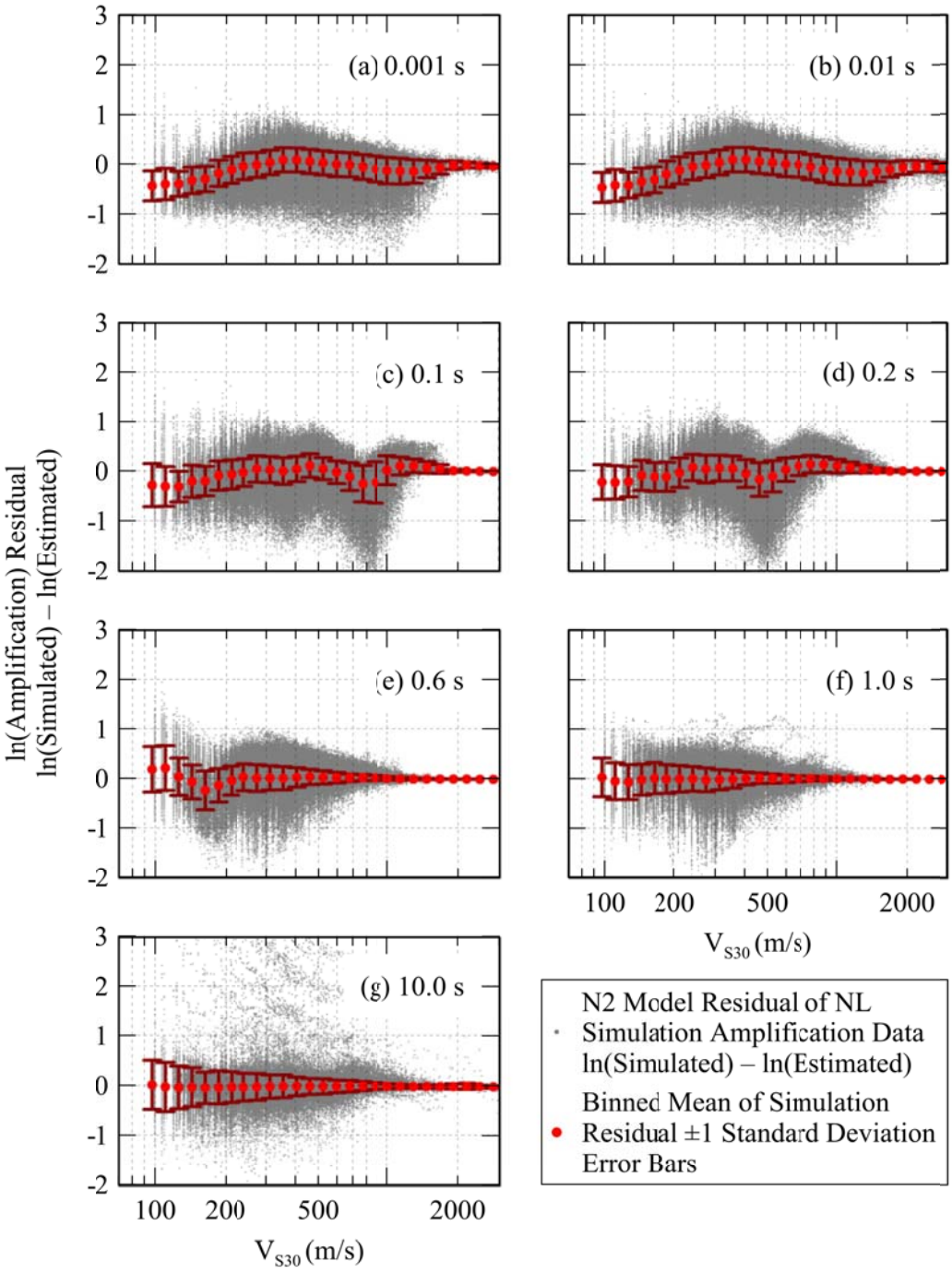

Figure B.18 N2 V_{S30} residuals for 0.001 s (a), 0.01 s (b), 0.1 s(c), 0.2 s (d), 0.6 s (e), 1.0 s (f), 10.0 s (g).

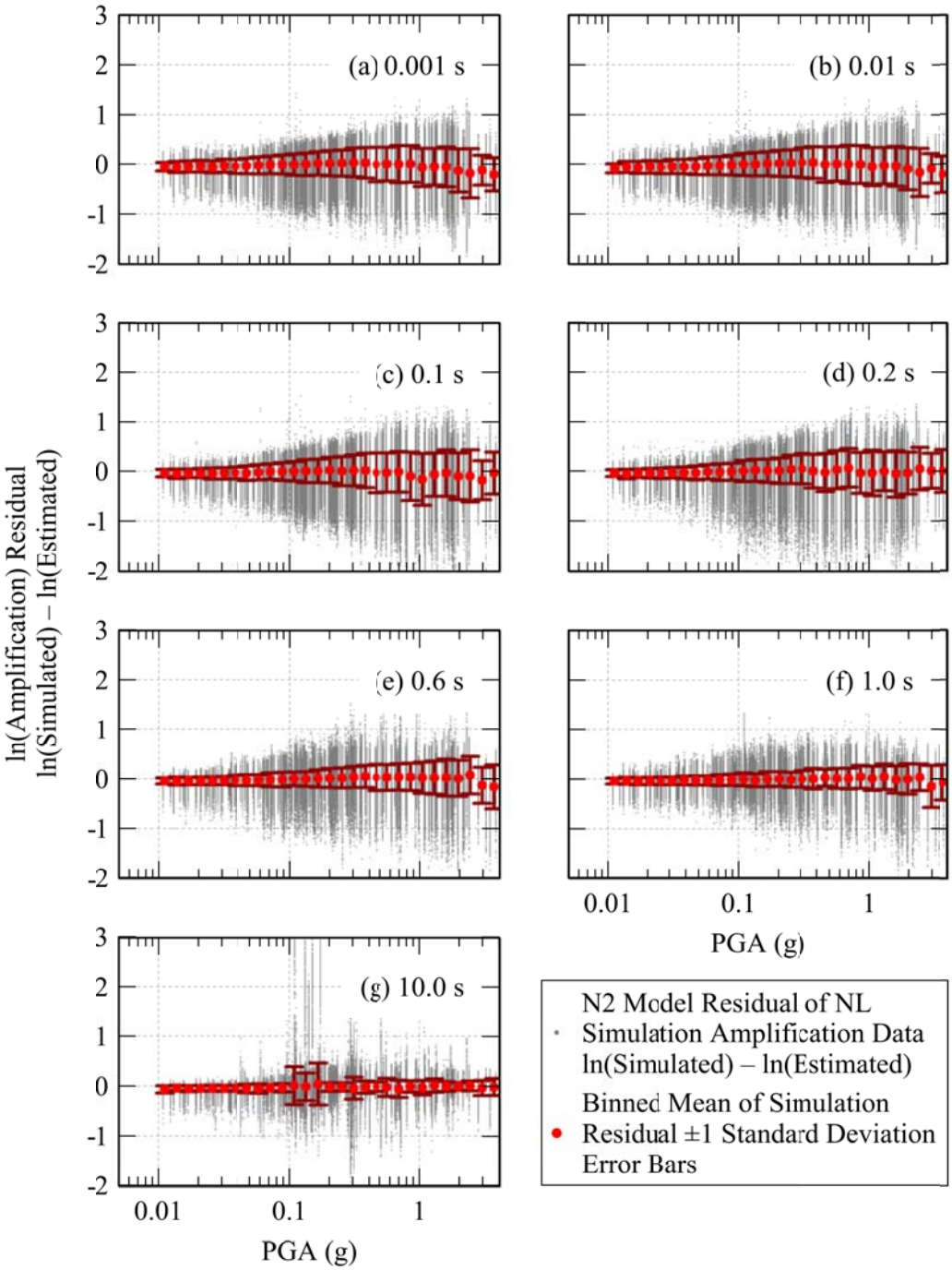

Figure B.19 N2 PGA residuals for 0.001 s (a), 0.01 s (b), 0.1 s(c), 0.2 s (d), 0.6 s (e), 1.0 s (f), 10.0 s (g).

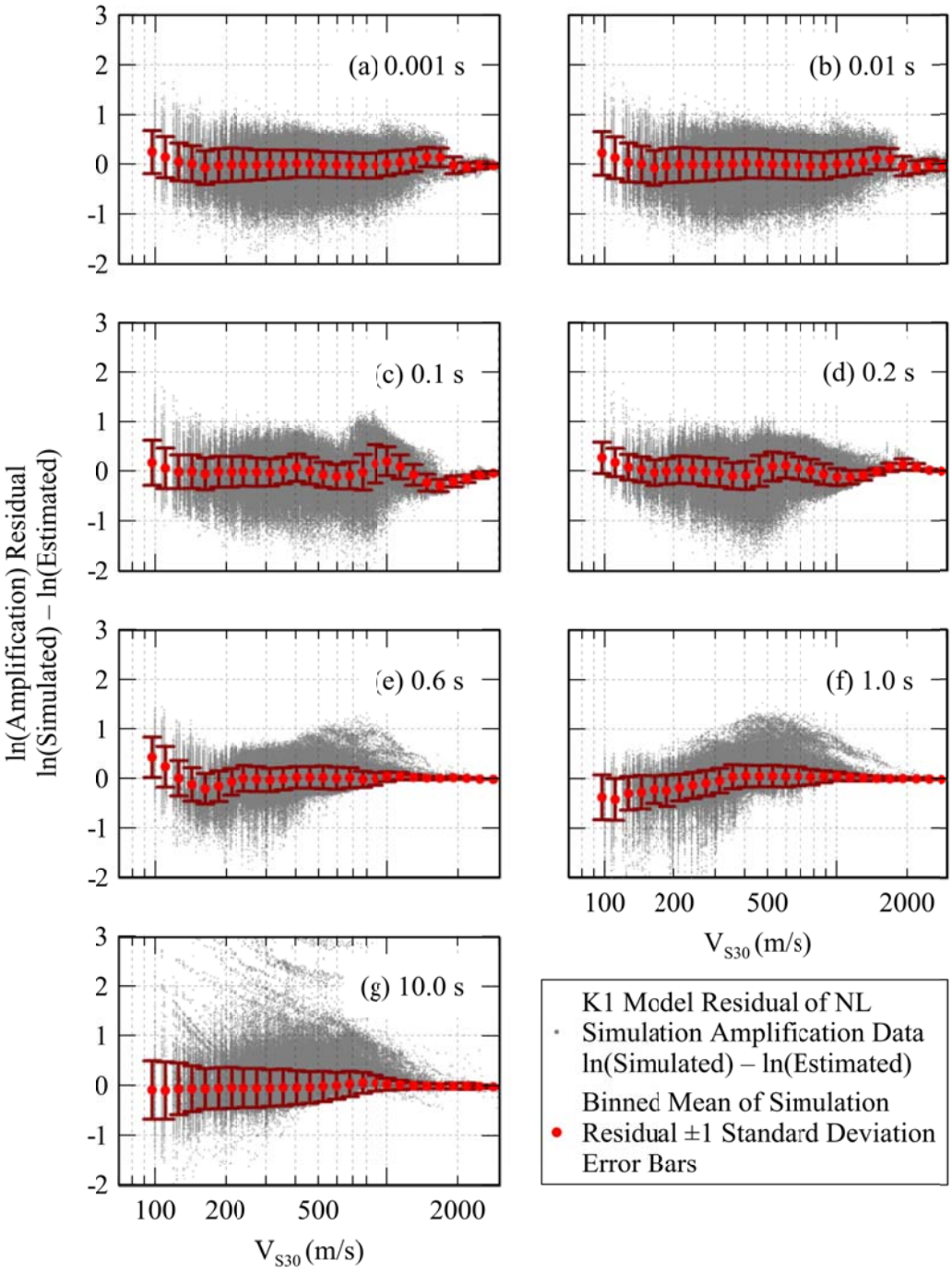

Figure B.20 K1 V_{S30} residuals for 0.001 s (a), 0.01 s (b), 0.1 s(c), 0.2 s (d), 0.6 s (e), 1.0 s (f), 10.0 s (g).

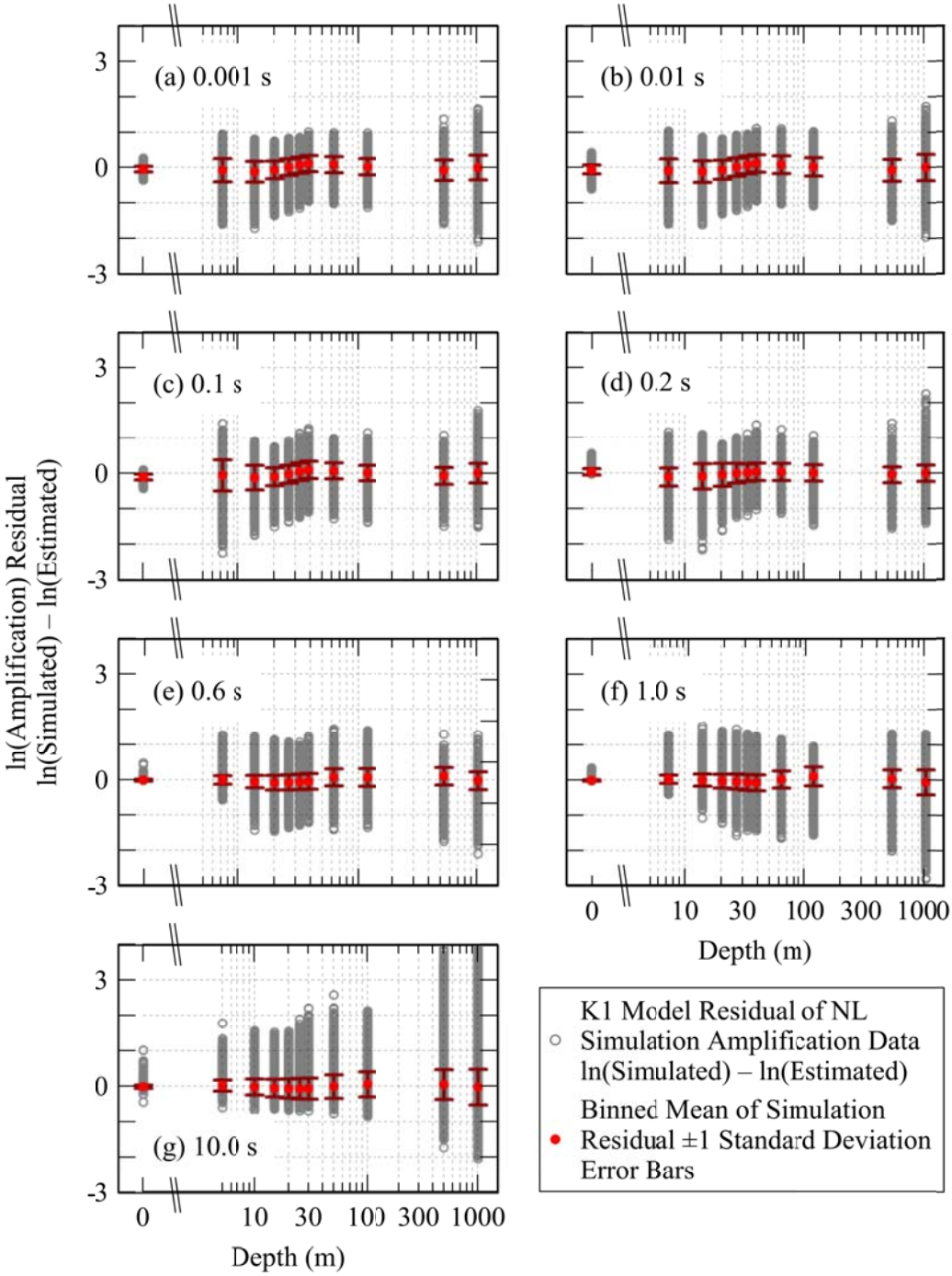

Figure B.21 K1 Z residuals for 0.001 s (a), 0.01 s (b), 0.1 s(c), 0.2 s (d), 0.6 s (e), 1.0 s (f), 10.0 s (g).

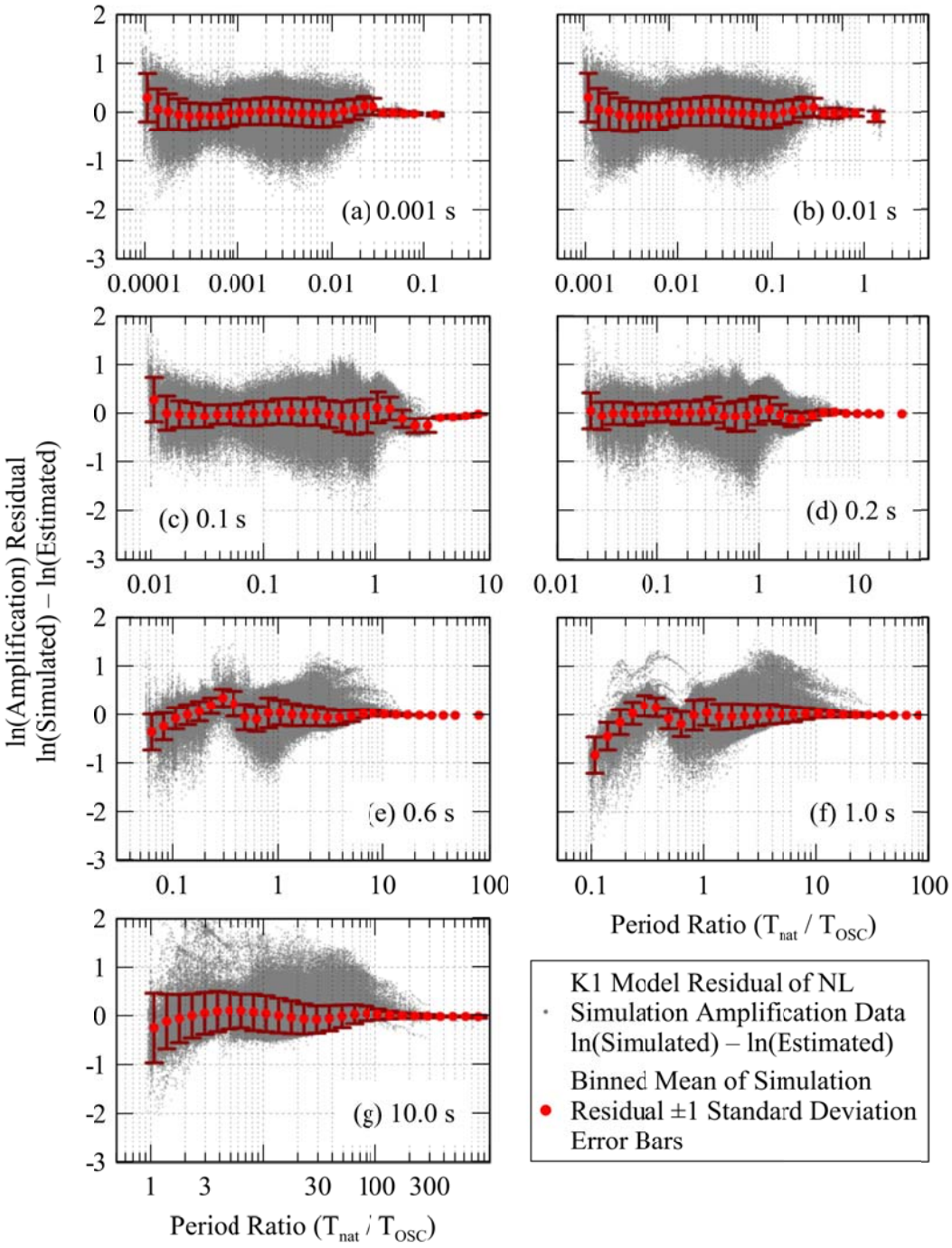

Figure B.22 K1 T_{OSC}/T_{nat} residuals for 0.001 s (a), 0.01 s (b), 0.1 s(c), 0.2 s (d), 0.6 s (e), 1.0 s (f), 10.0 s (g).

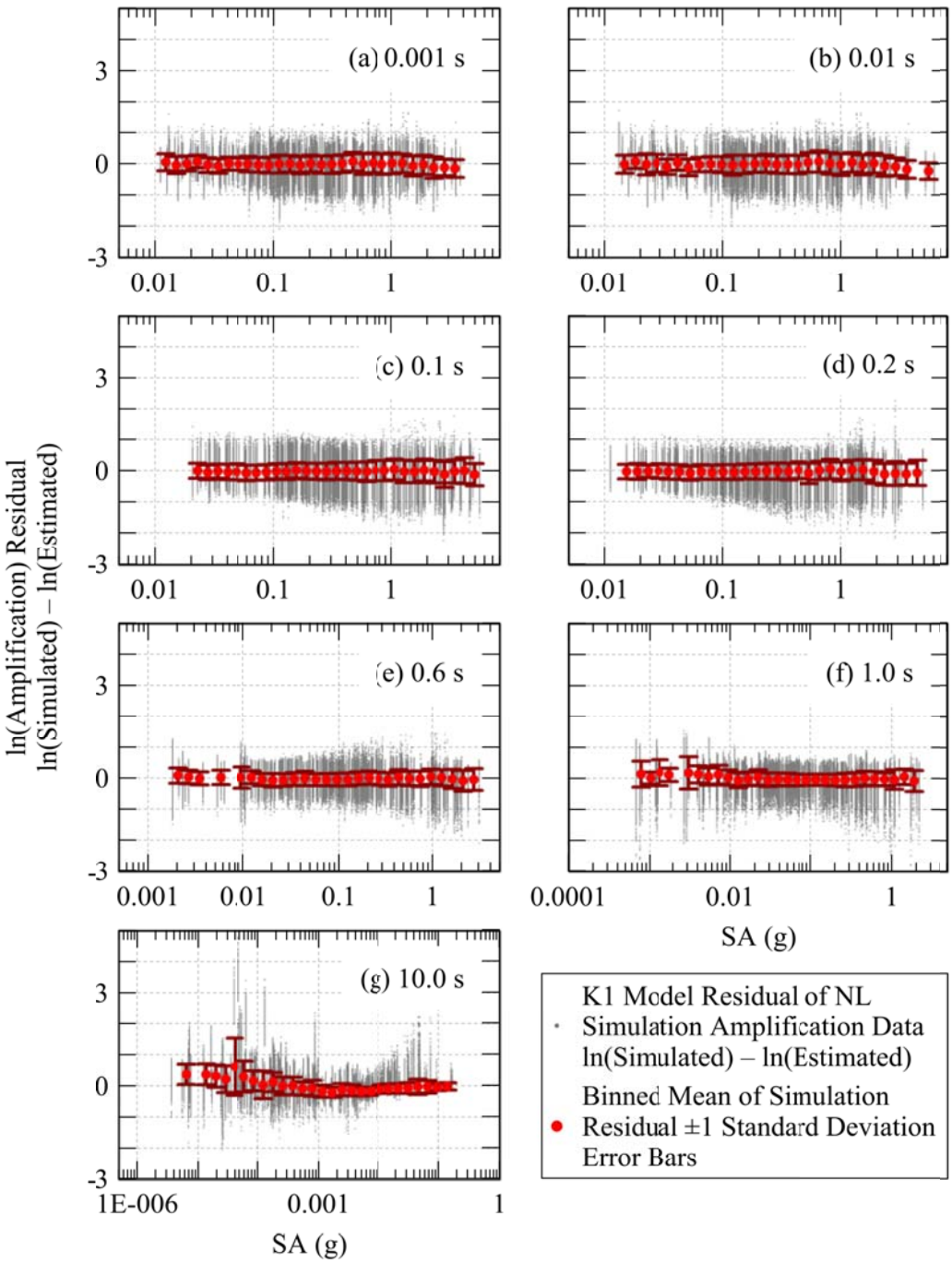

Figure B.23 K1 SA residuals for 0.001 s (a), 0.01 s (b), 0.1 s(c), 0.2 s (d), 0.6 s (e), 1.0 s (f), 10.0 s (g).

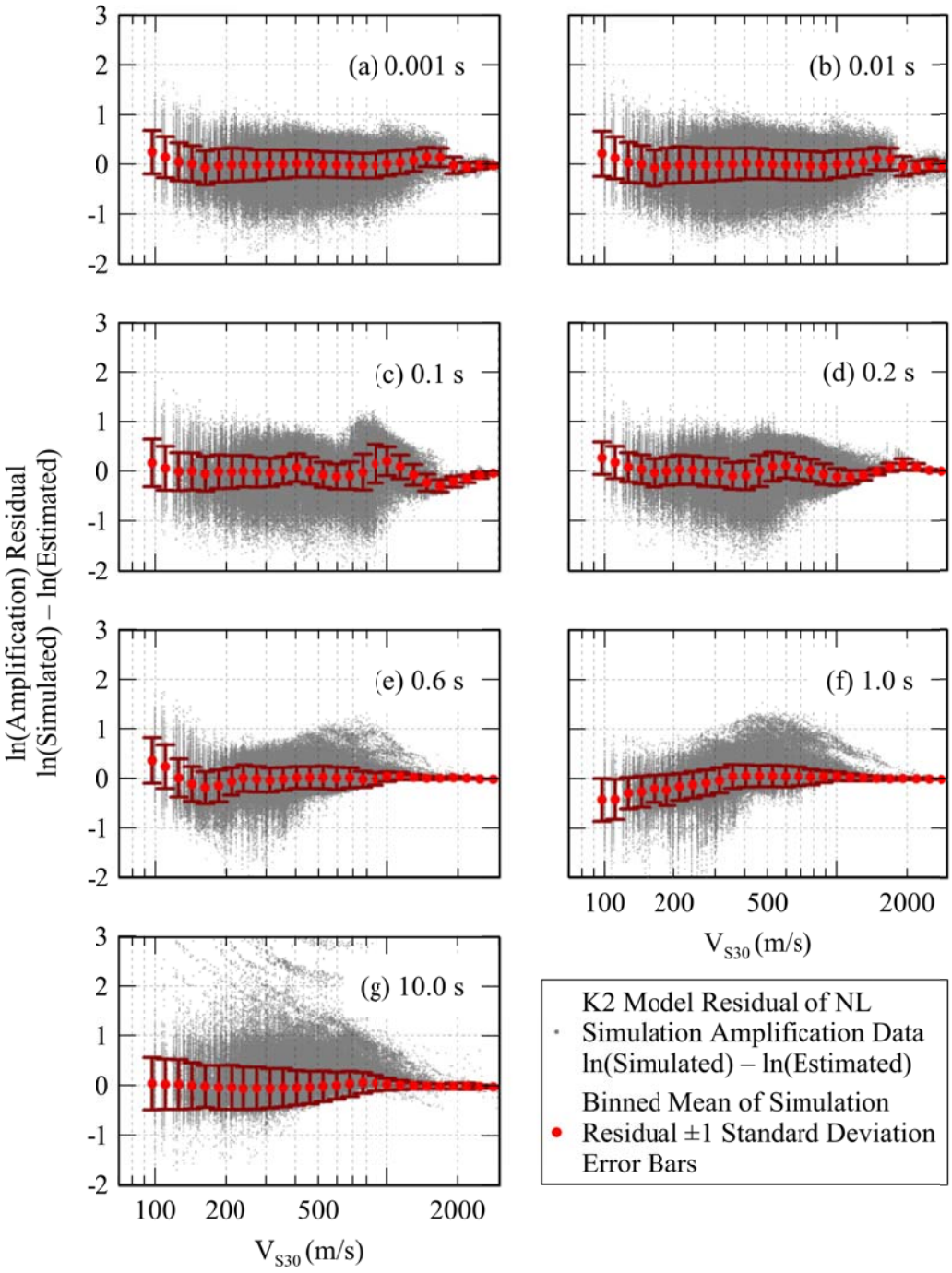

Figure B.24 K2 V_{S30} residuals for 0.001 s (a), 0.01 s (b), 0.1 s(c), 0.2 s (d), 0.6 s (e), 1.0 s (f), 10.0 s (g).

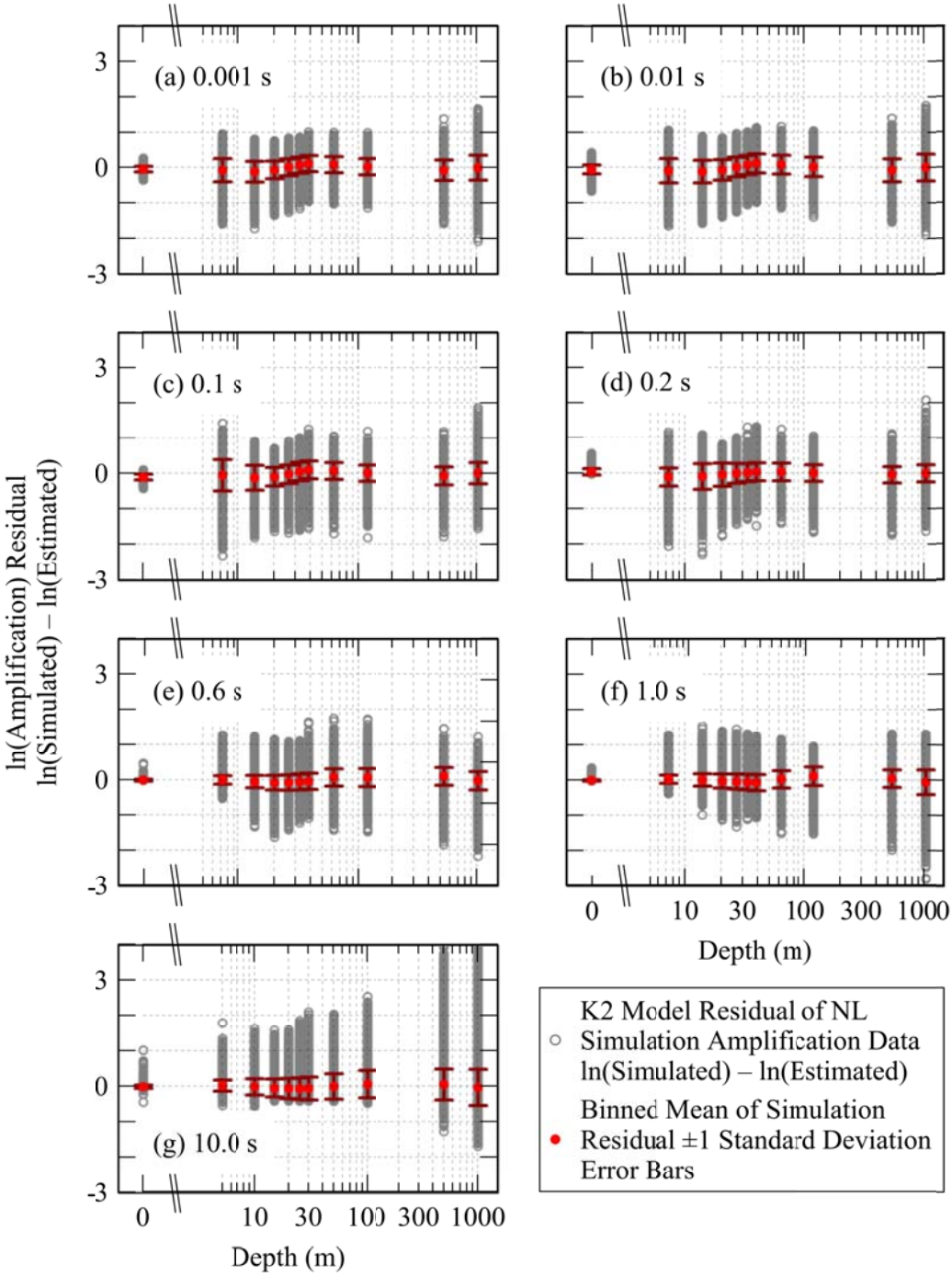

Figure B.25 K2 Z residuals for 0.001 s (a), 0.01 s (b), 0.1 s(c), 0.2 s (d), 0.6 s (e), 1.0 s (f), 10.0 s (g).

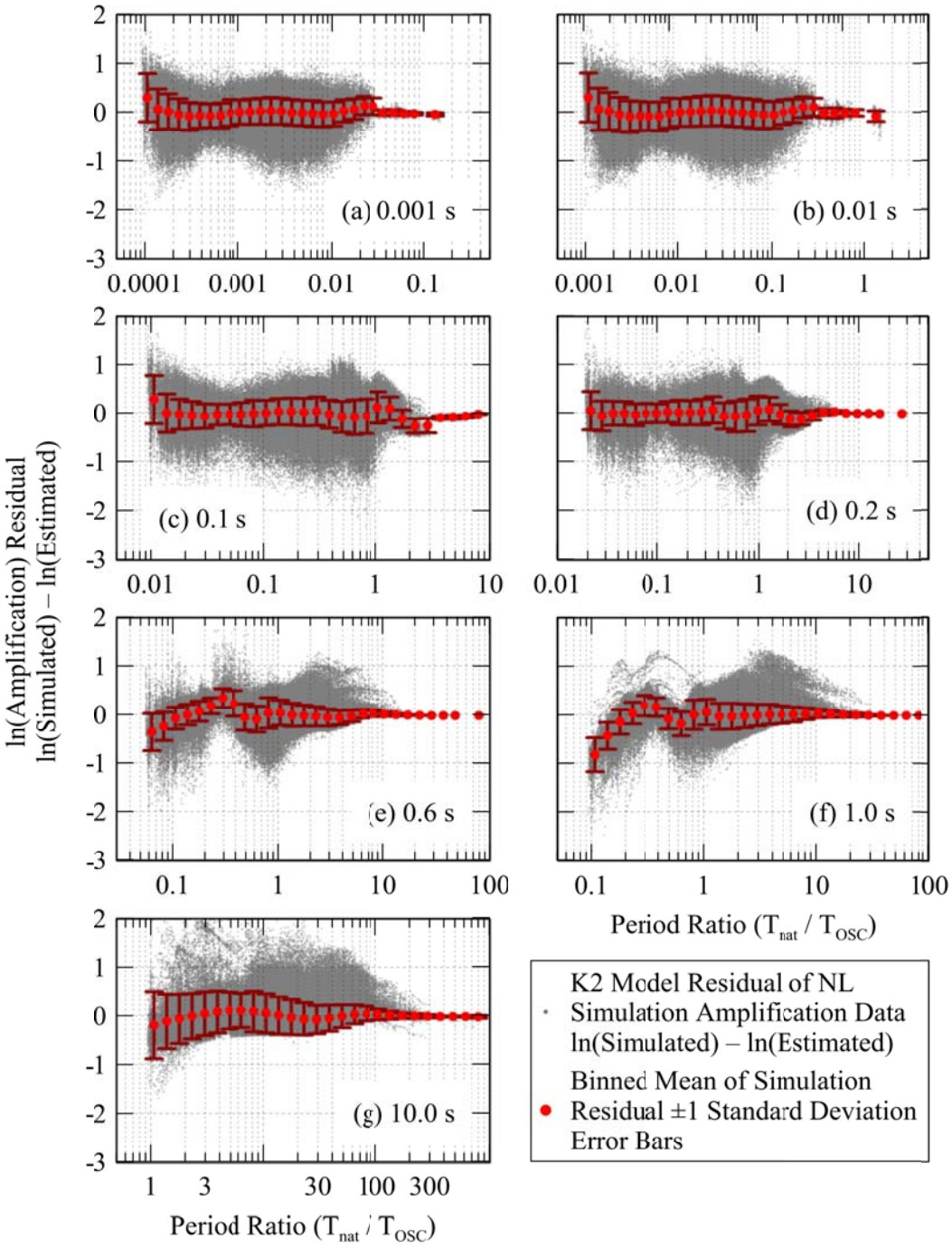

Figure B.26 K2 T_{OSC}/T_{nat} residuals for 0.001 s (a), 0.01 s (b), 0.1 s(c), 0.2 s (d), 0.6 s (e), 1.0 s (f), 10.0 s (g).

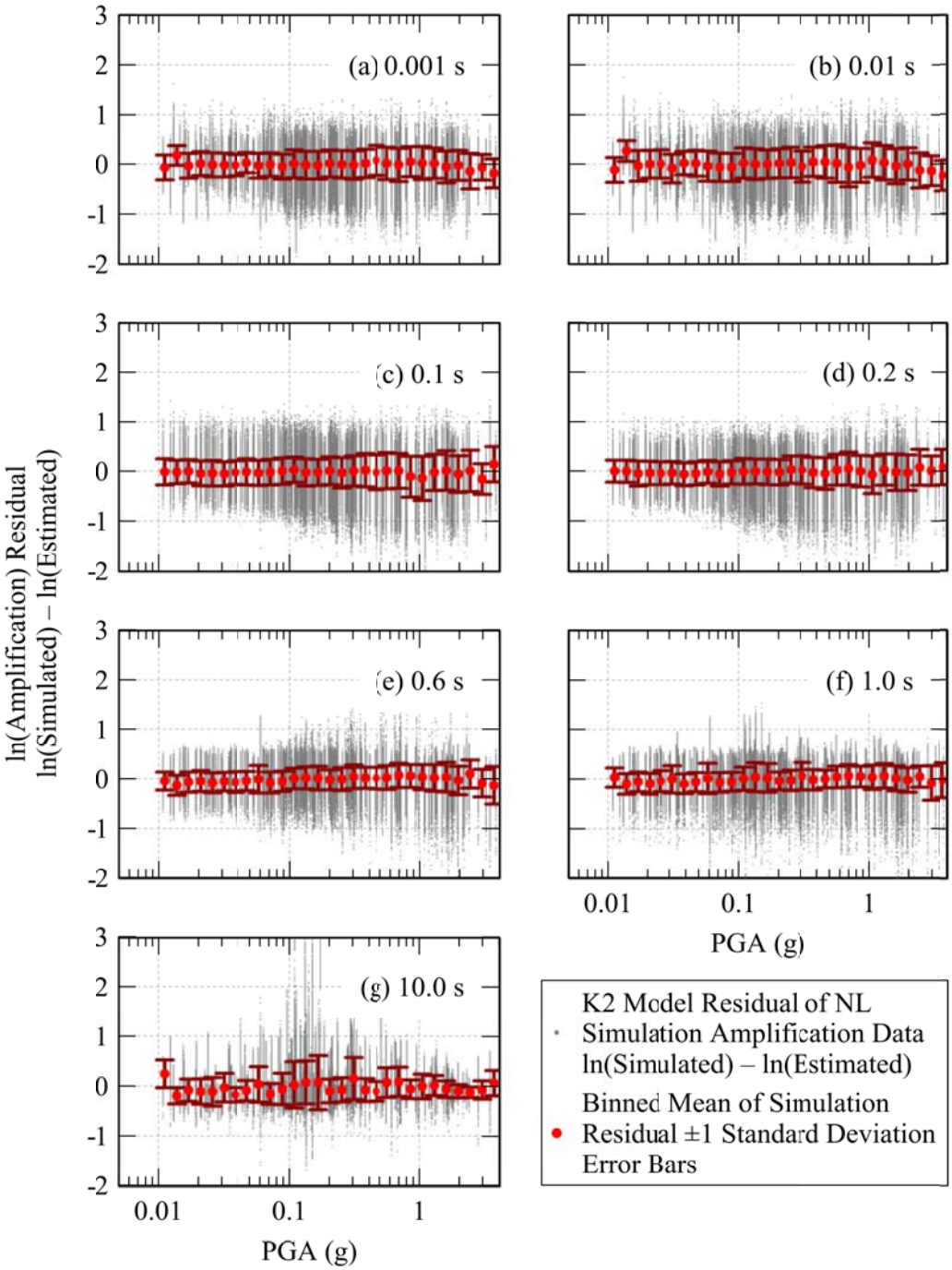

Figure B.27 K2 PGA residuals for 0.001 s (a), 0.01 s (b), 0.1 s(c), 0.2 s (d), 0.6 s (e), 1.0 s (f), 10.0 s (g).

APPENDIX C Depth Dependent Amplification of 760 m/s V_{S30} Sites

Table C.1: Period-dependent values of ln(amp) of linear elastic simulations of simulations with 700 m/s < V_{S30} < 800 m/s as a function of depth, denoted as $C_{760\text{-}3000}$ in eq 13.of the main body of this report. The DI (Depth-Independent) column is the average amplilfication of all simulations with 700 m/s < V_{S30} < 800 m/s.

T (s)	DI Correction	5 m	10 m	15 m	20 m	25 m	30 m	50 m	100 m	50 m	1000 m
0.001	0.822	0.913	0.861	0.838	0.811	0.792	0.773	0.756	0.710	0.466	0.285
0.006667	0.805	0.893	0.845	0.823	0.799	0.779	0.759	0.743	0.695	0.440	0.254
0.008	0.787	0.873	0.827	0.809	0.787	0.765	0.746	0.732	0.677	0.413	0.221
0.01	0.728	0.806	0.766	0.760	0.740	0.724	0.708	0.681	0.620	0.321	0.119
0.010526	0.712	0.790	0.751	0.747	0.727	0.711	0.694	0.669	0.602	0.290	0.089
0.011111	0.704	0.781	0.744	0.741	0.722	0.702	0.691	0.657	0.587	0.270	0.067
0.011749	0.697	0.771	0.740	0.738	0.715	0.697	0.682	0.648	0.577	0.253	0.044
0.0125	0.693	0.767	0.738	0.737	0.709	0.689	0.685	0.648	0.576	0.231	0.015
0.014125	0.677	0.744	0.729	0.713	0.682	0.701	0.701	0.652	0.586	0.189	-0.058
0.016218	0.662	0.724	0.713	0.684	0.711	0.711	0.682	0.646	0.579	0.129	-0.139
0.018182	0.665	0.727	0.718	0.697	0.716	0.707	0.694	0.647	0.579	0.118	-0.174
0.02	0.662	0.741	0.673	0.750	0.762	0.697	0.671	0.654	0.578	0.116	-0.209
0.022	0.667	0.770	0.657	0.725	0.734	0.765	0.727	0.674	0.600	0.133	-0.203
0.025	0.711	0.763	0.784	0.789	0.716	0.690	0.712	0.703	0.631	0.180	-0.169
0.029	0.740	0.737	0.780	0.866	0.871	0.800	0.721	0.697	0.646	0.242	-0.100
0.03	0.739	0.764	0.751	0.832	0.866	0.850	0.776	0.708	0.652	0.262	-0.069
0.032	0.734	0.834	0.723	0.756	0.782	0.847	0.832	0.753	0.657	0.285	-0.036
0.035	0.758	0.941	0.775	0.735	0.689	0.714	0.780	0.765	0.686	0.328	0.021
0.036	0.776	0.965	0.814	0.754	0.686	0.684	0.743	0.741	0.693	0.346	0.039
0.04	0.887	0.998	1.018	0.926	0.793	0.701	0.688	0.740	0.739	0.417	0.132
0.042	0.928	0.956	1.093	1.019	0.876	0.748	0.705	0.788	0.750	0.432	0.156
0.044	0.945	0.891	1.111	1.088	0.967	0.820	0.755	0.843	0.749	0.455	0.185
0.045	0.941	0.857	1.097	1.099	1.000	0.852	0.781	0.860	0.741	0.460	0.195
0.046	0.937	0.831	1.078	1.102	1.033	0.894	0.813	0.876	0.736	0.469	0.211
0.048	0.907	0.777	1.001	1.062	1.067	0.975	0.888	0.878	0.731	0.485	0.236
0.05	0.870	0.744	0.918	0.993	1.060	1.038	0.959	0.844	0.760	0.506	0.262

Table C.1: Period-dependent values of ln(amp) of linear elastic simulations of simulations with 700 m/s < V_{S30} < 800 m/s as a function of depth, denoted as $C_{760\text{-}3000}$ in eq 13.of the main body of this report. The DI (Depth-Independent) column is the average amplilfication of all simulations with 700 m/s < V_{S30} < 800 m/s.

T (s)	DI Correction	5 m	10 m	15 m	20 m	25 m	30 m	50 m	100 m	50 m	1000 m
0.055	0.767	0.705	0.749	0.797	0.890	1.002	1.020	0.734	0.831	0.543	0.320
0.06	0.710	0.721	0.681	0.693	0.749	0.850	0.920	0.731	0.791	0.584	0.373
0.065	0.707	0.782	0.680	0.663	0.683	0.739	0.800	0.823	0.774	0.612	0.417
0.066667	0.716	0.811	0.690	0.661	0.672	0.715	0.766	0.864	0.795	0.623	0.432
0.07	0.739	0.868	0.715	0.669	0.661	0.678	0.705	0.956	0.858	0.645	0.464
0.075	0.790	0.963	0.772	0.703	0.676	0.662	0.675	1.042	0.930	0.678	0.504
0.08	0.852	1.069	0.845	0.763	0.717	0.674	0.673	1.026	0.922	0.698	0.535
0.085	0.925	1.186	0.937	0.840	0.778	0.714	0.695	0.942	0.853	0.710	0.557
0.09	0.999	1.292	1.038	0.926	0.839	0.755	0.728	0.849	0.791	0.719	0.570
0.095	1.083	1.391	1.150	1.021	0.922	0.823	0.785	0.776	0.777	0.724	0.579
0.1	1.172	1.480	1.270	1.127	1.013	0.899	0.850	0.731	0.803	0.726	0.588
0.11	1.311	1.580	1.465	1.310	1.175	1.044	0.975	0.666	0.892	0.717	0.595
0.12	1.391	1.580	1.567	1.440	1.309	1.187	1.111	0.675	0.978	0.721	0.605
0.13	1.352	1.456	1.496	1.436	1.349	1.277	1.189	0.736	0.961	0.720	0.612
0.133333	1.317	1.398	1.443	1.404	1.335	1.282	1.198	0.760	0.931	0.715	0.612
0.14	1.226	1.271	1.317	1.306	1.277	1.264	1.193	0.810	0.849	0.714	0.620
0.15	1.088	1.098	1.137	1.151	1.156	1.185	1.140	0.886	0.734	0.737	0.627
0.16	0.981	0.973	1.005	1.025	1.041	1.089	1.055	0.968	0.670	0.729	0.641
0.17	0.880	0.861	0.888	0.904	0.927	0.976	0.956	1.038	0.628	0.708	0.635
0.18	0.788	0.761	0.779	0.797	0.824	0.871	0.859	1.078	0.610	0.717	0.637
0.19	0.723	0.692	0.704	0.719	0.746	0.787	0.784	1.097	0.608	0.733	0.638
0.2	0.667	0.630	0.643	0.656	0.678	0.719	0.719	1.090	0.624	0.727	0.629
0.22	0.566	0.522	0.530	0.543	0.561	0.598	0.600	1.015	0.697	0.662	0.629
0.24	0.496	0.451	0.456	0.466	0.479	0.509	0.504	0.884	0.775	0.660	0.602
0.25	0.471	0.423	0.426	0.436	0.448	0.475	0.470	0.832	0.826	0.685	0.600
0.26	0.435	0.383	0.386	0.397	0.408	0.433	0.434	0.775	0.852	0.698	0.604
0.28	0.389	0.336	0.336	0.344	0.354	0.380	0.378	0.689	0.909	0.685	0.591
0.29	0.371	0.319	0.318	0.325	0.336	0.360	0.358	0.650	0.930	0.646	0.573

Table C.1: Period-dependent values of ln(amp) of linear elastic simulations of simulations with 700 m/s < V_{S30} < 800 m/s as a function of depth, denoted as $C_{760\text{-}3000}$ in eq 13.of the main body of this report. The DI (Depth-Independent) column is the average amplilfication of all simulations with 700 m/s < V_{S30} < 800 m/s.

T (s)	DI Correction	5 m	10 m	15 m	20 m	25 m	30 m	50 m	100 m	50 m	1000 m
0.3	0.358	0.307	0.308	0.312	0.325	0.346	0.341	0.622	0.938	0.605	0.561
0.32	0.329	0.279	0.279	0.283	0.296	0.313	0.306	0.563	0.942	0.552	0.563
0.34	0.297	0.246	0.248	0.251	0.263	0.277	0.273	0.497	0.920	0.522	0.572
0.35	0.288	0.238	0.238	0.242	0.253	0.266	0.263	0.476	0.904	0.526	0.569
0.36	0.277	0.226	0.227	0.232	0.240	0.254	0.251	0.458	0.883	0.545	0.559
0.38	0.256	0.206	0.206	0.211	0.218	0.231	0.228	0.423	0.835	0.584	0.523
0.4	0.236	0.188	0.186	0.191	0.200	0.210	0.208	0.386	0.776	0.613	0.494
0.42	0.224	0.178	0.175	0.177	0.183	0.192	0.192	0.359	0.722	0.643	0.494
0.44	0.214	0.169	0.165	0.167	0.174	0.181	0.179	0.336	0.675	0.650	0.515
0.45	0.208	0.163	0.160	0.161	0.167	0.174	0.171	0.319	0.653	0.642	0.524
0.46	0.201	0.156	0.154	0.155	0.162	0.168	0.164	0.305	0.630	0.629	0.532
0.48	0.191	0.147	0.145	0.149	0.154	0.160	0.156	0.283	0.589	0.590	0.538
0.5	0.178	0.138	0.134	0.139	0.143	0.149	0.146	0.255	0.549	0.548	0.529
0.55	0.156	0.122	0.119	0.123	0.128	0.131	0.128	0.222	0.472	0.457	0.466
0.6	0.140	0.108	0.106	0.111	0.116	0.119	0.118	0.196	0.415	0.399	0.422
0.65	0.133	0.104	0.102	0.106	0.110	0.113	0.109	0.178	0.367	0.369	0.440
0.666667	0.128	0.100	0.098	0.101	0.105	0.109	0.105	0.175	0.350	0.361	0.451
0.7	0.125	0.096	0.093	0.096	0.099	0.102	0.100	0.166	0.337	0.363	0.485
0.75	0.120	0.091	0.088	0.091	0.094	0.095	0.091	0.150	0.296	0.386	0.529
0.8	0.118	0.088	0.085	0.087	0.091	0.092	0.088	0.143	0.270	0.422	0.543
0.85	0.114	0.084	0.082	0.082	0.087	0.087	0.082	0.132	0.246	0.458	0.530
0.9	0.112	0.083	0.081	0.081	0.085	0.084	0.079	0.125	0.230	0.497	0.490
0.95	0.111	0.082	0.080	0.079	0.083	0.080	0.078	0.120	0.216	0.538	0.453
1	0.106	0.077	0.075	0.075	0.079	0.077	0.074	0.114	0.203	0.576	0.416
1.1	0.107	0.078	0.077	0.075	0.079	0.077	0.075	0.112	0.187	0.639	0.359
1.2	0.102	0.074	0.072	0.071	0.074	0.072	0.070	0.102	0.168	0.666	0.344
1.3	0.100	0.071	0.070	0.070	0.072	0.070	0.067	0.097	0.150	0.675	0.348
1.4	0.097	0.068	0.067	0.066	0.069	0.067	0.064	0.092	0.144	0.654	0.367

Table C.1: Period-dependent values of ln(amp) of linear elastic simulations of simulations with 700 m/s < V_{S30} < 800 m/s as a function of depth, denoted as $C_{760\text{-}3000}$ in eq 13.of the main body of this report. The DI (Depth-Independent) column is the average amplilfication of all simulations with 700 m/s < V_{S30} < 800 m/s.

T (s)	DI Correction	5 m	10 m	15 m	20 m	25 m	30 m	50 m	100 m	50 m	1000 m
1.5	0.099	0.070	0.069	0.068	0.071	0.069	0.065	0.092	0.145	0.623	0.406
1.6	0.099	0.069	0.069	0.068	0.071	0.070	0.066	0.095	0.142	0.590	0.441
1.7	0.098	0.069	0.068	0.067	0.070	0.068	0.066	0.091	0.138	0.556	0.478
1.8	0.096	0.068	0.068	0.066	0.069	0.066	0.064	0.085	0.131	0.521	0.509
1.9	0.094	0.066	0.066	0.064	0.066	0.064	0.062	0.083	0.124	0.489	0.537
2	0.094	0.067	0.066	0.065	0.066	0.064	0.062	0.085	0.123	0.463	0.555
2.2	0.097	0.070	0.069	0.068	0.070	0.067	0.065	0.090	0.123	0.417	0.575
2.4	0.096	0.070	0.068	0.069	0.071	0.069	0.065	0.090	0.122	0.385	0.572
2.5	0.094	0.068	0.067	0.068	0.071	0.068	0.065	0.090	0.118	0.365	0.563
2.6	0.093	0.068	0.068	0.068	0.071	0.068	0.066	0.089	0.116	0.347	0.554
2.8	0.091	0.067	0.067	0.068	0.070	0.066	0.065	0.087	0.112	0.321	0.534
3	0.091	0.069	0.069	0.069	0.071	0.067	0.066	0.089	0.114	0.303	0.509
3.2	0.089	0.068	0.068	0.069	0.071	0.066	0.065	0.088	0.115	0.291	0.484
3.4	0.089	0.069	0.069	0.070	0.072	0.068	0.065	0.087	0.117	0.281	0.461
3.5	0.089	0.070	0.070	0.070	0.072	0.068	0.066	0.087	0.116	0.273	0.447
3.6	0.089	0.070	0.070	0.071	0.073	0.069	0.066	0.088	0.116	0.267	0.433
3.8	0.088	0.070	0.070	0.070	0.072	0.069	0.066	0.087	0.117	0.256	0.412
4	0.087	0.070	0.069	0.069	0.071	0.068	0.065	0.088	0.117	0.252	0.396
4.2	0.086	0.070	0.069	0.069	0.071	0.067	0.065	0.088	0.115	0.247	0.382
4.4	0.085	0.070	0.069	0.068	0.071	0.067	0.065	0.087	0.116	0.245	0.369
4.6	0.086	0.071	0.070	0.069	0.072	0.068	0.066	0.088	0.118	0.243	0.360
4.8	0.086	0.072	0.071	0.070	0.073	0.069	0.067	0.090	0.121	0.241	0.353
5	0.086	0.072	0.071	0.070	0.073	0.069	0.067	0.092	0.121	0.236	0.342
5.5	0.087	0.074	0.073	0.071	0.075	0.070	0.068	0.094	0.122	0.239	0.326
6	0.089	0.075	0.074	0.073	0.077	0.072	0.069	0.096	0.125	0.242	0.318
6.5	0.090	0.076	0.076	0.074	0.078	0.072	0.070	0.097	0.127	0.245	0.315
7	0.091	0.077	0.077	0.075	0.079	0.073	0.070	0.098	0.129	0.248	0.317
7.5	0.091	0.078	0.077	0.076	0.079	0.074	0.071	0.099	0.130	0.249	0.312

Table C.1: Period-dependent values of ln(amp) of linear elastic simulations of simulations with 700 m/s < V_{S30} < 800 m/s as a function of depth, denoted as $C_{760\text{-}3000}$ in eq 13.of the main body of this report. The DI (Depth-Independent) column is the average amplilfication of all simulations with 700 m/s < V_{S30} < 800 m/s.

T (s)	DI Correction	5 m	10 m	15 m	20 m	25 m	30 m	50 m	100 m	50 m	1000 m
8	0.092	0.078	0.078	0.077	0.080	0.075	0.071	0.100	0.133	0.248	0.311
8.5	0.093	0.080	0.078	0.077	0.081	0.075	0.072	0.101	0.135	0.248	0.311
9	0.093	0.080	0.079	0.078	0.081	0.076	0.072	0.101	0.137	0.250	0.313
9.5	0.093	0.080	0.079	0.078	0.081	0.076	0.072	0.101	0.136	0.253	0.316
10	0.094	0.080	0.079	0.078	0.081	0.076	0.072	0.102	0.137	0.256	0.322